VLIZ North Sea Award

Candidate: Dr. Jens Boyen

Date: 30/12/2023

List of contributions

POLYUNSATURATED FATTY ACID BIOSYNTHESIS IN COPEPODS

A MECHANISM FOR CLIMATE CHANGE RESILIENCE

Jens Boyen

Marine Biology Research Group, Faculty of Sciences, Ghent University
Campus Sterre S8, Krijgslaan 281
9000, Gent, Belgium

Dutch translation of the title
Biosynthese van meervoudig onverzadigde vetzuren in roeipootkreeftjes – een mechanisme voor weerstand tegen klimaatverandering

Cover
Copepod drawings from: Khodami, S., McArthur, J. V., Blanco-Bercial, L., & Martinez Arbizu, P. (2017). Molecular Phylogeny and Revision of Copepod Orders (Crustacea: Copepoda). *Scientific Reports, 7*(1), 1–11. https://doi.org/10.1038/s41598-017-06656-4

Climate stripes: Visualization of global ocean temperature change (1850-2022) relative to average of 1971-2000 [°C]. The warming stripes graphics have been created by Professor Ed Hawkins (University of Reading) to start conversations about our warming world and the risks of climate change. https://showyourstripes.info/ #ShowYourStripes

Citation
Boyen, J. (2023) Polyunsaturated fatty acid biosynthesis in copepods - A mechanism for climate change resilience. PhD Thesis, Ghent University, Belgium

For citations to published work reprinted in this thesis, please refer to the original publication, as mentioned in the beginning of each chapter.

Defended in public on October 27, 2023

PROMOTORS

Prof. Dr. Marleen De Troch
Marine Biology Research Group, Faculty of Sciences, Gent University

PD Dr. Patrick Fink
Department of River Ecology and Department of Aquatic Ecosystem Analysis and Management, Helmholtz Centre for Environmental Research - UFZ, Magdeburg, Germany

Aquatic Chemical Ecology, Institute for Zoology, University of Cologne, Cologne, Germany

Prof. Dr. Pascal I. Hablützel
Flanders Marine Institute (VLIZ), Oostende

Biology Department, Vrije Universiteit Brussel, Brussels, Belgium

MEMBERS OF THE EXAMINATION COMMITTEE

Prof. Dr. Tom Moens (chair)
Marine Biology Research Group, Faculty of Sciences, Gent University

Prof. Dr. Jana Asselman (secretary)
Blue Growth Research Lab, Faculty of Biosciences Engineering, Ghent University

Prof. Dr. Olivier De Clerck
Phycology Research Group, Faculty of Sciences, Ghent Univesity

Dr. Sigrún H. Jónasdóttir
National Institute of Aquatic Resources, Technical University of Denmark, Denmark

Dr. Óscar Monroig
Instituto de Acuicultura Torre de la Sal (CSIC), Ribera de Cabanes, Castellón, Spain

« Ecosystems are so similar to human societies – they're built on relationships. The stronger those are, the more resilient the system. And since our world's systems are composed of individual organisms, they have the capacity to change. We creatures adapt, our genes evolve, and we can learn from experience. A system is ever changing because its parts […] are constantly responding to one another and to the environment. Our success in coevolution – our success as a productive society – is only as good as the strength of these bonds with other individuals and species. Out of the resulting adaptation and evolution emerge behaviours that help us survive, grow and thrive. »

Suzanne Simard (2021) *Finding the Mother Tree*

TABLE OF CONTENTS

ACKNOWLEDGMENTS

Six years, what a ride it's been. As the world slowly navigates through its many crises, I've been spending a significant amount of these years at this little corner of Earth called Sterre, trying to make a small contribution to the science of fatty acid biosynthesis. Luckily I was not alone. Along the way have been numerous people that I've got to meet for a short or longer period, many of whom don't properly grasp the impact they've had on my personal life, or on this thesis. I'm definitely not the best with putting the words and ideas from my always racing brain down to paper, but anyway here's my attempt at thanking all of you.

First of all, **Marleen**, thank you for the opportunity to conduct my PhD at the Marine Biology Research Group. You've always given me the freedom to come up with new research ideas and kick-start new scientific collaborations, which I'm grateful for. **Patrick**, you've been there from the very beginning as well. Thank you for your insightful advice and contributions. I fondly remember my short but successful RNA sequencing visits, which for some unexplainable reason always coincided with the Köln Christmas Market. **Pascal**, I'm so glad I took the bold step of asking you as a third co-promotor: your guidance on all things molecular and statistical have been challenging but finally rewarding, as you've helped me become a better, more critical scientist. I also very much enjoyed our chats about life inside and outside academia. Remind me to give back the book I stole from you all those years ago.

I would also very much like to thank the members of my examination committee **Tom, Jana, Olivier, Sigrún** and **Óscar**. Your feedback was highly valuable and insightful, and significantly improved many aspects of this thesis. **Olivier**, I've always appreciated the small bits of advice and challenging but engaging questions in these past years.

Óscar and **Naoki**, how can I ever properly thank the two of you, without whom I would likely have never finished this PhD. I'm forever grateful for the trust you've placed in this early-career PhD student from Ghent with his copepod transcriptome. My stay at Torre de la Sal was such a gift, and I'm very happy that we continue our collaboration

with Naoki's project. You infected me with a passion for fatty acid biosynthesis research that to this day keeps me going! And apart from the science, I'm so happy that I get along so well with both of you on a personal level as well. I hope we stay connected for many more years. Naoki, I wish you many moments of joy with Yui! **Juan Carlos**, many thanks to you as well for making my stay at Torre de la Sal so pleasurable and easy-going. I'll never forget your saying that "these copepods are like crazy little omega-3 factories!"

My main place of work was of course the Marbiol research group at Sterre. My continuous presence in the offices and labs was not so much due to my dislike of teleworking, but all the more because I loved hanging out with all of you. **Ann**, an earnest thank you for your relentless commitment to keep the Marbiol ship afloat, your heartfelt empathy and your strong sense of justice. You are an inspiration to generations of marine biologists. **Ulrike**, all the best with everything ahead. Know that myself and many others admire the way you seamlessly combine your scientific rigor with an engaging, positive and caring mind-set. Many thanks as well **Annick, Guy, Bart** and **Isolde** for all your help, whether it was by picking copepods, joining fieldwork at Paulina or assisting chaotic me with university administration. Also a heartfelt thank you to **Olga**, for teaching me and many others the ins and outs of algae culturing, and **Sofie**, for your tips and advice at the CeMoFE. **Bruno** and **Annelien**, this PhD thesis belongs to you as well. You've helped me so much with all the fatty acid and molecular work, and always joined in enthusiastically on my wild ideas for novel analyses. You are both invaluable pieces of Marbiol whose critical importance cannot be overstated.

After six years, entire generations of colleagues departed, and new ones arrived. **Thomas**, as your Master thesis student, you helped me gain the molecular experience I needed to embark on this PhD, which I'm very grateful for. Needless to say I was very happy when I became your officemate, together with **Ee Zin**, **Mirta** and the fish. **Siel,** what a ride we had together, how to put this down in words. The many (many!) hours of picking copepods, teaching practicals and eating koffiekoeken in Biervliet together

have been a joy because of you. Your (and **Nele**'s!) incredible teaching skills have been inspirational, and you can be really proud at everything you've accomplished. **Christoph** and **Laurien**, thank you so much for planting the seeds of this PhD. Siel, Laurien and **Robyn**, this PhD belongs as much to you as it belongs to me.

Ellen V, Ivan, Helena, Sebastiaan, Brecht, Tim D, Tim V, Freija, Nele, Liesbet, Lisa, Yana, An-Sofie, Ninon, Lidia, Inne, Inge, Qian and **Evelyn**, it was a pleasure being your colleague, and I very much enjoyed all the WinMon sampling, conferences, summer schools and parties with you. **Pieterjan**, I had great fun with our eel genetics side project, and I'm hoping for a positive outcome soon! **Gabriella, Lara, Anna-Maria, Ellen P, Rodgee, Francesca, Marleen R, Tania, Luana and Tim T**, I wish you many more happy moments at Marbiol, whether that's at a sunny lunch break around our picnic tables, or during one of our Marbiol parties. **Carl** and **Ee Zin,** thank you so much for all your help and advice with the ocean acidification experiments! **Quinten** and **Willem:** your tips, advice with bioinformatics and experiments were very much appreciated. After covid, a fresh wave of colleagues arrived at Marbiol, revitalising the lab with an energetic atmosphere. **Bram, Lotte, Iene, Abril, Christelle, Esther, Jordan, Marie C, Marie R, Yens, Yen, Tuan-Anh** and of course **Mario**: I wish you all the best in the years ahead, and I'm confident that the Marbiol spirit continues to thrive.

Many, many thanks as well to my thesis and internship students **Teresa, Cynthia, Benjamin, Robyn, Nisa** and **Asatsa**. Not only did you all contribute to the successful completion of this research, you were also amazing people to work with. Good luck with all your future plans! **Alberto, Marc** and **Andrea**, my stay at Torre de la Sal became even more wonderful with your company. I very much enjoyed our many hikes together in the Castellón mountains. Also a big thank you to my VLIZ colleagues **Anouk, Michiel, Sarah, Steven** and more to welcome me into your group, and for the fun evenings and writing week we had together. Many thanks as well to **Samuel** for your invaluable help with the compound-specific stable isotope analysis, and to **Ilias** for all your advice and your assistance with Robyn's thesis. I really enjoyed our collaboration!

Whenever my frustrations about work were getting to much, I had the privilege to count on my friends to cheer me up again. The entire amazing **EMBC+** 2015-2017 cohort and especially my housemates **Eli, Emilie, Stephan, Aude** and **Emma**: you shaped me into the person I am today. Many thanks as well to my Ledeberg housemates **Emma, Miriam** and **Femke** for enduring my complaints after another day of failed RNA extractions. Femke, I can never thank you enough for introducing me to the world of activism. Your fight for a more sustainable and just university is admirable! **Luz** and **Soria**, our journey in Ghent started together, and six years later it seems we're still here. We learned a lot from each other along the way, and I'm very grateful for your company, and the good times together (including getting stuck in the snow in Norway). **Joren, Jens, Giel** and **Gert,** our friendship dating back from our time in Leuven means so much to me. Our hangouts, evenings and weekends together are always great fun, even if they mean crossing half of Belgium each time.

But who cares about proper work/life balance when you're able to call your colleagues your friends. **Jolien**, your fight for justice is so inspirational. **Nene**, I promise the Wingspan game night is coming soon! **Marius**, my fellow narwhal, you're one of the funniest people I know. I truly believe you're capable to do great things. **Mirta**, your captivating energy made me entering the Jungle Office with a big smile each morning. **Robyn**, the moment you approached me for a thesis I knew you weren't just another student. I'm so glad it turned into this friendship. **Juli**, who are you kidding, of course you're going to stay in Ghent forever. **Ricca**, I'm already looking forward to many more late evenings together! You're all wonderful beings!

To my family, **Ruben, Robbe, Jelle, mama** and **papa**, for your support all these years. Also many thanks you **Annick** and **Paul** for welcoming me to your wonderful family and inviting me into your home after long days at Sterre.

And finally, of course, **Liselotte**. My fellow adventurer, hiking companion, late-night workaholic colleague, life advisor, crazy impulsive idea generator, emotional support Labrador, and my biggest supporter of all. Met u heb ik wel het beste Lotje getrokken!

LIST OF ABBREVIATIONS

AIC	Akaike Information Criterion	glm	generalized linear model
ALA	α-linolenic acid; 18:3n-3	GO	Gene Ontology
ANOVA	Analysis of Variance	GST	global surface temperature
AR5	IPCC's Fifth Assessment Report	HGT	horizontal gene transfer
AR6	IPCC's Sixth Assessment Report	IPCC	Intergovernmental Panel on Climate Change
ARA	arachidonic acid; 20:4n-6	IRMS	isotope ratio mass spectrometry
BEB	Bayes Emperical Bayes method	LA	linoleic acid; 18:2n-6
BUSCO	Benchmarking Universal Single-Copy Ortholog	LC-PUFA	long-chain polyunsaturated fatty acid
CDS	coding sequence	LRT	likelihood ratio test
CMIP	Coupled Model Intercomparison Project	med	methyl-end desaturase
CO_2	carbon dioxide	MS	mass spectrometry
COUSIN	COdon Usage Similarity INdex	MUFA	monounsaturated fatty acid
CS-SIA	compound-specific stable isotope analysis	nMDS	non-metric multidimensional scaling
DE	differential expression	OA	ocean acidification OR oleic acid; 18:1n-9
DHA	docosahexaenoic acid; 22:6n-3	ORF	open reading frame
elovl	fatty acyl elongase	OW	ocean warming
EPA	eicosapentaenoic acid; 20:5n-3	PCR	polymerase chain reaction
FA	fatty acid	POC	particulate organic carbon
FAME	fatty acid methyl ester	ppm	parts per million
FATM	fatty acid trophic marker	PUFA	polyunsaturated fatty acid
fed	front-end desaturase	qPCR	quantitative reverse-transcription PCR
FID	flame ionization detector	RCP	Representative Concentration Pathway
FNSW	filtered and autoclaved natural seawater	scd	stearoyl-CoA-desaturase
GC3	GC content (%) at the third codon position	SFA	saturated fatty acid
GC	gas chromatography	SRA	Short Read Archive
GEO	Gene Expression Omnibus	SSP	Shared Socioeconomic Pathway
GHG	greenhouse gas	SST	sea surface temperature
gllvm	generalized linear latent variable model	TSA	transcriptome shotgun assembly

SUMMARY

Since the Industrial Revolution, increasing global human activities detrimentally impacted the environment to such an extent that many ecosystems can no longer provide the services that human populations rely on in order to thrive. Growing emissions of greenhouse gasses (GHG) such as CO_2 causes an increase in global surface temperatures, further leading to ocean warming (OW) and ocean acidification (OA). Marine ecosystems have already been profoundly impacted by OW and OA, with detrimental effects continuing to intensify depending on future emission scenarios.

One such effect, also reported in the latest Assessment Report of the Intergovernmental Panel on Climate Change, is the multifactorial decline in production of long-chain polyunsaturated fatty acids (LC-PUFAs) by (mainly marine) microalgae. These fatty acids (FAs) are important lipid biomolecules for humans and other animals, as they ensure proper growth, reproduction and fitness. Particularly, omega-3 LC-PUFAs such as eicosapentaenoic acid (EPA) and docosahexaenoic acid (DHA) are highly abundant in marine ecosystems. They play crucial physiological roles for phospholipid membrane fluidity, energy storage and provisioning, gene regulation, and as precursors for various cell signalling and hormone molecules.

Until recently, it was widely believed that LC-PUFAs are primarily produced by autotrophic microorganisms such as microalgae and bacteria. These LC-PUFAs are subsequently transferred through the food web towards higher trophic levels including fish and humans, who acquire them from their diets. It is now well established however that many animal consumers can at least to some extent synthesize their own PUFAs and LC-PUFAs (endogenously or from other FA precursors) via a repertoire of fatty acid desaturase and elongase enzymes, marking a paradigm shift in trophic ecology research.

Among the animals with suspected PUFA biosynthesis capabilities are the small pancrustacean class of Copepoda. They are an ecologically and morphologically extremely diverse group, are dominant and abundant members of many pelagic and

benthic communities in marine and freshwater systems. Copepods generally contain high levels of omega-3 LC-PUFAs. As key primary consumers at the basis of aquatic food webs, they are crucial in ensuring LC-PUFA provisioning to higher trophic levels. However, the extent to which their PUFA biosynthesis capacity can buffer the LC-PUFA production decline in microalgae following climate change remains unknown.

In this PhD research, I investigated the molecular mechanisms of PUFA biosynthesis in copepods as consumers at the base of aquatic foodwebs, how it relates to their past evolutionary diversification, and how it responds towards future anthropogenic ocean warming and acidification. In Chapters 2 to 4, I specifically focussed on the benthic harpacticoid copepod *Platychelipus littoralis* (Brady, 1880), a dominant inhabitant of marine and brackish Northeast Atlantic mudflats. While previous work indicated at least some capacity for biosynthesis of EPA and DHA, no genetic resources were as of yet available for this species.

In Chapter 2, I performed RNA sequencing and *de novo* assembled the transcriptome of *P. littoralis* specimens exposed to a combination of OW (+3 °C) and dietary LC-PUFA limitation. LC-PUFA levels remained unaltered even under dietary LC-PUFA limitation. Temperature however, decreased both the total FA content as well as the absolute concentration of DHA. While I did find transcriptional changes of a limited number of genes when exposed to dietary LC-PUFA limitation and/or OW, none of the putative front-end desaturase or elongase transcripts identified were found to be differentially expressed.

Following this, I decided to further identify and functionally characterize the PUFA biosynthesis genes of *P. littoralis* using a heterologous expression system. In Chapter 3, I show that the putative front-end desaturase identified in Chapter 2 is related to non-functional desaturase-like sequences of decapods. However, I identified a novel *P. littoralis* front-end desaturase closely related to a functional front-end desaturase of the harpacticoid copepod *Tigriopus californicus*. I also found one methyl-end desaturase, only recently discovered in animals, and a number of fatty acid elongases.

The *P. littoralis* methyl-end desaturase has Δ15/17/19 desaturation activity, enabling biosynthesis of α-linolenic acid, EPA and DHA from various omega-6 PUFA precursors. The *P. littoralis* front-end desaturase has Δ4 desaturation activity from docosapentaenoic acid to DHA, implying that *P. littoralis* has multiple pathways to produce this physiologically important fatty acid. All characterized *P. littoralis* elongases were shown to possess varying degrees of elongation activity towards both saturated and unsaturated fatty acids, even producing aliphatic hydrocarbon chains with lengths of up to 30 carbons. While this implied that the gene repertoire of *P. littoralis* identified so far does not allow full endogenous LC-PUFA biosynthesis from monounsaturated precursors, other harpacticoid species such as *T. californicus* did exhibit this capacity.

In Chapter 4, I improved upon the experiment in Chapter 2 by performing a similar experiment that included OA (-0.4 pH) as a third climate change driver next to OW (+3 °C) and dietary LC-PUFA limation. I used reverse transcription quantitative PCR to assess the expression of the PUFA biosynthesis genes identified earlier (as well as an additionally identified stearoyl-CoA desaturase), and combined this with FA profiling. I found that generally, *P. littoralis* had fatty acids with shorter chains and fewer unsaturations when exposed to multiple stressors. While they were able to maintain relative DHA concentrations when fed *Dunaliella tertiolecta* at current temperatures (compared to when fed a LC-PUFA rich diet), these concentrations dropped when simultaneously exposed to OW. Similarly, expression of the DHA biosynthesis genes fed and elovl1a increased to compensate with dietary LC-PUFA limitation, but did not exceed control levels when the copepods were simultaneously exposed to OA, indicating the limitations of *P. littoralis* to cope with compound climate impacts. I also showed that PUFA biosynthesis gene expression was correlated positively with C_{18} precursors and negatively with LC-PUFAs, further proving their role as LC-PUFA biosynthesis enzymes.

In Chapter 5, I leveraged all publically available copepod transcriptomes to investigate differences in PUFA biosynthesis capacity between ecologically different copepod orders. Investigating genome anchoring, GC content, intron number and codon usage bias, I provided further evidence for the previously suggested hypothesis that methyl-end desaturases and front-end desaturases both appeared in a common copepod ancestor following two separate horizontal gene transfers (HGT). Both types of desaturases were subsequently retained in most copepod orders, but lost in the (mainly marine pelagic) Calanoida, except for some *Calanus* and *Neocalanus* species that still have one front-end desaturase. In contrast, elongase copy number did not differ between orders, although elongase expression was shown to be higher than average in benthic harpacticoids but lower in pelagic calanoids. All desaturase and elongase gene families exhibited non-clustered distribution in the assessed genomes, and positive selection on specific codons following HGT and duplication events.

Overall, in this PhD research I show that copepods, through their unique but varying PUFA biosynthesis capacity, can supply aquatic ecosystems with additional LC-PUFAs, even following projected declines in autotroph-derived LC-PUFA production. Combining this capacity with their high potential for rapid adaption, I argue that PUFA biosynthesis in copepods can be a mechanism for climate change resilience. However, the exact amount of LC-PUFAs that copepods can contribute with remains to be properly quantified. In addition, copepods themselves are also impacted by multiple direct and indirect effects of climate change, and biophysical phospholipid membrane adjustments are bound to occur in all trophic levels regardless of adaptation.

Further increases in OW and OA are likely to limit future LC-PUFA provisioning to both ecosystems and the global human population, and should therefore be avoided. In this regard, LC-PUFA provisioning can be envisioned as an ecosystem service with quantifiable social justice and environmental boundaries, and a number of components along the LC-PUFA supply chain can be improved in order to maintain sufficient LC-PUFA provisioning for all, both now, and in a future climate.

SAMENVATTING

Sinds de Industriële Revolutie hebben toenemende menselijke activiteiten wereldwijd de omgeving zodanig aangetast, dat ondertussen veel ecosystemen niet langer de diensten kunnen leveren waar onze maatschappij op vertrouwt. De nog steeds toenemende uitstoot van broeikasgassen zoals CO_2 veroorzaakt een stijging van de globale temperatuur, en zorgt ervoor dat de oceanen niet alleen opwarmen maar ook verzuren. Mariene ecosystemen zijn ondertussen al verregaand aangetast door oceaanopwarming en -verzuring, en afhankelijk van toekomstige emissiescenario's zullen deze nadelige effecten blijven toenemen.

Eén zo'n effect, dat ook wordt gerapporteerd in het laatste Assessment Report van het Intergovernmental Panel on Climate Change, is de multifactoriële afname van de productie van meervoudig onverzadigde vetzuren met lange ketens door (voornamelijk mariene) microalgen. Dit soort vetten zijn belangrijke biomoleculen voor mensen en andere dieren, omdat ze zorgen voor een goede groei, voortplanting en fitness. Met name de zogenaamde omega-3 vetzuren zoals eicosapentaeenzuur (EPA) en docosahexaeenzuur (DHA) zijn overvloedig aanwezig in mariene ecosystemen. Ze spelen cruciale fysiologische rollen in de structuur van fosfolipidemembranen, de opslag en voorziening van energie, genregulatie en als voorlopers voor verschillende signalerings- en hormoonmoleculen.

Tot voor kort werd algemeen aangenomen dat omega-3 vetzuren hoofdzakelijk worden geproduceerd door autotrofe micro-organismen zoals microalgen en bacteriën. Deze vetzuren worden vervolgens doorgegeven via het voedselweb aan hogere trofische niveaus (zoals vissen en mensen), die zo de vetzuren via hun voeding binnenkregen. Het is nu echter duidelijk vastgesteld dat veel dieren tot op zekere hoogte hun eigen omega-3 vetzuren kunnen aanmaken (endogeen of uit andere vetzuurprecursoren), aan de hand van enzymen genaamd vetzuurdesaturases en vetzuurelongases. Deze vaststelling betekende een paradigmaverschuiving in het trofische ecologieonderzoek.

Voornamelijk ongewervelden worden gedacht dat ze in staat zijn om omega-3 vetzuren aan te maken, waaronder kleine kreeftachtigen genaamd roeipootkreeftjes of Copepoda. Deze vormen een ecologisch en morfologisch zeer diverse groep. Ze zijn dominant en abundant binnen veel pelagische en benthische gemeenschappen in oceanen en zoetwatersystemen, en bevatten over het algemeen hoge gehaltes aan omega-3 vetzuren. Als primaire consumenten aan de basis van aquatische voedselwebben, zijn roeipootkreeftjes van cruciaal belang voor de voorziening van omega-3 vetzuren naar hogere trofische niveaus toe. Het is echter nog niet goed geweten in hoeverre hun capaciteit voor biosynthese van omega-3 vetzuren de (door klimaatverandering) verwachte afname van deze vetzuren in microalgen kan bufferen.

In dit doctoraatsonderzoek heb ik de moleculaire mechanismen achter vetzuurbiosynthese binnen roeipootkreeftjes onderzocht. Ik keek in welke mate dit mechanisme verband houdt met hun vroegere evolutionaire diversificatie, en onderzocht de impact van de verwachte oceaanopwarming en –verzuring. In hoofdstukken 2 tot en met 4 richtte ik me specifiek op het benthische harpacticoïde roeipootkreeftje *Platychelipus littoralis* (Brady, 1880), een dominante bewoner van mariene en brakke moddervlaktes rond de Noord-Atlantische oceaan. Hoewel uit eerder werk bleek dat zij enige capaciteit hadden voor de biosynthese van EPA en DHA, is er tot nu toe geen genetische informatie beschikbaar voor deze soort.

In hoofdstuk 2 heb ik aan de hand van RNA-sequencing het transcriptoom aangemaakt van *P. littoralis*. Ik stelde individuen van deze soort bloot aan een combinatie van oceaanopwarming (+3 °C) en vetzuurlimitatie in het dieet. Ondanks deze vetzuurlimitatie in het dieet bleef de relatieve vetzuursamenstelling onveranderd. Wel verminderde oceaanopwarming zowel de totale hoeveelheid vetzuren als de absolute concentratie van DHA. Hoewel ik veranderingen in expressie vond van een beperkt aantal genen door vetzuurlimitatie en/of oceaanopwarming, bleek geen enkel van de vermeende front end desaturases of elongases differentieel tot expressie te komen.

Vervolgens besloot ik om de genen voor vetzuurbiosynthese van *P. littoralis* verder te identificeren en functioneel te karakteriseren met behulp van heterologe expressie in gist. In hoofdstuk 3 toonde ik dat het vermeende front-end desaturase geïdentificeerd in hoofdstuk 2 verwant is aan niet-functionele desaturase-achtige sequenties van kreeften en krabben. Ik vond echter een nieuw *P. littoralis* front end desaturase dat nauw verwant is aan een functioneel front-end desaturase van het roeipootkreeftje *Tigriopus californicus*. Ook vond ik een methyl-end desaturase, een type dat pas recent ontdekt is bij dieren, alsook een aantal vetzuurelongases. Het *P. littoralis* methyl-end desaturase heeft de capaciteit voor Δ15/17/19 desaturatie, waardoor biosynthese van α-linoleenzuur, EPA en DHA uit verschillende omega-6 mogelijk is. Het *P. littoralis* front-end desaturase heeft de capaciteit voor Δ4 desaturatie van docosapentaeenzuur naar DHA. Dit impliceert dat *P. littoralis* meerdere routes heeft om het fysiologisch belangrijke vetzuur DHA te produceren. Van de gekarakteriseerde *P. littoralis* elongases werd aangetoond dat ze in verschillende mate elongatieactiviteit voor zowel verzadigde als onverzadigde vetzuren bezitten, en sommige zelfs vetzuren kunnen produceren met lengtes tot 30 koolstofatomen. Hoewel deze studie impliceert dat de tot nu toe geïdentificeerde genen van *P. littoralis* geen volledige endogene omega-3 vetzuurbiosynthese uit verzadigde vetzuurprecursoren toelaten, vertoonden andere harpacticoïde soorten zoals *T. californicus* deze capaciteit wel.

In hoofdstuk 4 voerde ik een vergelijkbaar experiment als uit hoofdstuk 2 uit, maar waarbij ik oceaanverzuring (-0,4 pH) in rekening bracht, naast oceaanopwarming (+3 °C) en vetzuurlimitatie in het dieet. Ik gebruikte quantitative PCR om de expressie van de eerder geïdentificeerde vetzuurbiosynthesegenen te bepalen (evenals het nieuw geïdentificeerde stearoyl-CoA desaturase), en combineerden dit opnieuw met vetzuurprofilering. Deze keer vond ik dat *P. littoralis* over het algemeen vetzuren met kortere ketens en minder onverzadigde vetzuren had bij blootstelling aan meerdere stressfactoren. Terwijl de soort in staat was om de relatieve DHA-concentraties op peil te houden wanneer ze gevoerd werden met *Dunaliella tertiolecta* bij de huidige temperaturen (in vergelijking met wanneer ze gevoerd werden met een dieet rijk in

EPA en DHA), daalden de DHA concentraties wanneer ze tegelijkertijd blootgesteld werden aan oceaanopwarming. Ook nam de expressie van de DHA-biosynthesegenen fed en elovl1a toe ter compensatie van de vetzuurlimitatie in het dieet, maar namen ze niet toe wanneer de roeipootkreeftjes gelijktijdig werden blootgesteld aan oceaanverzuring, wat erop wijst dat op *P. littoralis* slechts beperkt kan omgaan met meerdere, gecombineerde klimaatstressoren. Ik toonde ook aan dat expressie van vetzuurbiosynthesegenen positief gecorreleerd was met C_{18} precursoren, en negatief met EPA en DHA, wat hun rol als biosynthese-enzymen van deze omega-3 vetzuren verder bewijst.

In hoofdstuk 5 maakte ik gebruik van alle publiek beschikbare transcriptomen van roeipootkreeftjes om verschillen in vetzuurbiosynthese tussen ecologisch verschillende copepoden ordes te onderzoeken. Door genoomverankering, GC-gehalte, aantal introns en codon usage bias te onderzoeken, leverde ik verder bewijs voor de eerder gesuggereerde hypothese dat methyl-end desaturases en front-end desaturases beide verschenen in het DNA van een gemeenschappelijke voorouder van roeipootkreeftjes na twee afzonderlijke horizontal gene transfers. Beide typen desaturases werden vervolgens behouden in de meeste ordes roeipootkreeftjes, maar verdwenen in de (voornamelijk mariene pelagische) Calanoida, met uitzondering van enkele soorten *Calanus* en *Neocalanus* soorten die nog steeds één front-end desaturase bezitten. Het aantal kopieën van elongasegenen verschilde daarentegen niet tussen de ordes, maar de expressie van deze elongases bleek wel hoger dan gemiddeld te zijn bij benthische harpacticoïden, en lager bij pelagische calanoïden. Alle families van desaturase- en elongase-genen vertoonden een niet-geclusterde verdeling binnen de beoordeelde genomen. Ook vertoonden zij positieve selectie op specifieke codons na HGT en duplicatiegebeurtenissen.

Door dit doctoraatsonderzoek toonde ik aan dat roeipootkreeftjes, door hun unieke maar variërende capaciteit voor vetzuurbiosynthese, aquatische ecosystemen kunnen voorzien van extra omega-3 vetzuren, zelfs na de verwachte productieafname van deze

vetzuren door microalgen. Deze capaciteit, gecombineerd met hun groot potentieel om zich snel evolutionair aan te passen, zorgt er volgens mij voor dat dit een mechanisme kan zijn om bestand te zijn tegen klimaatverandering. De exacte hoeveelheid omega-3 vetzuren die roeipootkreeftjes kunnen produceren moet echter nog goed gekwantificeerd worden. Bovendien worden roeipootkreeftjes zelf ook beïnvloed door meerdere directe en indirecte effecten van klimaatverandering, en biofysische vetzuurmembraanaanpassingen zullen ongetwijfeld in alle trofische niveaus plaatsvinden, ongeacht potentiële toekomstige adaptie.

Verdere toenames van oceaanopwarming en -verzuring zal de toekomstige voorziening van omega-3 vetzuren voor zowel ecosystemen als de wereldbevolking waarschijnlijk belemmeren, en moeten daarom worden vermeden. In dit opzicht kan de omega-3 vetzuurvoorziening worden gezien als een ecosysteemdienst met kwantificeerbare sociaal rechtvaardige en ecologische grenzen, en een aantal onderdelen van de toeleveringsketen van vetzuren kan worden verbeterd om te voldoen aan de minimum omega-3 vetzuurbehoefte van iedereen, zowel nu als in een toekomstig klimaat.

CHAPTER 1

GENERAL INTRODUCTION

1.1 Anthropogenic global change: causes and consequences
    1.1.1   Welcome to the Anthropocene
    1.1.2   Anthropogenic greenhouse gas emissions and impacts on the biosphere
    1.1.3   Ocean warming and acidification
    1.1.4   Aquatic organisms and ecosystems: impact, vulnerability and responses
    1.1.5   Assessing biological impacts of and responses to global ocean change

1.2 Polyunsaturated fatty acids: vital biomolecules for a thriving biosphere
    1.2.1   Role, functions and demand of polyunsaturated fatty acids
    1.2.2   Polyunsaturated fatty acids in a changing ocean
    1.2.3   Transfer of polyunsaturated fatty acids throughout the food web
    1.2.4   Molecular mechanisms of polyunsaturated fatty acid biosynthesis
    1.2.5   Assessing polyunsaturated fatty acid biosynthesis and conversion in animals

1.3 Copepods: key microcrustaceans at the basis of aquatic food webs
    1.3.1   Evolution, phylogeny and biodiversity
    1.3.2   Role as primary consumers within aquatic food webs
    1.3.3   Copepods in a changing ocean
    1.3.4   Polyunsaturated fatty acid biosynthesis in copepods

1.4 Aims, objectives and outline of the thesis

1.1 Anthropogenic global change: causes and consequences

1.1.1 Welcome to the Anthropocene

Throughout their entire history, the actions of modern humans have had a profound impact on the environment. Approximately 13,000 years ago, as humans began practicing agriculture and domesticating plants and animals, they started exerting a significant influence on their local ecosystems. Over the centuries, deforestation, habitat loss and land-system changes increased alongside regional human population size increases, primarily at local and regional scales (Lewis & Maslin, 2015). An exponential population increase, especially after the Industrial Revolution (Roser et al., 2023), coupled with increased *per capita* resource production, consumption, and emissions, particularly by a small fraction of the global population, was a turning point. It resulted not only in local detrimental impacts on the environment, but marked the start of global-scale negative consequences for both the biosphere and human health (Steffen et al., 2015b).

Current global impacts range from the extraction of biotic (i.e. forests, fish populations) and non-biotic (i.e. mining) components from the environment, over the changes in land-use for agriculture and built infrastructure, to the emission of harmful pollutants in the soil, atmosphere and aquatic ecosystems. Since the 1950's, human activities and related environmental damages accelerated to such an extent – also known as *The Great Acceleration* (Steffen et al., 2015a) - that our current Earth system is at risk of becoming uninhabitable for future human generations. Humans are now seen as the dominant force contributing to changes on our planet, which led to the recognition of a new geological epoch termed the *Anthropocene* (Folke et al., 2021; Lewis & Maslin, 2015).

In order to assess and ensure Earth system stability and resilience, scientists from (among others) the Stockholm Resilience Centre have developed a framework with nine so-called *Planetary Boundaries* (Figure 1), which, when crossed, threaten the future of the global biosphere as a safe operating space for humanity (Richardson et al., 2023;

Rockström et al., 2009; Steffen et al., 2015b). This global biosphere provides a number of functions that allow life to thrive, such as food provisioning and water filtration, and these so-called *ecosystem services* can be quantified to define the need for society to keep certain ecosystems intact (Daily et al., 2000; FAO, 2023).
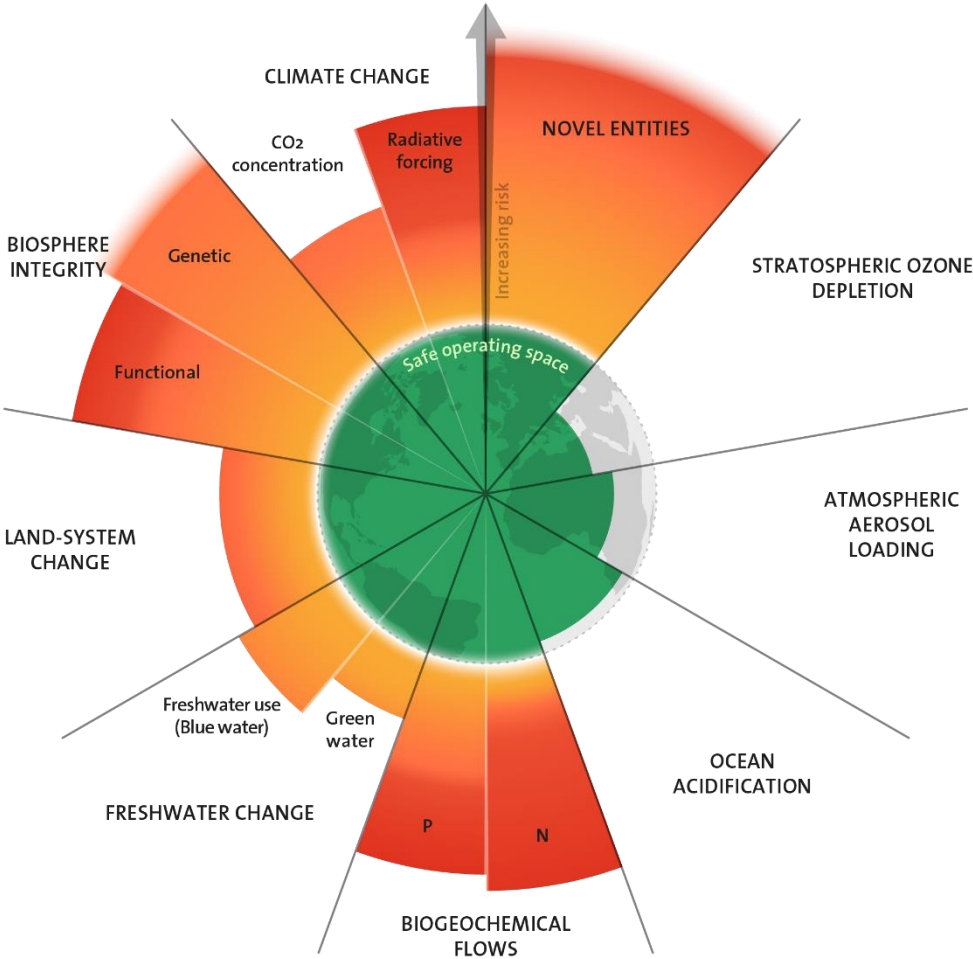
Figure 1 Current status of the nine planetary boundaries. Credit: Azote for Stockholm Resilience Centre, based on analysis in (Richardson et al., 2023). The green zone is the safe operating space (below the boundary), while orange and red represent the zone of uncertainty (increasing risk). P = Phosphorus; N = Nitrogen. Figure from (Stockholm Resilience Centre, 2023).

1.1.2 Anthropogenic greenhouse gas emissions and impacts on the biosphere

Human-induced climate change, as one of the 'core' planetary boundaries, is justifiably considered one of the great crises of the 21st century (Steffen et al., 2015b). Since around 1750, a number of exponentially increasing human activities resulted in the emission of greenhouse gasses (GHG) such as carbon dioxide (CO_2), methane (CH_4) and

nitrous oxide (N_2O) in the atmosphere (IPCC, 2021). These activities range from deforestation over infrastructure development to industrial cattle breeding, but by far the largest contribution to GHG emissions is the production and use of fossil fuels such as coal, oil and gas for energy generation (IPCC, 2022b). Atmospheric CO_2 concentration reached an annual average of 417.2 parts per million (ppm) in 2022, up from less than 300 ppm in the past two millions years before 1850 (Friedlingstein et al., 2022; IPCC, 2021). GHGs interfere with the amount of energy that leaves the Earth system by the reflection of sunlight and thermal radiation; the amount of interference is known as *effective radiative forcing*. As a result, atmospheric GHG concentrations and global surface temperature (GST) are strongly coupled, and therefore increasing GHG emissions unequivocally caused GSTs to reach levels that have been unprecedented in the past 125.000 years (IPCC, 2021). The science behind anthropogenic climate change is robust and well-established, and dates back to Foote's observations in 1856 that CO_2 retains heat (Foote, 1856). Fossil fuel companies such as ExxonMobil are now known to have been aware about the dangers of their products to the global climate since at least the 1950s, which they attempted to hide from the larger public (Supran et al., 2023). The United Nations' *Intergovernmental Panel on Climate Change* (IPCC) was established in 1988 to investigate the causes and consequences of climate change, and they compiled their findings into six *Assessment Reports*, with the latest coming out in 2021 and 2022 (IPCC, 2021, 2022a, 2022b).

GHG emissions caused GST to rise by an estimated 1.09 °C between 1850-1900 and 2011-2020 (IPCC, 2021). Multiple components of the Earth system are affected, which include sea level rise, sea ice and glacier retreat, ocean warming and acidification, permafrost thawing, and increases in heatwaves, heavy precipitation, drought and tropical cyclones. GHG emissions *per capita* have varied and continue to vary widely across regions and income levels, and are deeply linked with the capital appropriation of resources as well as histories of colonisation (Malm & Hornborg, 2014). Notably, people that are the least responsible for GHG emissions are often the most vulnerable and most impacted to the effects of climate change (IPCC, 2022a, 2022b). Global GHG

emissions have continued to increase in the last ten years (IPCC, 2022b), and the remaining *global carbon budget* for a 50% likelihood to limit global warming to 1.5 °C is set at 380 $GtCO_2$, or an equivalent of 9 years at 2022 emission levels (Friedlingstein et al., 2022).

To assess and project future climate change, a core set of emission scenarios are quantified using climate model simulations coordinated and collected as part of the World Climate Research Programme's *Coupled Model Intercomparison Project* (CMIP) (IPCC, 2021). IPCC's Fifth Assessment Report (AR5) used the four *Representative Concentration Pathways* (RCPs) from CMIP Phase 5 (CMIP5), which were RCP2.6, RCP4.5, RCP6, and RCP8.5, labelled after their expected level of anthropogenic radiative forcing (in watts $meter^{-2}$) by 2100 (IPCC, 2013). The Sixth Assessment Report (AR6) enhanced the RCP scenarios with five *Shared Socioeconomic Pathways* (SSPs) from CMIP Phase 6 (CMIP6), which better reflect narratives concerning socio-economic assumptions and developments (IPCC, 2021). The five scenarios are: SSP1-1.9/2.6, SSP2-4.5, SSP3-7.0, SSP4 (often not included in IPCC impact scenarios), and SSP5-8.5. While high emissions scenarios RCP8.5 and SSP5-8.5 are deemed by some unlikely to actually occur (Hausfather & Peters, 2020), cumulative GHG emmisions from 2005 to 2020 are most consistent with RCP8.5 (Schwalm et al., 2020). CMIP5 estimates of GST increases by 2081-2100 (relative to 1986-2005) range from 1.0 °C under RCP2.6 to 3.7 °C under RCP8.5 (IPCC, 2013). CMIP6 estimates of GST increases by 2081-2100 (relative to 1850-1900) range from 1.4 °C under SSP1-1.9 to 4.4 °C under SSP5-8.5, and projected GST increases compared to the current period (2011-2020) can be calculated by subtracting the already observed past GST increase of 1.09 °C (IPCC, 2021). Current mitigation policies and actions are estimated to result in global warming of 2.7 °C by 2100 compared to pre-industrial levels (Climate Action Tracker, 2022).

Both GHG emissions and the resulting global warming have caused, and will continue to cause, large-scale, detrimental impacts on the Earth biosphere well beyond natural climate variability (IPCC, 2022a). It has caused and will continue to cause severe

damages in terrestrial, freshwater and marine ecosystems, with many species already extinct at a local or global level. Species are increasingly being affected in their development, reproduction, physiology, phenology, behaviour and movement and ecology, with further indirect effects on their communities and ecosystems (Hoegh-Guldberg et al., 2018). Declines in key ecosystem goods and services threaten human health and wellbeing. For instance, climate change is projected to have severe consequences to food security and nutrition (Mirzabaev et al., 2023). Moreover, between 1970 and 2021, climate and water-related disasters resulted in over 2 million deaths and economic losses of US$4.3 trillion (World Meteorological Organization, 2022).

1.1.3 Ocean warming and acidification

The ocean, as one of the Earth systems covering 71% of its surface, is a hub of biodiversity (Appeltans et al., 2012). It provides a habitat for a large proportion of eukaryotic and prokaryotic species and delivers a number of Earth system functions such as climate and carbon regulation. The ocean and its marine ecosystems offer numerous benefits for humans such as food provision, photosynthetic oxygen production, coastline protection, recreation and cultural heritage (Barbier et al., 2011; Selig et al., 2019). It absorbs both heat and CO_2 from the atmosphere (Boyd et al., 2019), which causes *ocean warming* (OW) and *ocean acidification* (OA), respectively, resulting in increases in temperatures, heat waves, sea levels (caused by both thermosteric expansion and ice sheet melt) and upper-ocean stratification, decreases in oxygen and nutrient availability, and changes in ocean circulation patterns (IPCC, 2022a). Global mean *sea surface temperature* (SST) has increased by 0.88 °C between 1850–1900 and 2011–2020, and projected further SST increases between 1995-2014 and 2081-2100 range from 0.86 °C under SSP1-2.6 to 2.89 °C under SSP5-8.5 (IPCC, 2021). When SST increases are calculated relative to 1870–1899, they range from 1.42 °C under SSP1-2.6 to 3.47 °C under SSP5-8.5 (Kwiatkowski et al., 2020) (Figure 2a).
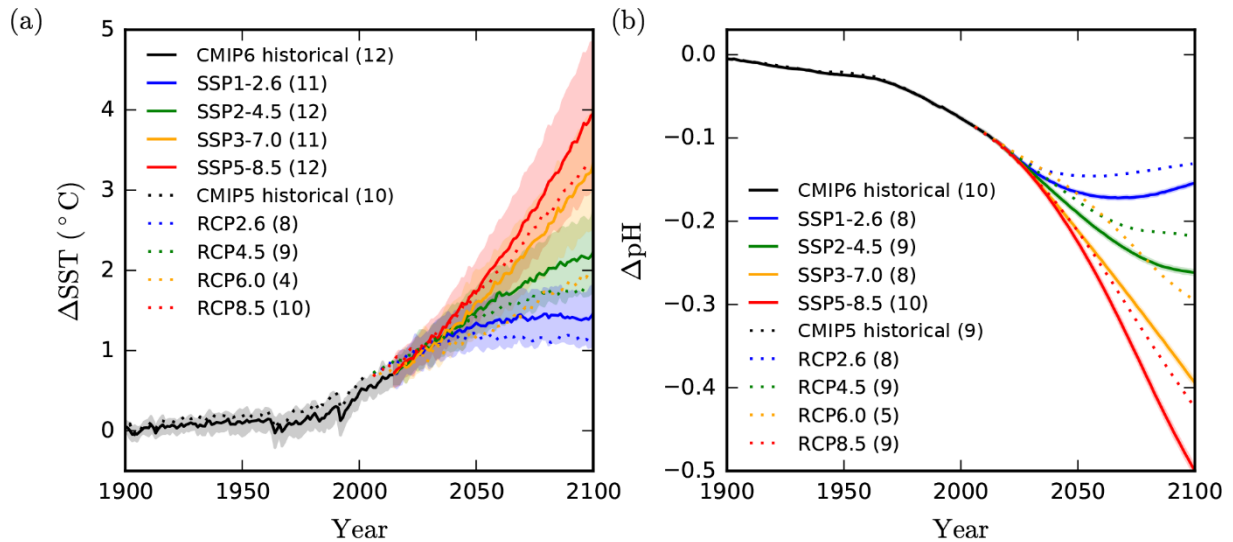
Figure 2 Past and future anomalies in global mean (a) sea surface temperature (SST) and (b) surface ocean pH, relative to 1870–1899. Couple Model Intercomparison Project (CMIP) Phase 6 (CMIP6) mean anomalies for the historical and Shared Socioeconomic Pathway (SSP) simulations are shown as solid lines with shading representing the inter-model standard deviation. CMIP Phase 5 (CMIP5) projections of Representative Concentration Pathways (RCPs) only show the multi-model mean as dashed lines. The model ensemble size for each scenario is given in parentheses. Figure from (Kwiatkowski et al., 2020).

Ocean acidification, i.e. a decrease in ocean pH, results from the oceanic uptake of CO_2. About 30% of current anthropogenic emissions of CO_2 has been taken up by oceans, reducing its contribution as a greenhouse gas in the atmosphere (i.e. acting as a *carbon sink*), but increasing the impacts on marine systems (IPCC, 2021). While higher CO_2 concentrations can increase growth, photosynthesis and primary production in heterotrophs, lower pH levels decrease calcification in calcifying species (Pörtner, 2008). As CO_2 dissolves in seawater, it reacts with water and forms carbonic acid (H_2CO_3), which quickly dissociates into bicarbonate (HCO_3^-) and hydrogen (H^+) ions (Equation 1). The increase in H^+ concentration not only raises the acidity of seawater (as $pH = -\log_{10}[H^+]$), it also in turn forms HCO_3^- by reacting with carbonate ions (CO_3^{2-}), and therefore reduces CO_3^{2-} concentrations (i.e. lowering the *calcium carbonate saturation state* or Ω), limiting calcification for marine shell-forming species such as coccolithophores, foraminera, molluscs, corals, echinoderms and crustaceans (Gattuso et al., 2015; IPCC, 2021, 2022a; Kwiatkowski et al., 2020).

$$CO_2(g) \leftrightarrow CO_2(aq) + H_2O \leftrightarrow H_2CO_3 \leftrightarrow HCO_3^- + H^+ \leftrightarrow CO_3^{2-} + 2H^+ \qquad (1)$$

Ocean surface pH has decreased by 0.1 pH units since pre-industrial levels, and projected decreases of global mean ocean surface pH between 1870–1899 and 2080-2099 range from 0.16 pH units under SSP1-2.6 to 0.44 pH units under SSP5-8.5 (Kwiatkowski et al., 2020) (Figure 2b). In shallow areas with low levels of stratification, the projected changes can be expected to be similar between the sea surface and the seafloor. However, changes in coastal seawater and freshwater pH due to anthropogenic CO_2 emissions are harder to detect and estimate compared to open ocean pH, due to larger natural variability as well as other (both anthropogenic and non-anthropogenic) significant drivers of local acidification (Kwiatkowski et al., 2020; Provoost et al., 2010; Schmidt & Boyd, 2016; Vargas et al., 2017). Furthermore, OW and OA occur together with and exacerbate the impacts of other anthropogenic (more local) stressors such as overfishing, deoxygenation, and the introduction of invasive species (Diaz & Rosenberg, 2008; IPCC, 2022a; Kwiatkowski et al., 2020; Molnar et al., 2008; Pauly et al., 1998).

1.1.4 Responses of aquatic organisms

The observed and projected OW and OA are and will greatly impact marine life. They reduce the fitness and performance of marine organisms, deteriorate ecosystem structure and function, and worsen their natural adaptive capacity (Birchenough et al., 2015; Doney et al., 2012; IPCC, 2022a; Pörtner, 2008; Pörtner & Farrell, 2008). To alleviate the impacts of global change, species respond in a variety of non-exclusive mechanisms and across different scales: they may (a) move to new regions with still tolerable conditions, (b) adjust by means of phenotypic plasticity and acclimation, or (c) adapt via genetic and evolutionary changes. Species with sufficient dispersal ability can move within the timespan of one (e.g. non-sessile organisms) or multiple generations, towards higher latitudes or depths with more favourable conditions, thereby expanding (i.e. *leading edge*) and contracting (i.e. *trailing edge*) their range (Pinsky et al., 2020). Examples of climate-driven range shifts have already been observed in primary producers (Neukermans et al., 2018), primary consumers (Chust et

al., 2014) and higher trophic levels (Drinkwater, 2005), with a recent estimated mean (± standard error) poleward shift of 5.92 ± 0.94 km year^{-1} for marine species (Lenoir et al., 2020), indirectly impacting other ecosystem components (Dam & Baumann, 2017).

Organisms can also cope with changing environmental conditions and exceeding thermal tolerance limits in the short term by altering their phenotype, i.e. *phenotypic plasticity*, such as adjusting their morphology, behaviour or physiology at the molecular, cellular and/or organismal level. When organisms reach a level of *physiological acclimation*, they may be able to persist novel environmental conditions and maintain fitness throughout their lifetime. Moreover, species with seasonal changes in population size can also shift their reproduction, growth and development towards more favourable periods of the year (i.e. *phenological shifts*), resulting in mismatches between trophic levels (Ji et al., 2010). Evolved differences in the capacity for phenotypic plasticity can differ between populations exposed to different conditions and depend on the degree and duration of exposure (Reusch, 2014; Somero, 2010). Coastal species and populations, for instance, are exposed to strong environmental fluctuations, which might have increased their tolerance to environmental stress (Dam, 2013).

Lastly, organisms can respond through *genetic adaptation* to novel conditions across multiple generations. The capacity for adaptation depends not only on the heritability and variation of a specific phenotypic trait, but also on the (effective) population size and connectivity, as well as the species' fecundity and generation time (Calosi et al., 2016; Reed et al., 2011). While rapid adaptation to OW and OA has been observed already in some species (see references), the rate of anthropogenic climate change is very likely too fast for adaptation to keep up for species with low genetic variation and large generation times (Dam, 2013; Munday et al., 2013).

1.1.5 Assessing biological impacts of and responses to global ocean change

Many approaches and strategies can be used to assess the impact and responses of marine organisms and ecosystems to certain global change drivers, such as using past

(i.e. fossil record) and present (e.g. CO_2 vents) proxies, contemporary observations, and (semi-)controlled manipulation experiments (Boyd et al., 2018; Riebesell et al., 2011). A *driver* is defined in this thesis as any changing environmental or biotic condition that impacts an organism, whether negatively (i.e. a *stressor*) or positively (Boyd et al., 2018). Drivers can affect an organism either *direct* (e.g. temperature, pH) or *indirect*, by affecting other organisms within the ecosystem, which, in turn, also impacts the first organism (von Elert & Fink, 2018). Manipulation experiments can range from small-sized (*microcosm*) to large-scale (*mesocosm*), short-term (acclimation) to long-term (adaptation), studies with one species (physiology) to many interacting species (ecosystems), and with single or multiple drivers (Riebesell & Gattuso, 2015). While currently a lot of knowledge is gained from short-term, single-species acclimation experiments with single drivers, ultimately more complex long-term adaptation studies with many species and multiple drivers are required (Boyd et al., 2018; Riebesell & Gattuso, 2015; Urban et al., 2016) (Figure 3). On top of this, other biological mechanisms such as dispersal and demography should be incorporated into forecasting models, as those would show a more complete picture of how global change affects ecosystem functioning, and allow policy advice based on the best available science (Boyd et al., 2018; Riebesell & Gattuso, 2015; Urban et al., 2016).

As global change effects such as OW and OA occur together, as well as with other global and local environmental changes, multiple driver research seeks to find out whether responses to these drivers are *additive* or *interactive* with respect to each other (Boyd et al., 2018; Orr et al., 2020; Piggott et al., 2015; Strain et al., 2014). According to Boyd et al. (2018), effects are additive when the presence/effect size of one driver does not alter the effect size of another driver, and interactive when they do. In the latter case, effects are *synergistic* when drivers act in the same direction and their combined effect on a response is greater than the sum of the effects of the individual drivers, or *antagonistic* when the combined effect of several drivers is smaller than the sum of the individual effects (Boyd et al., 2018). Piggott et al. (2015) further expanded upon this by proposing synergism that can be positive (more positive than predicted additively)

or negative (more negative than predicted additively), as well as antagonism that can be positive (less positive than predicted additively) or negative (less negative than predicted additively) (Piggott et al., 2015). While this framework helps in assessing impacts of multiple drivers, it still often assumes only two scenarios for each driver (e.g. control and impact, current and future). A balance between scenario-based approaches and gradient or mechanistic approaches would ideally allow modelling of biological impact under a wide variety of future global change scenarios: both those that already exist (i.e. RCPs and SSPs), but also those that would still need to be developed (Boyd et al., 2018).
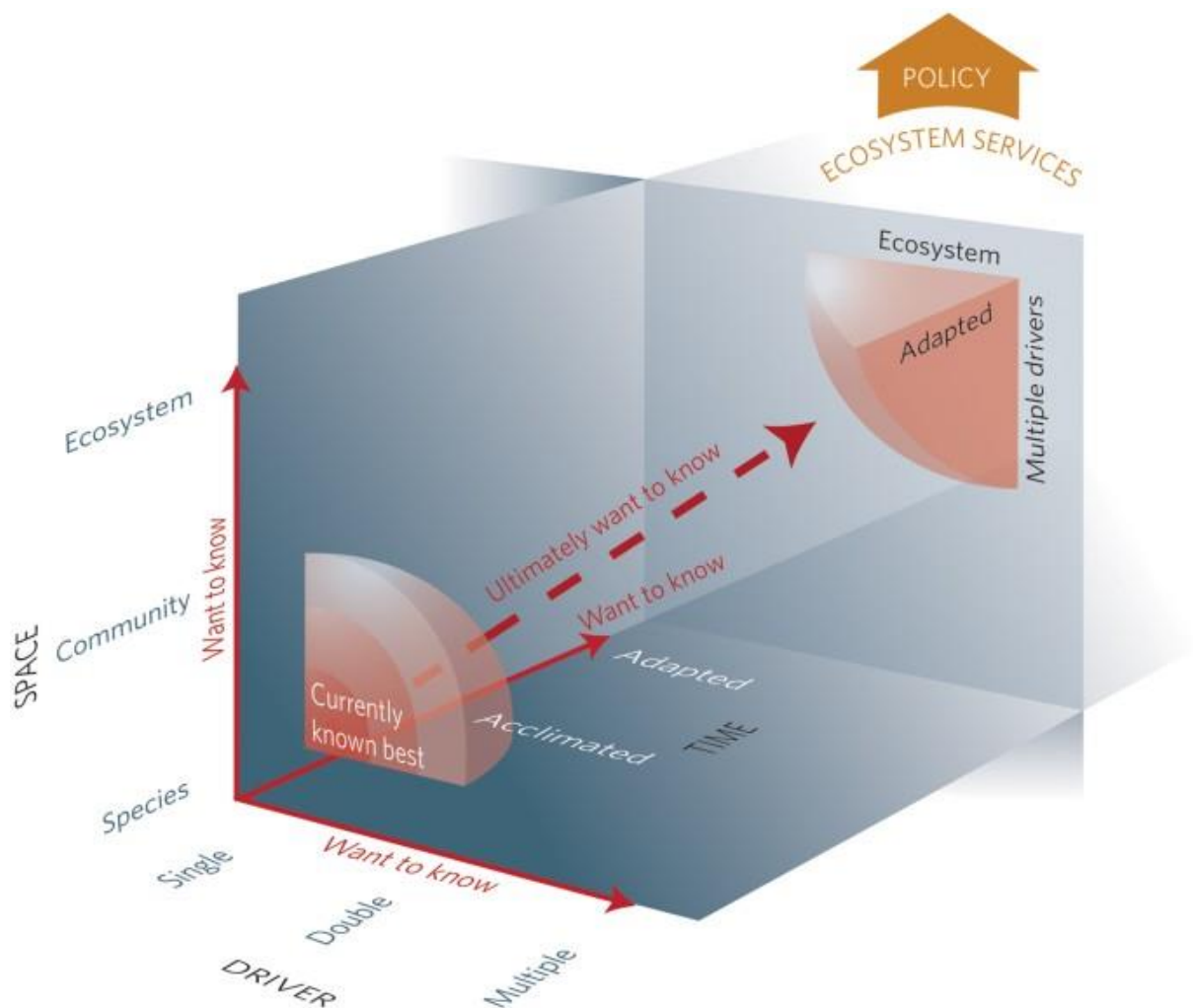
Figure 3 Present state of knowledge and knowledge needs in ocean change research. Red arrows indicate the direction where we need to expand our understanding. Assessment of impacts on ecosystem services, leading up to science-based policy advice, requires information on adapted responses to multiple drivers at the ecosystem level (upper right corner). Figure and caption from (Riebesell & Gattuso, 2015). *Original figure design by Rita Erven.*

1.2 Polyunsaturated fatty acids: vital biomolecules for a thriving biosphere

1.2.1 Nomenclature, role, functions and demand of polyunsaturated fatty acids

Life on Earth is sustained by different types of organic molecules. Global climate change severely impacts not only the availability and flow of these molecules for individual organisms, but also impairs the transfer of these molecules between different trophic levels. While autotrophs (or *primary producers*) such as plants and algae can create these biomolecules from inorganic nutrients such as carbon and an external energy source such as the sun (e.g. photosynthesis), heterotrophs (or *consumers*) such as animals and fungi need to obtain primary biomolecules and the energy therein by feeding on producers or other consumers and, if necessary and possible, modify them to other biomolecules (Lindeman, 1942). The most common biomolecules are grouped as either nucleic acids, peptides (including their building blocks amino acids), carbohydrates or *lipids*, the latter of which is a heterogeneous class of compounds grouped by their insolubility in water but solubility in organic solvents, and mainly constituted of fatty acids, sterols, or one of their derivatives (Parrish, 2013).

Fatty acids (FAs) are carboxylic acids with a hydrocarbon chain (usually unbranched and even-numbered), with a carboxyl group (-COOH) on one end of the chain (the *front* end), and a methyl group (-CH$_3$) on the other end (the *methyl* end) (Monroig et al., 2022). A FA is considered a *saturated fatty acid* (SFA) when its hydrocarbon chain does not contain ethylenic or double bonds, a *monounsaturated fatty acid* when it contains one double bond (usually in *cis* configuration), and a *polyunsaturated fatty acid* (PUFA) when it contains two or more double bonds, usually separated by a methylene (-CH$_2$-). The FA chain length and number and position of double bonds strongly determine their physicochemical characteristics as well as their role and functions in an organism (de Carvalho & Caramujo, 2018). While several systems for FA nomenclature exist and are defined by the International Union of Pure and Applied Chemistry, in this thesis we apply the n-x (or *omega-x*) system, where a FA is described with the formula *A:Bn-C*, with *A* the chain length, *B* the number of double bonds, and *C* the position of the first

double bond relative to the methyl end of the FA chain (Figure 4). Branched, uneven-numbered, non-methylene-interrupted and *trans* FAs are considered not as common in nature and sometimes the result of anthropogenic processing, however they might still be important for specific organisms (Monroig et al., 2013). FAs occur on their own, or as part of larger physiologically important biomolecules such as phospholipids, glycerolipids, glycolipids and wax esters (Parrish, 2013). They are usually identified and quantified in biological samples by transesterification to fatty acid methyl esters and subsequent analysis using *gas chromatography* (GC) combined with *mass spectroscopy* (MS) and/or *flame ionization detection* (FID) (Couturier et al., 2020).
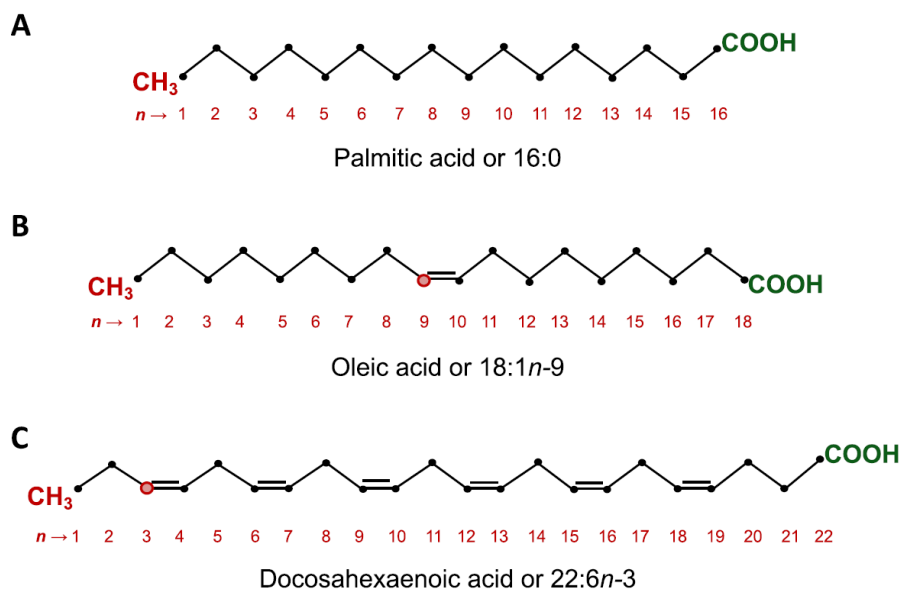
Figure 4 Composition and nomenclature of three example fatty acids (FAs). (A) the saturated FA 16:0 or palmitic acid, (B) the monounsaturated FA oleic acid or 18:1n-9, and (C) the omega-3 polyunsaturated FA docosahexaenoic acid or 22:6n-3. Positions of the first double bond relative to the methyl-end of the FA chain is indicated with a red dot in B and C. Figure and caption from (Monroig et al., 2022).

Many FAs, particularly PUFAs and *long-chain polyunsaturated fatty acids* (LC-PUFAs; C_{20}-C_{24}) such as *arachidonic acid* (ARA; 20:4n-6), *eicosapentaenoic acid* (EPA; 20:5n-3) and *docosahexaenoic acid* (DHA; 22:6n-3) and their derivatives occupy important physiological roles within an organism (de Carvalho & Caramujo, 2018; Glencross, 2009). First, phospholipids, more specifically glycerophospholipids, are the main components of biological membranes of cells and intracellular organelles. Due to the polar head group and the two nonpolar FA tails, they create a bilayer through which

biomolecules can still cross. The FA composition of the membranes determines their biophysical properties. Organisms adjust their membrane's FA composition to maintain biological functions under changing environmental conditions, a mechanism called *homeoviscous adaptation* (Sinensky, 1974). Short-chain SFAs form less viscous and more rigid membranes, while longer, more polyunsaturated FAs form more viscous membranes, and a balanced FA composition at a certain environmental condition (e.g. certain temperatures) is created to maintain proper membrane fluidity (de Carvalho & Caramujo, 2018). In neural systems as well as the retina, DHA is highly abundant in membrane phospholipids, and has particular roles in neuronal signalling (Bazinet & Layé, 2014; Pilecky et al., 2023).

Second, FAs, in the form of neutral lipids such as triacylglycerol (a type of glycerolipid) or wax esters, act as energy storage and provision. When oxidized, they yield about two-thirds more energy g^{-1} compared to proteins and carbohydrates (Parrish, 2013). This makes organisms rich in storage lipids attractive as an energy source to higher trophic levels. Third, LC-PUFAs such as EPA and ARA, DHA act as precursors for various cell signalling and hormone molecules, among which eicosanoids that contribute to inflammatory and anti-inflammatory responses (Bazinet & Layé, 2014; de Carvalho & Caramujo, 2018). Many LC-PUFAs are also involved in gene regulation (Monroig et al., 2022).

In humans and other chordates, although evidence suggests endogenous LC-PUFA synthesis from PUFA precursors *linoleic acid* (LA, 18:2n-6) and *α-linolenic acid* (ALA, 18:3n-3) (i.e. *essential fatty acids* for chordates) is sufficient to maintain brain function in healthy adults (Domenichiello et al., 2015; Prado-Cabrero & Nolan, 2021) (see below), the *omega-3* LC-PUFAs EPA and DHA are mainly to be obtained through the diet for proper physiological development, reproduction and health (Castro et al., 2016; Glencross, 2009). Humans typically obtain their dietary omega-3 LC-PUFAs requirements through seafood and/or freshwater sources (Hamilton et al., 2020). While the American Heart Association advises a minimal intake of 250 mg EPA+DHA d^{-1} for

adults (Rimm et al., 2018), both the International Society for the Study of Fatty Acids and Lipids and the corporate interest group Global Organization for EPA and DHA suggest a minimal intake of 500 mg d^{-1} (GOED, 2023; ISSFAL, 2004). Higher amounts are often recommended for certain health conditions, while lower amounts are recommended for children.

Based on those requirements, the current global aquatic supply of EPA and DHA from wild and farmed fish as well as krill, cephalopods, bivalves and crustaceans does not reach the global human demand, and as such there exists a strong *nutritional omega-3 gap* (Hamilton et al., 2020; Tocher, 2015) (Figure 5). This gap is particularly pronounced in countries in the Global South, where a strong reliance on fisheries for nutrition and livelihoods co-aligns with high rates of malnutrition and food insecurity (Shepon et al., 2022). Moreover, this human nutritional demand, while important, is paralleled by the omega-3 needs of other non-human species in our biosphere. Antarctic krill, for instance, is increasingly being fished to produce omega-3 supplements, while it is a key intermediate trophic level in the Southern Ocean food web and an important nutrient source for whales, penguins and seals (Prado-Cabrero & Nolan, 2021).
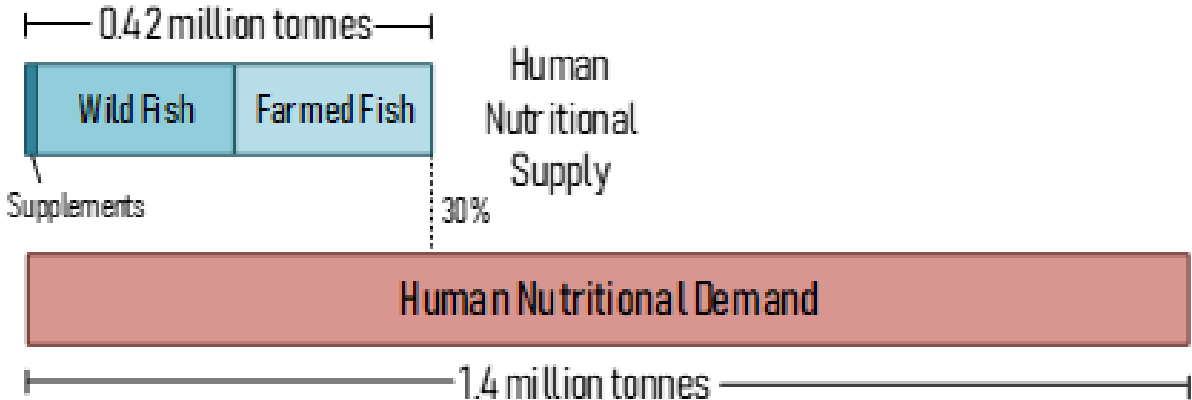

Figure 5 Human nutritional supply of EPA and DHA in million tonnes, calculated by material flow analysis (Hamilton et al., 2020). Human nutritional demand based on the average daily suggested intake of 500 mg EPA+DHA person^{-1} day^{-1}, as defined by the Global Organization for EPA and DHA Omega-3. Figure and caption from (Hamilton, 2020).

1.2.2 Polyunsaturated fatty acids in a changing ocean

Anthropogenic global change is predicted to significantly reduce LC-PUFA production by phytoplankton such as chlorophytes and diatoms (Hixson & Arts, 2016; Tan et al., 2022). Specifically, higher temperatures result in the homeoviscous adaptation of phospholipid membranes of primary producers, with relative increases in the proportion of SFA and omega-6 PUFAs, and relative decreases in the proportion of omega-3 LC-PUFAs (Sinensky, 1974). Additionally, at higher temperatures, LC-PUFAs are relatively more prone to FA oxidation compared to shorter, less saturated FAs (Hixson & Arts, 2016). Hixson and co-authors first brought this to attention in 2016 in their meta-analysis of lab-based FA profiles of six major groups of aquatic phytoplankton, estimating a reduction of 8.2% for EPA and 27.8% for DHA with a water temperature increase of 2.5°C (Hixson & Arts, 2016). A global-scale observational survey of plankton *lipidomes* (i.e. an organism's set of all its lipids) confirmed a high correlation between the mixed-layer temperature and suspended FA unsaturation levels, with predicted absolute EPA decreases (compared to current levels) of 2% globally and up to 7% at higher latitudes under SSP5-8.5 by 2081-2099 (Holm et al., 2022) (Figure 9). Moreover, OA is also suggested to negatively affect microalgal PUFA levels (Bermúdez et al., 2016; Marmillot et al., 2020; Rossoll et al., 2012). Worse, this physiological LC-PUFA decrease is predicted to co-occur with OA-driven declines of LC-PUFA rich diatoms (Taucher et al., 2022) and declining global net primary productivity (Kwiatkowski et al., 2020).

As LC-PUFAs are transferred throughout the food web (see below), higher trophic levels are profoundly impacted as well. In turn, reduced dietary LC-PUFA availability affecting the neurophysiology and behaviour of consumers could lead to shifts in trophic interactions and community composition, further disrupting global LC-PUFA supplies (Pilecky et al., 2021). Global levels of DHA available from marine and freshwater fish for human consumption are estimated to decline with 58% by 2100 under RCP8.5 (Colombo et al., 2020), with vulnerable communities in the Global South (e.g. inland

Africa) disproportionately affected. As such, the already currently reported nutritional omega-3 gap will only widen in the future.
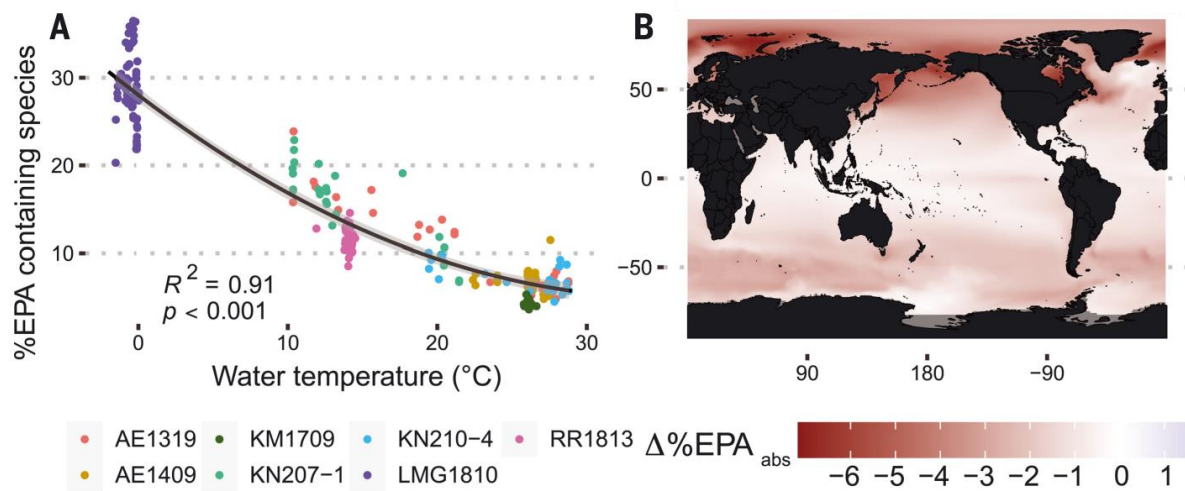
Figure 9 Future projections of eicosapentaenoic acid (EPA) abundance based on water temperature shows loss under high-emission (SSP5-8.5) scenario. (A) Percent abundance of all polar glycerolipids containing EPA species (% EPA) in mixed layer samples verse temperature. Samples coloured by cruise. Black line shows quadratic fit, grey area shows 99% confidence interval using SE. Statistics for the fit with least squares are shown in plot (n = 242 samples, p values from F-test). (B) Change in absolute %EPA ($\Delta\%EPA_{abs}$) at end of century from today using SST under SSP5-8.5 scenario (2080 to 2099). Adapted figure and caption from (Holm et al., 2022).

1.2.3 Transfer of polyunsaturated fatty acids throughout the food web

While C_{18} PUFAs are known to be produced by primary consumers from both terrestrial and aquatic environments, various research suggests that most LC-PUFAs are produced by marine primary producers such as algae, diatoms and bacteria (Colombo et al., 2017a, 2017b; Jónasdóttir, 2019; Twining et al., 2016, 2021) (Figure 6). Primary consumers such as zooplankton and herbivorous vertebrates obtain these energy-rich, physiologically important PUFAs by feeding on the primary producers, and higher trophic levels such as carnivorous fish and humans in turn obtain them by feeding on their respective diets (Glencross, 2009). This allows PUFAs to be transferred throughout the entire food web. Preferential accumulation of energy-dense lipids (compared to other carbon sources) occurs at each trophic level (e.g. lipids droplets in zooplankton, muscle tissue in salmon), resulting in increased efficiency in dietary uptake by higher levels, with about 10% of all energy transferred from one level to another (Pauly & Christensen, 1995). Transfers from marine to terrestrial and freshwater ecosystems also

occur, through diadromous migration (e.g. salmonids, eels), drift of carrion and seaweeds, riparian consumers (e.g. bears, birds, insects), or, in the case of humans, fisheries and mariculture (Gladyshev et al., 2013; Twining et al., 2021). However, levels of LC-PUFAs in terrestrial and freshwater primary producers remain relatively low and highly variable, resulting in nutritional constraints in metazoan consumers affecting their growth and survival (i.e. *fatty acid limitation*) (Boersma et al., 2008; Müller-Navarra et al., 2004).

The idea of transfer of specific FAs throughout the food web has developed into the concept of *fatty acid trophic markers* (FATM) in trophic ecology research. This concept presumes that the presence and quantity of certain FAs in a consumer can reveal its past diet and the relative importance of potential dietary resources (Dalsgaard et al., 2003). However, the concept has been challenged by research showing that consumers can selectively retain or oxidize some FAs, and endogenously produce others (e.g. LC-PUFAs) from dietary precursors (e.g. C_{18} PUFAs) – known as *trophic upgrading* (Bell & Tocher, 2009; Galloway & Budge, 2020; Monroig et al., 2013) (Figure 6). Moreover, consumer FA composition is shown to be strongly dependent on and modified under varying environmental conditions (Galloway & Budge, 2020).

Now, it is well established that many consumers have at least some ability for *LC-PUFA biosynthesis* from dietary C_{18} PUFAs, with certain primary consumers even having the complete capacity for C_{18} PUFA biosynthesis from endogenous carbon (Kabeya et al., 2018), challenging the long-held dogma that all (or nearly all) LC-PUFAs have an exclusively primary producer origin (Galloway & Budge, 2020) (Figure 6). Humans for instance are suggested to endogenously produce sufficient levels of DHA from dietary ALA to maintain healthy brain function (Prado-Cabrero & Nolan, 2021). While this paradigm shift demands the revaluation and improvement of the FATM concept by taking potential consumer modification into account (Jardine et al., 2020), it more importantly begs the question as to which extent consumers (in addition to producers) can contribute to global LC-PUFA production and availability. None of the current

models predicting LC-PUFA losses in higher trophic levels (Colombo et al., 2020; Holm et al., 2022) account for consumer LC-PUFA metabolism, which could potentially buffer the losses at the primary producer level. This also presses the need to better understand the molecular mechanisms behind PUFA biosynthesis within metazoans.
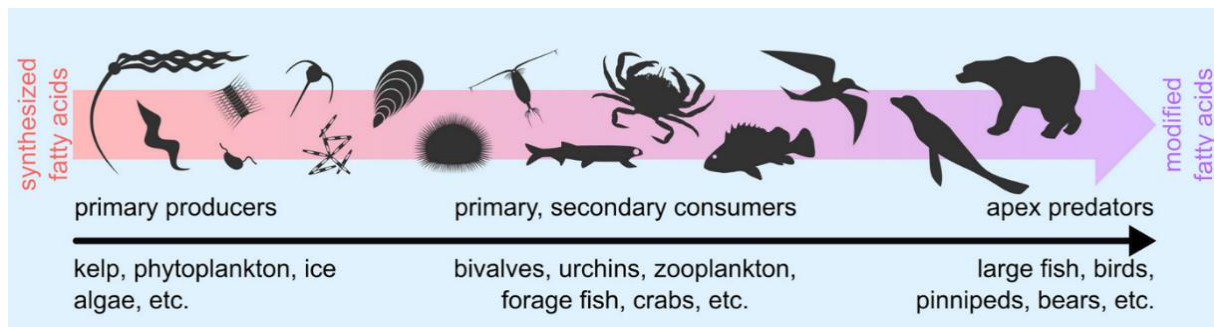
Figure 6 Continuum of algae-synthesized to highly modified fatty acids along the marine food web. Animals have differing, usually unknown, abilities to synthesize certain fatty acids de novo, resulting in higher predators having more derived, highly modified fatty acid profiles relative to basal consumers. Figure and caption from (Galloway & Budge, 2020). *Artwork by R. M. Yoshioka.*

1.2.4 Molecular mechanisms of polyunsaturated fatty acid biosynthesis

The molecular mechanisms behind PUFA biosynthesis in metazoans have been extensively described in a number of excellent reviews by Monroig and co-authors (Castro et al., 2016; Monroig et al., 2011, 2013, 2018, 2022; Monroig & Kabeya, 2018). Generally, prokaryotes (but also certain protists) use anaerobic pathways such as the polyketide pathway, which allow the biosynthesis of PUFAs but also of FAs with odd-numbered and branched carbon chains. On the other hand, most eukaryotes but also certain bacteria use the aerobic pathway, which exclusively allows the biosynthesis of even-numbered FAs because it uses C_2 units from acetyl-CoA as a carbon donor (Figure 7). This aerobic biosynthesis of PUFAs (and subsequently LC-PUFAs) from SFAs (when present in an animal) is performed by a sequential repertoire of (often alternating) membrane-bound enzymes termed *fatty acid desaturases* and *fatty acid elongases*, which are encoded by a range of genes such as (for example, in humans) *fatty acid desaturase 1* (FADS1) and *elongation of very long chain fatty acids 2* (ELOVL2). The presence, copy number, gene expression, and enzymatic activity of fatty acid desaturases and elongases all determine an organism's capacity for PUFA biosynthesis.

While this PUFA biosynthesis pathway is now well characterized in vertebrates, especially fish, research on the presence and diversification of the responsible genes and enzymes in invertebrates has only kick-started in the last few years (Monroig et al., 2022). The distribution of certain gene families or subfamilies is highly lineage-specific, differing between classes, families or even between species within the same genus. In contrast, the production of the SFA palmitic acid (16:0) from acetyl-CoA by the fatty acid synthase complex, the elongation of 16:0 to 18:0, and the subsequent production of the MUFA oleic acid (OA, 18:1n-9) by the *stearoyl-CoA-desaturase* (scd) with $\Delta 9$ desaturation capacity, are highly conserved in virtually all metazoans and do not limit potential PUFA biosynthesis (Monroig et al., 2022).

Fatty acid desaturases introduce a double bond within the FA chain, and their regioselectivities or functions (as they can be monofunctional or multifunctional) are named here according to the location of the inserted double bond relative to the carboxyl (front) end of the chain (e.g. $\Delta 4$, $\Delta 6$, $\Delta 12$, ...). They can further be divided between *front-end desaturases* with $\Delta 4$, $\Delta 5$, $\Delta 6$, or $\Delta 8$ desaturation capacity, which introduce a double bond between an existing double bond and the front end of the FA chain, and *methyl-end desaturases* with $\Delta 12$, $\Delta 15$, $\Delta 17$, or $\Delta 19$ desaturation capacity, which introduce a double bond between an existing double bond and the methyl end of the FA chain (Monroig et al., 2022). Front-end desaturases with $\Delta 4$ desaturation capacity are often, but should not be, confused with the phylogenetically and functionally unrelated $\Delta 4$ sphingolipid desaturases. Methyl-end and front-end desaturases can be distinguished from each other by the presence of a cytochrome b5 domain located at the N-terminus of a front-end desaturase enzyme, which methyl-end desaturases lack (Hashimoto et al., 2008). Fatty acid elongases on the other hand are responsible for the rate-limiting step in a complex metabolic process that elongates a FA chain by two carbon units at the front end of the chain (Monroig et al., 2022). Elongase naming follows, and expands upon, the eight currently identified elongase vertebrate elongase subfamilies elovl1 to elovl8, some of which likely have distinct substrate specificities (Hashimoto et al., 2008; Monroig et al., 2022).

PUFA biosynthesis from OA starts with two desaturations to LA and ALA by methyl-end desaturases with $\Delta 12$ and a $\Delta 15$ desaturation activities, respectively, whose presence therefore ultimately determines the capacity for *de novo* PUFA biosynthesis (Figure 7). Two potential pathways subsequently enable ARA and EPA biosynthesis from LA and ALA, respectively: the *$\Delta 6$ pathway* ($\Delta 6$ front-end desaturation – C_{18} to C_{20} elongation – $\Delta 5$ front-end desaturation), and the *$\Delta 8$ pathway* (C_{18} to C_{20} elongation – $\Delta 8$ front-end desaturation – $\Delta 5$ front-end desaturation) (Figure 7). Following one C_{20} to C_{22} elongation, the biosynthesis of DHA and 22:5n-6 from EPA and ARA, respectively, is again performed by two potential pathways: the *Sprecher pathway* (C_{22} to C_{24} elongation – $\Delta 6$ front-end desaturation – β-oxidation) discovered by (Sprecher et al., 1995), and the *$\Delta 4$ pathway* involving only one $\Delta 4$ front-end desaturation (Figure 7). Throughout, methyl-end desaturases with $\Delta 15$, $\Delta 17$ and $\Delta 19$ desaturation capacities enable the production of omega-3 PUFAs from their omega-6 counterparts (Monroig et al., 2022). While one enzyme can concurrently act on multiple substrates, it often exhibits a preferential mode of action (i.e. $\Delta 5$ desaturase preferring production of EPA over ARA) (Glencross, 2009), and this process is likely regulated by various external factors (Xie et al., 2021).
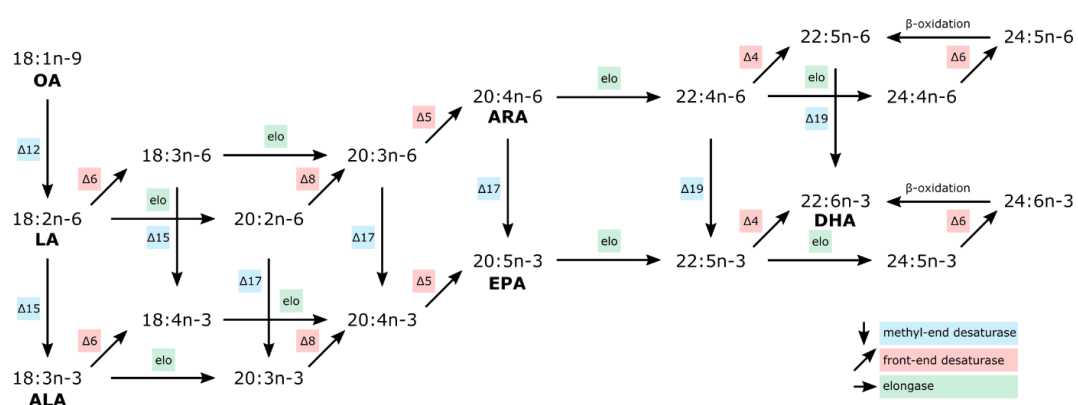
Figure 7 Putative theoretical polyunsaturated fatty acid biosynthesis pathway in metazoans. Note that the presence of each step depends on the presence of specific functional enzymes in a metazoan species, and that therefore, this entire pathway is not necessarily complete in all metazoans. Methyl-end desaturase reactions in blue (vertical arrows), front-end desaturase reactions in red (diagonal arrows), and elongase reactions in green (horizontal arrows). Desaturase reactions are further specified by "Δy", with "y" referring to the location of insertion of the double bond counting from the methyl-end of the carbon chain. β-oxidation reactions are shown as horizontal reverse arrows. OA, oleic acid; LA, linoleic acid; ALA, α-linolenic acid; ARA, arachidonic acid; EPA, eicosapentaenoic acid; DHA, docosahexaenoic acid. Figure and caption from (Boyen et al., 2023), adapted from (Monroig et al., 2022).

The molecular mechanism for PUFA biosynthesis has evolved closely with, and likely played a part in, animal diversification and transitions to novel environments with differing dietary LC-PUFA availability (Twining et al., 2021; Závorka et al., 2023). Events like gene duplication (or whole genome duplication), gene loss and gene retention are widespread through the evolution of fish, with the neofunctionalisation of PUFA biosynthesis genes enabling them to find new niches and opportunities to adapt (Castro et al., 2016; Lopes-Marques et al., 2018; Monroig et al., 2011; Oboh et al., 2017). For instance, a copy number increase and neofunctionalisation coincided with freshwater transitions of marine sticklebacks and flatfish (Ishikawa et al., 2019, 2022; Matsushita et al., 2020). In insects, the diversification of Δ9 desaturases and Δ12 desaturases (evolved following a Δ9 desaturase duplication), were linked to their ecological diversification (Helmkampf et al., 2015; Macháček et al., 2023; Malcicka et al., 2017). In contrast, the presence of methyl-end desaturases in certain metazoans is suggested to be the result of an ancestral *horizontal gene transfer* (transfer of genes between distantly related organisms) from non-metazoan eukaryotes, thereby obtaining the capacity for endogenous PUFA biosynthesis (Kabeya et al., 2018).

1.2.5 Assessing polyunsaturated fatty acid biosynthesis and conversion in animals

Here, I provide an overview of different methods to assess (environmentally-driven) PUFA biosynthesis, with references showing one or more examples or case-studies. The most simple yet elegant method to test consumer (LC-)PUFA biosynthesis under certain environmental conditions, is to feed them a diet devoid of (LC-)PUFAs (compared to a (LC-)PUFA rich control diet) and assess survival, growth and/or reproduction alongside analysing consumer FA composition (using GC-MS/FID), if possible across multiple generations (Nanton & Castell, 1998; Olive et al., 2009; Pajand et al., 2022; Ribes-Navarro et al., 2022). If, after a certain time (or after a number of generations), fitness parameters and consumer LC-PUFA levels remain high, endogenous LC-PUFA and/or PUFA biosynthesis should be present. More complex evidence can be gathered by

compound-specific stable isotope analysis (CS-SIA), whereby shifts in the $^{12}C/^{13}C$ ratio ($\delta^{13}C$) within individual FA compounds are investigated (Twining et al., 2020). Experiments can be performed using (a) diets with natural $\delta^{13}C$ levels to analyze (selective) enzymatic fractionation (Burian et al., 2020; Gladyshev et al., 2016), or (b) ^{13}C-labelled diets (whole organisms or liposomes with labelled MUFAs or C_{18} PUFAs) to asses ^{13}C uptake and incorporation in consumer LC-PUFAs (Boissonnot et al., 2016; De Troch et al., 2012; Graeve et al., 2020; Werbrouck et al., 2017). Both approaches are most commonly analyzed using GC coupled with isotope ratio mass spectrometry (GC-IRMS), but GC-MS or even liquid chromatography can be used as well (Bell et al., 2007; Helenius et al., 2019, 2020; Malcicka et al., 2017; Nielsen et al., 2020b).

Additionally, one can investigate the presence, functionality and expression of fatty acid desaturase and elongase genes of specific species using a number of advanced molecular techniques (Monroig et al., 2022). Full-length coding sequences of these genes can be discovered within the *genome* or *transcriptome* (an organism's set of all messenger RNA transcripts) obtained by *whole-genome sequencing* (Kabeya et al., 2018) or *RNA sequencing* (Lenz et al., 2014; Nielsen et al., 2019) respectively, or by rapid amplification of complementary DNA ends *polymerase chain reaction* (PCR) (Lin et al., 2018; Ribes-Navarro et al., 2021). The currently most common and successful method to assess the functionality and substrate specificity of a metazoan PUFA biosynthesis gene, adopted from biotechnology research, is the *cloning and heterologous expression* in transgenic baker's yeast *Saccharomyces cerevisiae* (which lacks PUFA biosynthesis genes) supplied with specific FA substrates (Figure 8). This method was first applied on an aquatic animal species in 2001 (Hastings et al., 2001), but has been highly optimized since (Monroig et al., 2022). To assess whether PUFA biosynthesis genes are differentially expressed under varying diets, environmental conditions, or between different organismal tissues, common methods include RNA sequencing (Nielsen et al., 2019) and *quantitative reverse-transcription PCR* (qPCR) (Lee et al., 2016, 2022a; Xu et al., 2020).
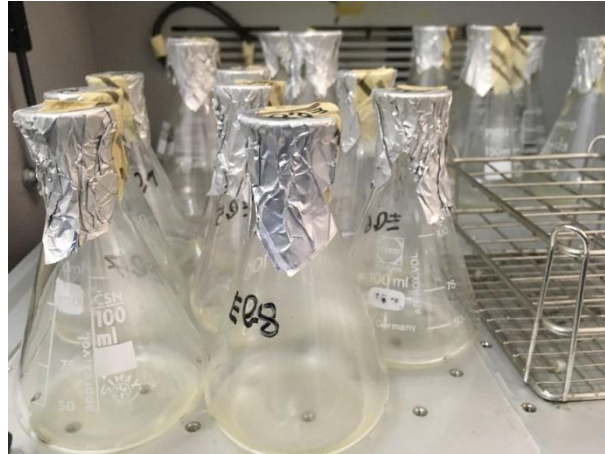
Figure 8 Transgenic baker's yeast (Saccharomyces cerevisiae) growing on different FA substrates.

1.3 Copepods: key microcrustaceans at the basis of aquatic food webs

1.3.1 Evolution, phylogeny and biodiversity

One of the most ecologically relevant groups of primary consumers at the basis of aquatic food webs are copepods. Copepoda (Milne Edwards, 1840) are a highly abundant, ecologically and morphologically diverse class of small pancrustaceans (Turner, 2004). As of July 2023, nearly 15000 extant species are accepted (Walter & Boxshall, 2023). Throughout their evolution, copepods managed to successfully inhabit a wide range of habitats: they are abundant members of pelagic and benthic communities in marine, brackish and freshwater ecosystems (Falk-Petersen et al., 2009; George et al., 2020), but are also found in the deep sea (Mathiske et al., 2021), submerged caves (Janssen et al., 2013), temporary rock pools (Snoeks et al., 2021), tropic phytotelmata (Mercado-Salas et al., 2021), groundwater (Galassi et al., 2009), and even Himalayan glacier pits (Kikuchi, 1994). Many species are associated with algae or seagrasses (Daudi et al., 2023; McAllen, 1999), while others have symbiotic or parasitic relationships with other metazoans such as anthozoans, echinoderms, fish, turtles and whales (Bass et al., 2021; Bernot et al., 2021; Domènech et al., 2017). Copepods are relatively small organisms (between 250 µm and ~3 cm adult body length), and its life cycle consists of six larval (naupliar) stages, five juvenile (copepodite) stages and one

adult stage (George et al., 2020). In terms of biomass, copepods dominate zooplankton assemblages in the open ocean more than any other taxa, with especially high planktonic copepod densities found in the polar regions (Drago et al., 2022).

While their exact placement within Pancrustacea remains debated (Lozano-Fernandez et al., 2019), copepods themselves form a monophyletic group with ten recognized orders (Walter & Boxshall, 2023). The four most species-rich and ecologically well-known orders are Calanoida and Harpacticoida, which are mainly marine pelagic and marine benthic, respectively (but there are many exceptions); the parasitic Siphonostomatoida; and the Cyclopoida, an order that encompasses diverse groups of marine, freshwater, free-living and parasitic species (Bass et al., 2021; George et al., 2020) (Figure 10).
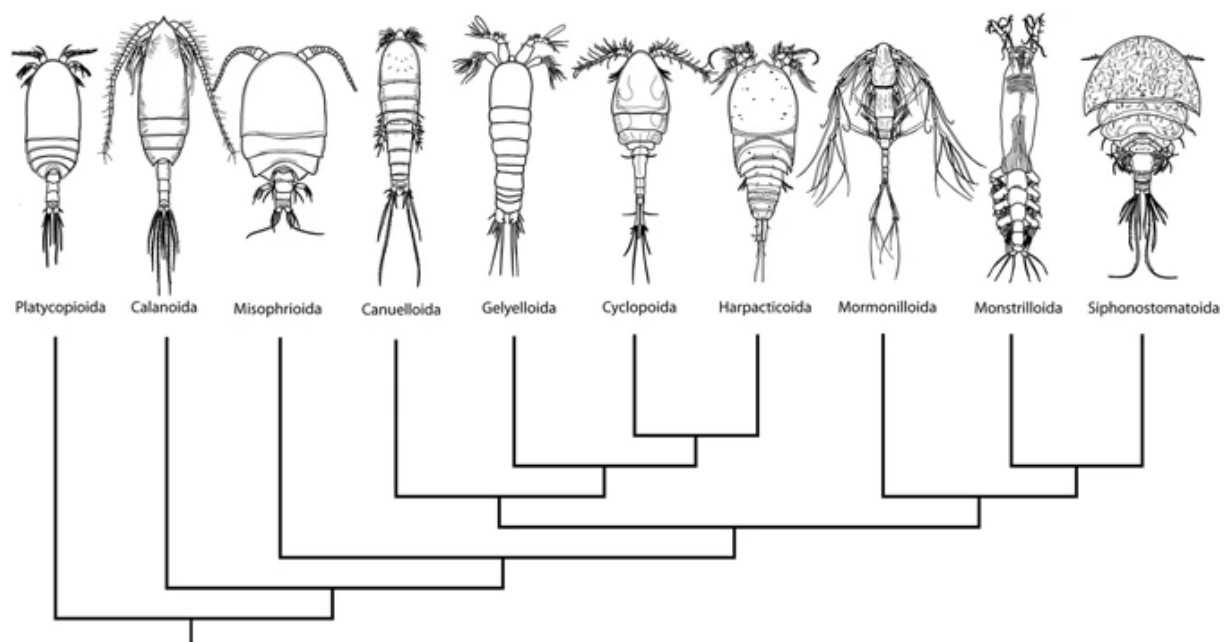
Figure 10 Cladogram of copepod orders. Figure from (Khodami et al., 2017)*, citations of original drawings found therein.*

Recently, a new order named Polyarthra (also known as Canuelloida) was suggested and is now widely accepted, containing species with morphological and ecological characteristics similar to benthic harpacticoids (Dahms, 2004; George et al., 2020; Khodami et al., 2017; Walter & Boxshall, 2023). However, as the study triggering the recognition of Polyarthra has since been retracted (Khodami et al., 2020), the exact

phylogeny of the ten copepod orders remains debated (Bass et al., 2021). Generally, most agree on the division between Progymnoplea (the single order Platycopioida) and Neocopepoda, and therein the two groups Gymnoplea (Calanoida) and Podoplea (all other orders) (Figure 10). Calanoida likely diverged from the other Neocopepoda about 400 million years ago following the Cambrian explosion (Schwentner et al., 2017). In line with the wide diversity of occupied habitats, the evolution of the different copepod orders likely involved adaptations to particular abiotic and biotic conditions such as temperature, salinity, oxygen levels, predation, competition as well as food availability and quality (Huys & Boxshall, 1991).

1.3.2 Role as primary consumers within aquatic food webs

Nonparasitic herbivorous copepods are primary consumers and provide a crucial link in the food web between primary producers and higher trophic levels (Turner, 2004). In marine and estuarine sediments, meiobenthic harpacticoid copepods mainly feed on benthic diatoms, but also on cyanobacteria, ciliates, bacteria, detritus and even exopolymers (Cnudde et al., 2015; Hicks & Coull, 1983), and in turn serve as a food source for juvenile fish such as flatfish and salmonids (Gee, 1987, 1989). In the water column of ocean and lakes, pelagic calanoids and cyclopoids, respectively, are an important dietary component of fish, seabirds and whales (Beaugrand et al., 2003; Bertram et al., 2017; Cronin et al., 2017; Isumbisho et al., 2004; Turner, 2004). Copepods are known to produce and store high levels of lipids, sometimes as lipid droplets or in a lipid sac (Falk-Petersen et al., 2009). Due to their high lipid accumulation (as wax esters) combined with their seasonal diapausing behaviour, calanoid copepods are considered crucial factors in the global carbon cycle, acting as a *seasonal lipid pump* that sequesters carbon into the deep ocean at potentially about 10% of the biological carbon pump (Boyd et al., 2019; Jónasdóttir et al., 2015). Within their lipids, copepods contain one of the highest levels of PUFAs and particularly omega-3 LC-PUFAs among all metazoans (Twining et al., 2021), transferring these physiologically important nutrients to higher levels.

Due to their high PUFA levels, herbivorous copepods are cultured as fish feed for aquaculture, and harvested for production of omega-3 supplements (Cutts, 2003; Long, 2016; Prado-Cabrero et al., 2022; Støttrup, 2000). They have a higher nutritional value than current dominant non-natural larviculture alternatives (*Artemia*, rotifers) and would in theory be a good substitute for fish meal and fish oil. However issues with large-scale production remain (Tocher, 2015). Moreover, wax esters, the dominant lipid type in calanoids, are physiologically difficult to metabolize for vertebrates. Much of the research around environmental and dietary modulation of copepod PUFA levels is performed in order to optimize LC-PUFA production for aquaculture applications (Arndt & Sommer, 2014; Lee et al., 2017b; Nanton & Castell, 1998, 1999; Nielsen et al., 2020a; Norsker & Støttrup, 1994). Ironically, parasitic siphonostomatoid copepods such as the salmon lice *Caligus rogercresseyi* and *Lepeophtheirus salmonis* pose widespread problems in the salmonid aquaculture industry (Burka et al., 2012), where large-scale infections can also cross to and devastate wild populations (Krkošek et al., 2007).

1.3.3 Copepods in a changing ocean

Copepods are, and will continue to be, profoundly impacted by anthropogenic climate change. Marine copepods specifically will have to face the consequences of both OW and OA (Semmouri et al., 2023), which will alter both zooplankton and meiofaunal communities and subsequently affect higher trophic levels (Dam & Baumann, 2017). On top of the direct impacts of OW and OA, they will also be impacted by changes in dietary availability and nutritional quality, i.e. indirect climate change effects. Observed responses of copepods to climate change encompass acclimation at transcriptional (Roncalli, Niestroy, et al., 2022; Semmouri et al., 2019; Smolina et al., 2015), physiological (Heine et al., 2019; Mayor et al., 2012, 2015; Thor et al., 2018), behavioral (Wyeth et al., 2022) and community levels, as well as shifts towards higher latitudes (Beaugrand et al., 2002; Chust et al., 2014; Ibarbalz et al., 2019). While pelagic calanoids are well able to move poleward (provided they do not already inhabit polar regions), benthic harpacticoids have limited dispersal capabilities and are thus unlikely to move

poleward in order to keep up with rapidly increasing SSTs. Since copepod exoskeletons have a relatively low calcium content, OA is expected to impact them less severely compared to other calcifying organisms (Engström-Öst et al., 2019; Kurihara & Ishimatsu, 2008), although other physiological responses might occur (Thor et al., 2022; Wang et al., 2018). Decreases in pH associated with OA may also interfere with their olfactory reception and chemical communication, leading to maladaptive food choices (Maibam et al., 2015). Moreover, environmental drivers might also impact different life stages differently (Horne et al., 2019; Mathews et al., 2018; Thor et al., 2018), although this does not always seem to be the case (Kurihara & Ishimatsu, 2008).

Multigenerational experiments have indicated that copepods have at least some ability for short-term acclimation at the transcriptional, epigenetic (Lee et al., 2022b), physiological level (Thor & Dupont, 2015) as well as long-term evolutionary adaptation (Brennan et al. 2022a, 2022b; Dam et al., 2021; De Wit et al., 2016; Langer et al., 2019), especially given their large population sizes, short generation times and high fecundity. However, these multigenerational adaptations might happen at the expense of growth and reproduction (de Juan et al., 2023; Fitzer et al., 2012; Langer et al., 2019).

1.3.4 Polyunsaturated fatty acid biosynthesis in copepods

Feeding experiments using natural and ^{13}C-labelled diets have shown that many copepod species might have a unique capacity for PUFA biosynthesis and/or bioconversion, with some at ecologically negligible levels, but others at levels sufficient to survive on LC-PUFA deficient diets for generations (Bell et al., 2007; Bell & Tocher, 2009; De Troch et al., 2012; Desvilettes et al., 1997; Moreno et al., 1979; Nanton & Castell, 1998; Nielsen et al., 2020a, 2020b; Norsker & Støttrup, 1994; Titocci & Fink, 2022; Werbrouck et al., 2017). Subsequent molecular studies have shown the presence of not only front-end desaturases and elongases in copepod genomes (Kabeya et al., 2021; Lee et al., 2016, 2020a, 2020b; Lenz et al., 2014; Nielsen et al., 2019), but also of methyl-end desaturases, implying the possibility for complete endogenous LC-PUFA biosynthesis from oleic acid (Kabeya et al., 2018, 2021).

Functional front-end and methyl-end desaturases are indicated to be absent from all other arthropod groups (Monroig et al., 2022; Ramos-Llorens et al., 2023b; Ribes-Navarro et al., 2021), except for Δ12 desaturases in hexapods which evolved from a stearoyl-CoA-desaturase (see before). Putative front-end desaturases in decapods (Chen et al., 2017; Lin et al., 2017; Wu et al., 2018; Yang et al., 2013) have still not been functionally characterized (Monroig et al., 2022). Therefore, the exact origin of copepod methyl-end and front-end desaturases remains peculiar. Functional front-end desaturases are also present in some non-crustacean metazoan groups (Monroig et al., 2022; Ramos-Llorens et al., 2023a; Surm et al., 2015, 2018), but these are phylogenetically unrelated to copepod front-end desaturases (Kabeya et al., 2021). As a result, Kabeya and co-authors hypothesized that both methyl-end desaturases (in specific metazoan groups) as well as front-end desaturases (in copepods) might be the result of multiple independent horizontal gene transfers from oomycetes and kinetoplasts, respectively (Kabeya et al., 2018, 2021).

Much research exists on how copepod LC-PUFA levels and biosynthesis are influenced by not only dietary LC-PUFA availability (Lee et al., 2020b; Titocci & Fink, 2022), but also by OW (Lee et al., 2017a; Pond et al., 2014) and OA (e.g. Almén et al., 2016; Bermúdez et al., 2016). However, studies investigating interactive effects are less common (Garzke et al., 2016; Rossoll et al., 2012). Furthermore, many copepod species, families and orders such as benthic harpacticoids and canuelloids remain little investigated, even though they often dominate sediment community assemblages and also serve as important diets for higher trophic levels (Gee, 1987; Vincx & Heip, 1979). Therefore, understanding how copepod LC-PUFA concentrations and also copepod LC-PUFA biosynthesis change under anthropogenic climate change (including reductions in microalgal LC-PUFA production) is crucial.

1.4 Aims, objectives and outline of the thesis

Despite some indications of the capacity for PUFA biosynthesis within copepods, detailed information on the molecular tools and mechanisms remains very limited. Current research identifying fatty acid desaturases and elongases have so far focussed on laboratory model species such as the rock pool harpacticoid *Tigriopus* (Kabeya et al., 2021; Lee et al., 2020a) as well as species relevant for aquaculture such as the parasitic siphonostomatoid *L. salmonis* (Kabeya et al., 2018) and the cyclopoid *Apocyclops royi* (Amparyup et al., 2022; Nielsen et al., 2019), while functional characterization has only been done on genes from *Tigriopus californicus* and *L. salmonis* (Kabeya et al., 2018, 2021). Furthermore, the impact of different climate change drivers on the PUFA biosynthesis of copepods remains unstudied, except for some work on the cyclopoid *Paracyclopina nana* (Lee et al., 2017a). This limited work, while relevant, does not reflect the remarkable phylogenetic, morphological and ecological diversity of the ~15000 copepod species, which have evolved a multitude of nutritional strategies in order to become one of the most ecologically successful and widespread animal groups.

Therefore, the overall aim of this PhD research is to improve our understanding on the **molecular basis behind polyunsaturated fatty acid biosynthesis in copepods as consumers at the basis of aquatic food webs, especially under future anthropogenic ocean warming and acidification scenarios.**

Much of the research within this thesis has been performed with the aid of our main species model *Platychelipus littoralis* (Brady, 1880). *Platychelipus littoralis* is a small (~800 μm) benthic harpacticoid copepod of the family Laophontidae (Figure 11). It is a dominant inhabitant of marine and brackish sediments, more specifically Northeast Atlantic intertidal and estuarine mudflats (Barnett, 1968, 1970). It can be considered representative for the general ecology of most (benthic, sediment-associated) harpacticoids, especially compared with the frequently studied genus *Tigriopus*, which occurs in intertidal rock pools. *Platychelipus littoralis* is a grazer on benthic microalgae

and bacteria (Cnudde et al., 2015) and itself serves as a food source for goby fishes and shore crabs (Gee, 1987; Gee et al., 1985). It has a restricted mobility (Barnett, 1966), and therefore needs to be able to quickly acclimatize to stochastic local environmental conditions (such as temperature) in the intertidal. Local population densities strongly fluctuate throughout the year, with highest densities recorded in April in one seasonal study (Barnett, 1970). It is shown to reproduce year-round but seasonal reproduction peaks might be present (Barnett, 1970). Its distribution spans from Spain to Iceland (Apostolov, 2014; Villate et al., 2004), however at the start of this research proper genetic confirmation using molecular barcoding was limited to one population in Germany (Rossel & Martínez Arbizu, 2019).

Figure 11 Adult Platychelipus littoralis specimens (~800 µm) as seen under a microscope (5x). Specimens were collected from a natural population at the Paulina mudflat of the Western Scheldt river in The Netherlands. Picture credit: Bram Martin.

Previous work performed at the Marine Biology Research Group by Werbrouck and co-authors has shown the effect of temperature on the lipid profile, FA composition and energy allocation of *P. littoralis* fed both single-species and multispecies diets (Werbrouck, et al., 2016a, 2016b). Moreover, they used CS-SIA to show that *P. littoralis* has at least some capacity for LC-PUFA biosynthesis when faced with both OW and dietary LC-PUFA limitation (Werbrouck et al., 2017). However, no genetic sequence information of *P. littoralis* has been obtained so far, aside for some COI barcoding sequences from a population in the German Part of the North Sea (Rossel & Martínez Arbizu, 2019). This project thus also serves to contribute to the publicly available

molecular data on harpacticoid copepods. In fact, most copepod transcriptomes currently available on the NCBI Sequence Set Browser are from calanoids, even though their species diversity (2709) is nearly only half that of harpacticoids (4771) or cyclopoids (4500) (Bernot et al., 2021).

The specific **objectives** of this thesis are as follows:

a) **Identify the repertoire** of fatty acid desaturase and elongase genes of *P. littoralis* using RNA sequencing and *de novo* transcriptome assembly.

b) **Functionally characterize** these PUFA biosynthesis genes using cloning and heterologous expression in yeast.

c) Evaluate the **gene expression** and **FA composition** of *P. littoralis* affected by indirect (dietary LC-PUFA deficiency) and direct (OW and OA) **climate drivers**.

d) Trace the **evolutionary origin and history** of PUFA biosynthesis within the different orders of copepods by identification and analysis of desaturases and elongases genes obtained from publicly available copepod transcriptomes.

Apart from the general introduction and discussion, each chapter within this PhD thesis discusses the outcomes of one or more of the above objectives (Figure 12). Each of them is an autonomous scientific article (published or in preparation for publication), and can be read separately from the other chapters. Inevitably, there is an overlap between the general introduction and discussion and those contained within the different chapters. Cited literature is compiled at the end of the thesis.

In **Chapter 2**, we sequenced and *de novo* assembled the transcriptome of *Platychelipus littoralis* (i.e. assembling a transcriptome without the availability of a genome). This transcriptome is the basis for the rest of the research within this PhD thesis. From this data, we identified a number of front-desaturase and elongase gene sequences. The biological samples were obtained from copepod specimens exposed to both OW and dietary LC-PUFA limitation in a full-factorial experiment. This experiment allowed us to additionally assess the transcriptional and FA response of *P. littoralis* to these two drivers. This chapter was published as "Fatty acid bioconversion in harpacticoid

copepods in a changing environment: a transcriptomic approach" in *Philosophical Transactions of the Royal Society B: Biological Sciences* (Boyen et al., 2020).

In **Chapter 3**, we redid the identification of the *P. littoralis* desaturases and elongases by comparing them with the functional desaturases and elongases of *Tigriopus californicus* (Kabeya et al., 2021). This allowed us to distinguish functional copepod front-end desaturases from the presumably non-functional sequences identified in Chapter 2, related to the (not yet functionally characterized) sequences of decapods (Monroig et al., 2022). We identified methyl-end and front-end desaturases as well as elongases within the *P. littoralis* transcriptome assembled in Chapter 2, and functionally characterized them by cloning and heterologous expression in yeast grown in the presence of different FA substrates. This allowed us to elucidate the precise capabilities of *P. littoralis* for biosynthesis of specific PUFAs. Additionally, we assessed the activities of *P. littoralis* elongases towards saturated fatty acids. This chapter was published as "Functional characterization reveals a diverse array of metazoan fatty acid biosynthesis genes" in *Molecular Ecology* (Boyen et al., 2023).

Chapter 4 details the results of a second incubation experiment that is an improvement to the one discussed in Chapter 2. We performed qPCR on the genes identified in Chapter 3 as well as an additionally identified *P. littoralis* stearoyl-CoA desaturase, and combined this with FA profiling (using GC-MS) to assess the copepod's response to multiple climate change drivers. We replaced Petri dishes with Duran bottles as incubation units, which allowed us to assess OA impacts next to OW and dietary LC-PUFA deficiency. Furthermore, obtaining FA and gene expression data from the same replicate enabled calculating correlations between the two replicates, further revealing the functionalities of the different desaturases and elongases. This chapter is being prepared for publication in a peer-review journal.

Although Chapters 2 to 4 reveal the unique PUFA biosynthesis capacities of *P. littoralis*, this work does not fully represent the ecological diversity of all copepods. Therefore in **Chapter 5**, we leveraged publicly available copepod transcriptome and genome data

to identify methyl-end desaturases, front-end desaturases and elongases within each species. We described differences in copy number and expression between orders, analysed the hypothesis of horizontal gene transfer as an origin of copepod front-end and methyl-end desaturases, and ran selection models to assess whether and how genes selectively adapted following emergence. This chapter is being prepared for publication in a peer-review journal.

To conclude, in **Chapter 6** I provide a general discussion of the results from the previous chapters. I attempt to answer whether copepod PUFA biosynthesis as a mechanism for climate change resilience, and provide a number of scientific recommendations for this specific research field. Finally, I provide some policy recommendations that follow the outcomes of my PhD research.
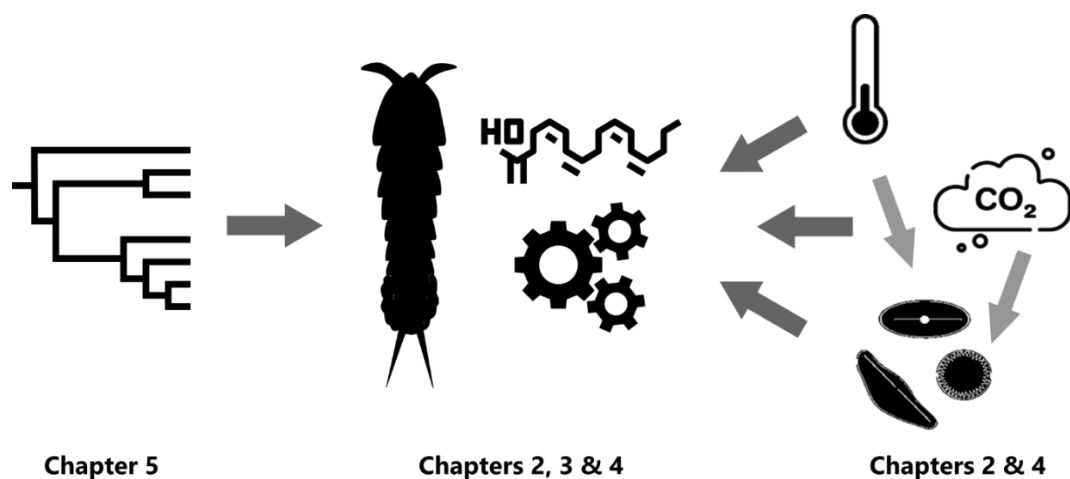
Figure 12 Outline of the thesis. We investigated the molecular mechanism behind polyunsaturated fatty acid biosynthesis of copepods (middle), within the evolutionary context of the different copepod orders (left) and within the context of future direct (ocean warming and ocean acidification) and indirect climate drivers (dietary LC-PUFA limitation due to direct drivers) (right). Icons obtained from the Noun Project and Phylopic websites.

CHAPTER 2

FATTY ACID BIOCONVERSION IN HARPACTICOID COPEPODS IN A CHANGING ENVIRONMENT: A TRANSCRIPTOMIC APPROACH

Jens Boyen[1], Patrick Fink[2, 3, 4], Christoph Mensens[1], Pascal I. Hablützel[5], Marleen De Troch[1]

[1]Marine Biology, Department of Biology, Ghent University, Krijgslaan 281 – S8, 9000 Gent, Belgium

[2]Cologne Biocenter, University of Cologne, Zülpicher Straße 47b, 50674 Köln, Germany

[3]Department Aquatic Ecosystem Analysis, Helmholtz Centre for Environmental Research, Brückstraße 3a, 39118 Magdeburg, Germany

[4]Department River Ecology, Helmholtz Centre for Environmental Research, Brückstraße 3a, 39118 Magdeburg, Germany

[5]Flanders Marine Institute (VLIZ), Wandelaarkaai 7, 8400 Oostende, Belgium

Abstract

By 2100, global warming is predicted to significantly reduce the capacity of marine primary producers for long-chain polyunsaturated fatty acid (LC-PUFA) synthesis. Primary consumers such as harpacticoid copepods (Crustacea) might mitigate the resulting adverse effects on the food web by increased LC-PUFA bioconversion. Here, we present a high-quality *de novo* transcriptome assembly of the copepod *Platychelipus littoralis,* exposed to changes in both temperature (+3°C) and dietary LC-PUFA availability. Using this transcriptome, we detected multiple transcripts putatively encoding for LC-PUFA-bioconverting front-end fatty acid desaturases and elongases, and performed phylogenetic analyses to identify their relationship with sequences of other (crustacean) taxa. While temperature affected the absolute fatty acid concentrations in copepods, LC-PUFA levels remained unaltered even when copepods were fed a LC-PUFA-deficient diet. While this suggests plasticity of LC-PUFA bioconversion within *P. littoralis*, none of the putative front-end desaturase or elongase transcripts were differentially expressed under the applied treatments. Nevertheless, the transcriptome presented here provides a sound basis for future ecophysiological research on harpacticoid copepods.

2.1 Introduction

Global climate change and the resulting increase in sea surface temperature over the past decades have profoundly impacted marine organisms and ecosystems (Doney et al., 2012). This trend is likely to continue for the next decades, with a projected global mean sea surface temperature (SST) increase of 2.73°C by 2090-2099 compared to 1990-1999 levels according to the business-as-usual Representative Concentration Pathway (RCP) 8.5 (Bopp et al., 2013). This temperature rise affects the physiological performance and fitness of marine organisms and consequently triggers adverse changes in marine ecosystems as well as the goods and services they provide (Gattuso et al., 2015). Indeed, prominent climate-related shifts in nutrient and food supplies have

already been observed in coastal areas worldwide (Drinkwater et al., 2010; Litzow et al., 2006). At the base of marine food webs, global warming is predicted to strongly impair the production of key nutritional fatty acids (FAs) by primary producers such as diatoms. These microalgae, like all living organisms, alter their FA composition due to temperature-dependent cell membrane restructuring, a process known as homeoviscous adaptation (Hixson & Arts, 2016; Sinensky, 1974). Specifically, proportions of long-chain polyunsaturated FAs (LC-PUFAs) such as eicosapentaenoic acid (20:5n-3, EPA) and docosahexaenoic acid (22:6n-3, DHA) in microalgae are projected to decline strongly in the coming century (Hixson & Arts, 2016). While the impact varies between taxa and LC-PUFA compounds, overall a reduced LC-PUFA availability is expected for higher trophic levels, many of which strongly rely on dietary LC-PUFAs to fulfil their metabolic requirements (Colombo et al., 2020; Litzow et al., 2006). Given the important role of LC-PUFAs in structural and physiological processes and as precursors for hormones and signalling molecules (Bell & Tocher, 2009), a reduced dietary LC-PUFA availability impacts growth, fecundity and fitness of consumers (Caramujo et al., 2008; Müller-Navarra et al., 2004). The relative contributions of the direct (increased SST) and the indirect (decreased dietary LC-PUFA availability) effect of global warming on higher trophic levels remains yet understudied (von Elert & Fink, 2018). Growth and FA composition of European sea bass *Dicentrarchus labrax* and European abalone *Haliotis tuberculata* were impacted by temperature but only to a lesser extent by diet (Gourtay et al., 2018; Hernández et al., 2013). This lesser dependency on dietary LC-PUFAs was attributed to the endogenous bioconversion of short-chain saturated FAs into LC-PUFAs. Numerous animal species, many of which aquatic invertebrates, are known to have at least some capacity for LC-PUFA bioconversion to cope with dietary changes (Monroig et al., 2013; Monroig & Kabeya, 2018). Benthic harpacticoid copepods (Crustacea) are key primary consumers in (coastal) marine and estuarine sediments (Hicks & Coull, 1983) and are known for their capacity for LC-PUFA bioconversion (De Troch et al., 2012; Nanton & Castell, 1998; Norsker & Støttrup, 1994; Werbrouck et al., 2017). Coastal and estuarine environments

undergo strong and stochastic fluctuations in temperature and nutrient availability. Harpacticoid copepods already adapted to such environments might be able to cope with the effects of global warming due to their LC-PUFA bioconversion capacity (Werbrouck et al., 2017). However, the environmental shifts driving this bioconversion are yet poorly understood (Monroig & Kabeya, 2018). Insights in the molecular aspects of LC-PUFA bioconversion are therefore required to understand this pivotal toolbox in crustaceans.

Converting short-chain saturated FAs to LC-PUFAs is achieved by a series of desaturase and elongase enzymes, which introduce a double bond or add two C-atoms to the FA chain, respectively (Monroig & Kabeya, 2018). Desaturase enzymes themselves can be split up in front-end and methyl-end (or ω-end) desaturases, depending on the location of the double bond insertion (Hashimoto et al., 2008). For crustaceans, genes encoding for front-end desaturase and elongase enzymes were so far mainly detected in decapods (Lin et al., 2017, 2018; Mah et al., 2019; Wu et al., 2018; Yang et al., 2013). Interestingly, a recent study discovered genes encoding w-end desaturases in many aquatic invertebrates including some orders of copepods, challenging the current dogma that *de novo* PUFA biosynthesis occurs exclusively in marine microbes (Kabeya et al., 2018). Nielsen et al. (2019) identified putative front-end desaturase genes in multiple copepod species (Nielsen et al., 2019). Understanding how changes in diet or temperature affect those genes at the transcriptomic (i.e. gene expression) level has so far only been investigated in cyclopoid copepods (Lee et al., 2017a; Nielsen et al., 2019). Within the order of Harpacticoida, transcriptomic resources are so far only available for *Tisbe holothuriae* (BioProject PRJEB23629) and three species of the *Tigriopus* genus (Kim et al., 2015, 2016; Schoville et al., 2012).

Given the ecological importance of benthic harpacticoid copepods at the plant-animal interface, there is a need to better characterize their physiological response to global change at the molecular level. To do so, we investigated the transcriptomic and FA-metabolic response of the benthic harpacticoid copepod *Platychelipus littoralis* (Brady,

1880) towards both direct and indirect effects of global warming within a multifactorial setting, combining a change in SST (current versus future scenario) with a change in the dietary LC-PUFA availability (LC-PUFA-rich diatoms versus LC-PUFA-deficient green algae as food sources (Renaud & Parry, 1994; Volkman et al., 1989)). *P. littoralis* is a common intertidal species in European estuaries, and temperature-dependent LC-PUFA turnover rates have been demonstrated previously using compound-specific stable isotope analysis, even within a short timeframe of six days (Werbrouck et al., 2017). This study presents a high-quality *de novo* transcriptome assembly from *P. littoralis* and reveals differentially expressed (DE) genes and FA profile changes towards both diet and temperature. Furthermore, putative PUFA desaturase and elongase genes are identified and compared phylogenetically with genes of other crustacean species.

2.2 Materials and Methods

2.2.1 Experiment

Nitzschia sp. (strain DCG0421, Bacillariophyceae) and *Dunaliella tertiolecta* (Chlorophyceae) were obtained from the BCCM/DCG Diatoms Collection (hosted by the Laboratory for Protistology & Aquatic Ecology - Ghent University) and the Aquaculture lab - Ghent University, respectively. Both algae were non-axenically cultured at $15 \pm 1°C$ in filtered (3 µm; Whatman Grade 6) and autoclaved natural seawater (FNSW), supplemented with Guillard's (F/2) Marine Water Enrichment solution (Sigma-Aldrich, Overijse, Belgium) and NutriBloom Plus (Necton) for *Nitzschia* sp. and *D. tertiolecta*, respectively. Food pellets were prepared through centrifugation and lyophilisation and stored at -80°C. In parallel, algae were stored in quadruplicate at -80°C for later FA analysis. Additional quadruplicate algae samples were filtered (Whatman GF/F) and lyophilized for particulate organic carbon determination using high temperature combustion. *Platychelipus littoralis* specimens were collected from the top sediment layer of the Paulina intertidal mudflat

(Westerscheldt estuary, The Netherlands; 51°21′N, 3°43′E) in August 2018. After sediment sieving (250 μm) and decantation, live adults were randomly collected using a glass Pasteur pipette under a stereo microscope. Copepods were cleaned by transferring them thrice to Petri dishes with clean FNSW and were kept in clean FNSW overnight to allow gut clearance prior to the start of the experiment.

The ten-day experiment had a fully crossed design with the factors temperature (19 ± 1 or 22 ± 1°C) and diet (*Nitzschia* sp. or *D. tertiolecta*). Temperature levels were based on the current mean August sea surface temperature at the sampling location (data obtained from www.scheldemonitor.be) and a global sea surface temperature increase of 3°C by 2100 as predicted by RCP8.5 (Collins et al., 2013). The food sources were offered as pre-thawed, rehydrated food pellets at a concentration of 3.69 ± 0.22 mg C l^{-1} day^{-1} and 5.10 ± 1.16 mg C l^{-1} day^{-1} for *Nitzschia* sp. and *D. tertiolecta* respectively, which are considered non-limiting food conditions (Werbrouck et al., 2017; Windisch & Fink, 2018). The combinations of diet and temperature yielded four treatments, each consisting of Petri dishes (52 mm diameter) filled with ten ml FNSW incubated in TC-175 incubators (Lovibond), with each treatment having four replicates for transcriptomic analysis (100 copepods per Petri dish) and three replicates for FA analysis (50 copepods per Petri dish). Each day, copepods were transferred to new units containing new temperature-equilibrated FNSW and were offered new pre-thawed food pellets. Triplicate copepod samples (50 specimens each) were collected from the field similarly as the specimens used in the experiment, and were stored at -80°C for analysis of the initial (field) FA composition. At the end of the experiment, mortality was assessed, and all live specimens were transferred to Petri dishes with clean FNSW to remove food particles from the cuticle. Copepods for transcriptomic analysis were immediately thereafter flash-frozen in liquid nitrogen and stored at -80°C. Copepods for FA analysis were stored overnight to allow gut clearance prior to storage at -80°C. Differences in copepod survival between diet and temperature treatments and due to initial density (100 vs. 50 copepods per Petri dish) was statistically assessed in R v.3.6.0

(R Core Team, 2020) using a type II three-way ANOVA, a Tukey normalization transformation, and a stepwise model selection by AIC.

2.2.2 FA analysis

FA methyl esters (FAMEs) were prepared from lyophilized algal and copepod samples using a direct transesterification procedure with 2.5 % (v:v) sulfuric acid in methanol as described by De Troch et al. (De Troch et al., 2012). The internal standard (nonadecanoic acid, Sigma-Aldrich, 2.5 µg) was added prior to the procedure. FAMEs were extracted twice with hexane. FA composition analysis was carried out with a gas chromatograph (HP 7890B, Agilent Technologies, Diegem, Belgium) equipped with a flame ionization detector (FID) and connected to an Agilent 5977A Mass Selective Detector (Agilent Technologies, Diegem, Belgium). The GC was further equipped with a PTV injector (CIS-4, Gerstel, Mülheim an der Ruhr, Germany). A HP88 fused-silica capillary column (60m×0.25mm×0.20µm film thickness, Agilent Technologies) was used at a constant Helium flow rate (2 ml min^{-1}). The injected sample (2 µl) was split equally between the MS and FID detectors using an Agilent capillary flow technology splitter. The oven temperature program was as follows: at the time of sample injection the column temperature was 50°C for 2 min, then gradually increased at 10°C min^{-1} to 150°C, followed by a second increase at 2°C min^{-1} to 230°C. The injector temperature was held at 30°C for 6 s and then ramped at 10°C s^{-1} to 250°C and held for ten min. The transfer line for the column was maintained at 250°C. The quadrupole and ion source temperatures were 150 and 230°C, respectively. Mass spectra were recorded at 70 eV ionization voltage over the mass range of 50-550 m/z units.

Data analysis was done with MassHunter Quantitative Analysis software (Agilent Technologies). The signal obtained with the FID detector was used to generate quantitative data of all compounds. Peaks were identified based on their retention times, compared with external standards as a reference (Supelco 37 Component FAME Mix, Sigma-Aldrich) and by the mass spectra obtained with the Mass Selective Detector. FAME quantification was based on the area of the internal standard and on the

conversion of peak areas to the weight of the FA by a theoretical response factor for each FA (Ackman & Sipos, 1964; Wolff et al., 1995). Statistical analyses were performed in R v.3.6.0 (R Core Team, 2020). Shapiro-Wilk test and Levene's test were used to check for normal distribution and homoscedasticity. The non-parametric Wilcoxon rank sum test was used to asses for the difference in absolute and relative concentration of the individual FA compounds between field and incubated copepods. The type II two-way ANOVA and the non-parametric Scheirer-Ray-Hare test were used to test for the effects of diet and temperature on the absolute and relative concentration for each FA compound. Multivariate statistics were performed to test the effects of incubation, diet and temperature on the overall FA composition. Non-metric multidimensional scaling (nMDS) with FAs as correlating vectors and PERMANOVA were performed after square root transformation (Bray-Curtis dissimilarity) using all FAs with mean relative concentration >1%. Mean values are presented with standard deviation (±s.d.). The FA shorthand notation A:Bn-X is used, where A represents the number of carbon atoms, B the number of double bonds, and X the position of the first double bond counting from the terminal methyl group.

2.2.3 Transcriptomic analysis

Total RNA from 45 to 97 pooled *P. littoralis* specimens per sample was isolated using the RNeasy Plus Micro Kit (QIAGEN) following an improved protocol (See Supplementary Methods). Total RNA was extracted from all four replicates from the two *Nitzschia* sp. treatments, but due to high copepod mortality, only three out of four replicates from each of the two *D. tertiolecta* treatments could be used. Total RNA quality and quantity were assessed by both a NanoDrop 2000 spectrophotometer (Thermo Scientific) and a 2100 Bioanalyzer (Agilent Technologies). RNA integrity numbers were between 6.5 and 10.0 (mean: 9.2), A260/280 ratios were between 1.7 and 2.2 (mean: 2.1), and A260/230 ratios were between 0.1 and 1.9 (mean: 1.0). cDNA libraries were constructed using the Illumina TruSeq Stranded mRNA kit and samples

were run on an Illumina HiSeq 4000 platform with 75 bp paired-end reads at the Cologne Centre for Genomics (University of Cologne).

Read quality was assessed using FASTQC v.0.11.7. The reads were quality-trimmed and adapter-clipped using Trimmomatic (Bolger et al., 2014), and the raw read files are available at the NCBI Short Read Archive under BioProject PRJNA575120. The transcriptome was assembled *de novo* using Trinity v.2.8.4 (Grabherr et al., 2011) including *in silico* read normalization. Multiple tools were used to assess assembly quality. First, the percentages of reads properly represented in the transcriptome assembly were calculated for each sample using Bowtie2 v.2.3.4 (Langmead & Salzberg, 2012). Second, the transcripts were aligned against proteins from the Swiss-Prot database (February 16, 2019) using blastx (cutoff of $1e^{-20}$), and the number of unique proteins represented with full-length or nearly full length transcripts (>90 %) was determined. Third, we performed Benchmarking Universal Single-Copy Orthologs (BUSCO) v.3.1.0 analysis using the arthropod dataset to estimate transcriptome assembly and annotation completeness (Simão et al., 2015). Lastly, both the N50 statistic and the E90N50 statistic (using only the set of transcripts representing 90 % of the total expression data) were determined based on transcript abundance estimation using salmon v.0.12.0 following the quasi-mapping procedure (Patro et al., 2017). The transcripts were annotated using Trinotate (Bryant et al., 2017), an open-source toolkit that compiles several analyses such as coding region prediction using TransDecoder (http://transdecoder.github.io), protein homology identification using BLAST and the Swiss-Prot database, protein domain identification using HMMER/Pfam (El-Gebali et al., 2019; Finn et al., 2011), and gene annotation using EggNOG, KEGG and Gene Ontology (GO) database resources (Huerta-Cepas et al., 2019; Kanehisa et al., 2012; The Gene Ontology Consortium et al., 2000). The transcriptome (GHXK0100001.1-GHXK01287339.1) is available at the NCBI TSA Database under BioProject PRJNA575120. Transcript abundance per sample was estimated using salmon v.0.12.0 following the quasi-mapping procedure (Patro et al., 2017). The R v.3.0.6 (R Core Team, 2020) package edgeR v.3.26.4 (Robinson et al., 2009) was used to identify significantly

DE transcripts. Transcripts with >5 counts per million in at least three samples were retained. TMM normalization was applied (Robinson & Oshlack, 2010), and differential expression was determined using a gene-wise negative binomial generalized linear model with quasi-likelihood F-tests (glmQLFit) with diet, temperature and the diet x temperature interaction as factors. Transcripts with an expression fold change ≥2 at a false discovery rate ≤0.05 (Benjamini-Hochberg method (Benjamini & Hochberg, 1995)) were considered significantly DE. The R package topGO v.2.36.0 (Alexa & Rahnenfuhrer, 2019) was used to test for enriched GO terms for both the diet and the temperature treatment. The enrichment tests were run using the weight01 algorithm and the Fisher's exact test statistic, with GO terms considered significantly enriched when p≤0.01.

A transcript was categorized as encoding a front-end desaturase when it contained the two essential Pfam domains *Cytb5* (PF00173) and *FA_desaturase* (PF00487), three diagnostic histidine boxes (HXXXH, HXXXHH, and QXXHH) and a heme-binding motif (HPGG) (Hashimoto et al., 2008). A transcript was categorized as encoding an elongase when it contained the Pfam domain *ELO* (PF01151) and the diagnostic histidine box (HXXHH) (Hashimoto et al., 2008). Nucleotide coding sequences of the transcripts were trimmed to those conserved regions and aligned using MAFFT v7.452 (Katoh & Standley, 2013) with default parameters. Sequences that did not align with the main multiple sequence alignment, contained long indels or were identical to other sequences after trimming were removed. Additional well-annotated (sometimes functionally characterized) crustacean sequences found to be most closely related to each of the *P. littoralis* transcripts through blastx were added to the alignment. We also included desaturase and elongase sequences from the hydrozoan *Hydra vulgaris*, copepod front-end desaturase sequences from Nielsen et al. (2019) and human elongase sequences Elovl1 to Elovl7. For each gene family, an unrooted maximum likelihood phylogenetic tree was built using RAxML v.8.2.4 (Stamatakis, 2014) with a General Time Reversible model of nucleotide substitution and CAT approximation. The

final tree was rooted (midpoint), visualized and edited with FigTree v.1.4.3 (http://tree.bio.ed.ac.uk/software/figtree).

2.3 Results

The two algal diets differed in their FA composition (Table S1). EPA and DHA were highly abundant in *Nitzschia* sp. (26.85 ± 2.26 % and 5.68 ± 0.29 %) while not detected in *D. tertiolecta*. On the contrary *D. tertiolecta* exhibited a high content of α-linolenic acid (ALA, 18:3n-3; 43.77 ± 1.29 %) compared to *Nitzschia* sp. (0.05 ± 0.03 %). Mean copepod survival after ten days was 75.46 ± 27.79 %. Besides high variation between replicates, no significant effects of diet, temperature, initial density or interactions on copepod survival were detected (three-way ANOVA; AIC = 1696.8; $F_{(7,20)}$ = 1.382; p = 0.2665).

2.3.1 Changes in FA content and composition

At the end of the experiment, total FA content in copepods in the treatments (149.47 ± 21.37 ng copepod^{-1}) declined compared to control values from the field (197.29 ± 4.50 ng copepod^{-1}) (p = $4.4e^{-3}$). Overall FA composition of the field copepods was significantly distinct from the ones of the incubated copepods ($F_{(1,14)}$ = 10.83; p = $3.0e^{-3}$), mainly due to lower PUFA concentrations in the latter ones (Fig. 1). In the experiment, overall copepod FA composition was significantly affected by temperature ($F_{(1,11)}$ = 4.30; p = 0.015) but not by diet ($F_{(1,11)}$ = 1.83; p = 0.13, no interaction), which was primarily correlated with short-chain, saturated fatty acids (Fig. 1). Temperature but not diet significantly affected total FA content, which was lower at 22°C compared to 19°C (Fig. 2, Table S2). Temperature but not diet also significantly affected absolute concentrations of anteiso-15:0, 15:0, 16:0, 18:1n-7, 24:0, DHA and total monounsaturated fatty acid concentration (∑MUFA), which were all lower at 22°C (Table S2). The diet only significantly affected the absolute ALA concentration, with copepods fed the ALA-rich diet *D. tertiolecta* having a higher absolute ALA

concentration compared with copepods fed with *Nitzschia* sp. (Fig. 2, Table S2). A significant temperature x diet interaction was found for oleic acid (OA, 18:1n-9). Absolute OA concentration was higher at 19°C when fed *Nitzschia* sp., an effect that reversed (higher at 22°C) when fed *D. tertiolecta* (Fig. 2, Table S2). Total polyunsaturated fatty acid concentration (∑PUFA), total saturated fatty acid concentration (∑SFA), or important LC-PUFAs such as EPA and arachidonic acid (ARA, 20:4n-6)were affected by neither temperature nor diet. Despite the absence of EPA and DHA in *D. tertiolecta*, copepods fed this diet were able to maintain similar relative EPA and DHA concentrations as in copepods fed with *Nitzschia* sp. (Table S3).
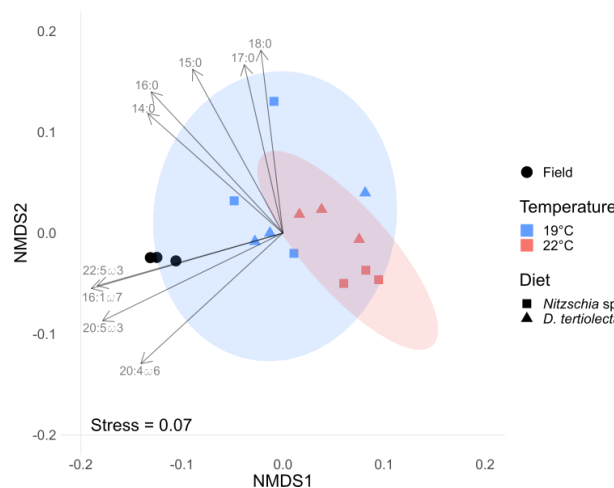
Figure 1 nMDS ordination using absolute FA concentrations (ng copepod^{-1}) of the four treatments and field samples. Ellipses indicate 95 % confidence levels of the temperature factor. Vectors were plotted for fatty acids with $r^2>0.7$.
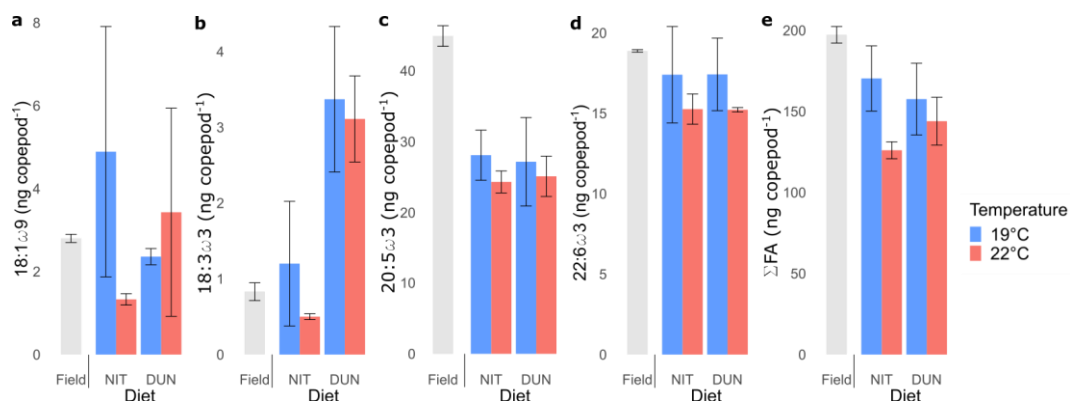
Figure 2 Mean absolute fatty acid concentration (ng copepod^{-1} ± s.d.; n=3) of P. littoralis prior (Field) and after ten days of incubation with Nitzschia sp. (NIT) or D. tertiolecta (DUN). a OA (18:1n-9) b ALA (18:3n-3) c EPA (20:6n-3) d DHA (22:6n-3) e ΣFA (total fatty acid concentration).

2.3.2 Transcriptome assembly and annotation

We sequenced 14 *P. littoralis* samples resulting in nearly 400 million paired-end Illumina reads. After quality filtering, an assembly was generated consisting of 287,753 transcript contigs (Table 1). 97.80 ± 0.44 % of the reads of each sample mapped back to the assembly, with 95.95 ± 0.68 % mapping as properly paired reads (aligning concordantly at least once). 7,088 proteins from the Swiss-Prot database were represented by transcripts with >90 % alignment coverage. 97.9 % of the BUSCO arthropod genes were represented by at least one complete copy (single: 26.1 %, duplicated: 71.8 %, fragmented: 1.1 %). The N50 and the E90N50 metrics were 1,360 and 2,657 respectively, and 90 % of the total expression data was represented by 35,540 transcripts. TransDecoder identified 296,142 putative open reading frame coding regions within the assembly, suggesting at least some transcripts contain multiple coding regions (Table 1). About a quarter of those putative ORFs were annotated with GO (24.9 %), KEGG (22.8 %) or EggNOG terms (16.0 %) or were found to contain at least one Pfam protein family domain (29.5 %, Table 1).

Table 1 Assembly and annotation characteristics of the P. littoralis transcriptome.

Assembly and annotation characteristics	Value
Assembly	
Number of raw reads	395,794,835
Average number of reads sample[-1]	28,271,060
Number of assembled bases (bp)	207,643,686
Number of assembled contigs	287,753
Average contig length (bp)	721.6
Median contig length (bp)	343
GC content (%)	47.54
Annotation	
Number of ORFs	296,142
ORFs with GO terms	73,836
ORFs with KEGG terms	67,484
ORFs with EggNOG terms	47,358
ORFs with Pfam protein family	87,319

2.3.3 Differential expression and gene set enrichment analysis

After filtering out low expression transcripts, 24,202 transcripts were retained for DE analysis. Seven transcripts were DE between the two diet treatments (Fig. 3a,b, Table S4). Four of them were upregulated when copepods were fed with *Nitzschia* sp., while three were upregulated when copepods were fed with *D. tertiolecta*. 29 transcripts were DE between the two temperature treatments (Fig. 3c,d, Table S4). Five transcripts were upregulated at 19°C, while 24 were upregulated at 22°C. Four transcripts were DE in both treatments. All but two DE transcripts contained at least one putative ORF. Gene set enrichment analysis using topGO identified 22 and 30 enriched GO terms under the diet and temperature treatment, respectively (Table S5). Notable enriched functions in both treatments were related to microtubuli and cilia organization (Table S5). Certain terms detected in both treatments and primarily related to the biological process "glycerophospholipid biosynthetic process" and the molecular function "transferring acyl groups" (Table S5), were all attributed to the transcript *Plit_DN1805_c0_g1_i18*, which was downregulated when fed *D. tertiolecta* (compared to *Nitzschia* sp.) and upregulated at 22°C (compared to 19°C, Fig. 3, Table S4, S5). This transcript contains six ORFS which, according to blastx, match against the chicken protein acetoacetyl-CoA synthetase and the human protein glycerol-3-phosphate acyltransferase, both involved in the phospholipid metabolism.
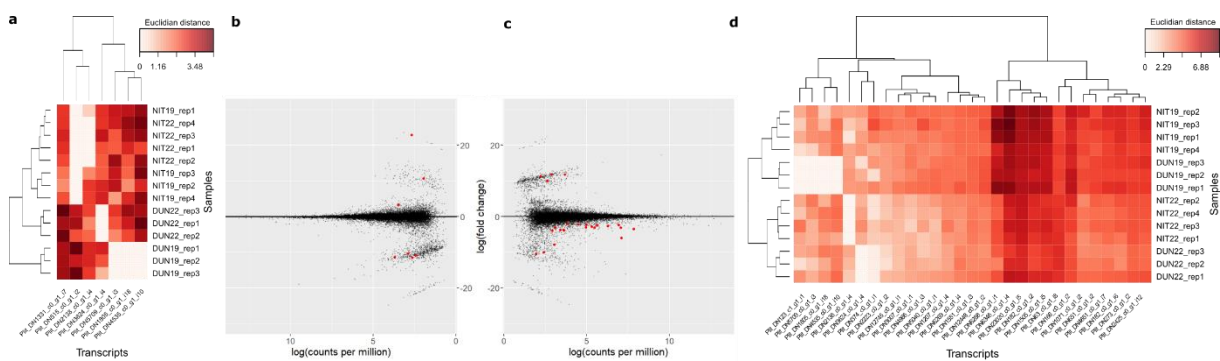
Figure 3 Heatmaps (a,d) and MA plots (b,c). MA plots show log fold change per transcript against its mean expression (in log counts per million) with diet (b) and temperature (c) as contrast. Red dots indicate significantly differentially expressed (DE) transcripts (i.e. log fold change ≥1 and false discovery rate ≤0.05). Black dots indicate non-significantly DE transcripts. Heatmaps show relative expression level (Euclidean distance) of each significantly DE transcript in each sample with diet (a) and temperature (d) as contrast. Transcripts and samples are hierarchically clustered.

2.3.4 Identification and phylogenetic analysis of desaturase and elongase genes

Respectively 19 and 17 unique putative front-end desaturase and elongase sequences were identified in the *P. littoralis* transcriptome since they all exhibited diagnostic characteristics and aligned properly to other sequences. A maximum likelihood phylogenetic tree was built for each gene family (Fig. 4). Concerning the front-end desaturase sequences, we identified two distinct clades with high bootstrap support (Fig. 4a). The first clade contained five front-end desaturases from *P. littoralis* as well as from all other crustacean taxa. While one transcript is related to the functionally characterized Δ6 front-end desaturase sequence from the decapod *Macrobrachium nipponense*, the phylogenetic relationship of the other *P. littoralis* transcripts as a sister clade of the sequences of other copepod species is poorly supported (bootstrap value <50). The second clade contained only sequences from *P. littoralis* and one sequence of *H. vulgaris* in a basal position. The phylogenetic analysis of elongase transcripts produced multiple subclades (Fig. 4b). Two *P. littoralis* sequences and one *Daphnia magna* elongase sequence formed a clade with the human Elovl3 and Elovl6, classifying them as putatively Elovl6/Elovl3-like. One *P. littoralis* sequence, one *D. magnia* sequence and one *H. vulgaris* sequence were found to be closely related with the human Elovl4 and the Elovl4-like sequence from *Scylla paramamosain*, classifying them as putatively Elovl4-like. Four *P. littoralis* sequences and sequences from *D. magna, Caligus rogercresseyi* and *Lepeophtheirus salmonis* formed a subclade with the functionally characterized Elovl7 sequence from *Scylla olivacea* which is also a sister clade with the human Elovl7 and Elovl1, classifying those as putatively Elovl7/Elovl1-like. None of the *P. littoralis* sequences formed a clade with human Elovl5 and Elovl2, while ten *P. littoralis* sequences were not related with any of the sequences included in the analysis (Fig. 4b).
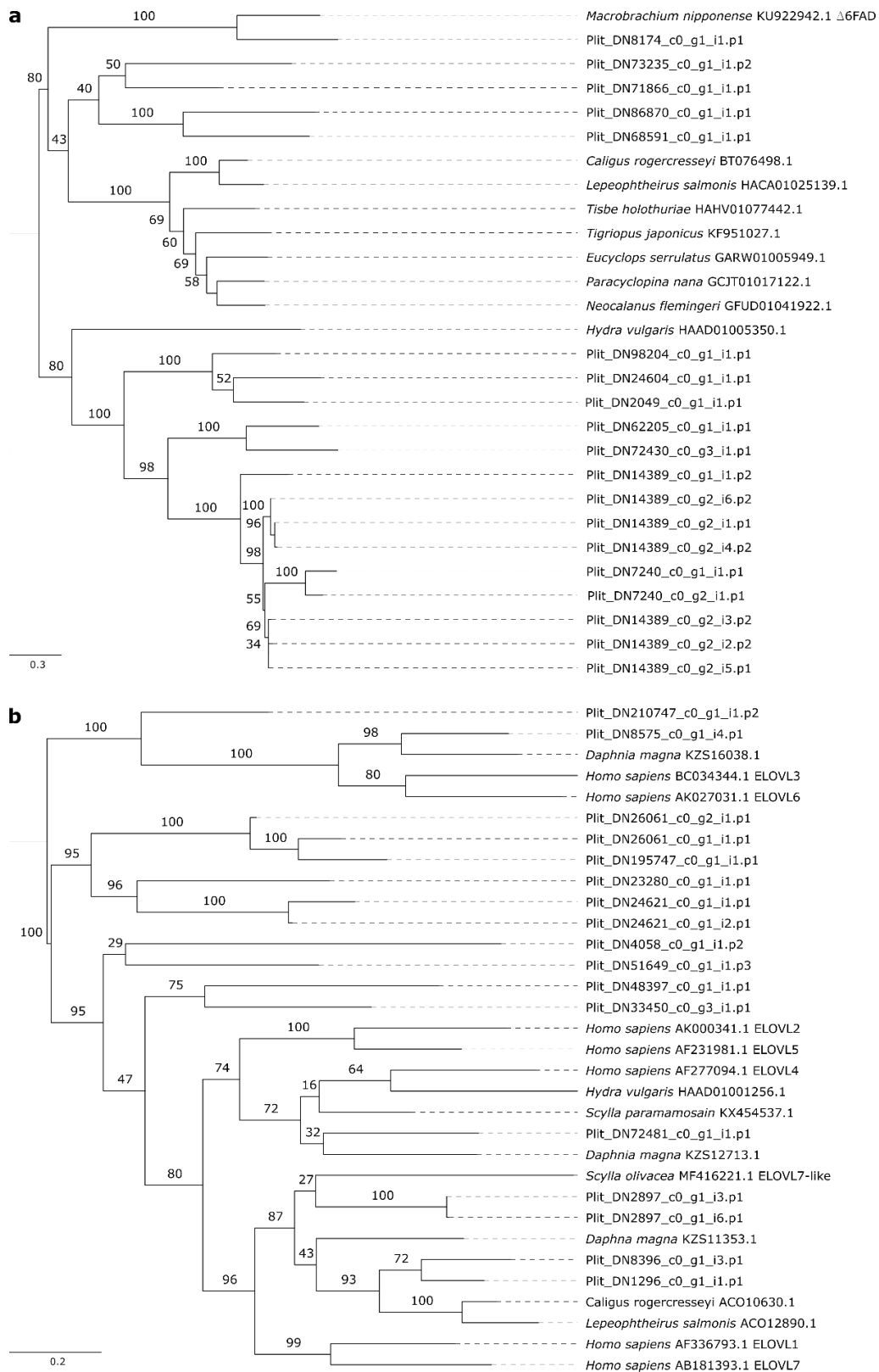
Figure 4 Maximum likelihood phylogenetic trees with midpoint root comparing trimmed nucleotide sequences of putative front-end desaturase (a) and elongase (b) transcripts of P. littoralis with sequences of other crustaceans, Homo sapiens and the hydrozoan Hydra vulgaris. Values above branches show bootstrap support after 100 RAxML iterations. Gene identification, when already functionally characterized, was added after each accession number.

2.4 Discussion

Several earlier studies indicated that harpacticoid copepods have a strong capacity for endogenous LC-PUFA bioconversion (De Troch et al., 2012; Nanton & Castell, 1998; Werbrouck et al., 2017). Meanwhile, our knowledge on the molecular pathways underlying this process is still limited (Monroig & Kabeya, 2018). Considering a global SST increase and a decline in LC-PUFA production by primary producers within this century (Hixson & Arts, 2016), LC-PUFA bioconversion potentially plays a unique role for primary consumers to physiologically mitigate the negative effects of climate change. Prior to our experiment, the algae were lyophilized to prevent temperature-dependent growth. Previous research found that harpacticoids ingest lyophilized algae, albeit at a lower assimilation rate than live algae (Cnudde et al., 2011). We showed that when fed with the LC-PUFA-deficient *D. tertiolecta*, *P. littoralis* had the physiological plasticity to maintain LC-PUFA levels relatively similar to copepods fed with *Nitzschia* sp. The high abundance of ALA in *D. tertiolecta*-fed *P. littoralis* indicates that the copepods efficiently ingested lyophilized *D. tertiolecta*. This likely counteracted the lack of LC-PUFA, since *P. littoralis* is able to use ALA as a precursor for desaturation and elongation towards EPA and DHA (Monroig & Kabeya, 2018). *D. tertiolecta*-derived 16:4n-3 and 16:3n-3 and *Nitzschia* sp.-derived 16:1n-7 were not sustained in *P. littoralis* (Supplementary Tables S2 and S3). Either way the lyophilized algae were not as efficiently assimilated as previously detected, or these compounds were bioconverted to other FAs or metabolized to provide energy. In contrast to diet, an increased SST of 3°C reduced the absolute total FA content, suggesting an increased use of storage FAs as energy providers (Bell & Tocher, 2009). Some FA compounds showed extensive variability between replicates, which can be explained by the low sample volume or the low number of replicates.

While the absolute concentrations of DHA and several monounsaturated FAs decreased, the relative concentrations of LC-PUFAs remained unaltered. Homeoviscous adaptation as a possible explanation cannot be confirmed nor rejected, as we do not

have any information on membrane FAs specifically (Sinensky, 1974). Decreased DHA concentrations can alternatively be linked to an increased stress response at the upper limits of *P. littoralis*' thermal range. In a previous experiment, increased temperatures indeed stimulated ARA and EPA bioconversion to allow enhanced eicosanoid biosynthesis in *P. littoralis* (Werbrouck et al., 2017). However, a comparison with the current results should be done with care since the previous experiment included an ecologically improbable SST increase of 10°C. These results thus clearly illustrate the importance of LC-PUFA bioconversion as a mechanism to cope with the direct and indirect effects of global warming. As such, fluctuations in temperature or food quality might be relatively less detrimental to *P. littoralis*, and its historical adaptation to a variable environment could have given this species useful adaptations to persist under future environmental changes.

To investigate the molecular mechanisms behind the FA metabolism of *P. littoralis*, we performed a *de novo* assembly of its transcriptome. The high N50 metric (1,360) and high number of complete arthropod BUSCO genes (97.9 %) compared to other copepod transcriptomes lead us to state that the transcriptome presented here is of high quality and can be confidently used for future studies (Semmouri et al., 2019). However, the high number of BUSCO duplicates (71.8%), expected in *de novo* transcriptome assemblies and when working with pools of individuals, might still indicate assembly errors. In our differential gene expression analysis, seven and 29 transcripts were found to be DE in the dietary and temperature contrasts, respectively. These low numbers can be attributed to the employed filtering threshold, or to the low number of replicates used, which reduced the power to detect significantly DE genes. Low numbers of DE genes were found in other transcriptomic studies on copepods as well (Semmouri et al., 2019). A gene set enrichment analysis identified GO terms mainly related to cytoskeleton organisation and phospholipid biosynthesis. Possible relations between temperature or dietary LC-PUFA availability and the cytoskeleton have been identified in vertebrates (Guzmán et al., 2000; Røsjø et al., 1994), yet further investigations on invertebrates are needed. GO terms related to phospholipid

biosynthesis were all attributed to one transcript which was downregulated when *P. littoralis* was fed *D. tertiolecta* and upregulated at 22°C, respectively. A temperature-driven reduction of membrane-bound phospholipid biosynthesis seems plausible (Sinensky, 1974) and is in line with both our own and previous findings (Werbrouck et al., 2017) at the FA level. It may be interpreted as increased mobilization of FAs for energy provision. The previous study however did not find membrane FA depletion when *P. littoralis* was fed the LC-PUFA deficient diet *D. tertiolecta* (Werbrouck et al., 2017), thereby contradicting our findings at the transcriptional level. As we sequenced bulk RNA from a pool of specimens, we were unable to determine whether some of the DE genes are tissue-specific regulated or not.

Importantly, we identified a high number of transcripts putatively encoding for front-end desaturases and elongases. While we are aware that a *de novo* assembly may artificially introduce an inflated number of contigs (Hölzer & Marz, 2019), most sequences were sufficiently distinct to confidently state that they belong to different paralogous genes. It is indeed known that gene duplication is an important driver of the diversity of desaturase and elongase genes (Ishikawa et al., 2019; Surm et al., 2018). We would therefore like to advance the hypothesis that an elevated front-end desaturase and elongase gene duplication frequency in harpacticoid copepods could be the key element for their high LC-PUFA bioconversion capacity. However, more exhaustive phylogenetic analyses are necessary to test this hypothesis. Our current analyses already show that putative front-end desaturases from *P. littoralis* grouped into two distinct phylogenetic clades, with one group of sequences clustering with other copepod desaturase sequences and a Δ6 desaturase sequence from *M. nipponense*, and another group of sequences clustering with a desaturase sequence from *H. vulgaris* (Fig. 4a). Corroborating the results of a previous study, copepod front-end desaturases grouped together in one monophyletic clade, however none of the *P. littoralis* sequences were found to cluster within this clade, but rather grouped separately as a sister clade. Including more functionally characterized front-end desaturases from other crustacean species might benefit our analyses, but are so far

not available (Monroig & Kabeya, 2018). In contrast, the maximum-likelihood tree of the elongase sequences corresponds more to earlier studies (Mah et al., 2019) (Fig. 4b). While ten *P. littoralis* sequences did not cluster with any of the additional sequences, we were able to assign seven *P. littoralis* sequences as well as seven other crustacean sequences to one of the three subclades Elovl3/Elvol6-like, Elovl4-like or Elovl1/Elovl7-like. Overall, our phylogenetic analyses of the front-end desaturase and elongase transcripts of *P. littoralis* provide a first glimpse at the high diversity of these genes and serve as a starting point to better comprehend the evolutionary history of LC-PUFA bioconversion within harpacticoid copepods.

Interestingly, none of the identified transcripts encoding a front-end desaturase or elongase were found to be DE due to temperature or dietary LC-PUFA availability. This contradicts the stressor-driven LC-PUFA bioconversion evidenced at the FA level. The majority of those transcripts (31 out of 36) were classified as lowly expressed (<5 counts per million sample^{-1}) and were therefore excluded from the DE analysis. Additionally, the applied correction for multiple testing might have resulted in potentially significantly DE transcripts to go undetected (Benjamini & Hochberg, 1995). A more gene-specific approach such as reverse transcriptase quantitative polymerase chain reaction (qPCR) (Freeman et al., 1999) might be better suited to analyse expression of LC-PUFA bioconversion genes following direct and indirect effects of global warming.

In conclusion, we combined two approaches – FA profiling and *de novo* transcriptome assembly – to expand the current knowledge on LC-PUFA bioconversion in harpacticoids. This study shows that LC-PUFA levels in *P. littoralis* remain high even on a LC-PUFA-deficient diet, yet transcripts putatively encoding for front-end desaturases and elongases were not found to be upregulated. The molecular pathways underlying this mechanism are thus more complex than previously assumed (also demonstrated by the recent discovery of w-end desaturases in multiple aquatic invertebrates (Kabeya et al., 2018)) and might not happen at the gene expression level. The *de novo* transcriptome of a non-model harpacticoid copepod presented here lays the

foundation for more targeted ecophysiological research to investigate the molecular basis of adaptation to cope with the effects of global change.

Acknowledgments

CHAPTER 3

FUNCTIONAL CHARACTERIZATION REVEALS A DIVERSE ARRAY OF METAZOAN FATTY ACID BIOSYNTHESIS GENES

Boyen Jens[1], Ribes-Navarro Alberto[2], Kabeya Naoki[3], Monroig Óscar[2], Rigaux Annelien[1], Fink Patrick[4, 5, 6], Hablützel Pascal[7], Navarro Juan Carlos[2]*, De Troch Marleen[1]*

*Juan Carlos Navarro and Marleen De Troch should be considered joint senior author.

[1]Marine Biology, Department of Biology, Ghent University, Gent, Belgium

[2]Instituto de Acuicultura Torre de la Sal (IATS), CSIC, Ribera de Cabanes, Castellón, Spain

[3]Department of Marine Biosciences, Tokyo University of Marine Science and Technology, Tokyo, Japan

[4]Department of River Ecology, Helmholtz Centre for Environmental Research - UFZ, Magdeburg, Germany

[5]Department of Aquatic Ecosystem Analysis and Management, Helmholtz Centre for Environmental Research - UFZ, Magdeburg, Germany

[6]Aquatic Chemical Ecology, Institute for Zoology, University of Cologne, Cologne, Germany

[7]Flanders Marine Institute (VLIZ), Oostende, Belgium

Previously published as:

Boyen, J., Ribes-Navarro, A., Kabeya, N., Monroig, Ó., Rigaux, A., Fink, P., Hablützel, P. I., Navarro, J. C., & De Troch, M. (2023). Functional characterization reveals a diverse array of metazoan fatty acid biosynthesis genes. *Molecular Ecology*, *32*(4), 970–982. https://doi.org/10.1111/mec.16808

Abstract

Long-chain ($\geq C_{20}$) polyunsaturated fatty acids (LC-PUFAs) are physiologically important fatty acids for most animals, including humans. Although most LC-PUFA production occurs in aquatic primary producers such as microalgae, recent research indicates the ability of certain groups of (mainly marine) invertebrates for endogenous LC-PUFA biosynthesis and/or bioconversion from dietary precursors. The genetic pathways for and mechanisms behind LC-PUFA biosynthesis remain unknown in many invertebrates to date, especially in non-model species. However, the numerous genomic and transcriptomic resources currently available can contribute to our knowledge of the LC-PUFA biosynthetic capabilities of metazoans. Within our previously generated transcriptome of the benthic harpacticoid copepod *Platychelipus littoralis*, we detected expression of one methyl-end desaturase, one front-end desaturase, and seven elongases, key enzymes responsible for LC-PUFA biosynthesis. To demonstrate their functionality, we characterized eight of them using heterologous expression in yeast. The *P. littoralis* methyl-end desaturase has $\Delta15/17/19$ desaturation activity, enabling biosynthesis of α-linolenic acid, eicosapentaenoic acid and docosahexaenoic acid (DHA) from 18:2n-6, 20:4n-6 and 22:5n-6, respectively. Its front-end desaturase has $\Delta4$ desaturation activity from 22:5n-3 to DHA, implying that *P. littoralis* has multiple pathways to produce this physiologically important fatty acid. All studied *P. littoralis* elongases possess varying degrees of elongation activity for saturated and unsaturated fatty acids, producing aliphatic hydrocarbon chains with lengths of up to 30 carbons. Our investigation revealed a functionally diverse range of fatty acid biosynthesis genes in copepods, which highlights the need to scrutinize the role that primary consumers could perform in providing essential nutrients to upper trophic levels.

3.1 Introduction

Long-chain ($\geq C_{20}$) polyunsaturated fatty acids (LC-PUFAs), including arachidonic acid (ARA, 20:4n-6), eicosapentaenoic acid (EPA, 20:5n-3) and docosahexaenoic acid (DHA, 22:6n-3), are key nutritional components that are particularly abundant in marine ecosystems but are also vital for the functioning of freshwater and terrestrial ecosystems (Bell & Tocher, 2009; Závorka et al., 2023). In animals specifically, LC-PUFAs play important roles in energy storage, lipid membrane structures, signalling pathways (as precursors of eicosanoids) and gene regulation (Bazinet & Layé, 2014; Tocher, 2015). While widely distributed, LC-PUFAs are particularly abundant in aquatic ecosystems, especially in marine waters (Colombo et al., 2017a). Due to global climate change and rising water temperatures, the production of LC-PUFAs in phytoplankton and other microalgae is expected to decrease significantly (Hixson & Arts, 2016; Holm et al., 2022). This predicted temperature-related LC-PUFA reduction occurs due to changes in the lipid composition of cell membranes through a process known as homeoviscous adaptation (Sinensky, 1974). Moreover, changes in phytoplankton community composition and declining net primary production could further impair global LC-PUFA availability (Bi et al., 2021; Kwiatkowski et al., 2020). This will consequently have an impact on organisms at higher trophic levels via trophic cascading (Colombo et al., 2020).

The increasing availability of genomic data on multiple invertebrate taxa facilitates the investigation of the LC-PUFA biosynthetic pathways at a molecular level by characterization of its key biosynthesizing enzymes (Fig. 1) (Monroig et al., 2022). Stearoyl-CoA-desaturase (*scd*), also known as Δ9 desaturase, is present in all eukaryotes and enables the first desaturation from stearic acid (18:0) to oleic acid (OA, 18:1n-9). It was long assumed that endogenous further *de novo* LC-PUFA biosynthesis is restricted to (micro-)algae, bacteria and heterotrophic protists, and that metazoans need to cover their LC-PUFA needs through their diet. In aquatic habitats microalgae supposedly synthesize the major LC-PUFAs, which are then transferred to higher trophic levels via

first-order consumers. However, this assumption has been challenged in recent years by the discovery of a particular type of enzyme termed "methyl-end desaturases" in numerous groups of (mainly marine) invertebrates such as cnidarians, nematodes, arthropods, annelids and molluscs (Kabeya et al., 2018; Malcicka et al., 2018; Zhou et al., 2008). Methyl-end desaturases, previously reported mostly in plants, algae and microbes, introduce a double bond between the pre-existing one and the methyl-end of the carbon chain. They are required for *de novo* biosynthesis of the C_{18} PUFAs linoleic acid (LA, 18:2n-6) and α-linolenic acid (ALA, 18:3n-3) from OA. Hence, these enzymes allow a consumer to not only depend upon exogenously (i.e. via their diet) supplied precursors required to biosynthesize LC-PUFAs (Monroig et al., 2022). The ecological implications of the occurrence of methyl-end desaturases in invertebrates have been largely disregarded so far, and many trophic ecology studies using FAs as trophic markers still assume that metazoans lack the capacity to endogenously produce LA and ALA, an issue also addressed by Galloway & Budge (2020).

The conversion of LA and ALA into ARA and EPA, respectively, occurs by the sequential reaction of front-end desaturases and elongases. While front-end desaturases introduce a double bond between the pre-existing one and the front-end of the carbon chain, elongases are the critical catalysing enzymes in the two-carbon chain elongation process (Bell & Tocher, 2009). Two possible pathways enabling ARA and EPA biosynthesis are known to exist, which are the so-called "Δ6 pathway" (Δ6 desaturation – elongation – Δ5 desaturation) and the "Δ8 pathway" (elongation – Δ8 desaturation – Δ5 desaturation) (Fig. 1). Similarly, the production of DHA from EPA can be performed via two pathways, namely the "Sprecher pathway" which involves two consecutive elongations and a Δ6 desaturation toward 24:6n-3 followed by a β-oxidation to DHA, and the "Δ4 pathway" involving only one elongation from EPA and one Δ4 desaturation (Fig. 1). The presence and activity of each of the enzymes determine an organism's capacity for LC-PUFA biosynthesis from endogenously produced or dietary obtained FAs (Monroig et al., 2022; Monroig & Kabeya, 2018).

Figure 1 Theoretical polyunsaturated fatty acid biosynthesis pathway in metazoans. Methyl-end desaturase reactions in blue (vertical arrows), front-end desaturase reactions in red (diagonal arrows), and elongase reactions in green (horizontal arrows). Desaturase reactions are further specified by "Δy", with "y" referring to the location of insertion of the double bond counting from the methyl-end of the car(Monroig et al., 2022)*bon chain. β-oxidation reactions are also shown (horizontal reverse arrows) but not included in this study. OA: oleic acid; LA: linoleic acid; ALA: α-linolenic acid; ARA: arachidonic acid; EPA: eicosapentaenoic acid; DHA: docosahexaenoic acid. Adapted from* (Monroig et al., 2022)*.*

Copepods are a globally distributed and highly abundant group of crustaceans that perform pivotal ecological functions at the basis of aquatic food webs (George et al., 2020). They are primary consumers of microalgae and are important prey for higher trophic levels, such as early life-cycle stages of fish (Gee, 1987) to which they provide essential nutrients including LC-PUFAs. Indeed, copepods generally have high levels of LC-PUFAs, particularly DHA, but whether these LC-PUFAs have an exclusive dietary origin or are, to some extent, produced endogenously remains unclear. Dietary studies in which copepods were fed diets lacking LC-PUFAs, or were given diets or specific FAs labelled with stable isotopes, suggest that multiple copepod species have the capacity for endogenous production of LC-PUFAs including DHA from ALA and/or possibly even OA (Arndt & Sommer, 2014; Caramujo et al., 2008; De Troch et al., 2012; Desvilettes et al., 1997; Farkas et al., 1981; Moreno et al., 1979; Nanton & Castell, 1998, 1999; Nielsen et al., 2020b; Titocci & Fink, 2022; Werbrouck et al., 2017). While similar evidence is scarce for other aquatic primary consumers, their potential ability for endogenous LC-PUFA biosynthesis and conversion raises questions about their role and importance in aquatic food webs, especially in the context of future environmental changes.

Recent extensive revisions of the repertoire and functions of desaturases and elongases involved in LC-PUFA biosynthesis of invertebrates illustrate the remarkably high diversity in comparison to vertebrates (Monroig et al., 2022; Monroig & Kabeya, 2018). Among copepods, our knowledge on the LC-PUFA biosynthesis pathways remains fragmentary as only a subset of genes has been scrutinized in few species (Kabeya et al., 2018, 2021). Heterologous expression in a model system such as the yeast *Saccharomyces cerevisiae* is an ideal benchmark method to verify the function of a candidate gene (Monroig et al., 2022). This method can eliminate the possibility of the gene being a defunct pseudogene, and/or that the observed LC-PUFA biosynthesis is performed by microbial activity (Kabeya et al., 2021). While LC-PUFA biosynthesis genes have been identified in harpacticoid, cyclopoid and siphonostomatoid copepods (Amparyup et al., 2022; Boyen et al., 2020; Kabeya et al., 2018, 2021; Lee et al., 2020a, 2020b; Nielsen et al., 2019), functional characterization has only been performed on genes from the parasitic siphonostomatoid *Lepeophtheirus salmonis* (methyl-end desaturases) and the rocky intertidal harpacticoid *Tigriopus californicus* (methyl-end desaturases, front-end desaturases and elongases) (Kabeya et al., 2018, 2021).

While phylogenetic analyses suggest that LC-PUFA elongase and desaturase activity might be common across a diverse range of metazoan taxa, we lack direct empirical evidence to generalize this finding even among closely related species. Therefore, the aim of this work was to perform a phylogenetic exploration of crustacean (mainly copepod) methyl-end desaturases, front-end desaturases and elongases, and clone and functionally characterize a total of eight desaturases and elongases of the benthic harpacticoid copepod *Platychelipus littoralis* (Brady, 1880), using heterologous expression in yeast. The transcriptome of *P. littoralis* has been generated in an earlier study (Boyen et al., 2020). While often disregarded due to their small size and subsequent difficulty to collect, study and cultivate in laboratory environments, harpacticoid copepods play a pivotal role at the algae-animal interface of benthic food webs and thus the overall functioning of marine sediment communities (Hicks & Coull, 1983). Knowing their LC-PUFA biosynthesis capacity will allow us to better understand

the role of not only *P. littoralis* but potentially benthic copepods in general as LC-PUFA providers within the marine ecosystem. *Platychelipus littoralis* was found to have a temperature-mediated capacity for endogenous LC-PUFA biosynthesis (Boyen et al., 2020; Werbrouck et al., 2017; Werbrouck et al., 2016b), yet functional molecular evidence is still lacking. Detailed knowledge of the metabolic pathways of LC-PUFA biosynthesis will allow the use of copepods as model organisms to study the effects of global warming on LC-PUFA-mediated food web interactions.

3.2 Materials and Methods

3.2.1 Protein identification and phylogenetic analysis

To perform the phylogenetic analysis, sequences from various crustacean species were retrieved from NCBI GenBank through BLAST (tblastn), using, as queries, the sequences of the functionally characterized *T. californicus* desaturases and elongases (Kabeya et al., 2018, 2021). Sequences were only selected when they contained the full-length open reading frame (ORF) and their predicted protein sequences contained specific features according to Hashimoto et al. (2008). Briefly, front-end desaturases had to contain three diagnostic histidine boxes (H-box) "HXXXH", "HXXXHH" and "QXXHH" and a heme binding motif (HPGG) in the cytochrome b5 domain. Putative desaturase sequences with the third box "HXXHH" instead of "QXXHH" were not regarded as front-end desaturases based on evidence collected from other crustaceans suggesting these enzymes lack fatty acyl desaturation capacity (Monroig et al., 2022; Monroig & Kabeya, 2018). Methyl-end desaturases had to contain the three H-boxes "HXXXH", "HXXHH" and "HXXHH" and had to lack the cytochrome b5 domain. Fatty acid elongases had to contain the H-box "HXXHH" or "QXXHH" (Boyen et al., 2020; Hashimoto et al., 2008; Kabeya et al., 2021). For *P. littoralis* specifically, sequences were retrieved from the previously assembled transcriptome (NCBI BioProject PRJNA575120). The phylogenetic analysis was completed with the addition of sequences of functionally characterized genes from *T. californicus*, *L. salmonis*, *Platynereis dumerilli*, *Hediste diversicolor,*

Leishmania major (Kabeya et al., 2018, 2020, 2021; Tripodi et al., 2006), as well as human sequences. The deduced protein sequences were aligned using MAFFT v. 7.490 (Katoh & Standley, 2013) using the E-INS-i method. For each gene family, a maximum-likelihood phylogenetic tree was built using RAxML v. 8.2.4 (Stamatakis, 2014) with a GAMMA model of rate heterogeneity, automatic selection of the best protein substitution model (MTZOA for methyl-end desaturases, LG for front-end desaturases and elongases), and 100 bootstrap replicates. The final trees were rooted with an outgroup (*P. dumerilli* and *H. diversicolor* for the methyl-end desaturases and *L. major* for the front-end desaturases) or using midpoint rooting (for the elongases). Trees were visualized and edited with FigTree v. 1.4.3 (http://tree.bio.ed.ac.uk/soft- ware/figtree).

3.2.2 Plasmid construction and transformation in yeast

Platychelipus littoralis adult specimens were collected from the top sediment layer of the Paulina intertidal mudflat (Westerscheldt estuary, The Netherlands; 51°21′ N, 3°43′ E) (Boyen et al., 2020). Total RNA was extracted from 50 pooled individuals using the RNeasy Plus Micro Kit (QIAGEN) following a modified protocol (Boyen et al., 2020). Total RNA quality and quantity were assessed by NanoDrop 2000 spectrophotometer (Thermo Fisher Scientific) and 2100 Bioanalyzer (Agilent Technologies). cDNA was synthesized using the Maxima H Minus First Strand cDNA Synthesis Kit (Thermo Fisher Scientific) with dsDNase treatment to remove potential genomic DNA contamination. The full-length ORF sequences of one methyl-end desaturase, one front-end desaturase and six elongases were amplified by PCR from *P. littoralis* cDNA using high-fidelity Phusion Hot Start II DNA Polymerase (Thermo Fisher Scientific) and primers containing restriction enzyme sites (Table 1). RestrictionMapper (www.restrictionmapper.org) was used to select restriction enzymes which would not cut internally within the corresponding ORF sequence. The calculation of the annealing temperature and GC content (ThermoFisher Scientific Tm Calculator) was done only using the primer sequence part specific to the DNA fragment to be amplified. All PCR runs consisted of an initial denaturation step of 30 s at 98 °C, 35 cycles of 10 s at 98 °C,

30 s at the sequence-specific amplification temperature (Table 1) and 30 s at 72 °C, ending with a final extension step of 10 min at 72 °C. The PCR products were purified with Purelink PCR Purification Kit (Thermo Fisher Scientific) and subsequently digested with the corresponding restriction enzymes (New England Biolabs) (Table 1). The restricted ORF fragments were ligated (T4 DNA ligase, Promega) into a similarly restricted pYES2 yeast expression vector and transformed into One Shot TOP10F´ chemically competent *E. coli* cells. Positive transformant colonies were grown overnight in LB broth containing ampicillin (50 µg/ml). Plasmids were purified with PureLink™ HiPure Plasmid Miniprep Kit, sequenced using T7 forward and CYC1 reverse primers (Macrogen Europe, The Netherlands) and compared with the original sequences from the transcriptome assembly. Concentrations of raw and restricted PCR products, ligated vectors and purified plasmids were all quantified using Qubit 2.0 dsDNA BR Assay Kit (Invitrogen).

Table 1 Original transcript contig (above) and coding sequence (below) NCBI accession numbers, restriction enzymes, sequences and annealing temperatures (TA) of each gene. Restriction sites are underlined.

Gene	Accession numbers	Enzyme	Primer name	Primer sequence (5'-3')	T_A (°C)
ωx	GHXK01184360	*Hind*III	plwxHF	CCC<u>AAGCTT</u>AAAATGTCGTCTAGAAGAAG	56.0
	ON075828	*Xho*I	plwxXR	CCG<u>CTCGAG</u>TCACTTAGACTTTGTATCGC	
fad	GHXK01205503	*Sac*I	plfadSF	CCC<u>GAGCTC</u>ACCATGGATCCCTCAATAGA	59.8
	ON075829	*Xho*I	plfadXR	CCG<u>CTCGAG</u>TTATGACAGAAGCTTGTTGAAG	
elovl1a	GHXK01177303	*Hind*III	ple1aHF	CCC<u>AAGCTT</u>AAGATGAACGTCGTTTCTGAAAAATGG	64.5
	ON075830	*Xho*I	ple1aXR	CCG<u>CTCGAG</u>TCAATGTTGCTTTTTGTCGCTAGA	
elovl1b	GHXK01255463	*Sac*I	ple1bSF	CCC<u>GAGCTC</u>ACCATGGCCACTCAGAA	61.1
	ON075831	*Xho*I	ple1bXR	CCG<u>CTCGAG</u>TCAATTTTCTTTTTTTGCAGCAGA	
elovl1c	GHXK01260983	*Sac*I	ple1cSF	CCC<u>GAGCTC</u>AAAATGAGTGAAACATTTTTGGACGG	61.9
	ON075832	*Xho*I	ple1cXR	CCG<u>CTCGAG</u>TTATGTACTTTTCTTCTTTTTCTGGTTG	
elovl1d	GHXK01228992	*Hind*III	ple1dHF	CCC<u>AAGCTT</u>AACATGCTGGATGTGTTAGTC	57.9
	ON075833	*Xho*I	ple1dXR	CCG<u>CTCGAG</u>TTATGTCACTTTTTTCTTGGAG	
elovl1e	GHXK01223266	*Hind*III	ple1eHF	CCC<u>AAGCTT</u>AGAATGACCAAGTCAGTGATCCC	65.1
	ON075834	*Xba*I	ple1eXbR	CCG<u>TCTAGA</u>TTAGTCCAATTTTGTTGCATTTAAATGCC	
elovl4	GHXK01149108	*Hind*III	ple4HF	CCC<u>AAGCTT</u>ACAATGGTTAGTGAAAATTTATATTCC	59.4
	ON075835	*Xho*I	ple4XR	CCG<u>CTCGAG</u>TCATTTCTTCTTTTTCTGAACAAC	

3.3.3 Functional characterization of *P. littoralis* desaturase and elongase genes

The plasmid constructs containing the ORF sequences of the *P. littoralis* desaturases and elongases were independently transformed into *S. cerevisiae* competent cells (strain INVSc1) using the *S.c.* EasyComp yeast transformation kit (Invitrogen). The recombinant yeast cells were grown on *S. cerevisiae* minimal medium minus uracil (hereafter referred to as "SCMM^{-ura}") agar plates for 3 d at 30 °C, the optimal temperature for growth of *S. cerivisiae*. One individual colony per gene was individually grown in SCMM^{-ura} broth for 48 h at 30 °C to produce a bulk culture with an OD_{600} of 8-10. Subsequently, an appropriate volume of the yeast bulk cultures was diluted to an OD_{600} of 0.4 in 5 ml of SCMM^{-ura} broth contained in a 250 ml Erlenmeyer flask. Each putative PUFA substrate was assayed in independent flasks. The Erlenmeyer flasks were incubated for 4 h at 30 °C under constant shaking (250 rpm) until they reached an OD_{600} of approximately 1. At that point, cultures were supplemented with 25% galactose to induce transgene expression, and one of the putative PUFA substrates as follows. For the methyl-end desaturase, the exogenously supplied PUFA substrates were 18:2n-6, 18:3n-6, 20:2n-6, 20:3n-6, 20:4n-6, 22:4n-6 and 22:5n-6. For the front-end desaturase, the PUFA substrates were 18:3n-3, 18:2n-6, 20:3n-3, 20:2n-6, 20:4n-3, 20:3n-6, 22:5n-3 and 22:4n-6. For the elongases, the PUFA substrates included 18:3n-3, 18:2n-6, 18:4n-3, 18:3n-6, 20:5n-3, 20:4n-6, 22:5n-3 and 22:4n-6. All PUFA substrates were purchased from Nu-Chek Prep, Inc. (Elysian, MN, USA), except 18:4n-3 from Larodan AB (Solna, Sweden) and 20:4n-3 from Cayman Chemicals (Ann Arbor, MI, USA). Each PUFA substrate was supplemented as sodium salts at concentrations of 0.5 mM (C_{18}), 0.75 mM (C_{20}) and 1.0 mM (C_{22}) as uptake efficiency decreases with increasing carbon chain length (Zheng et al., 2009). In addition, we wanted to determine the capacity of the *P. littoralis* methyl-end desaturase and elongases to utilize the yeast endogenous saturated and monounsaturated FAs as substrates. For this, transgenic yeast expressing either the methyl-end desaturase or one of the six elongases were grown in triplicate Erlenmeyer flasks supplemented with 2% galactose but without exogenously added FA substrates, in parallel with a control treatment consisting of

yeast transformed with an empty pYES2 vector (n=3). Yeast cultures were incubated again for 48 h at 30 °C under constant shaking (250 rpm), harvested by centrifugation (2 min, 2000 rpm) and washed twice with double distilled H_2O. Yeast pellets were subsequently homogenized in 8:4:3 (v/v/v) chloroform:methanol:saline solution (0.88% KCl) containing 0.01% (w/v) butylated hydroxytoluene (BHT, Sigma-Aldrich) as antioxidant, and stored at -20 °C under anaerobic conditions for a minimum of 24 h prior to FA analysis.

3.2.4 Fatty acid analysis

Total lipids were extracted from the homogenized yeast samples with 8:4:3 (v/v/v) chloroform:methanol:saline solution (0.88% KCl) according to the Folch method (Folch et al., 1957). Fatty acid methyl esters (FAMEs) were prepared through acid-catalyzed transesterification and subsequently purified by thin-layer chromatography. FAMEs from the desaturase functional assays were analyzed using a Thermo Trace GC Ultra (Thermo Electron Corporation, Waltham, MA, USA) equipped with a fused silica 30 m × 0.25 mm open tubular column (Tracer, TR-WAX (film thickness 0.25 μm); Teknokroma, Spain), coupled to a flame ionization detector. Identification was carried out by comparing the retention times with those from commercial FAME standards. Further confirmation of peaks and analysis of FAMEs from the elongase assays was carried out using an Agilent 6850 GC equipped with a mass spectrometry detector (5975 Series) and a 30 m × 0.25 mm open tubular column (Tracer, DB5-MS (film thickness 0.25 μm); Teknokroma, Spain), and comparing the spectra against those from the NIST library. The conversion efficiency of all assayed *P. littoralis* enzymes toward the exogenously supplied PUFA substrates was calculated as: (all product areas/(all product areas + substrate area)) × 100 (Kabeya et al., 2021).

3.2.5 Statistical analysis

The assays aiming to determine the ability of the *P. littoralis* methyl-end desaturase and elongases toward the yeast endogenous saturated and monounsaturated FAs were run in replicates (n=3) and the FA contents were expressed as mean percentages ±

standard deviation. Homogeneity of variances was checked using Levene's test. The FA profiles of control yeast and yeast expressing the methyl-end desaturase and the elongases were compared, and differences were statistically tested using Student's t-test for the methyl-end desaturase and Dunnett's multiple comparisons test for the elongases with p ≤ 0.05 indicating statistical significance. All statistical analyses were conducted in R v.4.0.2 (R Core Team, 2020).

3.3 Results

3.3.1 Protein identification and phylogenetic inference

We constructed three phylogenetic trees of the metazoan methyl-end desaturases, front-end desaturases and elongases respectively (Fig. 2). For each gene family, we found multiple subclades containing one or more sequences from different species. Each tree contains multiple well supported clades, however certain clades are not strongly supported. For *P. littoralis* specifically, we identified one putative methyl-end desaturase, one putative front-end desaturase and seven putative elongases. The *P. littoralis* methyl-end desaturase (ON075828) has the three specific H-boxes and lacks a cytochrome b5 domain. It clusters together with other harpacticoid sequences, including the functionally characterized *T. californicus* methyl-end desaturase "*ωx2*" with Δ15/Δ17/Δ19 activities (Fig. 2a). The front-end desaturase (ON075829) remained unnoticed in the initial phylogenetic analysis since its Pfam domain *Cyt-b5* (PF00173) had an E-score of 6.1E-05 and therefore did not pass the criteria at that time (Boyen et al., 2020). It was placed in the copepod-specific clade previously identified (Kabeya et al., 2021), with its closest functionally characterized sequence being the *T. californicus* Δ4 desaturase "*Fed2*" (Fig. 2b). In addition, we found a front-end desaturase in a transcriptome of the decapod *Eurypanopeus depressus* (GFJG01059607), which clustered inside the copepod-specific clade and contained the correct third histidine box "QIEHH" as opposed to previously identified decapod front-end desaturase sequences.

Figure 2 Maximum-likelihood phylogenetic trees of (a) methyl-end desaturases (blue), (b) front-end desaturases (red), and (c) elongases (green). Values below branches show bootstrap support after 100 RAxML iterations. P. littoralis sequences identified in this study are highlighted in bold. The different functions (when characterized) of each gene are indicated in unique colour shades, and are represented as desaturation activities ("Δ") for the methyl-end (a) and front-end (b) desaturases, and elongated PUFA substrates for the elongases (c).

One *P. littoralis* elongase (ON075836) aligned closely with the vertebrate elovl3/elovl6 subfamily, which is specifically known to elongate saturated FAs, and was therefore not included in the subsequent functional characterization. Another *P. littoralis* elongase (ON075835) formed a clade with the human and *T. californicus* elovl4 sequences. The five other *P. littoralis* elongase sequences all belonged within the Pancrustacea-specific elovl1/7-like clade identified earlier (Boyen et al., 2020; Kabeya et al., 2021) (Fig. 2c). Therefore, we subsequently labelled them elovl1a-e. *Platychelipus littoralis* elovl1a, elovl1b and elovl1e closely aligned with the functionally characterized *T. californicus* "*elo1*", "*elo5*" and "*elo2*" respectively, as well as the corresponding *Tigriopus japonicus* sequences. *Platychelipus littoralis* elovl1d does not have a direct relationship with any other copepod elongases, though it aligned most closely with the *P. littoralis* elovl1a/*T. californicus* "*elo1*" clade. The *P. littoralis* elovl1c did not match with any functionally characterized *T. californicus* elongase, but did align with elongase sequences from *L. salmonis, Caligus rogercresseyi* and *Caligus clemensi* (all siphonostomatoids). Remarkably, all sequences from the two subclades containing *P. littoralis* elovl1c (ON075832) and elovl1e (ON075834) contained a histidine box "QXXHH" instead of the typical "HXXHH" observed in other FA elongases.

3.3.2 Functional characterization

The functions of all putative desaturases and elongases identified from *P. littoralis,* except for elovl3/6, were characterized in yeast by heterologous expression of the corresponding coding region and growing in the presence of potential PUFA substrates. The FA profiles of the transgenic yeast expressing the *P. littoralis* methyl-end desaturase and grown in the presence of exogenously added C_{18}, C_{20} and C_{22} n-6 PUFA substrates showed n-3 desaturation products denoting that this enzyme has $\Delta15$, $\Delta17$ and $\Delta19$ desaturation capacity, respectively (Table 2). No $\Delta12$ desaturation capacity was detected for the *P. littoralis* methyl-end desaturase, since levels of the $\Delta12$ desaturation product 18:2n-6 were not statistically different when compared with yeast transformed with the empty pYES2 vector (Student's t-test, p>0.05) (Supp. Table 1).

Table 2 Substrate conversions of the transgenic yeast expressing the P. littoralis methyl-end desaturase. The results are presented as a percentage of the fatty acid (FA) substrate converted into the corresponding desaturated product.

FA substrate	Product	Conversion (%)	Activity
18:2n-6	18:3n-3	29.6	Δ15
18:3n-6	18:4n-3	25.7	Δ15
20:2n-6	20:3n-3	10.7	Δ17
20:3n-6	20:4n-3	13.7	Δ17
20:4n-6	20:5n-3	57.0	Δ17
22:4n-6	22:5n-3	13.4	Δ19
22:5n-6	22:6n-3	7.4	Δ19

Functional characterization assays of the *P. littoralis* front-end desaturase showed this enzyme has Δ4 desaturation capacity since transgenic yeast expressing its coding region were able to convert 22:5n-3 and 22:4n-6 into 22:6n-3 and 22:5n-6, respectively (Table 3). No activity toward 18:3n-3, 18:2n-6, 20:3n-3, 20:2n-6, 20:4n-3 and 20:3n-6 was detected, confirming that the *P. littoralis* front-end desaturase does not have Δ5, Δ6 or Δ8 desaturation capacities (Table 3).

Table 3 Substrate conversions of the transgenic yeast expressing the P. littoralis front-end desaturase. The results are presented as a percentage of the fatty acid (FA) substrate converted into the corresponding desaturated product.

FA substrate	Product	Conversion (%)	Activity
18:3n-3	18:4n-3	-	Δ6
18:2n-6	18:3n-6	-	Δ6
20:3n-3	20:4n-3	-	Δ8
20:2n-6	20:3n-6	-	Δ8
20:4n-3	20:5n-3	-	Δ5
20:3n-6	20:4n-6	-	Δ5
22:5n-3	22:6n-3	7.8	Δ4
22:4n-6	22:5n-6	7.3	Δ4

- : not detected (<0.1%).

The capacity of the *P. littoralis* elongases to act toward saturated FAs was assessed by comparing the FA profiles of yeast transformed with the empty vector with those of yeast each expressing one of the six elongases under study (Fig. 3, Supp. Table 2). Yeast expressing *P. littoralis* elovl4 showed a significant increase of 20:0 and production of 28:0 and 30:0 (Dunnett's test, $p < 0.05$), while levels of other FAs were not different from those of the control yeast. Yeast expressing *P. littoralis* elovl1a showed significantly lower levels of 16:0, 17:0, 18:0 and 20:0 and higher levels of 22:0, 24:0 and 26:0

compared to the control yeast. Expression of *P. littoralis* elovl1d resulted in significantly reduced levels of 16:0 and 18:0 and increased levels of 26:0, 28:0 and 30:0, while expression of *P. littoralis* elovl1e resulted in significantly reduced levels of 16:0 and increased levels of 26:0. *Platychelipus littoralis* elovl1b and elovl1c did not show any capacity for elongation of yeast endogenous FAs (Dunnett's test, $p > 0.05$) (Fig. 3, Supp. Table 2).

The activities of the *P. littoralis* elongases toward PUFA substrates were assessed by growing transgenic yeast expressing each elongase in the presence of exogenously added PUFA substrates. *Platychelipus littoralis* elovl4 was able to elongate all of the supplied substrates, with additional elongation of the product 24:5n-3 toward 26:5n-3 (Table 4). *Platychelipus littoralis* elovl1a was able to elongate all of the supplied substrates except 18:2n-6 (Table 4). The *P. littoralis* elovl1b had a relatively low elongation capacity toward C_{18} substrates and particularly high elongation capacity toward C_{20} substrates, with up to 84.7% and 57.2% conversion of 20:5n-3 (EPA) and 20:4n-6 (ARA) toward 22:5n-3 and 22:5n-3, respectively, yet no detectable activity toward C_{22} substrates (Table 4). Similarly, *P. littoralis* elovl1c and elovl1e had elongation capacity of C_{18} and C_{20} substrates, but no detectable activity toward C_{22} substrates (Table 4). While *P. littoralis* elovl1d was able to elongate C_{18} and C_{20} substrates to some extent, it was found to have particularly high elongation capacity of C_{22} substrates, enabling the production of polyenes up to C_{28} via stepwise elongations from exogenously added substrates (Table 4).

Table 4 Substrate conversions of the transgenic yeast expressing the P. littoralis elongases. The results are presented as a percentage of the fatty acid (FA) substrate converted into the corresponding elongated product.

FA substrate	Product	Conversion (%)						Activity
		elovl4	elovl1a	elovl1b	elovl1c	elovl1d	elovl1e	
18:3n-3	20:3n-3	5.9	0.5	2.2	14.2	1.2	13.2	$C_{18} \rightarrow C_{20}$
	22:3n-3	-	2.6	-	0.2	6.6	0.1	$C_{20} \rightarrow C_{22}$
18:2n-6	20:2n-6	2.2	-	0.3	3.0	0.3	1.6	$C_{18} \rightarrow C_{20}$
	22:2n-6	-	-	-	-	9.2	3.0	$C_{20} \rightarrow C_{22}$
18:4n-3	20:4n-3	3.7	2.9	1.5	11.0	3.7	10.6	$C_{18} \rightarrow C_{20}$
	22:4n-3	2.0	1.2	-	-	3.1	0.8	$C_{20} \rightarrow C_{22}$
	24:4n-3	-	-	-	-	12.1	-	$C_{22} \rightarrow C_{24}$
18:3n-6	20:3n-6	2.5	2.9	1.0	6.4	4.9	4.7	$C_{18} \rightarrow C_{20}$
	22:3n-6	3.0	1.0	0.8	0.5	2.7	0.5	$C_{20} \rightarrow C_{22}$
	24:4n-3	-	-	-	-	40.9	-	$C_{22} \rightarrow C_{24}$
20:5n-3	22:5n-3	8.3	4.6	84.7	0.7	4.3	5.2	$C_{20} \rightarrow C_{22}$
	24:5n-3	4.4	3.3	-	-	20.4	-	$C_{22} \rightarrow C_{24}$
20:4n-6	22:4n-6	6.0	2.3	57.2	0.1	4.0	0.4	$C_{20} \rightarrow C_{22}$
	24:4n-6	4.1	4.0	-	-	55.6	-	$C_{22} \rightarrow C_{24}$
	26:4n-6	-	-	-	-	57.5	-	$C_{24} \rightarrow C_{26}$
	28:4n-6	-	-	-	-	9.3	-	$C_{26} \rightarrow C_{28}$
22:5n-3	24:5n-3	3.5	2.4	-	-	14.5	-	$C_{22} \rightarrow C_{24}$
	26:5n-3	8.3	-	-	-	18.7	-	$C_{24} \rightarrow C_{26}$
	28:5n-3	-	-	-	-	9.9	-	$C_{26} \rightarrow C_{28}$
22:4n-6	24:4n-6	1.7	0.9	-	-	18.7	-	$C_{22} \rightarrow C_{24}$
	26:4n-6	-	-	-	-	58.8	-	$C_{24} \rightarrow C_{26}$
	28:4n-6	-	-	-	-	13.1	-	$C_{26} \rightarrow C_{28}$

- : not detected (<0.1%).
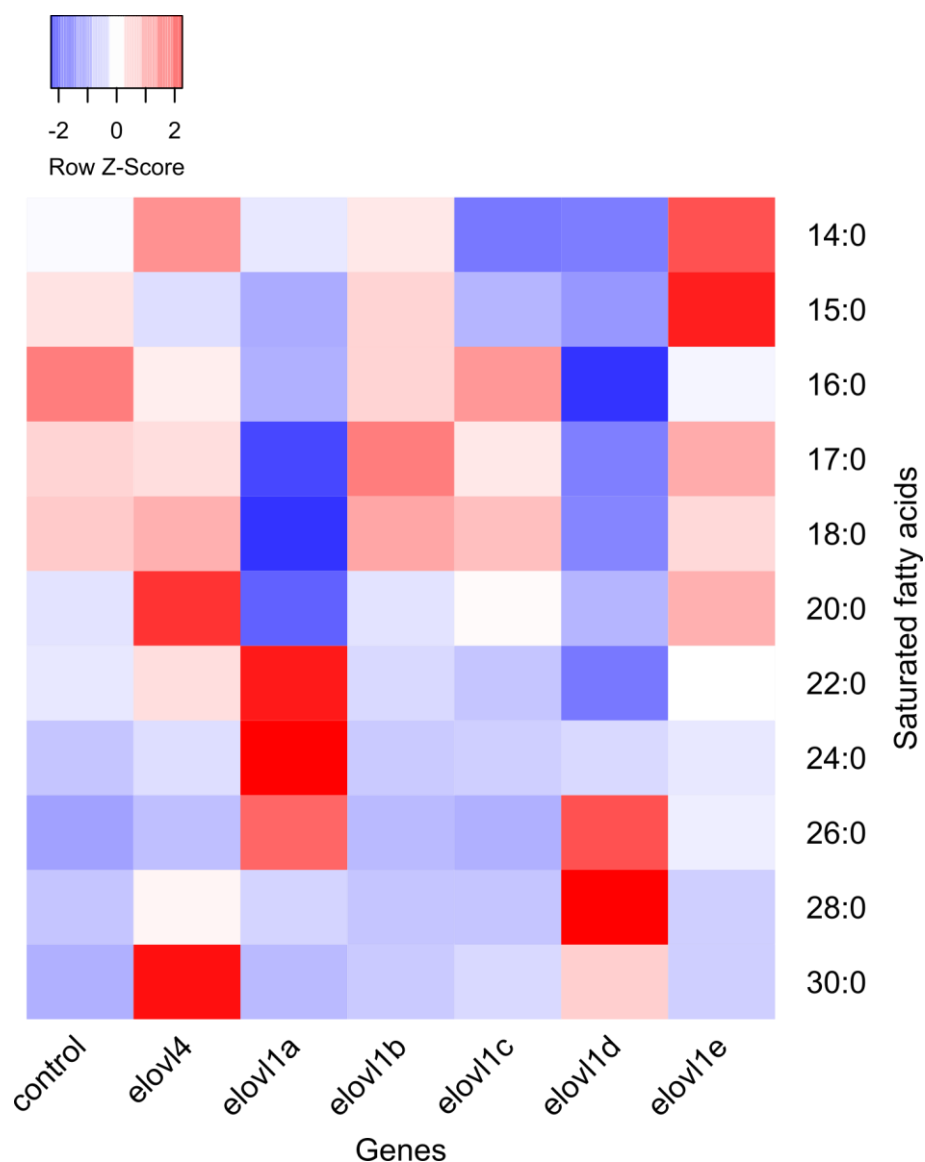
Figure 3 Heatmap illustrating mean endogenous saturated fatty acid levels of the transgenic yeast expressing the P. littoralis elongases as well as the control yeast (n=3). Fatty acids percentages (%) were scaled to z-scores per fatty acid, with blue indicating lower and red indicating higher than average percentages. Data used to generate this heatmap can be found in Supplementary Table 2.

3.4 Discussion

In this study, we identified nine *P. littoralis* desaturases and elongases and demonstrated the functions of eight of them. We found that these enzymes exhibited highly diverse enzymatic capacities enabling biosynthesis of not only LC-PUFAs but also very long-chain FAs (up to C_{30}). We found one *P. littoralis* methyl-end desaturase with a multifunctional Δ15, Δ17 and Δ19 desaturation capacity similar to the

T. californicus "ωx2" and *L. salmonis* "ω3" orthologs (Kabeya et al., 2018, 2021). Additionally, we found that the *P. littoralis* methyl-end desaturase is able to convert both 22:4n-6 and 22:5n-6 into 22:5n-3 and 22:6n-3 (DHA) respectively. This contrasts with the *T. californicus* "ωx2" methyl-end desaturase, which is only able to desaturate 22:4n-6 but not 22:5n-6 (Kabeya et al., 2021). While *T. californicus, T. japonicus* and *L. salmonis* have been found to possess two methyl-end desaturases (Kabeya et al., 2018, 2021), other copepods such as *C. rogercresseyi, Eucyclops serrulatus, Paracyclopina nana, Tigriopus kingsejongensis* and now also the benthic harpacticoid *P. littoralis* seem to possess only one (Fig. 2). While improved transcriptomic resources from the latter species might reveal a second methyl-end desaturase, a broader investigation including genomic data from more copepod species could disclose whether one or two methyl-end desaturases is the dominating trait among copepods. If assumed that *P. littoralis* only contains one sole methyl-end desaturase lacking Δ12 desaturation capacity, this implies that *P. littoralis* is not able to convert OA into LA and therefore does not have the capacity for complete *de novo* LC-PUFA biosynthesis from endogenously produced saturated and monounsaturated FAs. Such capacity has been reported to exist in specific species of Cnidaria, Mollusca, Annelida, Rotifera and Arthropoda, including the copepods *L. salmonis* and *T. californicus* (Kabeya et al., 2018, 2020, 2021). On the other hand, our results show that the *P. littoralis* methyl-end desaturase has Δ17 and Δ19 desaturation capacity, including a capacity for biosynthesis of EPA and DHA from ARA and 22:5n-6, respectively. This Δ17 and Δ19 desaturation of omega-6 FAs could be an important alternative pathway toward omega-3 LC-PUFAs, enabling their production from an increased variety of dietary precursors.

The copepod front-end desaturase gene family is distinct from other metazoan front-end desaturase clades (Kabeya et al., 2021; Lee et al., 2020a; Nielsen et al., 2019). It is more closely related to protists and algae such as *Leishmania major*, which was previously hypothesized to be a result of horizontal gene transfer (Kabeya et al., 2021). We found that the *P. littoralis* front-end desaturase had a single Δ4 desaturation capacity enabling the production of 22:5n-6 and, more importantly, DHA. This is the

second Δ4 desaturase found in harpacticoids, further supporting the hypothesis that they use the so-called "Δ4 pathway" as opposed to the Sprecher pathway to synthesize DHA (Kabeya et al., 2021). Functional characterization of more front-end desaturases will allow us to verify the potential universal presence of the Δ4 pathway in other copepod orders. The *P. littoralis* Δ4 desaturase is phylogenetically placed in the previously discovered copepod-specific clade, within a subclade that also contains the *T. californicus* Δ4 desaturase. The four other *T. californicus* front-end desaturases all cluster within a second subclade mostly containing harpacticoid species (*Tigriopus* and *Tisbe*), further speculating that more *P. littoralis* front-end desaturases with Δ5, Δ6 or Δ8 desaturation capacity remain to be discovered. While our phylogenetic inference of the front-end desaturases is similar to Nielsen et al. (2019), the phylogenetic tree of Kabeya et al. (2021) does not separate the *T. californicus* Δ4 desaturase "*Fed2*" from the other sequences. Therefore, a more substantial phylogenetic analysis involving even more putative copepod sequences coupled with additional functional characterization of front-end desaturases from other copepod species is essential to clarify the evolution and diversification of this gene family, including its potential origin from horizontal gene transfer (Kabeya et al., 2021).

The phylogenetic analysis of the *P. littoralis* elongases indicated extensive gene differentiation prior to copepod species differentiation. A large expansion of the elongase gene family was found in the harpacticoid genus *Tigriopus* as well (Kabeya et al., 2021; Lee et al., 2020a). Two *P. littoralis* elongases each clustered with the known "vertebrate" elovl3/6 and elovl4 clades, with *P. littoralis* elovl4 having a rather general elongation capacity similar to the *T. californicus* ortholog. Five *P. littoralis* elongases (elovl1a-e) clustered within the recently discovered Pancrustacea-specific elovl1/7-like clade (Ribes-Navarro et al., 2021), and the detected strong elongation capacities of the tested elongases further emphasize the importance of this clade. The results from *P. littoralis* elovl1c and elovl1e as well as *T. californicus* "elo2" show that elongases with a "QXXHH" histidine box instead of the usual "HXXHH" histidine box can still exhibit elongation capacities. While elovl1c and elovl1d do not have *T. californicus* orthologs,

P. littoralis elovl1b and elovl1e mirrored the C_{18} and C_{20} elongation capacities of their functionally characterized *T. californicus* orthologs "elo5" and "elo2" (Kabeya et al., 2021). Furthermore, while *P. littoralis* elovl1a matched its *T. californicus* ortholog "elo1" in its ability to elongate all C_{18} and C_{20} substrates except 18:2n-6, it was additionally able to elongate C_{22} substrates toward C_{24} products. We found a combination of general (elovl4) and specific (elovl1b and elovl1d) elongases, illustrating a large functional diversity. We acknowledge that cautious interpretation of these data is warranted as heterologous expression of single genes in a yeast system - while being a very robust system to establish the substrate specificities of the assayed enzymes - does not necessarily mirror the extent to which that enzyme is active in a more complex multicellular *in vivo* scenario where numerous competing enzymes, regulatory mechanisms (e.g. via transcription factors or epigenetic signals) and environmental drivers interact (Monroig et al., 2022; Xie et al., 2021).

Overall, our results show that gene family expansion can lead to an improved elongation capacity. The gene copy number increase of the elovl1/7-like elongase family found in *P. littoralis* and other harpacticoids can be considered an important evolutionary response enabling them to synthesize their well-documented high levels of LC-PUFAs, e.g. when compared to calanoids (Twining et al., 2020). Additionally, having multiple gene copies could lead to certain copies becoming tissue- or development stage-specific, or acquiring substrate-specific enzymatic functions, as seen in *P. littoralis* elovl1a (selective elongation of omega-3 instead of omega-6 substrates), and previously demonstrated in vertebrates (Ishikawa et al., 2019). Understanding the gene family diversity of these harpacticoids will help us to better understand the adaptions of copepods within their nutritional landscape. This could be an important driver of evolutionary divergence and copepod diversity, as observed in other species (Ishikawa et al., 2019, 2021, 2022; Twining et al., 2021).

While PUFA elongases have been successfully functionally characterized in other crustacean lineages such as decapods, branchiopods and amphipods (Mah et al., 2019;

Ribes-Navarro et al., 2021; Sun et al., 2020; Ting et al., 2020), the occurrence and functionality of methyl-end and front-end desaturases in these lineages remains highly questionable (Chen et al., 2017; Kabeya et al., 2021; Lin et al., 2017; Monroig & Kabeya, 2018; Nielsen et al., 2019; Ting et al., 2021; Wu et al., 2018; Yang et al., 2013). In our phylogenetic study, we detected a putative front-end desaturase in a transcriptome of the decapod *Eurypanopeus depressus* clustering together with the *T. californicus* Δ5 front-end desaturase "*Fed5*" with high bootstrap support (86%). Importantly, the *E. depressus* putative front-end desaturase identified in the present study has all correct signatures including the three H-boxes "HXXXH", "HXXXHH" and "QXXHH" and a heme binding motif (HPGG) in the cytochrome b5 domain (Hashimoto et al., 2008). Assuming this was not due to contamination during RNA sequencing, the *E. depressus* putative front-end desaturase could be the first report of this type of LC-PUFA biosynthesizing enzymes in decapods. Further functional assays will be required to test this hypothesis.

3.5 Conclusion

The present study demonstrates that the benthic copepod *P. littoralis* has the genes for biosynthesis of EPA from ARA (using its Δ15/Δ17/Δ19 methyl-end desaturase), as well as the synthesis of DHA from either EPA (using its elovl1b elongase and its Δ4 front-end desaturase) or 22:5n-6 (using its methyl-end desaturase). However, due to the lack of a Δ12 methyl-end desaturase and Δ5, Δ6 or Δ8 front-end desaturases, we could not confirm the capacity for full *de novo* endogenous LC-PUFA synthesis from MUFAs or short-chain PUFAs, as found in *T. californicus* (Kabeya et al., 2021). Since *P. littoralis* was shown to synthesize DHA from stable-isotope labelled diets containing high amounts of ALA and no LC-PUFAs (Werbrouck et al., 2017), at least enzymes with Δ5, Δ6 or Δ8 desaturation activity should theoretically be present but remain yet undetected.

Thus, copepods such as *P. littoralis* and *T. californicus* could play an important role as LC-PUFA producers in marine and estuarine food webs. Endogenous biosynthesis of EPA and DHA by primary consumers - even when synthesized from other LC-PUFAs

such as ARA as evidenced here - has large-scale implications for global food webs. In aquatic ecosystems, where LC-PUFA production by microalgae is expected to decrease due to climate change, LC-PUFA production by primary consumers could potentially still provide secondary and tertiary consumers with their required LC-PUFA levels (Závorka et al., 2021). Future research should examine a number of impacts and consequences resulting from this observation. First, this biosynthetic capacity in benthic and intertidal harpacticoids is unlikely to be representative for other copepod orders, such as pelagic calanoids, freshwater cyclopoids or parasitic siphonostomatoids, or even other primary consumers. Therefore, absolute quantities of LC-PUFA production in different taxa should be calculated and an assessment should be made whether this could significantly contribute to overall LC-PUFA biomass worldwide. Second, in a warming ocean, copepods not only face declining LC-PUFA from their diet, but also face climate change effects directly. Direct negative effects of ocean warming on LC-PUFA content and production have been demonstrated in *P. littoralis* (Boyen et al., 2020; Sahota et al., 2022; Werbrouck et al., 2017) and other primary consumers (Lee et al., 2017a, 2022a; Masclaux et al., 2012). These impacts should be considered, as they can severely limit the consumer's biosynthesis ability (when present) to make up for a reduced dietary LC-PUFA provision due to climate change. Third, endogenous LC-PUFA synthesis means facing higher metabolic costs, and the potentially associated reduced fitness should be accounted for as well. Finally, studies using FAs as biomarkers should integrate consumer FA metabolism into their considerations. For instance, Jardine et al. (2020) calculated FA regression equations and used those to correct for trophic modification. Updated knowledge on specific conversion capacities of certain species as well as controlled feeding experiments can further improve future models.

Author contributions

Jens Boyen, Naoki Kabeya, Óscar Monroig, Juan Carlos Navarro and Marleen De Troch conceptualized the study. Jens Boyen, Naoki Kabeya, Óscar Monroig and Pascal I.

Hablützel performed the phylogenetic analysis. Jens Boyen and Annelien Rigaux constructed the plasmids. Jens Boyen, Alberto Ribes- Navarro, Óscar Monroig and Juan Carlos Navarro performed the functional assays and fatty acid analysis. Jens Boyen performed the statistical analysis and prepared the initial version of the manuscript. All authors assisted in the interpretation of the results and the revision of the manuscript.

Conflict of interest

The authors have no conflict of interest to declare.

Data availability statement

All isolated sequences from *P. littoralis* in the present study were deposited at NCBI GenBank with the accession numbers ON075828 to ON075835.

Benefit-sharing statement

There are no benefits outlined in the Nagoya protocol associated with this study to report.

CHAPTER 4

MULTIPLE CLIMATE DRIVERS INTERACTIVELY AFFECT BIOSYNTHESIS OF POLYUNSATURATED FATTY ACIDS IN THE BENTHIC HARPACTICOID COPEPOD *PLATYCHELIPUS LITTORALIS*

Boyen Jens[1], Rodríguez María T.[1], Vlaeminck Bruno[1], Fink Patrick[3,4,5], Hablützel Pascal I.[6,7], De Troch Marleen[1]

[1] Marine Biology, Department of Biology, Ghent University, Ghent, Belgium

[2] Department of River Ecology, Helmholtz Centre for Environmental Research - UFZ, Magdeburg, Germany

[3] Department of Aquatic Ecosystem Analysis and Management, Helmholtz Centre for Environmental Research - UFZ, Magdeburg, Germany

[4] Aquatic Chemical Ecology, Institute for Zoology, University of Cologne, Cologne, Germany

[5] Flanders Marine Institute, Ostend, Belgium

[6] Biology Department, Vrije Universiteit Brussel, Brussels, Belgium

Keywords: ocean warming, ocean acidification, polyunsaturated fatty acid biosynthesis, copepods, microalgae, multifactorial experiments

Abstract

Excess greenhouse gas emissions and the resulting global warming and ocean acidification heavily impacts marine organisms and their functioning. One major consequence is the reduction in long-chain polyunsaturated fatty acid (LC-PUFA) production by marine microalgae due to ocean warming. Copepods, as primary consumers of microalgae, have been found to possess a unique capacity for endogenous LC-PUFA biosynthesis, and thus might be able to cope with a reduced dietary LC-PUFA availability. However, this LC-PUFA biosynthesis mechanism may also be itself negatively impacted by changes in oceanographic conditions. In this study, we performed a laboratory experiment to assess the interactive effects of two projected direct (ocean warming of +3 °C and ocean acidification of -0.4 pH) and one indirect (dietary LC-PUFA deficiency) climate drivers on the fatty acid composition and LC-PUFA biosynthesis (measured by quantitative RT-PCR) of the benthic harpacticoid copepod *Platychelipus littoralis* (Brady, 1880), and hypothesized increased LC-PUFA biosynthesis for all three drivers. We found that when exposed to multiple stressors, the lipid profile of copepods contained fatty acids with shorter chains and fewer unsaturations. Specifically, copepods were able to maintain the relative concentration of the physiologically important LC-PUFA docosahexaenoic acid (DHA) at base-line levels on a LC-PUFA deficient diet at contemporary temperatures, but DHA concentrations dropped significantly when exposed to higher temperatures. Similarly, expression of the DHA biosynthesis genes fed and elovl1a increased to compensate with dietary LC-PUFA deficiency, but did not exceed base-line levels when the copepods were simultaneously exposed to ocean acidification. The expression of the front-end desaturase and multiple elongases was correlated positively with concentrations of C_{18} precursors and negatively with those of LC-PUFAs such as DHA, further proving their role as LC-PUFA biosynthesis enzymes. Overall, our findings suggest that ocean warming and acidification may limit the capacity of benthic copepods to biosynthesize their own LC-PUFAs when dietary inputs are disrupted, impairing their contribution towards global LC-PUFA availability for higher trophic levels.

4.1 Introduction

There is a strong scientific consensus that global climate change is threatening coastal marine species and ecosystems (Doney et al., 2012; Harley et al., 2006). Increasing greenhouse gas (GHG) emissions cause unprecedented rapid changes in oceanographic conditions such as ocean warming (OW) and ocean acidification (OA; increased absorption of atmospheric CO_2 leading to a pH decrease). Under the Shared Socioeconomic Pathway 5 (SSP5) high GHG emissions scenario, projected global mean sea surface temperature (SST) increase is $+3.47 \pm 0.78$ °C from 1870-1899 to 2080-2099, while global mean surface ocean pH is projected to decline by -0.44 ± 0.005 (Kwiatkowski et al., 2020). These changes affect the physiological performance of marine organisms (Pörtner & Farrell, 2008). It further impacts their fitness and functional roles and consequently triggers potentially adverse changes in community composition and overall ecosystem functioning (Gattuso et al., 2015; Van Colen et al., 2020). Many biological responses to climate change are not well characterized yet, often because they are dependent on complex interactions of multiple effects and require a variety of strategic experimental approaches (Boyd et al., 2018; Piggott et al., 2015; Riebesell & Gattuso, 2015).

Anthropogenic global change is predicted to reduce the production of long-chain (C_{20}-C_{24}) polyunsaturated fatty acids (LC-PUFAs) by phytoplankton such as chlorophytes and diatoms (Hixson & Arts, 2016; Tan et al., 2022). LC-PUFAs, for instance eicosapentaenoic acid (EPA, 20:5n-3), and docosahexaenoic acid (DHA, 22:6n-3), are key nutrients providing a number of structural, physiological and energy-related functions for aquatic and terrestrial organisms, thereby influencing fitness, growth and reproduction (de Carvalho & Caramujo, 2018). Near-future OW is predicted to decrease the proportion of omega-3 LC-PUFAs and increase omega-6 LC-PUFAs and saturated fatty acids (SFAs) in microalgae (Hixson & Arts, 2016; Holm et al., 2022). At increased temperatures, phospholipids with less unsaturated fatty acids (FAs) are preferentially retained to maintain membrane fluidity (a process known as homeoviscous adaptation)

(Sinensky, 1974) and LC-PUFAs are relatively more prone to oxidation (Hixson & Arts, 2016). OA is also suggested to negatively affect PUFAs in microalgae (Bermúdez et al., 2016; Marmillot et al., 2020; Rossoll et al., 2012), yet not all studies confirm this (Leu et al., 2013). Moreover, changes in phytoplankton community composition and declining net primary production could even further impair global LC-PUFA levels (Bi et al., 2021; Kwiatkowski et al., 2020; Taucher et al., 2022) which is estimated to have profound negative impacts on higher trophic levels such as zooplankton, fish and humans (Colombo et al., 2020; Jin et al., 2020). In turn, reduced dietary LC-PUFA availability affecting neurophysiological and behavioral aspects of consumers could lead to shifts in trophic interactions and community composition, further disrupting global LC-PUFA supplies (Pilecky et al., 2021).

Many consumers however are at least to some extent able to convert dietary obtained PUFAs into longer, more unsaturated FAs, using a series of front-end desaturase and elongase enzymes, which introduce a double bond or add two C-atoms to the FA chain, respectively (Monroig et al., 2022). Certain animals, mainly marine primary consumers such as copepods, annelids, rotifers and nematodes, even have the potential for full endogenous *de novo* PUFA biosynthesis due to the presence of methyl-end desaturase enzymes (Kabeya et al., 2018). However, the contribution of this endogenous synthesis to total LC-PUFA provision remains unclear. Moreover, environmental pressures such as temperature, salinity, pressure, pH/pCO^2 and food quality and quantity, directly affect LC-PUFA levels and biosynthesis within aquatic consumers as well (Anacleto et al., 2014; Ericson et al., 2019; Y. Gao et al., 2018; Lee et al., 2018, 2022a; Madeira et al., 2021; Pajand et al., 2022; Schlechtriem et al., 2006). As a result, the total amount of LC-PUFAs in primary consumers is likely affected by a combination of multiple direct (on the consumer itself) and indirect (on its diet) environmental effects (Alma et al., 2020; Fernandes et al., 2021; Rossoll et al., 2012; Valles-Regino et al., 2015).

Copepods are small crustaceans and key primary consumers in aquatic environments, as they provide an energetic link between primary producers and higher trophic levels

such as fish (George et al., 2020). They occupy a wide range of habitats, including pelagic, benthic, freshwater, epiphytic and parasitic lifestyles, which in turn has led to a wide diversity of nutritional strategies (Huys & Boxshall, 1991). Currently, only little research has been performed on how copepod LC-PUFA levels and biosynthesis are influenced by diet (Lee et al., 2020b), OW (Lee et al., 2017a; Pond et al., 2014), or OA (Almén et al., 2016; Bermúdez et al., 2016; Thor et al., 2022), and even fewer on their interactive effects (Garzke et al., 2016; Rossoll et al., 2012).

A copepod species that has been studied extensively as of late is the harpacticoid copepod *Platychelipus littoralis* (Brady, 1880; Laophontidae). This species is a dominant (epi)benthic inhabitant of Northeast Atlantic intertidal and estuarine mudflats (Barnett, 1968). It has a restricted mobility (Barnett, 1966), and therefore needs to be able to quickly acclimatize to stochastic local environmental conditions in the intertidal. Recent work using isotopic labelled diets and compound-specific stable isotope analysis have shown that *P. littoralis* has some – albeit potentially modest – capacity for LC-PUFA biosynthesis and that this biosynthesis mechanism is influenced by both diet and temperature (Sahota et al., 2022; Werbrouck et al., 2017).

In this species, eight PUFA biosynthesis enzymes were identified and functionally characterized (Boyen et al., 2023). These enzymes are: one Δ15/17/19 methyl-end desaturase converting n-6 PUFAs in n-3 PUFAs, one Δ4 front-end desaturase converting 22:5n-3 in 22:6n-3 and 22:4n-6 in 22:5n-6, and six FA elongases (elovl) with rather general (elovl1a and elovl4) or more specific (elovl1b, elovl1c, elovl1d and elovl1e) substrate preferences (Boyen et al., 2023). Other participating enzymes are elovl6, which was phylogenetically identified but not functionally characterized (Boyen et al., 2023), and Δ9 stearoyl-coenzyme A desaturase (scd), which is responsible for the first desaturation in the PUFA biosynthesis pathway, converting 18:0 in oleic acid (18:1n-9) (Monroig et al., 2022). While previous work found diet and temperature effects on the FA levels, no significant differential expression of the FA biosynthesis genes was detected using RNA sequencing (Boyen et al., 2020).

In this study we aimed to evaluate the effect of two direct – OW and OA – and one indirect – dietary LC-PUFA deficiency – climate change drivers as well as their interactions on both the FA composition and PUFA biosynthesis gene expression of *P. littoralis*. We applied quantitative reverse transcription PCR (qPCR) to the 10 *P. littoralis* genes mentioned above. We hypothesize that while all three future conditions (dietary LC-PUFA deficiency, OW and OA) negatively impact copepod LC-PUFA levels, the copepods' biosynthetic capacity will be able to counteract these impacts, allowing *P. littoralis* to maintain high LC-PUFA levels (Boyen et al., 2020).

4.2 Materials and Methods

4.2.1 Multiple driver experiment

Platychelipus littoralis specimens were collected at low tide from the top sediment layer of the Paulina intertidal mudflat (Westerscheldt estuary, The Netherlands; 51°210 N, 3°430 E) in August 2019 (SST: 19.9 °C; salinity: 29.0). The sediment was sieved through a 250 µm mesh, and adult individuals were collected using a glass Pasteur pipette under a Wild Heerbrugg M5 stereomicroscope. Copepods were transferred to Petri dishes with autoclaved and filtered (3 µm; Whatman Grade 6) natural sea water (FNSW) and kept overnight to allow gut clearance prior to the start of the experiment. The antibiotic streptomycin (18 mg l^{-1}, Sigma-Aldrich) was added during this overnight period to temporarily suppress bacterial growth. Additionally, four samples of 40 copepods each were stored at -80 °C to analyze the FA composition of the natural population. The LC-PUFA rich diatom *Nitzschia* sp. A.H. Hassall, 1845 (DCG 0421) was selected as a control diet, and was obtained from the BCCM/DCG Diatoms Collection (hosted by the Laboratory for Protistology & Aquatic Ecology, Ghent University), and cultured at 15 °C and 12:12h light:dark conditions in autoclaved FNSW supplemented with Guillard's (F/2) Marine Water Enrichment solution (20 ml l^{-1}, Sigma-Aldrich, Overijse, Belgium). The chlorophyte *Dunaliella tertiolecta* Butcher, 1959 was selected as a LC-PUFA deficient diet based on previous research (Boyen et al., 2020). It was

obtained from the Laboratory of Aquaculture & Artemia Reference Center at Ghent University, and cultured at 15 °C and 12:12h light:dark conditions in autoclaved FNSW supplemented with NutriBloom Plus (2 ml l^{-1}, Necton). Food pellets of each diet were prepared through centrifugation and lyophilization of 75 ml culture aliquots and stored at -80 °C. Parallel culture flasks (n = 4) were subsampled to measure cell concentration (Beckman Coulter counter Multisizer 3; three technical replicates per biological replicate), determine particulate organic carbon (POC) using filtration (Whatman GF/F) and high-temperature combustion, and analyze FA composition (storage at -80°C until FA extraction).

The experiment lasted for 10 d and its design was fully crossed (Figure 1). Pools of 85 copepods were placed in experimental units (100 ml Duran bottles) and were exposed to two levels ("ambient" or "future") of each of the following three factors: temperature (19 °C (ambient) or 22 °C (OW)), pH/pCO$_2$ (pH 8.0 (ambient) or 7.6 (OA)) and diet (LC-PUFA rich *Nitzschia* sp. or LC-PUFA deficient *D. tertiolecta*). This resulted in eight distinct treatments that were a combination of all possible scenarios. With four replicate units per treatment, the total amount of copepods in the experiment was 2720 (32 units x 85 copepods unit^{-1}). Ambient temperature and pH target levels were based on the 2019 mean August SST and pH at the sampling location, which were obtained from ScheldeMonitor (ScheldeMonitor, 2019). Future target levels were based on the Representative Concentration Pathway RCP8.5 high GHG emissions scenario, which projects a global SST increase of 3.04 °C and a global pH decrease (pCO$_2$ increase) of 0.38 by 2080-2099 (Collins et al., 2013; Kwiatkowski et al., 2020).

Temperature levels were maintained by placing the experimental units in Lovibond TC-175 incubators and monitored every 30 min using HI144 temperature loggers (Hanna Instruments). Target pH levels were achieved by manually mixing normal FNSW with highly acidified FNSW (pH$_{NBS}$ 5) previously bubbled with pure CO$_2$ gas, and were measured using a Metrohm 914 pH/Conductometer (pH$_{NBS}$ scale). The glass pH electrode was two-point calibrated daily with buffer solutions (pH 4.01 and 7.01; Hanna

Instruments). Each stock FNSW (ambient and OA) was then distributed over the appropriate experimental units and the bottles were filled and closed immediately without leaving headspace to prevent water-atmosphere gas exchange. Experimental units were refreshed daily by discarding old FNSW and leftover diet pellets and adding new pre-thawed diet pellets and FNSW with appropriate pH and temperature levels. pH_{NBS} levels were randomly monitored prior to each refreshment to assess pH stability over the past 24 h. A Tris buffer (salinity = 36.2 ± 0.23) was used daily to convert the pH_{NBS} values to total scale (pH_T) (Riebesell et al., 2011). A 200 ml aliquot was collected daily from the stock FNSW and filtered (Whatman GF/F) for total alkalinity (A_T) quantification using a HydroFIA titrator (Kongsberg Maritime Contros GmbH) calibrated with CO_2 in Seawater Reference Material Batch 183 (Dickson et al., 2003). The carbonate chemistry parameters pCO_2, Ω_{Ca} and Ω_{Ar} were calculated from the obtained values for temperature, pH_T, A_T and salinity (Metrohm 914 pH/Conductometer) with CO2SYS version 25 (Pelletier et al., 2005) using the constants of Lueker et al. (2000).
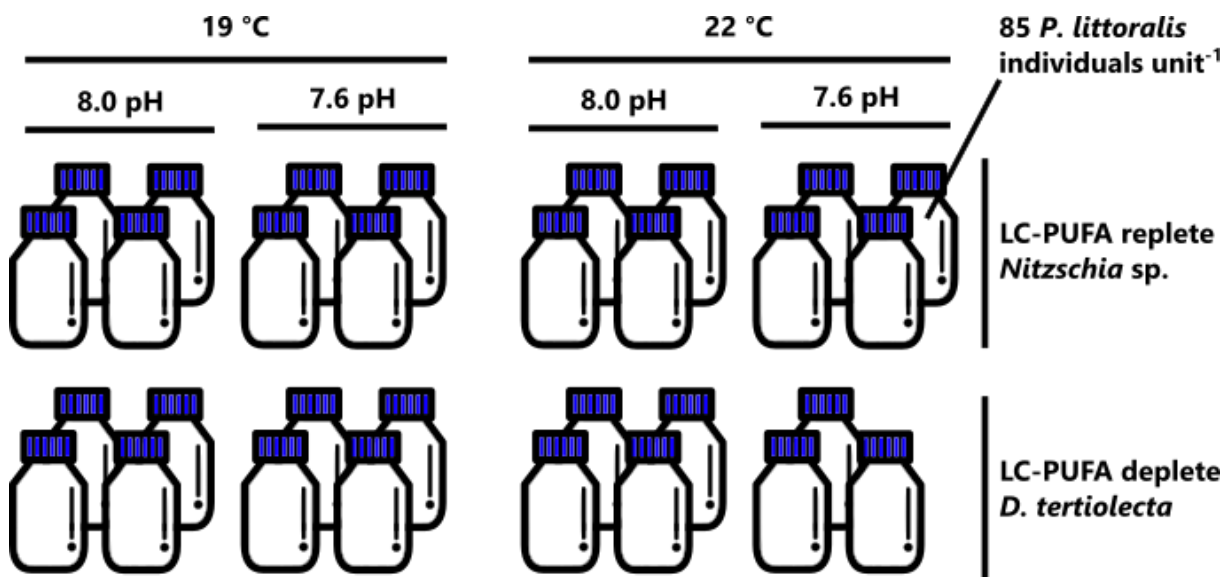

Figure 1 Design of the experiment.

After ten days of incubation, copepod specimens were transferred to Petri dishes with clean FNSW to remove food particles from the cuticle and assess mortality. A total of 40 copepods per unit were randomly picked and immediately flash-frozen in liquid

nitrogen, and stored at −80 °C for RNA extraction. The remaining copepods were returned to their experimental units and kept overnight under the same temperature and pH conditions but without food to allow gut clearance. The next day, 40 copepods per unit were randomly picked and stored at −80 °C for FA analysis. One replicate unit in the treatment with the combination of all three 'future' levels (OW, OA and *D. tertiolecta*) had >95% mortality and was excluded from further analyses.

4.2.2 Gene expression analysis

Total RNA was isolated using the RNeasy Micro Kit (QIAGEN) following a modified protocol (Boyen et al., 2020). RNA extractions were randomized over different days to prevent batch effects. Total RNA quality and quantity were assessed by a NanoDrop 2000 spectrophotometer (Thermo Scientific) and a 2100 Bioanalyzer (Agilent Technologies). RNA integrity numbers were between 4.0 and 9.4 (mean: 7.4), A260/280 ratios were between 1.4 and 3.0 (mean: 2.0), and A260/230 ratios were between 0.01 and 1.37 (mean: 0.56). The A260/230 ratios are likely due to saltwater presence during RNA extraction, but are similar throughout the samples, and total RNA quantity was sufficient for all samples for first strand cDNA synthesis. Conversion of total RNA to cDNA was performed using the Maxima H Minus First Strand cDNA Synthesis Kit (ThermoScientific) according to manufacturer's instructions.

In order to perform qPCR, primers for target genes were designed from the nine PUFA biosynthesis gene sequences identified in our previous study (Boyen et al., 2023). Additionally, we retrieved the *P. littoralis* stearoyl-CoA desaturase (scd) coding sequence (GHXK01165927) from the previously assembled transcriptome (PRJNA575120) using BLAST (tblastn) with the protein sequence of the functionally characterized Δ9 desaturase of *Calanus hyperboreus* (AHL21605) as query (Meesapyodsuk & Qiu, 2014). Its legitimacy as a true Δ9 desaturase was validated by the presence of the three diagnostic conserved histidine boxes "HRXXXH", "HRXHH" and "HNXHH" (Hashimoto et al., 2008). The peptide sequence was aligned with other copepod and metazoan scd peptide sequences using MAFFT version 7.490 (Katoh &

Standley, 2013) with the L-INS-i method, and a maximum-likelihood phylogenetic tree was built using RAxML version 8.2.12 (Stamatakis, 2014) with a GAMMA model of rate heterogeneity, automatic selection of the best protein substitution model (LG), and 100 bootstrap replicates. The final tree was rooted using midpoint rooting and visualized with Figtree version 1.4.3 (Rambaut, 2009). Additionally, sequences of four reference genes, namely 18S, 28S, β-actin and myosin, were retrieved from the *P. littoralis* transcriptome using BLAST (tblastx) with nucleotide sequences from *Tigriopus californicus* (AY599491), *Harpacticus nipponicus* (KR048873), *Tigriopus japonicus* (AF466280) and *Eurytemora affinis* (GQ885386) respectively as queries. For all 14 genes, we used Primer-BLAST (Ye et al., 2012) to design qPCR primers and included a specificity check (using the *P. littoralis* transcriptome as a search database) to prevent non-specific amplification. The primers were synthesized at Integrated DNA Technologies (Leuven, Belgium) (supp. table 1).

The qPCR amplifications were carried out using two technical replicates per gene/sample combination on a LightCycler 480 System (Roche), in a volume of 10 μl containing 1 μl of cDNA, 0.5 μM of each primer, 5 μl of SensiFAST SYBR No-ROX Mix (Roche) and 3 μl of PCR-grade water. The qPCR assays started with an initial activation step at 95 °C for 10 min, followed by 40 cycles: 15 s at 95 °C, 20 s at 60 °C, and 20 s at 72 °C, and ended with a melting curve from 65 °C to 95 °C (0.11 °C s^{-1}) to confirm a single product amplification. Cq values were converted in normalized relative expression values using qbase+ (Hellemans et al., 2007). GeNorm found the most stable expression when using only 18S, 28S and β-actin as reference genes (M = 0.432), therefore myosin was excluded from further analysis. Amplification efficiencies were all set at 100%. When the difference between the two technical replicates was >1, the gene/sample combination was removed (95.3% pass rate) (i.e. NA). Final relative expression values were log-transformed prior to further analysis.

4.2.3 Fatty acid analysis

Methylation of FA was performed in a one-step method according to Abdulkadir & Tsuchiya (2008) and De Troch et al. (2012). An internal standard (19:0, 5 μg) was added to the freeze-dried samples, then FA methyl esters (FAME) were prepared via a direct transesterification procedure with 2.5% (v:v) sulfuric acid in methanol. FAMEs were extracted twice with hexane. FA composition analysis was carried out with a gas chromatograph (GC; HP 7890B, Agilent Technologies, Diegem, Belgium) equipped with both a Flame Ionization Detector (FID) and an Agilent 5977A Mass Selective Detector (MSD; Agilent Technologies, Diegem, Belgium). The GC was further equipped with a PTV injector (CIS-4, Gerstel, Mülheim an der Ruhr, Germany). An HP88 fused-silica capillary column (60 m× 0.25 mm× 0.20 μm film thickness, Agilent Technologies) was used at a constant helium flow rate (2 ml min^{-1}). The injected sample (2 μl) was split equally between the MSD and FID using an Agilent Capillary Flow Technology Splitter. The oven temperature programme was as follows: at the time of sample injection, the column temperature was 50 °C for 2 min, then gradually increased at 10 °C min^{-1} to 150 °C, followed by a second increase at 2 °C min^{-1} to 230 °C. The injector temperature was held at 30 °C for 6 s and then ramped at 10 °C s^{-1} to 250 °C and held for 10 min. The transfer line for the column was maintained at 250 °C. The quadrupole and ion source temperatures were 150 and 230 °C, respectively. Mass spectra were recorded at 70 eV ionization voltage over the mass range of 50-550 m/z units.

Chromatogram analysis was done with MassHunter Qualitative Analysis and Quantitative Analysis (Agilent Technologies). Peaks were identified based on their retention times, compared with external standards as a reference (Supelco 37 Component FAME Mix, Sigma-Aldrich), and by the mass spectra obtained with the MSD. The signal obtained with the FID was used to generate quantitative data of all identified compounds. FAME quantification was based on the area of the internal standard and on the conversion of peak areas to the weight of the FA by a theoretical response factor for each FA (Ackman & Sipos, 1964; Wolff et al., 1995). Relative FA

concentrations were defined as the percentage contribution of each FA to the total concentration of all quantified FAs. Shorthand FA notations of the form A:Bn-X were used, where A represents the number of carbon atoms, B gives the number of double bonds and X gives the position of the first double bond counting from the terminal methyl group.

4.2.4 Statistical analysis

All statistical analyses were conducted with R version 4.0.2 (R Core Team, 2020) applying the statistical significance threshold $\alpha = 0.05$. The normality of data distributions was checked with a Shapiro-Wilk test and homoscedasticity was tested using Levene's test. Results are given as mean ± SD. In accordance with the data distribution, Wilcoxon rank sum test or Welch Two Sample t-test were used to test the effects of the diet, temperature and pH treatments on the experimental conditions, carbonate chemistry parameters and dietary FA levels. The effect of the three treatments on copepod survival was tested with generalized linear models with quasibinomial distributions and F-tests. Differences in total FA content were assessed using a t-test to test between natural population and experiment copepods, and multifactorial analysis of variance (ANOVA) to test between experimental treatments.

In view of the presumed correlations between response variables due to the biosynthesis processes, we used generalized linear latent variable models (gllvm) to test the effects of the three treatments on the relative FA concentrations and gene expressions (Niku et al., 2019). Small-sample corrected Akaike Information Criterion (AICc) and ANOVAs were used for backward stepwise selection between models with differing factors and interactions. For the absolute FA concentrations, we fitted gllvms with a gamma distribution, two latent variables and random starting values for latent variables and their coefficients. The same type of models were fitted for the relative FA concentrations, but here factorial analysis was applied to the residuals to obtain starting values. For the gene expression data, we fitted gllvms with a Gaussian distribution, two latent variables and random starting values. The genes methyl-end

desaturase and elovl4 were discarded from the analysis due to the high presence of NAs. For genes fed, elovl1a, elovl1c, elovl1e (containing 1 NA out of 31), NAs were replaced with the median expression value of that gene. Posterior fits based on 500 simulations were built according to Byrnes (2021) to obtain the predictor errors. We used a means-based approach and applied the framework of Piggott et al. (2015) to define interactive effects, when observed. The log2 change in relative FA levels between the 'all future levels' treatment and the control treatment were visualized according to FA chain length and unsaturation level, with the average log2 change calculated for FAs with identical number of carbon atoms and unsaturations. Residual covariate correlations were visualized using the R package corrplot (Wei & Viliam, 2021). To assess the relationships between genes and FAs, we applied regularised canonical correlation analysis using the R package mixOmics, including the cross-validation approach to optimize the regularization parameters $\lambda1$ and $\lambda2$ (Rohart et al., 2017).

4.3 Results

During the experiment, mean temperature levels significantly differed between treatments (18.4 ± 0.23 °C (CTRL) and 22.3 ± 0.30 °C (OW), W = 0, $p < 2.2e^{-16}$) (fig. 2a). Mean pH_T levels of the stock FNSW were 8.00 ± 0.03 (pCO_2 = 501 ± 41 μatm, Ω_{Ca} = 4.90 ± 0.50, Ω_{Ar} = 3.21 ± 0.34) and 7.59 ± 0.03 (pCO_2 = 1469 ± 117 μatm, Ω_{Ca} = 2.20 ± 0.16, Ω_{Ar} = 1.44 ± 0.11) for CTRL and OA treatments, respectively (fig. 2b, supp. fig. 1a), and both pH_T (t(26.99) = 36.71, $p < 2.2e^{-16}$) and pCO_2 (W = 0, $p < 2.58e^{-8}$) significantly differed between treatments. A_T did not significantly differ between CTRL and OA treatments (mean = 2509 ± 54, W = 71, p = 0.1456). After each 24 h of incubation, mean pH_{NBS} levels of the experimental units remained significantly different between pH treatments (t(24.89) = 33.56, $p < 2.2e^{-16}$) at 7.96 ± 0.04 (CTRL) and 7.57 ± 0.03 (OA) (supp. fig. 1b). While the estimated number of cells administered to each experiment unit was significantly lower (t(3.18) = -6.38, p = 0.006527) for *Nitzschia* sp. (0.17e^{-6} ± 0.06e^{-6} cells day^{-1}) than for *D. tertiolecta* (1.30e^{-6} ± 0.35e^{-6} cells day^{-1}), POC per feeding

event did not differ significantly (t(4.87) = -1.37, p = 0.231) between the two treatments (*Nitzschia* sp.: 0.06 ± 0.02 mg C day^{-1}, *D. tertiolecta*: 0.07 ± 0.01 mg C day^{-1}) (supp. fig. 2). The two algal diets differed in their FA composition (supp. table 2), with the LC-PUFAs 20:3n-6 (0.11 ± 0.02 %), 20:4n-6 (1.50 ± 0.30 %), 20:5n-3 (26.86 ± 1.87 %), 22:5n-3 (0.21 ± 0.01 %) and 22:6n-3 (3.34 ± 0.15 %) present in *Nitzschia* sp. but absent (≤ 0.1%) in *D. tertiolecta* (fig. 2c), and 18:4n-3 significantly higher (t(3.04) = 4.47, p = 0.02032) in *Nitzschia* sp. (2.94 ± 0.71 %) than in *D. tertiolecta* (1.35 ± 0.05 %). In contrast, 18:3n-3 was absent (≤ 0.1%) in *Nitzschia* sp. but highly abundant in *D. tertiolecta* (39.24 ± 0.89 %), and 18:1n-9 (t(5.21) = -25.22, p = 1.204e^{-6}) and 18:2n-6 (t(5.97) = -14.71, p = 6.507e^{-6}) were significantly lower in *Nitzschia* sp. (0.30 ± 0.16 % and 1.24 ± 0.28 % respectively) than in *D. tertiolecta* (3.85 ± 0.23 % and 4.00 ± 0.26 % respectively). Moreover, 18:3n-6 was not significantly different (t(6) = -0.45, p = 0.6709) between *Nitzschia* sp. (3.11 ± 0.30 %) and *D. tertiolecta* (3.20 ± 0.30 %) (supp. table 2).
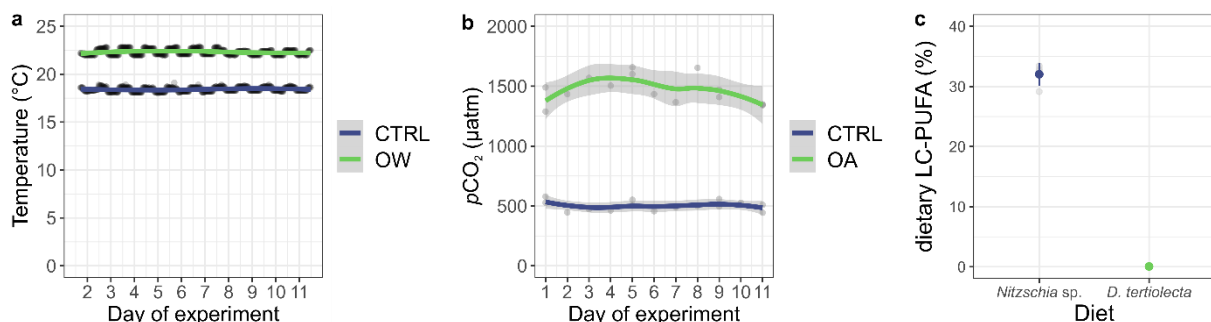
Figure 2 Experimental conditions: (a) temperature and (b) pCO$_2$ between ambient (CTRL) and future (OW/OA) levels, and (c) dietary LC-PUFA concentration (% of total FA measured) of the two diet treatments. Loess smooth lines (span = 0.75) were added to figures a and b using ggplot2 package in R, with 95% confidence intervals in grey.

Copepod survival after 10 d was high overall (92.23 ± 4.15 %) and not significantly affected by diet (F(29) = 4.03, p = 0.05416), temperature (F(29) = 1.43, p = 0.2418), pH (F(29) = 0.9783, p = 0.3308) or their interactions. The putative *P. littoralis* scd (GHXK01165927) shared 50.15% sequence identity with the homologous *C. hyperboreus* sequence, and the phylogenetic assessment showed that the *P. littoralis* sequences clustered within a copepod-specific clade, which more closely related (72% bootstrap support) to vertebrate sequences than to other non-copepod arthropod sequences (supp. fig. 3). After variable selection, the final fitted model for the gene

expressions included the single factors diet and pH but not temperature, as well as the interaction factor between diet and pH. The model detected significant positive antagonistic interaction effects between diet and pH on the genes fed ($z = -2.22$, $p = 0.0265$) and elovl1a ($z = -2.03$, $p = 0.0427$). At control pH (pH 8.0) both genes were upregulated in copepods fed *D. tertiolecta* compared to those fed *Nitzschia* sp., while at pH 7.6 there was no difference between the two diets (fig. 3, supp. fig 6). No significant interactive effect of diet and pH was found for the genes scd, elovl6, elovl1b, elovl1c, elovl1d or elovl1e.

Figure 3 (a) Gene expression (scaled to linear predictors of the best-fitting model). Means and error bars (2.5% to 97.5% quantiles) are built from 500 simulations of normally distributed model parameters. Factors: CTRL: control; OA: ocean acidification. (b) Covariate coefficients and 95% confidence intervals of gene expression. Negative or positive coefficients represent whether there is a decrease or increase respectively due to the 'future' treatment. Grey lines: not significant effect, black lines: significant effect (p<0.05).

Total FA content did not significantly differ between *P. littoralis* copepods sampled before (122.18 ± 10.80 ng copepod^{-1}) and after incubation (126.95 ± 17.90 ng copepod^{-1}) (t(4.84) = 0.68, p = 0.5287). Within the experiment, there was a significant

positive synergistic interactive effect of diet and temperature on total FA content, with *D. tertiolecta* and OW each leading to a decrease separately, but to an increase when combined ($F_{(1,27)}$ = 6.629, p = 0.0158, supp. fig 4, supp. table 3 and 4). The final fitted model for the absolute FA concentrations included all three single factors (diet, temperature and pH) as well as the interaction factor between diet and temperature. Absolute concentrations of most FAs had a positive synergistic diet and temperature effect similar to total FA content (supp. fig 5 and 7, supp. table 3 and 4), expect for 18:3n-3 (additional positive effect of OA, z = 2.03, p = 0.042712) and 22:6n-3 (negative effect of OW but no interaction effect, z = -2.30, p = 0.021732).

The final fitted model for the relative FA concentrations included the single factors diet and temperature but not pH, as well as the interaction factor between diet and temperature. According to this model, in copepods fed *D. tertiolecta*, 18:3n-3 was significantly higher (0.75 ± 0.3 %, z = 2.28, p = 0.022390) than those fed *Nitzschia* sp. (0.51 ± 0.11 %), while 18:3n-6 was significantly lower (z = -3.74, p = 0.000184) in copepods fed *D. tertiolecta* (0.43 ± 0.04 %) than in those fed *Nitzschia* sp. (0.52 ± 0.07 %) (fig. 4, supp. fig 6, supp. table 5 and 6). Interactive effects of diet and temperature were detected on both 18:0 (z = -2.30, p = 0.007011) and 22:6n-3 (z = -2.870, p = 0.004107). There was a slight increase in 18:0 in both copepods fed *D. tertiolecta* and those kept at 22°C, but when the two effects were combined no increase (i.e. an antagonistic response) was observed (fig. 4, supp. fig 6). In contrast, for 22:6n-3, there was no (*D. tertiolecta*) or a minor increase (OW), but a decrease when both effects were combined (i.e. a negative synergistic response) (fig. 4, supp. fig 6). Of the FAs involved in the LC-PUFA biosynthesis pathway, 18:1n-9, 18:4n-3, 20:3n-6, 20:4n-6 and 22:5n-3 were not observed to be significantly affected by any of the three drivers (supp. tables 5 and 6). Concentrations of FA not involved in the LC-PUFA pathway can be found in supp. tables 3, 4, 5, and 6. Overall, when comparing the treatment with all 'future' levels combined with the control treatment, relative levels of short-chain (≥ 18 C-atoms) SFAs increased, while levels of LC-PUFAs generally decreased (fig. 5).

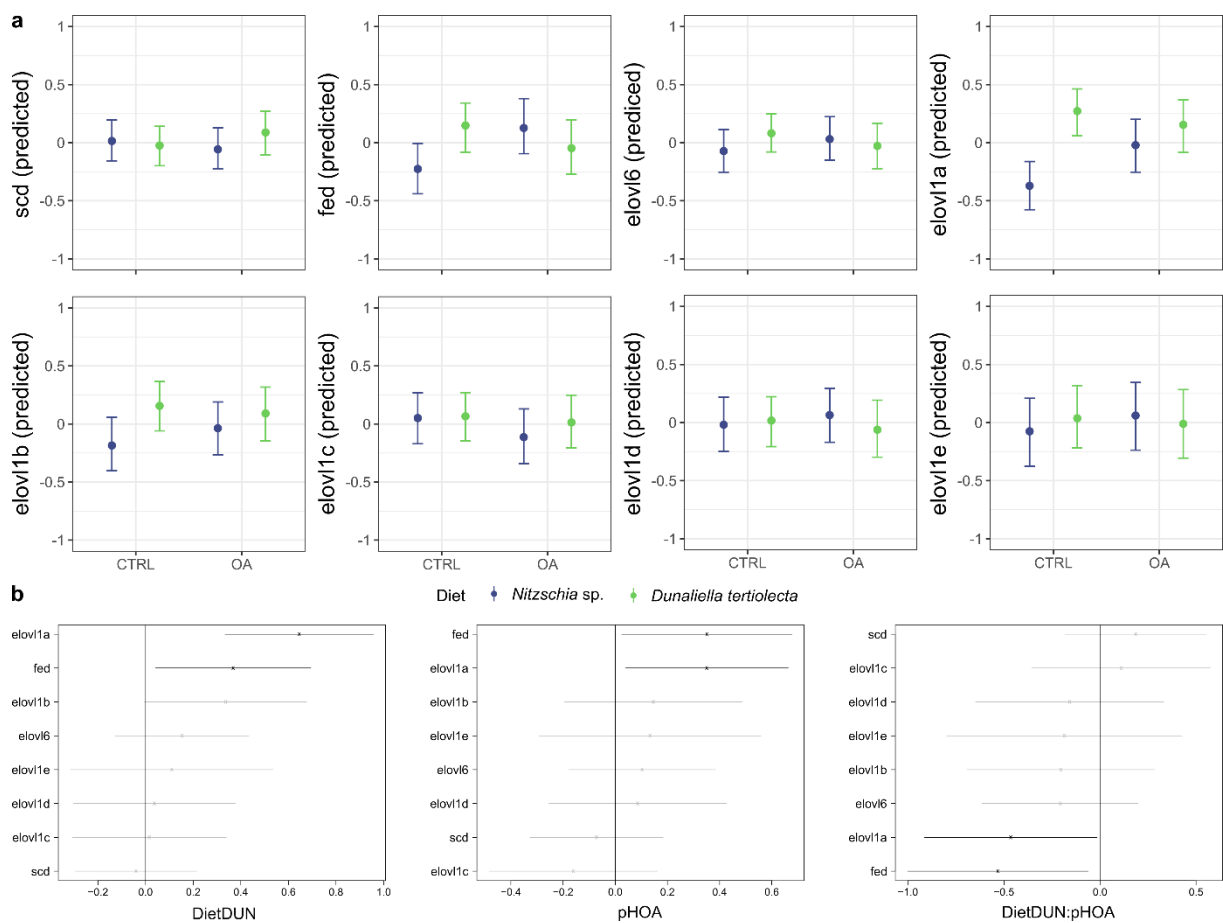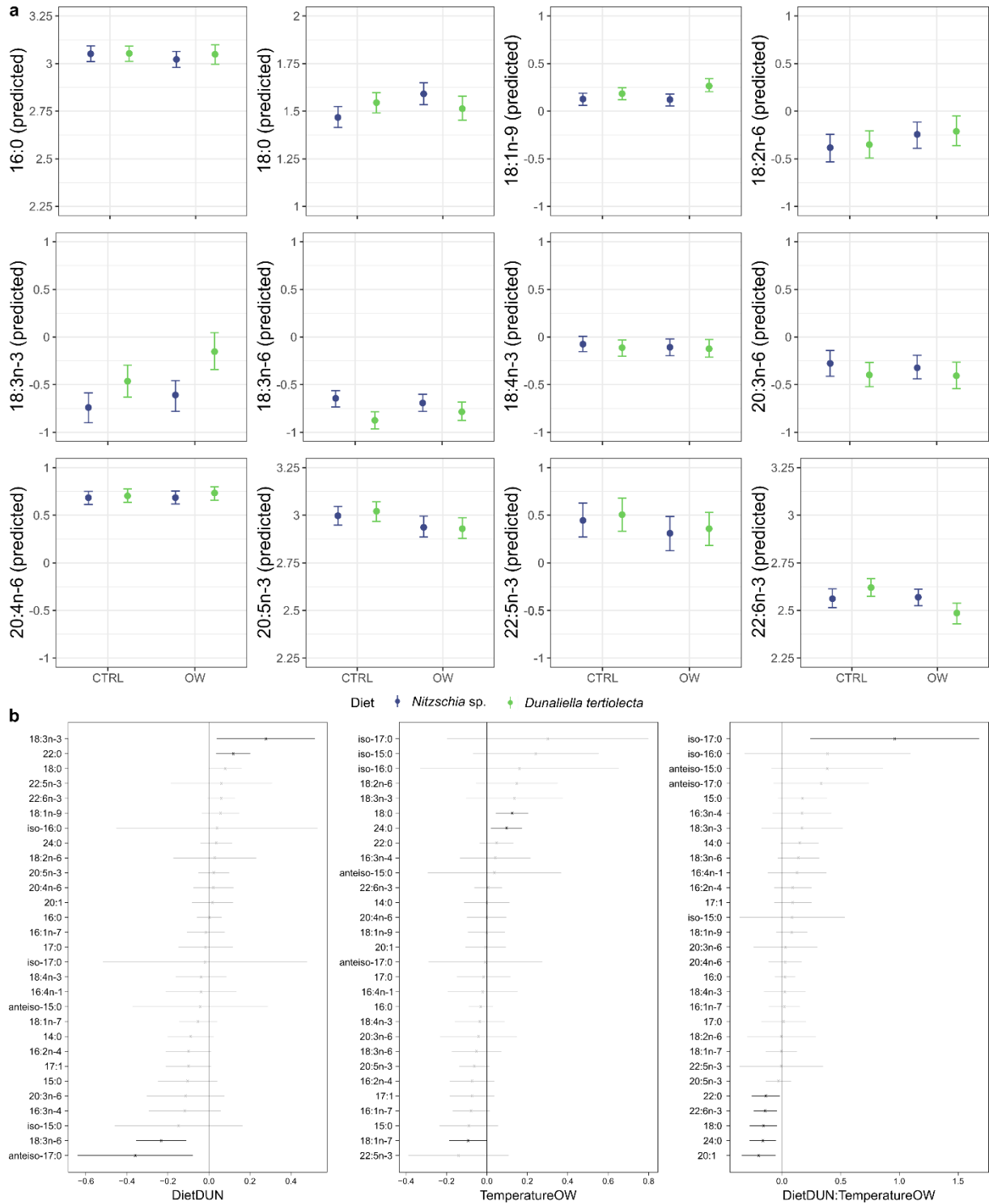*Figure 4 (a) Relative fatty acid composition (scaled to linear predictors of the best-fitting model). Means and error bars (2.5% to 97.5% quantiles) are built from 500 simulations of normally distributed model parameters. Factors: CTRL: control; OW: ocean warming. (b) Covariate coefficients and 95% confidence intervals of fatty acids (% of total FA measured). Negative or positive coefficients represent whether there is a decrease or increase respectively due to the 'future' treatment. Grey lines: not significant, black lines: significant effect (p<0.05).*
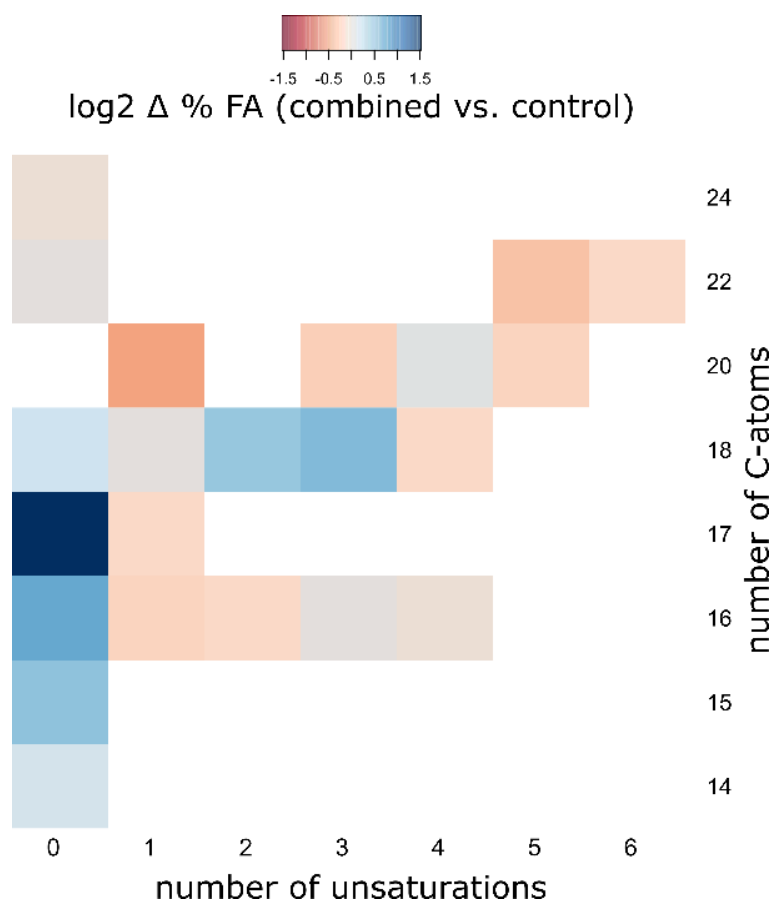
Figure 5 Differences in ratio % between relative FA levels of control treatment and future treatment with all three factors combined across FA length (number of C-atoms) and unsaturation level (number of unsaturations). Red: lower relative FA levels in future treatment compared to control: blue higher FA levels in future treatment compared to control.

The expression of most genes was found to be highly positively correlated with each other, except elovl1c, which had slightly lower positive correlation with the other genes (fig. 6a). The FAs can be roughly grouped into two groups with moderate to strong positive within-group correlation but negative correlation between each other (fig. 6b). The first group contained among others the PUFAs 18:3n-6, 18:4n-3, 20:4n-6, 20:5n-3, 22:5n-3 and 22:6n-3. The second group, negatively correlated with the first group, contained the precursor PUFAs 18:1n-9, 18:2n-6 and 18:3n-3, as well as the LC-PUFA 20:3n-6. The SFA 18:0 is negatively correlated with all previously mentioned FAs, except for 20:4n-6 and 22:6n-3, with which it is positively correlated (fig. 6b). Applying a canonical correlation threshold of 0.2 on the gene-FA correlation network revealed positive correlations between 18:1n-9 and elovl1a, elovl1b, elovl1d and elovl6, and between 18:2n-6 and fed, elovl1b and elovl6 (fig. 7). Furthermore, fed, elovl1b, elovl1d

and elovl6 were negatively correlated with 20:4n-6 and – together with elovl1a – with 22:6n-3. No correlation > 0.2 was observed between the genes elovl1c, elovl1e and scd and any of the FAs part of the LC-PUFA biosynthesis pathway (fig. 7, supp. table 7).
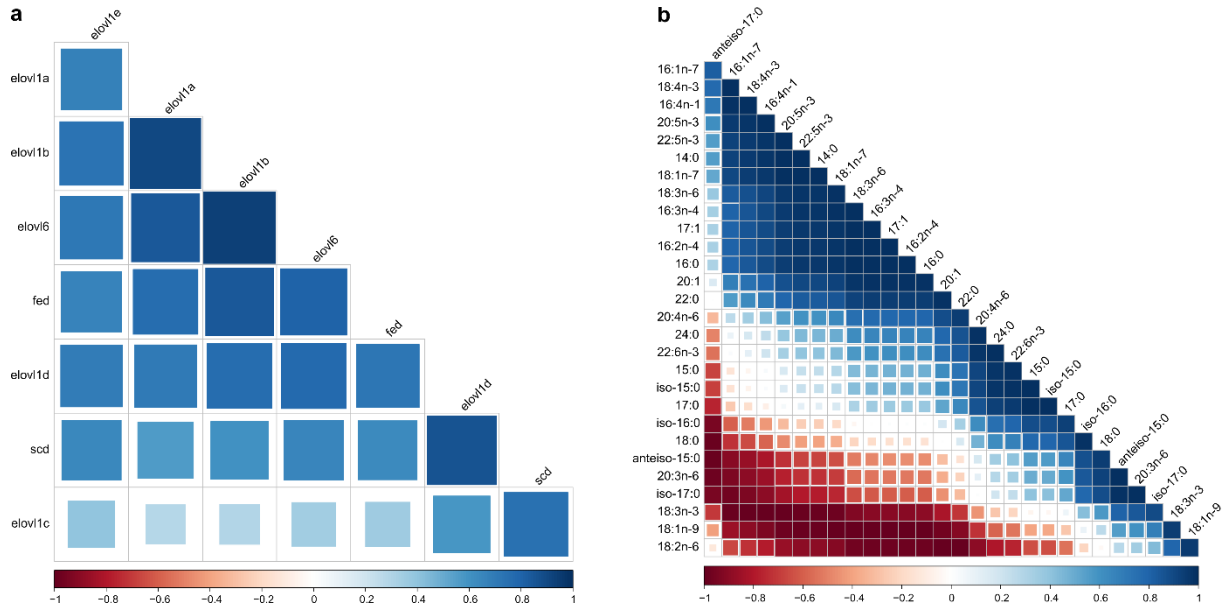
Figure 6 Residual correlation plots (a) between genes and (b) between FAs, with the effects of the drivers taken into account.
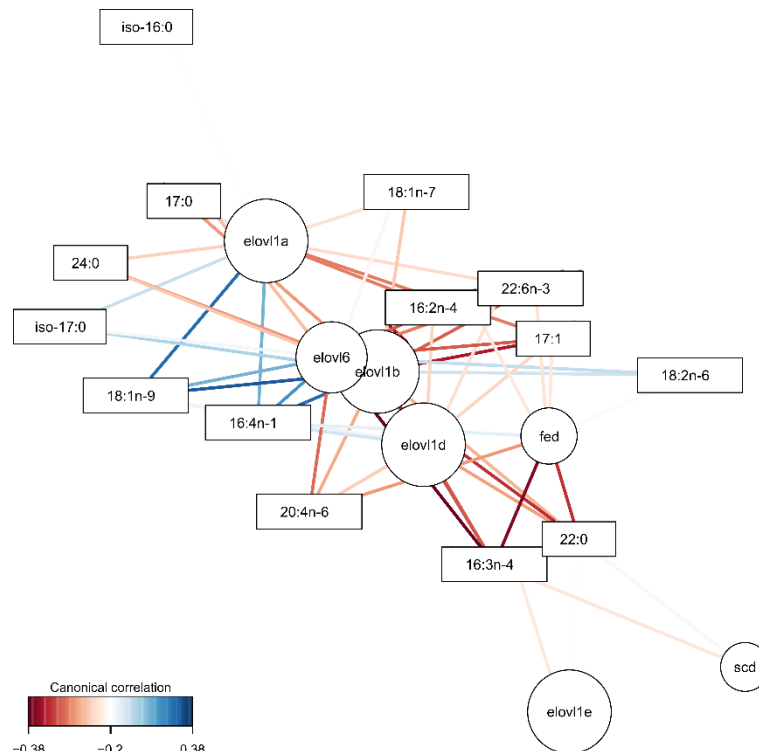
Figure 7 Bivariate relevance network of gene-FA regularized canonical correlations (minimum correlation = 0.2).

4.4 Discussion

Our study demonstrated significant interactive effects of diet, temperature, and pH/pCO$_2$ on PUFA biosynthesis gene expression and FA composition in *P. littoralis*, while copepod survival was unaffected. Specifically, we observed a significant diet-pH interaction effect on the expression of fed - a Δ4 front-end desaturase - and elovl1a, which produces C$_{20}$, C$_{22}$ and C$_{24}$ LC-PUFAs (Boyen et al., 2023). Both are key genes involved in the last two steps of the biosynthesis pathway to produce DHA from EPA (Boyen et al., 2023). This contrasts with our previous transcriptome-wide study on *P. littoralis*, were we found no environmental effects on PUFA biosynthesis gene expression (Boyen et al., 2020). However, one should exercise caution when comparing this study with the previous one, due to the different experimental setup (Petri dishes versus Duran bottles), as well as the different technologies used (RNA sequencing versus qPCR). While RNA sequencing allows the assessment of expression of (almost) all genes, qPCR is a more targeted approach that allows a more accurate detection of differential expression of a smaller number of genes.

Despite the increase in *P. littoralis* fed and elovl1a expression when the diet lacked LC-PUFA, this upregulation was nullified when combined with OA. Similarly, the relative proportion of DHA was not affected by one single stressor alone, but significantly decreased when faced with both the LC-PUFA deficient diet and OW. Although not significant, the lowest proportions of both EPA (17.54 ± 2.04 %) and DHA (11.84 ± 0.81 %) were found when all three near-future stressors were applied. While ALA was relatively higher and LA lower when fed ALA-rich *D. tertiolecta*, similar to Boyen et al. (2020), diet alone did not affect LC-PUFA proportions, potentially due to the upregulation of fed and elovl1a. These findings suggest that near-future OW and OA may limit the capacity of copepods to biosynthesize their own LC-PUFAs when dietary inputs are limited. However, the reduced levels of 18:3n-6 when fed *D. tertiolecta* regardless of OW and OA might indicate that this FA was used to produce LC-PUFAs via elongation and possibly even Δ15 desaturation (Boyen et al., 2023).

Current findings on environmental effects of copepod PUFA biosynthesis are still unresolved and likely taxon-specific. In one comparative study, PUFA biosynthesis genes were upregulated in *T. japonicus* but downregulated in *Paracyclopina nana* when fed the LC-PUFA deficient *Chlorella* sp. for 24 h (Lee et al., 2020b). Moreover, unlike *P. littoralis* in our study, OW decreased expression of both front-end desaturases and elongases in the cyclopoid *P. nana* after 120 min (Lee et al., 2017a). Temperature increases were previously found to impact LC-PUFA concentrations in both *P. littoralis* as well as other copepod species (Boyen et al., 2020; Garzke et al., 2016; Lee et al., 2017a; Pond et al., 2014; Sahota et al., 2022; Werbrouck et al., 2017), although effects may still be diet-dependent, time-dependent or only significant on specific LC-PUFA such as DHA. In another particularly noteworthy study on *P. nana*, one of the genes downregulated due to OA was annotated as APH81349 or 'elongase 3', a member of the elovl1 clade (Lee et al., 2022b). This contrasts with the OA-induced upregulation of elovl1a found in our study.

The impairment of LC-PUFA biosynthesis under conditions of increased temperature and pCO$_2$ can probably be attributed to various factors. These environmental stressors, coupled with dietary LC-PUFA deficiency, may trigger a stress response and increase the energy requirements necessary for normal cellular function, resulting in the downregulation of processes with lower priority such as LC-PUFA biosynthesis. At elevated temperatures for instance, cellular lipid membranes preferentially incorporate shorter, more saturated FAs, reducing the requirement for LC-PUFAs (Sinensky, 1974). Determining whether this is an active response or a passive side-effect will be challenging however. The absence of significant differential expression of the other elongases may suggest that they are less involved in the biosynthesis pathway compared to elovl1a. However, considerable caution in interpreting potential false negatives is needed due to the limited statistical power of our analysis.

A positive antagonistic effect between diet and temperature was observed on the total FA content, which decreased when faced with only OW or *D. tertiolecta*, but increased

when combined. This pattern was observed to some extent as well in most individual FAs, with DHA as notable exception (negative effect of only OW). Higher total FA content might have occurred due to increased energy requirements at higher temperatures, leading to increased ingestion and carbon assimilation rates (Helenius et al., 2020; Sahota et al., 2022). *Platychelipus littoralis* then could subsequently have ingested more *D. tertiolecta* than *Nitzschia* sp., perhaps due its (although insignificantly) higher POC or preferential uptake, which led to increased levels of total FA (but not DHA).

The fitted models provided residual correlations between genes and between FAs that were not attributable to the drivers. The strong positive correlation between all genes confirms that they participate in the same biological processes and pathways, and is consistent with previous observations of lipogenesis genes in other copepods such as *Calanus finmarchicus* (Tarrant et al., 2008). Moreover, negative correlations were found between C_{18} precursors (18:1n-9, 18:2n-6, and 18:3n-3) on the one hand, and their PUFA and LC-PUFA products on the other hand. The regularized canonical correlation analysis showed that the expression of certain genes (fed, elovl1a, elovl1b, elovl1d and elovl6) were positively correlated with C_{18} precursors (18:1n-9 and 18:2n-6) and negatively correlated with LC-PUFAs (20:4n-6 and 22:6n-3). These results suggest that when – potentially due to one of the three assessed drivers or other unassessed environmental effects– LC-PUFA proportion in *P. littoralis* is lower relative to C_{18} precursors, biosynthesis genes are upregulated as a response to endogenously produce LC-PUFAs. Additionally, all genes except elovl1c displayed correlations (> 0.2) with multiple other FAs that are not involved in the LC-PUFA biosynthesis pathway, highlighting that their functions extend beyond the production of LC-PUFAs (Boyen et al., 2023).

The research designs and strategies to investigate the multifaceted impacts of and responses to climate change are justifiably being discussed, as they determine the accuracy of predictions and can ultimately influence policy decisions and actions

regarding climate change mitigation and adaptation efforts (Boyd et al., 2018; Orr et al., 2020). Multistressor approaches have been identified as still underutilised in climate impact research (Boyd et al., 2018; Riebesell & Gattuso, 2015). Building on previous studies on the combined impact of OW and OA on copepod FAs (Garzke et al., 2016; Mayor et al., 2012), our experiment is the first to combine three climate drivers with two sets of response variables (gene expression and FA concentrations) to make predictions about near-future LC-PUFA biosynthesis. Combining a multidriver approach with gradient experiments with more than two levels per driver (e.g. Sahota et al., 2022) even further increases the accuracy of predictions, as it allows for modelling the impacts of a range of future scenarios and pathways (Boyd et al., 2018). Moreover, the intensity of stressors or drivers is of crucial importance. In our study, we applied temperature and pH treatments concurrent with RCP8.5 and SSP3-7.5 scenarios (Kwiatkowski et al., 2020), and followed OA research best practices (Dickson et al., 2007; Riebesell et al., 2011). Our 'future diet' treatment (a LC-PUFA deficient diet) may have been less realistic, as primary consumers are more likely to face reduced dietary LC-PUFA levels than no LC-PUFAs at all (Hixson & Arts, 2016). More realistic dietary LC-PUFA treatments would be using diet mixtures or live diets exposed to projected environmental conditions themselves (Bermúdez et al., 2016; Meyers et al., 2022; Rossoll et al., 2012; von Elert & Fink, 2018). Lastly, the choice of appropriate statistical analyses needs to be considered. Gene expression levels and cellular biochemistry (FAs) are intertwined through various biosynthetic processes, which makes them highly dependent on each other. Multiple separate univariate analyses may not be the most suitable approach compared to more advanced techniques, such as generalized linear latent variable models or regularized canonical analysis (Boyd et al., 2018; Rohart et al., 2017).

From the present multistressor study we conclude that OW and OA significantly impact LC-PUFA biosynthesis in the harpacticoid copepod *P. littoralis*, especially when the animals are facing a dietary LC-PUFA deficiency. While previous studies found no or limited impacts of OA on FAs in other crustaceans (Ericson et al., 2019), we here

demonstrate that OA, due to its effect on fed and elovl1a, is an important stressor that needs to be taken into account when investigating LC-PUFA levels and biosynthesis in primary consumers. In copepods however, genetic adaptations to environmental stressors can occur within only a few generations (De Wit et al., 2016; Lee et al., 2022b; Thor & Dupont, 2015), so addressing how their LC-PUFA biosynthesis mechanism will adapt over time is an important next research question (Twining et al., 2021; Závorka et al., 2023). As copepods play a major role in providing essential nutrients to higher trophic levels, impairments to their ability to endogenously produce LC-PUFAs can have profound ecosystem-wide effects that should be further quantified.

Acknowledgments

CHAPTER 5

EVOLUTION OF POLYUNSATURATED FATTY ACID BIOSYNTHESIS IN COPEPODS

Boyen Jens[1], Kabeya Naoki[2], Monroig Óscar[3], Fink Patrick[4, 5, 6], Hablützel Pascal I.[7, 8], De Troch Marleen[1]

[1]Marine Biology, Department of Biology, Ghent University, Gent, Belgium

[2]Department of Marine Biosciences, Tokyo University of Marine Science and Technology, Tokyo, Japan

[3]Instituto de Acuicultura Torre de la Sal (IATS), CSIC, Ribera de Cabanes, Castellón, Spain

[4]Department of River Ecology, Helmholtz Centre for Environmental Research - UFZ, Magdeburg, Germany

[5]Department of Aquatic Ecosystem Analysis and Management, Helmholtz Centre for Environmental Research - UFZ, Magdeburg, Germany

[6]Aquatic Chemical Ecology, Institute for Zoology, University of Cologne, Cologne, Germany

[7]Flanders Marine Institute (VLIZ), Oostende, Belgium

[8]Biology Department, Vrije Universiteit Brussel, Brussels, Belgium

Keywords: copepods, polyunsaturated fatty acid biosynthesis, evolution, horizontal gene transfer, codon usage preference, selection analysis

Abstract

Throughout their evolution, copepods have successfully inhabited a wide range of marine and freshwater habitats, each characterized by differing levels of dietary quality and quantity. Copepods are generally known to contain high levels of polyunsaturated fatty acids (PUFAs), notably omega-3 long-chain PUFAs such as eicosapentaenoic acid (EPA) and docosahexaenoic acid (DHA). Recent research indicates that at least some copepod species are capable of biosynthesizing these PUFAs endogenously. However, the extent to which the copepods' perceived capacity of PUFA biosynthesis coincides with their diversification and niche specialization remains uninvestigated. Leveraging publicly available copepod transcriptomes and genomes, we demonstrate significant copy number variations within the PUFA gene repertoire among ecologically different copepod orders. Following two presumable horizontal gene transfer (HGT) events in a common copepod ancestor, methyl-end desaturases and front-end desaturases were retained in Cyclopoida, Harpacticoida and Siphonostomatoida but lost in Calanoida, except for certain *Calanus* and *Neocalanus* species which still have one front-end desaturase. All orders show strong expansion of the elovl1/7 subfamily, with two distinct clades each containing gymnoplean (Calanoida) or podoplean elongases. While total elongase copy number did not differ among orders, the expression of these genes was higher than average in harpacticoids and lower in calanoids. All desaturase and elongase gene families exhibited non-clustered distribution in the assessed genomes, and positive selection on specific codons following HGT and duplication events. Overall, the unique but varying PUFA biosynthesis capacity of copepods enables at least some of them to maintain high PUFA levels even under dietary constraints, and further to ensure PUFA provisioning to higher trophic levels.

5.1 Introduction

Species evolution and natural selection is driven by a number of evolutionary forces. At the molecular level, gene sequence mutations historically garnered considerable attention, yet other modifications also assist in adaptation. For instance, gene copy number increases (through gene, chromosome or whole genome multiplication) allows increased transcriptional outputs of beneficial genes (Dimos et al., 2022; Kondrashov, 2012). Further neofunctionalisation or subfunctionalisation of novel genes can promote adaptation and diversification of certain traits. Deep-sea fishes for example were found to have independently expanded and diversified the repertoire of a rhodopsin gene in order to maximise their vision (Musilova et al., 2019). Even gene losses can be adaptive when these are no longer energetically beneficial (Albalat & Cañestro, 2016).

While these mechanisms are well-established in several taxa, some areas of the biological world still lack comprehensive exploration, particularly in terms of gene copy number variation as an adaptive mechanism. This gap in knowledge is exemplified in the case of copepods, a highly abundant and ecologically diverse class of small pancrustaceans (Turner, 2004), with, as of August 2023, nearly 15000 accepted species (Walter & Boxshall, 2023). Throughout their evolution, copepods have managed to successfully inhabit a wide range of habitats: they are abundant members of pelagic and benthic communities in marine, brackish and freshwater ecosystems (George et al., 2020), but are also found in the deep sea (Mathiske et al., 2021), submerged caves (Janssen et al., 2013), temporary rock pools (Snoeks et al., 2021), phytotelmata (Mercado-Salas et al., 2021), groundwater (Galassi et al., 2009) and even glacier pits (Kikuchi, 1994). Many species are associated with algae or seagrasses (Daudi et al., 2023; McAllen, 1999), while others have symbiotic or parasitic relationships with other metazoans (Bass et al., 2021; Bernot et al., 2021; Domènech et al., 2017).

While their exact placement within Pancrustacea remains debated (Lozano-Fernandez et al., 2019), copepods form a monophyletic group with ten recognized orders (Walter & Boxshall, 2023). The most ecologically well-known orders are Calanoida and

Harpacticoida, which are mainly marine pelagic and marine benthic, respectively (with many exceptions); the parasitic Siphonostomatoida; and the Cyclopoida, which encompasses diverse groups of marine, freshwater, free-living and parasitic species (Bass et al., 2021). Recently, a new order of copepods, Polyarthra (also known as Canuelloida) was suggested and recognized, containing species with similar morphological and ecological characteristics as benthic harpacticoids (Dahms, 2004; Khodami et al., 2017; Walter & Boxshall, 2023). However, as the study triggering the official recognition of Polyarthra has since been retracted (Khodami et al., 2020), the exact placement of Polyarthra within copepods remains debated (Bass et al., 2021). In line with the wide diversity of occupied habitats, the evolution of copepod orders likely involved adaptations to particular environmental conditions such as temperature, salinity, oxygen levels, and food availability and quality.

Nonparasitic copepods are primary consumers and provide a crucial link in the food web between primary producers (i.e. micro-algae, bacteria) and higher trophic levels (Gee, 1987; Hicks & Coull, 1983; Turner, 2004). Many are known to produce and store high levels of lipids (sometimes as lipid droplets or in a lipid sac) (Falk-Petersen et al., 2009), which makes them highly important in the global carbon cycle (Jónasdóttir et al., 2015) and an emerging candidate for aquaculture feed (Støttrup, 2000). Within their lipids, copepods contain one of the highest levels of polyunsaturated fatty acids (PUFAs) among all metazoans (Twining et al., 2021). Long-chain (C_{20}-C_{24}) PUFAs (LC-PUFAs) such as arachidonic acid (ARA, 20:4n-6), eicosapentaenoic acid (EPA, 20:5n-3) and docosahexaenoic acid (DHA, 22:6n-3) are vital biomolecules ensuring proper consumer development, physiological functioning and reproduction (Twining et al., 2016; Závorka et al., 2023). PUFAs are modulators of phospholipid membrane fluidity, components of storage neutral lipids for energy production, and precursors of cell signalling molecules called eicosanoids (de Carvalho & Caramujo, 2018). EPA and DHA are especially abundant in the marine environment (Colombo et al., 2017a; Twining et al., 2021).

Until recently, the common assumption was that most LC-PUFAs in metazoans originated from their diet (Bell & Tocher, 2009). Meanwhile, it is well established that many copepods, along with other metazoans, possess the ability to endogenously produce LC-PUFAs from saturated (SFA) and/or polyunsaturated fatty acid (PUFA) precursors (Monroig et al., 2022). This biosynthesis capacity relies on a group of enzymes known as fatty acid desaturases and elongases. Since stearoyl-CoA-desaturase or Δ9 desaturase, which converts SFAs into monounsaturated fatty acids (MUFAs), is universally present in all eukaryotes, the precise ability for LC-PUFA biosynthesis is determined by the presence, copy number, gene expression, and enzymatic activities of other desaturases and elongases (Kabeya et al., 2021).

Among those enzymes, methyl-end desaturases or ωx desaturases enable the crucial production of omega-6 and omega-3 PUFAs from omega-9 MUFAs and omega-6 PUFAs, respectively, by adding a double bond at the methyl-end of the carbon chain (Figure 1 Chapter 3). In metazoans, these enzymes are currently only found in a limited number of invertebrate groups, including copepods (Kabeya et al., 2018; Monroig et al., 2022). The conversion towards LC-PUFAs further progresses through a series of substrate-specific front-end desaturase and elongase enzymes, which add a double bond at the front-end of the carbon chain and enable the elongation of the FA chain with two carbon atoms, respectively (Boyen et al., 2023; Kabeya et al., 2021; Monroig et al., 2022). While functional front-end desaturases are found in vertebrates, molluscs, cnidarians, nematodes, annelids and echinoderms (Monroig et al., 2022; Ramos-Llorens et al., 2023a; Surm et al., 2015, 2018), they are believed to be absent in most arthropods (Monroig et al., 2022; Ramos-Llorens et al., 2023b; Ribes-Navarro et al., 2021), but uniquely present in copepods (Boyen et al., 2023; Kabeya et al., 2021; Lee et al., 2020a, 2020b; Nielsen et al., 2019). This has led to the hypothesis that methyl-end and front-end desaturases originated through horizontal gene transfer (HGT) in copepods from oomycetes and kinetoplastids, respectively (Kabeya et al., 2018, 2021). Elongases on the other hand are ubiquitous throughout the entire animal kingdom, however the

presence and absence of specific subfamilies (ranging from elovl1 to elovl11) differs between groups (Monroig et al., 2022).

The capacity for LC-PUFA biosynthesis, determined by the presence, copy number and expression of fatty acid biosynthesis genes, is indicated to play a significant role in the speciation and adaptive evolution of metazoans (Twining et al., 2021). For instance, Fads2 duplication and neofunctionalization was found enable freshwater transition of marine sticklebacks, flatfish and other fish lineages (Ishikawa et al., 2019, 2022; Matsushita et al., 2020). In insects, the evolution of Δ9 desaturases and Δ12 methyl-end desaturases (evolved independently from other invertebrate methyl-end desaturases through expansion of a Δ9 desaturase), have been linked to their ecological diversification (Helmkampf et al., 2015; Macháček et al., 2023). However, the specific role of desaturases and elongases involved in LC-PUFA biosynthesis in the ecological diversification of copepods and their evolutionary or environmental drivers remain uninvestigated.

Within copepods, functional methyl-end desaturases have been found in harpacticoids, cyclopoids and siphonostomatoids, but as of yet not in calanoids (Boyen et al., 2023; Kabeya et al., 2018, 2021). Multiple subclades of elongases were found to exist in multiple species of copepods (Boyen et al., 2023; Kabeya et al., 2021; Lee et al., 2020a, 2020b; Lenz et al., 2014), similar to other arthropods (Finck et al., 2016; Ramos-Llorens et al., 2023b; Ribes-Navarro et al., 2021). A comparable extensive diversification was observed for front-end desaturases (up to six) in species of the harpacticoid genus *Tigriopus* (Kabeya et al., 2021; Lee et al., 2020a, 2020b) but not to this extent in other copepods (Boyen et al., 2023; Lenz et al., 2014; Nielsen et al., 2019). While previous studies mainly focused on individual species, the increasing availability of numerous copepod transcriptomic and genomic datasets (Hartline et al., 2023; Lizano et al., 2022), presents an opportunity for a systematic investigation into the origin and diversification of desaturases and elongases during copepod diversification, encompassing transitions towards freshwater habitats and parasitism. Insights in the

capacity of LC-PUFA biosynthesis of different groups of copepods are essential to better understand their potential contribution towards global LC-PUFA production, especially given that production of EPA and DHA in microalgae is expected to decrease under ocean warming (Colombo et al., 2020; Hixson & Arts, 2016; Holm et al., 2022; Tan et al., 2022).

In this study, we conducted a meta-analysis of publicly available transcriptomic and genomic data of copepods to address several research questions that help us understand the role that LC-PUFA biosynthesis has played in ecological diversification of copepods. We explored differences in gene occurrence and copy number of desaturases and elongases among copepod orders, lifestyles (free-living or parasitic) and habitats (presence or absence of freshwater populations). Phylogenetic analyses were performed to investigate the diversification of gene families throughout copepod evolution. We also examined differences in expression among orders and analyzed synteny of LC-PUFA biosynthesis genes within copepod genomes. Furthermore, we explored the possibility of HGT by assessing a number of codon characteristics of both fatty acid biosynthesis genes and other copepod genes, as deviation from the 'core' characteristics can point to HGT events (Matriano et al., 2021; Nguyen et al., 2015). Finally, we investigated the potential influence of positive selection on the diversification of the three gene families.

5.2 Materials and Methods

5.2.1 Gene dataset

We compiled a dataset of all 62 publicly available copepod transcriptome resources (available as of February 2023) containing copepod transcriptome shotgun assemblies (TSA) obtained from the NCBI Sequence Set Browser or other sources specified in the referenced studies (Acebal et al., 2023; Barrick et al., 2022; De Wit et al., 2016). Additionally, 10 transcriptomes were *de novo* assembled from RNA sequencing studies where Short Read Archive (SRA) data but no TSA was available. The SRA data were

retrieved from the European Nucleotide Archive and read quality was assessed using FastQC version 0.11.5 (Andrews, 2010). Trimmomatic version 0.40 (Bolger et al., 2014) was used to perform quality trimming and adapter clipping of the reads, with parameters set as follows: ILLUMINACLIP: TruSeq3-PE-2.fa:2:30:10:2:True, LEADING: 3, TRAILING: 3, SLIDINGWINDOW: 4:15, and MINLEN: 50. After trimming, FastQC was run again to confirm quality trimming and adapter removal. Transcriptomes were assembled using Trinity version 2.15.1 (Grabherr et al., 2011) with default parameters and in silico read normalization.

Previously functionally characterized methyl-end and front-end desaturases and elongases from the copepod species *Platychelipus littoralis*, *Lepeophtheirus salmonis* and *Tigriopus californicus* (Boyen et al., 2023; Kabeya et al., 2018, 2021) were blasted individually as translated queries (tblastx) against each of the transcriptomes of our dataset using the online version of BLAST for the transcriptomes available at NCBI and local BLAST for all the other transcriptomes (Altschul et al., 1990). Transcripts with max e-value 1e-10 were collected, and for transcripts with multiple isoforms and/or transcripts with (near-)identical coding sequences (CDS), only one transcript was collected. Untranslated regions were removed, and further filtering was done by only selecting (near-) full length CDS for which the protein sequence contains the diagnostic features: methyl-end desaturases had to contain the three histidine boxes (H-boxes) "HXXXH", "HXXHH" and "HXXHH" but no cytochrome b5 domain, front-end desaturases had to contain a cytochrome b5 domain with a heme binding motif (HPGG) and the three H-boxes "HXXXH", "HXXXHH" and "QXXHH", and elongases had to contain the single H-box "HXXHH" or "QXXHH" (Boyen et al., 2023; Hashimoto et al., 2008; Kabeya et al., 2021). We also included sequences that were previously identified and publicly available on the NCBI nucleotide database (*Apocyclops royi, Paracyclopina nana, L. salmonis, Caligus rogercresseyi* and *Caligus clemensi*), as well as sequences obtained from three transcriptome assemblies (*Canuella perplexa*, *Tisbe* sp. and *A. panamensis*) from unpublished studies. Additionally, sequences from *Tigriopus japonicus* and *Tigriopus kingsejongensis* have been identified (Lee et al., 2020a, 2020b)

but are not publicly unavailable. We obtained those by blasting their qPCR primer sequences (blastn) and protein sequences (tblastn) respectively (available in supplementary information of each study) against the corresponding transcriptomes.

To detect putative contaminated or erroneous sequences, sequences were aligned for each gene family using ClustalW (Thompson et al., 2003) and simple neighbor-joining trees were built iteratively using MEGA version 7.0.26 (Kumar et al., 2016) with oomycete and annelid (for methyl-end desaturases), kinetoplast (for front-end desaturases) or human (for elongases) sequences included. Copepod sequences that placed outside the copepod-specific clades were blasted (blastn) against the NCBI Nucleotide collection (nr) and those that matched with non-copepod metazoan (in the case of parasitic copepods: vertebrate or mollusc hosts) or non-metazoan sequences were excluded from the analysis. Additionally, when sequences were not located on genomes from species with available genome data, they were excluded. For *Temora longicornis*, no desaturase or elongase sequences of the transcriptomes GINW01 and GGQN02 were retrieved from the Gene Expression Omnibus (GEO) files GSE115472 associated with the corresponding study (Semmouri et al., 2019). Therefore only sequences of the *T. longicornis* transcriptome GKAP01, which all matched with sequences in the GEO files, were considered valid.

5.2.2 Phylogenetic analysis

Using the final datasets for each gene family, codon-based multiple sequence alignments were built using MUSCLE version 3.7 (Edgar, 2004) and maximum likelihood (ML) phylogenetic inference was performed using RAxML version 8.2.12 with a generalized time-reversible model of nucleotide substitution, a gamma model of rate heterogeneity, 100 rapid bootstrap replicates and nine ML searches (Stamatakis, 2014). Oomycetes and kinetoplasts were included in the methyl-end and front-end desaturase inferences, respectively, as they were previously suggested as the likely horizontal origin of copepods desaturases (Kabeya et al., 2018, 2021). For elongases,

no outgroups were included and midpoint rooting was performed. Phylogenetic trees were visualized and edited with FigTree version 1.4.3 (Rambaut, 2009).

5.2.3 Copy number variation

Habitat information (with regard to presence or absence of freshwater populations) of each species was obtained from the World Register of Marine Species (WoRMs Editorial Board, 2023) and lifestyle (free-living or parasitic) was obtained from literature (Bernot et al., 2021). For each gene family, copy number variation was calculated per species, and statistical differences between orders, habitat and lifestyle were tested in R version 4.2.3 (R Core Team, 2023) using generalized linear models (GLMs), goodness-of-fit tests and the χ^2 statistic. Poisson or negative binomial regression was used depending on whether overdispersion was rejected or detected respectively using the package overdisp version 0.1.1 (De Freitas Souza et al., 2022). The emmeans and pairs functions of the *emmeans* package version 1.8.6 were used for post-hoc analysis of the GLMS. Tukey p-value multiple comparisons adjustments were applied, and estimated marginal means and standard error were backtransformed to the response scale.

5.2.4 Elongase gene expression

Next, we assessed whether genes were over- or underexpressed relative to the average gene expression of each species. Only expression of elongase genes was considered, since data availability for methyl-end and front-end desaturases was limited. When available, RNA sequencing files containing expression values (in RPKM, CPM, FPKM or 'Mreads') were retrieved from each studies' supplementary information or from personal unpublished data (Barreto et al., 2015; Berger et al., 2021; Boyen et al., 2020; De Wit et al., 2016; Maas et al., 2018; Roncalli, Cieslak, et al., 2022; Semmouri et al., 2019; Tarrant et al., 2014). If needed, the correct sequence names were retrieved by blasting (megablast) the sequences in our databases against the transcriptome belonging to the expression file. We first calculated the average expression per isoform across all samples in each study (regardless of experimental or observations factors), and then either way summed or averaged the expression value of multiple isoforms

(for 9 out of 37 sequences there was more than one isoform according to the used assembly method), divided this by the average expression of all transcripts and $\log_2$ transformed to obtain the $\log_2$ fold change of each desaturase or elongase gene, with values above or below 0 indicating higher or lower expression than the average expression of each species respectively. A nested additive Analysis of Variance was used to assess differences in $\log_2$ fold change between orders, species (nested within order) or elongase subfamilies (elovl1, elovl4, elovl11 or elovl6).

5.2.5 Genome localization

Sequences of the five copepod species for which chromosome-level genome data were available (*P. nana, T. californicus, T. japonicus, C. rogercresseyi* and *L. salmonis*) were aligned against the genome using BLAST (megablast) to infer the chromosomal location of each gene. Chromosomes and gene locations were visualized using the R package chromoMap version 4.1.1 (Anand & Rodriguez Lopez, 2022). For the three species where the chromosome-level genome was also functionally annotated (*T. californicus*, *C. rogercresseyi* and *L. salmonis*), we inferred proper genome anchoring by retrieving the four left and four right open reading frames (ORFs) using the NCBI Genome Data Viewer and blasting (megablast) against the NCBI nucleotide database.

5.2.6 Codon sequence characteristics

Next, we investigated differences in GC content and codon usage preference between fatty acid biosynthesis genes and other copepod genes, as these are characteristics pointing to HGT (Bourret et al., 2019; Matriano et al., 2021; Nguyen et al., 2015). A 'core' copepod database was compiled by downloading 1972 copepod sequences from the NCBI nucleotide database, filtered using the following parameters: species: Copepoda; molecular type: mRNA; sequence length: 200 to 5000 bp; sequence name: includes "complete cds". From this dataset, 29 methyl-end, front-end desaturase and elongase sequences were removed, resulting in a final dataset of 1943 'core' copepod sequences. Codon usage metrics of 'core', desaturase and elongase full-length coding sequences were calculated using the COdon Usage Similarity INdex (COUSIN) tool (Bourret et al.,

2019). Specifically, we measured total GC content (%), GC content (%) at the third codon position (GC3) and the COUSIN$_{59}$ index, which compares the codon usage preference of a gene with the average codon usage of, in this case, the core copepod genes. With the COUSIN$_{59}$ index, each family of synonymous codons contributes proportionally to the frequency of the corresponding amino acid in the query (Bourret et al., 2019). Finally, number of introns per sequence was determined for all species with chromosome-level (*P. nana, T. californicus, T. japonicus, C. rogercresseyi* and *L. salmonis*) and scaffold-level (*Acartia tonsa, Eurytemora affinis, Apocyclops royi, Oithona nana, T. kingsejongensis* and *Tisbe holothuriae*) genomes by blasting (megablast) the sequence against the corresponding genome, and normalizing to number of introns per 1000 base pairs (bp) to account for gene family differences in sequence length. For species with scaffold-level genomes, sequences were only included when they were found only once (in full-length) in the genome. Analysis of Variance and Tukey's post-hoc multiple comparisons tests (using the *emmeans* package) including p-value adjustments were used to assess differences in GC and GC3 content and normalized number of introns. One-sided t-tests (lower or higher than one) were used to test the COUSIN$_{59}$ index.

5.2.7 Selection models

To detect the occurrence of positive selection (nonsynonymous/synonymous substitution rate ratio d_N/d_S (or ω) > 1) throughout the evolution of copepod LC-PUFA biosynthesis genes, selection models were run using the codeML program in the PAML package version 4.9 (Yang, 2007) with the MUSCLE alignments and maximum likelihood trees as input. All sites with ambiguous alignment and gaps were excluded from the analysis. For each of the three gene families, we ran site models (M0, M1a and M2a for the elongases; M0, M1a, M2a, M7, M8 and M8a for the desaturases) as well as branch-site models (ω assumed to vary both among lineages and across sites, or ω assumed to be fixed at 1). Likelihood ratio tests (LRT; twice the log-likelihood difference) were used to compare models, and the Bayes empirical Bayes (BEB) method was used to calculate the posterior probability of positive selection for each site

(Álvarez-Carretero et al., 2023). For the methyl-end and front-end desaturases, branch-site models were run with the copepod sequences as foreground branch and the outgroup (oomycetes and kinetoplasts respectively) as background branch to infer positive selection following (potential) HGT. For the elongases, branch-site models were run with each subfamily (elovl1, elovl4, elovl6 and elovl11) separately as foreground branch to infer positive selection following elongase diversification. Conversion of fasta alignment files to pml files and labelling of foreground branches was done using EasyCodeML version 1.41 (F. Gao et al., 2019).

5.3 Results

In our study, we collected transcriptomic (TSA or SRA) or sequence (EST or unpublished studies) data from a total of 50 copepod species, including 31 calanoids, 1 canuelloid, 7 cyclopoids, 7 harpacticoids and 4 siphonostomatoids (Supp. Table 1). After filtering out sequences that had uncertain origins, did not contain the correct diagnostic features, or were not present on the genome (when available), we identified a total of 23 methyl-end desaturase sequences in 14 copepod species, 39 front-end desaturase sequences in 22 species and 245 elongase sequences in 48 species (Supp. Table 2). The transcriptomic data of two calanoid species (*Epischura baikalensis* and *Eucalanus bungii*) did not contain any of the genes of interest.

Methyl-end desaturases were absent in calanoids and *Canuella perplexa* but present in cyclopoids, harpacticoids and siphonostomatoids (Figure 1), with no significant variation in copy number detected between the latter three orders (χ^2 (2) = 0.80454, p = 0.6688). Front-end desaturases were present in all orders (Figure 1), but the copy number variation significantly differed between them (χ^2 (4) = 35.856, p = 3.098e^{-07}). Cyclopoids (1.14 ± 1.42, z = -3.133, p = 0.0149), harpacticoids (2.43 ± 1.28, z = -5.290, p < 0.0001), and siphonostomatoids (1.25 ± 1.56, z = -2.923, p = 0.0286) had significantly more copies of front-end desaturases compared to calanoids (0.23 ± 1.46). In calanoids, a single copy was only found in some, but not all, species of the family

Calanidae, and absent in species from other families. Elongases were present in all orders (Figure 1), and although copy number variation significantly differed between them (χ^2 (4) = 10.664, p = 0.03061), no significant differences were detected.
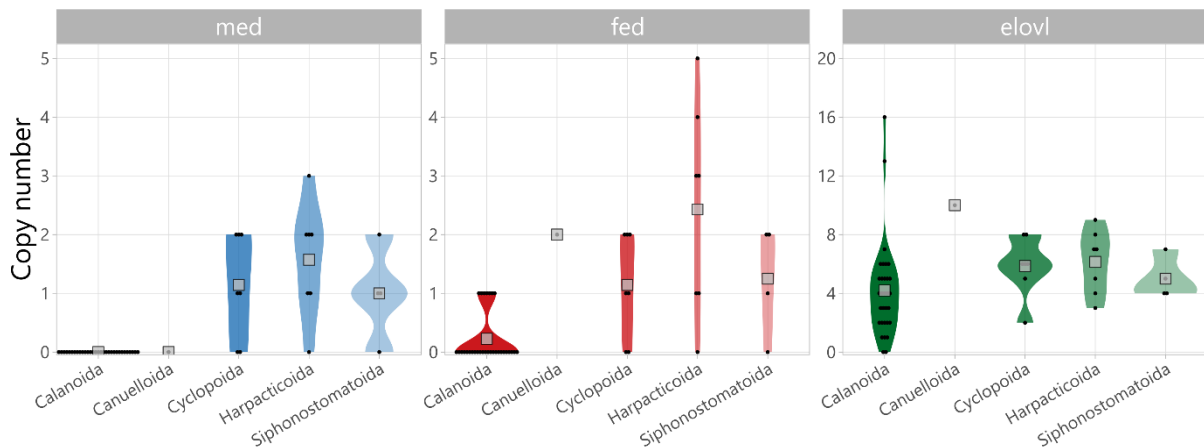
Figure 1 Violin plots of copy number of methyl-end desaturases (med), front-end desaturases (fed) and elongases (elovl) per copepod species, with grey squares indicating the mean copy number per order.

Habitat and lifestyle did not significantly influence copy number variation of methyl-end or front-end desaturases, both in models with single independent variables and in models including the interaction with the order variable (Supp. Figs. 1 to 4). However, order-specific generalized linear models showed that habitat significantly influenced the number of elongases in calanoids (χ^2 (1) = 6.365, p = 0.01164), with fewer elongase copies found in calanoid species with freshwater populations (2.00 ± 1.42) than in those without (4.52 ± 1.09) (Supp. Fig. 3). This contrasts with cyclopoids, where, although not significant (χ^2 (1) = 2.1475, p = 0.1428), more elongase copies were found in freshwater and/or brackish species (7.03 ± 1.21) than in marine species (4.35 ± 1.32).

The copepod methyl-end desaturases clustered weakly (42% bootstrap) with two annelid methyl-end desaturases, which in turn clustered strongly (100%) with another *Platynereis dumerilii* sequence (Figure 2a). The copepod methyl-end desaturase monophyletic clade itself had weak support (59%), which separated into two weakly supported clades (fig. 2a). In contrast, the copepod front-end desaturase formed a strongly supported (100%) monophyletic clade, but again composed of weakly supported subclades (Figure 2b). Notably, the calanoid front-end desaturase formed a

strongly supported (100%) monophyletic clade but was nested within a larger clade comprising harpacticoid sequences. Another interesting clade was the moderately supported (62%) clade consisting of multiple copies per species of the harpacticoid genus *Tigriopus* and *Tisbe* sp., except for *T. holothuriae* that only has one copy.

Figure 2 Maximum-likelihood phylogenetic trees of (a) methyl-end desaturases and (b) front-end desaturases. Node labels show bootstrap support after 100 RAxML iterations. Different colour shades of branches indicate different copepod orders. Outgroups are coloured black.

Figure 3 Maximum-likelihood phylogenetic tree of copepod fatty acid elongases. Node labels show bootstrap support after 100 RAxML iterations. Different colour shades of branches indicate different copepod orders.

Regarding the elongase subfamilies, elovl6 was found in all five orders. When present, only one elovl6 copy per species was found, except for *Calanus helgolandicus* (4 copies), *C. sinicus* (3 copies), *Rhincalanus gigas* (3 copies) and *Eucyclops serrulatus* (2 copies). Similarly, elovl4 was found as a single copy in all orders except Canuelloida (*C. perplexa*), and eight single-copy sequences from the recently discovered elovl11 elongase subfamily were found in cyclopoids and harpacticoids (including the functionally characterized *T. californicus* "elo4"), but not in calanoids, *C. perplexa* or siphonostomatoids. The elovl1/7 subfamily in copepods exhibited extensive diversification, forming two large, well-supported monophyletic clades: one (77%) comprising exclusively gymnoplean (calanoid) sequences, and the other (93%) comprising exclusively podoplean sequences (Figure 3). The gymnoplean subclade further divided into three strongly supported subclades, hereafter referred to as elovl1α (90%), elovl1β (92%) and elovl1γ (90%), with many calanoid species possessing at least one or more copies of the elovl1α and elovl1γ subclades. The podoplean clade was roughly comprised of four subclades with moderate to high bootstrap support (Figure 3). Elongases elovl1δ (80%) and elovl1η (62%) were retrieved in all four podoplean orders, while elovl1ε (61%) was only found in harpacticoids, cyclopoids and *C. perplexa*, and elovl1ζ (100%) only in the harpacticoids *Tigriopus* and *Tisbe*. Elongase elovl1δ showed further duplication in two weakly supported clades (50% and 33%), with more subsequent order-, genus- or species-specific duplications (Figure 3). Furthermore, 18 out of 29 sequences of the elovl1δ subclade contained the recently discovered conserved histidine box "QXXHH" (Boyen et al., 2023) as opposed to "HXXHH" found in other elongases, however this feature was not monophyletic.

When comparing elongase gene expression (sum of expression of all isoforms per gene) with the mean expression per species (for the eight studies with count data available; Supp. Table 3), a significant difference was found between orders ($F_{(1, 27)}$ = 8.8998, p = 0.005986, Figure 4) but not between species (nested in order) ($F_{(5, 27)}$ = 2.1164, p = 0.094107, Supp. Fig. 5) or between subfamilies ($F_{(3, 27)}$ = 2.5784, p = 0.074385, Supp. Fig. 6). On average, calanoids (n = 6) exhibited lower expression (in

log$_2$ fold change) of elongase genes than the average gene expression (-2.05 ± 0.43), whereas harpacticoids (n = 2) showed higher expression than average (0.51 ± 0.74). This remained consistent (order: (F(1, 27) = 6.1353, p = 0.01981); species: F(5, 27) = 1.4905, p = 0.22577; subfamily: F(3, 27) = 2.6616, p = 0.06818) when considering the average isoform expression per gene instead of the sum (Supp. Figs. 7 to 9).
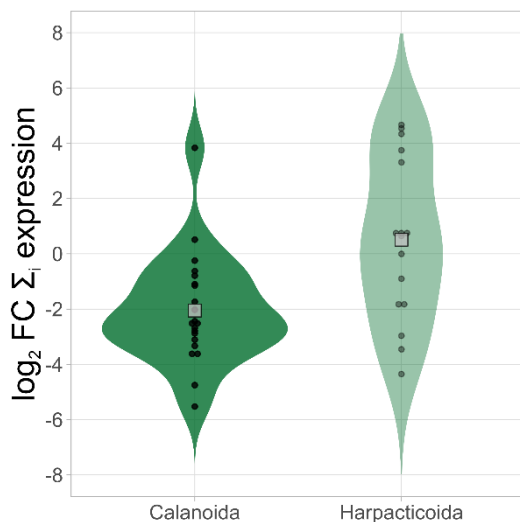
Figure 4 Violin plots of log$_2$ fold change (FC) of elongase gene expression (sum of isoform expression, Σ$_i$) relative to average expression per species. Grey squares indicate the mean expression over all elongases per order.

In the five species where chromosome-level genomes were available (Supp. Table 4), the functionally related genes failed to exhibit a clear clustering and were found to be dispersed across multiple chromosomes, with substantial variation observed among the different species (Figure 5). For instance, in siphonostomatoids, *C. rogercresseyi* displayed eight identified genes distributed across four chromosomes, whereas *L. salmonis* exhibited the same number of genes but across eight chromosomes. An exception to this trend was observed in the case of recently duplicated genes, which were found to be in close proximity to one another (Figure 5). Specifically, duplicated elovl1δ genes in *P. nana*, *T. californicus*, *T. japonicus* and (albeit with some distance) *C. rogercresseyi*, as well as two recently duplicated front-end desaturases (fed3 and fed4) in *T. californicus* and *T. japonicus*, were localized near each other (Figure 5). Three genes of *T. japonicus* (fed3, fed4 and elovl6) failed to map to one of the linkage groups, and were found on two scaffolds instead. In the three species with well-annotated

153

chromosome-level genomes (Supp. Table 4), their LC-PUFA biosynthesis genes were flanked with various genes previously observed in other metazoans and copepods (Supp. Table 5). Except for recently duplicated genes located next to each other, none of the flanking genes identified were related to fatty acid metabolism processes.
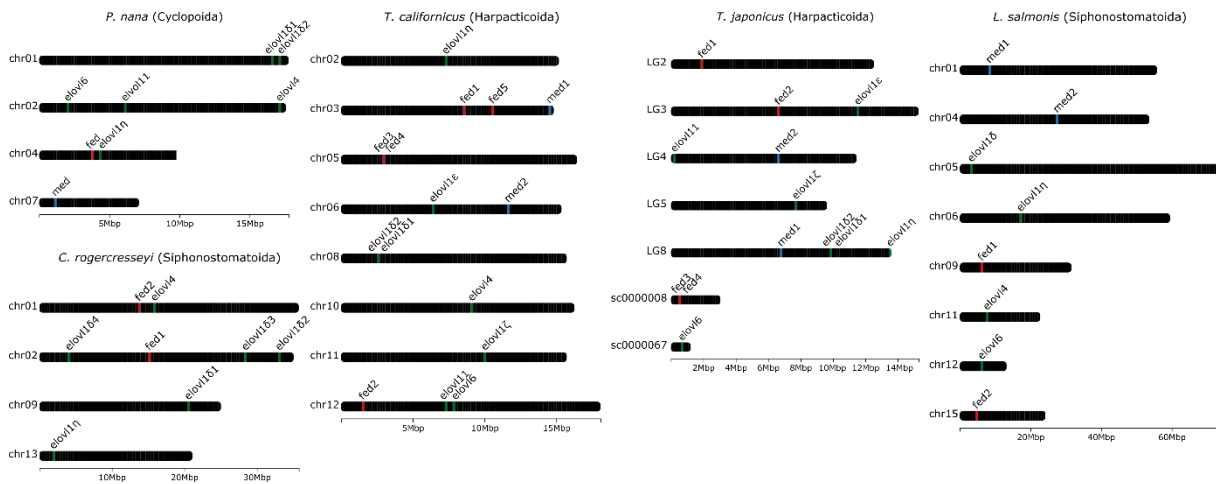
Figure 5 Chromosome locations of copepod genes. Elongases are named according to their subfamily, methyl-end desaturases (med) and front-end desaturases (fed) are numbered arbitrarily. Chromosome numbers are arbitrarily and do not correspond between species.

Next, we assessed multiple sequence characteristics that might indicate a gene origin through HGT. Total GC content significantly differed ($F_{(3, 2224)}$ = 38.437, $p < 2.2e^{-16}$) between core copepod genes (50.88 ± 0.13 %) and methyl-end desaturases (47.12 ± 1.15 %, t = -3.256, p = 0.0063), front-end desaturases (47.37 ± 0.89 %, t = -3.889, p = 0.0006) and elongases (47.22 ± 0.35 %, t = -9.764, p < 0.0001) (Supp. Fig. 10). Furthermore, the GC3 content significantly differed between gene families ($F_{(3, 2224)}$ = 3.0033, p = 0.02938) (Figure 6a). While the GC3 content in elovl (62.41 ± 0.87 %, t = 0.016, p = 1.000) was nearly equal compared to core genes (62.39 ± 0.31 %), it was lower but not significantly in methyl-end desaturases (58.48 ± 2.83 %, t = -1.374, p = 0.5156), and significantly lower in front-end desaturases (56.42 ± 2.20 %, t = -2.682, p = 0.037). Total GC content and GC3 content did not significantly differ among the three LC-PUFA biosynthesis gene families. The COUSIN$_{59}$ index, calculated against the codon usage of the core copepod genes, was lower but not significantly different than 1 for methyl-end desaturases (0.79 ± 0.19, t(22) = -1.2045, p = 0.1206), significantly lower than 1 for front-end desaturases (0.74 ± 0.14, t(37) = -2.3698, p = 0.01156), and

154

significantly higher than 1 for elongases (1.07 ± 0.06, t(242) = 1.7342, p = 0.04208) (Figure 6b). Number of introns per 1000 bp, assessed using only sequences of species with chromosome- or scaffold-level genome data, significantly differed between gene families (F(2, 84) = 3.5616, p = 0.03276), with significantly more introns in elongases (3.02 ± 0.30) compared to methyl-end desaturases (1.19 ± 0.65, t = -2.569, p = 0.0317), but not compared to front-end desaturases (2.28 ± 0.51, t = -1.248, p = 0.4282) (Figure 6c).
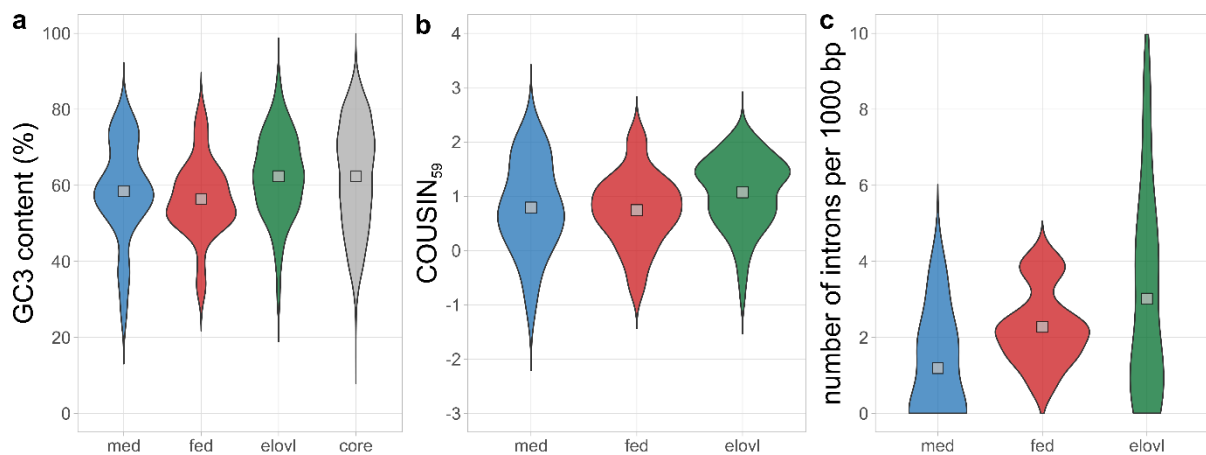
Figure 6 Violin plots of (a) GC content at the third codon position (GC3, %), (b) COUSIN$_{59}$ index, and (c) number of introns per 1000 base pairs (bp) of methyl-end desaturases (med), front-end desaturases (fed), elongases (elovl) and (for GC3 content) core copepod genes. Grey squares indicate the mean per gene family.

For all three gene families, no positive selection was detected by the site model comparisons (Supp. Table 6). Under the branch-site models, both methyl-end desaturases and front-end desaturases showed significant positive selection following presumed HGT. However, only for methyl-end desaturases we found specific sites (n = 6) with a probability of positive selection higher than 95% according to the BEB analysis (Table 1). The branch-site models of elongases showed significant positive selection for all four subclades, although only for the elovl4 branch there were two sites with a probability of positive selection higher than 95% (Table 1).

Table 1 Log likelihood values (Ln L), parameter estimations, likelihood ratio test (LRT) p-values and Bayes empirical Bayes (BEB) analysis output under the branch-site models (A and A₀) of the different gene (sub)families. np: number of free parameters; p: proportion of sites belonging to each site class; ω_0: background branch ω ratio; ω_1: foreground branch ω ratio; Pr(ω>1) > 95%: sites with probability higher than 95% to be under positive selection according to Bayes empirical Bayes (BEB) analysis. Amino acid sites are relative to the Aphanomyces invadans methyl-end desaturase and the Platychelipus littoralis elovl4 elongase sequences in the respective codon alignment.

Gene family	Model	np	Ln L	Estimates of parameters					LRT p-value	Pr(ω>1) > 95%
med	A	67	-19741.69	Site class	0	1	2a	2b		
				p:	0.769	0.126	0.090	0.015		
				ω_0	0.072	1	0.072	1		13, 17, 100, 138, 218, 234
				ω_1	0.072	1	999	999		
	A₀	66	-19748.32	ω	1				**2.70e⁻⁴**	
fed	A	85	-33549.48	Site class	0	1	2a	2b		
				p	0.606	0.042	0.329	0.023		
				ω_0	0.062	1	0.062	1		
				ω_1	0.062	1	999	999		-
	A₀	84	-33553.06	ω	1				**7.43e⁻³**	
elovl6	A	495	-145797.57	Site class	0	1	2a	2b		
				p	0.443	0.290	0.161	0.105		
				ω_0	0.097	1	0.097	1		
				ω_1	0.097	1	333.688	333.688		-
	A₀	494	-145803.89	ω	1.000				**3.77e⁻⁴**	
elovl11	A	495	-145800.50	Site class	0	1	2a	2b		
				p	0.368	0.241	0.236	0.155		
				ω_0	0.097	1	0.097	1		
				ω_1	0.097	1	21.556	21.556		149, 269
	A₀	494	-145803.05	ω	1.000				**2.38e⁻²**	
elovl4	A	495	-145790.66	Site class	0	1	2a	2b		
				p	0.450	0.294	0.155	0.101		
				ω_0	0.097	1	0.097	1		
				ω_1	0.097	1	499.892	499.892		-
	A₀	494	-145800.78	ω	1.000				**6.87e⁻⁶**	
elovl1	A	495	-145800.00	Site class	0	1	2a	2b		
				p	0.426	0.277	0.180	0.117		
				ω_0	0.097	1	0.097	1		
				ω_1	0.097	1	600.079	600.079		-
	A₀	494	-145804.69	ω	1				**2.18e⁻³**	

5.4 Discussion

As copepods radiated to a diversity of habitats and lifestyles, it remained unclear to which extent their fatty acid metabolism and biosynthesis capacity evolved along with this ecological diversification process. In this study, we provide evidence that supports previous hypotheses that calanoids, as opposed to cyclopoids, harpacticoids and siphonostomatoids, do not contain methyl-end desaturases and front-end desaturases, with the sole exception of a single-copy front-end desaturase in species of the Calanidae genera *Calanus* and *Neocalanus*. Considering the existence of orthologous methyl-end desaturases in annelids, rotifers and molluscs (Kabeya et al., 2018), and front-end desaturases in Calanidae, a plausible hypothesis is that of HGT from oomycetes and kinetoplasts preceding the gymnoplean-podoplean divergence about 400 million years ago (Schwentner et al., 2017), and a subsequent gene loss of both groups of desaturases within calanoids. However, other evolutionary processes might also be at play. The absence of desaturases in most calanoids would imply that they, as opposed to other copepods, have no capacity for endogenous *de novo* PUFA synthesis, and a minimal or non-existent capacity for LC-PUFA bioconversion from dietary precursors. While some laboratory incubation experiments confirm this trait loss (Bell et al., 2007), others do not (Helenius et al., 2020; Nielsen et al., 2019; Titocci & Fink, 2022). As predominantly zooplankton species, calanoids primarily rely on consuming high-quality, LC-PUFA-rich pelagic diatoms during seasonal blooms (Falk-Petersen et al., 2009). Many store the acquired fatty acids as wax esters in a specialized lipid sac, which serves as their primary energy source during overwintering diapause, potentially reducing the need for endogenous biosynthesis. This contrasts with the general habitats of harpacticoids (benthos) and cyclopoids (freshwater), with lower and more stochastic levels of LC-PUFA availability (Twining et al., 2021) and a higher need for endogenous biosynthesis, and therefore both groups of desaturases were possibly retained in these orders (Boyen et al., 2023; Kabeya et al., 2021).

The single-copy front-end desaturase retained in *Calanus* and *Neocalanus* species aligned closely with the functionally characterized Δ4 front-end desaturase of the harpacticoids *P. littoralis* and *T. californicus*, which, together with a fatty acid elongase, enables the conversion of EPA towards DHA (Boyen et al., 2023; Kabeya et al., 2021). If the calanoid desaturases would also be Δ4 front-end desaturases, this would mean that these high-latitude calanoids retained the ability to obtain their observed high levels of phospholipid DHA from pelagic diatoms high in EPA but low in DHA (Falk-Petersen et al., 2009; Scott et al., 2002). However, the low bootstrap support of subclades found in the phylogenetic analyses of both desaturases does not allow us to discern whether specific regioselectivities and substrate preferences have evolved monophyletically following duplication and neofunctionalisation, as suggested previously for Δ4 front-end desaturases (Boyen et al., 2023).

As for the elongase gene family, while elovl4, elovl6 and elovl11 appear to have mostly single copies across most orders, we found extensive diversification of the elovl1/7 (hereafter referred to as elovl1) subclade, with two divergences for the gymnopleans (calanoids) and podopleans separately. It is noteworthy that while elovl1 experienced this significant diversification, other elongases genes mostly maintained a more conservative pattern with single-copy representation. Among pancrustaceans, this elovl1 radiation has also occurred independently in Hexapoda and Branchiopoda (Finck et al., 2016; Kabeya et al., 2021; Ramos-Llorens et al., 2023b) but not to this extent in Malacostraca (Mah et al., 2019; Ribes-Navarro et al., 2021). The specific reasons behind this extraordinary expansion of elovl1 and its subsequent divergence into gymnoplean and podoplean subgroups remains to be further explored. While harpacticoid elovl1 elongases are shown to elongate PUFAs and LC-PUFA (Boyen et al., 2023; Kabeya et al., 2021), the functionality of the three different calanoid elovl1 subfamilies remains unknown. The increased elongase copy number found in marine calanoids compared to freshwater ones (but not in cyclopoids) disputes observations in fish, where desaturase duplications following transitions to LC-PUFA poor freshwater environments were observed (Ishikawa et al., 2019; Matsushita et al., 2020). However,

as more transcriptomes with also more recent release dates and a relatively higher quality were found in marine calanoids compared to freshwater ones, especially for *Calanus* species (Hartline et al., 2023; Lizano et al., 2022), a more targeted study comparing marine and freshwater copepods could better resolve this question. It is also interesting to note that parasitic copepods (siphonostomatoids but also certain cyclopoids) retained similar copy numbers of all three genes families despite parasitizing on hosts with high LC-PUFA levels, such as marine fish and mussels (Twining et al., 2021). Potentially, the emergence of parasitic copepods is too recent that the potentially redundant PUFA biosynthesis genes have not yet disappeared from their genomes (Bernot et al., 2021, 2023). Alternatively, parasitic copepods might not easily have access to host LC-PUFA deposits in muscle, liver or brain tissues, and therefore could still benefit from having PUFA biosynthesis genes.

Furthermore, the calanoid copepods *C. helgolandicus* and *C. sinicus* were found to have 16 and 11 elongase copies, respectively. As there is no genome data for these species, we cannot unequivocally confirm that these are true elongases belonging to those species as we were able to do for, for instance, *Oithona nana*. Alternatively, these could potentially be attributed to species misidentification, cryptic species and/or poor transcriptome assembly. Moreover, since the transcriptome of only one species of Canuelloida (*Canuella perplexa*) was available, any claims about the absence of methyl-end desaturases and a high number of elongases (10 in *Canuella perplexa*) as a common feature of canuelloids can only be resolved with additional transcriptomic and/or genomic data. Importantly, it is plausible that many desaturase and elongase sequences remain undetected in many copepod species using our comparative transcriptomic approach. Additional high-quality transcriptomic and genomic data, together with functional characterization studies, could possibly uncover even more copepod LC-PUFA biosynthesis genes. Moreover, here we discovered new genes based on sequence (dis)similarity and assumed that near-identical sequences were transcript variants. Therefore, while this tree-based approach is considered a valid method for

detecting gene duplication (Lallemand et al., 2020), recently duplicated genes at the species level with high sequence similarity might be missed.

Even more compelling evidence on the differences in LC-PUFA biosynthesis between calanoids and other copepods could be found when analysing the expression level of elongases relative to the species-specific gene expression, where harpacticoid elongases were higher expressed than calanoid elongases. However, comparing gene expression between studies and species should be done with care (Romero et al., 2012). To more accurately infer possible differences in expression between orders (not only for elongases, but also for methyl-end and front-end desaturases), count data can be calculated using the SRA data from all 72 transcriptome studies in our dataset, as opposed to using count data gathered from supplementary files, as was done here. In a comparative study, Lee, et al. (2020b) showed elongase upregulation in the harpacticoid copepod *T. japonicus* but not in the cyclopoid *P. nana* as a response to the LC-PUFA deficient diet *Chlorella* sp. Moreover, comparative studies using fatty acid specific stable isotope analysis have also shown differences in LC-PUFA biosynthesis rates between calanoids and cyclopoids (Nielsen et al., 2020b) or between calanoids and harpacticoids (Sahota et al., 2022) under dietary LC-PUFA limitation.

Apart from recently duplicated genes, no genome clustering was observed between or within the three gene families in species with chromosome-level genomes. While the lack of clustering can be attributed to poor resolution in genomes with linkage maps as proxy for chromosomes (e.g. *T. japonicus*), the non-clustering witnessed in the other four genomes as well suggests this is a consistent biological feature among copepods. In contrast, the insect Δ15 desaturase gene family, derived from a Δ9 desaturase duplication, was found to be clustered on a limited number of chromosomes/scaffolds in most species tested (Helmkampf et al., 2015). The non-clustering of functionally related genes indicates that they are likely governed by distinct regulatory mechanisms, often leading to specific gene activities in different locations within the organism. In fish for instance, specific front-end desaturases and elongases are shown to be

differentially expressed in different tissues (De la Cruz-Alvarado et al., 2021; Xu et al., 2020). Since no chromosome-level genome was available for any calanoid species, we could not investigate synteny of desaturases and elongases for this order. Increased calanoid genome data are therefore imperative, especially when considering that this order currently has more species with available transcriptome data than all other orders combined. While the flanking regions of desaturases and elongases do not seem to be related to fatty acid metabolism processes, they are classified as genuine metazoan or copepod genes (or non-coding DNA), affirming that genes from all three gene families are appropriately genome-anchored. This provides evidence that methyl-end and front-end desaturases are likely horizontally transferred, and not merely a result of non-metazoan contamination during sampling.

Further indications of HGT of the methyl-end desaturases and front-end desaturases, apart from the phylogenetic patterns detected earlier (Kabeya et al., 2018, 2021), was found by the reduced GC3 content and COUSIN$_{59}$ index compared to elongases and other 'core' copepod genes. However, differences were small and only significant in front-end desaturases. In contrast, increased GC3 content was found in HGT genes of other organisms (Matriano et al., 2021; Nguyen et al., 2015). Estimated GC3 content of the oomycete *Phytophthora* (55.67%) is lower than all four copepod gene groups (Jiang & Govers, 2006), while high variation in GC3 content (~51-86%) exists in kinetoplasts (Alvarez et al., 1994). It is plausible to assume that, since the event of HGT happened already at least 400 million ago (prior to the divergence of gymnopleans and podopleans), the codon usage selectively evolved and converged over time towards the codon usage preference of the core copepod genome, improving efficiency of gene translation (Callens et al., 2021; Tuller, 2011), and resulting in only limited evidence of horizontal transfer. Horizontal transfer of other types of desaturases was also found in other arthropods (Bryon et al., 2017) as well as fungi (Herzog et al., 2020). Horizontal transfer often occurs via retrotransposition and therefore HGT genes generally lack introns immediately after transferring (Kabeya et al., 2018). However, many copepod desaturases contain introns (albeit significantly fewer in methyl-end desaturases than

elongases), which can be a result of the long evolutionary timescale during which introns were inserted.

While no positive selection was detected on the entirety of each of the three gene families (site models), positive selection of specific sites was detected for both desaturases following HGT and for elongases following divergence into specific subclades (branch-site models). This is similar with selection analyses on desaturases and elongases in Actinaria, where site models and branch models detected mainly pervasive purifying (i.e. negative) selection but, branch-site models mainly detected positive selection (Surm et al., 2018). Intriguingly, branch-site models indicated strong positive selection on the independently evolved hexapod Δ15 desaturase in *Drosophila*, particularly directly after gene duplication (Fang et al., 2009), but not in other insects (Helmkampf et al., 2015). Overall, our results imply considerable evolutionary constraints on the gene families as a whole, but positive (diversifying) selection on specific codons following HGT and duplication events, which potentially led to altered substrate specificity, improving fitness in the process.

Overall, we provided the first large-scale assessment of all three PUFA biosynthesis gene families (methyl-end desaturases, front-end desaturases and elongases) of an entire class of animals. As we showed that calanoids (as opposed to other copepods) have evolved to be less dependent on endogenous LC-PUFA biosynthesis and more dependent on dietary LC-PUFA provision and subsequent storage, the projected decline of LC-PUFA production in microalgae will predominantly affect them over other orders (Hixson & Arts, 2016; Holm et al., 2022). Since calanoids are dominant members of marine zooplankton communities and an important source of nutrients for fish and other marine animals, higher trophic levels will likely be profoundly affected as well (Colombo et al., 2020). However, copepod orders with suspected complete LC-PUFA biosynthesis capabilities such as harpacticoids and cyclopoids are also known to be important food sources for, for instance, juvenile fish, especially at inshore nursery grounds (Gee, 1987, 1989). Nevertheless, apart from dietary LC-PUFA limitations, ocean

warming and ocean acidification might also directly impair copepod LC-PUFA levels and biosynthesis (Alma et al., 2020; Boyen et al., 2020; Rossoll et al., 2012; Sahota et al., 2022). The potential LC-PUFA biosynthesis capabilities of specific copepod orders and other primary consumers, and their response towards environmental changes should not only be integrated in trophic web modelling studies using fatty acids as trophic markers (Galloway & Budge, 2020), but also in projection models estimating climate-driven declines in LC-PUFA availabilities for higher trophic levels and, ultimately, humans (Colombo et al., 2020).

CHAPTER 6

GENERAL DISCUSSION

6.1 Overall findings
  6.1.1 PUFA biosynthesis capacity evolved alongside copepod diversification
  6.1.2 Harpacticoids possess a functionally diverse repertoire of PUFA biosynthesis genes
  6.1.3 Copepod PUFA biosynthesis is affected by multiple climate drivers
  6.1.4 A mechanism for climate change resilience?

6.2 Scientific recommendations
  6.2.1 Quantify potential contribution of copepods to LC-PUFA provisioning, in both a present and a future climate
  6.2.2 Sequence additional copepod genomes and transcriptomes
  6.2.3 Explore short-term adaptation potential of copepods and their LC-PUFA biosynthesis metabolism to climate drivers
  6.2.4 Establish a scientifically robust definition of daily recommended intake of EPA and DHA

6.3 Policy recommendations
  6.3.1 Reach net zero greenhouse gas emissions by 2050 to limit warming below 1.5°C
  6.3.2 Restore aquatic habitats and remove compound stressors
  6.3.3 Ensure sufficient LC-PUFA provisioning for all within environmentally safe boundaries

6.4 General conclusions

6.1 Overall findings

As the Earth warms and oceans absorb heat and CO_2, ocean food webs are profoundly affected (Doney et al., 2012). At the base of these food webs, changes in primary producer community assemblages (Taucher et al., 2022) coincide with organism-level physiological reductions in production of long-chain polyunsaturated fatty acids (LC-PUFAs) (Hixson & Arts, 2016). During this PhD project, I set out to assess the capacity of copepods as pivotal primary consumers (at the basis of aquatic food webs) for LC-PUFA biosynthesis, considering that this mechanism might partially compensate for the reduction of LC-PUFA availability in microalgae, and subsequent provisioning for higher trophic levels (humans and other animals). In this discussion, I commence with how copepods obtained their polyunsaturated fatty acid (PUFA) biosynthesis capacity throughout their evolution. Then, I continue with the finding that harpacticoids have not only a phylogenetically but also a functionally diverse repertoire of PUFA biosynthesis genes. Afterwards, I discuss how this PUFA biosynthesis mechanism is utilised as a response to multiple climate drivers, and argue whether copepod LC-PUFA biosynthesis could be a mechanism for climate change resilience. Finally, I provide a number of scientific and policy-related recommendations that result from my PhD research and the insights I obtained.

6.1.1 PUFA biosynthesis capacity evolved alongside copepod diversification

In **Chapter 5**, we found that the presence of PUFA biosynthesis genes in copepods is highly determined by phylogenetic descendence. Since copepods diverged from other pancrustaceans about 500 million years ago (Schwentner et al., 2017), they have adapted to a wide variety of marine, freshwater and even terrestrial habitats (Walter & Boxshall, 2023). Through what were possibly horizontal gene transfer (HGT) events, a copepod ancestor obtained the methyl-end desaturases and front-end desaturases that are critical for endogenous LC-PUFA biosynthesis, in addition to the already acquired elongase genes likely conserved among metazoans. In Chapter 5, we suggest that both desaturase genes families were transferred prior to the gymnoplean-

podoplean divergence about 400 million years ago, given the presence of orthologous methyl-end desaturases in certain other protostomes (annelids, rotifers and molluscs), and front-end desaturases in species of the calanoid family Calanidae (Table 1).

*Table 1 Overview of fatty acid desaturase and elongase genes in metazoans and sources of information. Colored boxes indicate presence in all (or some) species per clade. For copepods, we added the minimum and maximum copy number per species as determined in Chapter 5. * In calanoids, front-end desaturases are only present in some Calanidae species. ** Since only one Polyarthran transcriptome was assessed, the absence of methyl-end desaturases in the entire order remains to be confirmed. *** Hexapod Δ12 desaturases evolved independently from stearoyl-CoA desaturases. "Some" refers to the fact that methyl-end desaturases have so far been discovered in only a fraction of species within each group (Kabeya et al., 2018).*

	med	fed	elovl	sources
Copepoda				
Calanoida	-	0/1 *	0-16	Chapter 5
Polyarthra	- ? **	2	10	Chapter 5
Cyclopoida	0-2	0-2	2-8	Chapter 5
Harpacticoida	0-3	0-5	3-9	Chapters 2, 3 and 5
Siphonostomatoida	0-2	0-2	4-7	Chapter 5
Other Pancrustacea				
Malacostraca	-	-		(Ribes-Navarro et al., 2021; Ting et al., 2020)
Brachiopoda	-	-		(Finck et al., 2016; Ramos-Llorens et al., 2023b)
Hexapoda	***	-		(Finck et al., 2016; Helmkampf et al., 2015)
Other animal phyla				
Cnidaria	some			(Kabeya et al., 2018; Surm et al., 2018)
Nematoda	some			(Beaudoin et al., 2000; Kabeya et al., 2018; Menzel et al., 2019)
Annelida	some			(Kabeya et al., 2018; Ramos-Llorens et al., 2023a)
Rotifera	some			(Kabeya et al., 2018; Lee et al., 2019b, 2022a)
Mollusca	some			(Kabeya et al., 2018; Surm et al., 2015)
Echinodermata	-			(Kabeya et al., 2017; Liu et al., 2017)
Chordata	-			(Lopes-Marques et al., 2018; Monroig et al., 2022)

Although we provided additional evidence for the possibility of horizontal desaturase gene transfers in Chapter 5 (genome anchoring, GC3 content, intron number and codon usage bias), the precise timing and definitive origin of these transfers remain elusive, requiring additional genomic/transcriptomic data from rare copepod taxa (such as the basal Platycopioida), other pancrustacean taxa, and possible gene donor taxa, which are not currently available. Complicating matters is the current unresolved

phylogeny of Pancrustacea (Lozano-Fernandez et al., 2019; Schwentner et al., 2017), which does not allow us to assess the closest relatives of copepods and the potential presence of fatty acid desaturases. Recent improved analyses might resolve this issue (Bernot et al., 2023). Additionally, time-calibrated gene trees of the desaturase genes could be constructed, which seems to be possible even on highly duplicating gene families (Musilova et al., 2019). Time-calibrated desaturase gene trees, when cross-referenced with species trees, could shed novel light on the precise timing of the horizontal gene transfers.

Notably, a horizontal gene transfer of methyl-end desaturases prior to pancrustacean diversification would imply the loss of this gene family in all Pancrustacea except for (podoplean) Copepoda (Table 1). While the loss of PUFA biosynthesis capacity seems reasonable from an ecological perspective for marine pelagic species such as calanoids and euphasiids (krill) with generally LC-PUFA-rich diets, it likely posed ecological challenges for groups occupying benthic and/or freshwater habitats with dietary LC-PUFA limitations (decapods, cladocerans,...) (Twining et al., 2021). Consequently the question remains on what actually caused this gene loss. An alternative hypothesis could be that methyl-end desaturases transferred to podoplean copepods independently from the methyl-end desaturases that transferred to the lophotrochozoan phyla (annelids, molluscs and rotifers) (Kabeya et al., 2018), with a subsequent convergent evolution. The existence of methyl-end desaturases solely in certain species within each lophotrochozoan phylum, while absent in others, possibly substantiates this hypothesis (Table 1).

In contrast, front-end desaturases were likely only transferred to the most recent common ancestor of copepods (or Neocopepoda), with a subsequent gene loss in all assessed calanoids except for some (but not all) Calanidae species (Table 1). In Chapter 5, we show that the front-end desaturases retained in *Calanus* and *Neocalanus* species are homologous to harpacticoid front-end desaturases with known Δ4 desaturation activity, enabling conversion from 22:4n-6 to 22:5n-6, and, more

importantly, from 22:5n-3 to docosahexaenoic acid (DHA). If the *Calanus* and *Neocalanus* front-end desaturases also have this Δ4 desaturation activity, it would enable these species to produce DHA from dietary obtained eicosapentaenoic acid (EPA). *Calanus* and *Neocalanus* species occur in high latitude areas in the Northern Atlantic, Northern Pacific and Arctic Oceans (Hartline et al., 2023; Lizano et al., 2022), and the ability to produce fatty acids (FAs) with more than five double bonds could be an adaptation mechanism to maintain phospholipid membrane viscosity at very low sea surface temperatures (SSTs). Pond and co-authors also highlight the importance of DHA for vertically migrating and diapausing calanoids to withstand both high pressures and low temperatures at great depths (Pond et al., 2014).

The third PUFA biosynthesis gene family considered herein, the elongases, is consistently present across all copepod groups, mirroring their ubiquitous presence in all metazoans (Table 1). Note, however, that the presence of only elongases does not enable production of the physiologically important LC-PUFAs arachidonic acid (ARA), EPA and DHA by itself, as the biosynthesis of these LC-PUFAs from any FA precursor always necessitates the presence of some kind of desaturase (see Chapter 1 Figure 7). Nevertheless, in Chapter 5 we find that all copepod orders have increased elongase copy numbers, with substantial diversification and gene duplication of the elovl1 subfamily. This impressive diversification of elovl1 is also observed in Branchiopoda and Hexapoda (Finck et al., 2016; Ramos-Llorens et al., 2023b), while in malacostracans only one (Amphipoda) or at most two (Decapoda) elovl1/7 elongases are found (Ribes-Navarro et al., 2021; Ting et al., 2020). Fatty acyl elongase multiplication possibly enabled copepods to elongate a high diversity of FA substrates, both PUFAs and saturated fatty acids (SFAs), to create very-long-chain ($>C_{24}$) FAs with maybe as of yet unknown functions (see Chapter 3). Moreover, fatty acyl elongases in calanoids (which would still need to be functionally characterized) would allow these species to build up carbon-dense lipid reserves with long-chain or very-long-chain FAs, further contributing to the seasonal lipid pump when they hibernate and transport these

carbon-dense lipids below the permanent pycnocline (Boyd et al., 2019; Jónasdóttir et al., 2015).

Fatty acid desaturases and elongases are suggested as *ecological keystone genes* that have "disproportionately large effects on community and ecosystem functions" (Závorka et al., 2023). Indeed, the significance of methyl-end and front-end desaturases as well as elongases in many copepods transcends individual species, and concerns the functioning of entire aquatic ecosystems. As many copepods are pivotal and abundant primary consumers within meiofauna and zooplankton community assemblages, it is reasonable that a substantial proportion of the LC-PUFA supply for higher trophic levels is provided by the endogenous biosynthesis and/or bioconversion within copepods. A critical next step is quantifying this amount, and comparing it with the LC-PUFA production of primary consumers (see Scientific Recommendations).

6.1.2 Harpacticoids possess a functionally diverse repertoire of PUFA biosynthesis genes

Based on our research on *P. littoralis* in **Chapter 3** (Boyen et al., 2023) as well as work on *T. californicus* (Kabeya et al., 2021), we now know that these two harpacticoid species have not only a phylogenetically, but also a functionally diverse PUFA biosynthesis gene repertoire. PUFA biosynthesis genes have been functionally characterized in only one other copepod species, being the siphonostomatoid *L. salmonis*, which possess one Δ12/15 and one Δ15/17/19 (or ω3) methyl-end desaturase (Kabeya et al., 2018). While all genes and functions necessary for complete endogenous LC-PUFA biosynthesis from oleic acid were found and characterized in *T. californicus*, this was not the case for *P. littoralis*, in which we failed to find a Δ12 methyl-end desaturase or Δ5/6/8 front-end desaturases. Unless these genes would be uncovered in *P. littoralis* and characterized using updated sequencing and transcriptome assemblies, this indicates that *P. littoralis* does not have complete LC-PUFA biosynthesis capacity. In the latter case, it would always need to obtain its observed high LC-PUFA levels from diets containing pre-formed (LC-)PUFA, some of which can serve as biosynthetic

precursors. Functional characterization of other PUFA biosynthesis genes in other harpacticoids with available transcriptomes such as *Tisbe* sp. but also RNA sequencing of other harpacticoid genera would reveal whether complete endogenous biosynthesis is common in harpacticoids, or is a unique feature of only few species including *T. californicus* (Kabeya et al., 2021).

Not only is the presence of front-end desaturases in copepods unique among all pancrustaceans, harpacticoid copepods such as *Tigriopus* and *Tisbe* sp. have front-end desaturase copy numbers that are unparalleled in other copepod orders (Boyen et al., 2023; Kabeya et al., 2021; Lee et al., 2020a) and possibly all other animal phyla. High front-end desaturase copy numbers are also found but not yet functionally characterized in *Brachionus* rotifers (Lee et al., 2019a). However, the eight proposed FA desaturases also include first desaturases and (likely) functionally unrelated sphingolipid desaturases, bringing the number of putative front-end desaturases ('Δ5/6' according to the authors) to five.

Overall, we found that the presence of multiple functional front-end desaturases and elongases allows *P. littoralis* to produce highly unsaturated FAs as well as very-long-chain SFA and PUFAs, which are often disregarded in analyses due to their low quantities and measurement complexity (Serrano et al., 2021). However, these likely serve critical neurological or other still unknown functions, as PUFAs up to 44 carbons units are present in the vertebrate brain and retina, and are produced by means of the elovl4 elongase (Morais et al., 2020; Serrano et al., 2021). This shows an additional role of dietary EPA and DHA to serve as precursors for very-long-chain FAs. Moreover, our findings on *P. littoralis* open up new research areas concerning very-long-chain FA importance and capacity for biosynthesis in invertebrates.

6.1.3 Copepod PUFA biosynthesis is affected by multiple climate drivers

As we uncover the molecular mechanism behind PUFA biosynthesis in copepods, it is tempting to consider that copepods might (partially) alleviate the projected LC-PUFA decreases in primary producers due to climate change (Hixson & Arts, 2016; Holm et

al., 2022). However, these projections do not take into account (a) the fraction of copepod PUFA biosynthesis versus dietary acquisition; (b) the metabolic costs and trade-offs associated with PUFA biosynthesis (Twining et al., 2021; Závorka et al., 2023); and (c) the direct impacts of climate change drivers (OW and OA) on consumer's PUFA levels and biosynthesis. In this PhD research, we performed two full-factorial short-term experiments exposing *P. littoralis* fed a LC-PUFA deficient diet (*Dunaliella tertiolecta*) to projected ocean warming (OW) (**Chapters 2 and 4**) and ocean acidification (OA) (**Chapter 4**). Survival remained unaltered across all combinatorial treatments in both experiments, and *P. littoralis* was able to maintain LC-PUFA levels even when fed the low LC-PUFA microalgae *D. tertiolecta*. However, in both experiments absolute levels of DHA (but not EPA or ARA) decreased following exposure to OW (+3.0 °C) regardless of diet, from 17.14 to 15.24 ng copepod^{-1} (-11%) in the first experiment (Boyen et al., 2020), and from 16.70 to 16.00 ng copepod^{-1} (-4%) in the second experiment (Chapter 4). Moreover, while in the first experiment we did not find differential expression of any PUFA biosynthesis genes (using RNA sequencing), in the second experiment (using quantitative PCR or qPCR) we detected increased expression of both the Δ4 fad and elovl1a when fed *D. tertiolecta* or exposed to OA (but not when combined).

From both of these results, we conclude that *P. littoralis* has some ability to use its PUFA biosynthesis mechanisms to maintain LC-PUFA levels when individually faced with either dietary LC-PUFA deficiency or OA (but not when combined). This copepod however does not seem to activate such mechanisms to a sufficient extent when faced with OW, resulting in reduced absolute levels of DHA. Potentially, this is done to maintain membrane fluidity through homeoviscous adaptation similar to microalgae and bacteria (Hixson & Arts, 2016; Sinensky, 1974). However, whether this DHA reduction occurs in the membranes or in the neutral lipids (or both) cannot be concluded from our data. Werbrouck and co-authors did find that DHA decreased in the membranes but increased in the storage lipids at higher temperatures, when fed a mixed (LC-PUFA rich) diet (Werbrouck et al., 2016a). Combining these findings with

compound-specific stable isotope analyses (CS-SIA) of *P. littoralis* and other copepods (De Troch et al., 2012; Helenius et al., 2020; Moreno et al., 1979; Nielsen et al., 2020b; Sahota et al., 2022; Werbrouck et al., 2017), we hypothesize that while certain copepods can to some extent buffer against future shifts in dietary LC-PUFA availability as well as OA, complete maintenance of present-day LC-PUFA provisioning for higher trophic levels is unlikely, due to the temperature-driven biophysical changes in membrane phospholipid FA composition. However, the observed temperature-driven decreases of DHA in *P. littoralis* (-4 to -11% with +3 °C) are still substantially lower than the decreases in DHA observed in primary producers (-27.8% with +2.5 °C) (Hixson & Arts, 2016). Importantly, as mentioned before, little is still known on the long-term metabolic costs and trade-offs of PUFA biosynthesis, potentially affecting growth and reproduction (Twining et al., 2021; Závorka et al., 2023). Furthermore, the impacts of projected environmental change on a copepod species strongly depends on its regional habitat characteristics; marine pelagic copepods will be exposed to different levels of warming and acidification than benthic, coastal or freshwater copepods (Kwiatkowski et al., 2020). This variability would need to be taken into account when assessing species-specific responses in their PUFA biosynthesis (Schmidt & Boyd, 2016).

6.1.4 A mechanism for climate change resilience?

Considering the now evident capacity of certain copepods for PUFA and/or LC-PUFA biosynthesis when faced with dietary LC-PUFA limitations due to OW and OA, I propose here that the PUFA biosynthesis capacity of copepods can be considered a *mechanism for climate change resilience*. IPCC's Working Group II defines resilience as follows:

'Resilience in this report is defined as the capacity of social, economic and ecosystems to cope with a hazardous event or trend or disturbance, responding or reorganising in ways that maintain their essential function, identity and structure as well as biodiversity in case of ecosystems while also maintaining the capacity for adaptation, learning and transformation' (IPCC, 2022a).

Copepods are potentially the most abundant, widespread and dominant primary consumers at the base of food webs of both pelagic and benthic aquatic ecosystems. Therefore, their potential capacity for PUFA biosynthesis does not only concern their own populations and communities, but the entire ecosystems in which they play a fundamental role. Providing sufficient levels of LC-PUFAs to higher trophic levels contributes at least to some extent not only to the maintenance of essential functions, identities, structure and biodiversity within these ecosystems, but also in terrestrial ecosystems and in human systems. Importantly, while it is likely that podopleans (harpacticoids and cyclopoids) but not gymnopleans (calanoids) have a complete or near-complete capacity for endogenous PUFA biosynthesis, the limited trophic upgrading exhibited by certain calanoids (e.g. EPA to DHA) can still be a crucial trait ensuring ecosystem maintenance.

The second condition for resilience as defined by Working Group II is the capacity for adaptation. Due to their large population sizes, high fecundity and short generation times, copepods have a high potential for rapid genetic adaptation to climate change compared to many other animals (Brennan et al., 2022a, 2022b; Dam et al., 2021; De Wit et al., 2016). Whether their PUFA biosynthesis mechanisms will also be a target of adaptation remains to be investigated.

While biophysical membrane adjustments will inevitably lead to phospholipid LC-PUFA reductions in both primary producers and primary consumers following OW (potential for genetic adaption or not), these thermal laws likely also apply to many higher trophic levels including poikilothermic vertebrates (Monroig et al., 2018), potentially reducing their LC-PUFA demands at least to some extent. Additionally, not only primary consumers but also higher trophic level vertebrates still have some (albeit likely limited) capacity for trophic upgrading themselves when necessary (Colombo et al., 2023), which is not taken into account when estimating present and future LC-PUFA availability for human consumption (Colombo et al., 2020; Hamilton et al., 2020).

6.2 Scientific recommendations

6.2.1 Quantify potential contribution of copepods to LC-PUFA provisioning in present and future climates

Although we successfully uncovered the unique molecular mechanism behind PUFA biosynthesis in copepods, the analyses performed here do not allow the proper quantification (or estimation) of total LC-PUFA biomass production and subsequent contribution to total LC-PUFA availability to higher trophic levels. Quantification might be feasible using CS-SIA (Nielsen, Van Someren Gréve, et al., 2020; Sahota et al., 2022; Závorka et al., 2023), however, calculations are complex and issues remain concerning selective FA oxidation and possible retroconversion from DHA back to EPA, among others (Metherel & Bazinet, 2019). Current research indicates only a limited production of DHA in *P. littoralis* (Sahota et al., 2022; Werbrouck et al., 2017). Nielsen and co-authors were able to show that the cyclopoid *A. royi* and the calanoid *Pseudodiaptomus annandelei* both produced about 1 µg ^{13}C-DHA mgC$_{copepod}$$^{-1}$ after 48 h (Nielsen et al., 2020b). While ^{13}C has been used predominantly in past FA modification research, the use of deuterium (^{2}H) might offer some interesting benefits due to the large natural stable isotope fractionations of ^{2}H/H as well as strong depletion following FA biosynthesis (Pilecky et al., 2022). Moreover, CS-SIA analyses are highly suited to integrate consumer FA modification in trophic ecology studies (Burian et al., 2020; Pilecky et al., 2022; Závorka et al., 2023).

To attempt quantifying the global contribution of all copepods, one should start with calculating the global LC-PUFA biosynthesis potential of a dominant copepod with high total biomass and a relatively simple LC-PUFA biosynthesis capacity (e.g. *Calanus* spp.), and subsequently model the total LC-PUFA biomass production of the entire species across its range, similar to what has been done before for the estimation of the *C. finmarchicus* lipid pump (Jónasdóttir et al., 2015). Extending this effort to other highly abundant copepod species (including benthic harpacticoids and freshwater cyclopoids), integration of these estimates into global LC-PUFA availability models, and

including responses to future climate drivers, would ultimately allow the inference of the contribution of copepods to the entire LC-PUFA provisioning for humans in both present and future climates.

6.2.2 Sequence additional copepod genomes and transcriptomes

Despite our transcriptomic analysis of 50 copepod species (of which 31 calanoid species), this number is still low compared to the nearly 15000 currently accepted copepod species (Walter & Boxshall, 2023). Transcriptomic data and functional evidence from orders with no or only few assessed species (e.g. Platycopioida, Polyarthra, Gelyelloida,...) would help to paint a more complete picture of the evolution of PUFA biosynthesis in copepods, especially following transitions from marine free-living lifestyles to freshwater and parasitism.

More genomic resources from copepod species would bring even more added value. Not only would these better confirm the presence of (potentially horizontally transferred) front-end desaturase genes in certain calanoids, they would also allow the detection recently duplicated (at the species-level) genes with high sequence similarity. High-quality genomes would also enable research on long-term adaptations to climate change at the molecular level (see further). However, assembling such high-quality genomes is still a daunting task, that – while cost is no longer an issue – requires high-level bioinformatic knowledge and expertise to overcome technical hurdles. In this regard, *de novo* transcriptome assembly is more feasible without advanced prior knowledge, and especially useful for obtaining information from many species in a short timeframe.

6.2.3 Explore adaptation potential of copepods and their LC-PUFA biosynthesis metabolism to climate drivers

Incubation experiments following two or three generations have indicated the potential for transgenerational acclimation towards climate change in copepods via (grand)maternal effects or epigenetic modifications (Lee et al., 2022b; Thor & Dupont,

2015). Other long-term studies demonstrated successful rapid adaptation at the population level (Brennan et al., 2022a, 2022b; Dam et al., 2021; De Wit et al., 2016), while other studies contest this (Fitzer et al., 2012; Langer et al., 2019). Rapid multigenerational adaptation towards OW might not have a cost on fitness traits such as egg hatching success (de Juan et al., 2023), however, the question of whether this trend holds true when combined with reduced dietary LC-PUFA levels remains open (Brennan et al., 2022a).

Future studies could investigate the transgenerational acclimation and adaptive potential of the PUFA biosynthesis mechanism, especially given the past positive selection acting upon the desaturase and elongase genes, as shown in Chapter 5. In humans, the promotor region of the ELOVL2 gene is shown to be a candidate for epigenetic modifications, which might allow transgenerational plasticity of PUFA biosynthesis (Garagnani et al., 2012). In the cyclopoid *Paracyclopina nana*, the expression of one transcript considered a fatty acid elongase (Pn_01_20990T) was significantly downregulated in the F1 generation exposed to pH 7.3 (relative to F0 at pH 8.0) (Lee et al., 2022b). However, no elongases were found to be differentially methylated. Epigenetic modifications or long-term adaptations to dietary LC-PUFA limitation and interaction with OW and/or OA remain to be investigated. Moreover, multigenerational incubations could also indicate whether temperature-driven biophysical phospholipid membrane adjustments remain consistent over time, as these would influence total future LC-PUFA provisioning for higher trophic levels.

6.2.4 Establish a scientifically robust definition of daily recommended intake of EPA and DHA

The assessment of the global human demand for EPA and DHA (1400 kt year^{-1}) by Hamilton and co-authors was calculated assuming a minimum requirement of 500 mg day^{-1} (Hamilton et al., 2020). However, a more recent model by Shepon and co-authors estimating both current and future demand used lower requirements, and differentiated between adults (250 mg day^{-1}) and children (100-200 mg day^{-1}), thereby

substantially reducing the current global human demand to ~650 kt year^{-1} (Shepon et al., 2022). Dietary recommendations from Australia and New Zealand are as low as 90-160 mg day^{-1} (NHMRC, 2005), which would bring the global human demand for EPA and DHA substantially below the estimated current global supply (420 kt year^{-1}). If this would actually be the case, the global fishery sector would be able to decrease instead of having to expand, alleviating pressures on aquatic ecosystems.

Clearly, the global scientific community should provide a scientifically robust minimal daily requirement, that is consistent among countries, based on the most updated information on cardio-vascular, neurological and developmental processes, and that includes a limited, but potentially sufficient, degree of human EPA and DHA biosynthesis from ALA (Domenichiello et al., 2015). A definitive minimal requirement is urgently needed, as it would influence policy directions (especially in regions facing nutritional deficiencies), counteract misleading health claims of omega-3 supplementations, and ultimately prevent unnecessary ecosystem impacts (Prado-Cabrero & Nolan, 2021). For instance, The Flanders Institute for Healthy Living specifically recommends to consume seafood only once a week, not only to avoid potential toxic contaminants (e.g. heavy metals such as mercury), but also to minimize negative impacts on aquatic ecosystems (Flanders Institute for Healthy Living, 2023).

6.3 Policy recommendations

6.3.1 Reach net zero greenhouse gas emissions by 2050 to limit warming below 1.5°C

As we now know that many groups of primary and even secondary consumers such as cephalopods (Kabeya et al., 2018; Monroig et al., 2012) have the capacity for endogenous LC-PUFA biosynthesis (Table 1), it becomes alluring to assume that global LC-PUFA provisioning towards human populations is safeguarded, even in a future climate. However, as indicated in this thesis, OW and OA are bound to have large-scale

direct and indirect impacts on marine ecosystems that are currently still underinvestigated and underestimated. Moreover, the potential for migration, acclimation and evolutionary adaptation is limited to only a subset of animal species, and will diminish with every further increase in global surface temperatures on top of the already established global increase of 1.09 °C (IPCC, 2021, 2022a). Additionally, biophysical reductions of LC-PUFAs in membrane phospholipids are likely bound to occur with OW, regardless of trophic level and capacity for evolutionary adaptation.

Therefore, further increases in OW and OA should be evaded, not only to maintain global LC-PUFA availability (Tan et al., 2022), but also to prevent the multitudes of other climate change impacts on ecosystems and human systems (IPCC, 2022a). Limiting warming to 1.5°C, as decided by the Paris agreement in 2015, is possible by immediate action and by reaching net-zero CO_2 emissions by around 2050 (IPCC, 2022b). Tools such as carbon sequestration, carbon capture and storage and CO_2 removal can be considered to help with offsetting hard-to-abate GHG emission sectors, but should not be used to delay mitigation. One of these proposed CO_2 removal mechanisms, ocean iron fertilization, would enhance the biological carbon pump. However, it is shown to have a very limited potential for drawing down atmospheric CO_2, at the cost of even further impacting marine animals already affected by climate change (Tagliabue et al., 2023).

6.3.2 Restore aquatic habitats and remove compound stressors

While we focussed in this research on global impacts (OW and OA) on LC-PUFA provisioning, other studies have also shown the detrimental impacts of other, often more local, anthropogenic stressors, such as chemical pollution and eutrophication-driven deoxygenation (Lee et al., 2018; Závorka et al., 2023). Often, these stressors interact synergistically with and exacerbate climate change impacts (Yoon et al., 2022). Bottom trawling fisheries for instance heavily disrupt marine sediments and the meiofaunal communities therein, reducing LC-PUFA provisioning to higher trophic levels (Schratzberger & Jennings, 2002). Intertidal ecosystems along the Western

Scheldt estuary, the habitat from which we sampled *P. littoralis*, are heavily exposed to both chemical runoff from the Antwerp port (including PFAS chemicals), continuous dredging to allow ships to pass, as well as ongoing habitat squeezing due to sea level rise (Van de Vijver et al., 2003; van Dijk et al., 2021). Removing the ecosystem exposure to stressors whose removal have an immediate impact, would allow aquatic organisms to better cope with the impacts of stressors, which will remain present despite rapid, large-scale action (e.g. OW).

To provide aquatic consumers with the best conditions to adapt to future climate conditions, well preserved habitats should be protected and safeguarded, and impoverished habitats should be restored, with putting attention not only on large (easy-to-study) animals such as fish and birds, but also on the ecologically important meiofauna and microphytobenthos. The spaces should be large enough to sustain large population sizes, and devoid of potential anthropogenic stressors as much as possible. A good example that can be replicated is the Sigmaplan for the Belgian part of the Scheldt River, which is a large-scale project to restore riverine and estuarine ecosystems (including mudflats and salt marshes) while at the same time preventing floods (Sigmaplan, 2023).

6.3.3 Ensure sufficient LC-PUFA provisioning for all within environmentally safe boundaries

As indicated throughout this PhD thesis, humans rely for their dietary LC-PUFA requirements not only on the seafood itself, but on the healthy functioning of entire aquatic ecosystems. To allow for more system-thinking to this complex topic, I propose to envisage *LC-PUFA provisioning as an ecosystem service* that allows human life to thrive. This provisioning, and the demand for it, can be quantified (Hamilton et al., 2020; Shepon et al., 2022), although challenges to this quantification remain (see Scientific recommendations). Importantly, this quantification would help create policies to sustain ecosystems providing this service.

Specifically, the framework of social and planetary boundaries (O'Neill et al., 2018; Raworth, 2017; Steffen et al., 2015b) can be applied this LC-PUFA provisioning ecosystem service (Figure 1). The lower social threshold would then equate to the global human demand for LC-PUFAs from seafood and other dietary sources, which in itself depends on the minimal daily requirements, and is most recently defined at 650 kt yr^{-1} for EPA and DHA (Hamilton et al., 2020; Shepon et al., 2022). The upper biophysical/ecological boundary would be the maximum amount of food we can appropriate from aquatic ecosystems to fulfil our LC-PUFA needs without severely impacting these ecosystems. This boundary is not yet exactly quantified, but has possibly been already crossed in certain ecosystems (Prado-Cabrero & Nolan, 2021).
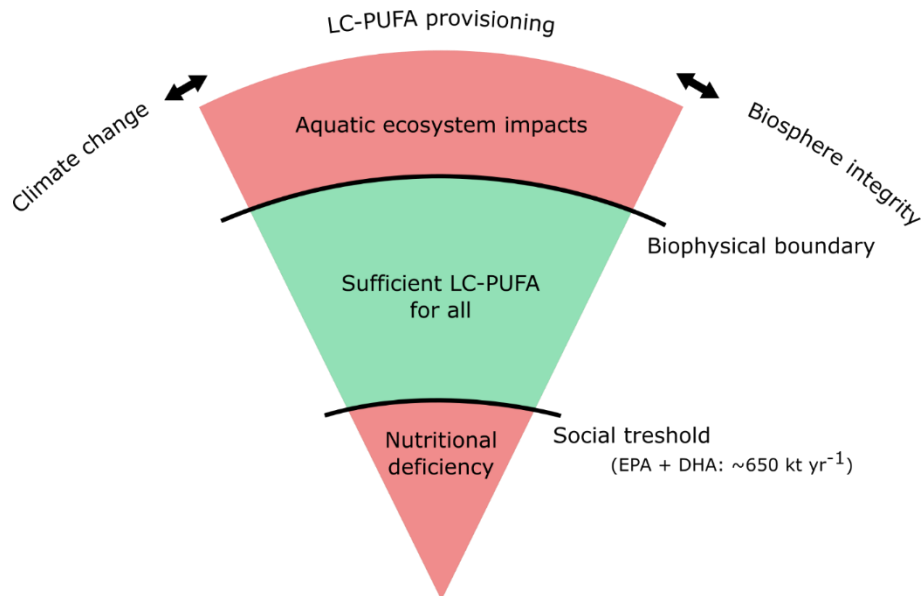
Figure 1 LC-PUFA provisioning as an ecosystem service following (O'Neill et al., 2018; Steffen et al., 2015b), *with a social threshold above which the minimal dietary requirement is met for all, and a biophysical boundary below which aquatic ecosystems are not detrimentally affected. LC-PUFA provisioning is tightly linked with the core planetary boundaries climate change and biosphere integrity* (Steffen et al., 2015b). *The global human demand for EPA and DHA is estimated to be 650 kt yr-1* (Shepon et al., 2022).

Moreover, LC-PUFA provisioning highly interacts with the core planetary boundaries climate change and biosphere integrity (Steffen et al., 2015b). While detrimental changes in these two processes will negatively affect LC-PUFA provisioning, disrupting aquatic ecosystems to obtain dietary LC-PUFAs will also impact both climate and biosphere (Figure 1). For instance, harvesting large amounts of *C. finmarchicus* to produce omega-3 supplements with dubious health benefits (Prado-Cabrero & Nolan,

2021), will also reduce the contribution that this species has towards the seasonal lipid pump (Jónasdóttir et al., 2015), thereby worsening climate change. Although the social threshold (650 kt yr^{-1}) for EPA and DHA is based on an ambiguous assumption of the minimal daily requirements, the current estimated demand from aquatic foods (420 kt yr^{-1}) does not meet this threshold (Hamilton et al., 2020; Shepon et al., 2022). Moreover, EPA and DHA availabilities widely vary among regions, with many countries deeply below this requirement (Colombo et al., 2020).

To ensure sufficient LC-PUFA provisioning for all within environmentally safe boundaries, a number of measures can be taken. First, Shepon and co-authors indicate that optimizing the supply chain by culturing fish rich in LC-PUFAs, improving byproduct utilization and reducing food waste would already increase the total EPA and DHA supply to 630 kt yr^{-1} (Shepon et al., 2022). Second, improving aquaculture sustainably would increase LC-PUFA supplies while reducing the need for wild food harvesting. Aquaculture feeds, despite the rise of vegetable feeds, are still heavily based on fish meal and fish oil from capture fisheries (Hamilton et al., 2020; Prado-Cabrero & Nolan, 2021), or on species with low LC-PUFA biosynthesis capabilities such as *Artemia* (Ramos-Llorens et al., 2023b), and should be shifted to the industrial production of alternative feeds with better biosynthesis capacities such as copepods (Nanton & Castell, 1998; Prado-Cabrero et al., 2022). Certain marine invertebrates such as annelids and amphipods, despite some of them seemingly having no functional front-end or methyl-end desaturases (Table 1), might also be a promising sustainable aquaculture feed alternative, as they can thrive on different bioindustry side streams while maintaining high LC-PUFAs levels, increasing circularity principles within the aquaculture sector (Kabeya et al., 2020; Pajand et al., 2022; Ribes-Navarro et al., 2022). Other novel sources of EPA and DHA that should be considered are microalgae or genetically modified organisms (Napier et al., 2019; Sato et al., 2023; Tocher et al., 2019).

In addition, humans should consume fewer (unsustainable) higher trophic level species such as predatory fish, and instead rely more on consumers with proven LC-PUFA biosynthesis capacities such as cephalopods (Monroig et al., 2012), or, even better, diversify their seafood options by including macroalgae and even microalgae with high levels of EPA and DHA in their diets. Importantly, meeting global LC-PUFA demand does not mean that dietary requirements are met everywhere; likely large nutritional deficiencies would remain in many countries (Colombo et al., 2020). Multilateral collaborations and international policy is therefore crucial to ensure that each person across the globe has access to sufficient dietary LC-PUFA intake.

A last point to note here is that the scientific community, particularly those working on omega-3 LC-PUFA research, should be cautious concerning the broader application and utilization of their research beyond the confines of academia. While there is a clear link between LC-PUFAs and optimal human development and health (Bazinet & Layé, 2014), the need for dietary LC-PUFAs in healthy adults remains a point of uncertainty. This uncertainty is occasionally exploited, leading to unsubstantiated health claims concerning omega-3 nutraceuticals at the expense of marine ecosystems (Prado-Cabrero & Nolan, 2021). Providing healthy individuals with superfluous and unnecessary amounts of EPA and DHA should be avoided. Instead, focus should be directed toward populations with demonstrable nutritional needs, such as preterm infants and undernourished communities. A fair distribution of global EPA and DHA supplies is thus essential to prevent regional deficiencies while at same time mitigating strain on aquatic ecosystems. Researchers investigating omega-3 FAs therefore have an ethical responsibility to remain critical towards their own work, and always ask themselves who is benefitting from their research.

6.4 General conclusions

As continuous anthropogenic greenhouse gas (GHG) emissions cause our oceans to warm and absorb CO_2, global LC-PUFA levels supplied by primary producers are set to diminish. Copepods, as primary consumers, occupy a key point within aquatic food webs, and their underinvestigated PUFA biosynthesis capacities might to some extent contribute to sufficient LC-PUFA provisioning in a future climate. Within this PhD project, I set out to investigate the PUFA biosynthesis capabilities of the benthic harpacticoid copepod *Platychelipus littoralis*.

- We **successfully sequenced and *de novo* assembled the *P. littoralis* transcriptome**. While we did find transcriptional changes of a limited number of genes when exposed to dietary LC-PUFA deficiency and OW, the identified LC-PUFA biosynthesis genes were not found to be significantly differentially expressed.

- Further investigations, including heterologous expression in yeast, showed that *P. littoralis* **has a large number of functionally relevant PUFA biosynthesis genes**, with at least one Δ15/17/19 methyl-end desaturase, one Δ4 front-end desaturase and five fatty acid elongases. While the *P. littoralis* gene repertoire identified so far does not allow full endogenous LC-PUFA biosynthesis from monounsaturated fatty acid precursors, other harpacticoid species do exhibit this capacity.

- A second incubation experiment showed that **both direct (dietary LC-PUFA deficiency) and indirect (ocean warming (OW) and acidification (OA)) climate change drivers interactively affect LC-PUFA levels and PUFA gene expression**. Relative levels of DHA decreased when fed the LC-PUFA deficient *Dunaliella tertiolecta* and simultaneously exposed to OW. Expression of the DHA-producing genes Δ4 front-end desaturase and elovl1a increased when fed *D. tertiolecta* under control pH but not under future pH.

- The three PUFA biosynthesis genes families have considerably evolved throughout copepod evolution, including evidence for positive selection. **The potentially horizontally transferred methyl-end and front-end desaturases were lost in (most) calanoids but retained in other copepod orders**. Moreover, **harpacticoid elongases were more highly expressed than calanoid elongases**, showing that species from the former order likely have higher capabilities for PUFA biosynthesis than species from latter one.

We concluded by arguing that the **unique PUFA biosynthesis capacities of copepods** (whether *de novo* or from another PUFA precursor) **might act as a mechanism that helps aquatic ecosystems to maintain resilience following climate change.** However, biophysical phospholipid membrane adjustments are still bound to happen following OW across all trophic levels of the food web. LC-PUFA provisioning to human populations can be regarded as an ecosystem service with both social justice and environmental boundaries, and the future provision of sufficient global LC-PUFA supplies depends as much on the response of copepods as it does on the near-future actions of humans.

REFERENCES

Abdulkadir, S., & Tsuchiya, M. (2008). One-step method for quantitative and qualitative analysis of fatty acids in marine animal samples. *Journal of Experimental Marine Biology and Ecology*, *354*(1), 1–8. https://doi.org/10.1016/j.jembe.2007.08.024

Acebal, M. C., Dalgaard, L. T., Jørgensen, T. S., & Hansen, B. W. (2023). Embryogenesis of a calanoid copepod analyzed by transcriptomics. *Comparative Biochemistry and Physiology - Part D: Genomics and Proteomics*, *45*, 101054. https://doi.org/10.1016/j.cbd.2022.101054

Ackman, R. G., & Sipos, J. C. (1964). Application of specific response factors in the gas chromatographic analysis of methyl esters of fatty acids with flame ionization detectors. *Journal of the American Oil Chemists Society*, *41*(5), 377–378. https://doi.org/10.1007/BF02654818

Albalat, R., & Cañestro, C. (2016). Evolution by gene loss. *Nature Reviews Genetics*, *17*(7), 379–391. https://doi.org/10.1038/nrg.2016.39

Alexa, A., & Rahnenfuhrer, J. (2019). *topGO - Enrichment analysis for gene ontology* (2.37.0). https://doi.org/10.18129/B9.bioc.topGO

Alma, L., Kram, K. E., Holtgrieve, G. W., Barbarino, A., Fiamengo, C. J., & Padilla-Gamiño, J. L. (2020). Ocean acidification and warming effects on the physiology, skeletal properties, and microbiome of the purple-hinge rock scallop. *Comparative Biochemistry and Physiology - Part A: Molecular and Integrative Physiology*, *240*, 110579. https://doi.org/10.1016/j.cbpa.2019.110579

Almén, A. K., Vehmaa, A., Brutemark, A., Bach, L., Lischka, S., Stuhr, A., Furuhagen, S., Paul, A., Rafael Bermúdez, J., Riebesell, U., & Engström-Öst, J. (2016). Negligible effects of ocean acidification on *Eurytemora affinis* (Copepoda) offspring production. *Biogeosciences*, *13*(4), 1037–1048. https://doi.org/10.5194/bg-13-1037-2016

Altschul, S. F., Gish, W., Miller, W., Myers, E. W., & Lipman, D. J. (1990). Basic Local Alignment Search Tool. *Journal of Molecular Biology*, *215*, 403–410. https://doi.org/10.1016/S0022-2836(05)80360-2

Álvarez-Carretero, S., Kapli, P., & Yang, Z. (2023). Beginner's Guide on the Use of PAML to Detect Positive Selection. *Molecular Biology and Evolution*, *40*(4), 1–18. https://doi.org/10.1093/molbev/msad041

Alvarez, F., Robello, C., & Vignali, M. (1994). Evolution of codon usage and base contents in kinetoplastid protozoans. *Molecular Biology and Evolution*, *11*(5), 790–802. https://doi.org/10.1093/oxfordjournals.molbev.a040159

Amparyup, P., Sungkaew, S., Charoensapsri, W., Tapaneeyaworawong, P., Chumtong, P., Yocawibun, P., Pantong, P., Wongpanya, R., Imjongjirak, C., & Powtongsook, S. (2022). Molecular characterization of biosynthesis of polyunsaturated fatty acids

during different developmental stages in the copepod *Apocyclops royi*. *Aquaculture Reports*, *23*, 101064. https://doi.org/10.1016/j.aqrep.2022.101064

Anacleto, P., Maulvault, A. L., Bandarra, N. M., Repolho, T., Nunes, M. L., Rosa, R., & Marques, A. (2014). Effect of warming on protein, glycogen and fatty acid content of native and invasive clams. *Food Research International*, *64*, 439–445. https://doi.org/10.1016/j.foodres.2014.07.023

Anand, L., & Rodriguez Lopez, C. M. (2022). ChromoMap: an R package for interactive visualization of multi-omics data and annotation of chromosomes. *BMC Bioinformatics*, *23*(1), 1–9. https://doi.org/10.1186/s12859-021-04556-z

Andrews, S. (2010). *FastQC: a quality control tool for high throughput sequence data* (0.11.5). http://www.bioinformatics.babraham.ac.uk/projects/fastqc/

Apostolov, A. (2014). Contribution to the study of marine harpacticoid fauna (Crustacea, Copepoda) of Iceland. *ZooNotes*, 62, 1–5.

Appeltans, W., Ahyong, S. T., Anderson, G., Angel, M. V., Artois, T., Bailly, N., Bamber, R., Barber, A., Bartsch, I., Berta, A., Błazewicz-Paszkowycz, M., Bock, P., Boxshall, G., Boyko, C. B., Brandão, S. N., Bray, R. A., Bruce, N. L., Cairns, S. D., Chan, T. Y., … Costello, M. J. (2012). The magnitude of global marine species diversity. *Current Biology*, *22*(23), 2189–2202. https://doi.org/10.1016/j.cub.2012.09.036

Arndt, C., & Sommer, U. (2014). Effect of algal species and concentration on development and fatty acid composition of two harpacticoid copepods, *Tisbe* sp. and *Tachidius discipes*, and a discussion about their suitability for marine fish larvae. *Aquaculture Nutrition*, *20*(1), 44–59. https://doi.org/10.1111/anu.12051

Barbier, E. B., Hacker, S. D., Kennedy, C., Koch, E. W., Stier, A. C., & Silliman, B. R. (2011). The value of estuarine and coastal ecosystem services. *Ecological Monographs*, *81*(2), 169–193. https://doi.org/10.1890/10-1510.1

Barnett, P. R. O. (1966). The comparative development of two species of *Platychelipus* Brady (Harpacticoida). *Some Contemporary Studies in Marine Science*, 113–127.

Barnett, P. R. O. (1968). Distribution and Ecology of Harpacticoid Copepods of an Intertidal Mudflat. *Internationale Revue Der Gesamten Hydrobiologie Und Hydrographie*, *53*(2), 177–209. https://doi.org/10.1002/iroh.19680530202

Barnett, P. R. O. (1970). The Life Cycles of two Species of *Platychelipus* Brady (Harpacticoida) on an Intertidal Mudflat. *Internationale Revue Der Gesamten Hydrobiologie Und Hydrographie*, *55*(2), 169–175.

Barreto, F. S., Pereira, R. J., & Burton, R. S. (2015). Hybrid dysfunction and physiological compensation in gene expression. *Molecular Biology and Evolution*, *32*(3), 613–622. https://doi.org/10.1093/molbev/msu321

Barrick, A., Laroche, O., Boundy, M., Pearman, J. K., Wiles, T., Butler, J., Pochon, X., Smith,

K. F., & Tremblay, L. A. (2022). First transcriptome of the copepod *Gladioferens pectinatus* subjected to chronic contaminant exposures. *Aquatic Toxicology*, *243*, 106069. https://doi.org/10.1016/j.aquatox.2021.106069

Bass, D., Rueckert, S., Stern, R., Cleary, A. C., Taylor, J. D., Ward, G. M., & Huys, R. (2021). Parasites, pathogens, and other symbionts of copepods. *Trends in Parasitology*, *37*(10), 875–889. https://doi.org/10.1016/j.pt.2021.05.006

Bazinet, R. P., & Layé, S. (2014). Polyunsaturated fatty acids and their metabolites in brain function and disease. *Nature Reviews Neuroscience*, *15*(12), 771–785. https://doi.org/10.1038/nrn3820

Beaudoin, F., Michaelson, L. V., Lewis, M. J., Shewry, P. R., Sayanova, O., & Napier, J. A. (2000). Production of C20 polyunsaturated fatty acids (PUFAs) by pathway engineering: Identification of a PUFA elongase component from *Caenorhabditis elegans*. *Biochemical Society Transactions*, *28*(6), 661–663. https://doi.org/10.1042/bst0280661

Beaugrand, G., Brander, K. M., Lindley, J. A., Souissi, S., & Reid, P. C. (2003). Plankton effect on cod recruitment in the North Sea. *Nature*, *426*, 661–664. https://doi.org/10.1038/nature02164

Beaugrand, G., Reid, P. C., Ibañez, F., Alistair Lindley, J., & Edwards, M. (2002). Reorganization of North Atlantic Marine Copepod Biodiversity and Climate. *Science*, *296*, 1692–1694.

Bell, M. V., Dick, J. R., Anderson, T. R., & Pond, D. W. (2007). Application of liposome and stable isotope tracer techniques to study polyunsaturated fatty acid biosynthesis in marine zooplankton. *Journal of Plankton Research*, *29*(5), 417–422. https://doi.org/10.1093/plankt/fbm025

Bell, M. V, & Tocher, D. R. (2009). Biosynthesis of polyunsaturated fatty acids in aquatic ecosystems: General pathways and new directions. In *Lipids in Aquatic Ecosystems* (pp. 211–236). Springer. https://doi.org/10.1007/978-0-387-89366-2_9

Benjamini, Y., & Hochberg, Y. (1995). Controlling the False Discovery Rate: A Practical and Powerful Approach to Multiple Testing. *Journal of the Royal Statistical Society Series B*, *57*(1), 289–300. https://doi.org/10.1111/j.2517-6161.1995.tb02031.x

Berger, C. A., Steinberg, D. K., Copley, N. J., & Tarrant, A. M. (2021). De novo transcriptome assembly of the Southern Ocean copepod *Rhincalanus gigas* sheds light on developmental changes in gene expression. *Marine Genomics*, *58*, 100835. https://doi.org/10.1016/j.margen.2021.100835

Bermúdez, J. R., Riebesell, U., Larsen, A., & Winder, M. (2016). Ocean acidification reduces transfer of essential biomolecules in a natural plankton community. *Scientific Reports*, *6*, 1–8. https://doi.org/10.1038/srep27749

Bernot, J. P., Boxshall, G. A., & Crandall, K. A. (2021). A synthesis tree of the Copepoda:

Integrating phylogenetic and taxonomic data reveals multiple origins of parasitism. *PeerJ*, *9*. https://doi.org/10.7717/peerj.12034

Bernot, J. P., Owen, C. L., Olesen, J., Crandall, K. A., Wolfe, J. M., & Meland, K. (2023). Major Revisions in Pancrustacean Phylogeny and Evidence of Sensitivity to Taxon Sampling. *Molecular Biology and Evolution*, *40*(8), 1–22. https://doi.org/10.1093/molbev/msad175

Bertram, D. F., Mackas, D. L., Welch, D. W., Boyd, W. S., Ryder, J. L., Galbraith, M., Hedd, A., Morgan, K., & O'Hara, P. D. (2017). Variation in zooplankton prey distribution determines marine foraging distributions of breeding Cassin's Auklet. *Deep-Sea Research Part I: Oceanographic Research Papers*, *129*, 32–40. https://doi.org/10.1016/j.dsr.2017.09.004

Bi, R., Cao, Z., Ismar-Rebitz, S. M. H., Sommer, U., Zhang, H., Ding, Y., & Zhao, M. (2021). Responses of marine diatom-dinoflagellate competition to multiple environmental drivers: abundance, elemental, and biochemical aspects. *Frontiers in Microbiology*, *12*, 731786. https://doi.org/10.3389/fmicb.2021.731786

Birchenough, S. N. R., Reiss, H., Degraer, S., Mieszkowska, N., Borja, Á., Buhl-Mortensen, L., Braeckman, U., Craeymeersch, J., De Mesel, I., Kerckhof, F., Kröncke, I., Parra, S., Rabaut, M., Schröder, A., Van Colen, C., Van Hoey, G., Vincx, M., & Wätjen, K. (2015). Climate change and marine benthos: A review of existing research and future directions in the North Atlantic. *Wiley Interdisciplinary Reviews: Climate Change*, *6*(2), 203–223. https://doi.org/10.1002/wcc.330

Boersma, M., Aberle, N., Hantzsche, F. M., Schoo, K. L., Wiltshire, K. H., & Malzahn, A. M. (2008). Nutritional limitation travels up the food chain. *International Review of Hydrobiology*, *93*(4–5), 479–488. https://doi.org/10.1002/iroh.200811066

Boissonnot, L., Niehoff, B., Hagen, W., Søreide, J. E., & Graeve, M. (2016). Lipid turnover reflects life-cycle strategies of small-sized Arctic copepods. *Journal of Plankton Research*, *38*, 1420–1432. https://doi.org/10.1093/plankt/fbw076

Bolger, A. M., Lohse, M., & Usadel, B. (2014). Trimmomatic: A flexible trimmer for Illumina sequence data. *Bioinformatics*, *30*(15), 2114–2120. https://doi.org/10.1093/bioinformatics/btu170

Bopp, L., Resplandy, L., Orr, J. C., Doney, S. C., Dunne, J. P., Gehlen, M., Halloran, P., Heinze, C., Ilyina, T., Séférian, R., Tjiputra, J., & Vichi, M. (2013). Multiple stressors of ocean ecosystems in the 21st century: Projections with CMIP5 models. *Biogeosciences*, *10*, 6225–6245. https://doi.org/10.5194/bg-10-6225-2013

Bourret, J., Alizon, S., & Bravo, I. G. (2019). COUSIN (COdon Usage Similarity INdex): A Normalized Measure of Codon Usage Preferences. *Genome Biology and Evolution*, *11*(12), 3523–3528. https://doi.org/10.1093/gbe/evz262

Boyd, P. W., Claustre, H., Levy, M., Siegel, D. A., & Weber, T. (2019). Multi-faceted

particle pumps drive carbon sequestration in the ocean. *Nature*, *568*(7752), 327–335. https://doi.org/10.1038/s41586-019-1098-2

Boyd, P. W., Collins, S., Dupont, S., Fabricius, K., Gattuso, J. P., Havenhand, J., Hutchins, D. A., Riebesell, U., Rintoul, M. S., Vichi, M., Biswas, H., Ciotti, A., Gao, K., Gehlen, M., Hurd, C. L., Kurihara, H., McGraw, C. M., Navarro, J. M., Nilsson, G. E., … Pörtner, H. O. (2018). Experimental strategies to assess the biological ramifications of multiple drivers of global ocean change—A review. *Global Change Biology*, *24*(6), 2239–2261. https://doi.org/10.1111/gcb.14102

Boyen, J., Fink, P., Mensens, C., Hablützel, P. I., & De Troch, M. (2020). Fatty acid bioconversion in harpacticoid copepods in a changing environment: a transcriptomic approach. *Philosophical Transactions of the Royal Society B: Biological Sciences*, *375*(1804), 20190645. https://doi.org/10.1098/rstb.2019.0645

Boyen, J., Ribes-Navarro, A., Kabeya, N., Monroig, Ó., Rigaux, A., Fink, P., Hablützel, P. I., Navarro, J. C., & De Troch, M. (2023). Functional characterization reveals a diverse array of metazoan fatty acid biosynthesis genes. *Molecular Ecology*, *32*(4), 970–982. https://doi.org/10.1111/mec.16808

Brady, G. S. (1880). *A monograph of the free and semi-parasitic Copepoda of the British Islands: Vol. II*. The Ray Society.

Brennan, R. S., deMayo, J. A., Dam, H. G., Finiguerra, M. B., Baumann, H., & Pespeni, M. H. (2022a). Loss of transcriptional plasticity but sustained adaptive capacity after adaptation to global change conditions in a marine copepod. *Nature Communications*, *13*(1), 1–13. https://doi.org/10.1038/s41467-022-28742-6

Brennan, R. S., deMayo, J. A., Dam, H. G., Finiguerra, M., Baumann, H., Buffalo, V., & Pespeni, M. H. (2022b). Experimental evolution reveals the synergistic genomic mechanisms of adaptation to ocean warming and acidification in a marine copepod. *Proceedings of the National Academy of Sciences of the United States of America*, *119*(38), 1–10. https://doi.org/10.1073/pnas.2201521119

Bryant, D. M., Johnson, K., DiTommaso, T., Tickle, T., Couger, M. B., Payzin-Dogru, D., Lee, T. J., Leigh, N. D., Kuo, T. H., Davis, F. G., Bateman, J., Bryant, S., Guzikowski, A. R., Tsai, S. L., Coyne, S., Ye, W. W., Freeman, R. M., Peshkin, L., Tabin, C. J., … Whited, J. L. (2017). A Tissue-Mapped Axolotl De Novo Transcriptome Enables Identification of Limb Regeneration Factors. *Cell Reports*, *18*(3), 762–776. https://doi.org/10.1016/j.celrep.2016.12.063

Bryon, A., Kurlovs, A. H., Dermauw, W., Greenhalgh, R., Riga, M., Grbic, M., Tirry, L., Osakabe, M., Vontas, J., Clark, R. M., & Leeuwen, T. Van. (2017). Disruption of a horizontally transferred phytoene desaturase abolishes carotenoid accumulation and diapause in *Tetranychus urticae*. *Proceedings of the National Academy of Sciences of the United States of America*, *114*(29), E5871–E5880. https://doi.org/10.1073/pnas.1706865114

Burian, A., Nielsen, J. M., Hansen, T., Bermudez, R., & Winder, M. (2020). The potential of fatty acid isotopes to trace trophic transfer in aquatic food-webs. *Philosophical Transactions of the Royal Society B: Biological Sciences*, *375*(1804). https://doi.org/10.1098/rstb.2019.0652

Burka, J. F., Fast, M. D., & Revie, C. W. (2012). *Lepeophtheirus salmonis* and *Caligus rogercresseyi*. In P. T. K. Woo & K. Buchmann (Eds.), *Fish Parasites: Pathobiology and Protection*. https://doi.org/10.1079/9781845938062.0350

Byrnes, J. (2021). get_sim_fit_gllvm.R. https://gist.github.com/jebyrnes/a60ec172a391ed8dd3d44cbe1eed0bed

Callens, M., Scornavacca, C., & Bedhomme, S. (2021). Evolutionary responses to codon usage of horizontally transferred genes in *Pseudomonas aeruginosa*: Gene retention, amelioration and compensatory evolution. *Microbial Genomics*, *7*(6). https://doi.org/10.1099/MGEN.0.000587

Calosi, P., De Wit, P., Thor, P., & Dupont, S. (2016). Will life find a way? Evolution of marine species under global change. *Evolutionary Applications*, *9*(9), 1035–1042. https://doi.org/10.1111/eva.12418

Caramujo, M. J., Boschker, H. T. S., & Admiraal, W. (2008). Fatty acid profiles of algae mark the development and composition of harpacticoid copepods. *Freshwater Biology*, *53*(1), 77–90. https://doi.org/10.1111/j.1365-2427.2007.01868.x

Castro, L. F. C., Tocher, D. R., & Monroig, O. (2016). Long-chain polyunsaturated fatty acid biosynthesis in chordates: Insights into the evolution of Fads and Elovl gene repertoire. *Progress in Lipid Research*, *62*, 25–40. https://doi.org/10.1016/j.plipres.2016.01.001

Chen, K., Li, E., Li, T., Xu, C., Xu, Z., Qin, J. G., & Chen, L. (2017). The expression of the Δ6 fatty acyl desaturase-like gene from Pacific white shrimp (*Litopenaeus vannamei*) under different salinities and dietary lipid compositions. *Journal of Shellfish Research*, *36*(2), 501–509. https://doi.org/10.2983/035.036.0221

Chust, G., Castellani, C., Licandro, P., Ibaibarriaga, L., Sagarminaga, Y., & Irigoien, X. (2014). Are *Calanus* spp. shifting poleward in the North Atlantic? A habitat modelling approach. *ICES Journal of Marine Science*, *71*, 241–253. https://doi.org/10.1093/icesjms/fst147

Climate Action Tracker. (2022). *Warming Projections Global Update November 2022*.

Cnudde, C., Moens, T., Werbrouck, E., Lepoint, G., Van Gansbeke, D., & De Troch, M. (2015). Trophodynamics of estuarine intertidal harpacticoid copepods based on stable isotope composition and fatty acid profiles. *Marine Ecology Progress Series*, *524*, 225–239. https://doi.org/10.3354/meps11161

Cnudde, C., Willems, A., Van Hoorde, K., Vyverman, W., Moens, T., & De Troch, M. (2011). Effect of food preservation on the grazing behavior and on the gut flora of the

harpacticoid copepod *Paramphiascella fulvofasciata*. *Journal of Experimental Marine Biology and Ecology*, *407*(1), 63–69. https://doi.org/10.1016/j.jembe.2011.07.007

Collins, M., Knutti, R., Arblaster, J., Dufresne, J.-L., Fichefet, T., Friedlingstein, P., Gao, X., Gutowski, W. J., Johns, T., Krinner, G., Shongwe, M., Tebaldi, C., Weaver, A. J., & Wehner, M. (2013). Long-term climate change: projections, commitments and irreversibility. In *Climate Change 2013: The Physical Science Basis. Contribution of Working Group I to the Fifth Assessment Report of the Intergovernmental Panel on Climate Change* (pp. 1029–1136). https://doi.org/10.1017/CBO9781107415324.024

Colombo, S. M., Budge, S. M., Hall, J. R., Kornicer, J., & White, N. (2023). Atlantic salmon adapt to low dietary n-3 PUFA and warmer water temperatures by increasing feed intake and expression of n-3 biosynthesis-related transcripts. *Fish Physiology and Biochemistry*, *49*(1), 39–60. https://doi.org/10.1007/s10695-022-01157-2

Colombo, S. M., Rodgers, T. F. M., Diamond, M. L., Bazinet, R. P., & Arts, M. T. (2020). Projected declines in global DHA availability for human consumption as a result of global warming. *Ambio*, *49*(4), 865–880. https://doi.org/10.1007/s13280-019-01234-6

Colombo, S. M., Wacker, A., Parrish, C. C., Kainz, M. J., & Arts, M. T. (2017a). A fundamental dichotomy in long-chain polyunsaturated fatty acid abundance between and within marine and terrestrial ecosystems. *Environmental Reviews*, *25*(2), 163–174.

Colombo, S. M., Wacker, A., Parrish, C. C., Kainz, M. J., & Arts, M. T. (2017b). A fundamental dichotomy in long-chain polyunsaturated fatty acid abundance between and within marine and terrestrial ecosystems. *Environmental Reviews*, *25*(2), 163–174. https://doi.org/10.1139/er-2016-0062

Couturier, L. I. E., Michel, N., Amaro, T., Budge, S. M., Costa, E., De Troch, M., Dato, V. Di, Fink, P., Giraldo, C., Mathieu-resuge, M., Nichols, P. D., Grand, F. Le, Parrish, C. C., Sardenne, F., Vagner, M., Pernet, F., & Soudant, P. (2020). State of art and best practices for fatty acid analysis in aquatic sciences. *ICES Journal of Marine Science*, *fsaa121*, 21. https://doi.org/10.1093/icesjms/fsaa121

Cronin, T. W., Fasick, J. I., Schweikert, L. E., Johnsen, S., Kezmoh, L. J., & Baumgartner, M. F. (2017). Coping with copepods: Do right whales (*Eubalaena glacialis*) forage visually in dark waters? *Philosophical Transactions of the Royal Society B: Biological Sciences*, *372*(1717). https://doi.org/10.1098/rstb.2016.0067

Cutts, C. J. (2003). Culture of harpacticoid copepods: Potential as live feed for rearing marine fish. *Advances in Marine Biology*, *44*, 295–316. https://doi.org/10.1016/S0065-2881(03)44005-4

Dahms, H.-U. (2004). Exclusion of the Polyarthra from Harpacticoida and its reallocation as an underived branch of the Copepoda (Arthropoda, Crustacea). *Invertebrate Zoology*, *1*(1), 29–51. https://doi.org/10.15298/invertzool.01.1.03

Daily, G. C., Soderqvist, T., Aniyar, S., Arrow, K., & Dasgupta, P. (2000). The Value of Nature and Nature of Value. *Science*, *289*, 395–396.

Dalsgaard, J., Michael, S. J., Kattner, G., Müller-Navarra Dörthe, & Wilhelm, H. (2003). Fatty acid trophic markers in the pelagic marine environment. In *Advances in Marine Biology Volume 46* (pp. 225–340).

Dam, H. G. (2013). Evolutionary Adaptation of Marine Zooplankton to Global Change. *Annual Review of Marine Science*, *5*, 349–370. https://doi.org/10.1146/annurev-marine-121211-172229

Dam, H. G., & Baumann, H. (2017). Climate Change, Zooplankton and Fisheries. In B. F. Phillips & M. Pérez-Ramírez (Eds.), *Climate Change Impacts on Fisheries and Aquaculture: A Global Analysis* (Vol. 2, pp. 851–874). John Wiley & Sons Ltd. https://doi.org/10.1002/9781119154051.ch25

Dam, H. G., deMayo, J. A., Park, G., Norton, L., He, X., Finiguerra, M. B., Baumann, H., Brennan, R. S., & Pespeni, M. H. (2021). Rapid, but limited, zooplankton adaptation to simultaneous warming and acidification. *Nature Climate Change*, *11*(9), 780–786. https://doi.org/10.1038/s41558-021-01131-5

Daudi, L. N., Uku, J. N., & De Troch, M. (2023). Effects of habitat complexity on the abundance and diversity of seagrass leaf meiofauna communities in tropical Kenyan seagrass meadows. *Aquatic Botany*, *187*, 103651. https://doi.org/10.1016/j.aquabot.2023.103651

de Carvalho, C. C. C. R., & Caramujo, M. J. (2018). The various roles of fatty acids. *Molecules*, *23*(10). https://doi.org/10.3390/molecules23102583

De Freitas Souza, R., Fávero, L. P., Belfiore, P., & Corrêa, H. L. (2022). overdisp: An R Package for Direct Detection of Overdispersion in Count Data Multiple Regression Analysis. *International Journal of Business Intelligence and Data Mining*, *20*(3), 327–344. https://doi.org/10.1504/IJBIDM.2022.122157

de Juan, C., Griffell, K., Calbet, A., & Saiz, E. (2023). Multigenerational physiological compensation and body size reduction dampen the effects of warming on copepods. *Limnology and Oceanography*, *68*(5), 1037–1047. https://doi.org/10.1002/lno.12327

De la Cruz-Alvarado, F. J., Álvarez-González, C. A., Llera-Herrera, R., Monroig, Ó., Kabeya, N., Rodríguez-Morales, S., Concha-Frias, B., Guerrero-Zárate, R., Jiménez-Martínez, L. D., & Peña-Marín, E. S. (2021). Expression of long-chain polyunsaturated fatty acids biosynthesis genes during the early life-cycle stages of the tropical gar *Atractosteus tropicus*. *Comparative Biochemistry and Physiology Part B: Biochemistry and Molecular Biology*, *256*, 110628. https://doi.org/10.1016/j.cbpb.2021.110628

De Troch, M., Boeckx, P., Cnudde, C., Van Gansbeke, D., Vanreusel, A., Vincx, M., & Caramujo, M. J. (2012). Bioconversion of fatty acids at the basis of marine food webs:

Insights from a compound-specific stable isotope analysis. *Marine Ecology Progress Series*, *465*, 53–67. https://doi.org/10.3354/meps09920

De Wit, P., Dupont, S., & Thor, P. (2016). Selection on oxidative phosphorylation and ribosomal structure as a multigenerational response to ocean acidification in the common copepod *Pseudocalanus acuspes*. *Evolutionary Applications*, *9*(9), 1112–1123. https://doi.org/10.1111/eva.12335

Desvilettes, C., Bourdier, G., & Breton, J. C. (1997). On the occurrence of a possible bioconversion of linolenic acid into docosahexaenoic acid by the copepod *Eucyclops serrulatus* fed on microalgae. *Journal of Plankton Research*, *19*(2), 273–278. https://doi.org/10.1093/plankt/19.2.273

Diaz, R. J., & Rosenberg, R. (2008). Spreading dead zones and consequences for marine ecosystems. *Science*, *321*(5891), 926–929. https://doi.org/10.1126/science.1156401

Dickson, A. G., Afghan, J. D., & Anderson, G. C. (2003). Reference materials for oceanic CO_2 analysis: A method for the certification of total alkalinity. *Marine Chemistry*, *80*(2–3), 185–197. https://doi.org/10.1016/S0304-4203(02)00133-0

Dickson, A. G., Sabine, C. L., & Christian, J. R. (2007). *Guide to Best Practices for Ocean CO_2 Measurements*. North Pacific Marine Science Organization.

Dimos, B., Emery, M., Beavers, K., MacKnight, N., Brandt, M., Demuth, J., & Mydlarz, L. (2022). Adaptive variation in homologue number within transcript families promotes expression divergence in reef-building coral. *Molecular Ecology*, *31*(9), 1–17. https://doi.org/10.1111/mec.16414

Domènech, F., Tomás, J., Crespo-Picazo, J. L., García-Párraga, D., Raga, J. A., & Aznar, F. J. (2017). To swim or not to swim: Potential transmission of *Balaenophilus manatorum* (Copepoda: Harpacticoida) in marine turtles. *PLoS ONE*, *12*(1), 1–15. https://doi.org/10.1371/journal.pone.0170789

Domenichiello, A. F., Kitson, A. P., & Bazinet, R. P. (2015). Is docosahexaenoic acid synthesis from α-linolenic acid sufficient to supply the adult brain? *Progress in Lipid Research*, *59*, 54–66. https://doi.org/10.1016/j.plipres.2015.04.002

Doney, S. C., Ruckelshaus, M., Emmett Duffy, J., Barry, J. P., Chan, F., English, C. A., Galindo, H. M., Grebmeier, J. M., Hollowed, A. B., Knowlton, N., Polovina, J., Rabalais, N. N., Sydeman, W. J., & Talley, L. D. (2012). Climate Change Impacts on Marine Ecosystems. *Annual Review of Marine Science*, *4*, 11–37. https://doi.org/10.1146/annurev-marine-041911-111611

Drago, L., Panaïotis, T., Irisson, J. O., Babin, M., Biard, T., Carlotti, F., Coppola, L., Guidi, L., Hauss, H., Karp-Boss, L., Lombard, F., McDonnell, A. M. P., Picheral, M., Rogge, A., Waite, A. M., Stemmann, L., & Kiko, R. (2022). Global Distribution of Zooplankton Biomass Estimated by In Situ Imaging and Machine Learning. *Frontiers in Marine Science*, *9*, 1–22. https://doi.org/10.3389/fmars.2022.894372

Drinkwater, K. F. (2005). The response of Atlantic cod (*Gadus morhua*) to future climate change. *ICES Journal of Marine Science*, *62*(7), 1327–1337. https://doi.org/10.1016/j.icesjms.2005.05.015

Drinkwater, K. F., Beaugrand, G., Kaeriyama, M., Kim, S., Ottersen, G., Perry, R. I., Pörtner, H. O., Polovina, J. J., & Takasuka, A. (2010). On the processes linking climate to ecosystem changes. *Journal of Marine Systems*, *79*, 374–388. https://doi.org/10.1016/j.jmarsys.2008.12.014

Edgar, R. C. (2004). MUSCLE: Multiple sequence alignment with high accuracy and high throughput. *Nucleic Acids Research*, *32*(5), 1792–1797. https://doi.org/10.1093/nar/gkh340

El-Gebali, S., Mistry, J., Bateman, A., Eddy, S. R., Luciani, A., Potter, S. C., Qureshi, M., Richardson, L. J., Salazar, G. A., Smart, A., Sonnhammer, E. L. L., Hirsh, L., Paladin, L., Piovesan, D., Tosatto, S. C. E., & Finn, R. D. (2019). The Pfam protein families database in 2019. *Nucleic Acids Research*, *47*, D427–D432. https://doi.org/10.1093/nar/gky995

Engström-Öst, J., Glippa, O., Feely, R. A., Kanerva, M., Keister, J. E., Alin, S. R., Carter, B. R., McLaskey, A. K., Vuori, K. A., & Bednaršek, N. (2019). Eco-physiological responses of copepods and pteropods to ocean warming and acidification. *Scientific Reports*, *9*, 4748. https://doi.org/10.1038/s41598-019-41213-1

Ericson, J. A., Hellessey, N., Kawaguchi, S., Nichols, P. D., Nicol, S., Hoem, N., & Virtue, P. (2019). Near-future ocean acidification does not alter the lipid content and fatty acid composition of adult Antarctic krill. *Scientific Reports*, *9*(1), 12375. https://doi.org/10.1038/s41598-019-48665-5

Falk-Petersen, S., Mayzaud, P., Kattner, G., & Sargent, J. R. (2009). Lipids and life strategy of Arctic *Calanus*. *Marine Biology Research*, *5*(1), 18–39. https://doi.org/10.1080/17451000802512267

Fang, S., Ting, C. T., Lee, C. R., Chu, K. H., Wang, C. C., & Tsaur, S. C. (2009). Molecular evolution and functional diversification of fatty acid desaturases after recurrent gene duplication in *Drosophila*. *Molecular Biology and Evolution*, *26*(7), 1447–1456. https://doi.org/10.1093/molbev/msp057

FAO. (2023). *Ecosystem services*. https://www.fao.org/ecosystem-services-biodiversity

Farkas, T., Kariko, K., & Csengeri, I. (1981). Incorporation of [1-14C] acetate into fatty acids of the crustaceans *Daphnia magna* and *Cyclops strenus* in relation to temperature. *Lipids*, *16*(6), 418–422. https://doi.org/10.1007/BF02535008

Fernandes, J. F., Ricardo, F., Jerónimo, D., Santos, A., Domingues, M. R., Calado, R., & Madeira, D. (2021). Modulation of fatty acid profiles by global and local ocean change drivers in the ragworm *Hediste diversicolor*: implications for aquaculture production. *Aquaculture*, *542*, 736871. https://doi.org/10.1016/j.aquaculture.2021.736871

Finck, J., Berdan, E. L., Mayer, F., Ronacher, B., & Geiselhardt, S. (2016). Divergence of cuticular hydrocarbons in two sympatric grasshopper species and the evolution of fatty acid synthases and elongases across insects. *Scientific Reports*, *6*, 33695. https://doi.org/10.1038/srep33695

Finn, R. D., Clements, J., & Eddy, S. R. (2011). HMMER web server: Interactive sequence similarity searching. *Nucleic Acids Research*, *39*, W29–W37. https://doi.org/10.1093/nar/gkr367

Fitzer, S. C., Caldwell, G. S., Close, A. J., Clare, A. S., Upstill-Goddard, R. C., & Bentley, M. G. (2012). Ocean acidification induces multi-generational decline in copepod naupliar production with possible conflict for reproductive resource allocation. *Journal of Experimental Marine Biology and Ecology*, *418–419*, 30–36. https://doi.org/10.1016/j.jembe.2012.03.009

Flanders Institute for Healthy Living. (2023). *Vis*. https://www.gezondleven.be/themas/voeding/voedingsdriehoek/vis

Folch, J., Lees, M., & Sloane Stanley, G. H. (1957). A simple method for the isolation and purification of total lipids from animal tissues. *Journal of Biological Chemistry*, *226*(1), 497–509.

Folke, C., Polasky, S., Rockström, J., Galaz, V., Westley, F., Lamont, M., Scheffer, M., Österblom, H., Carpenter, S. R., Chapin, F. S., Seto, K. C., Weber, E. U., Crona, B. I., Daily, G. C., Dasgupta, P., Gaffney, O., Gordon, L. J., Hoff, H., Levin, S. A., … Walker, B. H. (2021). Our future in the Anthropocene biosphere. *Ambio*, *50*(4), 834–869. https://doi.org/10.1007/s13280-021-01544-8

Foote, E. (1856). Circumstances affecting the Heat of the Sun's Rays. *The American Journal of Science and Arts*, *22*(56), 382–383.

Freeman, W. M., Walker, S. J., & Vrana, K. E. (1999). Quantitative RT-PCR: Pitfalls and potential. *BioTechniques*, *26*(1), 112–125. https://doi.org/10.2144/99261rv01

Friedlingstein, P., O'sullivan, M., Jones, M. W., Andrew, R. M., Gregor, L., Hauck, J., Le Quéré, C., Luijkx, I. T., Olsen, A., Peters, G. P., Peters, W., Pongratz, J., Schwingshackl, C., Sitch, S., Canadell, J. G., Ciais, P., Jackson, R. B., Alin, S. R., Alkama, R., … Zheng, B. (2022). Global Carbon Budget 2022. *Earth System Science Data*, *14*(11), 4811–4900. https://doi.org/10.5194/essd-14-4811-2022

Galassi, D. M. P., Huys, R., & Reid, J. W. (2009). Diversity, ecology and evolution of groundwater copepods. *Freshwater Biology*, *54*(4), 691–708. https://doi.org/10.1111/j.1365-2427.2009.02185.x

Galloway, A. W. E., & Budge, S. M. (2020). The critical importance of experimentation in biomarker-based trophic ecology. *Philosophical Transactions of the Royal Society B: Biological Sciences*, *375*(1804), 20190638. https://doi.org/10.1098/rstb.2019.0638

Gao, F., Chen, C., Arab, D. A., Du, Z., He, Y., & Ho, S. Y. W. (2019). EasyCodeML: A visual

tool for analysis of selection using CodeML. *Ecology and Evolution*, *9*(7), 3891–3898. https://doi.org/10.1002/ece3.5015

Gao, Y., Zheng, S., Zheng, C., Shi, Y., Xie, X., Wang, K., & Liu, H. (2018). The immune-related fatty acids are responsive to CO_2 driven seawater acidification in a crustacean brine shrimp *Artemia sinica. Developmental and Comparative Immunology*, *81*, 342–347. https://doi.org/10.1016/j.dci.2017.12.022

Garagnani, P., Bacalini, M. G., Pirazzini, C., Gori, D., Giuliani, C., Mari, D., Di Blasio, A. M., Gentilini, D., Vitale, G., Collino, S., Rezzi, S., Castellani, G., Capri, M., Salvioli, S., & Franceschi, C. (2012). Methylation of ELOVL2 gene as a new epigenetic marker of age. *Aging Cell*, *11*(6), 1132–1134. https://doi.org/10.1111/acel.12005

Garzke, J., Hansen, T., Ismar, S. M. H., & Sommer, U. (2016). Combined Effects of Ocean Warming and Acidification on Copepod Abundance, Body Size and Fatty Acid Content. *Plos One*, *11*(5), e0155952. https://doi.org/10.1371/journal.pone.0155952

Gattuso, J.-P., Magnan, A., Bille, R., Cheung, W. W. L., Howes, E. L., Joos, F., Allemand, D., Bopp, L., Cooley, S. R., Eakin, C. M., Hoegh-Guldberg, O., Kelly, R. P., Portner, H.-O., Rogers, A. D., Baxter, J. M., Laffoley, D., Osborn, D., Rankovic, A., Rochette, J., … Turley, C. (2015). Contrasting futures for ocean and society from different anthropogenic CO_2 emissions scenarios. *Science*, *349*(6243), aac4722. https://doi.org/10.1126/science.aac4722

Gee, J. M. (1987). Impact of epibenthic predation on estuarine intertidal harpacticoid copepod populations. *Marine Biology*, *96*(4), 497–510. https://doi.org/10.1007/BF00397967

Gee, J. M. (1989). An ecological and economic review of meiofauna as food for fish. *Zoological Journal of the Linnean Society*, *96*(3), 243–261. https://doi.org/10.1111/j.1096-3642.1989.tb02259.x

Gee, J. M., Warwick, R. M., Davey, J. T., & George, C. L. (1985). Field experiments on the role of epibenthic predators in determining prey densities in an estuarine mudflat. *Estuarine, Coastal and Shelf Science*, *21*(3), 429–448. https://doi.org/10.1016/0272-7714(85)90022-8

George, K. H., Khodami, S., Kihara, T. C., Martínez Arbizu, P., Martínez, A., Mercado Salas, N., Pointner, K., & Veit-Köhler, G. (2020). Copepoda. In A. Schmidt-Rhaesa (Ed.), *Guide to the identification of marine meiofauna* (pp. 465–533). Verlag Dr. Friedrich Pfeil.

Gladyshev, M. I., Makhutova, O. N., Kravchuk, E. S., Anishchenko, O. V., & Sushchik, N. N. (2016). Stable isotope fractionation of fatty acids of *Daphnia* fed laboratory cultures of microalgae. *Limnologica*, *56*, 23–29. https://doi.org/10.1016/j.limno.2015.12.001

Gladyshev, M. I., Sushchik, N. N., & Makhutova, O. N. (2013). Production of EPA and

DHA in aquatic ecosystems and their transfer to the land. *Prostaglandins and Other Lipid Mediators*, *107*, 117–126. https://doi.org/10.1016/j.prostaglandins.2013.03.002

Glencross, B. D. (2009). Exploring the nutritional demand for essential fatty acids by aquaculture species. *Aquaculture Research*, *48*(7), 71–124. https://doi.org/10.1111/J.1753-5131.2009.01006.X

GOED. (2023). *About EPA and DHA*. https://goedomega3.com/about-epa-and-dha

Gourtay, C., Chabot, D., Audet, C., Le Delliou, H., Quazuguel, P., Claireaux, G., & Zambonino-Infante, J. L. (2018). Will global warming affect the functional need for essential fatty acids in juvenile sea bass (*Dicentrarchus labrax*)? A first overview of the consequences of lower availability of nutritional fatty acids on growth performance. *Marine Biology*, *165*(9), 1–15. https://doi.org/10.1007/s00227-018-3402-3

Grabherr, M. G., Haas, B. J., Yassour, M., Levin, J. Z., Thompson, D. A., Amit, I., Adiconis, X., Fan, L., Raychowdhury, R., Zeng, Q., Chen, Z., Mauceli, E., Hacohen, N., Gnirke, A., Rhind, N., Di Palma, F., Birren, B. W., Nusbaum, C., Lindblad-Toh, K., … Regev, A. (2011). Full-length transcriptome assembly from RNA-Seq data without a reference genome. *Nature Biotechnology*, *29*(7), 644–652. https://doi.org/10.1038/nbt.1883

Graeve, M., Boissonnot, L., Niehoff, B., Hagen, W., & Kattner, G. (2020). Assimilation and turnover rates of lipid compounds in dominant Antarctic copepods fed with ^{13}C-enriched diatoms. *Philosophical Transactions of the Royal Society B: Biological Sciences*, *375*(1804). https://doi.org/10.1098/rstb.2019.0647

Guzmán, M., Velasco, G., & Geelen, M. J. H. (2000). Do cytoskeletal components control fatty acid translocation into liver mitochondria? *Trends in Endocrinology and Metabolism*, *11*(2), 49–53. https://doi.org/10.1016/S1043-2760(99)00223-4

Hamilton, H. A. (2020). *The omega-3 gap*. https://www.iffo.com/node/1619

Hamilton, H. A., Newton, R., Auchterlonie, N. A., & Müller, D. B. (2020). Systems approach to quantify the global omega-3 fatty acid cycle. *Nature Food*, *1*(1), 59–62. https://doi.org/10.1038/s43016-019-0006-0

Harley, C. D. G., Randall Hughes, A., Hultgren, K. M., Miner, B. G., Sorte, C. J. B., Thornber, C. S., Rodriguez, L. F., Tomanek, L., & Williams, S. L. (2006). The impacts of climate change in coastal marine systems. *Ecology Letters*, *9*(2), 228–241. https://doi.org/10.1111/j.1461-0248.2005.00871.x

Hartline, D. K., Cieslak, M. C., Castelfranco, A. M., Lieberman, B., Roncalli, V., & Lenz, P. H. (2023). De novo transcriptomes of six calanoid copepods (Crustacea): a resource for the discovery of novel genes. *Scientific Data*, *10*(1), 1–15. https://doi.org/10.1038/s41597-023-02130-1

Hashimoto, K., Yoshizawa, A. C., Okuda, S., Kuma, K., Goto, S., & Kanehisa, M. (2008). The repertoire of desaturases and elongases reveals fatty acid variations in 56

eukaryotic genomes. *Journal of Lipid Research*, *49*(1), 183–191. https://doi.org/10.1194/jlr.m700377-jlr200

Hastings, N., Agaba, M., Tocher, D. R., Leaver, M. J., Dick, J. R., Sargent, J. R., & Teale, A. J. (2001). A vertebrate fatty acid desaturase with Δ5 and Δ6 activities. *Proceedings of the National Academy of Sciences of the United States of America*, *98*(25), 14304–14309. https://doi.org/10.1073/pnas.251516598

Hausfather, Z., & Peters, G. P. (2020). Emissions - the "business as usual" story is misleading. *Nature*, *577*, 618–620. https://doi.org/10.1038/d41586-020-00177-3

Heine, K. B., Abebe, A., Wilson, A. E., & Hood, W. R. (2019). Copepod respiration increases by 7% per °C increase in temperature: A meta-analysis. *Limnology and Oceanography Letters*, *4*(3), 53–61. https://doi.org/10.1002/lol2.10106

Helenius, L., Budge, S., Duerksen, S., Devred, E., & Johnson, C. L. (2019). Lipids at the plant-animal interface: A stable isotope labelling method to evaluate the assimilation of essential fatty acids in the marine copepod *Calanus finmarchicus*. *Journal of Plankton Research*, *41*(6), 909–924. https://doi.org/10.1093/plankt/fbz062

Helenius, L., Budge, S. M., Nadeau, H., & Johnson, C. L. (2020). Ambient temperature and algal prey type affect essential fatty acid incorporation and trophic upgrading in a herbivorous marine copepod. *Philosophical Transactions of the Royal Society B: Biological Sciences*, *375*(1804). https://doi.org/10.1098/rstb.2020.0039

Hellemans, J., Mortier, G., De Paepe, A., Speleman, F., & Vandesompele, J. (2007). qBase relative quantification framework and software for management and automated analysis of real-time quantitative PCR data. *Genome Biology*, *8*, R19. https://doi.org/10.1186/gb-2007-8-2-r19

Helmkampf, M., Cash, E., & Gadau, J. (2015). Evolution of the insect desaturase gene family with an emphasis on social hymenoptera. *Molecular Biology and Evolution*, *32*(2), 456–471. https://doi.org/10.1093/molbev/msu315

Hernández, J., de la Parra, A. M., Lastra, M., & Viana, M. T. (2013). Effect of lipid composition of diets and environmental temperature on the performance and fatty acid composition of juvenile European abalone (*Haliotis tuberculata* L. 1758). *Aquaculture*, *412–413*, 34–40. https://doi.org/10.1016/j.aquaculture.2013.07.005

Herzog, S., Brinkmann, H., Vences, M., & Fleißner, A. (2020). Evidence of repeated horizontal transfer of sterol C-5 desaturase encoding genes among dikarya fungi. *Molecular Phylogenetics and Evolution*, *150*, 106850. https://doi.org/10.1016/j.ympev.2020.106850

Hicks, G. R. F., & Coull, B. C. (1983). The ecology of marine meiobenthic harpacticoid copepods. *Oceanography and Marine Biology - An Annual Review*, *21*, 67–175.

Hixson, S. M., & Arts, M. T. (2016). Climate warming is predicted to reduce omega-3, long-chain, polyunsaturated fatty acid production in phytoplankton. *Global Change*

Biology, *22*(8), 2744–2755. https://doi.org/10.1111/gcb.13295

Hoegh-Guldberg, O., Jacob, D., Taylor, M., Bindi, M., Brown, S., Camilloni, I., Diedhiou, A., Djalante, R., Ebi, K. L., Engelbrecht, F., Guiot, J., Hijioka, Y., Mehrotra, S., Payne, A., Seneviratne, S. I., Thomas, A., Warren, R., & Zhou, G. (2018). Impacts of 1.5°C of Global Warming on Natural and Human Systems. In V. Masson-Delmotte, P. Zhai, H.-O. Pörtner, D. Roberts, J. Skea, P. R. Shukla, A. Pirani, W. Moufouma-Okia, C. Péan, R. Pidcock, S. Connors, J. B. R. Matthews, Y. Chen, X. Zhou, M. I. Gomis, E. Lonnoy, T. Maycock, M. Tignor, & T. Waterfield (Eds.), *Global Warming of 1.5°C. An IPCC Special Report on the impacts of global warming of 1.5°C above pre-industrial levels and related global greenhouse gas emission pathways, in the context of strengthening the global response to the threat of climate change,* (pp. 175–312). Cambridge University Press. https://doi.org//10.1017/9781009157940.005

Holm, H. C., Fredricks, H. F., Bent, S. M., Lowenstein, D. P., Ossolinski, J. E., Becker, K. W., Johnson, W. M., Schrage, K., & Mooy, B. A. S. Van. (2022). Global ocean lipidomes show a universal relationship between temperature and lipid unsaturation. *Science*, *376*, 1487–1491. https://doi.org/10.1126/science.abn7455

Hölzer, M., & Marz, M. (2019). De novo transcriptome assembly: A comprehensive cross-species comparison of short-read RNA-Seq assemblers. *GigaScience*, *8*(5), 1–16. https://doi.org/10.1093/gigascience/giz039

Horne, C. R., Hirst, A. G., Atkinson, D., Almeda, R., & Kiørboe, T. (2019). Rapid shifts in the thermal sensitivity of growth but not development rate causes temperature–size response variability during ontogeny in arthropods. *Oikos, 128*(6), 823–835. https://doi.org/10.1111/oik.06016

Huerta-Cepas, J., Szklarczyk, D., Heller, D., Hernández-Plaza, A., Forslund, S. K., Cook, H., Mende, D. R., Letunic, I., Rattei, T., Jensen, L. J., Von Mering, C., & Bork, P. (2019). EggNOG 5.0: A hierarchical, functionally and phylogenetically annotated orthology resource based on 5090 organisms and 2502 viruses. *Nucleic Acids Research*, *47*(D1), D309–D314. https://doi.org/10.1093/nar/gky1085

Huys, R., & Boxshall, G. A. (1991). *Copepod evolution*. Ray Society.

Ibarbalz, F. M., Henry, N., Brandão, M. C., Martini, S., Busseni, G., Byrne, H., Coelho, L. P., Endo, H., Gasol, J. M., Gregory, A. C., Mahé, F., Rigonato, J., Royo-Llonch, M., Salazar, G., Sanz-Sáez, I., Scalco, E., Soviadan, D., Zayed, A. A., Zingone, A., … Zinger, L. (2019). Global Trends in Marine Plankton Diversity across Kingdoms of Life. *Cell*, *179*(5), 1084–1097. https://doi.org/10.1016/j.cell.2019.10.008

IEA. (2021). *Net Zero by 2050: A Roadmap for the Global Energy Sector*. https://www.iea.org/reports/net-zero-by-2050

IPCC. (2013). *Climate change 2013: The Physical Science Basis. Contribution of Working Group I to the Fifth Assessment Report of the Intergovernmental Panel on Climate Change* (T. F. Stocker, D. Qin, G.-K. Plattner, M. Tignor, S. K. Allen, J. Boschung, A.

Nauels, Y. Xia, V. Bex, & P. M. Midgley (eds.)). Cambridge University Press.

IPCC. (2021). *Climate Change 2021: The Physical Science Basis. Contribution of Working Group I to the Sixth Assessment Report of the Intergovernmental Panel on Climate Change* (V. Masson-Delmotte, P. Zhai, A. Pirani, S. L. Connors, C. Péan, S. Berger, N. Caud, Y. Chen, L. Goldfarb, M. I. Gomis, M. Huang, K. Leitzell, E. Lonnoy, J. B. R. Matthews, T. K. Maycock, T. Waterfield, O. Yelekçi, R. Yu, & B. Zhou (eds.)). Cambridge University Press. https://doi.org/10.1017/9781009157896

IPCC. (2022a). *Climate Change 2022: Impacts, Adaptation and Vulnerability. Working Group II contribution to the Sixth Assessment Report of the Intergovernamental Panel on Climate Change* (H.-O. Pörtner, D. C. Roberts, M. Tignor, E. S. Poloczanska, K. Mintenbeck, A. Alegría, M. Craig, S. Langsdorf, S. Löschke, V. Möller, A. Okem, & B. Rama (eds.)). Cambridge University Press. https://doi.org/10.1017/9781009325844

IPCC. (2022b). *Climate Change 2022: Mitigation of Climate Change. Working Group III Contribution to the Sixth Assessment Report of the Intergovernmental Panel on Climate Change*. Cambridge University Press.

Ishikawa, A., Kabeya, N., Ikeya, K., Kakioka, R., Cech, J. N., Osada, N., Leal, M. C., Inoue, J., Kume, M., Toyoda, A., Tezuka, A., Nagano, A. J., Yamasaki, Y. Y., Suzuki, Y., Kokita, T., Takahashi, H., Lucek, K., Marques, D., Takehana, Y., … Kitano, J. (2019). A key metabolic gene for recurrent freshwater colonization and radiation in fishes. *Science*, *364*, 886–889. https://doi.org/10.1126/science.aau5656

Ishikawa, A., Stuart, Y. E., Bolnick, D. I., & Kitano, J. (2021). Copy number variation of a fatty acid desaturase gene Fads2 associated with ecological divergence in freshwater stickleback populations. *Biology Letters*, *17*(8), 20210204. https://doi.org/10.1098/rsbl.2021.0204

Ishikawa, A., Yamanouchi, S., Iwasaki, W., & Kitano, J. (2022). Convergent copy number increase of genes associated with freshwater colonisation in fishes. *Philosophical Transactions of the Royal Society B: Biological Sciences*, *377*, 20200509. https://doi.org/10.1098/rstb.2020.0509

ISSFAL. (2004). *Recommendations for intake of polyunsaturated fatty acids in healthy adults*. https://doi.org/10.1016/j.plipres.2004.05.003

Isumbisho, M., Kaningini, M., Descy, J. P., & Baras, E. (2004). Seasonal and diel variations in diet of the young stages of the fish *Limnothrissa miodon* in Lake Kivu, Eastern Africa. *Journal of Tropical Ecology*, *20*, 1–11. https://doi.org/10.1017/S0266467403001056

Janssen, A., Chevaldonné, P., & Arbizu, P. M. (2013). Meiobenthic copepod fauna of a marine cave (NW Mediterranean) closely resembles that of deep-sea communities. *Marine Ecology Progress Series*, *479*, 99–113. https://doi.org/10.3354/meps10207

Jardine, T. D., Galloway, A. W. E., & Kainz, M. J. (2020). Unlocking the power of fatty

acids as dietary tracers and metabolic signals in fishes and aquatic invertebrates. *Philosophical Transactions of the Royal Society B: Biological Sciences*, *375*(1804), 20190639. https://doi.org/10.1098/rstb.2019.0639

Ji, R., Edwards, M., MacKas, D. L., Runge, J. A., & Thomas, A. C. (2010). Marine plankton phenology and life history in a changing climate: Current research and future directions. *Journal of Plankton Research*, *32*(10), 1355–1368. https://doi.org/10.1093/plankt/fbq062

Jiang, R. H. Y., & Govers, F. (2006). Nonneutral GC3 and retroelement codon mimicry in Phytophthora. *Journal of Molecular Evolution*, *63*(4), 458–472. https://doi.org/10.1007/s00239-005-0211-3

Jin, P., Hutchins, D. A., & Gao, K. (2020). The Impacts of Ocean Acidification on Marine Food Quality and Its Potential Food Chain Consequences. *Frontiers in Marine Science*, *7*, 543979. https://doi.org/10.3389/fmars.2020.543979

Jónasdóttir, S. H. (2019). Fatty acid profiles and production in marine phytoplankton. *Marine Drugs*, *17*(3), 1–20. https://doi.org/10.3390/md17030151

Jónasdóttir, S. H., Visser, A. W., Richardson, K., & Heath, M. R. (2015). Seasonal copepod lipid pump promotes carbon sequestration in the deep North Atlantic. *Proceedings of the National Academy of Sciences of the United States of America*, *112*(39), 12122–12126. https://doi.org/10.1073/pnas.1512110112

Kabeya, N., Fonseca, M. M., Ferrier, D. E. K., Navarro, J. C., Bay, L. K., Francis, D. S., Tocher, D. R., Castro, L. F. C., & Monroig, Ó. (2018). Genes for de novo biosynthesis of omega-3 polyunsaturated fatty acids are widespread in animals. *Science Advances*, *4*(5), eaar6849. https://doi.org/10.1126/sciadv.aar6849

Kabeya, N., Gür, İ., Oboh, A., Evjemo, J. O., Malzahn, A. M., Hontoria, F., Navarro, J. C., & Monroig, Ó. (2020). Unique fatty acid desaturase capacities uncovered in *Hediste diversicolor* illustrate the roles of aquatic invertebrates in trophic upgrading. *Philosophical Transactions of the Royal Society B: Biological Sciences*, *375*(1804), 20190654. https://doi.org/10.1098/rstb.2019.0654

Kabeya, N., Ogino, M., Ushio, H., Haga, Y., Satoh, S., Navarro, J. C., & Monroig, Ó. (2021). A complete enzymatic capacity for biosynthesis of docosahexaenoic acid (DHA, 22:6n-3) exists in the marine Harpacticoida copepod *Tigriopus californicus*. *Open Biology*, *11*(4), 200402. https://doi.org/10.1098/rsob.200402

Kabeya, N., Sanz-Jorquera, A., Carboni, S., Davie, A., Oboh, A., & Monroig, O. (2017). Biosynthesis of polyunsaturated fatty acids in sea urchins: Molecular and functional characterisation of three fatty acyl desaturases from *Paracentrotus lividus* (Lamark 1816). *PLoS ONE*, *12*(1), 1–15. https://doi.org/10.1371/journal.pone.0169374

Kanehisa, M., Goto, S., Sato, Y., Furumichi, M., & Tanabe, M. (2012). KEGG for integration and interpretation of large-scale molecular data sets. *Nucleic Acids Research*, *40*(D1),

109–114. https://doi.org/10.1093/nar/gkr988

Katoh, K., & Standley, D. M. (2013). MAFFT multiple sequence alignment software version 7: Improvements in performance and usability. *Molecular Biology and Evolution*, *30*(4), 772–780. https://doi.org/10.1093/molbev/mst010

Khodami, S., McArthur, J. V., Blanco-Bercial, L., & Arbizu, P. M. (2020). Retraction Note: Molecular Phylogeny and Revision of Copepod Orders (Crustacea: Copepoda). *Scientific Reports*, *10*, 17602. https://doi.org/10.1038/s41598-020-74404-2

Khodami, S., McArthur, J. V., Blanco-Bercial, L., & Martinez Arbizu, P. (2017). Molecular Phylogeny and Revision of Copepod Orders (Crustacea: Copepoda). *Scientific Reports*, *7*(1), 1–11. https://doi.org/10.1038/s41598-017-06656-4

Kikuchi, Y. (1994). *Glaciella*, a new genus of freshwater Canthocamptidae (Copepoda, Harpacticoida) from a glacier in Nepal, Himalayas. *Hydrobiologia*, *292–293*(1), 59–66. https://doi.org/10.1007/BF00229923

Kim, H. S., Lee, B. Y., Han, J., Lee, Y. H., Min, G. S., Kim, S., & Lee, J. S. (2016). De novo assembly and annotation of the Antarctic copepod (*Tigriopus kingsejongensis*) transcriptome. *Marine Genomics*, *28*, 37–39. https://doi.org/10.1016/j.margen.2016.04.009

Kim, H. S., Lee, B. Y., Won, E. J., Han, J., Hwang, D. S., Park, H. G., & Lee, J. S. (2015). Identification of xenobiotic biodegradation and metabolism-related genes in the copepod *Tigriopus japonicus* whole transcriptome analysis. *Marine Genomics*, *24*, 207–208. https://doi.org/10.1016/j.margen.2015.05.011

Kondrashov, F. A. (2012). Gene duplication as a mechanism of genomic adaptation to a changing environment. *Proceedings of the Royal Society B: Biological Sciences*, *279*(1749), 5048–5057. https://doi.org/10.1098/rspb.2012.1108

Krkošek, M., Ford, J. S., Morton, A., Lele, S., Myers, R. A., & Lewis, M. A. (2007). Declining Wild Salmon Populations in Relation to Parasites from Farm Salmon. *American Association for the Advancement of Science*, *318*, 1772–1775. https://doi.org/10.1126/science.1148744

Kumar, S., Stecher, G., & Tamura, K. (2016). MEGA7: Molecular Evolutionary Genetics Analysis version 7.0 for bigger datasets. *Molecular Biology and Evolution*, *33*(7), msw054. https://doi.org/10.1093/molbev/msw054

Kurihara, H., & Ishimatsu, A. (2008). Effects of high CO_2 seawater on the copepod (*Acartia tsuensis*) through all life stages and subsequent generations. *Marine Pollution Bulletin*, *56*(6), 1086–1090. https://doi.org/10.1016/j.marpolbul.2008.03.023

Kwiatkowski, L., Torres, O., Bopp, L., Aumont, O., Chamberlain, M., R. Christian, J., P. Dunne, J., Gehlen, M., Ilyina, T., G. John, J., Lenton, A., Li, H., S. Lovenduski, N., C. Orr, J., Palmieri, J., Santana-Falcón, Y., Schwinger, J., Séférian, R., A. Stock, C., ... Ziehn, T.

(2020). Twenty-first century ocean warming, acidification, deoxygenation, and upper-ocean nutrient and primary production decline from CMIP6 model projections. *Biogeosciences*, *17*(13), 3439–3470. https://doi.org/10.5194/bg-17-3439-2020

Lallemand, T., Leduc, M., Landès, C., Rizzon, C., & Lerat, E. (2020). An overview of duplicated gene detection methods: Why the duplication mechanism has to be accounted for in their choice. *Genes, 11,* 1046. https://doi.org/10.3390/genes11091046

Langer, J. A. F., Meunier, C. L., Ecker, U., Horn, H. G., Schwenk, K., & Boersma, M. (2019). Acclimation and adaptation of the coastal calanoid copepod *Acartia tonsa* to ocean acidification: A long-term laboratory investigation. *Marine Ecology Progress Series*, *619*, 35–51. https://doi.org/10.3354/meps12950

Langmead, B., & Salzberg, S. L. (2012). Fast gapped-read alignment with Bowtie 2. *Nature Methods*, *9*(4), 357–359. https://doi.org/10.1038/nmeth.1923

Lee, M.-C., Choi, B.-S., Kim, M.-S., Yoon, D.-S., Park, J. C., Kim, S., & Lee, J.-S. (2020a). An improved genome assembly and annotation of the Antarctic copepod *Tigriopus kingsejongensis* and comparison of fatty acid metabolism between *T. kingsejongensis* and the temperate copepod *T. japonicus*. *Comparative Biochemistry and Physiology - Part D: Genomics and Proteomics*, *35*, 100703. https://doi.org/10.1016/j.cbd.2020.100703

Lee, M.-C., Choi, H., Park, J. C., Yoon, D.-S., Lee, Y., Hagiwara, A., Park, H. G., Shin, K.-H., & Lee, J.-S. (2020b). A comparative study of food selectivity of the benthic copepod *Tigriopus japonicus* and the pelagic copepod *Paracyclopina nana*: A genome-wide identification of fatty acid conversion genes and nitrogen isotope investigation. *Aquaculture*, *521*, 734930. https://doi.org/10.1016/j.aquaculture.2020.734930

Lee, M.-C., Hagiwara, A., Park, H. G., & Lee, J.-S. (2019a). Genome-wide identification and expression of eight fatty acid desaturase genes, and the fatty acid profile, in the marine rotifer *Brachionus koreanus* fed the alga *Tetraselmis suecica*. *Fisheries Science*, *85*, 397–406. https://doi.org/10.1007/s12562-018-01286-9

Lee, M.-C., Han, J., Lee, S.-H., Kim, D.-H., Kang, H. M., Won, E. J., Hwang, D. S., Park, J. C., Om, A. S., & Lee, J. S. (2016). A brominated flame retardant 2,2′,4,4′ tetrabrominated diphenyl ether (BDE-47) leads to lipogenesis in the copepod *Tigriopus japonicus*. *Aquatic Toxicology*, *178*, 19–26. https://doi.org/10.1016/j.aquatox.2016.07.002

Lee, M.-C., Park, J.-C., Yoon, D.-S., Choi, H., Kim, H.-J., Shin, K.-H., Hagiwara, A., Han, J., Park, H. G., & Lee, J.-S. (2019b). Genome-wide characterization and expression of the elongation of very long chain fatty acid (Elovl) genes and fatty acid profiles in the alga (*Tetraselmis suecica*) fed marine rotifer *Brachionus koreanus*. *Comparative Biochemistry and Physiology - Part D: Genomics and Proteomics*, *30*, 179–185. https://doi.org/10.1016/j.cbd.2019.03.001

Lee, M.-C., Park, J. C., & Lee, J. S. (2018). Effects of environmental stressors on lipid metabolism in aquatic invertebrates. *Aquatic Toxicology*, *200*, 83–92. https://doi.org/10.1016/j.aquatox.2018.04.016

Lee, M.-C., Yoon, D.-S., Park, J. C., Choi, H., Shin, K.-H., Hagiwara, A., Lee, J.-S., & Park, H. G. (2022a). Effects of salinity and temperature on reproductivity and fatty acid synthesis in the marine rotifer *Brachionus rotundiformis*. *Aquaculture*, *546*, 737282. https://doi.org/10.1016/j.aquaculture.2021.737282

Lee, S.-H., Lee, M.-C., Puthumana, J., Park, J. C., Kang, S., Han, J., Shin, K.-H., Park, H. G., Om, A.-S., & Lee, J.-S. (2017a). Effects of temperature on growth and fatty acid synthesis in the cyclopoid copepod *Paracyclopina nana*. *Fisheries Science*, *83*(5), 725–734. https://doi.org/10.1007/s12562-017-1104-2

Lee, S.-H., Lee, M. C., Puthumana, J., Park, J. C., Kang, S., Hwang, D. S., Shin, K. H., Park, H. G., Souissi, S., Om, A. S., Lee, J. S., & Han, J. (2017b). Effects of salinity on growth, fatty acid synthesis, and expression of stress response genes in the cyclopoid copepod *Paracyclopina nana*. *Aquaculture*, *470*, 182–189. https://doi.org/10.1016/j.aquaculture.2016.12.037

Lee, Y. H., Kim, M.-S., Wang, M., Bhandari, R. K., Park, H. G., Wu, R. S.-S., & Lee, J.-S. (2022b). Epigenetic plasticity enables copepods to cope with ocean acidification. *Nature Climate Change*, *12*, 918–927. https://doi.org/10.1038/s41558-022-01477-4

Lenoir, J., Bertrand, R., Comte, L., Bourgeaud, L., Hattab, T., Murienne, J., & Grenouillet, G. (2020). Species better track climate warming in the oceans than on land. *Nature Ecology and Evolution*, *4*(8), 1044–1059. https://doi.org/10.1038/s41559-020-1198-2

Lenz, P. H., Roncalli, V., Hassett, R. P., Wu, L. S., Cieslak, M. C., Hartline, D. K., & Christie, A. E. (2014). De novo assembly of a transcriptome for *Calanus finmarchicus* (Crustacea, Copepoda) - The dominant zooplankter of the North Atlantic Ocean. *PLoS ONE*, *9*(2), e88589. https://doi.org/10.1371/journal.pone.0088589

Leu, E., Daase, M., Schulz, K. G., Stuhr, A., & Riebesell, U. (2013). Effect of ocean acidification on the fatty acid composition of a natural plankton community. *Biogeosciences*, *10*(2), 1143–1153. https://doi.org/10.5194/bg-10-1143-2013

Lewis, S. L., & Maslin, M. A. (2015). Defining the Anthropocene. *Nature*, *519*(7542), 171–180. https://doi.org/10.1038/nature14258

Lin, Z., Hao, M., Huang, Y., Zou, W., Rong, H., & Wen, X. (2018). Cloning, tissue distribution and nutritional regulation of a fatty acyl Elovl4-like elongase in mud crab, *Scylla paramamosain* (Estampador, 1949). *Comparative Biochemistry and Physiology - Part B: Biochemistry and Molecular Biology*, *217*, 70–78. https://doi.org/10.1016/j.cbpb.2017.12.010

Lin, Z., Hao, M., Zhu, D., Li, S., & Wen, X. (2017). Molecular cloning, mRNA expression and nutritional regulation of a Δ6 fatty acyl desaturase-like gene of mud crab, *Scylla*

paramamosain. Comparative Biochemistry and Physiology - Part B: Biochemistry and Molecular Biology, *208–209*, 29–37. https://doi.org/10.1016/j.cbpb.2017.03.004

Lindeman, R. L. (1942). The Trophic-Dynamic Aspect of Ecology Author. *Ecology*, *23*(4), 399–417. https://doi.org/10.2307/1930126

Litzow, M. A., Bailey, K. M., Prahl, F. G., & Heintz, R. (2006). Climate regime shifts and reorganization of fish communities: the essential fatty acid limitation hypothesis. *Marine Ecology Progress Series*, *315*, 1–11. https://doi.org/10.3354/meps315001

Liu, X., Wang, L., Feng, Z., Song, X., & Zhu, W. (2017). Molecular cloning and functional characterization of the fatty acid delta 6 desaturase (FAD6) gene in the sea cucumber *Apostichopus japonicus*. *Aquaculture Research*, *48*(9), 4991–5003. https://doi.org/10.1111/are.13317

Lizano, A. M., Smolina, I., Choquet, M., Kopp, M., & Hoarau, G. (2022). Insights into the species evolution of *Calanus* copepods in the northern seas revealed by de novo transcriptome sequencing. *Ecology and Evolution*, *12*(2), 1–15. https://doi.org/10.1002/ece3.8606

Long, A. P. (2016). *Coping with aquaculture*. National University of Ireland, Galway.

Lopes-Marques, M., Kabeya, N., Qian, Y., Ruivo, R., Santos, M. M., Venkatesh, B., Tocher, D. R., Castro, L. F. C., & Monroig, Ó. (2018). Retention of fatty acyl desaturase 1 (fads1) in Elopomorpha and Cyclostomata provides novel insights into the evolution of long-chain polyunsaturated fatty acid biosynthesis in vertebrates. *BMC Evolutionary Biology*, *18*(1), 1–9. https://doi.org/10.1186/s12862-018-1271-5

Lozano-Fernandez, J., Giacomelli, M., Fleming, J. F., Chen, A., Vinther, J., Thomsen, P. F., Glenner, H., Palero, F., Legg, D. A., Iliffe, T. M., Pisani, D., & Olesen, J. (2019). Pancrustacean Evolution Illuminated by Taxon-Rich Genomic-Scale Data Sets with an Expanded Remipede Sampling. *Genome Biology and Evolution*, *11*(8), 2055–2070. https://doi.org/10.1093/gbe/evz097

Lueker, T. J., Dickson, A. G., & Keeling, C. D. (2000). Ocean pCO$_2$ calculated from dissolved inorganic carbon, alkalinity, and equations for K1 and K2: Validation based on laboratory measurements of CO$_2$ in gas and seawater at equilibrium. *Marine Chemistry*, *70*(1–3), 105–119. https://doi.org/10.1016/S0304-4203(00)00022-0

Maas, A. E., Blanco-Bercial, L., Lo, A., Tarrant, A. M., & Timmins-Schiffman, E. (2018). Variations in copepod proteome and respiration rate in association with diel vertical migration and circadian cycle. *Biological Bulletin*, *235*(1), 30–42. https://doi.org/10.1086/699219

Macháček, S., Tupec, M., Horáček, N., Halmová, M., Roy, A., Machara, A., Kyjaková, P., Lukšan, O., Pichová, I., & Hanus, R. (2023). Evolution of Linoleic Acid Biosynthesis Paved the Way for Ecological Success of Termites. *Molecular Biology and Evolution*, *40*(4), 1–19. https://doi.org/10.1093/molbev/msad087

Madeira, C., Madeira, D., Ladd, N., Schubert, C. J., Diniz, M. S., Vinagre, C., & Leal, M. C. (2021). Conserved fatty acid profiles and lipid metabolic pathways in a tropical reef fish exposed to ocean warming – An adaptation mechanism of tolerant species? *Science of the Total Environment*, *782*, 146738. https://doi.org/10.1016/j.scitotenv.2021.146738

Mah, M., Kuah, M., Yeat, S., Merosha, P., Janaranjani, M., Goh, P., Jaya-ram, A., & Shu-chien, A. C. (2019). Molecular cloning , phylogenetic analysis and functional characterisation of an Elovl7-like elongase from a marine crustacean, the orange mud crab (*Scylla olivacea*). *Comparative Biochemistry and Physiology - Part B: Biochemistry and Molecular Biology*, *232*, 60–71. https://doi.org/10.1016/j.cbpb.2019.01.011

Maibam, C., Fink, P., Romano, G., Buia, M. C., Butera, E., & Zupo, V. (2015). *Centropages typicus* (Crustacea, Copepoda) reacts to volatile compounds produced by planktonic algae. *Marine Ecology*, *36*(3), 819–834. https://doi.org/10.1111/maec.12254

Malcicka, M., Ruther, J., & Ellers, J. (2017). De novo Synthesis of Linoleic Acid in Multiple Collembola Species. *Journal of Chemical Ecology*, *43*(9), 911–919. https://doi.org/10.1007/s10886-017-0878-0

Malcicka, M., Visser, B., & Ellers, J. (2018). An evolutionary perspective on linoleic acid synthesis in animals. *Evolutionary Biology*, *45*(1), 15–26. https://doi.org/10.1007/s11692-017-9436-5

Malm, A., & Hornborg, A. (2014). The geology of mankind? A critique of the Anthropocene narrative. *The Anthropocene Review*, *1*(1), 62–69. https://doi.org/10.1177/2053019613516291

Marmillot, V., Parrish, C. C., Tremblay, J. É., Gosselin, M., & MacKinnon, J. F. (2020). Environmental and Biological Determinants of Algal Lipids in Western Arctic and Subarctic Seas. *Frontiers in Environmental Science*, *8*, 538635. https://doi.org/10.3389/fenvs.2020.538635

Masclaux, H., Bec, A., Kainz, M. J., Perrière, F., Desvilettes, C., & Bourdier, G. (2012). Accumulation of polyunsaturated fatty acids by cladocerans: Effects of taxonomy, temperature and food. *Freshwater Biology*, *57*(4), 696–703. https://doi.org/10.1111/j.1365-2427.2012.02735.x

Mathews, L., Faithfull, C. L., Lenz, P. H., & Nelson, C. E. (2018). The effects of food stoichiometry and temperature on copepods are mediated by ontogeny. *Oecologia, 188*(1), 75–84. https://doi.org/10.1007/s00442-018-4183-6

Mathiske, A., Thistle, D., Gheerardyn, H., & Veit-Köhler, G. (2021). Deep sea without limits-four new closely related species of *Emertonia* Wilson, 1932 (Copepoda: Harpacticoida: Paramesochridae) show characters with a worldwide distribution. *Zootaxa*, *5051*(1), 443–486. https://doi.org/10.11646/zootaxa.5051.1.18

Matriano, D. M., Alegado, R. A., & Conaco, C. (2021). Detection of horizontal gene transfer in the genome of the choanoflagellate *Salpingoeca rosetta*. *Scientific Reports, 11*, 5993. https://doi.org/10.1038/s41598-021-85259-6

Matsushita, Y., Miyoshi, K., Kabeya, N., Sanada, S., Yazawa, R., Haga, Y., Satoh, S., Yamamoto, Y., Strüssmann, C. A., Luckenbach, J. A., & Yoshizaki, G. (2020). Flatfishes colonised freshwater environments by acquisition of various DHA biosynthetic pathways. *Communications Biology*, *3*(1), 4–5. https://doi.org/10.1038/s42003-020-01242-3

Mayor, D. J., Everett, N. R., & Cook, K. B. (2012). End of century ocean warming and acidification effects on reproductive success in a temperate marine copepod. *Journal of Plankton Research*, *34*(3), 258–262. https://doi.org/10.1093/plankt/fbr107

Mayor, D. J., Sommer, U., Cook, K. B., & Viant, M. R. (2015). The metabolic response of marine copepods to environmental warming and ocean acidification in the absence of food. *Scientific Reports*, *5*, 1–12. https://doi.org/10.1038/srep13690

McAllen, R. (1999). *Enteromorpha intestinalis*-a refuge for the supralittoral rockpool harpacticoid copepod *Tigriopus brevicornis*. *Journal of the Marine Biological Association of the United Kingdom*, *79*, 1125–1126.

Meesapyodsuk, D., & Qiu, X. (2014). Structure determinants for the substrate specificity of Acyl-CoA Δ9 desaturases from a marine copepod. *ACS Chemical Biology*, *9*(4), 922–934. https://doi.org/10.1021/cb400675d

Menzel, R., von Chrzanowski, H., Tonat, T., van Riswyck, K., Schliesser, P., & Ruess, L. (2019). Presence or absence? Primary structure, regioselectivity and evolution of Δ12/ω3 fatty acid desaturases in nematodes. *Biochimica et Biophysica Acta - Molecular and Cell Biology of Lipids*, *1864*(9), 1194–1205. https://doi.org/10.1016/j.bbalip.2019.05.001

Mercado-Salas, N. F., Khodami, S., & Arbizu, P. M. (2021). Copepods and ostracods associated with bromeliads in the Yucatán Peninsula, Mexico. *PLoS ONE*, *16*, 1–20. https://doi.org/10.1371/journal.pone.0248863

Meyers, M., Décima, M., Law, C. S., Gall, M., Barr, N., Miller, M. R., Safi, K., Robinson, K., Sabadel, A., Wing, S., & Hoffmann, L. (2022). No evidence of altered relationship between diet and consumer fatty acid composition in a natural plankton community under combined climate drivers. *Journal of Experimental Marine Biology and Ecology*, *551*, 151734. https://doi.org/10.1016/j.jembe.2022.151734

Mirzabaev, A., Bezner Kerr, R., Hasegawa, T., Pradhan, P., Wreford, A., Cristina Tirado von der Pahlen, M., & Gurney-Smith, H. (2023). Severe climate change risks to food security and nutrition. *Climate Risk Management*, *39*, 100473. https://doi.org/10.1016/j.crm.2022.100473

Molnar, J. L., Gamboa, R. L., Revenga, C., & Spalding, M. D. (2008). Assessing the global

threat of invasive species to marine biodiversity. *Frontiers in Ecology and the Environment*, *6*(9), 485–492. https://doi.org/10.1890/070064

Monroig, Ó., & Kabeya, N. (2018). Desaturases and elongases involved in polyunsaturated fatty acid biosynthesis in aquatic invertebrates: a comprehensive review. *Fisheries Science*, *84*(6), 911–928. https://doi.org/10.1007/s12562-018-1254-x

Monroig, Ó., Navarro, J. C., Dick, J. R., Alemany, F., & Tocher, D. R. (2012). Identification of a Δ5-like Fatty Acyl Desaturase from the Cephalopod *Octopus vulgaris* (Cuvier 1797) Involved in the Biosynthesis of Essential Fatty Acids. *Marine Biotechnology*, *14*(4), 411–422. https://doi.org/10.1007/s10126-011-9423-2

Monroig, Ó., Navarro, J. C., & Tocher, D. R. (2011). Long-Chain Polyunsaturated Fatty Acids in Fish: Recent Advances on Desaturases and Elongases Involved in Their Biosynthesis. In L. E. Cruz-Suárez, D. Ricque-Marie, M. Tapia-Salazar, M. G. Nieto-López, D. A. Villarreal-Cavazos, J. Gamboa-Delgado, & L. Hernández-Hernández (Eds.), *Avances en Nutrición Acuícola XI – Memorias del Décimo Primer Simposio Internacional de Nutrición Acuícola, 23-25 de Noviembre, San Nicolás de los Garza, N. L., México* (pp. 257–283). Universidad Autónoma de Nuevo León.

Monroig, Ó., Shu-Chien, A. C., Kabeya, N., Tocher, D. R., & Castro, L. F. C. (2022). Desaturases and elongases involved in long-chain polyunsaturated fatty acid biosynthesis in aquatic animals: from genes to functions. *Progress in Lipid Research*, *86*, 127248. https://doi.org/10.1016/j.plipres.2022.101157

Monroig, Ó., Tocher, D. R., & Castro, L. F. C. (2018). Polyunsaturated Fatty Acid Biosynthesis and Metabolism in Fish. In *Polyunsaturated fatty acid metabolism* (pp. 31–60). AOCS Press. https://doi.org/10.1016/B978-0-12-811230-4.00003-X

Monroig, Ó., Tocher, D. R., & Navarro, J. C. (2013). Biosynthesis of polyunsaturated fatty acids in marine invertebrates: Recent advances in molecular mechanisms. *Marine Drugs*, *11*(10), 3998–4018. https://doi.org/10.3390/md11103998

Monroig, Ó., Zheng, X., Morais, S., Leaver, M. J., Taggart, J. B., & Tocher, D. R. (2010). Multiple genes for functional 6 fatty acyl desaturases (Fad) in Atlantic salmon (*Salmo salar* L.): Gene and cDNA characterization, functional expression, tissue distribution and nutritional regulation. *Biochimica et Biophysica Acta - Molecular and Cell Biology of Lipids*, *1801*(9), 1072–1081. https://doi.org/10.1016/j.bbalip.2010.04.007

Morais, S., Torres, M., Hontoria, F., Monroig, Ó., Varó, I., Agulleiro, M. J., & Navarro, J. C. (2020). Molecular and functional characterization of elovl4 genes in *Sparus aurata* and *Solea senegalensis* pointing to a critical role in very long-chain (>C24) fatty acid synthesis during early neural development of fish. *International Journal of Molecular Sciences*, *21*(10), 1–18. https://doi.org/10.3390/ijms21103514

Moreno, V. J., De Moreno, J. E. A., & Brenner, R. R. (1979). Fatty acid metabolism in the calanoid copepod *Paracalanus parvus*: 1. Polyunsaturated fatty acids. *Lipids*, *14*(4),

313–317. https://doi.org/10.1007/BF02533413

Müller-Navarra, D. C., Brett, M. T., Park, S., Chandra, S., Ballantyne, A. P., Zorita, E., & Goldman, C. R. (2004). Unsaturated fatty acid content in seston and tropho-dynamic coupling in lakes. *Nature*, *427*, 69–72. https://doi.org/10.1038/nature02210

Munday, P. L., Warner, R. R., Monro, K., Pandolfi, J. M., & Marshall, D. J. (2013). Predicting evolutionary responses to climate change in the sea. *Ecology Letters*, *16*(12), 1488–1500. https://doi.org/10.1111/ele.12185

Musilova, Z., Cortesi, F., Matschiner, M., Davies, W. I. L., Patel, J. S., Stieb, S. M., De Busserolles, F., Malmstrøm, M., Tørresen, O. K., Brown, C. J., Mountford, J. K., Hanel, R., Stenkamp, D. L., Jakobsen, K. S., Carleton, K. L., Jentoft, S., Marshall, J., & Salzburger, W. (2019). Vision using multiple distinct rod opsins in deep-sea fishes. *Science*, *364*(6440), 588–592. https://doi.org/10.1126/science.aav4632

Nanton, D. A., & Castell, J. D. (1998). The effects of dietary fatty acids on the fatty acid composition of the harpacticoid copepod, *Tisbe* sp., for use as a live food for marine fish larvae. *Aquaculture*, *163*, 251–261. https://doi.org/10.1016/S0044-8486(98)00236-1

Nanton, D. A., & Castell, J. D. (1999). The effects of temperature and dietary fatty acids on the fatty acid composition of harpacticoid copepods, for use as a live food for marine fish larvae. *Aquaculture*, *175*(1–2), 167–181. https://doi.org/10.1016/S0044-8486(99)00031-9

Napier, J. A., Olsen, R. E., & Tocher, D. R. (2019). Update on GM canola crops as novel sources of omega-3 fish oils. *Plant Biotechnology Journal, 17*(4), 703–705. https://doi.org/10.1111/pbi.13045

Neukermans, G., Oziel, L., & Babin, M. (2018). Increased intrusion of warming Atlantic water leads to rapid expansion of temperate phytoplankton in the Arctic. *Global Change Biology*, *24*(6), 2545–2553. https://doi.org/10.1111/gcb.14075

Nguyen, M., Ekstrom, A., Li, X., & Yin, Y. (2015). HGT-finder: A new tool for horizontal gene transfer finding and application to *Aspergillus* genomes. *Toxins, 7*(10), 4035–4053. https://doi.org/10.3390/toxins7104035

NHMRC. (2005). *Nutrient Reference Values for Australia and New Zealand Including Recommended Dietary Intakes*.

Nielsen, B. L. H., Gøtterup, L., Jørgensen, T. S., Hansen, B. W., Hansen, L. H., Mortensen, J., & Jepsen, P. M. (2019). n-3 PUFA biosynthesis by the copepod *Apocyclops royi* documented using fatty acid profile analysis and gene expression analysis. *Biology Open*, *8*(2), bio038331. https://doi.org/10.1242/bio.038331

Nielsen, B. L. H., Van Someren Gréve, H., & Hansen, B. W. (2020a). Cultivation success and fatty acid composition of the tropical copepods *Apocyclops royi* and *Pseudodiaptomus annandalei* fed on monospecific diets with varying PUFA profiles.

Aquaculture Research, *52*(3), 1127–1138. https://doi.org/10.1111/are.14970

Nielsen, B. L. H., Van Someren Gréve, H., Rayner, T. A., & Hansen, B. W. (2020b). Biochemical adaptation by the tropical copepods *Apocyclops royi* and *Pseudodiaptomus annandalei* to a PUA-poor brackish water habitat. *Marine Ecology Progress Series*, *655*(655), 77–89. https://doi.org/10.3354/meps13536

Niku, J., Hui, F. K. C., Taskinen, S., & Warton, D. I. (2019). gllvm: Fast analysis of multivariate abundance data with generalized linear latent variable models in r. *Methods in Ecology and Evolution*, *10*(12), 2173–2182. https://doi.org/10.1111/2041-210X.13303

Norsker, N. H., & Støttrup, J. G. (1994). The importance of dietary HUFAs for fecundity and HUFA content in the harpacticoid, *Tisbe holothuriae* Humes. *Aquaculture*, *125*(1–2), 155–166. https://doi.org/10.1016/0044-8486(94)90292-5

O'Neill, D. W., Fanning, A. L., Lamb, W. F., & Steinberger, J. K. (2018). A good life for all within planetary boundaries. *Nature Sustainability*, *1*(2), 88–95. https://doi.org/10.1038/s41893-018-0021-4

Oboh, A., Kabeya, N., Carmona-Antoñanzas, G., Castro, L. F. C., Dick, J. R., Tocher, D. R., & Monroig, O. (2017). Two alternative pathways for docosahexaenoic acid (DHA, 22:6n-3) biosynthesis are widespread among teleost fish. *Scientific Reports*, *7*(1), 1–10. https://doi.org/10.1038/s41598-017-04288-2

Olive, P. J. W., Duangchinda, T., Ashforth, E., Craig, S., Ward, A. C., & Davies, S. J. (2009). Net gain of long-chain polyunsaturated fatty acids (PUFA) in a lugworm *Arenicola marina* bioturbated mesocosm. *Marine Ecology Progress Series*, *387*, 223–239. https://doi.org/10.3354/meps08088

Orr, J. A., Vinebrooke, R. D., Jackson, M. C., Kroeker, K. J., Kordas, R. L., Mantyka-Pringle, C., Van Den Brink, P. J., De Laender, F., Stoks, R., Holmstrup, M., Matthaei, C. D., Monk, W. A., Penk, M. R., Leuzinger, S., Schäfer, R. B., & Piggott, J. J. (2020). Towards a unified study of multiple stressors: Divisions and common goals across research disciplines. *Proceedings of the Royal Society B: Biological Sciences*, *287*(1926). https://doi.org/10.1098/rspb.2020.0421

Pajand, Z. O., Haddadi Moghaddam, K., Chubian, F., Farzaneh, E., & Hosseinnia, E. (2022). Effects of dietary various oil sources on zootechnical performance, sexual maturation, whole-body proximate composition and fatty acid profile of *Hediste diversicolor*. *Aquaculture Research*, *53*(8), 3078–3089. https://doi.org/10.1111/are.15820

Parrish, C. C. (2013). Lipids in Marine Ecosystems. *ISRN Oceanography*, *2013*, 1–16. https://doi.org/10.5402/2013/604045

Patro, R., Duggal, G., Love, M. I., Irizarry, R. A., & Kingsford, C. (2017). Salmon provides fast and bias-aware quantification of transcript expression. *Nature Methods*, *14*(4),

417–419. https://doi.org/10.1038/nmeth.4197

Pauly, D., & Christensen, V. (1995). Primary production required to sustain global fisheries. *Nature*, *374*(6519), 255–257. https://doi.org/10.1038/374255a0

Pauly, D., Christensen, V., Dalsgaard, J., Froese, R., & Torres, F. (1998). Fishing down marine food webs. *Science*, *279*(5352), 860–863. https://doi.org/10.1126/science.279.5352.860

Pelletier, G., Lewis, E., & Wallace, D. (2005). *CO2Sys.xls: A calculator for the CO_2 system in seawater for Microsoft Excel/VBA* (25).

Persson, L., Carney Almroth, B. M., Collins, C. D., Cornell, S., de Wit, C. A., Diamond, M. L., Fantke, P., Hassellöv, M., MacLeod, M., Ryberg, M. W., Søgaard Jørgensen, P., Villarrubia-Gómez, P., Wang, Z., & Hauschild, M. Z. (2022). Outside the Safe Operating Space of the Planetary Boundary for Novel Entities. *Environmental Science and Technology*, *56*(3), 1510–1521. https://doi.org/10.1021/acs.est.1c04158

Piggott, J. J., Townsend, C. R., & Matthaei, C. D. (2015). Reconceptualizing synergism and antagonism among multiple stressors. *Ecology and Evolution*, *5*(7), 1538–1547. https://doi.org/10.1002/ece3.1465

Pilecky, M., Fink, P., Kämmer, S. K., Schott, M., Zehl, M., & Kainz, M. J. (2023). Mass spectrometry imaging reveals the spatial distribution of essential lipids in *Daphnia magna* – potential implications for trophic ecology. *Inland Waters*, *13*(1), 111–120. https://doi.org/10.1080/20442041.2022.2127609

Pilecky, M., Kämmer, S. K., Mathieu-Resuge, M., Wassenaar, L. I., Taipale, S. J., Martin-Creuzburg, D., & Kainz, M. J. (2022). Hydrogen isotopes (δ2H) of polyunsaturated fatty acids track bioconversion by zooplankton. *Functional Ecology*, *36*(3), 538–549. https://doi.org/10.1111/1365-2435.13981

Pilecky, M., Závorka, L., Arts, M. T., & Kainz, M. J. (2021). Omega-3 PUFA profoundly affect neural, physiological, and behavioural competences – implications for systemic changes in trophic interactions. *Biological Reviews*, *96*(5), 2127–2145. https://doi.org/10.1111/brv.12747

Pinsky, M. L., Selden, R. L., & Kitchel, Z. J. (2020). Climate-Driven Shifts in Marine Species Ranges: Scaling from Organisms to Communities. *Annual Review of Marine Science*, *12*, 153–179. https://doi.org/10.1146/annurev-marine-010419-010916

Pond, D. W., Tarling, G. A., & Mayor, D. J. (2014). Hydrostatic pressure and temperature effects on the membranes of a seasonally migrating marine copepod. *PLoS ONE*, *9*(10). https://doi.org/10.1371/journal.pone.0111043

Pörtner, H.-O. (2008). Ecosystem effects of ocean acidification in times of ocean warming: A physiologist's view. *Marine Ecology Progress Series*, *373*, 203–217. https://doi.org/10.3354/meps07768

Pörtner, H.-O., & Farrell, A. P. (2008). Physiology and Climate Change. *Science*, *322*(5902), 690–692. https://doi.org/10.1126/science.1163156

Prado-Cabrero, A., Herena-Garcia, R., & Nolan, J. M. (2022). Intensive production of the harpacticoid copepod *Tigriopus californicus* in a zero-effluent 'green water' bioreactor. *Scientific Reports*, *12*(1), 1–12. https://doi.org/10.1038/s41598-021-04516-w

Prado-Cabrero, A., & Nolan, J. M. (2021). Omega-3 nutraceuticals, climate change and threats to the environment: The cases of Antarctic krill and *Calanus finmarchicus*. *Ambio*, *50*(6), 1184–1199. https://doi.org/10.1007/s13280-020-01472-z

Provoost, P., Van Heuven, S., Soetaert, K., Laane, R. W. P. M., & Middelburg, J. J. (2010). Seasonal and long-term changes in pH in the Dutch coastal zone. *Biogeosciences*, *7*(11), 3869–3878. https://doi.org/10.5194/bg-7-3869-2010

R Core Team. (2020). *R: A language and environment for statistical computing* (4.0.2). R Foundation for Statistical Computing. https://www.r-project.org/

R Core Team. (2023). *R: A language and environment for statistical computing*. R Foundation for Statistical Computing. https://www.r-project.org/

Rambaut, A. (2009). *Figtree v. 1.4.3* (1.4.3). http://tree.bio.ed.ac.uk/software/figtree/

Ramos-Llorens, M., Hontoria, F., Navarro, J. C., Ferrier, D. E. K., & Monroig, Ó. (2023a). Functionally diverse front-end desaturases are widespread in the phylum Annelida. *BBA - Molecular and Cell Biology of Lipids*. https://doi.org/10.1016/j.bbalip.2023.159377

Ramos-Llorens, M., Ribes-Navarro, A., Navarro, J. C., Hontoria, F., Kabeya, N., & Monroig, Ó. (2023b). Can *Artemia franciscana* produce essential fatty acids? Unveiling the capacity of brine shrimp to biosynthesise long-chain polyunsaturated fatty acids. *Aquaculture*, *563*, 738869. https://doi.org/10.1016/j.aquaculture.2022.738869

Raworth, K. (2017). A Doughnut for the Anthropocene: humanity's compass in the 21st century. *The Lancet Planetary Health*, *1*(2), e48–e49. https://doi.org/10.1016/S2542-5196(17)30028-1

Reed, T. E., Schindler, D. E., & Waples, R. S. (2011). Interacting Effects of Phenotypic Plasticity and Evolution on Population Persistence in a Changing Climate. *Conservation Biology* *25*(1), 56–63. https://doi.org/10.1111/j.1523-1739.2010.01552.x

Renaud, S. M., & Parry, D. L. (1994). Microalgae for use in tropical aquaculture. 2. Effect of salinity on growth, gross chemical composition and fatty acid composition of 3 species of marine microalgae. *Journal of Applied Phycology*, *6*(3), 347–356. https://doi.org/10.1007/BF02181949

Reusch, T. B. H. (2014). Climate change in the oceans: evolutionary versus phenotypically plastic responses of marine animals and plants. *Evolutionary Applications*, *7*(1). https://doi.org/10.1111/eva.12109

Ribes-Navarro, A., Alberts-Hubatsch, H., Monroig, Ó., Hontoria, F., & Navarro, J. C. (2022). Effects of diet and temperature on the fatty acid composition of the gammarid *Gammarus locusta* fed alternative terrestrial feeds. *Frontiers in Marine Science*, *9*, 931991. https://doi.org/10.3389/fmars.2022.931991

Ribes-Navarro, A., Navarro, J. C., Hontoria, F., Kabeya, N., Standal, I. B., Evjemo, J. O., & Monroig, Ó. (2021). Biosynthesis of long-chain polyunsaturated fatty acids in marine gammarids: Molecular cloning and functional characterisation of three fatty acyl elongases. *Marine Drugs*, *19*, 226. https://doi.org/10.3390/MD19040226

Riebesell, U., Fabry, V. J., Hansson, L., & Gattuso, J.-P. (2011). Guide to best practices for ocean acidification research and data reporting. In *Office for Official Publications of the European Communities*. https://doi.org/10.2777/66906

Riebesell, U., & Gattuso, J. P. (2015). Lessons learned from ocean acidification research. *Nature Climate Change*, *5*(1), 12–14. https://doi.org/10.1038/nclimate2456

Rimm, E. B., Appel, L. J., Chiuve, S. E., Djoussé, L., Engler, M. B., Kris-Etherton, P. M., Mozaffarian, D., Siscovick, D. S., & Lichtenstein, A. H. (2018). Seafood Long-Chain n-3 Polyunsaturated Fatty Acids and Cardiovascular Disease: A Science Advisory From the American Heart Association. *Circulation*, *138*(1), e35–e47. https://doi.org/10.1161/CIR.0000000000000574

Robinson, M. D., McCarthy, D. J., & Smyth, G. K. (2009). edgeR: A Bioconductor package for differential expression analysis of digital gene expression data. *Bioinformatics*, *26*(1), 139–140. https://doi.org/10.1093/bioinformatics/btp616

Robinson, M. D., & Oshlack, A. (2010). A scaling normalization method for differential expression analysis of RNA-seq data. *Genome Biology*, *11*(3), R25. https://doi.org/10.1186/gb-2010-11-3-r25

Rockström, J., Steffen, W., Noone, K., Persson, Å., Chapin III, F. S., Lambin, E. F., Lenton, T. M., Scheffer, M., Folke, C., Schellnhuber, H. J., Nykvist, B., de Wit, C. A., Hughes, T., van der Leeuw, S., Rodhe, H., Sörlin, S., Snyder, P. K., Costanza, R., Svedin, U., … Foley, J. A. (2009). A Safe Operating Space for Humanity. *Nature*, *461*, 472–475. https://doi.org/10.1038/461472a

Rohart, F., Gautier, B., Singh, A., & Lê Cao, K. A. (2017). mixOmics: An R package for 'omics feature selection and multiple data integration. *PLoS Computational Biology*, *13*(11), 1–19. https://doi.org/10.1371/journal.pcbi.1005752

Romero, I. G., Ruvinsky, I., & Gilad, Y. (2012). Comparative studies of gene expression and the evolution of gene regulation. *Nature Reviews Genetics*, *13*(7), 505–516. https://doi.org/10.1038/nrg3229

Roncalli, V., Cieslak, M. C., Castelfranco, A. M., Hartline, D. K., & Lenz, P. H. (2022). Postponing development: dormancy in the earliest developmental stages of a high-latitude calanoid copepod. *Journal of Plankton Research*, *44*(6), 923–935. https://doi.org/10.1093/plankt/fbac039

Roncalli, V., Niestroy, J., Cieslak, M. C., Castelfranco, A. M., Hopcroft, R. R., & Lenz, P. H. (2022). Physiological acclimatization in high-latitude zooplankton. *Molecular Ecology*, *January*, 1753–1765. https://doi.org/10.1111/mec.16354

Roser, M., Ritchie, H., Ortiz-Ospina, E., & Hasell, J. (2023). *World population growth*. Our World in Data. https://ourworldindata.org/population-growth

Røsjø, C., Berg, T., Manum, K., Gjøen, T., Magnusson, S., & Thomassen, M. S. (1994). Effects of temperature and dietary n-3 and n-6 fatty acids on endocytic processes in isolated rainbow trout (*Oncorhynchus mykiss*, Walbaum) hepatocytes. *Fish Physiology and Biochemistry*, *13*(2), 119–132. https://doi.org/10.1007/BF00004337

Rossel, S., & Martínez Arbizu, P. (2019). Revealing higher than expected diversity of Harpacticoida (Crustacea:Copepoda) in the North Sea using MALDI-TOF MS and molecular barcoding. *Scientific Reports*, *9*(1), 1–14. https://doi.org/10.1038/s41598-019-45718-7

Rossoll, D., Bermúdez, R., Hauss, H., Schulz, K. G., Riebesell, U., Sommer, U., & Winder, M. (2012). Ocean acidification-induced food quality deterioration constrains trophic transfer. *PLoS ONE*, *7*(4), 2–7. https://doi.org/10.1371/journal.pone.0034737

Sahota, R., Boyen, J., Semmouri, I., Bodé, S., & De Troch, M. (2022). An inter-order comparison of copepod fatty acid composition and biosynthesis in response to a long-chain PUFA-deficient diet along a temperature gradient. *Marine Biology*, *169*, 133. https://doi.org/10.1007/s00227-022-04121-z

Sato, M., Ota, R., Kobayashi, S., Yamakawa-Kobayashi, K., Miura, T., Ido, A., & Ohhara, Y. (2023). Bioproduction of n-3 polyunsaturated fatty acids by nematode fatty acid desaturases and elongase in *Drosophila melanogaster*. *Transgenic Research*. https://doi.org/10.1007/s11248-023-00363-9

ScheldeMonitor. (2019). ScheldeMonitor. https://www.scheldemonitor.be/

Schlechtriem, C., Arts, M. T., & Zellmer, I. D. (2006). Effect of temperature on the fatty acid composition and temporal trajectories of fatty acids in fasting *Daphnia pulex* (Crustacea, Cladocera). *Lipids*, *41*(4), 397–400. https://doi.org/10.1007/s11745-006-5111-9

Schmidt, D., & Boyd, P. W. (2016). Forecast ocean variability. *Nature, 539*, 162–163. https://doi.org/10.1038/539162a

Schoville, S. D., Barreto, F. S., Moy, G. W., Wolff, A., & Burton, R. S. (2012). Investigating the molecular basis of local adaptation to thermal stress: Population differences in gene expression across the transcriptome of the copepod *Tigriopus californicus*. *BMC*

Evolutionary Biology, *12*, 170. https://doi.org/10.1186/1471-2148-12-170

Schratzberger, M., & Jennings, S. (2002). Impacts of chronic trawling disturbance on meiofaunal communities. *Marine Biology*, *141*(5), 991–1000. https://doi.org/10.1007/s00227-002-0895-5

Schwalm, C. R., Glendon, S., & Duffy, P. B. (2020). RCP8.5 tracks cumulative CO_2 emissions. *Proceedings of the National Academy of Sciences of the United States of America*, *117*(33), 19656–19657. https://doi.org/10.1073/PNAS.2007117117

Schwentner, M., Combosch, D. J., Pakes Nelson, J., & Giribet, G. (2017). A Phylogenomic Solution to the Origin of Insects by Resolving Crustacean-Hexapod Relationships. *Current Biology*, *27*(12), 1818-1824.e5. https://doi.org/10.1016/j.cub.2017.05.040

Scott, C. L., Kwasniewski, S., Falk-Petersen, S., & Sargent, J. R. (2002). Species differences, origins and functions of fatty alcohols and fatty acids in the wax esters and phospholipids of *Calanus hyperboreus*, *C. glacialis* and *C. finmarchicus* from Arctic waters. *Marine Ecology Progress Series*, *235*, 127–134. https://doi.org/10.3354/meps235127

Selig, E. R., Hole, D. G., Allison, E. H., Arkema, K. K., McKinnon, M. C., Chu, J., de Sherbinin, A., Fisher, B., Glew, L., Holland, M. B., Ingram, J. C., Rao, N. S., Russell, R. B., Srebotnjak, T., Teh, L. C. L., Troëng, S., Turner, W. R., & Zvoleff, A. (2019). Mapping global human dependence on marine ecosystems. *Conservation Letters*, *12*(2), 1–10. https://doi.org/10.1111/conl.12617

Semmouri, I., Asselman, J., Van Nieuwerburgh, F., Deforce, D., Janssen, C. R., & De Schamphelaere, K. A. C. (2019). The transcriptome of the marine calanoid copepod *Temora longicornis* under heat stress and recovery. *Marine Environmental Research*, *143*, 10–23. https://doi.org/10.1016/j.marenvres.2018.10.017

Semmouri, I., De Schamphelaere, K. A. C., Mortelmans, J., Mees, J., Asselman, J., & Janssen, C. R. (2023). Decadal decline of dominant copepod species in the North Sea is associated with ocean warming: Importance of marine heatwaves. *Marine Pollution Bulletin*, *193*, 115159. https://doi.org/10.1016/j.marpolbul.2023.115159

Serrano, R., Navarro, J. C., Portolés, T., Sales, C., Beltrán, J., Monroig, Ó., & Hernández, F. (2021). Identification of new, very long-chain polyunsaturated fatty acids in fish by gas chromatography coupled to quadrupole/time-of-flight mass spectrometry with atmospheric pressure chemical ionization. *Analytical and Bioanalytical Chemistry*, *413*(4), 1039–1046. https://doi.org/10.1007/s00216-020-03062-0

Shepon, A., Makov, T., Hamilton, H. A., Müller, D. B., Gephart, J. A., Henriksson, P. J. G., Troell, M., & Golden, C. D. (2022). Sustainable optimization of global aquatic omega-3 supply chain could substantially narrow the nutrient gap. *Resources, Conservation and Recycling*, *181*, 106260. https://doi.org/10.1016/j.resconrec.2022.106260

Sigmaplan. (2023). *Sigmaplan*. https://sigmaplan.be/nl/

Simão, F. A., Waterhouse, R. M., Ioannidis, P., Kriventseva, E. V., & Zdobnov, E. M. (2015). BUSCO: Assessing genome assembly and annotation completeness with single-copy orthologs. *Bioinformatics*, *31*(19), 3210–3212. https://doi.org/10.1093/bioinformatics/btv351

Sinensky, M. (1974). Homeoviscous adaptation: a homeostatic process that regulates the viscosity of membrane lipids in *Escherichia coli*. *Proceedings of the National Academy of Sciences of the United States of America*, *71*(2), 522–525. https://doi.org/10.1073/pnas.71.2.522

Smolina, I., Kollias, S., Møller, E. F., Lindeque, P., Sundaram, A. Y. M., Fernandes, J. M. O., & Hoarau, G. (2015). Contrasting transcriptome response to thermal stress in two key zooplankton species, *Calanus finmarchicus* and *C. glacialis*. *Marine Ecology Progress Series*, *534*, 79–93. https://doi.org/10.3354/meps11398

Snoeks, J. M., Driesen, M., Porembski, S., Aristizábal-Botero, Á., & Vanschoenwinkel, B. (2021). Contrasting biodiversity and food web structure of three temporary freshwater habitats in a tropical biodiversity hotspot. *Aquatic Conservation: Marine and Freshwater Ecosystems*, *31*(9), 2603–2620. https://doi.org/10.1002/aqc.3670

Somero, G. N. (2010). The physiology of climate change: how potentials for acclimatization and genetic adaptation will determine "winners" and "losers." *Journal of Experimental Biology*, *213*(6), 912–920. https://doi.org/10.1242/jeb.037473

Sprecher, H., Luthria, D. L., Mohammed, B. S., & Baykousheva, S. P. (1995). Reevaluation of the pathways for the biosynthesis of polyunsaturated fatty acids. *Journal Lipid Research*, *36*(12), 2471–2477. https://doi.org/10.1016/S0022-2275(20)41084-3

Stamatakis, A. (2014). RAxML version 8: A tool for phylogenetic analysis and post-analysis of large phylogenies. *Bioinformatics*, *30*(9), 1312–1313. https://doi.org/10.1093/bioinformatics/btu033

Steffen, W., Broadgate, W., Deutsch, L., Gaffney, O., & Ludwig, C. (2015a). The trajectory of the Anthropocene: The great acceleration. *The Anthropocene Review*, *2*(1), 81–98. https://doi.org/10.1177/2053019614564785

Steffen, W., Richardson, K., Rockström, J., Cornell, S. E., Fetzer, I., Bennett, E. M., Biggs, R., Carpenter, S. R., De Vries, W., De Wit, C. A., Folke, C., Gerten, D., Heinke, J., Mace, G. M., Persson, L. M., Ramanathan, V., Reyers, B., & Sörlin, S. (2015b). Planetary boundaries: Guiding human development on a changing planet. *Science*, *347*(6223). https://doi.org/10.1126/science.1259855

Stockholm Resilience Centre. (2023). *Planetary boundaries*. https://www.stockholmresilience.org/research/planetary-boundaries.html

Støttrup, J. G. (2000). The elusive copepods: Their production and suitability in marine aquaculture. *Aquaculture Research*, *31*(8–9), 703–711. https://doi.org/10.1046/j.1365-2109.2000.00488.x

Strain, E. M. A., Thomson, R. J., Micheli, F., Mancuso, F. P., & Airoldi, L. (2014). Identifying the interacting roles of stressors in driving the global loss of canopy-forming to mat-forming algae in marine ecosystems. *Global Change Biology, 20*(11), 3300–3312. https://doi.org/10.1111/gcb.12619

Sun, P., Zhou, Q., Monroig, Ó., Navarro, J. C., Jin, M., Yuan, Y., Wang, X., & Jiao, L. (2020). Cloning and functional characterization of an elovl4-like gene involved in the biosynthesis of long-chain polyunsaturated fatty acids in the swimming crab *Portunus trituberculatus. Comparative Biochemistry and Physiology - Part B: Biochemistry and Molecular Biology, 242*, 110408. https://doi.org/10.1016/j.cbpb.2020.110408

Supran, G., Rahmstorf, S., & Oreskes, N. (2023). Assessing ExxonMobil's global warming projections. *Science, 379*(6628). https://doi.org/10.1126/science.abk0063

Surm, J. M., Prentis, P. J., & Pavasovic, A. (2015). Comparative Analysis and Distribution of Omega-3 lcPUFA Biosynthesis Genes in Marine Molluscs. *PLoS ONE*, 1–20. https://doi.org/10.1371/journal.pone.0136301

Surm, J. M., Toledo, T. M., Prentis, P. J., & Pavasovic, A. (2018). Insights into the phylogenetic and molecular evolutionary histories of Fad and Elovl gene families in Actiniaria. *Ecology and Evolution, 8*(11), 5323–5335. https://doi.org/10.1002/ece3.4044

Tagliabue, A., Twining, B. S., Barrier, N., Maury, O., Berger, M., & Bopp, L. (2023). Ocean iron fertilization may amplify climate change pressures on marine animal biomass for limited climate benefit. *Global Change Biology, June*, 1–11. https://doi.org/10.1111/gcb.16854

Tan, K., Zhang, H., & Zheng, H. (2022). Climate change and n-3 LC-PUFA availability. *Progress in Lipid Research, 86*, 101161. https://doi.org/10.1016/j.plipres.2022.101161

Tarrant, A. M., Baumgartner, M. F., Hansen, B. H., Altin, D., Nordtug, T., & Olsen, A. J. (2014). Transcriptional profiling of reproductive development, lipid storage and molting throughout the last juvenile stage of the marine copepod *Calanus finmarchicus. Frontiers in Zoology, 11*(1), 1–15. https://doi.org/10.1186/s12983-014-0091-8

Tarrant, A. M., Baumgartner, M. F., Verslycke, T., & Johnson, C. L. (2008). Differential gene expression in diapausing and active *Calanus finmarchicus* (Copepoda). *Marine Ecology Progress Series, 355*, 193–207. https://doi.org/10.3354/meps07207

Taucher, J., Bach, L. T., Prowe, A. E. F., Boxhammer, T., Kvale, K., & Riebesell, U. (2022). Enhanced silica export in a future ocean triggers global diatom decline. *Nature, 605*(7911), 696–700. https://doi.org/10.1038/s41586-022-04687-0

The Gene Ontology Consortium, Ashburner, M., Ball, C. A., Blake, J. A., Botstein, D., Butler, H., Cherry, J. M., Davis, A. P., Dolinski, K., Dwight, S. S., Eppig, J. T., Harris, M.

A., Hill, D. P., Issel-Tarver, L., Kasarskis, A., Lewis, S., Matese, J. C., Richardson, J. E., Ringwald, M., ... Sherlock, G. (2000). Gene Ontology: tool for the unification of biology. *Nature Genetics*, *25*(1), 25–29. https://doi.org/10.1038/75556

Thompson, J. D., Gibson, T. J., & Higgins, D. G. (2003). Multiple Sequence Alignment Using ClustalW and ClustalX. *Current Protocols in Bioinformatics*, *00*(1), 1–22. https://doi.org/10.1002/0471250953.bi0203s00

Thor, P., Bailey, A., Dupont, S., Calosi, P., Søreide, J. E., De Wit, P., Guscelli, E., Loubet-Sartrou, L., Deichmann, I. M., Candee, M. M., Svensen, C., King, A. L., & Bellerby, R. G. J. (2018). Contrasting physiological responses to future ocean acidification among Arctic copepod populations. *Global Change Biology*, *24*(1), e365–e377. https://doi.org/10.1111/gcb.13870

Thor, P., & Dupont, S. (2015). Transgenerational effects alleviate severe fecundity loss during ocean acidification in a ubiquitous planktonic copepod. *Global Change Biology*, *21*(6), 2261–2271. https://doi.org/10.1111/gcb.12815

Thor, P., Vermandele, F., Bailey, A., Guscelli, E., Loubet-Sartrou, L., Dupont, S., & Calosi, P. (2022). Ocean acidification causes fundamental changes in the cellular metabolism of the Arctic copepod *Calanus glacialis* as detected by metabolomic analysis. *Scientific Reports*, *12*(1), 1–15. https://doi.org/10.1038/s41598-022-26480-9

Ting, S. Y., Janaranjani, M., Merosha, P., Sam, K. K., Wong, S. C., Goh, P. T., Mah, M. Q., Kuah, M. K., & Chong Shu-Chien, A. (2020). Two Elongases, Elovl4 and Elovl6, Fulfill the Elongation Routes of the LC-PUFA Biosynthesis Pathway in the Orange Mud Crab (*Scylla olivacea*). *Journal of Agricultural and Food Chemistry*, *68*(14), 4116–4130. https://doi.org/10.1021/acs.jafc.9b06692

Ting, S. Y., Lau, N. S., Sam, K. K., Quah, E. S. H., Ahmad, A. B., Mat-Isa, M. N., & Shu-Chien, A. C. (2021). Long-Read Sequencing Reveals the Repertoire of Long-Chain Polyunsaturated Fatty Acid Biosynthetic Genes in the Purple Land Crab, *Gecarcoidea lalandii* (H. Milne Edwards, 1837). *Frontiers in Marine Science*, *8*, 713928. https://doi.org/10.3389/fmars.2021.713928

Titocci, J., & Fink, P. (2022). Food quality impacts on reproductive traits, development and fatty acid composition of the freshwater calanoid copepod *Eudiaptomus* sp. *Journal of Plankton Research*, *44*(4), 1–14. https://doi.org/10.1093/plankt/fbac030

Tocher, D. R. (2015). Omega-3 long-chain polyunsaturated fatty acids and aquaculture in perspective. *Aquaculture*, *449*, 94–107. https://doi.org/10.1016/j.aquaculture.2015.01.010

Tocher, D. R., Betancor, M. B., Sprague, M., Olsen, R. E., & Napier, J. A. (2019). Omega-3 long-chain polyunsaturated fatty acids, EPA and DHA: Bridging the gap between supply and demand. *Nutrients, 11*, 89. https://doi.org/10.3390/nu11010089

Tripodi, K. E. J., Buttigliero, L. V., Altabe, S. G., & Uttaro, A. D. (2006). Functional

characterization of front-end desaturases from trypanosomatids depicts the first polyunsaturated fatty acid biosynthetic pathway from a parasitic protozoan. *FEBS Journal*, *273*(2), 271–280. https://doi.org/10.1111/j.1742-4658.2005.05049.x

Tuller, T. (2011). Codon bias, tRNA pools, and horizontal gene transfer. *Mobile Genetic Elements*, *1*(1), 75–77. https://doi.org/10.4161/mge.1.1.15400

Turner, J. T. (2004). The importance of small planktonic copepods and their roles in pelagic marine food webs. *Zoological Studies*, *43*(2), 255–266.

Twining, C. W., Bernhardt, J., Derry, A., Hudson, C., Ishikawa, A., Kabeya, N., Kainz, M., Kitano, J., Kowarik, C., Ladd, S. N., Leal, M., Scharnweber, K., Shipley, J., & Matthews, B. (2021). The evolutionary ecology of fatty-acid variation: implications for consumer adaptation and diversification. *Ecology Letters*, 1–31. https://doi.org/10.1111/ele.13771

Twining, C. W., Brenna, J. T., Hairston, N. G., & Flecker, A. S. (2016). Highly unsaturated fatty acids in nature: What we know and what we need to learn. *Oikos*, *125*(6), 749–760. https://doi.org/10.1111/oik.02910

Twining, C. W., Taipale, S. J., Ruess, L., Bec, A., Martin-Creuzburg, D., & Kainz, M. J. (2020). Stable isotopes of fatty acids: current and future perspectives for advancing trophic ecology. *Philosophical Transactions of the Royal Society B: Biological Sciences*, *375*(1804), 20190641. https://doi.org/10.1098/rstb.2019.0641

Urban, M. C., Bocedi, G., Hendry, A. P., Mihoub, J. B., Pe'er, G., Singer, A., Bridle, J. R., Crozier, L. G., De Meester, L., Godsoe, W., Gonzalez, A., Hellmann, J. J., Holt, R. D., Huth, A., Johst, K., Krug, C. B., Leadley, P. W., Palmer, S. C. F., Pantel, J. H., … Travis, J. M. J. (2016). Improving the forecast for biodiversity under climate change. *Science, 353*, aad8466. https://doi.org/10.1126/science.aad8466

Valles-Regino, R., Tate, R., Kelaher, B., Savins, D., Dowell, A., & Benkendorff, K. (2015). Ocean warming and CO_2-induced acidification impact the lipid content of a marine predatory gastropod. *Marine Drugs*, *13*(10), 6019–6037. https://doi.org/10.3390/md13106019

Van Colen, C., Ong, E. Z., Briffa, M., Wethey, D. S., Abatih, E., Moens, T., & Woodin, S. A. (2020). Clam feeding plasticity reduces herbivore vulnerability to ocean warming and acidification. *Nature Climate Change*, *10*(2), 162–166. https://doi.org/10.1038/s41558-019-0679-2

Van de Vijver, K. I., Hoff, P. T., Van Dongen, W., Esmans, E. L., Blust, R., & De Coen, W. M. (2003). Exposure patterns of perfluorooctane sulfonate in aquatic invertebrates from the Western Scheldt estuary and the southern North Sea. *Environmental Toxicology and Chemistry*, *22*(9), 2037–2041. https://doi.org/10.1897/02-385

van Dijk, W. M., Cox, J. R., Leuven, J. R. F. W., Cleveringa, J., Taal, M., Hiatt, M. R., Sonke, W., Verbeek, K., Speckmann, B., & Kleinhans, M. G. (2021). The vulnerability of tidal

flats and multi-channel estuaries to dredging and disposal. *Anthropocene Coasts*, *4*(1), 36–60. https://doi.org/10.1139/anc-2020-0006

van Leeuwen, S., Tett, P., Mills, D., & Van Der Molen, J. (2015). Stratified and nonstratified areas in the North Sea: Long-term variability and biological and policy implications. *Journal of Geophysical Research: Oceans, 120*, 4670–4686. https://doi.org/10.1002/2014JC010485

Vargas, C. A., Lagos, N. A., Lardies, M. A., Duarte, C., Manríquez, P. H., Aguilera, V. M., Broitman, B., Widdicombe, S., & Dupont, S. (2017). Species-specific responses to ocean acidification should account for local adaptation and adaptive plasticity. *Nature Ecology and Evolution, 1*, 0084. https://doi.org/10.1038/s41559-017-0084

Villate, F., Uriarte, I., Irigoien, X., Beaugrand, G., & Cotano, U. (2004). Zooplankton communities. In *Oceanography and marine environment of the Basque Country* (pp. 395–423).

Vincx, M., & Heip, C. (1979). Larval development and biology of *Canuella perplexa* T. and A. Scott, 1893 (Copepoda, Harpacticoida). *Cahiers De Biologie Marine*, *XX*, 281–299.

Volkman, J. K., Jeffrey, S. W., Nichols, P. D., Rogers, G. I., & Garland, C. D. (1989). Fatty acid and lipid composition of ten species of microalgae used in mariculture. *J. Exp. Mar. Biol. Ecol.*, *128*, 219–240. https://doi.org/10.1016/0022-0981(89)90029-4

von Elert, E., & Fink, P. (2018). Global warming: Testing for direct and indirect effects of temperature at the interface of primary producers and herbivores is required. *Frontiers in Ecology and Evolution*, *6*, 1–10. https://doi.org/10.3389/fevo.2018.00087

Walter, T. C., & Boxshall, G. (2023). *World of Copepods database*. https://doi.org/10.14284/356

Wang-Erlandsson, L., Tobian, A., van der Ent, R. J., Fetzer, I., te Wierik, S., Porkka, M., Staal, A., Jaramillo, F., Dahlmann, H., Singh, C., Greve, P., Gerten, D., Keys, P. W., Gleeson, T., Cornell, S. E., Steffen, W., Bai, X., & Rockström, J. (2022). A planetary boundary for green water. *Nature Reviews Earth & Environment*, *3*, 380–392.

Wang, M., Jeong, C. B., Lee, Y. H., & Lee, J. S. (2018). Effects of ocean acidification on copepods. *Aquatic Toxicology*, *196*, 17–24. https://doi.org/10.1016/j.aquatox.2018.01.004

Wei, T., & Viliam, S. (2021). *R package "corrplot": Visualization of a Correlation Matrix* (0.90). https://github.com/taiyun/corrplot

Werbrouck, E., Bodé, S., Van Gansbeke, D., Vanreusel, A., & De Troch, M. (2017). Fatty acid recovery after starvation: insights into the fatty acid conversion capabilities of a benthic copepod (Copepoda, Harpacticoida). *Marine Biology*, *164*(7), 151. https://doi.org/10.1007/s00227-017-3181-2

Werbrouck, E., Van Gansbeke, D., Vanreusel, A., & De Troch, M. (2016a). Temperature Affects the Use of Storage Fatty Acids as Energy Source in a Benthic Copepod (*Platychelipus littoralis*, Harpacticoida). *PloS One*, *11*(3), e0151779. https://doi.org/10.1371/journal.pone.0151779

Werbrouck, E., Van Gansbeke, D., Vanreusel, A., Mensens, C., & De Troch, M. (2016b). Temperature-induced changes in fatty acid dynamics of the intertidal grazer *Platychelipus littoralis* (Crustacea, Copepoda, Harpacticoida): Insights from a short-term feeding experiment. *Journal of Thermal Biology*, *57*, 44–53. https://doi.org/10.1016/j.jtherbio.2016.02.002

Windisch, H. S., & Fink, P. (2018). The molecular basis of essential fatty acid limitation in *Daphnia magna* - a transcriptomic approach. *Molecular Ecology*, *27*(4), 871–885. https://doi.org/10.1111/mec.14498

Wolff, R. L., Bayard, C. C., & Fabien, R. J. (1995). Evaluation of sequential methods for the determination of butterfat fatty acid composition with emphasis on trans-18:1 acids. Application to the study of seasonal variations in french butters. *Journal of the American Oil Chemists' Society*, *72*(12), 1471–1483. https://doi.org/10.1007/BF02577840

World Meteorological Organization. (2022). *WMO atlas of mortality and economic losses from weather, climate and water extremes - 2022 update* (Issue 1267). https://library.wmo.int/index.php?lvl=notice_display&id=21930

WoRMs Editorial Board. (2023). *World Register of Marine Species*. https://doi.org/10.14284/170

Wu, D. L., Huang, Y. H., Liu, Z. Q., Yu, P., Gu, P. H., Fan, B., & Zhao, Y. L. (2018). Molecular cloning, tissue expression and regulation of nutrition and temperature on Δ6 fatty acyl desaturase-like gene in the red claw crayfish (*Cherax quadricarinatus*). *Comparative Biochemistry and Physiology - Part B: Biochemistry and Molecular Biology*, *225*, 58–66. https://doi.org/10.1016/j.cbpb.2018.07.003

Wyeth, A., Grünbaum, D., & Keister, J. (2022). Effects of hypoxia and acidification on *Calanus pacificus*: behavioral changes in response to stressful environments. *Marine Ecology Progress Series*, *697*, 15–29. https://doi.org/10.3354/meps14142

Xie, D., Chen, C., Dong, Y., You, C., Wang, S., Monroig, Ó., Tocher, D. R., & Li, Y. (2021). Regulation of long-chain polyunsaturated fatty acid biosynthesis in teleost fish. *Progress in Lipid Research*, *82*, 101095. https://doi.org/10.1016/j.plipres.2021.101095

Xu, W., Wang, S., You, C., Zhang, Y., Monroig, Ó., Tocher, D. R., & Li, Y. (2020). The catadromous teleost *Anguilla japonica* has a complete enzymatic repertoire for the biosynthesis of docosahexaenoic acid from α-linolenic acid: Cloning and functional characterization of an Elovl2 elongase. *Comparative Biochemistry and Physiology - Part B: Biochemistry and Molecular Biology*, *240*(July 2019), 110373. https://doi.org/10.1016/j.cbpb.2019.110373

Yang, Z. (2007). PAML 4: Phylogenetic analysis by maximum likelihood. *Molecular Biology and Evolution*, *24*(8), 1586–1591. https://doi.org/10.1093/molbev/msm088

Yang, Z., Guo, Z., Ji, L., Zeng, Q., Wang, Y., Yang, X., & Cheng, Y. (2013). Cloning and tissue distribution of a fatty acyl Δ6-desaturase-like gene and effects of dietary lipid levels on its expression in the hepatopancreas of Chinese mitten crab (*Eriocheir sinensis*). *Comparative Biochemistry and Physiology - Part B: Biochemistry and Molecular Biology*, *165*(2), 99–105. https://doi.org/10.1016/j.cbpb.2013.03.010

Ye, J., Coulouris, G., Zaretskaya, I., Cutcutache, I., Rozen, S., & Madden, T. L. (2012). Primer-BLAST: A tool to design target-specific primers for polymerase chain reaction. *BMC Bioinformatics*, *13*, 134. https://doi.org/10.1186/1471-2105-13-134

Yoon, D. S., Byeon, E., Kim, D. H., Lee, M. C., Shin, K. H., Hagiwara, A., Park, H. G., & Lee, J. S. (2022). Effects of temperature and combinational exposures on lipid metabolism in aquatic invertebrates. *Comparative Biochemistry and Physiology Part - C: Toxicology and Pharmacology*, *262*, 109449. https://doi.org/10.1016/j.cbpc.2022.109449

Závorka, L., Blanco, A., Chaguaceda, F., Cucherousset, J., Killen, S. S., Liénart, C., Mathieu-Resuge, M., Němec, P., Pilecky, M., Scharnweber, K., Twining, C. W., & Kainz, M. J. (2023). The role of vital dietary biomolecules in eco-evo-devo dynamics. *Trends in Ecology and Evolution*, *38*(1), 72–84. https://doi.org/10.1016/j.tree.2022.08.010

Závorka, L., Crespel, A., Dawson, N. J., Papatheodoulou, M., Killen, S. S., & Kainz, M. J. (2021). Climate change-induced deprivation of dietary essential fatty acids can reduce growth and mitochondrial efficiency of wild juvenile salmon. *Functional Ecology*, *35*(9), 1960–1971. https://doi.org/10.1111/1365-2435.13860

Zheng, X., Ding, Z., Xu, Y., Monroig, O., Morais, S., & Tocher, D. R. (2009). Physiological roles of fatty acyl desaturases and elongases in marine fish: Characterisation of cDNAs of fatty acyl Δ6 desaturase and elovl5 elongase of cobia (*Rachycentron canadum*). *Aquaculture*, *290*(1–2), 122–131. https://doi.org/10.1016/j.aquaculture.2009.02.010

Zhou, X. R., Horne, I., Damcevski, K., Haritos, V., Green, A., & Singh, S. (2008). Isolation and functional characterization of two independently-evolved fatty acid Δ12-desaturase genes from insects. *Insect Molecular Biology*, *17*(6), 667–676. https://doi.org/10.1111/j.1365-2583.2008.00841.x

SUPPLEMENTARY MATERIALS

Supplementary Materials Chapter 2

Supplementary Method: RNA extraction

At the end of the experiment, after mortality assessment and cleaning in filtered and autoclaved natural seawater (FNSW) to remove food particles, *P. littoralis* individuals from each replicate were pooled and transferred to a 1.5 ml Eppendorf tube. Copepods were concentrated by allowing them to settle and leftover FNSW in the Eppendorf was removed. Immediately thereafter (within minutes after removal from the Lovibond incubator), samples were flash-frozen in liquid nitrogen prior to storage at -80 °C. Total RNA was extracted using the RNeasy Plus Micro Kit (QIAGEN), with slight modifications to the manufacturer's protocol. Samples were disrupted and simultaneously homogenized in 350 µl Buffer RTL using one stainless steel bead (5 mm) per sample and a TissueLyser II (Qiagen) for two times 45 s at 30 Hz, with the samples placed on ice for one minute after each disruption step. The sample was centrifuged for 3 min at 8,000 g, after which the lysate was transferred to a new 1.5 ml microcentrifuge by pipetting. 350 µl 70 % ethanol was added and mixed with lysate, and the mixture (700 µl) was immediately transferred to an RNeasy MinElute spin column placed in a 2 ml collection tube. The spin column was centrifuged for 15 s at 8,000 g, 350 µl Buffer RW1 was added, and the spin column was centrifuged again for 15 s at 8,000 g. A mixture of DNase I solution (10 µl) and Buffer RDD (70 µl) was added to the spin column for 15 min. The subsequent extraction steps were similar to the ones in the manufacturer's protocol. At the final step, RNase-free water (19 µl) was added to the spin column and the spin column was centrifuged for 1 min at 8,000 g, resulting in a total RNA solution with a volume of about 17 µl. After quality and quantity assessment using a NanoDrop 2000 spectrophotometer (Thermo Scientific) and a 2100 Bioanalyzer (Agilent Technologies), samples (15 µl) were diluted to ensure equal total RNA concentrations prior to cDNA library construction. Final total RNA concentration per sample (17 µl) was 79.93 ± 6.68 ng µl^{-1}.

Supplementary Table 1 Mean relative FA concentration (% ± s.d.; n = 4) of Nitzschia sp. and D. tertiolecta

Fatty acid	*Nitzschia* sp.	*D. tertiolecta*
14:0	9.09 ± 0.29	0.35 ± 0.03
iso-15:0	0.19 ± 0.06	0.06 ± 0.04
anteiso-15:0	0.10 ± 0.03	0.01 ± 0.01
15:0	0.54 ± 0.09	n.d.
iso-16:0	n.d.	0.01 ± 0.01
16:0	9.07 ± 0.55	18.65 ± 0.78
16:1	3.46 ± 0.10	2.03 ± 0.14
16:1w7	10.14 ± 0.38	0.21 ± 0.07
16:2w4	6.20 ± 0.14	n.d.
16:2w6	n.d.	0.69 ± 0.05
16:2w7	1.53 ± 0.10	n.d.
16:3w3	0.07 ± 0.02	3.66 ± 0.34
16:3w4	3.59 ± 0.93	0.05 ± 0.02
16:3w6	n.d.	0.65 ± 0.11
16:4w1	7.14 ± 0.63	0.02 ± 0.01
16:4w3	n.d.	18.37 ± 0.81
18:0	0.91 ± 0.26	0.43 ± 0.10
18:1w7	8.95 ± 2.10	n.d.
18:1w9	0.14 ± 0.05	2.97 ± 0.46
18:2w6	0.65 ± 0.15	3.13 ± 0.37
18:3w3	0.05 ± 0.03	43.77 ± 1.29
18:3w6	1.82 ± 0.38	2.92 ± 0.22
18:4w3	1.26 ± 0.29	1.80 ± 0.06
20:4w6	0.41 ± 0.08	0.18 ± 0.02
20:5w3	26.85 ± 2.26	n.d.
22:0	0.07 ± 0.01	0.01 ± 0.01
22:5w3	0.13 ± 0.01	0.01 ± 0.00
22:6w3	5.68 ± 0.29	n.d.
24:0	1.98 ± 0.25	0.03 ± 0.00
∑SFA	21.94 ± 0.91	19.54 ± 0.95
∑MUFA	22.68 ± 2.44	5.22 ± 0.66
∑PUFA	55.39 ± 3.34	75.24 ± 1.51

n.d. = not detected

Supplementary Table 2 Mean absolute FA concentration (ng copepod^{-1} ± s.d.; n = 3) of P. littoralis prior (field) and after ten days of incubation with Nitzschia sp. or D. tertiolecta. - : not significant

	Field	*Nitzschia* sp.		D. tertiolecta		Two-way ANOVA/Scheirer-Ray-Hare test		
		19°C	22°C	19°C	22°C	Diet	Temperature	Interaction
14:0	8.94 ± 0.23	6.84 ± 3.65	3.61 ± 0.32	4.86 ± 0.25	4.19 ± 0.62	-	-	-
iso-15:0	0.28 ± 0.04	1.43 ± 0.41	1.01 ± 0.11	1.67 ± 0.40	1.41 ± 0.26	-	-	-
anteiso-15:0*	0.15 ± 0.01	0.36 ± 0.26	0.15 ± 0.03	0.32 ± 0.16	0.19 ± 0.02	-	p < 0.01	-
15:0	2.58 ± 0.20	2.49 ± 0.99	1.38 ± 0.11	2.19 ± 0.30	1.80 ± 0.22	-	p < 0.05	-
iso-16:0	0.34 ± 0.04	0.64 ± 0.48	0.24 ± 0.02	0.38 ± 0.07	0.27 ± 0.04	-	-	-
16:0	42.63 ± 0.90	38.88 ± 9.96	26.21 ± 1.44	34.82 ± 2.82	31.22 ± 3.29	-	p < 0.05	-
iso-17:0	0.38 ± 0.45	2.47 ± 1.91	0.85 ± 0.19	1.35 ± 0.08	1.23 ± 0.24	-	-	-
16:1w7*	30.66 ± 1.31	19.82 ± 0.68	16.07 ± 0.89	19.91 ± 4.29	17.60 ± 1.60	-	-	-
16:1	0.19 ± 0.02	0.43 ± 0.10	0.19 ± 0.02	0.34 ± 0.24	0.31 ± 0.05	-	-	-
17:0	1.53 ± 0.12	1.83 ± 0.33	1.39 ± 0.05	1.60 ± 0.19	1.61 ± 0.14	-	-	-
16:2w4	2.36 ± 0.13	1.96 ± 0.86	1.36 ± 0.09	1.45 ± 0.34	1.76 ± 0.44	-	-	-
17:1	2.36 ± 0.13	1.96 ± 0.86	1.36 ± 0.09	1.45 ± 0.34	1.76 ± 0.44	-	-	-
18:0	7.29 ± 0.15	9.68 ± 4.94	6.00 ± 0.30	7.48 ± 0.85	7.00 ± 0.87	-	-	-
16:3w4	1.77 ± 0.15	1.59 ± 0.11	1.82 ± 0.19	1.67 ± 0.62	1.87 ± 0.19	-	-	-
18:1w7	9.37 ± 0.74	14.02 ± 0.79	11.23 ± 0.90	13.98 ± 1.42	12.08 ± 1.63	-	p < 0.01	-
18:1w9	2.80 ± 0.09	4.89 ± 2.67	1.33 ± 0.13	2.36 ± 0.17	3.43 ± 2.21	-	-	p < 0.05
16:4w1*	1.65 ± 0.08	1.50 ± 0.34	1.22 ± 0.10	1.32 ± 0.50	1.22 ± 0.08	-	-	-
18:2w6	1.91 ± 0.11	1.11 ± 0.14	0.85 ± 0.04	1.21 ± 0.32	1.28 ± 0.22	-	-	-
18:3w6	1.25 ± 0.03	0.72 ± 0.10	0.59 ± 0.04	0.83 ± 0.30	0.79 ± 0.02	-	-	-
20:0	0.22 ± 0.03	0.43 ± 0.41	0.15 ± 0.02	0.30 ± 0.10	0.20 ± 0.07	-	-	-
18:3w3	0.83 ± 0.10	1.20 ± 0.72	0.50 ± 0.04	3.37 ± 0.85	3.11 ± 0.50	p < 0.001	-	-
18:4w3	2.76 ± 0.07	1.46 ± 0.23	1.19 ± 0.08	1.49 ± 0.45	1.50 ± 0.14	-	-	-
22:0*	1.74 ± 0.49	1.43 ± 0.06	1.19 ± 0.04	1.45 ± 0.18	1.30 ± 0.10	-	-	-
20:4w6	3.85 ± 0.24	2.89 ± 0.68	2.64 ± 0.23	2.76 ± 0.58	2.58 ± 0.15	-	-	-
20:5w3*	44.78 ± 1.28	27.99 ± 3.11	24.22 ± 1.36	27.06 ± 5.50	25.01 ± 2.51	-	-	-
24:0	2.56 ± 0.11	2.68 ± 0.16	2.21 ± 0.05	2.31 ± 0.24	2.19 ± 0.16	-	p < 0.05	-
22:5w3	3.24 ± 0.14	2.24 ± 0.05	1.80 ± 0.09	2.23 ± 0.81	1.81 ± 0.29	-	-	-
22:6w3	18.88 ± 0.08	17.40 ± 2.64	15.26 ± 0.84	17.42 ± 1.99	15.22 ± 0.11	-	p < 0.05	-
∑SFA	68.64 ± 2.33	69.14 ± 23.39	44.37 ± 2.26	58.73 ± 1.83	52.60 ± 5.88	-	-	-
∑MUFA	45.38 ± 0.84	41.12 ± 4.17	30.17 ± 0.15	38.04 ± 5.89	35.18 ± 4.07	-	p < 0.05	-
∑PUFA	83.27 ± 2.13	60.07 ± 7.25	51.47 ± 2.34	60.82 ± 12.01	56.16 ± 3.78	-	-	-
DHA/EPA*	0.42 ± 0.01	0.62 ± 0.03	0.63 ± 0.04	0.65 ± 0.07	0.61 ± 0.07	-	-	-
∑FA	197.29 ± 4.50	170.33 ± 17.76	126.02 ± 4.63	157.59 ± 19.55	143.94 ± 13.05	-	p < 0.05	-

Differences were tested using type II two-way ANOVA, except for datasets without normal distribution (*), for which the Scheirer-Ray-Hare test was used.

Supplementary Table 3 Mean relative FA concentration (% ± s.d.; n = 3) of P. littoralis prior (field) and after ten days of incubation with Nitzschia sp. or D. tertiolecta.
- : not significant

	Field	*Nitzschia* sp.		*D. tertiolecta*		Two-way ANOVA/Scheirer-Ray-Hare test		
		19°C	22°C	19°C	22°C	Diet	Temperature	Interaction
14:0	4.53 ± 0.06	3.91 ± 1.71	2.86 ± 0.16	3.12 ± 0.42	2.9 ± 0.19	-	-	-
iso-15:0	0.14 ± 0.02	0.83 ± 0.17	0.80 ± 0.08	1.08 ± 0.36	0.98 ± 0.12	-	-	-
anteiso-15:0*	0.08 ± 0.00	0.20 ± 0.13	0.12 ± 0.02	0.22 ± 0.14	0.13 ± 0.00	-	-	-
15:0	1.31 ± 0.08	1.43 ± 0.43	1.10 ± 0.12	1.42 ± 0.35	1.25 ± 0.04	-	-	-
iso-16:0	0.17 ± 0.02	0.36 ± 0.24	0.19 ± 0.01	0.24 ± 0.08	0.19 ± 0.03	-	-	-
16:0*	21.61 ± 0.11	22.63 ± 3.66	20.79 ± 0.39	22.18 ± 1.06	21.67 ± 0.61	-	-	-
iso-17:0	0.19 ± 0.23	1.39 ± 0.96	0.67 ± 0.12	0.87 ± 0.16	0.85 ± 0.13	-	-	-
16:1w7	15.54 ± 0.44	11.74 ± 1.50	12.75 ± 0.45	12.53 ± 1.24	12.23 ± 0.01	-	-	-
16:1	0.10 ± 0.01	0.26 ± 0.08	0.15 ± 0.02	0.21 ± 0.14	0.22 ± 0.06	-	-	-
17:0	0.78 ± 0.04	1.07 ± 0.09	1.10 ± 0.05	1.02 ± 0.07	1.12 ± 0.04	-	-	-
16:2w4	1.20 ± 0.05	1.16 ± 0.50	1.08 ± 0.07	0.91 ± 0.11	1.22 ± 0.28	-	-	-
17:1	1.20 ± 0.05	1.16 ± 0.50	1.08 ± 0.07	0.91 ± 0.11	1.22 ± 0.28	-	-	-
18:0	3.69 ± 0.01	5.55 ± 2.30	4.76 ± 0.16	4.85 ± 1.22	4.86 ± 0.23	-	-	-
16:3w4	0.90 ± 0.07	0.95 ± 0.15	1.45 ± 0.15	1.04 ± 0.28	1.30 ± 0.02	-	p < 0.01	-
18:1w7	4.76 ± 0.49	8.31 ± 1.17	8.93 ± 0.97	8.9 ± 0.56	8.38 ± 0.60	-	-	-
18:1w9*	1.42 ± 0.08	2.82 ± 1.48	1.05 ± 0.09	1.52 ± 0.29	2.37 ± 1.48	-	-	p < 0.05
16:4w1	0.84 ± 0.03	0.90 ± 0.27	0.97 ± 0.05	0.82 ± 0.24	0.85 ± 0.04	-	-	-
18:2w6	0.97 ± 0.03	0.65 ± 0.01	0.67 ± 0.03	0.76 ± 0.12	0.89 ± 0.08	p < 0.01	-	-
18:3w6	0.63 ± 0.01	0.43 ± 0.09	0.47 ± 0.04	0.51 ± 0.14	0.55 ± 0.04	-	-	-
20:0*	0.11 ± 0.01	0.24 ± 0.21	0.12 ± 0.01	0.20 ± 0.10	0.14 ± 0.04	-	-	-
18:3w3	0.42 ± 0.05	0.68 ± 0.34	0.40 ± 0.04	2.12 ± 0.31	2.16 ± 0.23	p < 0.001	-	-
18:4w3*	1.40 ± 0.03	0.87 ± 0.19	0.95 ± 0.03	0.93 ± 0.19	1.04 ± 0.00	-	-	-
22:0	0.88 ± 0.24	0.85 ± 0.11	0.94 ± 0.02	0.92 ± 0.03	0.91 ± 0.06	-	-	-
20:4w6*	1.95 ± 0.08	1.73 ± 0.51	2.09 ± 0.14	1.74 ± 0.16	1.80 ± 0.22	-	-	-
20:5w3	22.69 ± 0.14	16.62 ± 3.05	19.22 ± 0.50	17.05 ± 1.57	17.37 ± 0.23	-	-	-
24:0*	1.30 ± 0.05	1.58 ± 0.10	1.75 ± 0.03	1.47 ± 0.06	1.52 ± 0.07	p < 0.05	-	-
22:5w3*	1.64 ± 0.03	1.33 ± 0.13	1.43 ± 0.06	1.39 ± 0.37	1.25 ± 0.12	-	-	-
22:6w3	9.57 ± 0.18	10.36 ± 2.30	12.11 ± 0.47	11.07 ± 0.17	10.64 ± 1.03	-	-	-
∑SFA*	34.79 ± 0.58	40.05 ± 9.65	35.20 ± 0.59	37.58 ± 3.83	36.51 ± 1.36	-	-	-
∑MUFA	23.01 ± 0.55	24.29 ± 3.11	23.96 ± 0.79	24.08 ± 0.84	24.41 ± 1.23	-	-	-
∑PUFA	42.21 ± 0.16	35.67 ± 6.64	40.84 ± 0.50	38.34 ± 3.15	39.07 ± 0.95	-	-	-
DHA/EPA*	0.42 ± 0.01	0.62 ± 0.03	0.63 ± 0.04	0.65 ± 0.07	0.61 ± 0.07	-	-	-

Differences were tested using type II two-way ANOVA, except for datasets without normal distribution (*), for which the Scheirer-Ray-Hare test was used.

Supplementary Table 4 Tested contrasts and corresponding significantly differentially expressed transcripts

Contrast	logFC	logCPM	F-statistic	p-value	FDR
Differentially expressed transcript					
Diet					
Plit_DN4535_c0_g1_i10	-11.46	3.70	140.42	4.95E-07	0.01
Plit_DN515_c0_g1_i2	22.86	2.67	384.29	2.38E-06	0.03
Plit_DN3624_c0_g1_i4	-10.94	2.40	91.79	3.27E-06	0.03
Plit_DN5709_c0_g1_i3	-11.60	2.63	72.75	8.94E-06	0.05
Plit_DN1805_c0_g1_i18	-10.39	2.89	69.50	1.09E-05	0.05
Plit_DN1331_c0_g1_i7	3.23	3.47	53.37	1.16E-05	0.05
Plit_DN2138_c0_g1_i4	10.63	1.95	77.39	1.42E-05	0.05
Temperature					
Plit_DN4535_c0_g1_i10	11.70	3.70	153.48	3.32E-07	0.01
Plit_DN3007_c0_g1_i1	-3.79	3.41	83.75	1.22E-06	0.01
Plit_DN12745_c0_g1_i1	-3.21	3.09	68.79	3.32E-06	0.02
Plit_DN1805_c0_g1_i18	11.78	2.89	91.11	3.38E-06	0.02
Plit_DN4651_c0_g1_i7	-2.85	5.32	66.60	3.90E-06	0.02
Plit_DN3624_c0_g1_i4	-10.05	2.40	84.37	4.72E-06	0.02
Plit_DN273_c0_g1_i2	-1.59	5.41	63.41	4.98E-06	0.02
Plit_DN6288_c0_g1_i1	-6.03	7.12	61.63	5.74E-06	0.02
Plit_DN63_c0_g1_i8	1.08	5.84	58.64	7.32E-06	0.02
Plit_DN182_c0_g1_i2	-3.19	7.07	55.79	9.34E-06	0.02
Plit_DN2425_c0_g1_i12	-2.47	5.65	53.50	1.14E-05	0.03
Plit_DN1505_c0_g1_i5	-2.37	6.95	50.93	1.45E-05	0.03
Plit_DN6346_c0_g1_i4	-3.57	7.85	49.69	1.63E-05	0.03
Plit_DN1207_c0_g1_i4	-2.03	3.84	48.85	1.77E-05	0.03
Plit_DN182_c0_g1_i6	-3.21	5.48	48.70	1.79E-05	0.03
Plit_DN5040_c0_g1_i1	-3.81	3.61	47.99	1.93E-05	0.03
Plit_DN374_c0_g1_i1	-7.88	3.06	47.61	2.00E-05	0.03
Plit_DN1071_c0_g1_i2	-3.06	4.96	47.56	2.01E-05	0.03
Plit_DN23020_c0_g1_i5	-1.54	7.27	47.23	2.08E-05	0.03
Plit_DN12448_c0_g1_i2	-2.25	4.50	47.11	2.10E-05	0.03
Plit_DN5709_c0_g1_i3	9.94	2.63	58.92	2.18E-05	0.03
Plit_DN2138_c0_g1_i4	-10.53	1.95	68.48	2.28E-05	0.03
Plit_DN6269_c0_g1_i4	-1.84	4.13	44.73	2.68E-05	0.03
Plit_DN123_c1_g1_i1	11.24	2.22	52.34	3.56E-05	0.04
Plit_DN166_c0_g1_i2	-2.73	6.28	41.84	3.66E-05	0.04
Plit_DN1551_c0_g1_i3	-1.39	4.28	41.04	4.00E-05	0.04
Plit_DN651_c0_g1_i2	-2.34	4.99	39.65	4.68E-05	0.04
Plit_DN4966_c0_g1_i3	-3.88	3.62	38.48	5.37E-05	0.05
Plit_DN2223_c0_g1_i2	-3.99	2.92	37.68	5.90E-05	0.05
Diet (temperature fixed at 19°C)					
Plit_DN4535_c0_g1_i10	-11.64	3.70	183.77	1.46E-07	0.00
Plit_DN1805_c0_g1_i18	-10.33	2.89	89.00	3.74E-06	0.04
Plit_DN5709_c0_g1_i3	-10.73	2.63	81.66	5.44E-06	0.04
Diet (temperature fixed at 22°C)					
Plit_DN3624_c0_g1_i4	-10.41	2.40	107.94	1.60E-06	0.04
Plit_DN1598_c0_g1_i9	13.73	4.58	211.68	3.06E-06	0.04
Temperature (diet fixed at *D. tertiolecta*)					
Plit_DN4535_c0_g1_i10	11.76	3.70	183.83	1.46E-07	0.00
Plit_DN3624_c0_g1_i4	-9.97	2.40	99.79	2.27E-06	0.02
Plit_DN1805_c0_g1_i18	11.02	2.89	96.89	2.58E-06	0.02
Plit_DN1598_c0_g1_i9	13.73	4.58	158.20	7.74E-06	0.05
Plit_DN5709_c0_g1_i3	9.91	2.63	71.05	9.89E-06	0.05
Temperature by diet interaction					
Plit_DN4535_c0_g1_i10	11.81	3.70	156.08	3.07E-07	0.01
Plit_DN1598_c0_g1_i9	26.31	4.58	320.58	8.08E-07	0.01
Plit_DN3624_c0_g1_i4	-9.88	2.40	82.01	5.34E-06	0.04

Differential expression was tested using the edgeR gene-wise negative binomial generalized linear model. LogFC: log fold change; logCPM: log counts per million; FDR: false discovery rate.

Supplementary Table 5 Gene Ontology (GO) terms enriched under the diet and temperature treatments

| Domain GO.ID	GO term	Fisher p-value
Diet		
Biological process		
GO:0032053	ciliary basal body organization	0.0017
GO:0010457	centriole-centriole cohesion	0.0022
GO:1903566	positive regulation of protein localization to cilium	0.0026
GO:0031053	primary miRNA processing	0.0050
GO:0006654	phosphatidic acid biosynthetic process	0.0054
GO:0030951	establishment or maintenance of microtubule cytoskeleton polarity	0.0066
GO:0016024	CDP-diacylglycerol biosynthetic process	0.0072
GO:0097711	ciliary basal body-plasma membrane docking	0.0075
GO:0045724	positive regulation of cilium assembly	0.0076
GO:0010669	epithelial structure maintenance	0.0096
Molecular function		
GO:0015232	heme transporter activity	0.0012
GO:0030729	acetoacetate-CoA ligase activity	0.0012
GO:0102420	sw1-glycerol-3-phosphate C16:0-DCA-CoA acyl transferase activity	0.0022
GO:0004366	glycerol-3-phosphate O-acyltransferase activity	0.0023
GO:0070878	primary miRNA binding	0.0026
GO:0003841	1-acylglycerol-3-phosphate O-acyltransferase activity	0.0041
GO:0051010	microtubule plus-end binding	0.0049
GO:0019894	kinesin binding	0.0085
Cellular component		
GO:0070877	microprocessor complex	0.0015
GO:0035253	ciliary rootlet	0.0027
GO:0005813	centrosome	0.0048
GO:0001917	photoreceptor inner segment	0.0094
Temperature		
Biological process		
GO:1903033	positive regulation of microtubule plus-end binding	0.0010
GO:1904825	protein localization to microtubule plus-end	0.0012
GO:0002149	hypochlorous acid biosynthetic process	0.0021
GO:1990268	response to gold nanoparticle	0.0021
GO:0034374	low-density lipoprotein particle remodeling	0.0025
GO:0032053	ciliary basal body organization	0.0029
GO:1905907	negative regulation of amyloid fibril formation	0.0030
GO:0010457	centriole-centriole cohesion	0.0037
GO:0001878	response to yeast	0.0041
GO:1903566	positive regulation of protein localization to cilium	0.0043
GO:0044130	negative regulation of growth of symbiont in host	0.0070
GO:0045737	positive regulation of cycliwdependent protein serine/threonine kinase activity	0.0076
GO:0031053	primary miRNA processing	0.0084
GO:0002679	respiratory burst involved in defense response	0.0088
GO:0006654	phosphatidic acid biosynthetic process	0.0091
Molecular function		
GO:0005509	calcium ion binding	0.0002
GO:0015232	heme transporter activity	0.0027
GO:0030021	extracellular matrix structural constituent conferring compression resistance	0.0029
GO:0030729	acetoacetate-CoA ligase activity	0.0029
GO:0008022	protein C-terminus binding	0.0034
GO:0004035	alkaline phosphatase activity	0.0042
GO:0102420	sw1-glycerol-3-phosphate C16:0-DCA-CoA acyl transferase activity	0.0051
GO:0004366	glycerol-3-phosphate O-acyltransferase activity	0.0053
GO:0070878	primary miRNA binding	0.0060
GO:0003841	1-acylglycerol-3-phosphate O-acyltransferase activity	0.0096
Cellular component		
GO:0070877	microprocessor complex	0.0025
GO:0065010	extracellular membrane-bounded organelle	0.0040
GO:0035253	ciliary rootlet	0.0045
GO:0035371	microtubule plus-end	0.0071
GO:0005796	Golgi lumen	0.0096

Supplementary Materials Chapter 3

Supplementary Table 1 Endogenous fatty acid (FA) levels of the transgenic yeast expressing the P. littoralis methyl-end desaturase (ωx) as well as the control yeast. The results are presented as mean percentages of total FAs (%) ± standard deviation (n = 3). No significant differences (p≤0.05) were detected.

FA	Control	ωx
14:0	1.4 ± 0.3	1.2 ± 0.1
15:0	0.8 ± 0.1	0.7 ± 0.1
16:1n-7	25 ± 5.8	30.3 ± 1.6
16:0	41 ± 6.5	32.4 ± 1.2
18:1n-9	16.4 ± 3.5	20.7 ± 0.5
18:1n-7	1.5 ± 0.2	1.4 ± 0.1
18:0	13.9 ± 2.3	13.4 ± 0.7

Supplementary Table 2 Endogenous saturated fatty acid (FA) levels of the transgenic yeast expressing the P. littoralis elongases as well as the control yeast. The results are presented as mean percentages of total saturated FAs (%) ± standard deviation (n = 3). Asterisks indicate significant differences (p≤0.05).

| FA	Control	elovl4	elovl1a	elovl1b	elovl1c	elovl1d	elovl1e
14:0	3.2 ± 0.8	4.1 ± 1.3	3.1 ± 1	3.4 ± 0.2	2.3 ± 0.2	2.3 ± 0.4	4.5 ± 1
15:0	0.9 ± 0.3	0.7 ± 0.2	0.5 ± 0.1	0.9 ± 0.4	0.5 ± 0.1	0.4 ± 0.1	1.5 ± 0.5
16:0	51.8 ± 5.6	40.2 ± 3.6	29.8 ± 11.5*	42.6 ± 1.8	48.9 ± 3.3	17.5 ± 2.3*	36.8 ± 2.1*
17:0	1 ± 0.3	1 ± 0.4	0.4 ± 0.1*	1.2 ± 0.2	0.9 ± 0.1	0.5 ± 0.2	1.1 ± 0.1
18:0	39.3 ± 4.1	41.8 ± 1.4	9.9 ± 2.4*	42.9 ± 1	40.4 ± 5.6	18.8 ± 0.9*	37 ± 2.5
20:0	0.6 ± 0.1	1.2 ± 0.2*	0.3 ± 0.1*	0.6 ± 0.1	0.7 ± 0.1	0.5 ± 0.1	0.9 ± 0
22:0	1.1 ± 0.2	1.3 ± 0.2	1.9 ± 0.4*	1.1 ± 0.2	1 ± 0.3	0.7 ± 0.2	1.2 ± 0.1
24:0	0.2 ± 0	0.6 ± 0.2	5 ± 1.7*	0.3 ± 0.1	0.4 ± 0.1	0.6 ± 0.1	0.7 ± 0.2
26:0	1.9 ± 0.9	7.7 ± 1.9	48.7 ± 14.3*	6.8 ± 2.1	4.9 ± 2.2	52.7 ± 2.7*	16 ± 1.5*
28:0	0 ± 0	1.4 ± 0.4*	0.4 ± 0.3	0.1 ± 0	0.1 ± 0	5.9 ± 0.4*	0.3 ± 0.1
30:0	0 ± 0	0.1 ± 0*	0 ± 0	0 ± 0	0 ± 0	0.1 ± 0*	0 ± 0

Supplementary Materials Chapter 4

Supplementary Table 1 Original transcript contig and coding sequence NCBI accession numbers, forward and reverse primer sequences and qPCR product length (bp) of each target and reference gene. Myosin was not used as a reference gene in the final analysis.

| Gene	Transcript contig	Coding seq.	Forward sequence (5'-3')	Reverse sequence (5'-3')	size (bp)
scd	GHXK01165927		ACCGTGATACCGGTTGTCTT	CCATGTTGCGTGCAAGGATA	93
med	GHXK01184360	ON075828	ACCACTCCACCATGTTCTGT	GTCCCAAAGCGGACAAGAAG	135
fed	GHXK01205503	ON075829	ACGACTGGAGACTCTCTGCT	CATGATTGGCATCGTGCTGG	78
elovl1a	GHXK01177303	ON075830	CCGGTGGTCATGCATCATTT	GTGGTCATGTGCTGTTTCCA	130
elovl1b	GHXK01255463	ON075831	TGCTGTTCAGCGTTTGGATT	TCTCATGGCCTTGGGATTGT	110
elovl1c	GHXK01260983	ON075832	TCGTTGACTTCACGGACACA	CCACCAGGAGCATACGTTGT	130
elovl1d	GHXK01228992	ON075833	TTGCTCGCAAAGTAGAGCCA	GGATGGGGAGGCGATTACAG	104
elovl1e	GHXK01223266	ON075834	TTTTGAAACTGCGGGCCAAG	GTCCTTTGGTGGCTTCCTCA	87
elovl4	GHXK01149108	ON075835	ACCACTCCACCATGTTCTGT	GTCCCAAAGCGGACAAGAAG	135
elovl6	GHXK01159412	ON075836	ACACCGTCTTCATCGTGCTA	CTGGCAGCAGCTGTGTATTC	115
18S	GHXK01254969		GGGAATCGCGAGCCAAATTC	GGAGTGGGAAAGTCTGTCGG	95
28S	GHXK01117689		GTTGCGTGAACAGGAGGAGA	TCAGGTTAGCGTTGGCTCTG	101
β-actin	GHXK01154926		GCTGGTCGTGACTTGACTGA	GGCCATCTCCTGCTCAAAGT	144
myosin	GHXK01233605		ACAAAATGAAGGGACGCTGTA	AACCGTGCAATCGAATTTGTTA	81
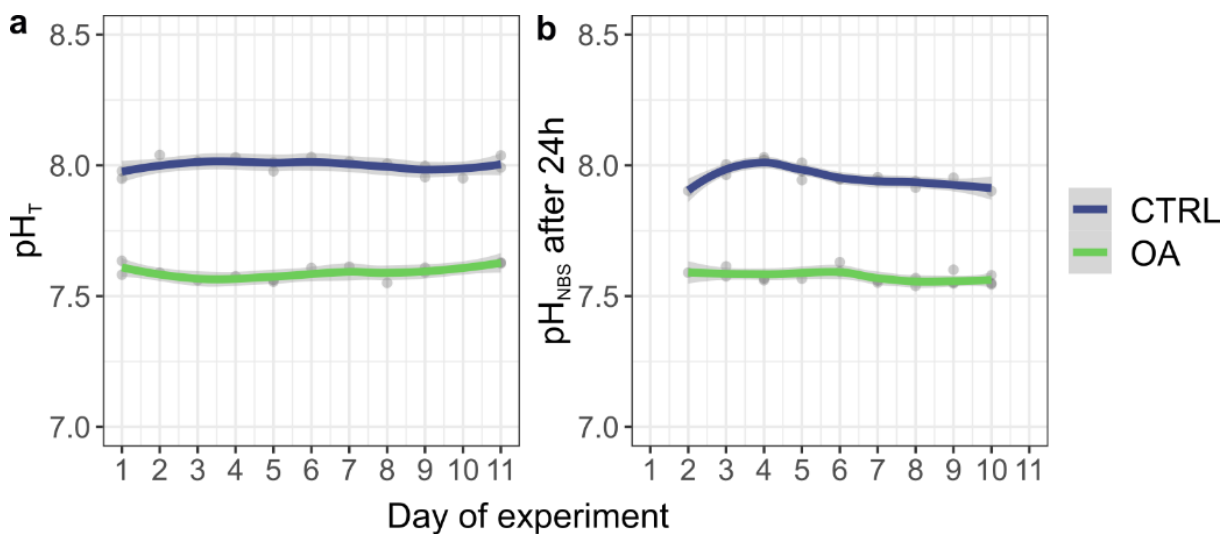
Supplementary Figure 1 Additional experimental conditions: (a) pH$_T$ of stock seawater and (b) pH$_{NBS}$ after 24h of incubation between ambient (CTRL) and future (OA) levels. Loess smooth lines (span = 0.75) were added using ggplot2 package in R, with 95% confidence intervals in grey.
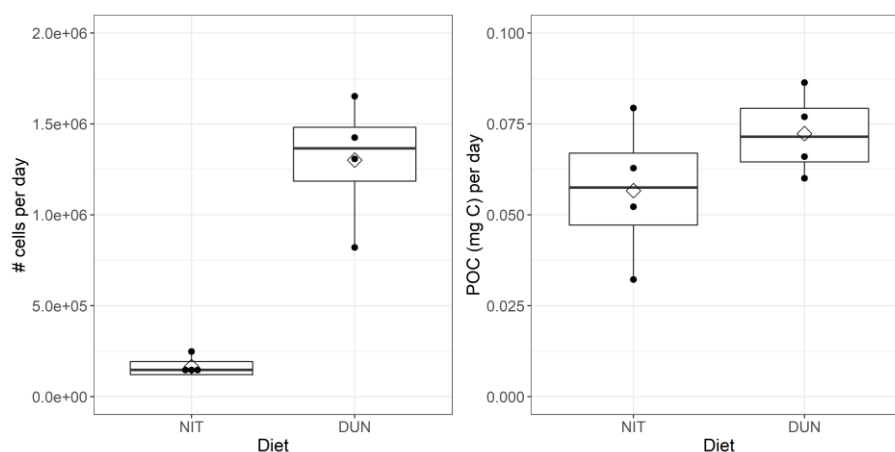
Supplementary Figure 2 Boxplots of estimated (a) number of cells and (b) particulate organic carbon (POC, in mg C) administered per experimental unit per day.

Supplementary Table 2 Relative fatty acid concentrations (mean ± sd) per diet (% of total FA).

|	*Nitzschia* sp.	*Dunaliella tertiolecta*
14:0	10.97 ± 0.49	0.39 ± 0.07
iso-15:0	0.4 ± 0.17	0.21 ± 0.07
anteiso-15:0	0.1 ± 0.03	0.02 ± 0
15:0	0.54 ± 0.11	0.06 ± 0.01
iso-16:0	0.04 ± 0.02	0.05 ± 0.01
16:0	10.4 ± 1.05	17.45 ± 0.77
16:1	0.49 ± 0.11	0.39 ± 0.11
16:1n-9	11.54 ± 0.52	1.25 ± 0.14
17:0	1.04 ± 0.2	0.07 ± 0.01
16:2n-7	0.74 ± 0.06	0 ± 0
16:2n-6	0 ± 0	1.2 ± 0.16
16:2n-4	5.28 ± 0.14	0 ± 0
16:3n-6	0 ± 0	0.94 ± 0.05
18:0	0.65 ± 0.16	0.97 ± 0.23
16:3n-4	6.27 ± 0.6	0 ± 0
16:3n-3	0 ± 0	3.65 ± 0.17
18:1n-9	0.3 ± 0.16	3.85 ± 0.23
18:1n-11	2.89 ± 1.71	3.7 ± 0.43
16:4n-3	0 ± 0	17.08 ± 0.68
16:4n-1	7.82 ± 0.9	0.81 ± 0.5
18:2n-6	1.24 ± 0.28	4 ± 0.26
18:3n-6	3.11 ± 0.3	3.2 ± 0.3
18:3n-3	0.04 ± 0.01	39.24 ± 0.89
18:4n-3	2.94 ± 0.71	1.35 ± 0.05
20:3n-6	0.11 ± 0.02	0.03 ± 0
22:0	0.1 ± 0.02	0.03 ± 0
20:4n-6	1.5 ± 0.3	0.03 ± 0.01
20:5n-3	26.86 ± 1.87	0 ± 0
24:0	1.1 ± 0.21	0.03 ± 0.01
22:5n-3	0.21 ± 0.01	0 ± 0
22:6n-3	3.34 ± 0.15	0 ± 0
ΣLC-PUFA	32.03 ± 1.95	0.06 ± 0.01
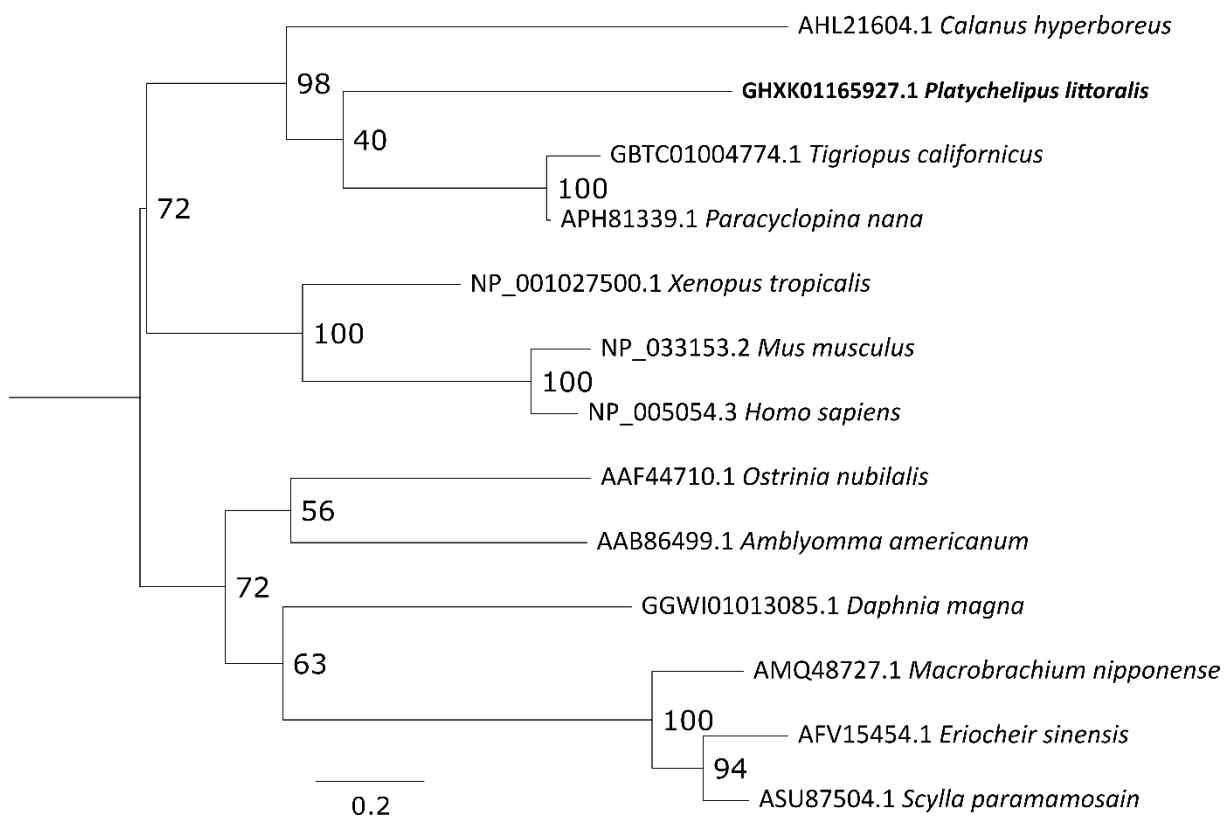
Supplementary Figure 3 Maximum-likelihood phylogenetic tree of stearoyl CoA desaturase, with the Platychelipus littoralis sequence highlighted in bold. Values next to nodes show bootstrap support (%) after 100 RAxML iterations.
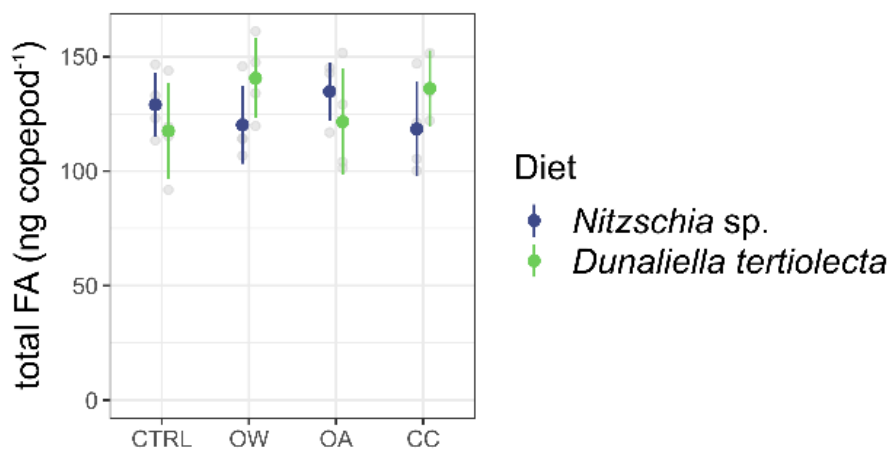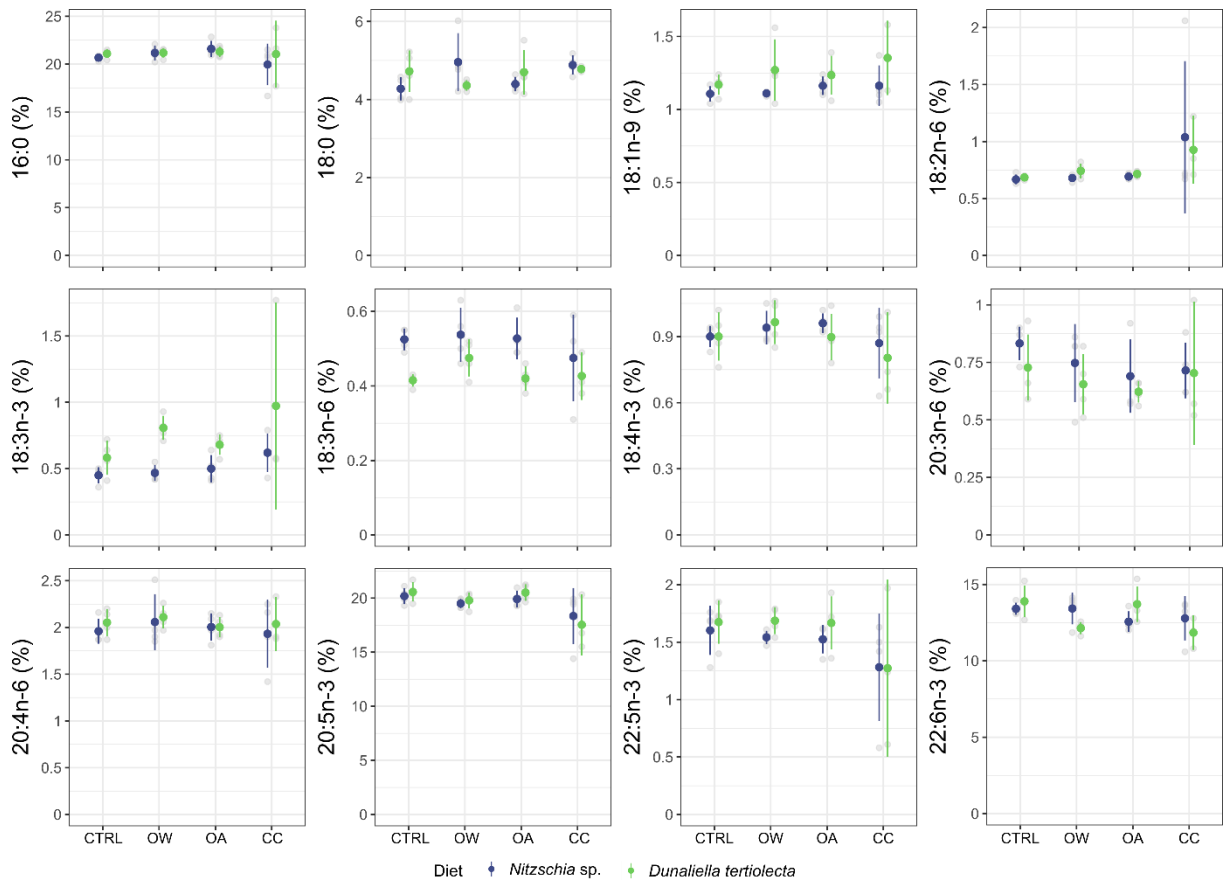

Supplementary Figure 4 Total FA content (sum of all quantified FAs, ng copepod^{-1}). Factors: CTRL: control; OW: ocean warming; OA: ocean acidification; CC: climate change (OW + OA).
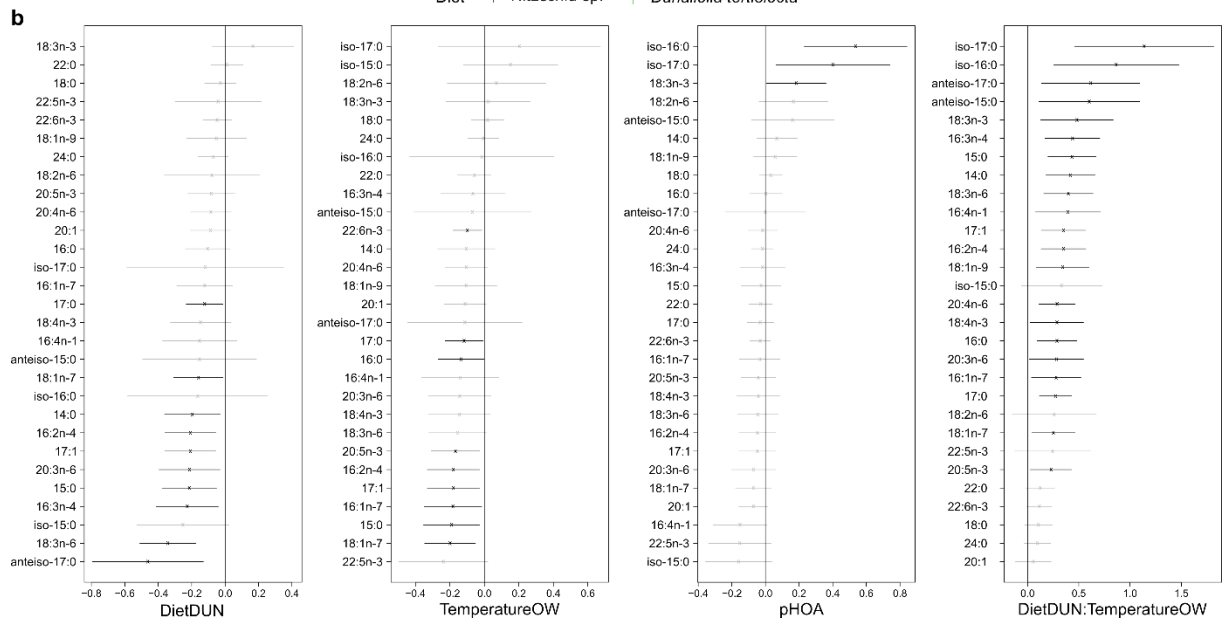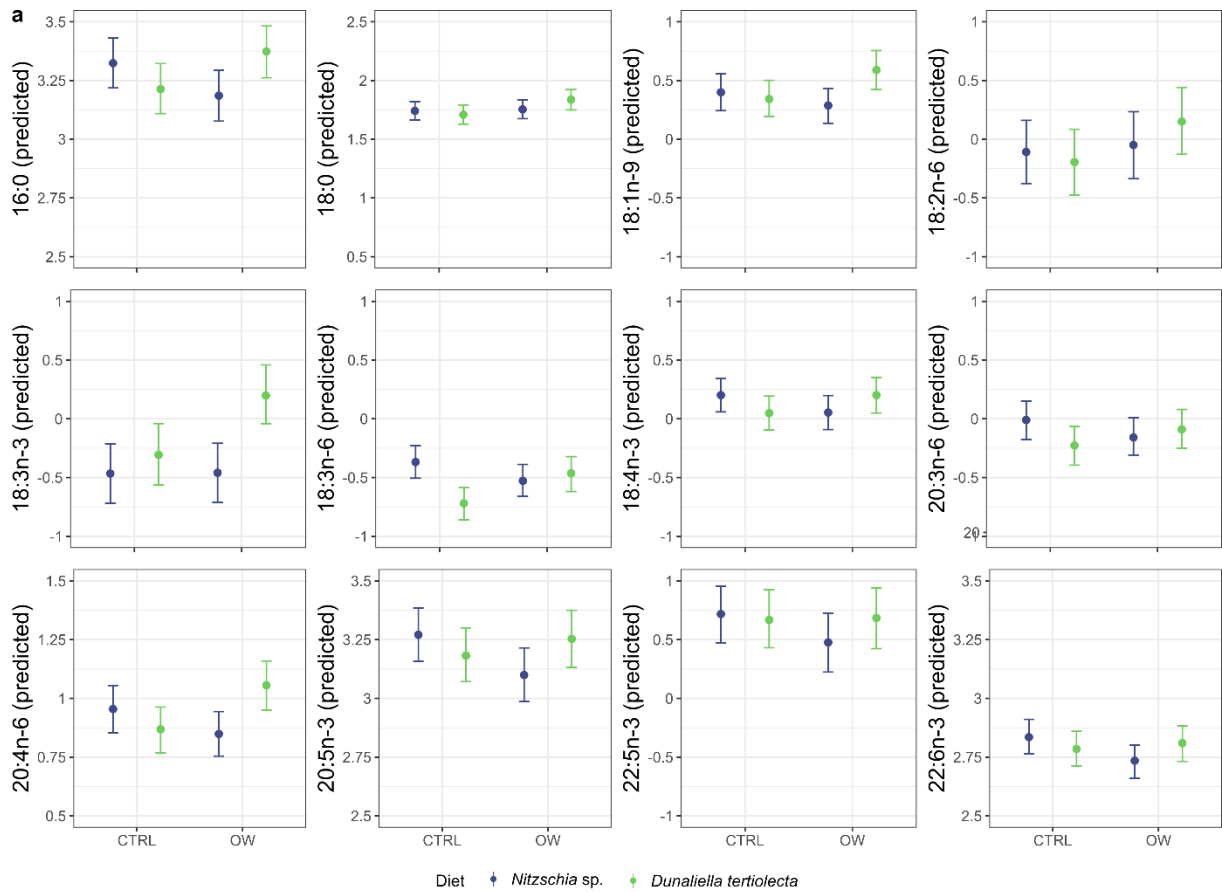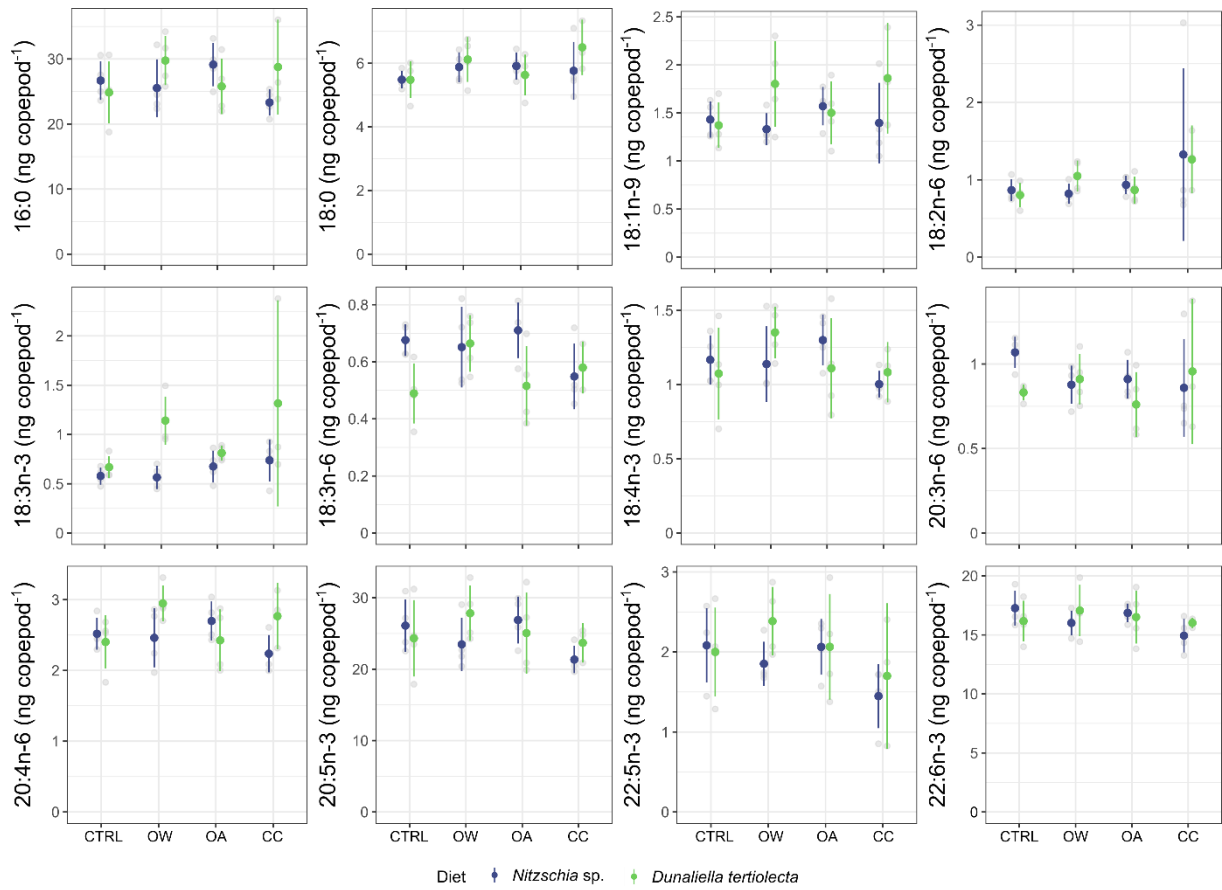
Supplementary Figure 5 (a) Absolute fatty acid concentrations (scaled to linear predictors of the best-fitting model). Means and error bars (2.5% to 97.5% quantiles) are built from 500 simulations of normally distributed model parameters. Factors: CTRL: control; OW: ocean warming. (b) Covariate coefficients and 95% confidence intervals of absolute fatty acid concentrations. Negative or positive coefficients represent whether there is a decrease or increase respectively due to the 'future' treatment. Grey lines: not significant effect, black lines: significant effect (p<0.05).
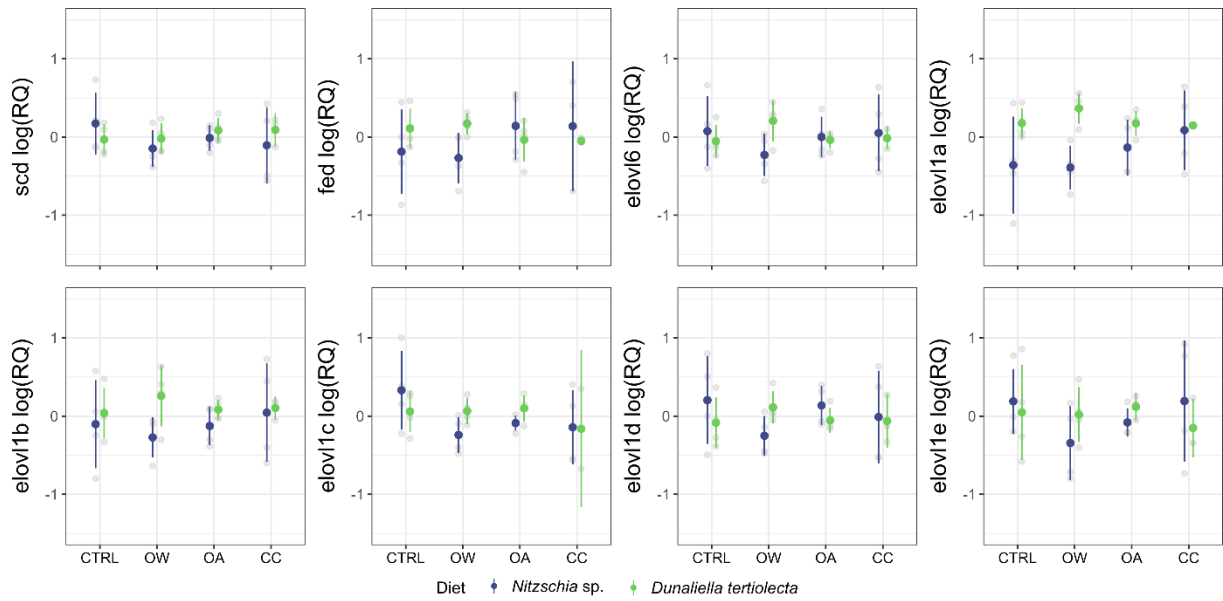
Supplementary Figure 6 Gene expression (relative quantities (RQ); observed variables). Factors: CTRL: control; OW: ocean warming; OA: 2800 ocean acidification; CC: climate change (OW + OA).

Supplementary Figure 7 Relative fatty acid composition (% of total FA measured) of the main FAs involved in the LC-PUFA biosynthesis pathway (observed variables). Factors: CTRL: control; OW: ocean warming; OA: ocean acidification; CC: climate change (OW + OA).

Supplementary Figure 8 Absolute fatty acid concentrations (ng copepod^{-1}) of the main FAs involved in the LC-PUFA biosynthesis pathway (observed variables). Factors: CTRL: control; OW: ocean warming; OA: ocean acidification; CC: climate change (OW + OA).

Supplementary Table 3 Absolute fatty acid concentrations (mean ± sd) per treatment (ng copepod^{-1}). CTRL: control; OW: ocean warming; OA: ocean acidification

diet	field	*Nitzschia* sp.				*Dunaliella tertiolecta*			
temperature		CTRL	OW	CTRL	OW	CTRL	OW	CTRL	OW
pH		CTRL		OA		CTRL		OA	
14:0	3.65 ± 0.53	3.32 ± 0.36	3.19 ± 0.6	3.84 ± 0.51	3.26 ± 0.28	2.79 ± 0.56	4.1 ± 0.58	3.13 ± 0.6	3.91 ± 0.4
iso-15:0	0.18 ± 0.01	0.27 ± 0.05	0.35 ± 0.03	0.23 ± 0.13	0.24 ± 0.08	0.21 ± 0.07	0.32 ± 0.06	0.19 ± 0.03	0.33 ± 0.03
anteiso-15:0	0.22 ± 0.02	0.14 ± 0.04	0.12 ± 0.02	0.14 ± 0.02	0.15 ± 0.03	0.12 ± 0.02	0.17 ± 0.04	0.12 ± 0.02	0.33 ± 0
15:0	4.4 ± 0.61	2.64 ± 0.35	2.35 ± 0.2	2.65 ± 0.2	2.01 ± 0.14	2.17 ± 0.23	2.67 ± 0.32	2.14 ± 0.37	2.94 ± 0.08
iso-16:0	0.66 ± 0.12	0.25 ± 0.04	0.17 ± 0.05	0.28 ± 0.18	0.39 ± 0.19	0.14 ± 0.01	0.47 ± 0.11	0.36 ± 0.17	0.6 ± 0.18
16:0	25.45 ± 2.26	26.69 ± 2.65	25.53 ± 3.91	29.14 ± 2.94	23.32 ± 1.77	24.85 ± 4.2	29.77 ± 3.35	25.79 ± 3.77	28.76 ± 1.85
iso-17:0	1.29 ± 0.24	0.39 ± 0.19	0.35 ± 0.06	0.41 ± 0.05	0.65 ± 0.17	0.32 ± 0.02	1.03 ± 0.36	0.4 ± 0.17	2.85 ± 0.18
16:1n-7	12.76 ± 1.5	14.59 ± 1.89	13.54 ± 2.87	15.93 ± 1.69	12 ± 0.89	13.44 ± 3.05	16.17 ± 2.15	14.07 ± 3.21	13.38 ± 1.38
anteiso-17:0	0.53 ± 0.07	0.56 ± 0.19	0.61 ± 0.16	0.6 ± 0.19	0.43 ± 0.16	0.35 ± 0.08	0.53 ± 0.17	0.39 ± 0.14	0.64 ± 0.2
17:0	2.56 ± 0.32	2 ± 0.14	1.9 ± 0.09	1.98 ± 0.15	1.63 ± 0.12	1.77 ± 0.1	2.01 ± 0.16	1.76 ± 0.26	2.17 ± 0.16
17:1	1.94 ± 0.29	1.82 ± 0.21	1.73 ± 0.28	1.98 ± 0.15	1.47 ± 0.15	1.57 ± 0.3	1.94 ± 0.21	1.57 ± 0.41	1.7 ± 0.07
16:2n-4	1.94 ± 0.29	1.82 ± 0.21	1.73 ± 0.28	1.98 ± 0.15	1.47 ± 0.15	1.57 ± 0.3	1.94 ± 0.21	1.57 ± 0.41	1.7 ± 0.07
18:0	4.77 ± 0.28	5.48 ± 0.24	5.88 ± 0.41	5.91 ± 0.37	5.76 ± 0.8	5.48 ± 0.51	6.12 ± 0.62	5.63 ± 0.56	6.5 ± 0.53
16:3n-4	1.07 ± 0.14	1.43 ± 0.09	1.4 ± 0.31	1.51 ± 0.14	1.37 ± 0.35	1.18 ± 0.19	1.81 ± 0.28	1.21 ± 0.31	1.54 ± 0.02
18:1n-9	1.88 ± 0.22	1.43 ± 0.17	1.33 ± 0.15	1.57 ± 0.18	1.4 ± 0.37	1.37 ± 0.21	1.8 ± 0.39	1.5 ± 0.29	1.86 ± 0.2
18:1n-7	5.95 ± 0.62	7.33 ± 1.09	6.71 ± 1	7.51 ± 0.97	5.47 ± 0.41	6.3 ± 0.9	7.11 ± 1.19	6.42 ± 1.38	6.16 ± 0.73
16:4n-1	0.73 ± 0.49	0.87 ± 0.09	0.93 ± 0.18	0.87 ± 0.05	0.64 ± 0.12	0.79 ± 0.23	1.08 ± 0.16	0.77 ± 0.22	0.9 ± 0.13
18:2n-6	0.95 ± 0.08	0.87 ± 0.12	0.82 ± 0.12	0.93 ± 0.11	1.33 ± 0.99	0.8 ± 0.14	1.05 ± 0.18	0.87 ± 0.15	1.26 ± 0.08
18:3n-6	0.53 ± 0.06	0.68 ± 0.05	0.65 ± 0.12	0.71 ± 0.09	0.55 ± 0.1	0.49 ± 0.09	0.66 ± 0.09	0.52 ± 0.12	0.58 ± 0.05
18:3n-3	0.81 ± 0.1	0.58 ± 0.08	0.56 ± 0.1	0.68 ± 0.14	0.74 ± 0.19	0.67 ± 0.1	1.14 ± 0.22	0.81 ± 0.07	1.32 ± 0.08
20:1	0.98 ± 0.07	1.13 ± 0.05	1 ± 0.07	1.08 ± 0.11	0.97 ± 0.07	1.02 ± 0.11	1.07 ± 0.16	1.02 ± 0.14	0.84 ± 0.1
18:4n-3	1.05 ± 0.13	1.17 ± 0.15	1.14 ± 0.23	1.3 ± 0.15	1 ± 0.08	1.07 ± 0.27	1.35 ± 0.15	1.11 ± 0.3	1.08 ± 0.13
20:3n-6	1.32 ± 0.24	1.07 ± 0.08	0.88 ± 0.1	0.91 ± 0.1	0.86 ± 0.26	0.83 ± 0.04	0.91 ± 0.13	0.76 ± 0.17	0.96 ± 0.12
22:0	1.1 ± 0.1	1.27 ± 0.09	1.28 ± 0.1	1.31 ± 0.1	1.16 ± 0.07	1.29 ± 0.14	1.45 ± 0.13	1.34 ± 0.19	1.34 ± 0.11
20:4n-6	2.78 ± 0.18	2.52 ± 0.2	2.46 ± 0.37	2.7 ± 0.24	2.24 ± 0.23	2.4 ± 0.33	2.95 ± 0.22	2.43 ± 0.39	2.77 ± 0.3
20:5n-3	24.47 ± 2.02	26.11 ± 3.26	23.48 ± 3.31	26.89 ± 2.91	21.35 ± 1.69	24.33 ± 4.74	27.83 ± 3.42	25.06 ± 4.99	23.7 ± 2.62
24:0	1.84 ± 0.08	2.15 ± 0.13	2.24 ± 0.13	2.22 ± 0.08	2.1 ± 0.22	2.06 ± 0.22	2.25 ± 0.12	2.03 ± 0.21	2.21 ± 0.1
22:5n-3	2.08 ± 0.22	2.08 ± 0.41	1.85 ± 0.24	2.06 ± 0.31	1.45 ± 0.35	2 ± 0.49	2.38 ± 0.38	2.06 ± 0.58	1.7 ± 0.29
22:6n-3	14.32 ± 0.78	17.26 ± 1.29	16.01 ± 0.91	16.86 ± 0.7	14.94 ± 1.25	16.17 ± 1.52	17.06 ± 1.92	16.51 ± 1.98	16.02 ± 1.54
ΣFA	122.18 ± 10.8	129 ± 12.26	120.19 ± 15.02	134.73 ± 11.09	118.35 ± 18.22	117.56 ± 18.45	140.52 ± 15.38	121.53 ± 20.45	136.03 ± 10.54

Supplementary Table 4 Absolute fatty acid concentrations (mean ± sd) per single driver (ng copepod⁻¹), including change (Δ%) from control to future level. CTRL: control; OW: ocean warming; OA: ocean acidification

driver	diet		Δ%	temperature		Δ%	pH		Δ%
level	NIT	DUN		CTRL	OW		CTRL	OA	
14:0	3.4 ± 0.52	3.45 ± 0.85	2	3.27 ± 0.56	3.59 ± 0.72	10	3.35 ± 0.72	3.51 ± 0.67	5
iso-15:0	0.28 ± 0.09	0.25 ± 0.08	-8	0.22 ± 0.07	0.31 ± 0.07	37	0.29 ± 0.08	0.24 ± 0.1	-16
anteiso-15:0	0.14 ± 0.03	0.18 ± 0.15	28	0.13 ± 0.03	0.18 ± 0.15	39	0.14 ± 0.04	0.18 ± 0.15	27
15:0	2.41 ± 0.35	2.45 ± 0.68	1	2.4 ± 0.35	2.46 ± 0.65	3	2.46 ± 0.35	2.4 ± 0.68	-2
iso-16:0	0.27 ± 0.16	0.38 ± 0.22	39	0.26 ± 0.15	0.4 ± 0.21	54	0.26 ± 0.14	0.4 ± 0.22	54
16:0	26.17 ± 3.6	27.19 ± 4.61	4	26.62 ± 3.72	26.72 ± 4.49	0	26.71 ± 4.04	26.62 ± 4.26	0
iso-17:0	0.45 ± 0.18	1.04 ± 1.63	131	0.38 ± 0.28	1.11 ± 1.61	192	0.52 ± 0.36	0.96 ± 1.62	85
16:1n-7	14.01 ± 2.44	14.33 ± 2.87	2	14.51 ± 2.64	13.8 ± 2.55	-5	14.44 ± 2.76	13.87 ± 2.51	-4
anteiso-17:0	0.55 ± 0.19	0.47 ± 0.18	-15	0.47 ± 0.13	0.55 ± 0.18	16	0.52 ± 0.18	0.51 ± 0.2	-2
17:0	1.88 ± 0.19	1.91 ± 0.31	2	1.88 ± 0.22	1.91 ± 0.3	2	1.92 ± 0.16	1.86 ± 0.33	-3
17:1	1.75 ± 0.28	1.7 ± 0.34	-3	1.74 ± 0.3	1.71 ± 0.28	-1	1.76 ± 0.29	1.68 ± 0.32	-5
16:2n-4	1.75 ± 0.28	1.7 ± 0.34	-3	1.74 ± 0.3	1.71 ± 0.28	-1	1.76 ± 0.29	1.68 ± 0.32	-5
18:0	5.76 ± 0.53	5.89 ± 0.7	2	5.63 ± 0.48	6.04 ± 0.69	7	5.74 ± 0.54	5.92 ± 0.68	3
16:3n-4	1.43 ± 0.25	1.43 ± 0.38	0	1.33 ± 0.22	1.53 ± 0.35	15	1.45 ± 0.33	1.4 ± 0.31	-4
18:1n-9	1.43 ± 0.25	1.62 ± 0.39	13	1.47 ± 0.24	1.58 ± 0.42	8	1.48 ± 0.31	1.56 ± 0.36	5
18:1n-7	6.76 ± 1.21	6.52 ± 1.12	-3	6.89 ± 1.11	6.38 ± 1.05	-7	6.86 ± 1.12	6.41 ± 1.18	-7
16:4n-1	0.83 ± 0.16	0.88 ± 0.25	7	0.82 ± 0.17	0.88 ± 0.25	7	0.92 ± 0.2	0.79 ± 0.2	-14
18:2n-6	0.99 ± 0.54	0.98 ± 0.26	-1	0.87 ± 0.14	1.11 ± 0.58	27	0.88 ± 0.17	1.09 ± 0.57	23
18:3n-6	0.65 ± 0.11	0.56 ± 0.12	-13	0.6 ± 0.11	0.61 ± 0.11	3	0.62 ± 0.12	0.59 ± 0.12	-5
18:3n-3	0.64 ± 0.15	0.96 ± 0.44	51	0.68 ± 0.13	0.91 ± 0.47	34	0.74 ± 0.27	0.86 ± 0.43	16
20:1	1.05 ± 0.1	1 ± 0.16	-5	1.06 ± 0.11	0.98 ± 0.14	-8	1.05 ± 0.12	0.99 ± 0.14	-6
18:4n-3	1.15 ± 0.19	1.16 ± 0.26	1	1.16 ± 0.23	1.15 ± 0.21	-1	1.18 ± 0.23	1.13 ± 0.22	-5
20:3n-6	0.93 ± 0.17	0.86 ± 0.19	-8	0.89 ± 0.16	0.9 ± 0.21	0	0.92 ± 0.13	0.87 ± 0.23	-6
22:0	1.26 ± 0.11	1.36 ± 0.16	8	1.3 ± 0.14	1.3 ± 0.15	0	1.32 ± 0.14	1.28 ± 0.15	-3
20:4n-6	2.48 ± 0.32	2.63 ± 0.4	6	2.51 ± 0.35	2.59 ± 0.41	3	2.58 ± 0.36	2.52 ± 0.37	-3
20:5n-3	24.46 ± 3.61	25.33 ± 4.36	4	25.6 ± 4.2	24.12 ± 3.67	-6	25.44 ± 4.09	24.29 ± 3.85	-5
24:0	2.18 ± 0.16	2.13 ± 0.24	-2	2.11 ± 0.17	2.2 ± 0.22	4	2.17 ± 0.18	2.13 ± 0.23	-2
22:5n-3	1.86 ± 0.42	2.06 ± 0.58	11	2.05 ± 0.45	1.86 ± 0.55	-10	2.08 ± 0.44	1.83 ± 0.55	-12
22:6n-3	16.27 ± 1.39	16.47 ± 1.68	1	16.7 ± 1.6	16 ± 1.5	-4	16.62 ± 1.56	16.08 ± 1.48	-3
ΣFA	125.57 ± 15.87	128.43 ± 19.73	2	125.7 ± 17.01	128.29 ± 18.34	2	126.82 ± 17.85	127.1 ± 17.94	0

Supplementary Table 5 Relative fatty acid composition (mean ± sd) per treatment (% of total FA). CTRL: control; OW: ocean warming; OA: ocean acidification

diet	field	*Nitzschia* sp.				*Dunaliella tertiolecta*			
temperature	field	CTRL	OW	CTRL	OW	CTRL	OW	CTRL	OW
pH		CTRL		OA		CTRL		OA	
14:0	2.98 ± 0.24	2.58 ± 0.26	2.63 ± 0.16	2.84 ± 0.22	2.79 ± 0.27	2.35 ± 0.13	2.91 ± 0.18	2.61 ± 0.46	2.86 ± 0.48
iso-15:0	0.15 ± 0.01	0.22 ± 0.04	0.3 ± 0.03	0.17 ± 0.1	0.21 ± 0.07	0.19 ± 0.09	0.23 ± 0.02	0.16 ± 0.04	0.24 ± 0.03
anteiso-15:0	0.18 ± 0.01	0.11 ± 0.03	0.1 ± 0.01	0.11 ± 0.02	0.13 ± 0.03	0.11 ± 0.02	0.12 ± 0.02	0.1 ± 0.02	0.23 ± 0.17
15:0	3.59 ± 0.25	2.05 ± 0.17	1.97 ± 0.2	1.99 ± 0.29	1.75 ± 0.31	1.86 ± 0.15	1.91 ± 0.15	1.76 ± 0.1	2.11 ± 0.64
iso-16:0	0.54 ± 0.07	0.2 ± 0.04	0.15 ± 0.05	0.21 ± 0.12	0.34 ± 0.17	0.12 ± 0.02	0.33 ± 0.06	0.31 ± 0.14	0.43 ± 0.12
16:0	20.83 ± 0.19	20.68 ± 0.22	21.18 ± 0.69	21.6 ± 0.74	19.97 ± 1.92	21.09 ± 0.4	21.18 ± 0.44	21.3 ± 0.5	21.05 ± 2.52
iso-17:0	1.05 ± 0.14	0.3 ± 0.14	0.29 ± 0.01	0.31 ± 0.04	0.55 ± 0.1	0.28 ± 0.03	0.73 ± 0.25	0.35 ± 0.18	1.94 ± 1.9
16:1n-7	10.42 ± 0.44	11.28 ± 0.48	11.16 ± 0.92	11.8 ± 0.37	10.29 ± 1.15	11.31 ± 0.79	11.5 ± 0.65	11.47 ± 0.8	9.9 ± 1.37
anteiso-17:0	0.43 ± 0.04	0.43 ± 0.13	0.51 ± 0.11	0.44 ± 0.14	0.36 ± 0.11	0.3 ± 0.05	0.38 ± 0.08	0.31 ± 0.07	0.48 ± 0.16
17:0	2.1 ± 0.17	1.55 ± 0.07	1.61 ± 0.21	1.49 ± 0.21	1.42 ± 0.26	1.54 ± 0.22	1.44 ± 0.12	1.45 ± 0.05	1.58 ± 0.2
17:1	1.59 ± 0.12	1.41 ± 0.04	1.43 ± 0.06	1.47 ± 0.11	1.28 ± 0.27	1.33 ± 0.06	1.39 ± 0.09	1.28 ± 0.14	1.25 ± 0.03
16:2n-4	1.59 ± 0.12	1.41 ± 0.04	1.43 ± 0.06	1.47 ± 0.11	1.28 ± 0.27	1.33 ± 0.06	1.39 ± 0.09	1.28 ± 0.14	1.25 ± 0.03
18:0	3.92 ± 0.16	4.28 ± 0.26	4.96 ± 0.66	4.4 ± 0.16	4.89 ± 0.22	4.72 ± 0.47	4.36 ± 0.12	4.7 ± 0.5	4.78 ± 0.06
16:3n-4	0.88 ± 0.07	1.12 ± 0.11	1.16 ± 0.17	1.12 ± 0.08	1.21 ± 0.43	1.01 ± 0.05	1.3 ± 0.25	0.99 ± 0.14	1.13 ± 0.11
18:1n-9	1.54 ± 0.08	1.11 ± 0.05	1.11 ± 0.01	1.16 ± 0.06	1.16 ± 0.12	1.17 ± 0.06	1.27 ± 0.19	1.24 ± 0.12	1.35 ± 0.18
18:1n-7	4.87 ± 0.26	5.66 ± 0.4	5.58 ± 0.2	5.55 ± 0.37	4.71 ± 0.59	5.39 ± 0.35	5.03 ± 0.33	5.24 ± 0.26	4.57 ± 0.47
16:4n-1	0.59 ± 0.39	0.68 ± 0.08	0.77 ± 0.07	0.65 ± 0.04	0.54 ± 0.06	0.66 ± 0.1	0.77 ± 0.06	0.62 ± 0.08	0.66 ± 0.19
18:2n-6	0.78 ± 0.01	0.67 ± 0.04	0.68 ± 0.03	0.69 ± 0.02	1.04 ± 0.59	0.69 ± 0.02	0.74 ± 0.06	0.72 ± 0.02	0.93 ± 0.22
18:3n-6	0.43 ± 0.01	0.53 ± 0.03	0.54 ± 0.06	0.53 ± 0.05	0.48 ± 0.1	0.42 ± 0.02	0.48 ± 0.04	0.42 ± 0.03	0.43 ± 0.05
18:3n-3	0.66 ± 0.04	0.45 ± 0.05	0.47 ± 0.05	0.5 ± 0.09	0.62 ± 0.13	0.58 ± 0.11	0.81 ± 0.08	0.68 ± 0.07	0.97 ± 0.56
20:1	0.8 ± 0.03	0.88 ± 0.06	0.84 ± 0.07	0.8 ± 0.03	0.83 ± 0.07	0.87 ± 0.05	0.76 ± 0.04	0.84 ± 0.04	0.62 ± 0.12
18:4n-3	0.85 ± 0.04	0.9 ± 0.04	0.94 ± 0.07	0.96 ± 0.04	0.87 ± 0.14	0.9 ± 0.1	0.97 ± 0.09	0.9 ± 0.09	0.8 ± 0.15
20:3n-6	1.08 ± 0.14	0.83 ± 0.06	0.75 ± 0.15	0.69 ± 0.14	0.72 ± 0.11	0.73 ± 0.13	0.66 ± 0.12	0.62 ± 0.04	0.7 ± 0.22
22:0	0.91 ± 0.08	0.99 ± 0.04	1.07 ± 0.06	0.98 ± 0.02	1 ± 0.16	1.11 ± 0.05	1.03 ± 0.03	1.1 ± 0.03	0.99 ± 0.12
20:4n-6	2.29 ± 0.15	1.96 ± 0.12	2.06 ± 0.26	2.01 ± 0.13	1.93 ± 0.32	2.05 ± 0.13	2.11 ± 0.11	2 ± 0.1	2.04 ± 0.21
20:5n-3	20.04 ± 0.42	20.19 ± 0.66	19.51 ± 0.39	19.92 ± 0.68	18.35 ± 2.29	20.57 ± 0.79	19.79 ± 0.65	20.52 ± 0.68	17.54 ± 2.04
24:0	1.52 ± 0.09	1.68 ± 0.07	1.88 ± 0.11	1.65 ± 0.09	1.81 ± 0.24	1.76 ± 0.1	1.61 ± 0.11	1.69 ± 0.11	1.62 ± 0.13
22:5n-3	1.7 ± 0.09	1.6 ± 0.19	1.54 ± 0.05	1.53 ± 0.11	1.28 ± 0.41	1.68 ± 0.17	1.69 ± 0.1	1.67 ± 0.2	1.27 ± 0.56
22:6n-3	11.76 ± 0.44	13.41 ± 0.35	13.43 ± 0.92	12.56 ± 0.6	12.79 ± 1.28	13.9 ± 0.9	12.14 ± 0.35	13.71 ± 1.03	11.84 ± 0.81

Supplementary Table 6 Relative fatty acid composition (mean ± sd) per single driver (% of total FA)., including change (Δ%) from control to future level. CTRL: control; OW: ocean warming; OA: ocean acidification

treatment level	diet NIT	DUN	Δ%	temperature CTRL	OW	Δ%	pH CTRL	OA	Δ%
14:0	2.71 ± 0.25	2.67 ± 0.41	-1	2.59 ± 0.34	2.79 ± 0.3	8	2.62 ± 0.27	2.77 ± 0.38	6
iso-15:0	0.22 ± 0.08	0.2 ± 0.06	-10	0.18 ± 0.07	0.24 ± 0.05	33	0.23 ± 0.07	0.19 ± 0.07	-16
anteiso-15:0	0.11 ± 0.02	0.13 ± 0.09	23	0.11 ± 0.02	0.14 ± 0.09	31	0.11 ± 0.02	0.13 ± 0.09	23
15:0	1.94 ± 0.27	1.9 ± 0.33	-2	1.91 ± 0.22	1.92 ± 0.37	0	1.95 ± 0.18	1.89 ± 0.39	-3
iso-16:0	0.22 ± 0.13	0.29 ± 0.15	30	0.21 ± 0.12	0.3 ± 0.15	46	0.2 ± 0.09	0.31 ± 0.16	57
16:0	20.86 ± 1.25	21.16 ± 1.2	1	21.17 ± 0.6	20.83 ± 1.65	-2	21.03 ± 0.51	20.97 ± 1.7	0
iso-17:0	0.36 ± 0.14	0.75 ± 1.06	108	0.31 ± 0.12	0.8 ± 1.04	160	0.4 ± 0.24	0.71 ± 1.06	78
16:1n-7	11.13 ± 0.96	11.12 ± 1.1	0	11.47 ± 0.67	10.77 ± 1.21	-6	11.31 ± 0.74	10.93 ± 1.24	-3
anteiso-17:0	0.43 ± 0.13	0.36 ± 0.12	-17	0.37 ± 0.12	0.43 ± 0.13	15	0.4 ± 0.12	0.39 ± 0.14	-3
17:0	1.52 ± 0.21	1.5 ± 0.17	-1	1.51 ± 0.16	1.51 ± 0.22	0	1.54 ± 0.18	1.48 ± 0.2	-4
17:1	1.4 ± 0.16	1.31 ± 0.11	-6	1.37 ± 0.12	1.34 ± 0.17	-2	1.39 ± 0.08	1.32 ± 0.19	-5
16:2n-4	1.4 ± 0.16	1.31 ± 0.11	-6	1.37 ± 0.12	1.34 ± 0.17	-2	1.39 ± 0.08	1.32 ± 0.19	-5
18:0	4.63 ± 0.48	4.63 ± 0.4	0	4.52 ± 0.43	4.74 ± 0.44	5	4.58 ± 0.51	4.68 ± 0.35	2
16:3n-4	1.15 ± 0.25	1.1 ± 0.21	-4	1.06 ± 0.12	1.2 ± 0.29	14	1.14 ± 0.2	1.11 ± 0.26	-3
18:1n-9	1.14 ± 0.08	1.25 ± 0.16	10	1.17 ± 0.09	1.22 ± 0.17	4	1.16 ± 0.12	1.22 ± 0.14	5
18:1n-7	5.37 ± 0.57	5.09 ± 0.46	-5	5.46 ± 0.38	5 ± 0.57	-8	5.41 ± 0.41	5.05 ± 0.59	-7
16:4n-1	0.66 ± 0.1	0.68 ± 0.12	3	0.65 ± 0.08	0.69 ± 0.14	5	0.72 ± 0.09	0.61 ± 0.11	-14
18:2n-6	0.77 ± 0.33	0.76 ± 0.13	-2	0.69 ± 0.03	0.84 ± 0.35	22	0.69 ± 0.05	0.84 ± 0.35	21
18:3n-6	0.52 ± 0.07	0.43 ± 0.04	-16	0.47 ± 0.06	0.48 ± 0.08	2	0.49 ± 0.06	0.46 ± 0.08	-5
18:3n-3	0.51 ± 0.11	0.75 ± 0.3	47	0.55 ± 0.12	0.7 ± 0.32	27	0.58 ± 0.16	0.67 ± 0.31	17
20:1	0.84 ± 0.07	0.78 ± 0.11	-6	0.85 ± 0.05	0.77 ± 0.11	-9	0.84 ± 0.07	0.79 ± 0.11	-6
18:4n-3	0.92 ± 0.09	0.9 ± 0.12	-2	0.91 ± 0.08	0.9 ± 0.13	-1	0.93 ± 0.08	0.89 ± 0.12	-4
20:3n-6	0.75 ± 0.13	0.68 ± 0.14	-10	0.72 ± 0.13	0.71 ± 0.15	-2	0.74 ± 0.13	0.68 ± 0.14	-8
22:0	1.01 ± 0.1	1.06 ± 0.08	5	1.04 ± 0.07	1.03 ± 0.11	-2	1.05 ± 0.07	1.02 ± 0.11	-3
20:4n-6	1.99 ± 0.23	2.05 ± 0.14	3	2.01 ± 0.12	2.03 ± 0.25	1	2.05 ± 0.18	1.99 ± 0.21	-3
20:5n-3	19.49 ± 1.44	19.74 ± 1.6	1	20.3 ± 0.75	18.88 ± 1.77	-7	20.01 ± 0.76	19.18 ± 1.95	-4
24:0	1.75 ± 0.17	1.67 ± 0.13	-5	1.69 ± 0.1	1.74 ± 0.2	2	1.73 ± 0.14	1.7 ± 0.17	-2
22:5n-3	1.49 ± 0.26	1.6 ± 0.33	7	1.62 ± 0.18	1.46 ± 0.38	-10	1.63 ± 0.15	1.45 ± 0.39	-11
22:6n-3	13.04 ± 0.94	12.97 ± 1.21	-1	13.39 ± 0.92	12.6 ± 1.09	-6	13.22 ± 0.95	12.78 ± 1.17	-3

Supplementary Table 7 Regularized canonical correlation between relative fatty acid concentrations and gene expression

	elovl1a	elovl1b	elovl1c	elovl1d	elovl1e	elovl6	fed	scd
14:0	0.156611	0.171184	-0.00965	0.109707	0.055321	0.14518	0.096329	0.049753
iso-15:0	-0.08929	-0.11986	-0.00709	-0.09085	-0.05423	-0.11609	-0.09192	-0.05227
anteiso-15:0	0.166745	0.187682	-0.00721	0.123697	0.064425	0.162686	0.111569	0.058793
15:0	-0.0449	0.001938	0.031609	0.033408	0.036133	0.034718	0.057151	0.040516
iso-16:0	0.200756	0.159343	-0.04635	0.064229	0.00967	0.096178	0.023631	-0.00075
16:0	-0.02168	-0.07967	-0.03031	-0.08634	-0.0647	-0.10385	-0.10633	-0.06699
iso-17:0	0.239866	0.253429	-0.01973	0.156893	0.075804	0.209253	0.132986	0.066799
16:1n-7	-0.06665	-0.1162	-0.0204	-0.1018	-0.06772	-0.12665	-0.11302	-0.06772
anteiso-17:0	0.021962	0.106536	0.045305	0.12031	0.091867	0.143857	0.150639	0.095596
17:0	-0.22954	-0.27821	-0.0013	-0.19552	-0.10892	-0.25366	-0.18657	-0.10225
17:1	-0.29208	-0.34532	0.003267	-0.23773	-0.12973	-0.30976	-0.22295	-0.12077
16:2n-4	-0.29208	-0.34532	0.003267	-0.23773	-0.12973	-0.30976	-0.22295	-0.12077
18:0	-0.05989	-0.15169	-0.04506	-0.15157	-0.10903	-0.18454	-0.18011	-0.11161
16:3n-4	-0.13411	-0.31613	-0.08759	-0.3095	-0.22016	-0.37803	-0.3642	-0.22466
18:1n-9	0.337305	0.350052	-0.03132	0.212586	0.100151	0.284792	0.176499	0.087142
18:1n-7	-0.22831	-0.24751	0.015227	-0.15733	-0.07856	-0.20858	-0.13703	-0.07033
16:4n-1	0.285026	0.338844	-0.00213	0.234365	0.128499	0.305067	0.220669	0.119859
18:2n-6	0.15546	0.235879	0.027707	0.19275	0.122129	0.242804	0.205207	0.120206
18:3n-6	-0.1951	-0.18197	0.029712	-0.09689	-0.03703	-0.13404	-0.06802	-0.02838
18:3n-3	-0.00262	-0.02774	-0.0139	-0.03345	-0.02627	-0.03964	-0.04293	-0.02753
20:1	-0.08022	-0.07462	0.012332	-0.03958	-0.01502	-0.05481	-0.02763	-0.01145
18:4n-3	-0.07509	-0.14751	-0.03237	-0.13579	-0.09321	-0.16752	-0.1549	-0.09411
20:3n-6	-0.17506	-0.11972	0.051282	-0.03156	0.011162	-0.0551	0.011341	0.021299
22:0	-0.08486	-0.26098	-0.08988	-0.27332	-0.20142	-0.3304	-0.33171	-0.20759
20:4n-6	-0.13677	-0.26603	-0.05746	-0.24397	-0.16708	-0.30117	-0.27776	-0.16859
20:5n-3	-0.11847	-0.1836	-0.02329	-0.15178	-0.09699	-0.19079	-0.16277	-0.09573
24:0	-0.23927	-0.27874	0.005013	-0.18949	-0.10206	-0.24756	-0.17577	-0.09449
22:5n-3	0.027937	-0.01409	-0.02695	-0.03716	-0.03561	-0.04088	-0.05696	-0.03904
22:6n-3	-0.23534	-0.30598	-0.01305	-0.22682	-0.1328	-0.29109	-0.22574	-0.1271

Supplementary Materials Chapter 5

Supplementary Table 1 Overview of publically available transcriptomic data assessed within this study. TSA: transcriptome shotgun assembly; SRA: short read archive; EST: expressed sequence tags. *data was obtained from a source indicated within the study rathen than from an NCBI database.

order	species	type	prefix	NCBI BioProject	year	DOI reference	size (Mb)	# contigs
Calanoida	*Acartia (Acartiura) clausii*	TSA	GKAA01	PRJNA824716	2023	10.1093/nargab/lqad007	31	23313
Calanoida	*Acartia fossae*	SRA	SRP036139	PRJNA236441	2014	10.1111/mec.12781		
Calanoida	*Acartia tonsa*	TSA	GKAB01	PRJNA824716	2023	10.1093/nargab/lqad007	31	22784
Calanoida	*Acartia tonsa*	TSA*	GSE210554	PRJNA866147	2022	10.1016/j.cbd.2022.101054	180	252212
Calanoida	*Acartia tonsa*	TSA	HAGX01	PRJEB20069	2017	10.1093/gbe/evz067	119	117406
Calanoida	*Acartia tonsa*	TSA	GFWY01	PRJNA407266	2017	10.3389/fmars.2018.00156	74	60662
Calanoida	*Calanoides acutus*	TSA	GJIZ01	PRJNA757455	2022		314	338109
Calanoida	*Calanus finmarchicus*	TSA	HBXF01	PRJEB51404	2022		111	154909
Calanoida	*Calanus finmarchicus*	TSA	GBXU01	PRJNA236983	2015	10.3354/meps11398	10	28954
Calanoida	*Calanus finmarchicus*	TSA	GAXK01	PRJNA236528	2014	10.1016/j.ygcen.2013.03.018	205	206012
Calanoida	*Calanus finmarchicus*	TSA	GBFB01	PRJNA231164	2014	10.1186/s12983-014-0091-8	161	241140
Calanoida	*Calanus glacialis*	TSA	GJQS01	PRJNA744376	2022	10.1002/ece3.8606	514	573399
Calanoida	*Calanus glacialis*	TSA	HBXE01	PRJEB51407	2022		99	111768
Calanoida	*Calanus glacialis*	TSA	HACJ01	PRJNA274584	2015	10.1016/j.margen.2015.03.014	33	54344
Calanoida	*Calanus glacialis*	TSA	GBXT01	PRJNA237014	2015	10.3354/meps11398	16	36880
Calanoida	*Calanus helgolandicus*	TSA	GKAC01	PRJNA824716	2023	10.1093/nargab/lqad007	48	43040
Calanoida	*Calanus helgolandicus*	TSA	GJQW01	PRJNA744376	2022	10.1002/ece3.8606	367	424432
Calanoida	*Calanus helgolandicus*	TSA	GJFL01	PRJNA640515	2021	10.3390/md18080392	43	30339
Calanoida	*Calanus hyperboreus*	TSA	GJRE01	PRJNA744376	2022	10.1002/ece3.8606	349	393435
Calanoida	*Calanus hyperboreus*	TSA	HBXD01	PRJEB51409	2022		89	93239
Calanoida	*Calanus marshallae*	TSA	GJRL01	PRJNA662858	2022	10.1038/s41597-023-02130-1	81	88923
Calanoida	*Calanus marshallae*	TSA	GJRF01	PRJNA662858	2022	10.1038/s41597-023-02130-1	66	73920
Calanoida	*Calanus marshallae*	TSA	GJQX01	PRJNA745090	2022	10.1002/ece3.8606	215	246945
Calanoida	*Calanus pacificus*	TSA	GJQY01	PRJNA745090	2022	10.1002/ece3.8606	365	419932
Calanoida	*Calanus pacificus*	SRA	SRX1981328	PRJNA335617	2016			
Calanoida	*Calanus propinquus*	TSA	GIVX01	PRJNA669816	2021		484	504547
Calanoida	*Calanus sinicus*	SRA	SRX372691	PRJNA225989	2014	10.1155/2014/493825		
Calanoida	*Centropages hamatus*	TSA	GKAD01	PRJNA824716	2023	10.1093/nargab/lqad007	34	23278
Calanoida	*Epischura baikalensis*	TSA	GFUA01	PRJNA395558	2017	10.1111/mec.14704	3	5413
Calanoida	*Eucalanus bungii*	TSA	GJRG01	PRJNA662858	2022	10.1038/s41597-023-02130-1	30	38410
Calanoida	*Eurytemora affinis*	TSA	GEAN01	PRJNA278152	2016	10.1111/mec.15681	142	107445
Calanoida	*Eurytemora affinis*	TSA	GBGO01	PRJNA242763	2015	10.1093/femsec/fiw072	144	138088
Calanoida	*Gladioferens pectinatus*	TSA*			2022	10.1016/j.aquatox.2021.106069		218769
Calanoida	*Hemidiaptomus amblyodon*	TSA	GCIW01	PRJNA254268	2020	10.1186/s12862-020-01699-0	31	35268
Calanoida	*Labidocera madurae*	TSA	GFWO01	PRJNA324849	2017	10.1371/journal.pone.0186794	184	210768

order	species	type	prefix	NCBI BioProject	year	DOI reference	size (Mb)	# contigs
Calanoida	*Metridia lucens*	SRA	SRR6956663	PRJNA449123	2018	10.7717/peerj.5506		
Calanoida	*Metridia pacifica*	TSA	GJAO01	PRJNA662858	2021	10.1038/s41597-023-02130-1	125	119911
Calanoida	*Neocalanus cristatus*	TSA	GJRH01	PRJNA662858	2022	10.1038/s41597-023-02130-1	90	91729
Calanoida	*Neocalanus flemingeri*	TSA	GJSD01	PRJNA662858	2022	10.1038/s41597-023-02130-1	82	88456
Calanoida	*Neocalanus flemingeri*	TSA	GJRT01	PRJNA662858	2022	10.1038/s41597-023-02130-1	59	66818
Calanoida	*Neocalanus flemingeri*	TSA	GJVQ	PRJNA681461	2022	10.1093/plankt/fbac039		150507
Calanoida	*Neocalanus flemingeri*	TSA	GHLB01	PRJNA496596	2019	10.1038/s42003-019-0565-5	45	51605
Calanoida	*Neocalanus flemingeri*	TSA	GFUD01	PRJNA324453	2017	10.1016/j.margen.2017.09.002	142	140535
Calanoida	*Neocalanus plumchrus*	TSA	GJRU01	PRJNA662858	2022	10.1038/s41597-023-02130-1	71	73912
Calanoida	*Pleuromamma robusta*	SRA	SRX3341162	PRJNA416202	2017	10.1186/1471-2164-14-167		
Calanoida	*Pleuromamma xiphias*	TSA	GFCI01	PRJNA352670	2017	10.1086/699219	247	554991
Calanoida	*Pseudocalanus acuspes*	TSA*	SRP063962	PRJNA296544	2015	10.1111/eva.12335		69555
Calanoida	*Pseudodiaptomus annandalei*	TSA	GHWV01	PRJNA558682	2019		173	183458
Calanoida	*Rhincalanus gigas*	TSA	GIVD01	PRJNA666170	2020	10.1016/j.margen.2021.100835	228	260930
Calanoida	*Rhincalanus gigas*	SRA	SRP267242	PRJNA639356	2020	10.3390/biology9110410		
Calanoida	*Temora longicornis*	TSA	GKAP01	PRJNA824716	2023	10.1093/nargab/lqad007	38	25723
Calanoida	*Temora longicornis*	TSA	GINW01	PRJNA577564	2021	10.1016/j.marenvres.2020.105037	484	504547
Calanoida	*Temora longicornis*	TSA	GGQN02	PRJNA475124	2019	10.1016/j.marenvres.2018.10.017	97	179569
Calanoida	*Temora stylifera*	TSA	GJGX01	PRJNA632714	2021	10.1186/s12864-020-07112-w	139	268582
Canuelloida	*Canuella perplexa*	TSA*	unpublished		2023		142	189334
Cyclopoida	*Apocyclops panamensis*	TSA*	unpublished		2023			
Cyclopoida	*Apocyclops royi*	TSA	GHAJ01	PRJEB28764	2018	10.1534/g3.119.400085	101	75477
Cyclopoida	*Eucyclops serrulatus*	TSA	GARW01	PRJNA231234	2014	10.1111/1755-0998.12368	37	51528
Cyclopoida	*Lernaea cyprinacea*	SRA		PRJNA232511	2013	10.1016/j.exppara.2015.03.014	54	50792
Cyclopoida	*Mytilicola intestinalis*	SRA		PRJNA430138	2018	10.1111/mec.14541		45645
Cyclopoida	*Oithona nana*	SRA		PRJEB34229	2021	10.3390/biology10070657		
Cyclopoida	*Paracyclopina nana*	SRA		PRJNA714788	2021	10.1038/s41558-022-01477-4		
Cyclopoida	*Paracyclopina nana*	TSA	GCJT01	PRJNA268783	2015	10.1016/j.cbd.2015.04.002	96	60687
Harpacticoida	*Platychelipus littoralis*	TSA	GHXK01	PRJNA575120	2019	10.1098/rstb.2019.0645	208	287339
Harpacticoida	*Tigriopus californicus*	TSA	GHUE01	PRJNA504307	2019	10.1073/pnas.1819874116	107	92866
Harpacticoida	*Tigriopus californicus*	TSA	GBSZ01	PRJNA263967	2015	10.1093/molbev/msu321	15	12067
Harpacticoida	*Tigriopus californicus*	TSA	GBTC01	PRJNA263967	2015	10.1093/molbev/msu321	15	12075
Harpacticoida	*Tigriopus japonicus*	TSA	GCHA01	PRJNA274317	2015	10.1016/j.margen.2015.05.011	83	54758
Harpacticoida	*Tigriopus kingsejongensis*	TSA	GDFW01	PRJNA283925	2015	10.1016/j.margen.2016.04.009	36	38250
Harpacticoida	*Tisbe furcata*	TSA	GCIT01	PRJNA254316	2020	10.1186/s12862-020-01699-0	24	33473
Harpacticoida	*Tisbe holothuriae*	TSA	HAHV01	PRJEB23629	2018	?	101	285984
Harpacticoida	*Tisbe* sp.	TSA*	unpublished		2023			
Siphonostomatoida	*Caligus clemensi*	EST	BT		2011	10.1007/s10126-011-9398-z		
Siphonostomatoida	*Caligus rogercresseyi*	TSA	GAZX01	PRJNA234316	2014	10.1016/j.cbd.2014.01.003	56	44089
Siphonostomatoida	*Lepeophtheirus salmonis*	TSA	HACA01	PRJEB1804	2015	10.1371/journal.pone.0137394	50	33933
Siphonostomatoida	*Tracheliastes polycolpus*	TSA	GGQW01	PRJNA476682	2018	10.1016/j.margen.2018.12.001	20	17157

244

Supplementary Table 2 Order, habitat, lifestyle and number of methyl-end desaturases (med), front-end desaturases (fed) and elongases (elovl) per copepod species. fresh: freshwater; free: free-living.

order	species	habitat	lifestyle	med	fed	elovl
Calanoida	*Acartia (Acartiura) clausi*	marine	free	0	0	4
Calanoida	*Acartia fossae*	marine	free	0	0	2
Calanoida	*Acartia tonsa*	marine, brackish	free	0	0	4
Calanoida	*Calanoides acutus*	marine	free	0	0	6
Calanoida	*Calanus finmarchicus*	marine	free	0	0	5
Calanoida	*Calanus glacialis*	marine	free	0	1	4
Calanoida	*Calanus helgolandicus*	marine	free	0	1	16
Calanoida	*Calanus hyperboreus*	marine	free	0	1	3
Calanoida	*Calanus marshallae*	marine	free	0	1	5
Calanoida	*Calanus pacificus*	marine	free	0	1	4
Calanoida	*Calanus propinquus*	marine	free	0	0	3
Calanoida	*Calanus sinicus*	marine	free	0	1	13
Calanoida	*Centropages hamatus*	marine	free	0	0	3
Calanoida	*Epischura baikalensis*	fresh	free	0	0	0
Calanoida	*Eucalanus bungii*	marine	free	0	0	0
Calanoida	*Eurytemora affinis*	brackish, fresh	free	0	0	5
Calanoida	*Gladioferens pectinatus*	marine, brackish	free	0	0	6
Calanoida	*Hemidiaptomus amblyodon*	fresh	free	0	0	1
Calanoida	*Labidocera madurae*	marine	free	0	0	2
Calanoida	*Metridia lucens*	marine	free	0	0	6
Calanoida	*Metridia pacifica*	marine	free	0	0	1
Calanoida	*Neocalanus cristatus*	marine	free	0	0	4
Calanoida	*Neocalanus flemingeri*	marine	free	0	1	3
Calanoida	*Neocalanus plumchrus*	marine	free	0	0	2
Calanoida	*Pleuromamma robusta*	marine	free	0	0	5
Calanoida	*Pleuromamma xiphias*	marine	free	0	0	2
Calanoida	*Pseudocalanus acuspes*	marine	free	0	0	5
Calanoida	*Pseudodiaptomus annandalei*	marine, brackish, fresh	free	0	0	2
Calanoida	*Rhincalanus gigas*	marine	free	0	0	6
Calanoida	*Temora longicornis*	marine	free	0	0	7
Calanoida	*Temora stylifera*	marine	free	0	0	1
Canuelloida	*Canuella perplexa*	marine	free	0	2	10
Cyclopoida	*Apocyclops royi*	brackish, fresh	free	2	2	8
Cyclopoida	*Apocyclops panamensis*	brackish, fresh	free	2	2	6
Cyclopoida	*Eucyclops serrulatus*	fresh	free	1	2	8
Cyclopoida	*Lernaea cyprinacea*	fresh	parasitic	0	1	6
Cyclopoida	*Mytilicola intestinalis*	marine	parasitic	2	0	2
Cyclopoida	*Oithona nana*	marine	free	0	0	5
Cyclopoida	*Paracyclopina nana*	marine	free	1	1	6
Harpacticoida	*Platychelipus littoralis*	marine, brackish	free	1	1	9
Harpacticoida	*Tigriopus californicus*	marine	free	2	5	8
Harpacticoida	*Tigriopus japonicus*	marine	free	2	4	7
Harpacticoida	*Tigriopus kingsejongensis*	marine	free	2	3	7
Harpacticoida	*Tisbe furcata*	marine	free	0	0	3
Harpacticoida	*Tisbe holothuriae*	marine	free	1	1	5
Harpacticoida	*Tisbe* sp.	marine	free	3	3	4
Siphonostomatoida	*Caligus clemensi*	marine	parasitic	0	0	5
Siphonostomatoida	*Caligus rogercresseyi*	marine	parasitic	1	2	7
Siphonostomatoida	*Lepeophtheirus salmonis*	marine	parasitic	2	2	4
Siphonostomatoida	*Tracheliastes polycolpus*	fresh	parasitic	1	1	4

Supplementary Table 3 Elongase transcripts (gene id and transcript id) with count data available. Overall average: average count value across all transcripts and samples; isoform average: average count value per isoform (in case of multiple isoforms per transcript); sum: sum of isoform counts; av: average of isoform counts.

species	clade	gene_id	doi reference	transcript id	overall average	isoform average	log$_2$FC (sum)	log$_2$FC (av)
C. finmarchicus	elovl1	GBFB01089547	10.1186/s12983-014-0091-8	comp260136_c0_seq1	27.578	393.335	3.834	3.834
C. finmarchicus	elovl1	HBXF01058729	10.1186/s12983-014-0091-8	comp257786_c0_seq1	27.578	15.941	-0.791	-0.791
P. xiphias	elovl1	GFCI01024781	10.1086/699219	TRINITY_DN199733_c0_g3_i1	11.027	3.310	-1.736	-1.736
P. xiphias	elovl4	GFCI01130892	10.1086/699219	TRINITY_DN198207_c0_g2_i8	11.027	0.030 0.950 0.360 0.080 0.080	-2.878	-5.200
P. acuspes	elovl4	comp81259_c1_seq1	10.1111/eva.12335		225.513	8.379	-4.750	-4.750
P. acuspes	elovl1	comp81302_c0_seq1	10.1111/eva.12335		225.513	26.176	-3.107	-3.107
P. acuspes	elovl1	comp79175_c0_seq1	10.1111/eva.12335		225.513	39.779	-2.503	-2.503
P. acuspes	elovl1	comp87030_c0_seq1	10.1111/eva.12335		225.513	105.491	-1.096	-1.096
R. gigas	elovl6	DN5702_c0_g1_i3	10.1016/j.margen.2021.100835	contig66844.2, 66844.1	375.180	64.972	-2.530	-2.530
R. gigas	elovl6	DN8473_c0_g1_i2	10.1016/j.margen.2021.100835	contig117624.1	375.180	316.156	-0.247	-0.247
R. gigas	elovl6	DN25022_c0_g1_i1	10.1016/j.margen.2021.100835	contig128465.1, 131028.1, 127367.1, 134079.2	375.180	54.320	-2.788	-2.788
R. gigas	elovl1	DN24013_c0_g1_i1	10.1016/j.margen.2021.100835	contig71184.1, 73152.1, 96508.1	375.180	30.409	-3.625	-3.625
R. gigas	elovl1	DN691_c0_g1_i6	10.1016/j.margen.2021.100835	contig114460.1, 144047.1, 178793.1, 169578.1	375.180	243.378	-0.624	-0.624
R. gigas	elovl1	DN88512_c0_g1_i1	10.1016/j.margen.2021.100835	contig84073.1	375.180	69.182	-2.439	-2.439
T. longicornis	elovl4	GKAP01000744	10.1016/j.marenvres.2018.10.017	TRINITY_DN184691_c0_g1_i1	533.278	43.583	-3.613	-3.613
T. longicornis	elovl6	GKAP01021940	10.1016/j.marenvres.2018.10.017	TRINITY_DN181084_c3_g1_i1	533.278	131.167	-2.023	-2.023
T. longicornis	elovl1	GKAP01002718	10.1016/j.marenvres.2018.10.017	TRINITY_DN172837_c3_g2_i	533.278	11.583	-5.525	-5.525
T. longicornis	elovl1	GKAP01004573	10.1016/j.marenvres.2018.10.017	TRINITY_DN180749_c0_g1_i2	533.278	18.583 64.500	-2.682	-3.682
T. longicornis	elovl1	GKAP01005026	10.1016/j.marenvres.2018.10.017	TRINITY_DN187924_c5_g7_i2	533.278	451.833 308.667	0.512	-0.488
T. longicornis	elovl1	GKAP01023627	10.1016/j.marenvres.2018.10.017	TRINITY_DN172140_c0_g2_i2	533.278	240.417	-1.149	-1.149
T. longicornis	elovl1	GKAP01005025	10.1016/j.marenvres.2018.10.017	TRINITY_DN181053_c2_g4_i9	533.278	53.000	-3.331	-3.331
P. littoralis	elovl1	GHXK01019362	10.1098/rstb.2019.0645	Plit_DN102518_c0_g2_i1	90.387	4.429	-4.351	-4.351
P. littoralis	elovl4	GHXK01149108	10.1098/rstb.2019.0645	Plit_DN72481_c0_g1_i1	90.387	11.571	-2.966	-2.966
P. littoralis	elovl6	GHXK01159412	10.1098/rstb.2019.0645	Plit_DN8575_c0_g1_i6	90.387	288.178 972.178 1031.144	4.664	3.079
P. littoralis	elovl1	GHXK01177303	10.1098/rstb.2019.0645	Plit_DN1296_c0_g1_i1	90.387	2097.786	4.537	4.537
P. littoralis	elovl1	GHXK01223266	10.1098/rstb.2019.0645	Plit_DN10074_c0_g1_i2	90.387	620.649 274.423	3.308	2.308

species	clade	gene_id	reference	transcript id	overall average	isoform average	log2FC (sum)	log2FC (av)
P. littoralis	elovl1	GHXK01228992	10.1098/rstb.2019.0645	Plit_DN8396_c0_g1_i4	90.387	0.918 2.019 63.136 85.856	0.749	-1.251
P. littoralis	elovl1	GHXK01255463	10.1098/rstb.2019.0645	Plit_DN2897_c0_g1_i8	90.387	10.555 20.627 224.365 315.140 610.948 31.151	3.746	1.161
P. littoralis	elovl1	GHXK01260983	10.1098/rstb.2019.0645	Plit_DN12057_c0_g1_i5	90.387	0.934 6.486 8.422 6.073 26.442	-0.902	-3.224
P. littoralis	elovl11	GHXK01195180	10.1098/rstb.2019.0645	Plit_DN4058_c0_g1_i2	90.387	117.866 24.347 189.212 1262.606 10.505 117.866 72.530 30.507	4.336	1.336
T. californicus	elovl6	JW526839	10.1093/molbev/msu321	SCN_Contig_12680	95.325	94.996	-0.005	-0.005
T. californicus	elovl1	MT757162	10.1093/molbev/msu321	SCN_C3_Contig2152	95.325	157.689	0.726	0.726
T. californicus	elovl1	MT757163	10.1093/molbev/msu321	SCN_C3_Contig1291	95.325	162.616	0.771	0.771
T. californicus	elovl1	MT757164	10.1093/molbev/msu321	SCN_Contig_50350	95.325	8.690	-3.455	-3.455
T. californicus	elovl11	MT757165	10.1093/molbev/msu321	SCN_Contig_33573	95.325	26.715	-1.835	-1.835
T. californicus	elovl1	MT757166	10.1093/molbev/msu321	SCN_Contig_19364	95.325	149.165	0.646	0.646
T. californicus	elovl1	JW505079	10.1093/molbev/msu321	SCN_Contig_1405	95.325	27.027	-1.818	-1.818

247

Supplementary Table 4 Overview of publically available genomic data assessed within this study. *The LsalAtl2s genome was used to assess flanking regions.

species name	Accession id	NCBI BioProject	year	reference	level	annotated
Acartia tonsa	OETC01	PRJEB20069	2018	10.1093/gbe/evz067	scaffold	
Eurytemora affinis	AZAI02	PRJNA203087	2017	10.1093/molbev/msx147	scaffold	
Apocyclops royi	UYDY01	PRJEB28764	2018	10.1534/g3.119.400085	scaffold	
Oithona nana	FTRT01	PRJEB18938	2017	doi.org/10.1111/mec.14214	scaffold	
Paracyclopina nana	JAGUCH01	PRJNA714788	2021	https://doi.org/10.1038/s41558-022-01477-4	chromosome	no
Tigriopus californicus	VCGU01	PRJNA237968	2019	10.1038/s41559-018-0588-1	chromosome	yes
Tigriopus japonicus	JAAGOF01	PRJNA592403	2020	10.1016/j.aquatox.2020.105462	chromosome	no
Tigriopus kingsejongensis	JABCAI01	PRJNA625855	2020	10.1016/j.cbd.2020.100703	scaffold	
Tisbe holothuriae	CAACVA01	PRJEB30601	2019		scaffold	
Caligus rogercresseyi	ASM1338718v1	PRJNA551027	2021	10.1038/s41597-021-00842-w	chromosome	yes
Caligus rogercresseyi	ASM1915635v1	PRJNA739385	2021	10.1038/s41597-021-00842-w	scaffold	
Lepeophtheirus salmonis	LSalAtl2s	PRJNA705827	2021	10.1016/j.ygeno.2021.08.002	chromosome	yes*
Lepeophtheirus salmonis	CAJNVT01	PRJEB43242	2021	https://www.ebi.ac.uk/ena/browser/view/PRJEB43242	chromosome	yes
Lepeophtheirus salmonis	JADKYV01	PRJNA673901	2022	10.1093/g3journal/jkac087	chromosome	yes

species	family	left4	left3	left2	left1	gene	right1	right2	right3	right4
T. californicus	med		cuticle protein 7		rotund	wx2		rotund	rotund	Glce
T. californicus	med	STK11	ataxin-3	obst-E	peroxidase	wx1	COA7	hig	hig	
L. salmonis	med	WDR46	PARG	Pdap1	lncrna	w3		JMJD8	AP3B2	BAF
L. salmonis	med	ENGASE	RBM45	CCDC124	CCDC124	wx			lncrna	PGBD4
T. californicus	fed	WDR55	ABCD4	NSE4A	GALNT1	fed1	CCND2	CCND2	Cad87A	
T. californicus	fed	gacK	U-scoloptoxin(05)-Sm1a	DNAJA2	MAT	fed2		SPARC	FBPase-2	MOB1
T. californicus	fed	KDM6B		pHCl-2	fed4	fed3	CLH2	TRPM	HS-2OST	
T. californicus	fed	D2R	KDM6B		pHCl-2	fed4	fed3	CLH2	TRPM	HS-2OST
T. californicus	fed	SASB_ANAPL	pyruvyl transferase 1	Q6TFL3	ABCD1	fed5	CCDC85C	ALG11	TXLNA	Mdm2
C. rogercresseyi	fed	KIF3A	KIF3A			fed		Prkab2	SUN1	SUN1
C. rogercresseyi	fed		ERD6-LIKE	ERD6-LIKE		fadsA	HTH_48 domain-containing protein			
L. salmonis	fed	FRMD8	lncrna			fed		NNT	lncrna	RNF170
L. salmonis	fed	ORP1C	TMEM53		PTPN1	fed		U6 spliceosomal RNA	ALPK1	ZBED4
T. californicus	elovl6		INTS4	FIS1		elovl6	MPDZ	CAPN7	PRIM2	IQCA1
T. californicus	elovl1			arm	elovl1e	elo1		UCH37	CI-MPR	AUH
T. californicus	elovl1	glsA		Fas3		elo2	Tret1		EHMT2	ATOH1
T. californicus	elovl1	Cad86C	NAP1L1	CaM		elo3	DAZAP2	RETREG3		
T. californicus	elovl11	NPT	PPAF2	LYSMD3	METTL3	elo4				DNAJB6
T. californicus	elovl1	obst-E	obst-E	SSUH2	KLC1	elo5	EPRS1	TRPV5	TRPV5	B-H1
T. californicus	elovl4		CHT1	SmydA-8	CPSF4	elovl4	Slowpoke		N4BP2L1	U-scoloptoxin(01)-Er1a
T. californicus	elovl1	CNPPD1			arm	elovl1	elo1		UCH37	CI-MPR
C. rogercresseyi	elovl1	NWD1	HS3ST6	RINT-1	MON2	elo1	PRSS41	PDIA4	PDIA4	PDIA4
C. rogercresseyi	elovl1	HDAC1	HDAC1	HDAC1	SFMBT2	elo2a		PPP4R1		
C. rogercresseyi	elovl1		MLX/ChREBP2	transposase		elo2b	transposase	SLC6A15S	SLC6A18	SLC6A18

C. rogercresseyi	elovl1	Homeobox domain	MafG	SETMAR		elo2c	Tcb2-L3	LIG	LIG	CHD1
C. rogercresseyi	elovl1	PDPR	tRNA-Trp	BLM		elo2d	MFN2			
C. rogercresseyi		UTRN	colt	GDI1		elovl4	DUF659 domain-containing protein			transposase
L. salmonis	elovl1		TIPIN	PPP4R1	SFMBT2	elo2a	TRIM71	HDAC1	ATP6V1G1	DNAJB11
L. salmonis	elovl1		lncrna	lncrna	lncrna	elo1	MON2	RINT-1	KCP	HS6ST3
L. salmonis	elovl4	lncrna	lncrna	lncrna	MUC2	elovl4	lncrna	SPTBN1	lncrna	FAM210A
L. salmonis	elovl6	PPP3CB	ATOH8	lncrna		elovl6	lncrna	lncrna	NADK	lncrna

Table 6 Log likelihood values (Ln L), number of free parameters (np) and parameter estimations of the different site models far each geny family, as well as likelihood ratio test (LRT) p-values for the different site model comparisons. M1a: p_0 is the proportion of sites with $\omega_0 < 1$, while p_1 is the proportion of sites with $\omega_1 = 1$. M2a: same as M1a but includes an additional class of sites with $\omega_2 > 1$ in proportion p_2. M7: the model uses a beta distribution with parameters p and q to describe variable ω for sites in the range $0 \leq \omega \leq 1$. M8: p_0 is the proportion of sites with ω from beta(p, q) as in M7, but an additional class is now added (with proportion p_1) with $\omega_1 > 1$. M8a: same as M8 but $\omega_1 = 1$.

Gene family	Model	np	Ln L	Estimates of parameters			Comparison	LRT p-value
med	M2a	67	-19755.999895	p_0: 0.85433 ω_0: 0.07233	p_1: 0.01437 ω_1: 1	p_2: 0.13130 ω_2: 1	M1a vs. M2a	1
	M1a	65	-19755.999895	p_0: 0.85433 ω_0: 0.07233	p_1: 0.14567 ω_1: 1			
	M8	67	-19055.989791	p_0: 0.99825 p_1: 0.00175	p: 0.57062 ω: 1	q: 8.93455	M7 vs. M8	0.91761
	M7	65	-19056.075775	p: 0.56897	q: 8.79451			
	M8a	66	-19055.989790	p_0: 0.99825 p_1: 0.00175	p: 0.57062 ω: 1	q: 8.93464	M8a vs. M8	0.99887
fed	M2a	85	-33580.087192	p_0: 0.93623 ω_0: 0.06055	p_1: 0.03693 ω_1: 1	p_2: 0.02684 ω_2: 1	M1a vs. M2a	1
	M1a	83	-33580.087192	p_0: 0.93623 ω_0: 0.06055	p_1: 0.06377 ω_1: 1			
	M8	85	-32256.868573	p_0: 0.99743 p_1: 0.00257	p: 0.55278 ω: 1	q: 9.64041	M7 vs. M8	0.08892
	M7	83	-32259.288550	p: 0.55282	q: 9.49567			
	M8a	84	-32256.868573	p_0: 0.99743 p_1: 0.00257	p: 0.55278 ω: 1	q: 9.64043	M8a vs. M8	1
elovl	M2a	495	-145811.007675	p_0: 0.60528 ω_0: 0.09663	p_1: 0.24386 ω_1: 1	p_2: 0.1509 ω_2: 1	M1a vs. M2a	1
	M1a	493	-145811.007675	p_0: 0.60527 ω_0: 0.09663	p_1: 0.3947 ω_1: 1			
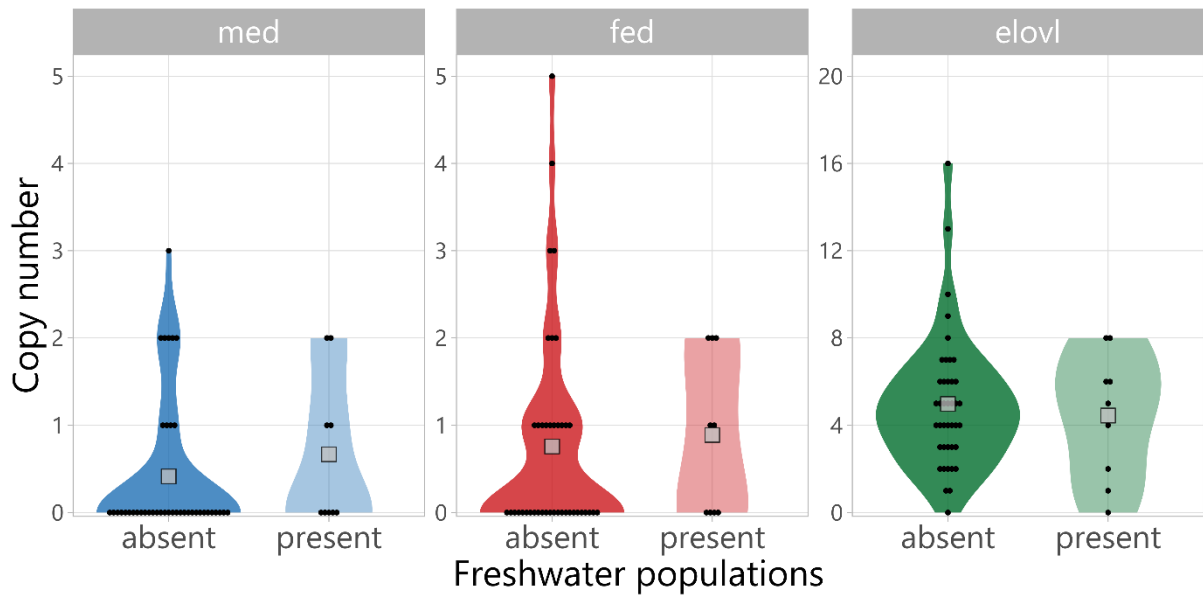
Supplementary Figure 1 Violin plots of copy number of methyl-end desaturases (med), front-end desaturases (fed) and elongases (elovl) per copepod species, with grey squares indicating the mean copy number of species with or without freshwater populations.
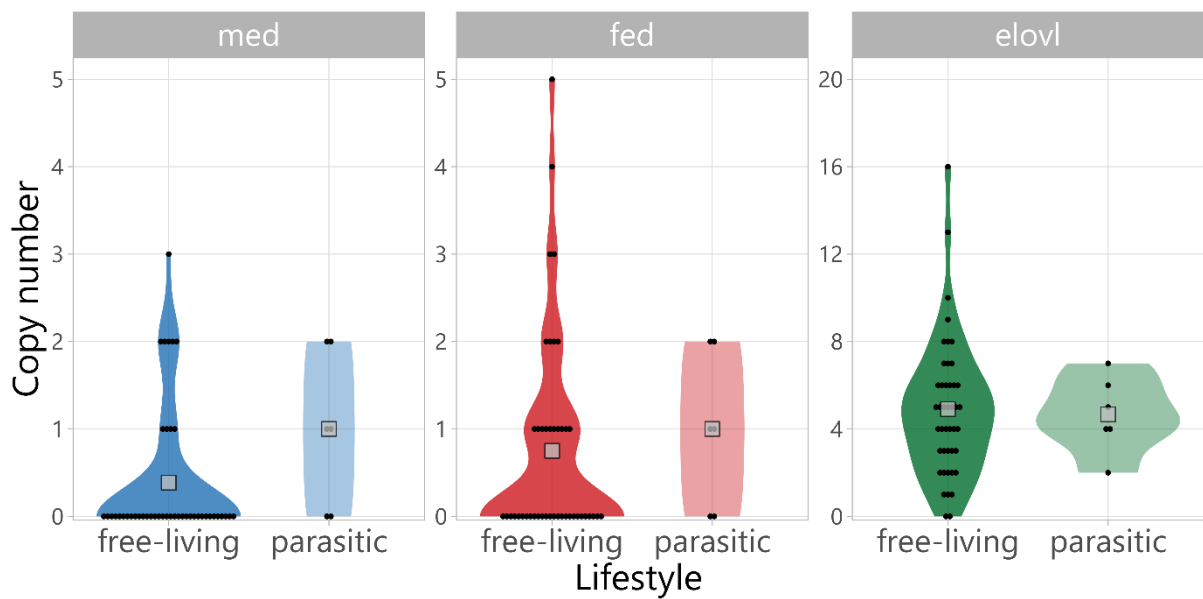
Supplementary Figure 2 Violin plots of copy number of methyl-end desaturases (med), front-end desaturases (fed) and elongases (elovl) per copepod species, with grey squares indicating the mean copy number of species with free-living or parasitic lifestyles.
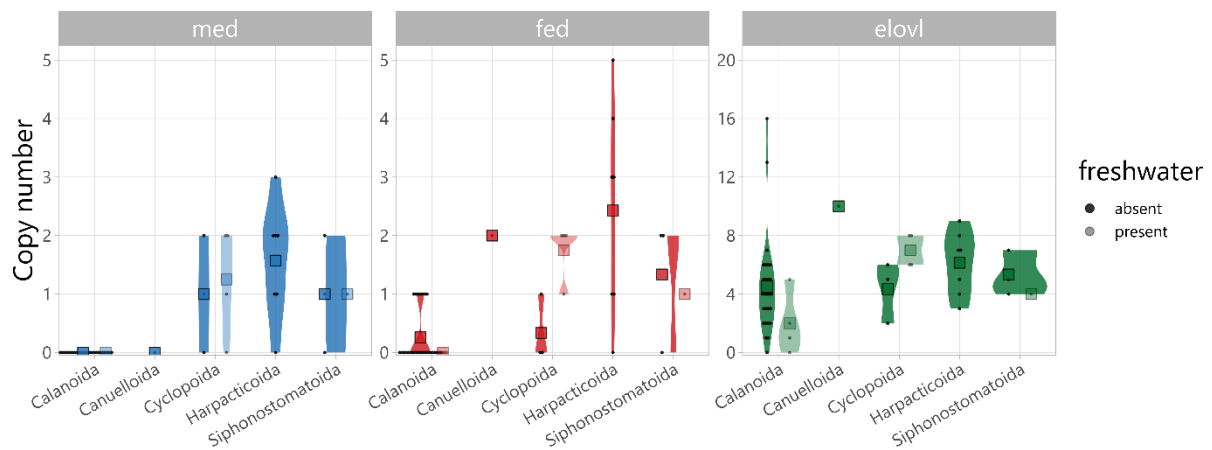
Supplementary Figure 3 Violin plots of copy number of methyl-end desaturases (med), front-end desaturases (fed) and elongases (elovl) per copepod species, with grey squares indicating the mean copy number of species with or without freshwater populations per order.
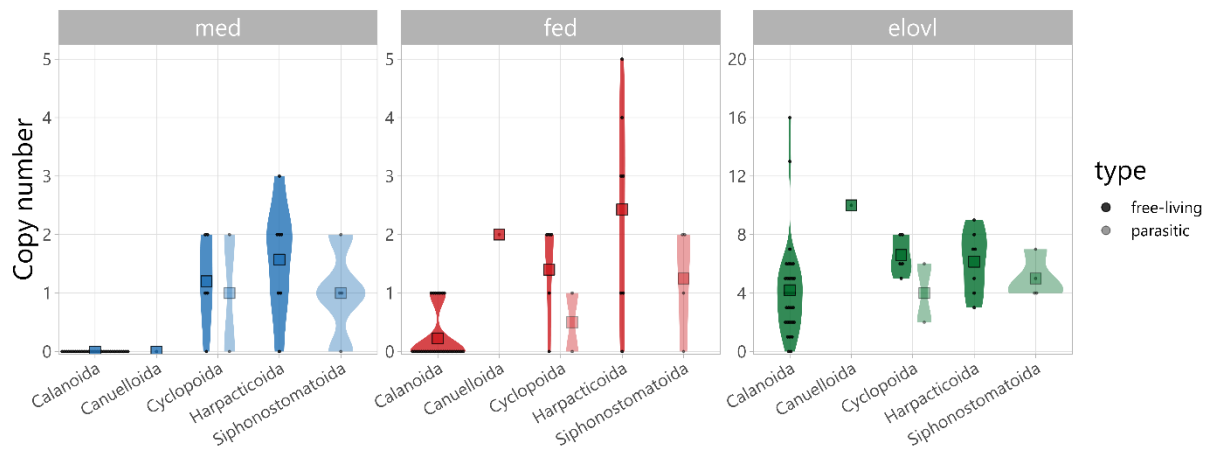
Supplementary Figure 4 Violin plots of copy number of methyl-end desaturases (med), front-end desaturases (fed) and elongases (elovl) per copepod species, with grey squares indicating the mean copy number of species with free-living or parasitic lifestyles per order.
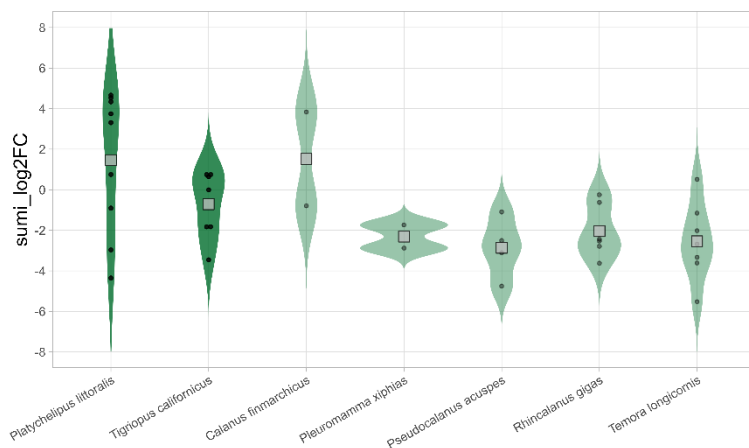
Supplementary Figure 5 Violin plots of log2 fold change (FC) of elongase gene expression (sum of isoform expression) relative to average expression per species. Grey squares indicate the mean expression over all elongases per species.
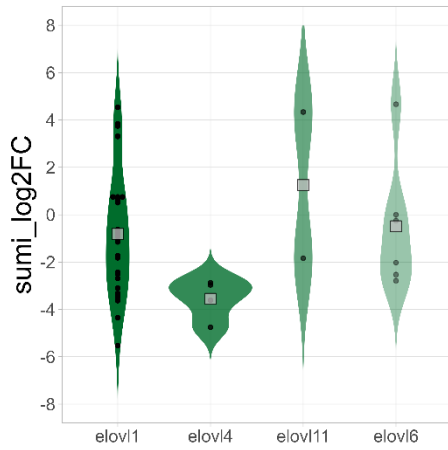
Supplementary Figure 6 Violin plots of log$_2$ fold change (FC) of elongase gene expression (sum of isoform expression) relative to average expression per species. Grey squares indicate the mean expression over all elongases per elongase subclade.
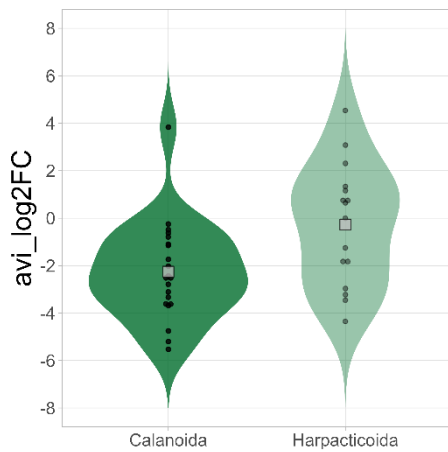
Supplementary Figure 7 Violin plots of log$_2$ fold change (FC) of elongase gene expression (average of isoform expression) relative to average expression per species. Grey squares indicate the mean expression over all elongases per order.
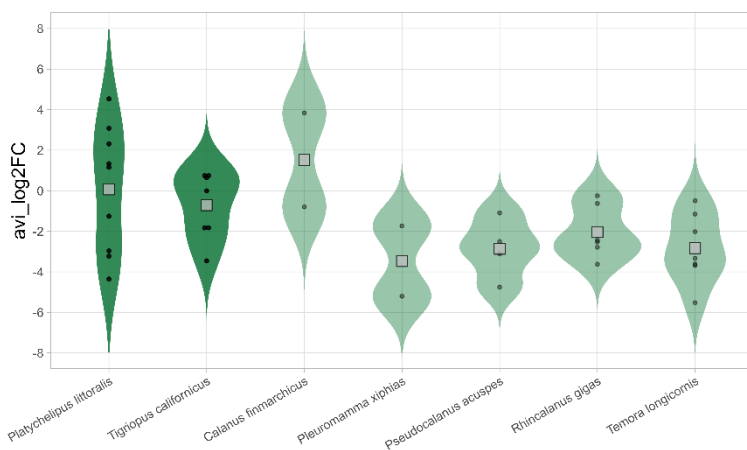
Supplementary Figure 8 Violin plots of log2 fold change (FC) of elongase gene expression (average of isoform expression) relative to average expression per species. Grey squares indicate the mean expression over all elongases per species.
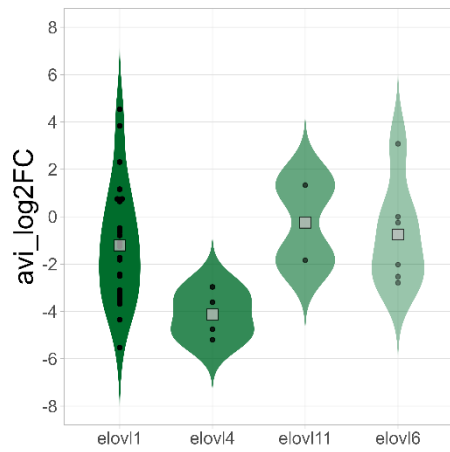
Supplementary Figure 9 Violin plots of log$_2$ fold change (FC) of elongase gene expression (average of isoform expression) relative to average expression per species. Grey squares indicate the mean expression over all elongases per elongase subclade.

Supplementary Figure 10 Violin plots of total GC content of methyl-end desaturases (med), front-end desaturases (fed), elongases (elovl) and core copepod genes. Grey squares indicate the mean content per gene family.

Fatty acid bioconversion in harpacticoid copepods in a changing environment: a transcriptomic approach

Jens Boyen[1], Patrick Fink[2,3,4], Christoph Mensens[1], Pascal I. Hablützel[5] and Marleen De Troch[1]

[1]Marine Biology, Department of Biology, Ghent University, Krijgslaan 281–S8, 9000 Gent, Belgium
[2]Cologne Biocenter, University of Cologne, Zülpicher Straße 47b, 50674 Köln, Germany
[3]Department Aquatic Ecosystem Analysis, and [4]Department River Ecology, Helmholtz Centre for Environmental Research, Brückstraße 3a, 39118 Magdeburg, Germany
[5]Flanders Marine Institute (VLIZ), Wandelaarkaai 7, 8400 Oostende, Belgium

JB, 0000-0001-5005-7724; PF, 0000-0002-5927-8977; PIH, 0000-0002-6739-4994; MD, 0000-0002-6800-0299

By 2100, global warming is predicted to significantly reduce the capacity of marine primary producers for long-chain polyunsaturated fatty acid (LC-PUFA) synthesis. Primary consumers such as harpacticoid copepods (Crustacea) might mitigate the resulting adverse effects on the food web by increased LC-PUFA bioconversion. Here, we present a high-quality de novo transcriptome assembly of the copepod *Platychelipus littoralis*, exposed to changes in both temperature (+3°C) and dietary LC-PUFA availability. Using this transcriptome, we detected multiple transcripts putatively coding for LC-PUFA-bioconverting front-end fatty acid (FA) desaturases and elongases, and performed phylogenetic analyses to identify their relationship with sequences of other (crustacean) taxa. While temperature affected the absolute FA concentrations in copepods, LC-PUFA levels remained unaltered even when copepods were fed an LC-PUFA-deficient diet. While this suggests plasticity of LC-PUFA bioconversion within *P. littoralis*, none of the putative front-end desaturase or elongase transcripts was differentially expressed under the applied treatments. Nevertheless, the transcriptome presented here provides a sound basis for future ecophysiological research on harpacticoid copepods.

This article is part of the theme issue 'The next horizons for lipids as 'trophic biomarkers': evidence and significance of consumer modification of dietary fatty acids'.

1. Introduction

Global climate change and the resulting increase in sea surface temperature (SST) over the past decades have profoundly impacted marine organisms and ecosystems [1]. This trend is likely to continue for the next decades, with a projected global mean SST increase of 2.73°C by 2090–2099 compared with 1990–1999 levels according to the business-as-usual Representative Concentration Pathway (RCP) 8.5 [2]. This temperature rise affects the physiological performance and fitness of marine organisms and consequently triggers adverse changes in marine ecosystems as well as the goods and services they provide [3]. Indeed, prominent climate-related shifts in nutrient and food supplies have already been observed in coastal areas worldwide [4,5]. At the base of marine food webs, global warming is predicted to strongly impair the production of key nutritional fatty acids (FAs) by primary producers such as diatoms. These microalgae, like all living organisms, alter their FA composition owing to temperature-dependent cell membrane restructuring, a process known as homeoviscous adaptation [6,7]. Specifically, proportions of long-chain polyunsaturated FAs (LC-PUFAs) such as eicosapentaenoic acid (20:5ω-3, EPA) and docosahexaenoic acid (22:6ω-3, DHA) in microalgae are

projected to decline strongly in the coming century [7]. While the impact varies between taxa and LC-PUFA compounds, overall a reduced LC-PUFA availability is expected for higher trophic levels, many of which strongly rely on dietary LC-PUFAs to fulfil their metabolic requirements [5,8]. Given the important role of LC-PUFAs in structural and physiological processes and as precursors for hormones and signalling molecules [9], a reduced dietary LC-PUFA availability impacts growth, fecundity and fitness of consumers [10,11]. The relative contributions of the direct (increased SST) and the indirect (decreased dietary LC-PUFA availability) effects of global warming on higher trophic levels remain understudied [12]. Growth and FA composition of European sea bass, *Dicentrarchus labrax*, and European abalone, *Haliotis tuberculata*, were shown to be impacted by temperature but only to a lesser extent by diet [13,14]. This lesser dependency on dietary LC-PUFAs was attributed to the endogenous bioconversion of short-chain saturated FAs into LC-PUFAs. Numerous animal species, many of which are aquatic invertebrates, are known to have at least some capacity for LC-PUFA bioconversion to cope with dietary changes [15,16]. Benthic harpacticoid copepods (Crustacea) are key primary consumers in (coastal) marine and estuarine sediments [17] and are known for their capacity for LC-PUFA bioconversion [18–21]. Coastal and estuarine environments undergo strong and stochastic fluctuations in temperature and nutrient availability. Harpacticoid copepods already adapted to such environments might be able to cope with the effects of global warming owing to their LC-PUFA bioconversion capacity [19]. However, the environmental shifts driving this bioconversion are yet poorly understood [16]. Insights into the molecular aspects of LC-PUFA bioconversion are therefore required to understand this pivotal toolbox in crustaceans.

Converting short-chain saturated FAs to LC-PUFAs is achieved by a series of desaturase and elongase enzymes, which introduce a double bond or add two C-atoms to the FA chain, respectively [16]. Desaturase enzymes themselves can be split up into front-end and methyl-end (or ω-end) desaturases, depending on the location of the double-bond insertion [22]. For crustaceans, genes encoding front-end desaturase and elongase enzymes have so far mainly been detected in decapods [23–27]. Interestingly, a recent study discovered genes encoding ω-end desaturases in many aquatic invertebrates, including some orders of copepods, challenging the current dogma that de novo PUFA biosynthesis occurs exclusively in marine microbes [28]. Nielsen *et al.* [29] identified putative front-end desaturase genes in multiple copepod species. Understanding how changes in diet or temperature affect those genes at the transcriptomic (i.e. gene expression) level has so far only been investigated in cyclopoid copepods [29,30]. Within the order Harpacticoida, transcriptomic resources are so far only available for *Tisbe holothuriae* (BioProject PRJEB23629) and three species of the *Tigriopus* genus [31–33].

Given the ecological importance of benthic harpacticoid copepods at the plant–animal interface, there is a need to better characterize their physiological response to global change at the molecular level. To do so, we investigated the transcriptomic and FA-metabolic response of the benthic harpacticoid copepod *Platychelipus littoralis* (Brady, 1880) towards both direct and indirect effects of global warming within a multifactorial setting, combining a change in SST (current versus future scenario) with a change in the dietary LC-PUFA availability (LC-PUFA-rich diatoms versus

LC-PUFA-deficient green algae as food sources [34,35]). *Platychelipus littoralis* is a common intertidal species in European estuaries, and temperature-dependent LC-PUFA turnover rates have been demonstrated previously using compound-specific stable isotope analysis, even within a short timeframe of 6 days [19]. This study presents a high-quality de novo transcriptome assembly from *P. littoralis* and reveals differentially expressed (DE) genes and FA profile changes in response to both diet and temperature. Furthermore, putative PUFA desaturase and elongase genes are identified and compared phylogenetically with genes of other crustacean species.

2. Material and methods

(a) Experiment

Nitzschia sp. (strain DCG0421, Bacillariophyceae) and *Dunaliella tertiolecta* (Chlorophyceae) were obtained from the BCCM/DCG Diatoms Collection (hosted by the Laboratory for Protistology & Aquatic Ecology, Ghent University) and the Aquaculture lab, Ghent University, respectively. Both algae were non-axenically cultured at $15 \pm 1°C$ in filtered (3 µm; Whatman Grade 6) and autoclaved natural seawater (FNSW), supplemented with Guillard's (F/2) Marine Water Enrichment solution (Sigma-Aldrich, Overijse, Belgium) and NutriBloom Plus (Necton) for *Nitzschia* sp. and *D. tertiolecta*, respectively. Food pellets were prepared through centrifugation and lyophilization and stored at −80°C. In parallel, quadruplicate algae samples were stored at −80°C for later FA analysis. Additional quadruplicate algae samples were filtered (Whatman GF/F) and lyophilized for particulate organic carbon determination using high-temperature combustion. *Platychelipus littoralis* specimens were collected from the top sediment layer of the Paulina intertidal mudflat (Westerscheldt estuary, The Netherlands; 51°21′ N, 3°43′ E) in August 2018. After sediment sieving (250 µm) and decantation, live adults were randomly collected using a glass Pasteur pipette under a stereo microscope. Copepods were cleaned by transferring them thrice to Petri dishes with clean FNSW and were kept in clean FNSW overnight to allow gut clearance prior to the start of the experiment.

The 10 day experiment had a fully crossed design with the factors temperature (19 ± 1 or $22 \pm 1°C$) and diet (*Nitzschia* sp. or *D. tertiolecta*). Temperature levels were based on the current mean August SST at the sampling location (data obtained from www.scheldemonitor.be) and a global SST increase of 3°C by 2100 as predicted by RCP8.5 [36]. The food sources were offered as pre-thawed, rehydrated food pellets at a concentration of 3.69 ± 0.22 mg C l^{-1} d^{-1} and 5.10 ± 1.16 mg C l^{-1} d^{-1} for *Nitzschia* sp. and *D. tertiolecta*, respectively, which are considered non-limiting food conditions [19,37]. The combinations of diet and temperature yielded four treatments, each consisting of Petri dishes (52 mm diameter) filled with 10 ml FNSW incubated in TC-175 incubators (Lovibond), with each treatment having four replicates for transcriptomic analysis (100 copepods per Petri dish) and three replicates for FA analysis (50 copepods per Petri dish). Each day, copepods were transferred to new units containing new temperature-equilibrated FNSW and were offered new pre-thawed food pellets. Triplicate copepod samples (50 specimens each) were collected from the field similarly to the specimens used in the experiment, and were stored at −80°C for analysis of the initial (field) FA composition. At the end of the experiment, mortality was assessed, and all live specimens were transferred to Petri dishes with clean FNSW to remove food particles from the cuticle. Copepods for transcriptomic analysis were immediately thereafter flash-frozen in liquid nitrogen and stored at −80°C. Copepods for FA analysis were stored overnight to allow gut clearance prior to storage at −80°C. Differences in

copepod survival between diet and temperature treatments and due to initial density (100 versus 50 copepods per Petri dish) were statistically assessed in R v. 3.6.0 [38] using a type II three-way ANOVA, a Tukey normalization transformation and a stepwise model selection by Akaike information criterion (AIC).

(b) Fatty acid analysis

FA methyl esters (FAMEs) were prepared from lyophilized algal and copepod samples using a direct transesterification procedure with 2.5% (v : v) sulfuric acid in methanol as described by De Troch *et al.* [18]. The internal standard (nonadecanoic acid, Sigma-Aldrich, 2.5 µg) was added prior to the procedure. FAMEs were extracted twice with hexane. FA composition analysis was carried out with a gas chromatograph (GC; HP 7890B, Agilent Technologies, Diegem, Belgium) equipped with a flame ionization detector (FID) and connected to an Agilent 5977A Mass Selective Detector (MSD; Agilent Technologies, Diegem, Belgium). The GC was further equipped with a PTV injector (CIS-4, Gerstel, Mülheim an der Ruhr, Germany). An HP88 fused-silica capillary column (60 m × 0.25 mm × 0.20 µm film thickness, Agilent Technologies) was used at a constant helium flow rate (2 ml min^{-1}). The injected sample (2 µl) was split equally between the MS and FID using an Agilent Capillary Flow Technology Splitter. The oven temperature programme was as follows: at the time of sample injection, the column temperature was 50°C for 2 min, then it was gradually increased at 10°C min^{-1} to 150°C, followed by a second increase at 2°C min^{-1} to 230°C. The injector temperature was held at 30°C for 6 s and then ramped at 10°C s^{-1} to 250°C and held for 10 min. The transfer line for the column was maintained at 250°C. The quadrupole and ion source temperatures were 150 and 230°C, respectively. Mass spectra were recorded at 70 eV ionization voltage over the mass range of 50–550 m/z units.

Data analysis was done with MassHunter Quantitative Analysis software (Agilent Technologies). The signal obtained with the FID detector was used to generate quantitative data of all compounds. Peaks were identified based on their retention times, compared with external standards as a reference (Supelco 37 Component FAME Mix, Sigma-Aldrich) and by the mass spectra obtained with the MS detector. FAME quantification was based on the area of the internal standard and on the conversion of peak areas to the weight of the FA by a theoretical response factor for each FA [39,40]. Statistical analyses were performed in R v. 3.6.0 [38]. The Shapiro–Wilk test and Levene's test were used to check for normal distribution and homoscedasticity. The non-parametric Wilcoxon rank-sum test was used to assess for the difference in absolute and relative concentration of the individual FA compounds between field and incubated copepods. The type II two-way ANOVA and the non-parametric Scheirer–Ray–Hare test were used to test for the effects of diet and temperature on the absolute and relative concentration for each FA compound. Multivariate statistics were performed to test the effects of incubation, diet and temperature on the overall FA composition. Non-metric multidimensional scaling (nMDS) with FAs as correlating vectors and PERMANOVA were performed after square root transformation (Bray–Curtis dissimilarity) using all FAs with mean relative concentration greater than 1%. The mean values are presented with standard deviation (±s.d.). The FA short-hand notation $A{:}B\omega\text{-}X$ is used, where A represents the number of carbon atoms, B the number of double bonds and X the position of the first double bond counting from the terminal methyl group.

(c) Transcriptomic analysis

Total RNA from 45 to 97 pooled *P. littoralis* specimens per sample was isolated using the RNeasy Plus Micro Kit (QIAGEN) following an improved protocol (see electronic supplementary material, Methods). Total RNA was extracted from all four replicates from

the two *Nitzschia* sp. treatments, but owing to high copepod mortality, only three out of four replicates from each of the two *D. tertiolecta* treatments could be used. Total RNA quality and quantity were assessed by both a NanoDrop 2000 spectrophotometer (Thermo Scientific) and a 2100 Bioanalyzer (Agilent Technologies). cDNA libraries were constructed using the Illumina TruSeq Stranded mRNA kit and samples were run on an Illumina HiSeq 4000 platform with 75 bp paired-end reads at the Cologne Centre for Genomics (University of Cologne).

Read quality was assessed using FASTQC v. 0.11.7. The reads were quality-trimmed and adapter-clipped using Trimmomatic [41], and the raw read files are available at the NCBI Short Read Archive under BioProject PRJNA575120. The transcriptome was assembled de novo using Trinity v. 2.8.4 [42] including *in silico* read normalization. Multiple tools were used to assess assembly quality. First, the percentages of reads properly represented in the transcriptome assembly were calculated for each sample using Bowtie2 v. 2.3.4 [43]. Second, the transcripts were aligned against proteins from the Swiss-Prot database (16 February 2019) using blastx (cut-off of 1×10^{-20}) and the number of unique proteins represented with full-length or nearly full length transcripts (greater than 90%) was determined. Third, we performed Benchmarking Universal Single-Copy Orthologs (BUSCO) v. 3.1.0 analysis using the arthropod dataset to estimate transcriptome assembly and annotation completeness [44]. Lastly, both the N50 statistic and the E90N50 statistic (using only the set of transcripts representing 90% of the total expression data) were determined based on transcript abundance estimation using salmon v. 0.12.0 following the quasi-mapping procedure [45]. The transcripts were annotated using Trinotate [46], an open-source toolkit that compiles several analyses such as coding region prediction using TransDecoder (http://transdecoder.github.io), protein homology identification using BLAST and the Swiss-Prot database, protein domain identification using HMMER/Pfam [47,48] and gene annotation using EggNOG, KEGG and Gene Ontology (GO) database resources [49–51]. The transcriptome (GHXK00000000) is available at the NCBI TSA Database under BioProject PRJNA575120. Transcript abundance per sample was estimated using Salmon v. 0.12.0 following the quasi-mapping procedure [45]. The R v. 3.0.6 [38] package edgeR v. 3.26.4 [52] was used to identify significantly DE transcripts. Transcripts with greater than 5 counts per million in at least three samples were retained. TMM normalization was applied [53], and differential expression was determined using a gene-wise negative binomial generalized linear model with quasi-likelihood F-tests (glmQLFit) with diet, temperature and the diet × temperature interaction as factors. Transcripts with an expression fold change ≥2 at a false discovery rate ≤0.05 (Benjamini–Hochberg method [54]) were considered significantly DE. The R package topGO v. 2.36.0 [55] was used to test for enriched GO terms for both the diet and the temperature treatment. The enrichment tests were run using the weight01 algorithm and the Fisher's exact test statistic, with GO terms considered significantly enriched when $p \le 0.01$.

A transcript was categorized as encoding a front-end desaturase when it contained the two essential Pfam domains *Cytb5* (PF00173) and *FA_desaturase* (PF00487), three diagnostic histidine boxes (HXXXH, HXXXHH and QXXHH) and a haem-binding motif (HPGG) [22]. A transcript was categorized as encoding an elongase when it contained the Pfam domain *ELO* (PF01151) and the diagnostic histidine box (HXXHH) [22]. Nucleotide coding sequences of the transcripts were trimmed to those conserved regions and aligned using MAFFT v. 7.452 [56] with default parameters. Sequences that aligned badly, contained long indels or were identical to other sequences after trimming were removed. Additional well-annotated (sometimes functionally characterized) crustacean sequences found to be most closely related to each of the *P. littoralis* transcripts through blastx were added to the alignment. We also included desaturase and elongase sequences from

the hydrozoan *Hydra vulgaris*, copepod front-end desaturase sequences from Nielsen *et al.* [29] and human elongase sequences Elovl1 to Elovl7. For each gene family, an unrooted maximum-likelihood phylogenetic tree was built using RAxML v. 8.2.4 [57] with a general time reversible model of nucleotide substitution and CAT approximation. The final tree was rooted (midpoint), visualized and edited with FigTree v. 1.4.3 (http://tree.bio.ed.ac.uk/software/figtree).

3. Results

The two algal diets differed in their FA composition (electronic supplementary material, table S1). EPA and DHA were highly abundant in *Nitzschia* sp. (26.85 ± 2.26 and 5.68 ± 0.29%) while not detected in *D. tertiolecta*. On the contrary, *D. tertiolecta* exhibited a high content of α-linolenic acid (ALA, 18:3w3; 43.77 ± 1.29%) compared with *Nitzschia* sp. (0.05 ± 0.03%). The mean copepod survival after 10 days was 75.46 ± 27.79%. Besides high variation between replicates, no significant effects of diet, temperature, initial density or interactions on copepod survival were detected (three-way ANOVA; AIC = 1696.8; $F_{7,20} = 1.382$; $p = 0.2665$).

(a) Changes in fatty acid content and composition

At the end of the experiment, total FA content in copepods in the treatments (149.47 ± 21.37 ng copepod^{-1}) declined compared with control values from the field (197.29 ± 4.50 ng copepod^{-1}) ($p = 4.4 \times 10^{-3}$). The overall FA composition of the field copepods was significantly distinct from the ones of the incubated copepods ($F_{1,14} = 10.83$; $p = 3.0 \times 10^{-3}$), mainly owing to lower PUFA concentrations in the latter (figure 1). In the experiment, the overall copepod FA composition was significantly affected by temperature ($F_{1,11} = 4.30$; $p = 0.015$) but not by diet ($F_{1,11} = 1.83$; $p = 0.13$, no interaction), which was primarily correlated with short-chain, saturated FAs (figure 1). Temperature but not diet significantly affected total FA content, which was lower at 22°C compared with 19°C (figure 2; electronic supplementary material, table S2). Temperature but not diet also significantly affected absolute concentrations of *anteiso*-15:0, 15:0, 16:0, 18:1ω-7, 24:0, DHA and total monounsaturated fatty acid concentration (ΣMUFA), which were all lower at 22°C (electronic supplementary material, table S2). The diet only significantly affected the absolute ALA concentration, with copepods fed the ALA-rich diet *D. tertiolecta* having a higher absolute ALA concentration compared with copepods fed with *Nitzschia* sp. (figure 2; electronic supplementary material, table S2). A significant temperature × diet interaction was found for oleic acid (OA, 18:1ω-9). The absolute OA concentration was higher at 19°C when copepods were fed *Nitzschia* sp., an effect that reversed (higher at 22°C) when fed *D. tertiolecta* (figure 2; electronic supplementary material, table S2). ΣPUFA, total saturated fatty acid concentration ΣSFA or important LC-PUFAs such as EPA and arachidonic acid (ARA, 20:4ω-6) were affected by neither temperature nor diet. Despite the absence of EPA and DHA in *D. tertiolecta*, copepods fed this diet were able to maintain similar relative EPA and DHA concentrations to those in copepods fed with *Nitzschia* sp. (electronic supplementary material, table S3).

(b) Transcriptome assembly and annotation

We sequenced 14 *P. littoralis* samples, resulting in nearly 400 million paired-end Illumina reads. After quality filtering, an
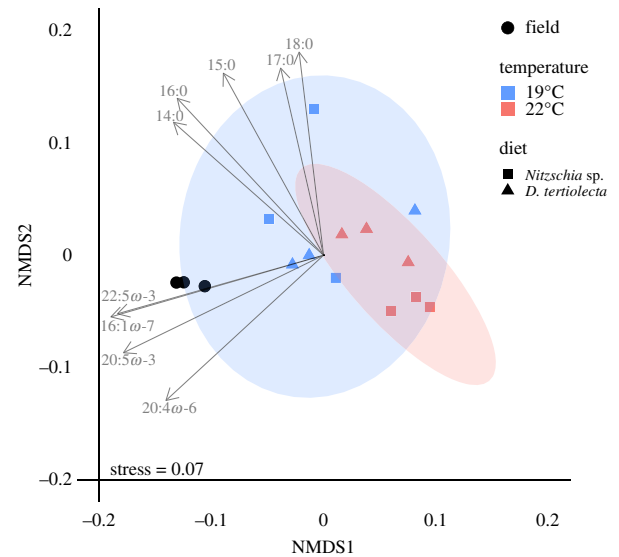
Figure 1. nMDS ordination using absolute fatty acid (FA) concentrations (ng copepod^{-1}) of the four treatments and field samples. Ellipses indicate 95% confidence levels of the temperature factor. Vectors were plotted for FAs with $r^2 > 0.7$.

assembly was generated consisting of 287 753 transcript contigs (table 1). 97.80 ± 0.44% of the reads of each sample mapped back to the assembly, with 95.95 ± 0.68% mapping as properly paired reads (aligning concordantly at least once). A total of 7088 proteins from the Swiss-Prot database were represented by transcripts with greater than 90% alignment coverage. 97.9% of the BUSCO arthropod genes were represented by at least one complete copy (single: 26.1%, duplicated: 71.8%, fragmented: 1.1%). The N50 and the E90N50 metrics were 1360 and 2657, respectively, and 90% of the total expression data was represented by 35 540 transcripts. TransDecoder identified 296 142 putative open reading frame (ORF) coding regions within the assembly, suggesting at least some transcripts contain multiple coding regions (table 1). About one-quarter of those putative ORFs were annotated with GO (24.9%), KEGG (22.8%) or EggNOG terms (16.0%) or were found to contain at least one Pfam protein family domain (29.5%, table 1).

(c) Differential expression and gene set enrichment analysis

After filtering out low expression transcripts, 24 202 transcripts were retained for DE analysis. Seven transcripts were DE between the two diet treatments (figure 3a,b; electronic supplementary material, table S4). Four of them were upregulated when copepods were fed with *Nitzschia* sp., while three were upregulated when copepods were fed with *D. tertiolecta*. Twenty-nine transcripts were DE between the two temperature treatments (figure 3c,d; electronic supplementary material, table S4). Five transcripts were upregulated at 19°C, while 24 were upregulated at 22°C. Four transcripts were DE in both treatments. All but two DE transcripts contained at least one putative ORF. Gene set enrichment analysis using topGO identified 22 and 30 enriched GO terms under the diet and temperature treatment, respectively (electronic supplementary material, table S5). Notable enriched functions in both treatments were related to microtubuli and cilia organization (electronic supplementary material, table S5). Certain terms detected in both treatments and primarily related to the biological process 'glycerophospholipid biosynthetic process'
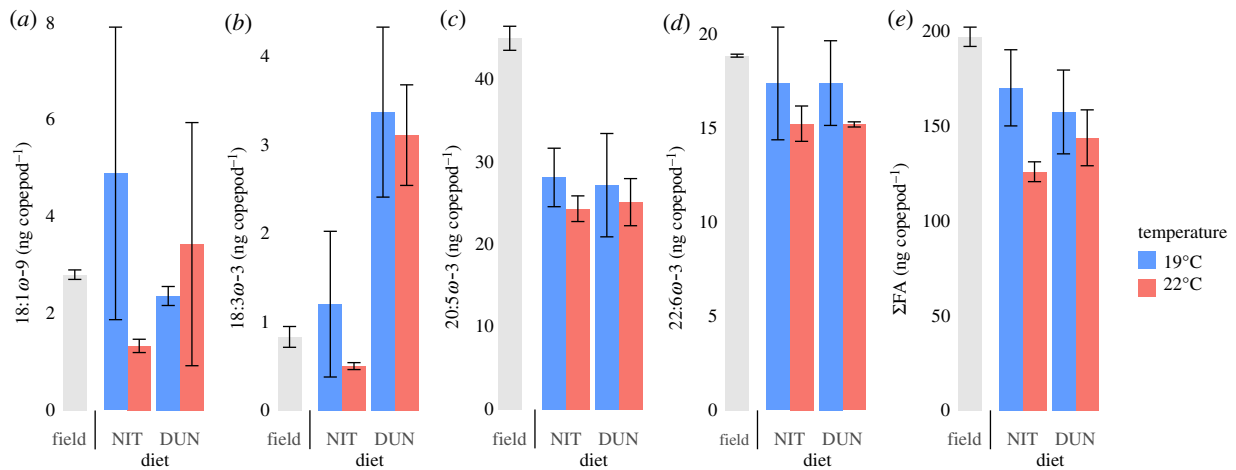
Figure 2. Mean absolute fatty acid concentration (ng copepod^{-1} ± s.d.; $n = 3$) of *P. littoralis* before (field) and after 10 days of incubation with *Nitzschia* sp. (NIT) or *D. tertiolecta* (DUN). (a) OA (18:1ω-9), (b) ALA (18:3ω-3), (c) EPA (20:6ω-3), (d) DHA (22:6ω-3) and (e) ΣFA (total fatty acid concentration).

Table 1. Assembly and annotation characteristics of the *P. littoralis* transcriptome.

assembly and annotation characteristics	value
assembly	
number of raw reads	395 794 835
average number of reads per sample	28 271 060
number of assembled bases (bp)	207 643 686
number of assembled contigs	287 753
average contig length (bp)	721.6
median contig length (bp)	343
GC content (%)	47.54
annotation	
number of ORFs	296 142
ORFs with GO terms	73 836
ORFs with KEGG terms	67 484
ORFs with EggNOG terms	47 358
ORFs with Pfam protein family	87 319

and the molecular function 'transferring acyl groups' (electronic supplementary material, table S5) were all attributed to the transcript *Plit_DN1805_c0_g1_i18*, which was down-regulated when copepods were fed *D. tertiolecta* (compared with *Nitzschia* sp.) and upregulated at 22°C (compared with 19°C, figure 3; electronic supplementary material, tables S4 and S5). This transcript contains six ORFS which, according to blastx, match against the chicken protein acetoacetyl-CoA synthetase and the human protein glycerol-3-phosphate acyltransferase, both involved in phospholipid metabolism.

(d) Identification and phylogenetic analysis of desaturase and elongase genes

Respectively, 19 and 17 unique putative front-end desaturase and elongase sequences were identified in the *P. littoralis* transcriptome since they all exhibited diagnostic characteristics and aligned properly to other sequences. A maximum-likelihood phylogenetic tree was built for each gene family

(figure 4). Concerning the front-end desaturase sequences, we identified two distinct clades with high bootstrap support (figure 4a). The first clade contained five front-end desaturases from *P. littoralis* as well as from all other crustacean taxa. While one transcript is related to the functionally characterized Δ6 front-end desaturase sequence from the decapod *Macrobrachium nipponense*, the phylogenetic relationship of the other *P. littoralis* transcripts as a sister clade of the sequences of other copepod species is poorly supported (bootstrap value less than 50). The second clade contained only sequences from *P. littoralis* and one sequence of *H. vulgaris* in a basal position. The phylogenetic analysis of elongase transcripts produced multiple subclades (figure 4b). Two *P. littoralis* sequences and one *Daphnia magna* elongase sequence formed a clade with the human Elovl3 and Elovl6, classifying them as putatively Elovl6/Elovl3-like. One *P. littoralis* sequence, one *D. magna* sequence and one *H. vulgaris* sequence were found to be closely related with the human Elovl4 and the Elovl4-like sequence from *Scylla paramamosain*, classifying them as putatively Elovl4-like. Four *P. littoralis* sequences and sequences from *D. magna*, *Caligus rogercresseyi* and *Lepeophtheirus salmonis* formed a subclade with the functionally characterized Elovl7 sequence from *Scylla olivacea*, which is also a sister clade with the human Elovl7 and Elovl1, classifying those as putatively Elovl7/Elovl1-like. None of the *P. littoralis* sequences formed a clade with human Elovl5 and Elovl2, while 10 *P. littoralis* sequences were not related with any of the sequences included in the analysis (figure 4b).

4. Discussion

Several earlier studies indicated that harpacticoid copepods have a strong capacity for endogenous LC-PUFA bioconversion [18,19,21]. Meanwhile, our knowledge on the molecular pathways underlying this process is still limited [16]. Considering a global SST increase and a decline in LC-PUFA production by primary consumers within this century [7], LC-PUFA bioconversion potentially plays a unique role for primary producers to physiologically mitigate the negative effects of climate change. Prior to our experiment, the algae were lyophilized to prevent temperature-dependent growth. Previous research found that harpacticoids ingest lyophilized algae, albeit at a lower assimilation rate than live algae [58]. We showed that when fed with the LC-PUFA-deficient
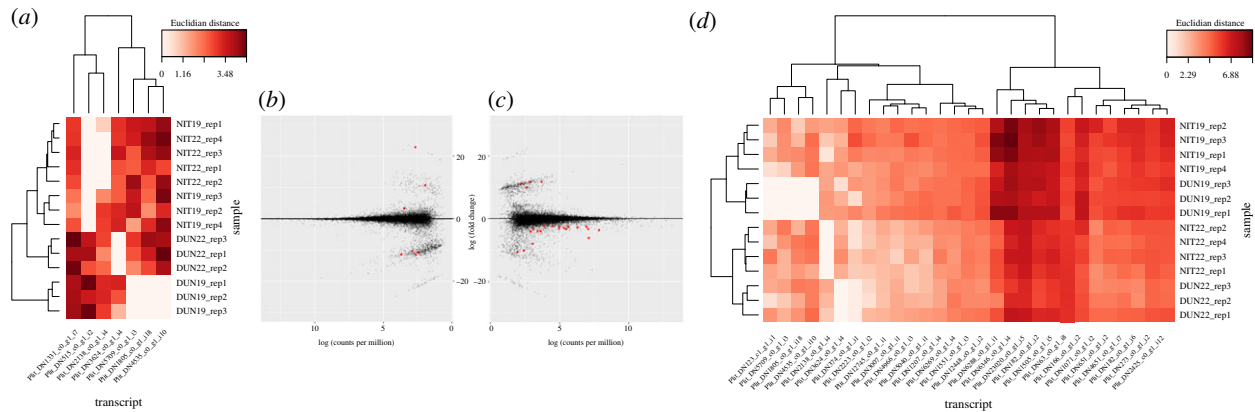
Figure 3. Heatmaps (*a,d*) and MA plots (*b,c*). MA plots show log-fold change per transcript against its mean expression (in log (counts per million)) with diet (*b*) and temperature (*c*) as contrast. Red dots indicate significantly DE transcripts (i.e. log-fold change ≥ 1 and false discovery rate ≤ 0.05). Black dots indicate non-significantly DE transcripts. Heatmaps show relative expression level (Euclidean distance) of each significantly DE transcript in each sample with diet (*a*) and temperature (*d*) as contrast. Transcripts and samples are hierarchically clustered.

D. tertiolecta, *P. littoralis* had the physiological plasticity to maintain LC-PUFA levels relatively similar to copepods fed with *Nitzschia* sp. The high abundance of ALA in *D. tertiolecta*-fed *P. littoralis* indicates that the copepods efficiently ingested lyophilized *D. tertiolecta*. This likely counteracted the lack of LC-PUFA, since *P. littoralis* is able to use ALA as a precursor for desaturation and elongation towards EPA and DHA [16]. *Dunaliella tertiolecta*-derived 16:4ω-3 and 16:3ω-3 and *Nitzschia* sp.-derived 16:1ω-7 were not sustained in *P. littoralis* (electronic supplementary material, tables S2 and S3). Either way the lyophilized algae were not as efficiently assimilated as previously detected, or these compounds were bioconverted to other FAs or metabolized to provide energy. In contrast with diet, an increased SST of 3°C reduced the absolute total FA content, suggesting an increased use of storage FAs as energy providers [9]. Some FA compounds showed extensive variability between replicates, which can be explained by the low sample volume or the low number of replicates. While the absolute concentrations of DHA and several monounsaturated FAs decreased, the relative concentrations of LC-PUFAs remained unaltered. Homeoviscous adaptation as a possible explanation cannot be confirmed nor rejected, as we do not have any information on membrane FAs specifically [6]. Decreased DHA concentrations can alternatively be linked to an increased stress response at the upper limits of *P. littoralis*'s thermal range. In a previous experiment, increased temperatures indeed stimulated ARA and EPA bioconversion to allow enhanced eicosanoid biosynthesis in *P. littoralis* [19]. However, comparison with the current results should be done with care since the previous experiment included an ecologically improbable SST increase of 10°C. These results thus clearly illustrate the importance of LC-PUFA bioconversion as a mechanism to cope with the direct and indirect effects of global warming. As such, fluctuations in temperature or food quality might be relatively less detrimental to *P. littoralis*, and its historical adaptation to a variable environment could have given this species useful adaptations to persist under future environmental changes.

To investigate the molecular mechanisms behind the FA metabolism of *P. littoralis*, we performed a de novo assembly of its transcriptome. The high N50 metric (1360) and high number of complete arthropod BUSCO genes (97.9%) compared with other copepod transcriptomes lead us to state that the transcriptome presented here is of high quality and can

be confidently used for future studies [59]. In our differential gene expression analysis, 7 and 29 transcripts were found to be DE in the dietary and temperature contrasts, respectively. These low numbers can be attributed to the employed filtering threshold, or to the low number of replicates used, which reduced the power to detect significantly DE genes. Low numbers of DE genes were found in other transcriptomic studies on copepods as well [59]. A gene set enrichment analysis identified GO terms mainly related to cytoskeleton organization and phospholipid biosynthesis. Possible relations between temperature or dietary LC-PUFA availability and the cytoskeleton have been identified in vertebrates [60,61], yet further investigations on invertebrates are needed. GO terms related to phospholipid biosynthesis were all attributed to one transcript which was downregulated when *P. littoralis* was fed *D. tertiolecta* and upregulated at 22°C, respectively. A temperature-driven reduction of membrane-bound phospholipid biosynthesis seems plausible [6] and is in line with both our own and previous findings [19] at the FA level. It may be interpreted as increased mobilization of FAs for energy provision. The previous study, however, did not find membrane FA depletion when *P. littoralis* was fed the LC-PUFA-deficient diet *D. tertiolecta* [19], thereby contradicting our findings at the transcriptional level. As we sequenced bulk RNA from a pool of specimens, we were unable to determine whether some of the DE genes are tissue-specific regulated or not. Importantly, we identified a high number of transcripts putatively coding for front-end desaturases and elongases. While we are aware that a de novo assembly may artificially introduce an inflated number of contigs [62], most sequences were sufficiently distinct to confidently state that they belong to different paralogous genes. It is indeed known that gene duplication is an important driver of the diversity of desaturase and elongase genes [63,64]. We would, therefore, like to advance the hypothesis that an elevated front-end desaturase and elongase gene duplication frequency in harpacticoid copepods could be the key element for their high LC-PUFA bioconversion capacity. However, more exhaustive phylogenetic analyses are necessary to test this hypothesis. Our current analyses already show that putative front-end desaturases from *P. littoralis* grouped into two distinct phylogenetic clades, with one group of sequences clustering with other copepod desaturase sequences and a Δ6 desaturase sequence from *M. nipponense*, and another group of sequences clustering with a desaturase sequence from
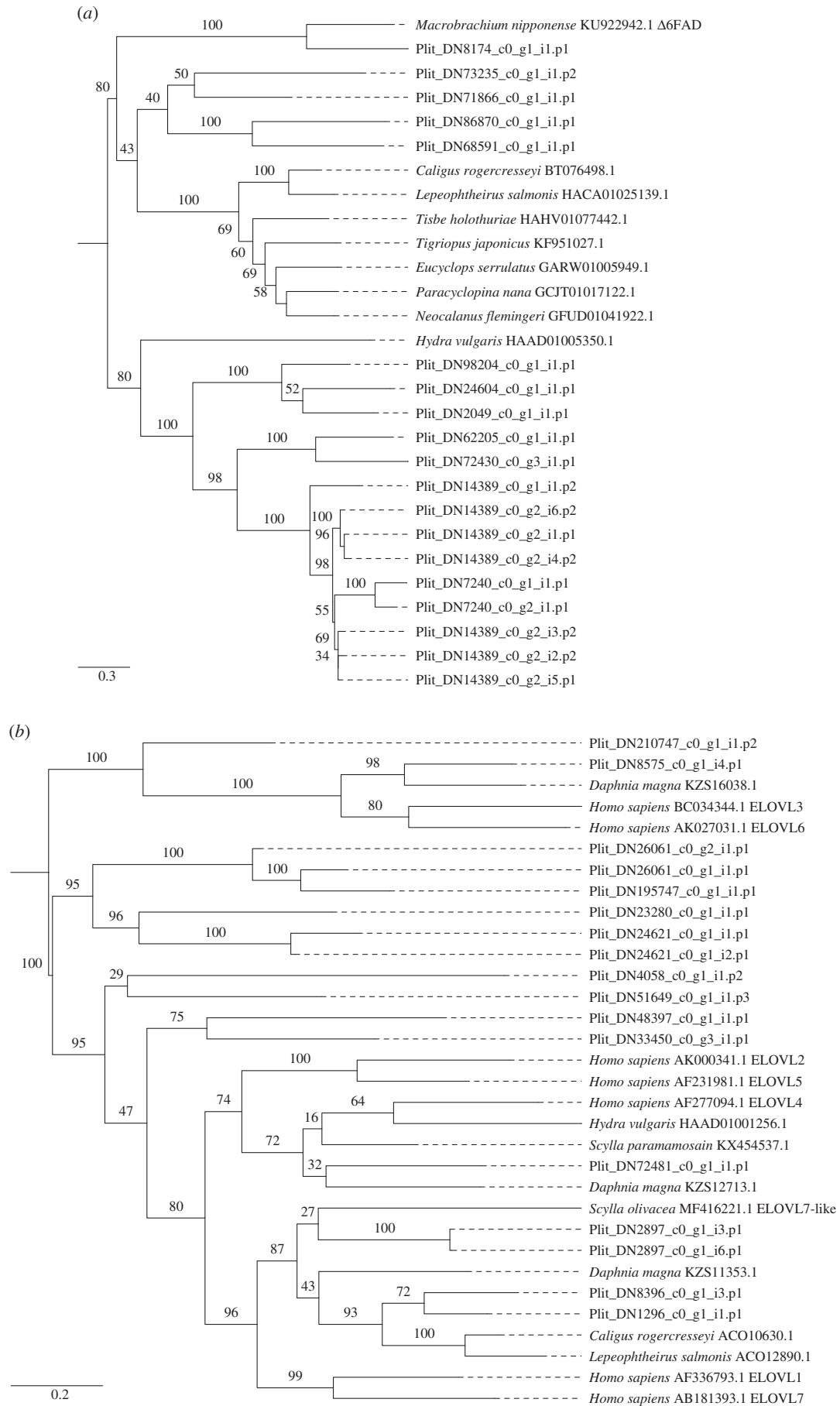
Figure 4. Maximum-likelihood phylogenetic trees with midpoint root comparing trimmed nucleotide sequences of putative front-end desaturase (*a*) and elongase (*b*) transcripts of *P. littoralis* with sequences of other crustaceans, *Homo sapiens* and the hydrozoan *H. vulgaris*. Values above branches show bootstrap support after 100 RAxML iterations. Gene identification, when already functionally characterized, is shown after each accession number.

H. vulgaris (figure 4*a*). Corroborating the results of a previous study, copepod front-end desaturases grouped together in one monophyletic clade; however, none of the *P. littoralis* sequences was found to cluster within this clade, but rather grouped separately as a sister clade. Including more functionally characterized front-end desaturases from other crustacean species might benefit our analyses, but these are so far not available [16]. By contrast, the maximum-likelihood tree of the elongase sequences corresponds more to earlier studies [27] (figure 4*b*). While 10 *P. littoralis* sequences did not cluster with any of the additional sequences, we were able to assign seven *P. littoralis* sequences as well as seven other crustacean sequences to one of the three subclades Elovl3/Elvol6-like, Elovl4-like or Elovl1/Elovl7-like. Overall, our phylogenetic analyses of the front-end desaturase and elongase transcripts of *P. littoralis* provide a first glimpse at the high diversity of these genes and serve as a starting point to better comprehend the evolutionary history of LC-PUFA bioconversion within harpacticoid copepods. Interestingly, none of the identified transcripts encoding a front-end desaturase or elongase was found to be DE owing to temperature or dietary LC-PUFA availability. This contradicts the stressor-driven LC-PUFA bioconversion evidenced at the FA level. The majority of those transcripts (31 out of 36) were classified as lowly expressed (less than 5 counts per million per sample) and were therefore excluded from the DE analysis. Additionally, the applied correction for multiple testing might have resulted in potentially significantly DE transcripts going undetected [54]. A more gene-specific approach such as reverse transcriptase quantitative polymerase chain reaction (RT-qPCR) [65] might be better suited to analyse expression of LC-PUFA bioconversion genes following direct and indirect effects of global warming.

In conclusion, we combined two approaches—FA profiling and de novo transcriptome assembly—to expand the current knowledge on LC-PUFA bioconversion in harpacticoids. This study shows that LC-PUFA levels in *P. littoralis* remained high even on a LC-PUFA-deficient diet, yet transcripts putatively encoding for front-end desaturases and elongases were not found to be upregulated. The molecular pathways underlying this mechanism are thus more complex than previously assumed (also demonstrated by the recent discovery of *ω*-end desaturases in multiple aquatic invertebrates [28]) and might not happen at the gene expression level. The de novo transcriptome of a non-model harpacticoid copepod presented here lays the foundation for more targeted ecophysiological research to investigate the molecular basis of adaption to cope with the effects of global change.

References

1. Doney SC *et al.* 2012 Climate change impacts on marine ecosystems. *Annu. Rev. Mar. Sci.* **4**, 11–37. (doi:10.1146/annurev-marine-041911-111611)

2. Bopp L *et al.* 2013 Multiple stressors of ocean ecosystems in the 21st century: projections with CMIP5 models. *Biogeosciences* **10**, 6225–6245. (doi:10.5194/bg-10-6225-2013)

3. Gattuso J-P *et al.* 2015 Contrasting futures for ocean and society from different anthropogenic CO$_2$ emissions scenarios. *Science* **349**, aac4722. (doi:10.1126/science.aac4722)

4. Drinkwater KF, Beaugrand G, Kaeriyama M, Kim S, Ottersen G, Perry RI, Polovina JJ, Takasuka A. 2010 On the processes linking climate to ecosystem changes. *J. Mar. Syst.* **79**, 374–388. (doi:10.1016/j.jmarsys.2008.12.014)

5. Litzow MA, Bailey KM, Prahl FG, Heintz R. 2006 Climate regime shifts and reorganization of fish communities: the essential fatty acid limitation hypothesis. *Mar. Ecol. Prog. Ser.* **315**, 1–11. (doi:10.3354/meps315001)

6. Sinensky M. 1974 Homeoviscous adaptation: a homeostatic process that regulates the viscosity of membrane lipids in *Escherichia coli*. *Proc. Natl Acad. Sci. USA* **71**, 522–525. (doi:10.1073/pnas.71.2.522)

7. Hixson SM, Arts MT. 2016 Climate warming is predicted to reduce omega-3, long-chain, polyunsaturated fatty acid production in phytoplankton. *Glob. Change Biol.* **22**, 2744–2755. (doi:10.1111/gcb.13295)

8. Colombo SM, Rodgers TFM, Diamond ML, Bazinet RP, Arts MT. 2020 Projected declines in global DHA availability for human consumption as a result of global warming. *Ambio* **49**, 865–880. (doi:10.1007/s13280-019-01234-6)

9. Bell MV, Tocher DR. 2009 Biosynthesis of polyunsaturated fatty acids in aquatic ecosystems: general pathways and new directions. In *Lipids in aquatic ecosystems* (eds M Kainz, MT Brett, MT Arts), pp. 211–236. Dordrecht, The Netherlands: Springer.

10. Müller-Navarra DC, Brett MT, Park S, Chandra S, Ballantyne AP, Zorita E, Goldman CR. 2004 Unsaturated fatty acid content in seston and trophodynamic coupling in lakes. *Nature* **427**, 69–72. (doi:10.1038/nature02210)

11. Caramujo MJ, Boschker HTS, Admiraal W. 2008 Fatty acid profiles of algae mark the development and composition of harpacticoid copepods. *Freshw. Biol.* **53**, 77–90. (doi:10.1111/j.1365-2427.2007.01868.x)

12. von Elert E, Fink P. 2018 Global warming: testing for direct and indirect effects of temperature at the interface of primary producers and herbivores is required. *Front. Ecol. Evol.* **6**, 87. (doi:10.3389/fevo.2018.00087)

13. Gourtay C, Chabot D, Audet C, Le Delliou H, Quazuguel P, Claireaux G, Zambonino-Infante J. 2018 Will global warming affect the functional need for essential fatty acids in juvenile sea bass (*Dicentrarchus labrax*)? A first overview of the consequences of lower availability of nutritional fatty acids on growth performance. *Mar. Biol.* **165**, 143. (doi:10.1007/s00227-018-3402-3)

14. Hernández J, de la Parra AM, Lastra M, Viana MT. 2013 Effect of lipid composition of diets and environmental temperature on the performance and fatty acid composition of juvenile European abalone (*Haliotis tuberculata* L. 1758). *Aquaculture* **412–413**, 34–40. (doi:10.1016/j.aquaculture.2013.07.005)

15. Monroig Ó, Tocher DR, Navarro JC. 2013 Biosynthesis of polyunsaturated fatty acids in marine invertebrates: recent advances in molecular mechanisms. *Mar. Drugs* **11**, 3998–4018. (doi:10.3390/md11103998)

16. Monroig Ó, Kabeya N. 2018 Desaturases and elongases involved in polyunsaturated fatty acid biosynthesis in aquatic invertebrates:

a comprehensive review. *Fish. Sci.* **84**, 911–928. (doi:10.1007/s12562-018-1254-x)

17. Hicks GR, Coull BC. 1983 The ecology of marine meiobenthic harpacticoid copepods. *Oceanogr. Mar. Biol. Annu. Rev.* **21**, 67–175.

18. De Troch M, Boeckx P, Cnudde C, Van Gansbeke D, Vanreusel A, Vincx M, Caramujo MJ. 2012 Bioconversion of fatty acids at the basis of marine food webs: insights from a compound-specific stable isotope analysis. *Mar. Ecol. Prog. Ser.* **465**, 53–67. (doi:10.3354/meps09920)

19. Werbrouck E, Bodé S, Van Gansbeke D, Vanreusel A, De Troch M. 2017 Fatty acid recovery after starvation: insights into the fatty acid conversion capabilities of a benthic copepod (Copepoda, Harpacticoida). *Mar. Biol.* **164**, 151. (doi:10.1007/s00227-017-3181-2)

20. Norsker NH, Støttrup JG. 1994 The importance of dietary HUFAs for fecundity and HUFA content in the harpacticoid, *Tisbe holothuriae* Humes. *Aquaculture* **125**, 155–166. (doi:10.1016/0044-8486(94)90292-5)

21. Nanton DA, Castell JD. 1998 The effects of dietary fatty acids on the fatty acid composition of the harpacticoid copepod, *Tisbe* sp., for use as a live food for marine fish larvae. *Aquaculture* **163**, 251–261. (doi:10.1016/s0044-8486(98)00236-1)

22. Hashimoto K, Yoshizawa AC, Okuda S, Kuma K, Goto S, Kanehisa M. 2008 The repertoire of desaturases and elongases reveals fatty acid variations in 56 eukaryotic genomes. *J. Lipid Res.* **49**, 183–191. (doi:10.1194/jlr.m700377-jlr200)

23. Yang Z, Guo Z, Ji L, Zeng Q, Wang Y, Yang X, Cheng Y. 2013 Cloning and tissue distribution of a fatty acyl Δ6-desaturase-like gene and effects of dietary lipid levels on its expression in the hepatopancreas of Chinese mitten crab (*Eriocheir sinensis*). *Comp. Biochem. Physiol. B Biochem. Mol. Biol.* **165**, 99–105. (doi:10.1016/j.cbpb.2013.03.010)

24. Lin Z, Hao M, Zhu D, Li S, Wen X. 2017 Molecular cloning, mRNA expression and nutritional regulation of a Δ6 fatty acyl desaturase-like gene of mud crab, *Scylla paramamosain*. *Comp. Biochem. Physiol. B Biochem. Mol. Biol.* **208–209**, 29–37. (doi:10.1016/j.cbpb.2017.03.004)

25. Wu DL, Huang YH, Liu ZQ, Yu P, Gu PH, Fan B, Zhao Y-L. 2018 Molecular cloning, tissue expression and regulation of nutrition and temperature on Δ6 fatty acyl desaturase-like gene in the red claw crayfish (*Cherax quadricarinatus*). *Comp. Biochem. Physiol. B Biochem. Mol. Biol.* **225**, 58–66. (doi:10.1016/j.cbpb.2018.07.003)

26. Lin Z, Hao M, Huang Y, Zou W, Rong H, Wen X. 2018 Cloning, tissue distribution and nutritional regulation of a fatty acyl Elovl4-like elongase in mud crab, *Scylla paramamosain* (Estampador, 1949). *Comp. Biochem. Physiol. B Biochem. Mol. Biol.* **217**, 70–78. (doi:10.1016/j.cbpb.2017.12.010)

27. Mah M, Kuah M, Yeat S, Merosha P, Janaranjani M, Goh P, Jaya-Ram A, Shu-Chien AC. 2019 Molecular cloning, phylogenetic analysis and functional characterisation of an Elovl7-like elongase from a marine crustacean, the orange mud crab (*Scylla olivacea*). *Comp. Biochem. Physiol. B* **232**, 60–71. (doi:10.1016/j.cbpb.2019.01.011)

28. Kabeya N *et al.* 2018 Genes for *de novo* biosynthesis of omega-3 polyunsaturated fatty acids are widespread in animals. *Sci. Adv.* **4**, eaar6849. (doi:10.1126/sciadv.aar6849)

29. Nielsen BLH *et al.* 2019 n-3 PUFA biosynthesis by the copepod *Apocyclops royi* documented using fatty acid profile analysis and gene expression analysis. *Biol. Open* **8**, bio038331. (doi:10.1242/bio.038331)

30. Lee SH *et al.* 2017 Effects of temperature on growth and fatty acid synthesis in the cyclopoid copepod *Paracyclopina nana*. *Fish. Sci.* **83**, 725–734. (doi:10.1007/s12562-017-1104-2)

31. Kim HS, Lee BY, Han J, Lee YH, Min GS, Kim S, Lee J-S. 2016 *De novo* assembly and annotation of the Antarctic copepod (*Tigriopus kingsejongensis*) transcriptome. *Mar. Genomics* **28**, 37–39. (doi:10.1016/j.margen.2016.04.009)

32. Kim HS, Lee BY, Won EJ, Han J, Hwang DS, Park HG, Lee J-S. 2015 Identification of xenobiotic biodegradation and metabolism-related genes in the copepod *Tigriopus japonicus* whole transcriptome analysis. *Mar. Genomics* **24**, 207–208. (doi:10.1016/j.margen.2015.05.011)

33. Schoville SD, Barreto FS, Moy GW, Wolff A, Burton RS. 2012 Investigating the molecular basis of local adaptation to thermal stress: population differences in gene expression across the transcriptome of the copepod *Tigriopus californicus*. *BMC Evol. Biol.* **12**, 170. (doi:10.1186/1471-2148-12-170)

34. Renaud SM, Parry DL. 1994 Microalgae for use in tropical aquaculture. II. Effect of salinity on growth, gross chemical composition and fatty acid composition of three species of marine microalgae. *J. Appl. Phycol.* **6**, 347–356. (doi:10.1007/bf02181949)

35. Volkman JK, Jeffrey SW, Nichols PD, Rogers GI, Garland CD. 1989 Fatty acid and lipid composition of ten species of microalgae used in mariculture. *J. Exp. Mar. Biol. Ecol.* **128**, 219–240. (doi:10.1016/0022-0981(89)90029-4)

36. Collins M *et al.* 2013 Long-term climate change: projections, commitments and irreversibility. In *Climate change 2013: the physical science basis contribution of Working Group I to the fifth assessment report of the Intergovernmental Panel on Climate Change*, pp. 1029–1136. Cambridge, UK: Cambridge University Press.

37. Windisch HS, Fink P. 2018 The molecular basis of essential fatty acid limitation in *Daphnia magna*—a transcriptomic approach. *Mol. Ecol.* **27**, 871–885. (doi:10.1111/mec.14498)

38. R Core Team. 2019 *R: a language and environment for statistical computing*. Vienna, Austria: R Foundation for Statistical Computing. See http://www.R-project.org/

39. Ackman RG, Sipos JC. 1964 Application of specific response factors in the gas chromatographic analysis of methyl esters of fatty acids with flame ionization detectors. *J. Am. Oil Chem. Soc.* **41**, 377–378. (doi:10.1007/bf02654818)

40. Wolff RL, Bayard CC, Fabien RJ. 1995 Evaluation of sequential methods for the determination of butterfat fatty acid composition with emphasis on *trans*-18:1 acids. Application to the study of seasonal variations in French butters. *J. Am. Oil Chem. Soc.* **72**, 1471–1483. (doi:10.1007/bf02577840)

41. Bolger AM, Lohse M, Usadel B. 2014 Trimmomatic: a flexible trimmer for Illumina sequence data. *Bioinformatics* **30**, 2114–2120. (doi:10.1093/bioinformatics/btu170)

42. Grabherr MG *et al.* 2011 Full-length transcriptome assembly from RNA-Seq data without a reference genome. *Nat. Biotechnol.* **29**, 644–652. (doi:10.1038/nbt.1883)

43. Langmead B, Salzberg SL. 2012 Fast gapped-read alignment with Bowtie 2. *Nat. Methods.* **9**, 357–359. (doi:10.1038/nmeth.1923)

44. Simão FA, Waterhouse RM, Ioannidis P, Kriventseva EV, Zdobnov EM. 2015 BUSCO: assessing genome assembly and annotation completeness with single-copy orthologs. *Bioinformatics* **31**, 3210–3212. (doi:10.1093/bioinformatics/btv351)

45. Patro R, Duggal G, Love MI, Irizarry RA, Kingsford C. 2017 Salmon provides fast and bias-aware quantification of transcript expression. *Nat. Methods* **14**, 417–419. (doi:10.1038/nmeth.4197)

46. Bryant DM *et al.* 2017 A tissue-mapped axolotl *de novo* transcriptome enables identification of limb regeneration factors. *Cell Rep.* **18**, 762–776. (doi:10.1016/j.celrep.2016.12.063)

47. Finn RD, Clements J, Eddy SR. 2011 HMMER web server: interactive sequence similarity searching. *Nucleic Acids Res.* **39**, 29–37. (doi:10.1093/nar/gkr367)

48. El-Gebali S *et al.* 2019 The Pfam protein families database in 2019. *Nucleic Acids Res.* **47**, D427–D432. (doi:10.1093/nar/gky995)

49. Huerta-Cepas J *et al.* 2019 EggNOG 5.0: a hierarchical, functionally and phylogenetically annotated orthology resource based on 5090 organisms and 2502 viruses. *Nucleic Acids Res.* **47**, D309–D314. (doi:10.1093/nar/gky1085)

50. Kanehisa M, Goto S, Sato Y, Furumichi M, Tanabe M. 2012 KEGG for integration and interpretation of large-scale molecular data sets. *Nucleic Acids Res.* **40**, 109–114. (doi:10.1093/nar/gkr988)

51. Ashburner M *et al.* 2000 Gene ontology: tool for the unification of biology. *Nat. Genet.* **25**, 25–29. (doi:10.1038/75556)

52. Robinson MD, McCarthy DJ, Smyth GK. 2009 edgeR: a Bioconductor package for differential expression analysis of digital gene expression data. *Bioinformatics* **26**, 139–140. (doi:10.1093/bioinformatics/btp616)

53. Robinson MD, Oshlack A. 2010 A scaling normalization method for differential expression analysis of RNA-seq data. *Genome Biol.* **11**, R25. (doi:10.1186/gb-2010-11-3-r25)

54. Benjamini Y, Hochberg Y. 1995 Controlling the false discovery rate: a practical and powerful approach to multiple testing. *J. R. Stat. Soc. Ser. B* **57**, 289–300. (doi:10.1111/j.2517-6161.1995.tb02031.x)

55. Alexa A, Rahnenfuhrer J. 2019 *topGO—enrichment analysis for gene ontology. R package version 2.37.0*. (doi:10.18129/b9.bioc.topgo)

56. Katoh K, Standley DM. 2013 MAFFT multiple sequence alignment software version 7: improvements in performance and usability. *Mol. Biol. Evol.* **30**, 772–780. (doi:10.1093/molbev/mst010)

57. Stamatakis A. 2014 RAxML version 8: a tool for phylogenetic analysis and post-analysis of large phylogenies. *Bioinformatics* **30**, 1312–1313. (doi:10.1093/bioinformatics/btu033)

58. Cnudde C, Willems A, Van Hoorde K, Vyverman W, Moens T, De Troch M. 2011 Effect of food preservation on the grazing behavior and on the gut flora of the harpacticoid copepod *Paramphiascella fulvofasciata*. *J. Exp. Mar. Biol. Ecol.* **407**, 63–69. (doi:10.1016/j.jembe.2011.07.007)

59. Semmouri I, Asselman J, Van Nieuwerburgh F, Deforce D, Janssen CR, De Schamphelaere KAC. 2018 The transcriptome of the marine calanoid copepod *Temora longicornis* under heat stress and recovery. *Mar. Environ. Res.* **143**, 10–23. (doi:10.1016/j.marenvres.2018.10.017)

60. Guzmán M, Velasco G, Geelen MJH. 2000 Do cytoskeletal components control fatty acid translocation into liver mitochondria? *Trends Endocrinol. Metab.* **11**, 49–53. (doi:10.1016/s1043-2760(99)00223-4)

61. Røsjø C, Berg T, Manum K, Gjøen T, Magnusson S, Thomassen MS. 1994 Effects of temperature and dietary n-3 and n-6 fatty acids on endocytic processes in isolated rainbow trout (*Oncorhynchus mykiss*, Walbaum) hepatocytes. *Fish Physiol. Biochem.* **13**, 119–132. (doi:10.1007/bf00004337)

62. Hölzer M, Marz M. 2019 *De novo* transcriptome assembly: a comprehensive cross-species comparison of short-read RNA-Seq assemblers. *Gigascience* **8**, giz039. (doi:10.1093/gigascience/giz039)

63. Surm JM, Toledo TM, Prentis PJ, Pavasovic A. 2018 Insights into the phylogenetic and molecular evolutionary histories of *Fad* and *Elovl* gene families in Actiniaria. *Ecol. Evol.* **8**, 5323–5335. (doi:10.1002/ece3.4044)

64. Ishikawa A *et al.* 2019 A key metabolic gene for recurrent freshwater colonization and radiation in fishes. *Science* **364**, 886–889. (doi:10.1126/science.aau5656)

65. Freeman WM, Walker SJ, Vrana KE. 1999 Quantitative RT-PCR: pitfalls and potential. *Biotechniques* **26**, 112–125. (doi:10.2144/99261rv01)

10

royalsocietypublishing.org/journal/rstb *Phil. Trans. R. Soc. B* **375**: 20190645

ORIGINAL PAPER

An inter-order comparison of copepod fatty acid composition and biosynthesis in response to a long-chain PUFA deficient diet along a temperature gradient

Robyn Sahota[1] · Jens Boyen[1] · Ilias Semmouri[2] · Samuel Bodé[3] · Marleen De Troch[1]

Abstract

Copepods serve as a major link in marine food webs, bridging the energy transfer from primary producers to higher trophic levels. Oceanic warming is linked to reduced concentrations of essential fatty acids (FA) in phytoplankton, namely eicosapentaenoic acid (EPA, 20:5ω3) and docosahexaenoic acid (DHA, 22:6ω3), and it remains largely unknown if copepods have the capacity to endure. The calanoid *Temora longicornis* and the harpacticoid *Platychelipus littoralis* were chosen to analyse their FA and biosynthesis activity in response to a long-chain polyunsaturated FA (LC-PUFA) deficient diet (*Dunaliella tertiolecta*) along a temperature gradient. Copepods were fed *D. tertiolecta* labelled with the stable isotope carbon-13 (^{13}C) to quantify carbon assimilation into their total FA and de novo EPA and DHA biosynthesis after 6 days incubated at 11, 14, 17, 20 and 23 °C. The calanoid had increased mortality with warming, whereas the harpacticoid exhibited high survival across the thermal gradient. After the incubation, *P. littoralis* assimilated minimal amounts of dietary carbon into its total FA in comparison to *T. longicornis*. *T. longicornis* depleted their field EPA and DHA stores more rapidly, whereas *P. littoralis* maintained its relative storage of EPA and DHA and absolute concentrations of DHA. *T. longicornis* displayed higher fractions of de novo EPA and DHA biosynthesis than *P. littoralis* at all temperatures, with the exception of DHA at 23 °C. Within our experimental incubation period both species were unable to meaningfully upgrade the LC-PUFA deficient algae to biosynthesize de novo EPA and DHA as a relevant source for higher trophic levels.

Keywords Biosynthesis · Calanoid copepod · Carbon assimilation · Climate change · Fatty acids · Harpacticoid copepod

Introduction

Record temperature increases and large fluctuations are undisputedly becoming more ordinary and frequent in marine ecosystems (Stenseth et al. 2002) pressuring the adaptive and acclimatization limits of organisms who have limited motility. These temperature changes can

✉ Robyn Sahota
robyn.sahota@ugent.be

[1] Marine Biology, Department of Biology, Ghent University, Krijgslaan 281-S8, 9000 Ghent, Belgium

[2] Laboratory of Environmental Toxicology and Aquatic Ecology, Faculty of Bioscience Engineering, Ghent University, Coupure Links 653-F, 9000 Ghent, Belgium

[3] Isotope Bioscience Laboratory (ISOFYS), Ghent University, Coupure Links 653, 9000 Ghent, Belgium

restructure the base of complex marine food webs notably through range-shifts (Beaugrand et al. 2002; McGinty et al. 2021), changes in reproductive timing (Daase et al. 2013), abundances and size (Garzke et al. 2015), and via the modification of individuals' fatty acids (FA) (Garzke et al. 2016). This adjustment of primary producer food quality, specifically the predicted reduction of omega(ω)-3 FA with warming, can have major implications on the availability of these important essential FA (EFA) (Hixson and Arts 2016; Colombo et al. 2020). EFA (e.g. eicosapentaenoic acid (EPA): 20:5ω3, docosahexaenoic acid (DHA): 22:6ω3) are critical for growth and survival and cannot be produced de novo by marine invertebrates in the considerable amounts required (Bell et al. 2007). However, through the recent development of detailed molecular and isotope tracing methods many metazoans have been shown to contain the critical enzymes with the capacity to perform biosynthetic pathways producing ω-3 FA (Kabeya et al. 2018, 2021). Calanoids were often believed

to have poor biosynthesis capacities (Moreno et al. 1979; Bell et al. 2007), more recent research suggest that at least some species have the ability to produce long-chain poly-unsaturated FA (LC-PUFA) from precursors in ecologically relevant quantities (Nielsen et al. 2019). Cyclopoid, calanoid, and harpacticoid copepod species were shown to possess these biosynthesis capabilities (De Troch et al. 2012; Nielsen et al. 2020), that intensified under warming pressures (Werbrouck et al. 2017; Helenius et al. 2020). LC-PUFA are defined by a FA chain length of 20 or more carbon units (Ratnayake and Galli 2009). LC-PUFA biosynthesis is enabled by a series of enzymes including fatty acyl desaturases, which introduce a double bond in the FA carbon chain, and elongases, that elongate very long-chain FA by introducing two additional carbon atoms (Bell and Tocher 2009; Monroig and Kabeya 2018). While front-end desaturases and elongases are present throughout copepod orders (Nielsen et al. 2019; Lee et al. 2020; Kabeya et al. 2021), methyl-end desaturases—enabling biosynthesis of monounsaturated FA (MUFA) towards LC-PUFA—have recently been detected in at least harpacticoid, cyclopoid and siphonostomatoid copepods, completely revising the current assumptions on global de novo LC-PUFA production within aquatic food webs (Kabeya et al. 2018). This ability for biosynthesis has been proposed to be a potential adaptive mechanism to overcome reduced dietary LC-PUFA availability (Nielsen et al. 2020); however, the triggers/circumstances for biosynthesis and the extent to which individuals can offset these deficiencies remains unknown.

Copepods are a dominant group of zooplankton and play an important role due to their high lipid concentrations in comparison to primary producers (Kattner and Hagen 2009), providing higher trophic levels with an energetic food source. In marine intertidal sediments the order Harpacticoida dominates, due to high inputs of detritus and nutrients stimulating microphytobenthos growth, and availability of benthic microbial communities (Meyer 1994; Cnudde et al. 2015). Harpacticoids are a lipid-rich dietary item for demersal and juvenile fish species (Gee 1987; Coull 1990), and can enrich sediment with organic matter, promoting biogeochemical cycling processes (Stock et al. 2014). Comparatively, in the pelagic environment the order Calanoida is the major group within the zooplankton community, serving as prey-items for (larval) fish (Beaugrand et al. 2003; Turner 2004), seabirds (Frederiksen et al. 2013; Bertram et al. 2017), and whales (Cronin et al. 2017). Apart from direct consumption, they also contribute to the detrital food web through the microbial remineralization (Lampitt et al. 1990), and to the biological carbon pump (Jónasdóttir et al. 2015). Although morphologically distinct, these two orders fill a similarly critical niche in energy transfer, within their respective oceanic realms, and will face analogous warming pressures.

Global sea surface temperatures (SSTs) are expected to rise between 1.2 and 3.47 °C by 2100 as per Shared Socio-economic Pathway (SSP) scenarios 2.6 and 8.5, respectively (Kwiatkowski et al. 2020). Since zooplankton have a relatively short generational time (< 1 year) and are poikilothermic, the population dynamics and energetics tied to environmental warming are meaningful (Hays et al. 2005; Richardson 2008). This environmental pressure can have an effect on both the organism itself and the algae they consume. Hence, assessing the effects of dietary LC-PUFA provision along a temperature gradient in these important primary consumers is relevant to understand future climate effects on the marine food web. Both temperature and food quality have been shown to be the stressors with the largest impact on individual FA composition (Deschutter et al. 2019), thereby impacting energy flow changes for higher trophic levels. A methodology being used to quantify the transfer of FA incorporation and biosynthesis in a consumer is compound-specific stable isotope analysis (CSIA). By labelling the food source with the stable isotope carbon-13 (^{13}C), we are able to track the percent of algae-derived FA under experimental conditions, and understand differential incorporation or modification/biosynthesis processes for each FA (Twining et al. 2020). These data are resolved via gas chromatography combustion-isotope ratio mass spectrometry (GC-c-IRMS), allowing us to ascertain the ^{13}C/^{12}C ratio of individual FA found within the copepod consumer. Accordingly, the amount of FA in the consumer, derived from the isotopically labelled food source can be determined. As LC-PUFA are absent in the chlorophyte *Dunaliella tertiolecta*, this alga was selected. As such, the LC-PUFA with *D. tertiolecta* derived carbon in the copepod consumer can be used to assess LC-PUFA biosynthesis during the lab incubation (de novo). This method is a proposed alternative FA tracer method to liposomes (Bell et al. 2007).

The objective of this study was to measure the effects of a LC-PUFA deficient diet on the FA composition, incorporation and de novo biosynthesis in two copepod species of different orders along a temperature gradient. Using 7-day lab treatments, we evaluated the temperature-specific response of carbon incorporation in consumer FA under LC-PUFA deficient conditions between *Platychelipus littoralis,* a benthic harpacticoid species with known temperature-dependent biosynthesis capabilities (Werbrouck et al. 2017), and the calanoid *Temora longicornis*, the dominant zooplankton species in the southern North Sea (Semmouri et al. 2021), with as of yet unknown biosynthesis capabilities.

Materials and methods

Sampling and experimental design

The calanoid copepod *T. longicornis* (Müller 1785) were collected from the Belgian part of the North Sea (BPNS), on the research vessel (RV) Simon Stevin on 15th February 2021 at sampling station 330 (51°25′ 995″ N, 2°48′41.5″ E) in the coastal waters near Ostend. Copepods were collected using a vertically towed WP2 net (57 cm diameter, 200 μm mesh size), towed from bottom to surface (SST: 4.8 °C, 32.997 PSU, 0 μg L^{-1} chlorophyll a). Individuals were transported and held in 35 L vessels, containing natural seawater obtained from the sampling station. The harpacticoid copepod *P. littoralis* (Brady, 1880) were obtained during low tide from the Paulina intertidal mudflat, Westerscheldt estuary, Netherlands (51°21′ 24″ N, 3° 42′ 51″E) on 9 March 2021. The top sediment layer was sampled (5.45 °C, 21.55 PSU), and individuals were isolated by sieving through a 250 μm mesh. Copepods (CV/CVI) were randomly selected under a Wild Heerbrugg M5 stereomicroscope (length *P. littoralis*: ~ 0.9 mm (Werbrouck et al. 2017), *T. longicornis*: 1.39 ± 0.27 mm (Semmouri 2022)). To characterize the FA profile of individuals in the field, quadruplicates of 50 copepods were sampled and stored at − 80 °C after allowing gut clearance for 12 h in autoclaved filtered natural seawater (FNSW). Following identification to species level, individuals (n = 60: *T. longicornis*, n = 70: *P. littoralis*) were placed directly in 1 L glass jars of autoclaved FNSW with aeration for 12 h at 11 °C to allow gut clearance before addition of the food. Based on previous laboratory experiments (*e.g.*, Werbrouck et al. 2017), no aeration was added to the *P. littoralis* jars to not disturb their benthic lifestyle as they could not hide in any sediment in the experimental unit.

The chlorophyte, *D. tertiolecta* (Butcher 1959)*,* was obtained from the Laboratory of Aquaculture & Artemia Reference Center at Ghent University, and cultured at 15 °C in autoclaved FNSW with NutriBloom Plus. *D. tertiolecta* cultures were isotopically labelled with 16.8 mg $NaH^{13}CO_3$ stock solution per 100 mL of growth medium (De Troch et al. 2012; Werbrouck et al. 2017), and grown in climate rooms (15 °C, 12:12 h light:dark, 17–46 μmol photons m^{-2} s^{-1}) for 10 days. Cell concentrations were monitored with a Beckman Coulter counter Multisizer 3. Prior to addition in experimental units, *D. tertiolecta* cultures were centrifuged, the supernatant containing the ^{13}C label and nutrients was removed, then *D. tertiolecta* was resuspended in autoclaved FNSW. This was repeated twice to inhibit further algal growth (De Troch et al. 2012; Werbrouck et al. 2017). Quadruplicate 10 mL samples of *D. tertiolecta* were taken for FA analysis in pre-combusted

glass vials, and for total carbon analysis by filtering 25 mL onto Whatman GF/F filter, both stored at − 80 °C. Algae concentrations were measured approximately 12 h after addition to the experimental units and after 6 days.

Four replicates of glass jars filled with 1 L of autoclaved FNSW per species (*P. littoralis*, 70 ind. $unit^{-1}$; *T. longicornis*, 60 ind. $unit^{-1}$) were placed at each of the five temperature treatments (11, 14, 17, 20, 23 °C), controlled Lovibond TC-175 incubators (temperature control ± 1 °C). Experimental units (total n = 40) were fed ad libitum (20 000–45 000 cells mL^{-1}, 0.248–1.098 mg carbon L^{-1}) with the prepared ^{13}C-labelled *D. tertiolecta* (above) for 6 days under a 12:12 h light:dark regime. These units were acclimated from 11 °C to their treatment temperature at a rate of 2 °C h^{-1}. To assess potential algae growth throughout the experiments, quadruplicate experimental units containing only *D. tertiolecta* were placed in the 14 °C incubator for the duration of the experiment. No increase in cell concentration was reported in these samples (Fig. S1), hereafter we assume algae growth was successfully inhibited. On day 6 individuals were sieved on a 38 μm mesh and living individuals were transferred to autoclaved FNSW to allow gut clearance for 24 h. After this period, surviving individuals were transferred to glass vials and stored at − 80 °C prior to FA analysis.

Total fatty acid extraction, quantification and CSIA

An internal standard (FA 19:0, 5 μg) was added to the freeze-dried samples, then FA methyl esters (FAME) were prepared via a direct transesterification procedure with 2.5% (v:v) sulfuric acid in methanol as described by De Troch et al. (2012) to achieve total FA analysis. FAME were extracted twice with hexane. Composition analysis of FA was carried out using a gas chromatograph (GC) (HP 7890B, Agilent Technologies, Diegem, Belgium) equipped with a flame ionization detector (FID) and connected to an Agilent 5977A Mass Selective (MS) Detector (Agilent Technologies). The GC was further equipped with a PTV injector (CIS-4, Gerstel, Mülheim an der Ruhr, Germany). A 60 m × 0.25 mm × 0.20 μm film thickness HP88 fused-silica capillary column (Agilent Technologies) was used for the GC analysis, at a constant Helium flow rate (2 mL min^{-1}). The injection sample volume was 2 μL, and the oven temperature program was set as described in Boyen et al. (2020). FAME were analysed with the GC–MS prior to CSIA due to the higher total FA profile resolution and detection capabilities. The signal obtained with the FID detector was used to generate quantitative data of all compounds (MassHunter Quantitative Analysis Software, Agilent Technologies). Chromatogram peaks were identified based on their retention times, the external standards (Supelco 37 Component FAME Mix, Sigma-Aldrich) and the mass spectra. Quantification

of FAME was based on the FID area of the internal standard (19:0), and the conversion of peak areas to the amount of the FA by a theoretical response factor for each FA (Ackman and Sipos 1964; Wolff et al. 1995).

To assess the ^{13}C within the FA, FAME from all treatments and field samples were analysed by capillary gas chromatography combustion-isotope ratio mass spectrometry (GC-c-IRMS) at the Isotope Bioscience Laboratory (ISOFYS), Ghent University. The GC-c-IRMS system consisted of a Trace GC 1310 equipped with a PTV injector and a VF23-MS column (length = 60 m, ID = 0.25 mm, film = 0.25 μm), connected to combustion/pyrolysis unit (GC-ISOLINK) where the FAME are converted to CO_2. The FAME is let by an automated open split system (Conflo IV) to an IRMS detector (DeltaV advantage, Thermo Scientific, Bremen Germany). ^{13}C abundance was calibrated using the F8-3 mix of Arndt Schimmelman. Typical precision of ^{13}C abundance is within 0.0005%. The GC-c-IRMS was not able to determine the position of the unsaturation in the carbon-20 chain (20:1), therefore its full notation is not indicated in the figures and tables reported in the results and supplementary information.

CSIA calculations

During GC-c-IRMS analysis the analytes are converted to CO_2 to be analysed by the IRMS detector where m/z 44, 45 and 46 are recorded simultaneously by three detectors. From the ratio of these three traces the $a^{13}C$ can be determined with high precision. The peak area (PA) of the individual FA can be used to also assess the FA content ([FA]). Commonly, in not artificially ^{13}C enriched material this is done using the combined peak area of the three mass traces. However, due to the high ^{13}C enrichments and the different amplifications of the detectors, the [FA] per copepod was determined as follows:

$$FAt = \left(\frac{PA_{44,FAME} \times (1 - a^{13}C_{IS})}{PA_{44,IS}} + \frac{PA_{45,FAME} \times (a^{13}C_{IS})}{PA_{45,IS}} \right)$$
$$\times \frac{m_{IS} \times (nC_{IS}) \times M_{FA}}{M_{IS} \times (nC_{FA} + 1) \times N} \tag{1}$$

with $PA_{X,FAME}$ and $PA_{X,IS}$ being the peak area at m/z = x of the FAME of interest and of the internal standard (IS), respectively, $a^{13}C_{IS}$ the ^{13}C abundance in the IS (1.08%), m_{IS} the mass of the C19:0-FAME added (50 μg), M_{FA} and M_{IS} the molar mass of the FA of interest and of the IS (312.54 g•mol^{-1}), respectively, nC_{FA} and nC_{IS} indicating the number of carbons in the FA of interest and in IS (20), and N being the number of copepods in the extracted sample.

The GC-c-IRMS measurements delivers the ^{13}C abundance of the individual FAME ($a^{13}C_{FAME}$). To obtain the

$a^{13}C$ of the corresponding FA ($a^{13}C_{FA}$), the measured $a^{13}C_{FAME}$ must be corrected for the contribution of the methyl ($a^{13}C_{MeOH}$), added during derivatization to FAME:

$$a^{13}C_{FA} = \frac{\left[a^{13}C_{FAME} \times (nC_{FA} + 1) - a^{13}C_{MeOH} \right]}{nC_{FA}} \tag{2}$$

The fraction of carbon assimilated ($f_{C\,assi}$) in consumer FA derived from the ^{13}C-labelled *D. tertiolecta* can be computed as:

$$f_{Cassi} = \frac{a^{13}C_{FA\text{-}exp.} - a^{13}C_{FA\text{-}control}}{a^{13}C_{labelled\,DUNA} - a^{13}C_{field\,food}} \tag{3}$$

with $a^{13}C_{FA\text{-}exp.}$ and $a^{13}C_{FA\text{-}control}$ representing the $a^{13}C_{FA}$ of the specific FA in copepods fed with ^{13}C-labelled *D. tertiolecta* and control copepod (directly collected on field site), respectively, $a^{13}C_{labelled\,DUNA}$ and $a^{13}C_{field\,food}$ (1.08%) indicating the bulk $a^{13}C$ of the ^{13}C-labelled *D. tertiolecta* and of the food prior to incubation, respectively (adapted from Werbrouck et al. 2017). The bulk ^{13}C of the labelled *D. tertiolecta*, was not measured due to instrumental limitations to measure very high enrichments, therefore the $a^{13}C_{labelled\,DUNA}$ was estimated using the $a^{13}C_{FA}$ of 18:3ω3 (46.45%) found in the calanoid copepod samples. This value was used as a proxy due to the high concentration of 18:3ω3 in *D. tertiolecta* (Thor et al. 2007), and high uptake by *T. longicornis*. Finally, the absolute amount of FA derived from the carbon assimilated of the ^{13}C-labelled *D. tertiolecta* ([FA]$_{C\,assi}$) could be computed as follows:

$$[FA]_{Cassi} = [FA] \times f_{Cassi} \tag{4}$$

For FA already present in *D. tertiolecta* (SFA, MUFA and PUFA < 20 carbon units), we assume that FA derived from the labelled feed in the copepods are a combination of direct unaltered incorporation, biosynthesis and conversion. LC-PUFA (ARA, EPA and DHA) are not present in *D. tertiolecta*, therefore LC-PUFA derived from the labelled feed in the copepod are the result of biosynthesis from dietary obtained FA precursors (see Supplementary Information, Table S1). The carbon assimilation from the algae into the total sum of all measured FA (TFA) relative to the absolute concentrations was additionally calculated.

Statistical analysis

All statistical analyses and visualizations were conducted in R, version 4.1.1 (R Core Team 2021). Intra-specific cell concentrations of *D. tertiolecta* between day 1 and 6 were compared using a Bonferroni corrected multiple pairwise *t*-test. No increase of algae concentrations during the experimental treatment was detected, therefore algae growth inhibition was considered successful (Fig. S1). Relative percent FA

composition data were analysed using non-parametric multidimensional scaling (nMDS), Bray–Curtis dissimilarity, on cube-root transformed data. A permutational analysis of variance (PERMANOVA) was conducted based on groups determined by hierarchical clustering. To discriminate which FA were contributing the most to these differences, a similarity percentages test (SIMPER) was conducted.

A quasi-binomial logistic generalized linear model (GLM) was used to model proportional copepod survival along temperature, considering species identity as a factor and weighted by the number of copepods in each sample, to account for an overdispersion of the data estimated by the ratio of the residuals deviance and the degrees of freedom (Haman 2020). Multiple comparisons of type Tukey were applied to the survival GLM, using the package 'multcomp' to determine significant differences considering species and temperature (Hothorn et al. 2008) (Table S2). Generalized additive models (GAM) were used to evaluate the significance of the non-linear relationship of the relative carbon assimilation into the TFA (C_{assi} TFA^{-1}) and the fraction of carbon assimilation into specific FA along a temperature gradient between species using the package 'mgcv' (Wood 2011). Non-parametric smoothers (s) by restricted maximum likelihood were applied to the temperature effects (T) by species identity (S), considering species as a factor: C_{assi} $TFA^{-1} \sim f(S) + s(T, by = S)$. If these data violated homogeneity assumptions evaluated by the dispersion of the residuals versus fitted values, due to zero-inflation, a gamma distribution family was assumed with a log-link function (Zuur et al. 2009) (Table S3). Due to high mortality the FA data from two *T. longicornis* replicates at 23 °C have been omitted. Model selection was done on the basis of the Akaike Information Criterion (AIC) and ANOVA. The significance of the smooth terms are reported, and explained deviance is listed on the GAM as it is considered as a generalized measurement of goodness of fit, rather than R^2-values (Wood 2011). Carbon assimilation per FA is listed in the supplementary information (Fig. S2, Table S4, Table S5), note some models could not be reliably interpreted for FA with numerous undetected values and were omitted from this analysis (*i.e.*, 15:0, 16:2ω4, 18:1ω9, 20:1). Due to size differences between species, the fraction of de novo FA was modelled rather than the absolute amount.

Results

Survival and diet characterization

The proportional survival could be predicted from the interaction between temperature (T) exposure and species (S) identity (GLM, $P = 0.003$) (Fig. 1). Accordingly, the effect of temperature on survival was species specific. The harpacticoid, *P. littoralis*, survival was not significantly
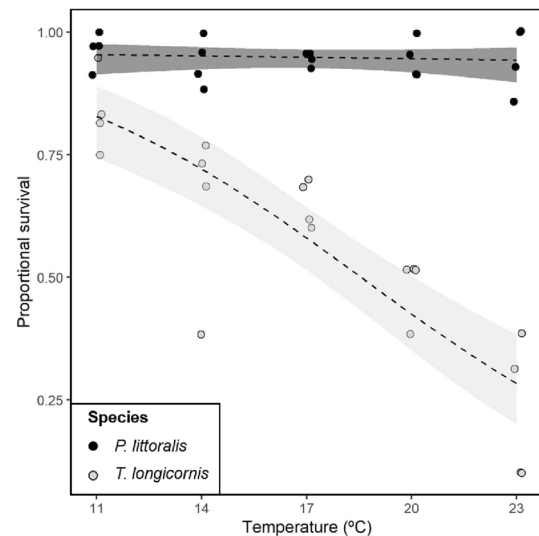
Fig. 1 Generalized linear model of proportional survival (ranging from 0 to 1, indicating complete mortality or survival of individuals within experimental units, respectively) for *Platychelipus littoralis* and *Temora longicornis* along a temperature gradient (11, 14, 17, 20, 23 °C). The shaded lines around the mean (dashed) per species, represent the 95% confidence interval

different (94.8 ± 4.1%) across all temperature treatments (GLM Tukey, 11:23 °C, $P = 0.999$) (Table S2). In contrast, the survival of the calanoid, *T. longicornis*, decreased with at higher temperature treatments, ranging from 83.8 ± 8.3% at 11 °C to 22.5 ± 14.7% at 23 °C (GLM Tukey, $P < 0.01$) (Table S2).

Interspecific comparison of FA composition

In *T. longicornis* FA 16:0, 20:5ω3 (EPA), and 22:6ω3 (DHA) were the most abundant, comprising of > 70% of the total FA composition (Table S6). Comparatively, in *P. littoralis* FA 16:0, 16:1ω5, 16:1ω7, EPA, and DHA were the most abundant, corresponding to > 70% of the total FA composition (Table S6). There were significant differences in FA composition between all temperature treatments and field samples among species (PERMANOVA, $P = 0.012$). However, hierarchical clustering and nMDS visualization of the data showed these did not fall into natural groups, therefore only significant differences (PERMANOVA, $P = 0.001$) between broad field and experimental species groups were considered (Fig. S3). Looking only at field samples between species, the FA that contributed the most to the differences are EPA, 14:0, 16:1ω5, DHA, and 16:1ω7 (Table S7). FA EPA, 14:0 and DHA were present in higher relative concentrations in field *T. longicornis* than in field *P. littoralis* (Table S6). Notably in field samples, *P. littoralis* contained 7.7% DHA whereas *T. longicornis* contained 29% DHA. Accordingly, these same FA also contributed largely to the

differences between the temperature incubation treatments per species, in addition to 18:3ω3, which was the dominant FA in the algal feed (*D. tertiolecta*, Table S1), 24:1ω9 and 18:1ω7 (Table S7).

Interestingly, there was no significant difference between the relative amounts of EPA in *P. littoralis* in the field and experimental samples, regardless of temperature treatment (Kruskal–Wallis, $P = 0.96$), whereas they decrease in *T. longicornis* (Kruskal–Wallis, $P = 0.031$) (Table S6). Between field and the incubated samples absolute EPA concentrations (ng ind.$^{-1}$) were significantly lower for both *P. littoralis* (Kruskal–Wallis, $P < 0.001$) (Fig. 2a) and *T. longicornis* (ANOVA, $P = 0.002$) (Fig. 2b, Table S8). There was no difference between the relative amount of DHA in *P. littoralis*' field and experimental incubation samples, with the exception of treatments at 17 (Pairwise t-test, $P = 0.042$) and 23 °C (Pairwise t-test, $P = 0.018$), similarly when considering the absolute DHA

values, with an exception at 20 °C (Pairwise Wilcox test, $P = 0.024$) (Fig. 2c). In *T. longicornis,* relative DHA values increased between field and experimental samples for temperatures 11 (Pairwise t-test, $P = 0.042$), 14 (Pairwise t-test, $P = 0.004$), 17 (Pairwise t-test, $P = 0.012$), and 20 °C (Pairwise t-test, $P = 0.013$) with the exception of the treatment at 23 °C (Pairwise t-test, $P = 0.22$). However, when considering *T. longicornis* absolute DHA values, they were significantly lower in temperature treatments 14, 17, 20 °C than the field samples and the 11 °C treatment (ANOVA, $P = 0.007$) (Fig. 2d). Therefore, with the exception of DHA in *P. littoralis*, EPA and DHA concentrations decrease in incubated samples fed *D. tertiolecta* after 6 days in comparison to the field (Fig. 2).
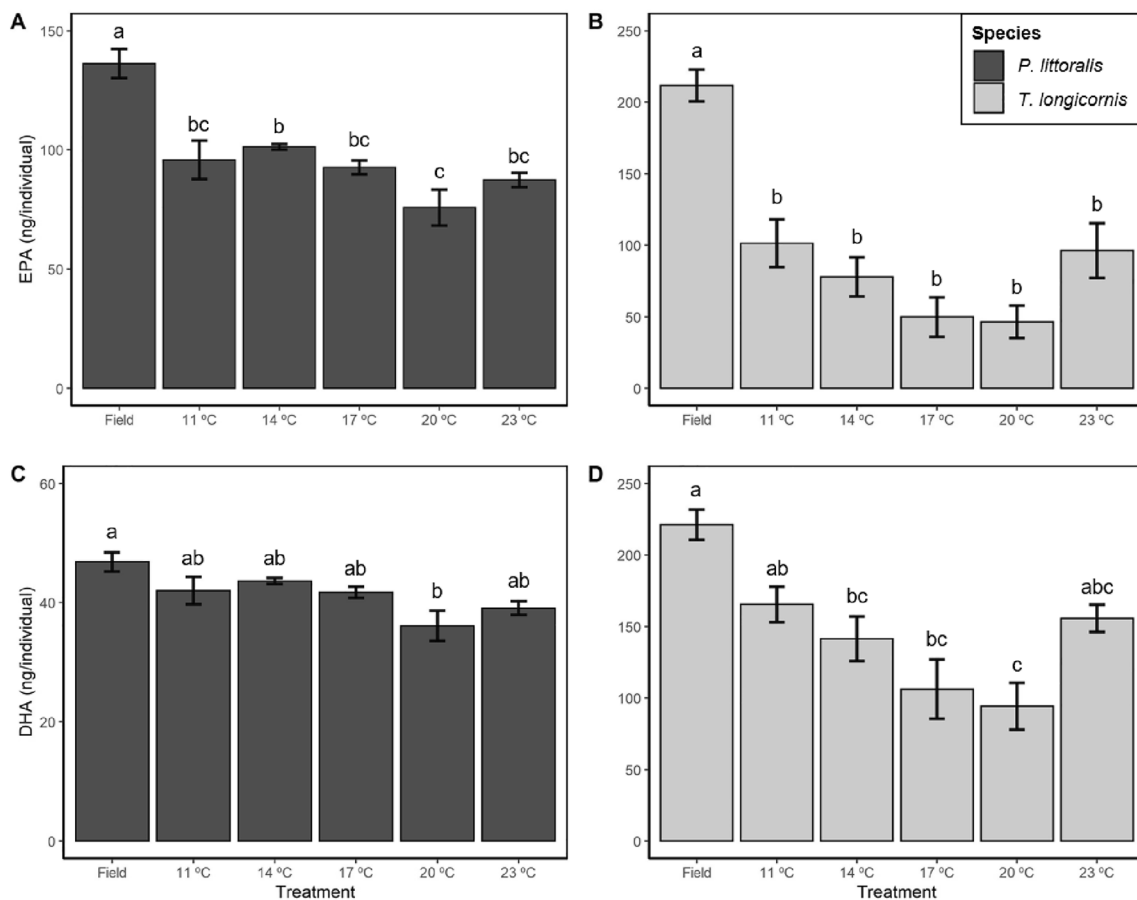
Fig. 2 Mean absolute **a–b** EPA (20:5ω3) and (c-d) DHA (22:6ω3) amounts (ng) per individual ± standard error in *P. littoralis* and *T. longicornis* samples from the field and in the incubated temperature treatments (11, 14, 17, 20 and 23 °C) after day 6. Visualization is divided per FA and species, note the differences of scale between panels. Pairwise post-hoc tests were performed for all temperature treatments against natural reference ('Field') group ($n = 4$) per FA and species after finding significant difference of global means, means sharing a letter are not significantly different ($P > 0.05$). Note, *T. longicornis* 23 °C treatment significance should be interpreted with caution due to high mortality (low number of individuals per sample), and low sample size ($n = 2$)

Carbon assimilated into total fatty acids

The total carbon assimilated by *P. littoralis* during the experimental incubation, indicated by carbon assimilation derived from ^{13}C-labelled *D. tertiolecta*, into the TFA (C_{assi} TFA^{-1}) varied with increasing temperature (Fig. 3a). Carbon assimilated into the total consumer FA decreased from $0.45 \pm 0.21\%$ at 11 °C to $0.28 \pm 0.07\%$ at 20 °C, then increased to $1.29 \pm 0.32\%$ at 23 °C (GAM, $P < 0.001$). Comparatively, *T. longicornis* displayed a significantly higher relative carbon assimilation than *P. littoralis* with a mean value of $12.08 \pm 4.62\%$, with no significant effect of temperature (GAM, $P = 0.34$) (Fig. 3b). Overall, *T. longicornis* displayed higher carbon assimilation into it's FA pool than *P. littoralis* per individual, derived from *D. tertiolecta* in 6 days. Similar patterns were observed in carbon assimilation per SFA (14:0, 16:0, 18:0), MUFA (16:1ω9, 18:1ω11), and short-chain PUFA (18:3ω3) (Fig. S2, Table S4).

Comparison of <u>de novo</u> production of EPA and DHA between species

T. longicornis displayed higher de novo production of both EPA and DHA than *P. littoralis* with an exception at 23 °C (Table S4). *T. longicornis* EPA production ranged from 0.226 ± 0.117 to 0.030 ± 0.060 ng ind.$^{-1}$ at 11 to 23 °C, respectively (Table S5). In comparison, EPA production in *P. littoralis* ranged from 0.015 ± 0.011 to 0.033 ± 0.008 ng ind.$^{-1}$ at 11 to 23 °C, respectively. Lower DHA than EPA production was observed ranging from 0.161 ± 0.043 to 0.012 ± 0.025 and from 0.009 ± 0.001 to 0.030 ± 0.019 ng ind.$^{-1}$ in the temperature range from 11 to 23 °C in *T. longicornis* and *P. littoralis*, respectively.

There is a significant effect of temperature on the fraction of de novo EPA in *T. longicornis* derived from the *D. tertiolecta* after 6 days (GAM, $P < 0.001$, explained deviance $= 91.6\%$) (Fig. 4a, Table S3). Comparatively, there is no relationship between temperature and fraction of EPA produced by *P. littoralis* with a mean value of 0.023 ± 0.007 ng ind.$^{-1}$ (no significant difference between treatments) (GAM, $P = 0.935$, explained deviance $= 91.6\%$). Despite showing significant relationships for both species for the fraction of de novo DHA with temperature, due to the numerous undetected values resulting from low concentrations, this model output should be interpreted with caution (Fig. 4b, Table S3). This is reflected in a low proportion of the variance and deviance explained ($R^2 = 0.219$, 68.0%).

Discussion

The aim of this study was to discern the effects of a poor quality diet on the FA composition, and evaluate the potential for LC-PUFA biosynthesis after 6 days in two copepod species along a temperature gradient. To compensate for poor quality food, organisms can increase ingestion rates (Malzahn and Boersma 2012), and their carbon incorporation efficiency (Gulati and Demott 1997). By choosing a labelled algal diet absent of LC-PUFA, we were able to discern the effect of poor food quality on assimilation and thereby what was retained by the individuals. Furthermore, we could evaluate the potential of LC-PUFA biosynthesis from labelled precursor compounds consumed within the duration of the experiment. *T. longicornis* displayed higher overall carbon assimilation than *P. littoralis,* and maintained this across all temperature treatments, likely to compensate
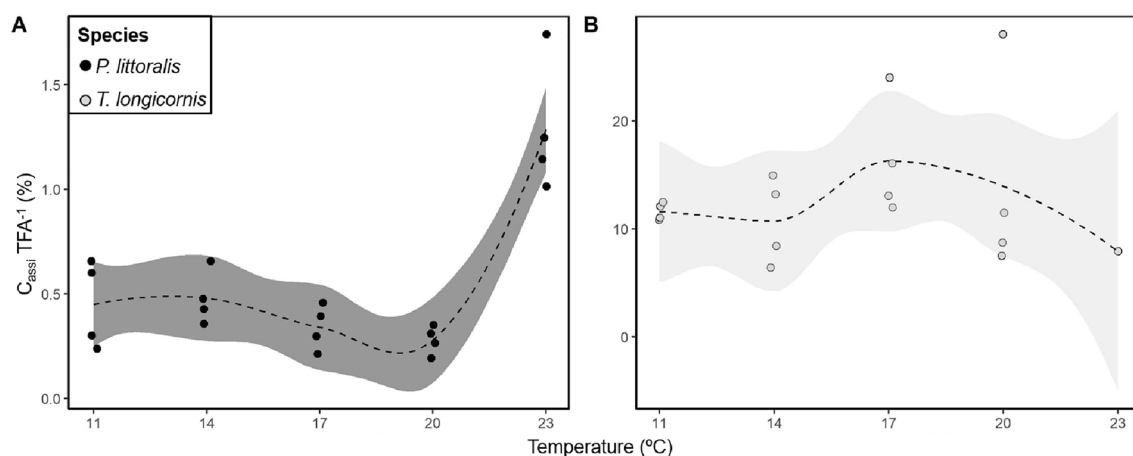
Fig. 3 Fraction of the total fatty acid carbon derived from the labelled *D. tertiolecta* (C_{assi} TFA^{-1}) after 6 days in **a** *P. littoralis* and **b** *T. longicornis* along an experimental temperature gradient. Data displayed are untransformed and separated by species factor. The shaded lines around the mean (dashed line), coloured per species, represent the 95% confidence interval. Note the difference of scale between the two panels
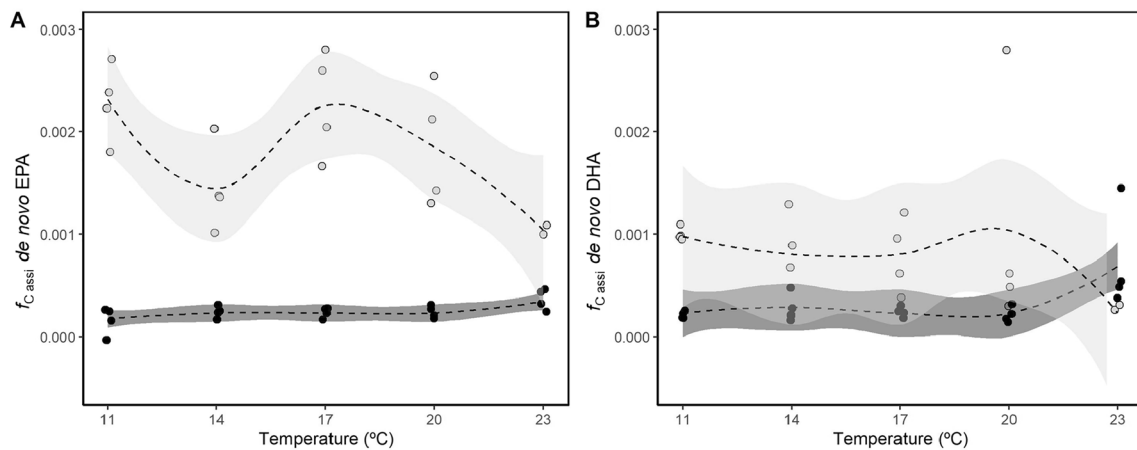
Fig. 4 De novo synthesized fraction of **a** EPA (20:5ω3) and **b** DHA (22:6ω3) derived from *D. tertiolecta* in *P. littoralis* '•' and *T. longicornis* '∘' along a temperature gradient after 6 days. The shaded lines around the mean (dashed) per species represent the 95% confidence interval

for the high metabolic costs associated with the LC-PUFA deficient diet and warming pressure. Since the calanoid carbon assimilation did not significantly vary across the temperature range, this indicates that either this process is not regulated (*i.e.*, independent of temperature), or the experimental stress was heightened enough at 11 °C to induce maximum ingestion rates, assumed from carbon assimilation, to compensate for the temperature and diet stressors. In comparison, *P. littoralis* has relatively low assimilation rates, only increasing at the highest temperature treatment (23 °C). This—in conjunction with the retention of the relative field LC-PUFA concentrations—may indicate that *P. littoralis* does not require to increase assimilation to meet their metabolic demands until the extreme of 23 °C. The carbon assimilation rate in *P. littoralis* ranges from 0.075 to 0.214% day^{-1} at 11 and 23 °C, respectively, whereas it is on average 2.014% day^{-1} for *T. longicornis*. This suggests that *P. littoralis* increased assimilation of the labelled *D. tertiolecta* as temperatures increased, whereas *T. longicornis* maintained the same uptake throughout. The variation of *T. longicornis* carbon assimilation per TFA increased with temperature, whereas for *P. littoralis* replicates were quite similar. This increased variability between replicates is recognized as a biochemical indicator of environmental stress (Werbrouck et al. 2017).

Higher observed assimilation rates have been recorded in Antarctic calanoid species *Calanoides acutus* and *Calanus propinquus* of 3.1 and 3.9% day^{-1}, respectively, when fed on a diatom diet under natural temperature conditions (Graeve et al. 2020). The small herbivorous arctic calanoid *Pseudocalanus minutus* has demonstrated a more similar carbon assimilation rate to *T. longicornis* of 2.6% day^{-1}, while the cyclopoid *Oithona similis* has a carbon assimilation rate more similar to *P. littoralis* at 0.5% day^{-1}, when fed on a diatom dinoflagellate mixture at 4 °C (Boissonnot et al.

2016). These studies reporting the assimilation efficiency have been conducted under ambient sampling temperature and with higher food quality (presence of LC-PUFA), therefore individuals may have increased their uptake in response to these favourable conditions. Reduced ingestion of carbon in *T. longicornis* fed on *D. tertiolecta* has been previously recorded (Arendt et al. 2005). We suggest that the combined stress of a LC-PUFA deficient diet and temperature resulted in reduced rates of carbon assimilation for the two species investigated in this study in comparison to those reported in the literature. The low assimilation rates recorded in *P. littoralis* may be due to the preferential use or ability to retain its own relative lipid content rather than utilization of the poor external food source.

Although *T. longicornis* exhibits higher carbon incorporation into its TFA than *P. littoralis*, this does not restore the absolute FA concentrations to the levels observed in the field samples. There was a considerable reduction of EPA concentrations between field and experimental samples for both *T. longicornis* (~60% reduced) and *P. littoralis* (~32% reduced) (Fig. 2). A similar reduction of 33% was observed in *T. longicornis* DHA concentrations between field and experimental samples. For *T. longicornis* DHA concentrations have been shown to be an important factor contributing to reproductive success (Arendt et al. 2005). Comparatively, *P. littoralis* was able to retain the same DHA concentrations between the field and the temperature exposed samples after 6 days. This retention of DHA in *P. littoralis* fed a LC-PUFA deficient diet was similarly recorded by Boyen et al. (2020), where this species was exposed to +3 °C warming conditions for four additional days to this study. Considering the low fractions of EPA and DHA derived from *D. tertiolecta* in both *T. longicornis* (<0.001–0.002) and *P. littoralis* (<0.001–0.001) (Fig. 4, Table S4), under the experimental conditions described *T. longicornis* was not able to

biosynthesize EPA and DHA to restore their ω3-stores. This is in accordance with the observed poor ability of calanoids to biosynthesize LC-PUFA (Bell et al. 2007). The minor amounts of biosynthesized EPA and DHA by *T. longicornis* are presumed to be derived from FA precursors modified via front-end desaturases and elongase genes present in calanoids (Monroig and Kabeya 2018). Monitoring the differential gene expression of these aforementioned biosynthesis genes can help elucidate the specific pathways utilized (Nielsen et al. 2019). Previously, under LC-PUFA deficient conditions *P. littoralis* has been shown to have high assimilation of carbon into their EPA and DHA, thus demonstrating strong biosynthesis capabilities (0.088 ng DHA ind.$^{-1}$) (Werbrouck et al. 2017). However, this was still not sufficient to recover the individuals DHA stores (Werbrouck et al. 2017). Under our experimental conditions we observed the opposite, rather *P. littoralis* was able to retain its DHA stores while at the same time exhibited poor biosynthesis abilities (0.023 ng DHA ind.$^{-1}$), and lower than *T. longicornis*. Both species exhibited a lower fraction of EPA and DHA (Fig. 4) derived from the labelled food in comparison to tropical cyclopoid *Apocyclops royi* (EPA: 1.64%, DHA: 2.35%) and calanoid *Pseudodiaptomus annandalei* (EPA: 0.55%, DHA: 3.09%) fed *D. tertiolecta* after 48 h (Nielsen et al. 2020). Nielsen et al. (2020) proposes that the biosynthesis pathways are more active in these two brackish species since they naturally inhabit a PUFA-poor environment. Thus, the life-history feeding conditions and field PUFA availability may contribute to the copepods ability to utilize these pathways. We suggest that since DHA levels were maintained, the need for additional de novo biosynthesis was not necessary for *P. littoralis*. Alternatively, *P. littoralis* could maintain its DHA concentrations through the conversion of EPA, previously obtained in the field, to DHA (Monroig and Kabeya 2018), rather than utilizing FA obtained from the labelled experimental feed. However, as we cannot trace the modification of the FA acquired in the field with CSIA, we suggest monitoring via a gene-specific approach, once it is confirmed that biosynthesis pathways are being employed, or over multiple generations.

The species-specific response may be attributed to the difference of functional traits resulting from the unique stressors in their respective natural environments. Our results indicate that the harpacticoid, *P. littoralis*, appears to be more suited to more variable conditions than the calanoid *T. longicornis*. The differing lifestyles of pelagic calanoids and benthic harpacticoids can be linked to the abiotic stressors faced, energy demands throughout their lifespan, prey types encountered, and frequency of feeding periods. Since *P. littoralis* occupies the benthos, this species is more sedentary and expends less energy in comparison to *T. longicornis'* vertical movement throughout the water column (Hays et al. 2001). In the harsher intertidal conditions that

the harpacticoids inhabit, the temperature change can be more stochastic, ranging between 4 and 22 °C throughout the year (Sahan et al. 2007). Comparatively, calanoids in the pelagic environment experience temperature buffering effects from the water column, with short-term temperature change occurring at a slower rate than in the exposed mudflats. Large-scale poleward calanoid population displacements have also been noted, linked closely to temperature changes (Beaugrand et al. 2002), in relation to their planktonic nature. This justifies *P. littoralis'* short-term eurythermic survival response, *i.e.,* ability to tolerate a wide temperature range, compared to *T. longicornis'* more stenothermic survival response.

Field *T. longicornis* contained higher amounts of both DHA and EPA than *P. littoralis*, the ratios of 16:1ω7/16:0 < 1 and EPA/DHA < 1 indicated a non-diatom dominated diet, and the higher amounts of 18:4ω3 suggested a dinoflagellate abundant diet (Kelly and Scheibling 2012). Harpacticoids exhibit differences in the way they take up food, due to their contact with the sediment, they are able to ingest microphytobenthos indirectly through the consumption of bacteria or ciliates (Cnudde et al. 2015). As such, *P. littoralis* from the field contained higher relative amounts of 16:1ω7 and 16:1ω5, suggesting herbivorous feeding on microphytobenthos (Graeve et al. 1994), and bacterial markers (18:1ω7, 17:1) (Conway and McDowell Capuzzo 1991; Kelly and Scheibling 2012). Therefore, the energy stores in which these individuals entered the experiment are contrasting as are their FA requirements for optimal functioning, which may be attributed to the differences in their available prey field and life histories. The overall outcome of this study suggests that based on their FA dynamics, *P. littoralis* has a greater potential for resilience than *T. longicornis* under more extreme conditions due to the higher variability in their natural environment.

As 18:3ω3 (ALA) is present in high quantities in *D. tertiolecta*, this implies we are unable to quantify copepod biosynthesis of MUFA (*i.e*., 18:1ω9) into short-chain PUFA (*i.e*., linoleic acid (LA, 18:2ω6), ALA) by methyl-end desaturases (Kabeya et al. 2021). Therefore, if you wish to follow this specific pathway, baker's yeast could be used as an alternative to *D. tertiolecta*, as it contains no or very little ALA and no other LC-PUFA (Payne and Rippingale 2000; Nielsen et al. 2020). Additionally, synthesis of FA from acetyl coenzyme A (2C) is possible and can be monitored via the gene expression of specific enzymes in the FA synthase pathway (Tarrant et al. 2016). In future harpacticoid studies we suggest monitoring the triggers resulting in high assimilation prior to investigating biosynthesis regulation. Potentially seasonality and field FA composition may play a role in regulating *P. littoralis* biosynthesis pathways, as these were the primary difference between our study and Werbrouck et al. (2017). Separation of the lipid classes into

non-polar and polar fractions prior to CSIA may be interesting to understand how individuals regulate their membrane versus storage lipids during the experimental treatment (Parrish 2013; Werbrouck et al. 2017). Measures of fitness, such as reproductive success, should be considered to quantify the significance of EPA and DHA loss and production.

Conclusions

This study fills the gap of the knowledge of the FA response and biosynthesis capabilities in two species of copepods under the same experimental temperature conditions. *P. littoralis* did not assimilate dietary carbon readily, and thus had a LC-PUFA biosynthesis rate that is lower than what is found in other copepods (Boissonnot et al. 2016; Graeve et al. 2020). *T. longicornis* displayed higher fractions of de novo biosynthesis of EPA and DHA than *P. littoralis* at all temperatures, with the exception of DHA at 23 °C. This temperature was the most stressful for the calanoid displaying a higher mortality with warming. Comparatively, the harpacticoid was eurythermal, with survival independent of temperature.

Although there may be a reduction in absolute ω3 LC-PUFA availability in primary producers (Hixson and Arts 2016; Colombo et al. 2020; Holm et al. 2022), it is important to consider that complete absence, as in our experiment, is not a realistic scenario. Despite the fact that *T. longicornis* demonstrated higher de novo production, albeit not in sufficient amounts, individuals depleted their field EPA and DHA stores more rapidly. This indicates that *T. longicornis* is not able to biosynthesize EPA and DHA at a rate necessary for basic metabolic functioning. Conversely, *P. littoralis* has maintained its relative storage of EPA and DHA and absolute concentrations of DHA, suggesting these extremes are within their coping capacity. Under the stressors imposed, *P. littoralis* has a greater potential for resilience when faced with extreme temperature conditions than *T. longicornis*. Within our experimental incubation both species were unable to meaningfully upgrade the LC-PUFA deficient algae to biosynthesize de novo EPA and DHA as a relevant source for higher trophic levels.

Declarations

References

Ackman RG, Sipos JC (1964) Application of specific response factors in the gas chromatographic analysis of methyl esters of fatty acids with flame ionization detectors. J Am Oil Chem Soc 41:377–378. https://doi.org/10.1007/BF02654818

Arendt KE, Jónasdóttir SH, Hansen PJ, Gärtner S (2005) Effects of dietary fatty acids on the reproductive success of the calanoid copepod Temora longicornis. Mar Biol. https://doi.org/10.1007/s00227-004-1457-9

Beaugrand G, Reid PC, Ibañez F, Lindley JA, Edwards M (2002) Reorganization of North Atlantic marine copepod biodiversity and climate. Science 296:1692–1694. https://doi.org/10.1126/science.1071329

Beaugrand G, Brander KM, Alistair Lindley J, Souissi S, Reid PC (2003) Plankton effect on cod recruitment in the North Sea. Nature 426:661–664. https://doi.org/10.1038/nature02164

Bell MV, Dick JR, Anderson TR, Pond DW (2007) Application of liposome and stable isotope tracer techniques to study polyunsaturated fatty acid biosynthesis in marine zooplankton. J Plankton Res 29:417–422. https://doi.org/10.1093/plankt/fbm025

Bell MV, Tocher DR (2009) Biosynthesis of polyunsaturated fatty acids in aquatic ecosystems: general pathways and new directions. In: Kainz M, Brett MT, Arts MT (eds) Lipids in Aquatic Ecosystems. Springer, New York, pp 211–236

Bertram DF, Mackas DL, Welch DW, Boyd WS, Ryder JL, Galbraith M, Hedd A, Morgan K, O'Hara PD (2017) Variation in zooplankton prey distribution determines marine foraging distributions of breeding Cassin's Auklet. Deep Sea Res Part I 129:32–40. https://doi.org/10.1016/j.dsr.2017.09.004

Boissonnot L, Niehoff B, Hagen W, Søreide JE, Graeve M (2016) Lipid turnover reflects life-cycle strategies of small-sized Arctic copepods. J Plankton Res. https://doi.org/10.1093/plankt/fbw076

Cnudde C, Moens T, Werbrouck E, Lepoint G, Van Gansbeke D, De Troch M (2015) Trophodynamics of estuarine intertidal harpacticoid copepods based on stable isotope composition and fatty acid profiles. Mar Ecol Prog Ser 524:225–239. https://doi.org/10.3354/meps11161

Colombo SM, Rodgers TFM, Diamond ML, Bazinet RP, Arts MT (2020) Projected declines in global DHA availability for human

consumption as a result of global warming. Ambio 49:865–880. https://doi.org/10.1007/s13280-019-01234-6

Conway N, McDowell Capuzzo J (1991) Incorporation and utilization of bacterial lipids in theSolemya velum symbiosis. Mar Biol 108:277–291. https://doi.org/10.1007/BF01344343

Coull BC (1990) Are members of the Meiofauna food for higher trophic levels? Trans Am Microsc Soc. https://doi.org/10.2307/3226794

Cronin TW, Fasick JI, Schweikert LE, Johnsen S, Kezmoh LJ, Baumgartner MF (2017) Coping with copepods: do right whales (Eubalaena glacialis) forage visually in dark waters? Philos Trans the Royal Soc Biol Sci 372:20160067–20160067. https://doi.org/10.1098/rstb.2016.0067

Daase M, Falk-Petersen S, Varpe Ø, Darnis G, Søreide JE, Wold A, Leu E, Berge J, Philippe B, Fortier L (2013) Timing of reproductive events in the marine copepod Calanus glacialis: A pan-Arctic perspective. Can J Fish Aquat Sci 70:871–884. https://doi.org/10.1139/cjfas-2012-0401

De Troch M, Boeckx P, Cnudde C, Van Gansbeke D, Vanreusel A, Vincx M, Caramujo MJ (2012) Bioconversion of fatty acids at the basis of marine food webs: Insights from a compound-specific stable isotope analysis. Mar Ecol Prog Ser. https://doi.org/10.3354/meps09920

Deschutter Y, De Schamphelaere K, Everaert G, Mensens C, De Troch M (2019) Seasonal and spatial fatty acid profiling of the calanoid copepods Temora longicornis and Acartia clausi linked to environmental stressors in the North Sea. Mar Environ Res. https://doi.org/10.1016/j.marenvres.2018.12.008

Frederiksen M, Anker-Nilssen T, Beaugrand G, Wanless S (2013) Climate, copepods and seabirds in the boreal Northeast Atlantic - current state and future outlook. Glob Change Biol. https://doi.org/10.1111/gcb.12072

Garzke J, Ismar SMH, Sommer U (2015) Climate change affects low trophic level marine consumers: warming decreases copepod size and abundance. Oecologia 177:849–860. https://doi.org/10.1007/s00442-014-3130-4

Garzke J, Hansen T, Ismar SMH, Sommer U (2016) Combined effects of ocean warming and acidification on copepod abundance, body size and fatty acid content. PLoS One. https://doi.org/10.1371/journal.pone.0155952

Gee JM (1987) Impact of epibenthic predation on estuarine intertidal harpacticoid copepod populations. Mar Biol. https://doi.org/10.1007/BF00397967

Graeve M, Kattner G, Hagen W (1994) Diet-induced changes in the fatty acid composition of Arctic herbivorous copepods: Experimental evidence of trophic markers. J Exp Mar Biol Ecol 182:97–110. https://doi.org/10.1016/0022-0981(94)90213-5

Graeve M, Boissonnot L, Niehoff B, Hagen W, Kattner G (2020) Assimilation and turnover rates of lipid compounds in dominant Antarctic copepods fed with 13 C-enriched diatoms. Philos Trans Royal Soc Biol Sci 375:20190647–20190647. https://doi.org/10.1098/rstb.2019.0647

Gulati R, Demott W (1997) The role of food quality for zooplankton: remarks on the state-of-the-art, perspectives and priorities. Freshw Biol 38:753–768

Haman J (2020) Quasibinomial model in R glm(). In: Random Effect. https://randomeffect.net/post/2020/10/12/quasi-binomial-in-r-glm/.

Hays GC, Kennedy H, Frost BW (2001) Individual variability in diel vertical migration of a marine copepod: Why some individuals remain at depth when others migrate. Limnol Oceanogr 46:2050–2054. https://doi.org/10.4319/lo.2001.46.8.2050

Hays G, Richardson A, Robinson C (2005) Climate change and marine plankton. Trends Ecol Evol 20:337–344. https://doi.org/10.1016/j.tree.2005.03.004

Helenius L, Budge SM, Nadeau H, Johnson CL (2020) Ambient temperature and algal prey type affect essential fatty acid incorporation and trophic upgrading in a herbivorous marine copepod. Philos Trans Royal Soc Biol Sci. https://doi.org/10.1098/rstb.2020.0039

Hixson SM, Arts MT (2016) Climate warming is predicted to reduce omega-3, long-chain, polyunsaturated fatty acid production in phytoplankton. Glob Change Biol. https://doi.org/10.1111/gcb.13295

Holm HC, Fredricks HF, Bent SM, Lowenstein DP, Ossolinski JE, Becker KW, Johnson WM, Schrage K, Van Mooy BAS (2022) Global ocean lipidomes show a universal relationship between temperature and lipid unsaturation. Science 376:1487–1491. https://doi.org/10.1126/science.abn7455

Hothorn T, Bretz F, Westfall P (2008) Simultaneous inference in general parametric models. Biom J 50:346–363

Jónasdóttir SH, Visser AW, Richardson K, Heath MR (2015) Seasonal copepod lipid pump promotes carbon sequestration in the deep North Atlantic. Proc Natl Acad Sci 112:12122–12126. https://doi.org/10.1073/pnas.1512110112

Kabeya N, Fonseca MM, Ferrier DEK, Navarro JC, Bay LK, Francis DS, Tocher DR, Filipe L, Castro C, Monroig Ó (2018) Genes for de novo biosynthesis of omega-3 polyunsaturated fatty acids are widespread in animals. Sci Adv. https://doi.org/10.1126/sciadv.aar6849

Kabeya N, Ogino M, Ushio H, Haga Y, Satoh S, Navarro JC, Monroig Ó (2021) A complete enzymatic capacity for biosynthesis of docosahexaenoic acid (DHA, 22: 6n–3) exists in the marine Harpacticoida copepod Tigriopus californicus. Open Biol. https://doi.org/10.1098/rsob.200402

Kattner G, Hagen W (2009) Lipids in marine copepods: latitudinal characteristics and perspective to global warming. Lipids in Aquatic Ecosystems. Springer, New York, pp 257–280

Kelly J, Scheibling R (2012) Fatty acids as dietary tracers in benthic food webs. Mar Ecol Prog Ser 446:1–22. https://doi.org/10.3354/meps09559

Kwiatkowski L, Torres O, Bopp L, Aumont O, Chamberlain M, Christian JR, Dunne JP, Gehlen M, Ilyina T, John JG, Lenton A, Li H, Lovenduski NS, Orr JC, Palmieri J, Santana-Falcón Y, Schwinger J, Séférian R, Stock CA, Tagliabue A, Takano Y, Tjiputra J, Toyama K, Tsujino H, Watanabe M, Yamamoto A, Yool A, Ziehn T (2020) Twenty-first century ocean warming, acidification, deoxygenation, and upper-ocean nutrient and primary production decline from CMIP6 model projections. Biogeosciences 17:3439–3470. https://doi.org/10.5194/bg-17-3439-2020

Lampitt RS, Noji T, Von Bodungen B (1990) What happens to zooplankton faecal pellets? Implications for material flux. Springer-Verlag, Berlin

Lee MC, Choi BS, Kim MS, Yoon DS, Park JC, Kim S, Lee JS (2020) An improved genome assembly and annotation of the Antarctic copepod Tigriopus kingsejongensis and comparison of fatty acid metabolism between T. kingsejongensis and the temperate copepod T. japonicus. Compar Biochem Physiol Part D Genom Proteom. https://doi.org/10.1016/j.cbd.2020.100703

Malzahn AM, Boersma M (2012) Effects of poor food quality on copepod growth are dose dependent and non-reversible. Oikos 121:1408–1416. https://doi.org/10.1111/j.1600-0706.2011.20186.x

McGinty N, Barton AD, Record NR, Finkel ZV, Johns DG, Stock CA, Irwin AJ (2021) Anthropogenic climate change impacts on copepod trait biogeography. Glob Change Biol 27:1431–1442. https://doi.org/10.1111/gcb.15499

Meyer JL (1994) The microbial loop in flowing waters. Microb Ecol. https://doi.org/10.1007/BF00166808

Monroig Ó, Kabeya N (2018) Desaturases and elongases involved in polyunsaturated fatty acid biosynthesis in aquatic invertebrates: a comprehensive review. Fish Sci 84:911–928. https://doi.org/10.1007/s12562-018-1254-x

Moreno VJ, De Moreno JEA, Brenner RR (1979) Fatty acid metabolism in the calanoid copepodParacalanus parvus: 1. Polyunsaturated fatty acids. Lipids 14:313–317. https://doi.org/10.1007/BF02533413

Nielsen BLH, Gøtterup L, Jørgensen TS, Hansen BW, Hansen LH, Mortensen J, Jepsen PM (2019) n-3 PUFA biosynthesis by the copepod Apocyclops royi documented using fatty acid profile analysis and gene expression analysis. Biol Open. https://doi.org/10.1242/bio.038331

Nielsen BLH, van Someren GH, Rayner TA, Hansen BW (2020) Biochemical adaptation by the tropical copepods apocyclops royi and pseudodiaptomus annandalei to a pufa-poor brackish water habitat. Mar Ecol Prog Ser 655:77–89. https://doi.org/10.3354/meps13536

Parrish CC (2013) Lipids in marine ecosystems. ISRN Oceanograp 2013:1–16. https://doi.org/10.5402/2013/604045

Payne MF, Rippingale RJ (2000) Evaluation of diets for culture of the calanoid copepod Gladioferens imparipes. Aquaculture 187:85–96. https://doi.org/10.1016/S0044-8486(99)00391-9

R Core Team (2021) R: A language and environment for statistical computing.

Ratnayake WMN, Galli C (2009) Fat and fatty acid terminology, methods of analysis and fat digestion and metabolism: a background review paper. Ann Nutr Metab 55:8–43. https://doi.org/10.1159/000228994

Richardson AJ (2008) In hot water: Zooplankton and climate change

Sahan E, Sabbe K, Creach V, Hernandez-Raquet G, Vyverman W, Stal LJ, Muyzer G (2007) Community structure and seasonal dynamics of diatom biofilms and associated grazers in intertidal mudflats. Aquat Microb Ecol. https://doi.org/10.3354/ame047253

Semmouri I, De Schamphelaere KAC, Willemse S, Vandegehuchte MB, Janssen CR, Asselman J (2021) Metabarcoding reveals hidden species and improves identification of marine zooplankton communities in the North Sea. ICES J Mar Sci 78:3411–3427. https://doi.org/10.1093/icesjms/fsaa256

Semmouri I (2022) Temporal effects of chemical and physical stressors on marine zooplankton: a molecular approach. Ghent University, Faculty of Bioscience Engineering

Stenseth NC, Mysterud A, Ottersen G, Hurrell JW, Chan K-S, Lima M (2002) Ecological effects of climate fluctuations. Science 297:1292–1296. https://doi.org/10.1126/science.1071281

Stock W, Heylen K, Sabbe K, Willems A, De Troch M (2014) Interactions between benthic copepods, bacteria and diatoms promote nitrogen retention in intertidal marine sediments. PLoS ONE. https://doi.org/10.1371/journal.pone.0111001

Tarrant AM, Baumgartner MF, Lysiak NSJ, Altin D, Størseth TR, Hansen BH (2016) Transcriptional profiling of metabolic transitions during development and diapause preparation in the copepod *Calanus finmarchicus*. Integr Comp Biol 56:1157–1169. https://doi.org/10.1093/icb/icw060

Thor P, Koski M, Tang K, Jónasdóttir S (2007) Supplemental effects of diet mixing on absorption of ingested organic carbon in the marine copepod Acartia tonsa. Mar Ecol Prog Ser 331:131–138. https://doi.org/10.3354/meps331131

Turner JT (2004) The importance of small planktonic copepods and their roles in pelagic marine food webs

Twining CW, Taipale SJ, Ruess L, Bec A, Martin-Creuzburg D, Kainz MJ (2020) Stable isotopes of fatty acids: current and future perspectives for advancing trophic ecology. Philos Trans R Soc B 375:20190641. https://doi.org/10.1098/rstb.2019.0641

Werbrouck E, Bodé S, Van Gansbeke D, Vanreusel A, De Troch M (2017) Fatty acid recovery after starvation: insights into the fatty acid conversion capabilities of a benthic copepod (Copepoda, Harpacticoida). Marine Biol https://doi.org/10.1007/s00227-017-3181-2

Wolff RL, Bayard CC, Fabien RJ (1995) Evaluation of sequential methods for the determination of butterfat fatty acid composition with emphasis on trans -18:1 acids. Application to the study of seasonal variations in french butters. J Am Oil Chem Soc 72:1471–1483. https://doi.org/10.1007/BF02577840

Wood SN (2011) Fast stable restricted maximum likelihood and marginal likelihood estimation of semiparametric generalized linear models. J Royal Statist Soc Series B Statist Methodol. https://doi.org/10.1111/j.1467-9868.2010.00749.x

ORIGINAL ARTICLE

MOLECULAR ECOLOGY WILEY

Functional characterization reveals a diverse array of metazoan fatty acid biosynthesis genes

Jens Boyen[1] | Alberto Ribes-Navarro[2] | Naoki Kabeya[3] | Óscar Monroig[2] | Annelien Rigaux[1] | Patrick Fink[4,5,6] | Pascal I. Hablützel[7] | Juan Carlos Navarro[2] | Marleen De Troch[1]

[1]Marine Biology, Department of Biology, Ghent University, Ghent, Belgium

[2]Instituto de Acuicultura Torre de la Sal (IATS), CSIC, Ribera de Cabanes, Spain

[3]Department of Marine Biosciences, Tokyo University of Marine Science and Technology, Tokyo, Japan

[4]Department of River Ecology, Helmholtz Centre for Environmental Research – UFZ, Magdeburg, Germany

[5]Department of Aquatic Ecosystem Analysis and Management, Helmholtz Centre for Environmental Research – UFZ, Magdeburg, Germany

[6]Aquatic Chemical Ecology, Institute for Zoology, University of Cologne, Cologne, Germany

[7]Flanders Marine Institute (VLIZ), Oostende, Belgium

Correspondence
Jens Boyen, Marine Biology, Department of Biology, Ghent University, Ghent, Belgium.
Email: jens.boyen@ugent.be

Funding information
Fonds Wetenschappelijk Onderzoek, Grant/Award Number: 11E2320N, I001621N and V431420N; Japan Society for the Promotion of Science, Grant/Award Number: JP19K15908 and JP20KK0348; Ministerio de Ciencia, Innovación y Universidades, Grant/Award Number: RTI2018-095119-B-100; Universiteit Gent, Grant/Award Number: GOA 01GA2617

Handling Editor: Sean Rogers

Abstract

Long-chain ($\geq C_{20}$) polyunsaturated fatty acids (LC-PUFAs) are physiologically important fatty acids for most animals, including humans. Although most LC-PUFA production occurs in aquatic primary producers such as microalgae, recent research indicates the ability of certain groups of (mainly marine) invertebrates for endogenous LC-PUFA biosynthesis and/or bioconversion from dietary precursors. The genetic pathways for and mechanisms behind LC-PUFA biosynthesis remain unknown in many invertebrates to date, especially in non-model species. However, the numerous genomic and transcriptomic resources currently available can contribute to our knowledge of the LC-PUFA biosynthetic capabilities of metazoans. Within our previously generated transcriptome of the benthic harpacticoid copepod *Platychelipus littoralis*, we detected expression of one methyl-end desaturase, one front-end desaturase, and seven elongases, key enzymes responsible for LC-PUFA biosynthesis. To demonstrate their functionality, we characterized eight of them using heterologous expression in yeast. The *P. littoralis* methyl-end desaturase has $\Delta15/17/19$ desaturation activity, enabling biosynthesis of α-linolenic acid, eicosapentaenoic acid and docosahexaenoic acid (DHA) from $18:2n-6$, $20:4n-6$ and $22:5n-6$, respectively. Its front-end desaturase has $\Delta4$ desaturation activity from $22:5n-3$ to DHA, implying that *P. littoralis* has multiple pathways to produce this physiologically important fatty acid. All studied *P. littoralis* elongases possess varying degrees of elongation activity for saturated and unsaturated fatty acids, producing aliphatic hydrocarbon chains with lengths of up to 30 carbons. Our investigation revealed a functionally diverse range of fatty acid biosynthesis genes in copepods, which highlights the need to scrutinize the role that primary consumers could perform in providing essential nutrients to upper trophic levels.

KEYWORDS
functional characterization, harpacticoids copepods, heterologous expression, polyunsaturated fatty acid biosynthesis

1 | INTRODUCTION

Long-chain (≥C_{20}) polyunsaturated fatty acids (LC-PUFAs), including arachidonic acid (ARA, 20:4n−6), eicosapentaenoic acid (EPA, 20:5n−3) and docosahexaenoic acid (DHA, 22:6n−3), are key nutritional components that are particularly abundant in marine ecosystems but are also vital for the functioning of freshwater and terrestrial ecosystems (Bell & Tocher, 2009; Závorka et al., 2023). In animals specifically, LC-PUFAs play important roles in energy storage, lipid membrane structures, signalling pathways (as precursors of eicosanoids) and gene regulation (Bazinet & Layé, 2014; Tocher, 2015). While widely distributed, LC-PUFAs are particularly abundant in aquatic ecosystems, especially in marine waters (Colombo et al., 2017). Due to global climate change and rising water temperatures, the production of LC-PUFAs in phytoplankton and other microalgae is expected to decrease significantly (Hixson & Arts, 2016; Holm et al., 2022). This predicted temperature-related LC-PUFA reduction occurs due to changes in the lipid composition of cell membranes through a process known as homeoviscous adaptation (Sinensky, 1974). Moreover, changes in phytoplankton community composition and declining net primary production could further impair global LC-PUFA availability (Bi et al., 2021; Kwiatkowski et al., 2020). This will consequently have an impact on organisms at higher trophic levels via trophic cascading (Colombo et al., 2020).

The increasing availability of genomic data on multiple invertebrate taxa facilitates the investigation of the LC-PUFA biosynthetic pathways at a molecular level by characterization of its key biosynthesizing enzymes (Figure 1) (Monroig et al., 2022). Stearoyl-CoA-desaturase (*scd*), also known as Δ9 desaturase, is present in all eukaryotes and enables the first desaturation from stearic acid (18:0) to oleic acid (OA, 18:1n−9). It was long assumed that endogenous further de novo LC-PUFA biosynthesis is restricted to (micro-)

algae, bacteria and heterotrophic protists, and that metazoans need to cover their LC-PUFA needs through their diet. In aquatic habitats microalgae supposedly synthesize the major LC-PUFAs, which are then transferred to higher trophic levels via first-order consumers. However, this assumption has been challenged in recent years by the discovery of a particular type of enzyme termed "methyl-end desaturases" in numerous groups of (mainly marine) invertebrates such as cnidarians, nematodes, arthropods, annelids and molluscs (Kabeya et al., 2018; Malcicka et al., 2018; Zhou et al., 2008). Methyl-end desaturases, previously reported mostly in plants, algae and microbes, introduce a double bond between the pre-existing one and the methyl-end of the carbon chain. They are required for de novo biosynthesis of the C_{18} PUFAs linoleic acid (LA, 18:2n−6) and α-linolenic acid (ALA, 18:3n−3) from OA. Hence, these enzymes allow a consumer to not only depend upon exogenously (i.e., via their diet) supplied precursors required to biosynthesize LC-PUFAs (Monroig et al., 2022). The ecological implications of the occurrence of methyl-end desaturases in invertebrates have been largely disregarded so far, and many trophic ecology studies using FAs as trophic markers still assume that metazoans lack the capacity to endogenously produce LA and ALA, an issue also addressed by Galloway and Budge (2020).

The conversion of LA and ALA into ARA and EPA, respectively, occurs by the sequential reaction of front-end desaturases and elongases. While front-end desaturases introduce a double bond between the pre-existing one and the front-end of the carbon chain, elongases are the critical catalysing enzymes in the two-carbon chain elongation process (Bell & Tocher, 2009). Two possible pathways enabling ARA and EPA biosynthesis are known to exist, which are the so-called "Δ6 pathway" (Δ6 desaturation – elongation – Δ5 desaturation) and the "Δ8 pathway" (elongation – Δ8 desaturation – Δ5 desaturation) (Figure 1). Similarly, the production of DHA from
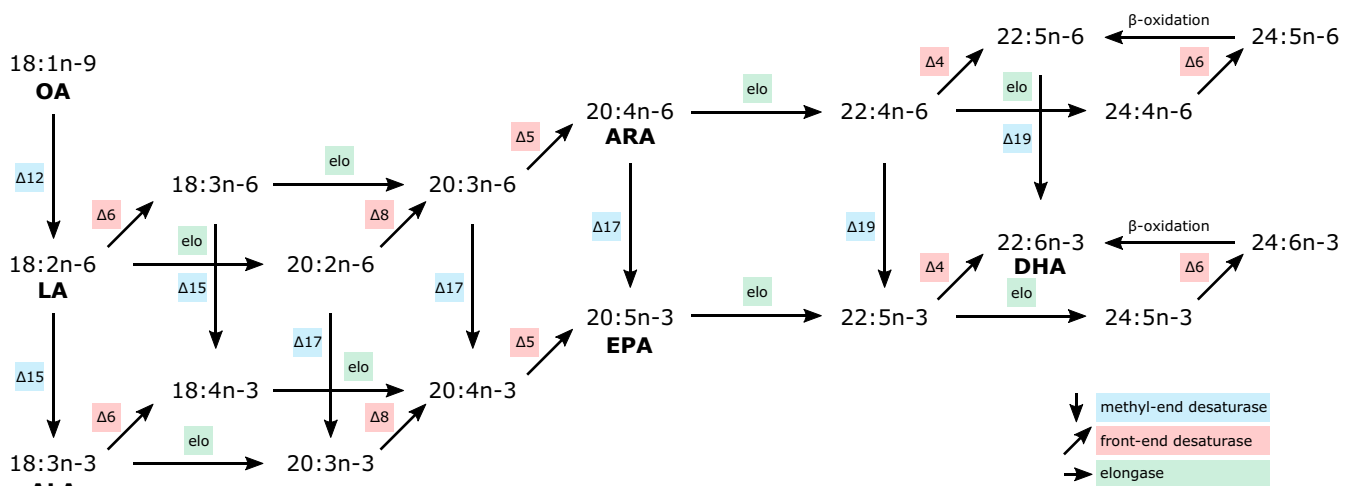

FIGURE 1 Theoretical polyunsaturated fatty acid biosynthesis pathway in metazoans. Methyl-end desaturase reactions in blue (vertical arrows), front-end desaturase reactions in red (diagonal arrows), and elongase reactions in green (horizontal arrows). Desaturase reactions are further specified by "Δy", with "y" referring to the location of insertion of the double bond counting from the methyl-end of the carbon chain. β-oxidation reactions are also shown (horizontal reverse arrows) but not included in this study. OA, oleic acid; LA, linoleic acid; ALA, α-linolenic acid; ARA, arachidonic acid; EPA, eicosapentaenoic acid; DHA, docosahexaenoic acid. Adapted from Monroig et al. (2022). [Colour figure can be viewed at wileyonlinelibrary.com]

EPA can be performed via two pathways, namely the "Sprecher pathway" which involves two consecutive elongations and a Δ6 desaturation toward 24:6n−3 followed by a β-oxidation to DHA, and the "Δ4 pathway" involving only one elongation from EPA and one Δ4 desaturation (Figure 1). The presence and activity of each of the enzymes determine an organism's capacity for LC-PUFA biosynthesis from endogenously produced or dietary obtained FAs (Monroig et al., 2022; Monroig & Kabeya, 2018).

Copepods are a globally distributed and highly abundant group of crustaceans that perform pivotal ecological functions at the basis of aquatic food webs (George et al., 2020). They are primary consumers of microalgae and are important prey for higher trophic levels, such as early life-cycle stages of fish (Gee, 1987) to which they provide essential nutrients including LC-PUFAs. Indeed, copepods generally have high levels of LC-PUFAs, particularly DHA, but whether these LC-PUFAs have an exclusive dietary origin or are, to some extent, produced endogenously remains unclear. Dietary studies in which copepods were fed diets lacking LC-PUFAs, or were given diets or specific FAs labelled with stable isotopes, suggest that multiple copepod species have the capacity for endogenous production of LC-PUFAs including DHA from ALA and/or possibly even OA (Arndt & Sommer, 2014; Caramujo et al., 2008; De Troch et al., 2012; Desvilettes et al., 1997; Farkas et al., 1981; Moreno et al., 1979; Nanton & Castell, 1998, 1999; Nielsen et al., 2020; Titocci & Fink, 2022; Werbrouck et al., 2017). While similar evidence is scarce for other aquatic primary consumers, their potential ability for endogenous LC-PUFA biosynthesis and conversion raises questions about their role and importance in aquatic food webs, especially in the context of future environmental changes.

Recent extensive revisions of the repertoire and functions of desaturases and elongases involved in LC-PUFA biosynthesis of invertebrates illustrate the remarkably high diversity in comparison to vertebrates (Monroig et al., 2022; Monroig & Kabeya, 2018). Among copepods, our knowledge on the LC-PUFA biosynthesis pathways remains fragmentary as only a subset of genes has been scrutinized in few species (Kabeya et al., 2018, 2021). Heterologous expression in a model system such as the yeast *Saccharomyces cerevisiae* is an ideal benchmark method to verify the function of a candidate gene (Monroig et al., 2022). This method can eliminate the possibility of the gene being a defunct pseudogene, and/or that the observed LC-PUFA biosynthesis is performed by microbial activity (Kabeya et al., 2021). While LC-PUFA biosynthesis genes have been identified in harpacticoid, cyclopoid and siphonostomatoid copepods (Amparyup et al., 2022; Boyen et al., 2020; Kabeya et al., 2018, 2021; Lee, Choi, Kim, et al., 2020; Lee, Choi, Park, et al., 2020; Nielsen et al., 2019), functional characterization has only been performed on genes from the parasitic siphonostomatoid *Lepeophtheirus salmonis* (methyl-end desaturases) and the rocky intertidal harpacticoid *Tigriopus californicus* (methyl-end desaturases, front-end desaturases and elongases) (Kabeya et al., 2018, 2021).

While phylogenetic analyses suggest that LC-PUFA elongase and desaturase activity might be common across a diverse range of metazoan taxa, we lack direct empirical evidence to generalize this finding even among closely related species. Therefore, the aim of this work was to perform a phylogenetic exploration of crustacean (mainly copepod) methyl-end desaturases, front-end desaturases and elongases, and clone and functionally characterize a total of eight desaturases and elongases of the benthic harpacticoid copepod *Platychelipus littoralis* (Brady, 1880), using heterologous expression in yeast. The transcriptome of *P. littoralis* has been generated in an earlier study (Boyen et al., 2020). While often disregarded due to their small size and subsequent difficulty to collect, study and cultivate in laboratory environments, harpacticoid copepods play a pivotal role at the algae-animal interface of benthic food webs and thus the overall functioning of marine sediment communities (Hicks & Coull, 1983). Knowing their LC-PUFA biosynthesis capacity will allow us to better understand the role of not only *P. littoralis* but potentially benthic copepods in general as LC-PUFA providers within the marine ecosystem. *Platychelipus littoralis* was found to have a temperature-mediated capacity for endogenous LC-PUFA biosynthesis (Boyen et al., 2020; Werbrouck et al., 2016, 2017), yet functional molecular evidence is still lacking. Detailed knowledge of the metabolic pathways of LC-PUFA biosynthesis will allow the use of copepods as model organisms to study the effects of global warming on LC-PUFA-mediated food web interactions.

2 | MATERIALS AND METHODS

2.1 | Protein identification and phylogenetic analysis

To perform the phylogenetic analysis, sequences from various crustacean species were retrieved from NCBI GenBank through BLAST (tblastn), using, as queries, the sequences of the functionally characterized *T. californicus* desaturases and elongases (Kabeya et al., 2018, 2021). Sequences were only selected when they contained the full-length open reading frame (ORF) and their predicted protein sequences contained specific features according to Hashimoto et al. (2008). Briefly, front-end desaturases had to contain three diagnostic histidine boxes (H-box) "HXXXH", "HXXXHH" and "QXXHH" and a heme binding motif (HPGG) in the cytochrome b5 domain. Putative desaturase sequences with the third box "HXXHH" instead of "QXXHH" were not regarded as front-end desaturases based on evidence collected from other crustaceans suggesting these enzymes lack fatty acyl desaturation capacity (Monroig et al., 2022; Monroig & Kabeya, 2018). Methyl-end desaturases had to contain the three H-boxes "HXXXH", "HXXHH" and "HXXHH" and had to lack the cytochrome b5 domain. Fatty acid elongases had to contain the H-box "HXXHH" or "QXXHH" (Boyen et al., 2020; Hashimoto et al., 2008; Kabeya et al., 2021). For *P. littoralis* specifically, sequences were retrieved from the previously assembled transcriptome (NCBI BioProject PRJNA575120). The phylogenetic analysis was completed with the addition of sequences of functionally characterized genes from *T. californicus*, *L. salmonis*, *Platynereis dumerilli*, *Hediste diversicolor*, *Leishmania major* (Kabeya et al., 2018, 2020,

2021; Tripodi et al., 2006), as well as human sequences. The deduced protein sequences were aligned using MAFFT version 7.490 (Katoh & Standley, 2013) using the E-INS-i method. For each gene family, a maximum-likelihood phylogenetic tree was built using RAxML version 8.2.4 (Stamatakis, 2014) with a GAMMA model of rate heterogeneity, automatic selection of the best protein substitution model (MTZOA for methyl-end desaturases, LG for front-end desaturases and elongases), and 100 bootstrap replicates. The final trees were rooted with an outgroup (*P. dumerilli* and *H. diversicolor* for the methyl-end desaturases and *L. major* for the front-end desaturases) or using midpoint rooting (for the elongases). Trees were visualized and edited with FigTree version 1.4.3 (http://tree.bio.ed.ac.uk/soft-ware/figtree).

2.2 | Plasmid construction and transformation in yeast

Platychelipus littoralis adult specimens were collected from the top sediment layer of the Paulina intertidal mudflat (Westerscheldt estuary, The Netherlands; 51°21' N, 3°43' E) (Boyen et al., 2020). Total RNA was extracted from 50 pooled individuals using the RNeasy Plus Micro Kit (QIAGEN) following a modified protocol (Boyen et al., 2020). Total RNA quality and quantity were assessed by NanoDrop 2000 spectrophotometer (Thermo Fisher Scientific) and 2100 Bioanalyser (Agilent Technologies). cDNA was synthesized using the Maxima H Minus First Strand cDNA Synthesis Kit (Thermo Fisher Scientific) with dsDNase treatment to remove potential genomic DNA contamination. The full-length ORF sequences of one methyl-end desaturase, one front-end desaturase and six elongases were amplified by PCR from *P. littoralis* cDNA using high-fidelity Phusion Hot Start II DNA Polymerase (Thermo

Fisher Scientific) and primers containing restriction enzyme sites (Table 1). RestrictionMapper (www.restrictionmapper.org) was used to select restriction enzymes which would not cut internally within the corresponding ORF sequence. The calculation of the annealing temperature and GC content (ThermoFisher Scientific Tm Calculator) was done only using the primer sequence part specific to the DNA fragment to be amplified. All PCR runs consisted of an initial denaturation step of 30s at 98°C, 35 cycles of 10 s at 98°C, 30s at the sequence-specific amplification temperature (Table 1) and 30s at 72°C, ending with a final extension step of 10 min at 72°C. The PCR products were purified with Purelink PCR Purification Kit (Thermo Fisher Scientific) and subsequently digested with the corresponding restriction enzymes (New England Biolabs) (Table 1). The restricted ORF fragments were ligated (T4 DNA ligase, Promega) into a similarly restricted pYES2 yeast expression vector and transformed into One Shot TOP10F´ chemically competent *E. coli* cells. Positive transformant colonies were grown overnight in LB broth containing ampicillin (50μg/ml). Plasmids were purified with PureLink HiPure Plasmid Miniprep Kit, sequenced using T7 forward and CYC1 reverse primers (Macrogen Europe) and compared with the original sequences from the transcriptome assembly. Concentrations of raw and restricted PCR products, ligated vectors and purified plasmids were all quantified using Qubit 2.0 dsDNA BR Assay Kit (Invitrogen).

2.3 | Functional characterization of *P. littoralis* desaturase and elongase genes

The plasmid constructs containing the ORF sequences of the *P. littoralis* desaturases and elongases were independently

TABLE 1 Original transcript contig (above) and coding sequence (below) NCBI accession numbers, restriction enzymes, sequences and annealing temperatures (T_A) of each gene

Gene	Accession numbers	Enzyme	Primer name	Primer sequence (5′-3′)	T_A (°C)
ωx	GHXK01184360	*Hind*III	plwxHF	CCCAAGCTTAAAATGTCGTCTAGAAGAAG	56.0
	ON075828	*Xho*I	plwxXR	CCGCTCGAGTCACTTAGACTTTGTATCGC	
fad	GHXK01205503	*Sac*I	plfadSF	CCCGAGCTCACCATGGATCCCTCAATAGA	59.8
	ON075829	*Xho*I	plfadXR	CCGCTCGAGTTATGACAGAAGCTTGTTGAAG	
elovl1a	GHXK01177303	*Hind*III	ple1aHF	CCCAAGCTTAAGATGAACGTCGTTTCTGAAAAATGG	64.5
	ON075830	*Xho*I	ple1aXR	CCGCTCGAGTCAATGTTGCTTTTTGTCGCTAGA	
elovl1b	GHXK01255463	*Sac*I	ple1bSF	CCCGAGCTCACCATGGCCACTCAGAA	61.1
	ON075831	*Xho*I	ple1bXR	CCGCTCGAGTCAATTTTCTTTTTTTGCAGCAGA	
elovl1c	GHXK01260983	*Sac*I	ple1cSF	CCCGAGCTCAAAATGAGTGAAACATTTTTGGACGG	61.9
	ON075832	*Xho*I	ple1cXR	CCGCTCGAGTTATGTACTTTTCTTCTTTTTCTGGTTG	
elovl1d	GHXK01228992	*Hind*III	ple1dHF	CCCAAGCTTAACATGCTGGATGTGTTAGTC	57.9
	ON075833	*Xho*I	ple1dXR	CCGCTCGAGTTATGTCACTTTTTTCTTGGAG	
elovl1e	GHXK01223266	*Hind*III	ple1eHF	CCCAAGCTTAGAATGACCAAGTCAGTGATCCC	65.1
	ON075834	*Xba*I	ple1eXbR	CCGTCTAGATTAGTCCAATTTTGTTGCATTTAAATGCC	
elovl4	GHXK01149108	*Hind*III	ple4HF	CCCAAGCTTACAATGGTTAGTGAAAATTTATATTCC	59.4
	ON075835	*Xho*I	ple4XR	CCGCTCGAGTCATTTCTTCTTTTTCTGAACAAC	

Note: Restriction sites are underlined.

transformed into *S. cerevisiae* competent cells (strain INVSc1) using the *S.c.* EasyComp yeast transformation kit (Invitrogen). The recombinant yeast cells were grown on *S. cerevisiae* minimal medium minus uracil (hereafter referred to as "SCMM⁻ᵘʳᵃ") agar plates for 3 days at 30°C, the optimal temperature for growth of *S. cerevisiae*. One individual colony per gene was individually grown in SCMM⁻ᵘʳᵃ broth for 48 h at 30°C to produce a bulk culture with an OD_{600} of 8–10. Subsequently, an appropriate volume of the yeast bulk cultures was diluted to an OD_{600} of 0.4 in 5 ml of SCMM⁻ᵘʳᵃ broth contained in a 250 ml Erlenmeyer flask. Each putative PUFA substrate was assayed in independent flasks. The Erlenmeyer flasks were incubated for 4 h at 30°C under constant shaking (250 rpm) until they reached an OD_{600} of approximately 1. At that point, cultures were supplemented with 2% galactose to induce transgene expression, and one of the putative PUFA substrates as follows. For the methyl-end desaturase, the exogenously supplied PUFA substrates were 18:2 n−6, 18:3 n−6, 20:2 n−6, 20:3 n−6, 20:4 n−6, 22:4 n−6 and 22:5 n−6. For the front-end desaturase, the PUFA substrates were 18:3 n−3, 18:2 n−6, 20:3 n−3, 20:2 n−6, 20:4 n−3, 20:3 n−6, 22:5 n−3 and 22:4 n−6. For the elongases, the PUFA substrates included 18:3 n−3, 18:2 n−6, 18:4 n−3, 18:3 n−6, 20:5 n−3, 20:4 n−6, 22:5 n−3 and 22:4 n−6. All PUFA substrates were purchased from Nu-Chek Prep, Inc. (Elysian), except 18:4 n−3 from Larodan AB and 20:4 n−3 from Cayman Chemicals. Each PUFA substrate was supplemented as sodium salts at concentrations of 0.5 mM (C_{18}), 0.75 mM (C_{20}) and 1.0 mM (C_{22}) as uptake efficiency decreases with increasing carbon chain length (Zheng et al., 2009). In addition, we wanted to determine the capacity of the *P. littoralis* methyl-end desaturase and elongases to utilize the yeast endogenous saturated and monounsaturated FAs as substrates. For this, transgenic yeast expressing either the methyl-end desaturase or one of the six elongases were grown in triplicate Erlenmeyer flasks supplemented with 2% galactose but without exogenously added FA substrates, in parallel with a control treatment consisting of yeast transformed with an empty pYES2 vector (n = 3). Yeast cultures were incubated again for 48 h at 30°C under constant shaking (250 rpm), harvested by centrifugation (2 min, 2000 rpm) and washed twice with double distilled H_2O. Yeast pellets were subsequently homogenized in 8:4:3 (v/v/v) chloroform:methanol:saline solution (0.88% KCl) containing 0.01% (w/v) butylated hydroxytoluene (BHT, Sigma-Aldrich) as antioxidant, and stored at −20°C under anaerobic conditions for a minimum of 24 h prior to FA analysis.

2.4 | Fatty acid analysis

Total lipids were extracted from the homogenized yeast samples with 8:4:3 (v/v/v) chloroform:methanol:saline solution (0.88% KCl)

according to the Folch method (Folch et al., 1957). Fatty acid methyl esters (FAMEs) were prepared through acid-catalysed transesterification and subsequently purified by thin–layer chromatography. FAMEs from the desaturase functional assays were analysed using a Thermo Trace GC Ultra (Thermo Electron Corporation) equipped with a fused silica 30 m × 0.25 mm open tubular column (Tracer, TR-WAX [film thickness 0.25 μm]; Teknokroma), coupled to a flame ionization detector. Identification was carried out by comparing the retention times with those from commercial FAME standards. Further confirmation of peaks and analysis of FAMEs from the elongase assays were carried out using an Agilent 6850 GC equipped with a mass spectrometry detector (5975 Series) and a 30 m × 0.25 mm open tubular column (Tracer, DB5-MS [film thickness 0.25 μm]; Teknokroma), and comparing the spectra against those from the NIST library. The conversion efficiency of all assayed *P. littoralis* enzymes toward the exogenously supplied PUFA substrates was calculated as: (all product areas/[all product areas + substrate area]) × 100 (Kabeya et al., 2021).

2.5 | Statistical analysis

The assays aiming to determine the ability of the *P. littoralis* methyl-end desaturase and elongases toward the yeast endogenous saturated and monounsaturated FAs were run in replicates (n = 3) and the FA contents were expressed as mean percentages ± standard deviation. Homogeneity of variances was checked using Levene's test. The FA profiles of control yeast and yeast expressing the methyl-end desaturase and the elongases were compared, and differences were statistically tested using Student's *t*-test for the methyl-end desaturase and Dunnett's multiple comparisons test for the elongases with $p ≤ .05$ indicating statistical significance. All statistical analyses were conducted in R version 4.0.2 (R Core Team, 2020).

3 | RESULTS

3.1 | Protein identification and phylogenetic inference

We constructed three phylogenetic trees of the metazoan methyl-end desaturases, front-end desaturases and elongases respectively (Figure 2). For each gene family, we found multiple subclades containing one or more sequences from different species. Each tree contains multiple well supported clades, however certain clades are not strongly supported. For *P. littoralis* specifically, we identified one putative methyl-end desaturase, one putative front-end desaturase and seven putative elongases. The *P. littoralis* methyl-end desaturase (ON075828) has the three specific H-boxes and lacks a cytochrome

FIGURE 2 Maximum-likelihood phylogenetic trees of (a) methyl-end desaturases (blue), (b) front-end desaturases (red), and (c) elongases (green). Values below branches show bootstrap support after 100 RAxML iterations. *P. littoralis* sequences identified in this study are highlighted in bold. The different functions (when characterized) of each gene are indicated in unique colour shades, and are represented as desaturation activities ("Δ") for the methyl-end (a) and front-end (b) desaturases, and elongated PUFA substrates for the elongases (c). [Colour figure can be viewed at wileyonlinelibrary.com]
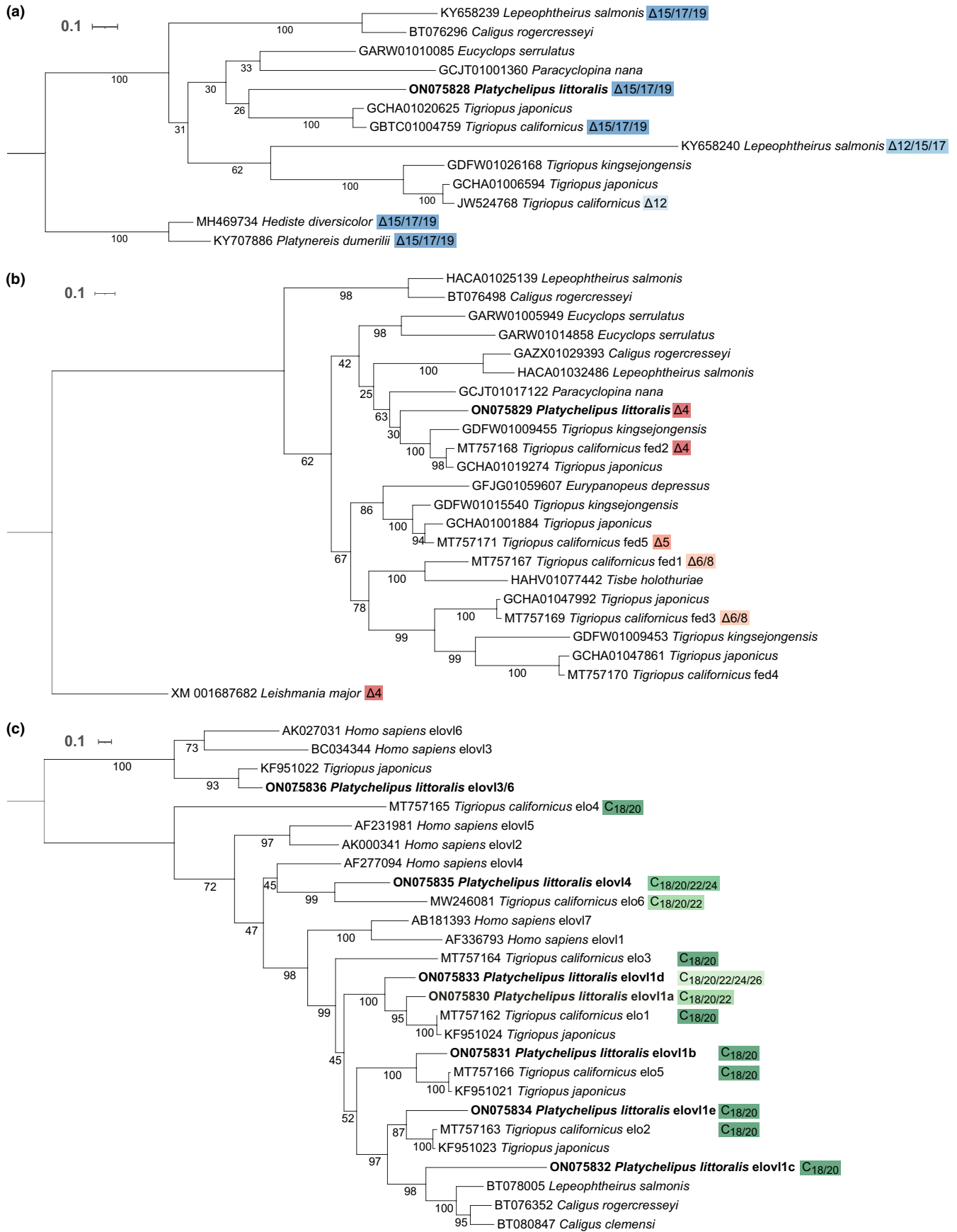
b5 domain. It clusters together with other harpacticoid sequences, including the functionally characterized *T. californicus* methyl-end desaturase "*ωx2*" with Δ15/Δ17/Δ19 activities (Figure 2a). The front-end desaturase (ON075829) remained unnoticed in the initial phylogenetic analysis since its Pfam domain *Cyt-b5* (PF00173) had an E-score of 6.1 E-05 and therefore did not pass the criteria at that time (Boyen et al., 2020). It was placed in the copepod-specific clade previously identified (Kabeya et al., 2021), with its closest functionally characterized sequence being the *T. californicus* Δ4 desaturase "*Fed2*" (Figure 2b). In addition, we found a front-end desaturase in a transcriptome of the decapod *Eurypanopeus depressus* (GFJG01059607), which clustered inside the copepod-specific clade and contained the correct third histidine box "QIEHH" as opposed to previously identified decapod front-end desaturase sequences. One *P. littoralis* elongase (ON075836) aligned closely with the vertebrate elovl3/elovl6 subfamily, which is specifically known to elongate saturated FAs, and was therefore not included in the subsequent functional characterization. Another *P. littoralis* elongase (ON075835) formed a clade with the human and *T. californicus* elovl4 sequences. The five other *P. littoralis* elongase sequences all belonged within the Pancrustacea-specific elovl1/7-like clade identified earlier (Boyen et al., 2020; Kabeya et al., 2021) (Figure 2c). Therefore, we subsequently labelled them elovl1a-e. *Platychelipus littoralis* elovl1a, elovl1b and elovl1e closely aligned with the functionally characterized *T. californicus* "*elo1*", "*elo5*" and "*elo2*" respectively, as well as the corresponding *Tigriopus japonicus* sequences. *Platychelipus littoralis* elovl1d does not have a direct relationship with any other copepod elongases, though it aligned most closely with the *P. littoralis* elovl1a/*T. californicus* "*elo1*" clade. The *P. littoralis* elovl1c did not match with any functionally characterized *T. californicus* elongase, but did align with elongase sequences from *L. salmonis*, *Caligus rogercresseyi* and *Caligus clemensi* (all siphonostomatoids). Remarkably, all sequences from the two subclades containing *P. littoralis* elovl1c (ON075832) and elovl1e (ON075834) contained a histidine box "QXXHH" instead of the typical "HXXHH" observed in other FA elongases.

3.2 | Functional characterization

The functions of all putative desaturases and elongases identified from *P. littoralis*, except for elovl3/6, were characterized in yeast by heterologous expression of the corresponding coding region and growing in the presence of potential PUFA substrates. The FA profiles of the transgenic yeast expressing the *P. littoralis* methyl-end desaturase and grown in the presence of exogenously added C_{18}, C_{20} and C_{22} n−6 PUFA substrates showed n−3 desaturation products denoting that this enzyme has Δ15, Δ17 and Δ19 desaturation capacity, respectively (Table 2). No Δ12 desaturation capacity was detected for the *P. littoralis* methyl-end desaturase, since levels of the Δ12 desaturation product 18:2 n−6 were not statistically different when compared with yeast transformed with the empty pYES2 vector (Student's *t*-test, $p > .05$) (Table S1).

Functional characterization assays of the *P. littoralis* front-end desaturase showed this enzyme has Δ4 desaturation capacity since transgenic yeast expressing its coding region were able to convert 22:5 n−3 and 22:4 n−6 into 22:6 n−3 and 22:5 n−6, respectively (Table 3). No activity toward 18:3 n−3, 18:2 n−6, 20:3 n−3, 20:2 n−6, 20:4 n−3 and 20:3 n−6 was detected, confirming that the *P. littoralis* front-end desaturase does not have Δ5, Δ6 or Δ8 desaturation capacities (Table 3).

The capacity of the *P. littoralis* elongases to act toward saturated FAs was assessed by comparing the FA profiles of yeast transformed with the empty vector with those of yeast each expressing one of the six elongases under study (Figure 3, Table S2). Yeast expressing *P. littoralis* elovl4 showed a significant increase of 20:0 and production of 28:0 and 30:0 (Dunnett's test, $p < .05$), while levels of other FAs were not different from those of the control yeast. Yeast expressing *P. littoralis* elovl1a showed significantly lower levels of 16:0, 17:0, 18:0 and 20:0 and higher levels of 22:0, 24:0 and 26:0 compared to the control yeast. Expression of *P. littoralis* elovl1d resulted in significantly reduced levels of 16:0 and 18:0 and increased levels of 26:0, 28:0 and 30:0, while expression of *P. littoralis* elovl1e resulted in significantly reduced levels of 16:0 and increased levels of 26:0. *Platychelipus littoralis* elovl1b and elovl1c did not show any capacity for elongation of yeast endogenous FAs (Dunnett's test, $p > .05$) (Figure 3, Table S2).

The activities of the *P. littoralis* elongases toward PUFA substrates were assessed by growing transgenic yeast expressing each elongase in the presence of exogenously added PUFA substrates. *Platychelipus littoralis* elovl4 was able to elongate all of the supplied substrates, with additional elongation of the product 24:5 n−3 toward 26:5 n−3 (Table 4). *Platychelipus littoralis* elovl1a was able to elongate all of the supplied substrates except 18:2 n−6 (Table 4). The *P. littoralis* elovl1b had a relatively low elongation capacity toward C_{18} substrates and particularly high elongation capacity toward C_{20} substrates, with up to 84.7% and 57.2% conversion of 20:5 n−3 (EPA) and 20:4 n−6 (ARA) toward 22:5 n−3 and 22:4 n−6, respectively, yet no detectable activity toward C_{22} substrates (Table 4). Similarly, *P. littoralis* elovl1c and elovl1e had elongation capacity of C_{18} and C_{20} substrates, but no detectable activity toward C_{22} substrates (Table 4). While *P. littoralis* elovl1d was able to elongate C_{18} and C_{20} substrates to some extent, it was found to have particularly high elongation capacity of C_{22} substrates, enabling the production of polyenes up to C_{28} via stepwise elongations from exogenously added substrates (Table 4).

4 | DISCUSSION

In this study, we identified nine *P. littoralis* desaturases and elongases and demonstrated the functions of eight of them. We found that these enzymes exhibited highly diverse enzymatic capacities enabling biosynthesis of not only LC-PUFAs but also very long-chain FAs (up to C_{30}). We found one *P. littoralis* methyl-end desaturase with a multifunctional Δ15, Δ17 and Δ19 desaturation capacity similar to the *T. californicus* "*ωx2*" and *L. salmonis* "*ω3*" orthologues (Kabeya

TABLE 2 Substrate conversions of the transgenic yeast expressing the *P. littoralis* methyl-end desaturase

FA substrate	Product	Conversion (%)	Activity
18:2n−6	18:3n−3	29.6	Δ15
18:3n−6	18:4n−3	25.7	Δ15
20:2n−6	20:3n−3	10.7	Δ17
20:3n−6	20:4n−3	13.7	Δ17
20:4n−6	20:5n−3	57.0	Δ17
22:4n−6	22:5n−3	13.4	Δ19
22:5n−6	22:6n−3	7.4	Δ19

Note: The results are presented as a percentage of the fatty acid (FA) substrate converted into the corresponding desaturated product.

TABLE 3 Substrate conversions of the transgenic yeast expressing the *P. littoralis* front-end desaturase

FA substrate	Product	Conversion (%)	Activity
18:3n−3	18:4n−3	–	Δ6
18:2n−6	18:3n−6	–	Δ6
20:3n−3	20:4n−3	–	Δ8
20:2n−6	20:3n−6	–	Δ8
20:4n−3	20:5n−3	–	Δ5
20:3n−6	20:4n−6	–	Δ5
22:5n−3	22:6n−3	7.8	Δ4
22:4n−6	22:5n−6	7.3	Δ4

Note: The results are presented as a percentage of the fatty acid (FA) substrate converted into the corresponding desaturated product. –, not detected (<0.1%).

FIGURE 3 Heatmap illustrating mean endogenous saturated fatty acid levels of the transgenic yeast expressing the *P. littoralis* elongases as well as the control yeast ($n = 3$). Fatty acids percentages (%) were scaled to z-scores per fatty acid, with blue indicating lower and red indicating higher than average percentages. Data used to generate this heatmap can be found in Table S2. [Colour figure can be viewed at wileyonlinelibrary.com]

et al., 2018, 2021). Additionally, we found that the *P. littoralis* methyl-end desaturase is able to convert both 22:4n−6 and 22:5n−6 into 22:5n−3 and 22:6n−3 (DHA), respectively. This contrasts with the *T. californicus* "ωx2" methyl-end desaturase, which is only able to desaturate 22:4n−6 but not 22:5n−6 (Kabeya et al., 2021). While *T. californicus*, *T. japonicus* and *L. salmonis* have been found to possess two methyl-end desaturases (Kabeya et al., 2018, 2021), other copepods such as *C. rogercresseyi*, *Eucyclops serrulatus*, *Paracyclopina nana*, *Tigriopus kingsejongensis* and now also the benthic harpacticoid *P. littoralis* seem to possess only one (Figure 2). While improved transcriptomic resources from the latter species might reveal a second methyl-end desaturase, a broader investigation including genomic data from more copepod species could disclose whether one or two methyl-end desaturases is the dominating trait among copepods. If assumed that *P. littoralis* only contains one sole methyl-end desaturase lacking Δ12 desaturation capacity, this implies that *P. littoralis* is not able to convert OA into LA and therefore does not have the capacity for complete de novo LC-PUFA biosynthesis from endogenously produced saturated and monounsaturated FAs. Such capacity has been reported to exist in specific species of Cnidaria, Mollusca, Annelida, Rotifera and Arthropoda, including the copepods *L. salmonis* and *T. californicus* (Kabeya et al., 2018, 2020, 2021). On the other hand, our results show that the *P. littoralis* methyl-end desaturase has Δ17 and
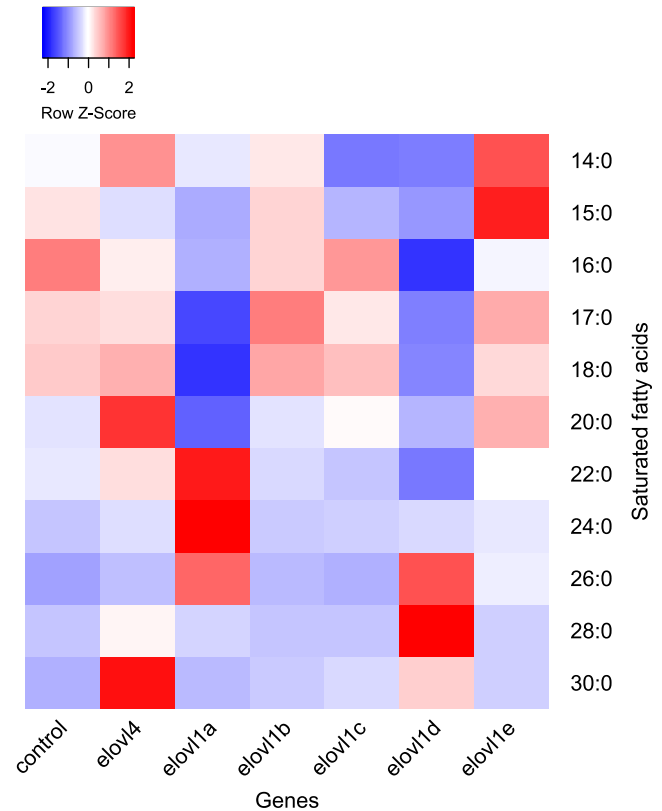
Δ19 desaturation capacity, including a capacity for biosynthesis of EPA and DHA from ARA and 22:5n−6, respectively. This Δ17 and Δ19 desaturation of omega-6 FAs could be an important alternative pathway toward omega-3 LC-PUFAs, enabling their production from an increased variety of dietary precursors.

The copepod front-end desaturase gene family is distinct from other metazoan front-end desaturase clades (Kabeya et al., 2021; Lee, Choi, Kim, et al., 2020; Nielsen et al., 2019). It is more closely related to protists and algae such as *Leishmania major*, which was previously hypothesized to be a result of horizontal gene transfer (Kabeya et al., 2021). We found that the *P. littoralis* front-end desaturase had a single Δ4 desaturation capacity enabling the production of 22:5n−6 and, more importantly, DHA. This is the second Δ4 desaturase found in harpacticoids, further supporting the hypothesis that they use the so-called "Δ4 pathway" as opposed to the Sprecher pathway to synthesize DHA (Kabeya et al., 2021). Functional characterization of more front-end desaturases will allow us to verify the potential universal presence of the Δ4 pathway in other copepod orders. The *P. littoralis* Δ4 desaturase is phylogenetically placed in the previously discovered copepod-specific clade, within a subclade that also contains the *T. californicus* Δ4 desaturase. The four other *T. californicus* front-end desaturases all cluster within a second subclade

TABLE 4 Substrate conversions of the transgenic yeast expressing the *P. littoralis* elongases

FA substrate	Product	Conversion (%)						Activity
		elovl4	elovl1a	elovl1b	elovl1c	elovl1d	elovl1e	
18:3n–3	20:3n–3	5.9	0.5	2.2	14.2	1.2	13.2	$C_{18} \rightarrow C_{20}$
	22:3n–3	–	2.6	–	0.2	6.6	0.1	$C_{20} \rightarrow C_{22}$
18:2n–6	20:2n–6	2.2	–	0.3	3.0	0.3	1.6	$C_{18} \rightarrow C_{20}$
	22:2n–6	–	–	–	–	9.2	3.0	$C_{20} \rightarrow C_{22}$
18:4n–3	20:4n–3	3.7	2.9	1.5	11.0	3.7	10.6	$C_{18} \rightarrow C_{20}$
	22:4n–3	2.0	1.2	–	–	3.1	0.8	$C_{20} \rightarrow C_{22}$
	24:4n–3	–	–	–	–	12.1	–	$C_{22} \rightarrow C_{24}$
18:3n–6	20:3n–6	2.5	2.9	1.0	6.4	4.9	4.7	$C_{18} \rightarrow C_{20}$
	22:3n–6	3.0	1.0	0.8	0.5	2.7	0.5	$C_{20} \rightarrow C_{22}$
	24:4n–3	–	–	–	–	40.9	–	$C_{22} \rightarrow C_{24}$
20:5n–3	22:5n–3	8.3	4.6	84.7	0.7	4.3	5.2	$C_{20} \rightarrow C_{22}$
	24:5n–3	4.4	3.3	–	–	20.4	–	$C_{22} \rightarrow C_{24}$
20:4n–6	22:4n–6	6.0	2.3	57.2	0.1	4.0	0.4	$C_{20} \rightarrow C_{22}$
	24:4n–6	4.1	4.0	–	–	55.6	–	$C_{22} \rightarrow C_{24}$
	26:4n–6	–	–	–	–	57.5	–	$C_{24} \rightarrow C_{26}$
	28:4n–6	–	–	–	–	9.3	–	$C_{26} \rightarrow C_{28}$
22:5n–3	24:5n–3	3.5	2.4	–	–	14.5	–	$C_{22} \rightarrow C_{24}$
	26:5n–3	8.3	–	–	–	18.7	–	$C_{24} \rightarrow C_{26}$
	28:5n–3	–	–	–	–	9.9	–	$C_{26} \rightarrow C_{28}$
22:4n–6	24:4n–6	1.7	0.9	–	–	18.7	–	$C_{22} \rightarrow C_{24}$
	26:4n–6	–	–	–	–	58.8	–	$C_{24} \rightarrow C_{26}$
	28:4n–6	–	–	–	–	13.1	–	$C_{26} \rightarrow C_{28}$

Note: The results are presented as a percentage of the fatty acid (FA) substrate converted into the corresponding elongated product. –: not detected (<0.1%).

mostly containing harpacticoid species (*Tigriopus* and *Tisbe*), further speculating that more *P. littoralis* front-end desaturases with Δ5, Δ6 or Δ8 desaturation capacity remain to be discovered. While our phylogenetic inference of the front-end desaturases is similar to Nielsen et al. (2019), the phylogenetic tree of Kabeya et al. (2021) does not separate the *T. californicus* Δ4 desaturase "Fed2" from the other sequences. Therefore, a more substantial phylogenetic analysis involving even more putative copepod sequences coupled with additional functional characterization of front-end desaturases from other copepod species is essential to clarify the evolution and diversification of this gene family, including its potential origin from horizontal gene transfer (Kabeya et al., 2021).

The phylogenetic analysis of the *P. littoralis* elongases indicated extensive gene differentiation prior to copepod species differentiation. A large expansion of the elongase gene family was found in the harpacticoid genus *Tigriopus* as well (Kabeya et al., 2021; Lee, Choi, Kim, et al., 2020). Two *P. littoralis* elongases each clustered with the known "vertebrate" elovl3/6 and elovl4 clades, with *P. littoralis* elovl4 having a rather general elongation capacity similar to the *T. californicus* orthologue. Five *P. littoralis* elongases (elovl1a-e) clustered within the recently discovered Pancrustacea-specific elovl1/7-like clade (Ribes-Navarro et al., 2021), and the detected strong elongation capacities of the tested elongases further emphasize the importance

of this clade. The results from *P. littoralis* elovl1c and elovl1e as well as *T. californicus* "elo2" show that elongases with a "QXXHH" histidine box instead of the usual "HXXHH" histidine box can still exhibit elongation capacities. While elovl1c and elovl1d do not have *T. californicus* orthologues, *P. littoralis* elovl1b and elovl1e mirrored the C_{18} and C_{20} elongation capacities of their functionally characterized *T. californicus* orthologues "elo5" and "elo2" (Kabeya et al., 2021). Furthermore, while *P. littoralis* elovl1a matched its *T. californicus* orthologue "elo1" in its ability to elongate all C_{18} and C_{20} substrates except 18:2n–6, it was additionally able to elongate C_{22} substrates toward C_{24} products. We found a combination of general (elovl4) and specific (elovl1b and elovl1d) elongases, illustrating a large functional diversity. We acknowledge that cautious interpretation of these data is warranted as heterologous expression of single genes in a yeast system - while being a very robust system to establish the substrate specificities of the assayed enzymes - does not necessarily mirror the extent to which that enzyme is active in a more complex multicellular in vivo scenario where numerous competing enzymes, regulatory mechanisms (e.g., via transcription factors or epigenetic signals) and environmental drivers interact (Monroig et al., 2022; Xie et al., 2021).

Overall, our results show that gene family expansion can lead to an improved elongation capacity. The gene copy number increase of

the elovl1/7-like elongase family found in *P. littoralis* and other harpacticoids can be considered an important evolutionary response enabling them to synthesize their well-documented high levels of LC-PUFAs, for example, when compared to calanoids (Twining et al., 2020). Additionally, having multiple gene copies could lead to certain copies becoming tissue- or development stage-specific, or acquiring substrate-specific enzymatic functions, as seen in *P. littoralis* elovl1a (selective elongation of omega-3 instead of omega-6 substrates), and previously demonstrated in vertebrates (Ishikawa et al., 2019). Understanding the gene family diversity of these harpacticoids will help us to better understand the adaptions of copepods within their nutritional landscape. This could be an important driver of evolutionary divergence and copepod diversity, as observed in other species (Ishikawa et al., 2019, 2021, 2022; Twining et al., 2021).

While PUFA elongases have been successfully functionally characterized in other crustacean lineages such as decapods, branchiopods and amphipods (Mah et al., 2019; Ribes-Navarro et al., 2021; Sun et al., 2020; Ting et al., 2020), the occurrence and functionality of methyl-end and front-end desaturases in these lineages remains highly questionable (Chen et al., 2017; Kabeya et al., 2021; Lin et al., 2017; Monroig & Kabeya, 2018; Nielsen et al., 2019; Ting et al., 2021; Wu et al., 2018; Yang et al., 2013). In our phylogenetic study, we detected a putative front-end desaturase in a transcriptome of the decapod *Eurypanopeus depressus* clustering together with the *T. californicus* Δ5 front-end desaturase "*Fed5*" with high bootstrap support (86%). Importantly, the *E. depressus* putative front-end desaturase identified in the present study has all correct signatures including the three H-boxes "HXXXH", "HXXXHH" and "QXXHH" and a heme binding motif (HPGG) in the cytochrome b5 domain (Hashimoto et al., 2008). Assuming this was not due to contamination during RNA sequencing, the *E. depressus* putative front-end desaturase could be the first report of this type of LC-PUFA biosynthesizing enzymes in decapods. Further functional assays will be required to test this hypothesis.

4.1 | Concluding remarks

The present study demonstrates that the benthic copepod *P. littoralis* has the genes for biosynthesis of EPA from ARA (using its Δ15/Δ17/Δ19 methyl-end desaturase), as well as the synthesis of DHA from either EPA (using its elovl1b elongase and its Δ4 front-end desaturase) or 22:5n−6 (using its methyl-end desaturase). However, due to the lack of a Δ12 methyl-end desaturase and Δ5, Δ6 or Δ8 front-end desaturases, we could not confirm the capacity for full de novo endogenous LC-PUFA synthesis from MUFAs or short-chain PUFAs, as found in *T. californicus* (Kabeya et al., 2021). Since *P. littoralis* was shown to synthesize DHA from stable-isotope labelled diets containing high amounts of ALA and no LC-PUFAs (Werbrouck et al., 2017), at least enzymes with Δ5, Δ6 or Δ8 desaturation activity should theoretically be present but remain yet undetected.

Thus, copepods such as *P. littoralis* and *T. californicus* could play an important role as LC-PUFA producers in marine and estuarine food webs. Endogenous biosynthesis of EPA and DHA by primary consumers - even when synthesized from other LC-PUFAs such as ARA as evidenced here - has large-scale implications for global food webs. In aquatic ecosystems, where LC-PUFA production by microalgae is expected to decrease due to climate change, LC-PUFA production by primary consumers could potentially still provide secondary and tertiary consumers with their required LC-PUFA levels (Závorka et al., 2021). Future research should examine a number of impacts and consequences resulting from this observation. First, this biosynthetic capacity in benthic and intertidal harpacticoids is unlikely to be representative for other copepod orders, such as pelagic calanoids, freshwater cyclopoids or parasitic siphonostomatoids, or even other primary consumers. Therefore, absolute quantities of LC-PUFA production in different taxa should be calculated and an assessment should be made whether this could significantly contribute to overall LC-PUFA biomass worldwide. Second, in a warming ocean, copepods not only face declining LC-PUFA from their diet, but also face climate change effects directly. Direct negative effects of ocean warming on LC-PUFA content and production have been demonstrated in *P. littoralis* (Boyen et al., 2020; Sahota et al., 2022; Werbrouck et al., 2017) and other primary consumers (Lee et al., 2017, 2022; Masclaux et al., 2012). These impacts should be considered, as they can severely limit the consumer's biosynthesis ability (when present) to make up for a reduced dietary LC-PUFA provision due to climate change. Third, endogenous LC-PUFA synthesis means facing higher metabolic costs, and the potentially associated reduced fitness should also be accounted for. Finally, studies using FAs as biomarkers should integrate consumer FA metabolism into their considerations. For instance, Jardine et al. (2020) calculated FA regression equations and used those to correct for trophic modification. Updated knowledge on specific conversion capacities of certain species as well as controlled feeding experiments can further improve future models.

AUTHOR CONTRIBUTIONS

Jens Boyen, Naoki Kabeya, Óscar Monroig, Juan Carlos Navarro and Marleen De Troch conceptualized the study. Jens Boyen, Naoki Kabeya, Óscar Monroig and Pascal I. Hablützel performed the phylogenetic analysis. Jens Boyen and Annelien Rigaux constructed the plasmids. Jens Boyen, Alberto Ribes-Navarro, Óscar Monroig and Juan Carlos Navarro performed the functional assays and fatty acid analysis. Jens Boyen performed the statistical analysis and prepared the initial version of the manuscript. All authors assisted in the interpretation of the results and the revision of the manuscript.

CONFLICT OF INTEREST

The authors have no conflict of interest to declare.

DATA AVAILABILITY STATEMENT

All isolated sequences from *P. littoralis* in the present study have been deposited at NCBI GenBank with the accession numbers ON075828 to ON075835.

BENEFIT-SHARING STATEMENT

There are no benefits outlined in the Nagoya protocol associated with this study to report.

ORCID

Jens Boyen https://orcid.org/0000-0001-5005-7724

Alberto Ribes-Navarro https://orcid.org/0000-0002-8293-7168

Naoki Kabeya https://orcid.org/0000-0002-2055-6554

Óscar Monroig https://orcid.org/0000-0001-8712-0440

Patrick Fink https://orcid.org/0000-0002-5927-8977

Pascal I. Hablützel https://orcid.org/0000-0002-6739-4994

Juan Carlos Navarro https://orcid.org/0000-0001-6976-6686

Marleen De Troch https://orcid.org/0000-0002-6800-0299

REFERENCES

Amparyup, P., Sungkaew, S., Charoensapsri, W., Tapaneeyaworawong, P., Chumtong, P., Yocawibun, P., Pantong, P., Wongpanya, R., Imjongjirak, C., & Powtongsook, S. (2022). Molecular characterization of biosynthesis of polyunsaturated fatty acids during different developmental stages in the copepod *Apocyclops royi*. *Aquaculture Reports*, 23, 101064. https://doi.org/10.1016/j.aqrep.2022.101064

Arndt, C., & Sommer, U. (2014). Effect of algal species and concentration on development and fatty acid composition of two harpacticoid copepods, *Tisbe* sp. and *Tachidius discipes*, and a discussion about their suitability for marine fish larvae. *Aquaculture Nutrition*, 20(1), 44–59. https://doi.org/10.1111/anu.12051

Bazinet, R. P., & Layé, S. (2014). Polyunsaturated fatty acids and their metabolites in brain function and disease. *Nature Reviews Neuroscience*, 15(12), 771–785. https://doi.org/10.1038/nrn3820

Bell, M. V., & Tocher, D. R. (2009). Biosynthesis of polyunsaturated fatty acids in aquatic ecosystems: General pathways and new directions. In M. Kainz, M. Brett, & M. Arts (Eds.), *Lipids in aquatic ecosystems* (pp. 211–236). Springer. https://doi.org/10.1007/978-0-387-89366-2_9

Bi, R., Cao, Z., Ismar-Rebitz, S. M. H., Sommer, U., Zhang, H., Ding, Y., & Zhao, M. (2021). Responses of marine diatom-dinoflagellate competition to multiple environmental drivers: Abundance, elemental, and biochemical aspects. *Frontiers in Microbiology*, 12, 731786. https://doi.org/10.3389/fmicb.2021.731786

Boyen, J., Fink, P., Mensens, C., Hablützel, P. I., & De Troch, M. (2020). Fatty acid bioconversion in harpacticoid copepods in a changing environment: A transcriptomic approach. *Philosophical Transactions of the Royal Society B: Biological Sciences*, 375(1804), 20190645. https://doi.org/10.1098/rstb.2019.0645

Brady, G. S. (1880). *A monograph of the free and semi-parasitic Copepoda of the British Islands* (Vol. II). The Ray Society.

Caramujo, M. J., Boschker, H. T. S., & Admiraal, W. (2008). Fatty acid profiles of algae mark the development and composition of harpacticoid copepods. *Freshwater Biology*, 53(1), 77–90. https://doi.org/10.1111/j.1365-2427.2007.01868.x

Chen, K., Li, E., Li, T., Xu, C., Xu, Z., Qin, J. G., & Chen, L. (2017). The expression of the Δ6 fatty acyl desaturase-like gene from Pacific white shrimp (*Litopenaeus vannamei*) under different salinities and dietary lipid compositions. *Journal of Shellfish Research*, 36(2), 501–509. https://doi.org/10.2983/035.036.0221

Colombo, S. M., Rodgers, T. F. M., Diamond, M. L., Bazinet, R. P., & Arts, M. T. (2020). Projected declines in global DHA availability for human consumption as a result of global warming. *Ambio*, 49(4), 865–880. https://doi.org/10.1007/s13280-019-01234-6

Colombo, S. M., Wacker, A., Parrish, C. C., Kainz, M. J., & Arts, M. T. (2017). A fundamental dichotomy in long-chain polyunsaturated fatty acid abundance between and within marine and terrestrial ecosystems. *Environmental Reviews*, 25(2), 163–174.

De Troch, M., Boeckx, P., Cnudde, C., Van Gansbeke, D., Vanreusel, A., Vincx, M., & Caramujo, M. J. (2012). Bioconversion of fatty acids at the basis of marine food webs: Insights from a compound-specific stable isotope analysis. *Marine Ecology Progress Series*, 465, 53–67. https://doi.org/10.3354/meps09920

Desvilettes, C., Bourdier, G., & Breton, J. C. (1997). On the occurrence of a possible bioconversion of linolenic acid into docosahexaenoic acid by the copepod *Eucyclops serrulatus* fed on microalgae. *Journal of Plankton Research*, 19(2), 273–278. https://doi.org/10.1093/plankt/19.2.273

Farkas, T., Kariko, K., & Csengeri, I. (1981). Incorporation of [1-14C] acetate into fatty acids of the crustaceans *Daphnia magna* and *Cyclops strenus* in relation to temperature. *Lipids*, 16(6), 418–422. https://doi.org/10.1007/BF02535008

Folch, J., Lees, M., & Sloane Stanley, G. H. (1957). A simple method for the isolation and purification of total lipids from animal tissues. *Journal of Biological Chemistry*, 226(1), 497–509.

Galloway, A. W. E., & Budge, S. M. (2020). The critical importance of experimentation in biomarker-based trophic ecology. *Philosophical Transactions of the Royal Society B: Biological Sciences*, 375(1804), 20190638. https://doi.org/10.1098/rstb.2019.0638

Gee, J. M. (1987). Impact of epibenthic predation on estuarine intertidal harpacticoid copepod populations. *Marine Biology*, 96(4), 497–510. https://doi.org/10.1007/BF00397967

George, K. H., Khodami, S., Kihara, T. C., Martínez Arbizu, P., Martínez, A., Mercado Salas, N., Pointner, K., & Veit-Köhler, G. (2020). Chapter 27: Copepoda. In A. Schmidt-Rhaesa (Ed.), *Guide to the identification of marine meiofauna* (pp. 465–533). Verlag Dr. Friedrich Pfeil. https://doi.org/10.1017/CBO9781107415324.004

Hashimoto, K., Yoshizawa, A. C., Okuda, S., Kuma, K., Goto, S., & Kanehisa, M. (2008). The repertoire of desaturases and elongases reveals fatty acid variations in 56 eukaryotic genomes. *Journal of Lipid Research*, 49(1), 183–191. https://doi.org/10.1194/jlr.m700377-jlr200

Hicks, G. R. F., & Coull, B. C. (1983). The ecology of marine meiobenthic harpacticoid copepods. *Oceanography and Marine Biology - An Annual Review*, 21, 67–175.

Hixson, S. M., & Arts, M. T. (2016). Climate warming is predicted to reduce omega-3, long-chain, polyunsaturated fatty acid production in phytoplankton. *Global Change Biology*, 22(8), 2744–2755. https://doi.org/10.1111/gcb.13295

Holm, H. C., Fredricks, H. F., Bent, S. M., Lowenstein, D. P., Ossolinski, J. E., Becker, K. W., Johnson, W. M., Schrage, K., & Van Mooy, B.

A. S. (2022). Global Ocean lipidomes show a universal relationship between temperature and lipid unsaturation. *Science*, 376, 1487–1491. https://doi.org/10.1126/science.abn7455

Ishikawa, A., Kabeya, N., Ikeya, K., Kakioka, R., Cech, J. N., Osada, N., Leal, M. C., Inoue, J., Kume, M., Toyoda, A., Tezuka, A., Nagano, A. J., Yamasaki, Y. Y., Suzuki, Y., Kokita, T., Takahashi, H., Lucek, K., Marques, D., Takehana, Y., … Kitano, J. (2019). A key metabolic gene for recurrent freshwater colonization and radiation in fishes. *Science*, 364, 886–889. https://doi.org/10.1126/science.aau5656

Ishikawa, A., Stuart, Y. E., Bolnick, D. I., & Kitano, J. (2021). Copy number variation of a fatty acid desaturase gene Fads2 associated with ecological divergence in freshwater stickleback populations. *Biology Letters*, 17(8), 20210204. https://doi.org/10.1098/rsbl.2021.0204

Ishikawa, A., Yamanouchi, S., Iwasaki, W., & Kitano, J. (2022). Convergent copy number increase of genes associated with freshwater colonisation in fishes. *Philosophical Transactions of the Royal Society B: Biological Sciences*, 377(1855), 20200509. https://doi.org/10.1098/rstb.2020.0509

Jardine, T. D., Galloway, A. W. E., & Kainz, M. J. (2020). Unlocking the power of fatty acids as dietary tracers and metabolic signals in fishes and aquatic invertebrates. *Philosophical Transactions of the Royal Society B: Biological Sciences*, 375(1804), 20190639. https://doi.org/10.1098/rstb.2019.0639

Kabeya, N., Fonseca, M. M., Ferrier, D. E. K., Navarro, J. C., Bay, L. K., Francis, D. S., Tocher, D. R., Castro, L. F. C., & Monroig, Ó. (2018). Genes for de novo biosynthesis of omega-3 polyunsaturated fatty acids are widespread in animals. *Science Advances*, 4(5), eaar6849. https://doi.org/10.1126/sciadv.aar6849

Kabeya, N., Gür, İ., Oboh, A., Evjemo, J. O., Malzahn, A. M., Hontoria, F., Navarro, J. C., & Monroig, Ó. (2020). Unique fatty acid desaturase capacities uncovered in *Hediste diversicolor* illustrate the roles of aquatic invertebrates in trophic upgrading. *Philosophical Transactions of the Royal Society B: Biological Sciences*, 375(1804), 20190654. https://doi.org/10.1098/rstb.2019.0654

Kabeya, N., Ogino, M., Ushio, H., Haga, Y., Satoh, S., Navarro, J. C., & Monroig, Ó. (2021). A complete enzymatic capacity for biosynthesis of docosahexaenoic acid (DHA, 22:6n−3) exists in the marine Harpacticoida copepod *Tigriopus californicus. Open Biology*, 11(4), 200402. https://doi.org/10.1098/rsob.200402

Katoh, K., & Standley, D. M. (2013). MAFFT multiple sequence alignment software version 7: Improvements in performance and usability. *Molecular Biology and Evolution*, 30(4), 772–780. https://doi.org/10.1093/molbev/mst010

Kwiatkowski, L., Torres, O., Bopp, L., Aumont, O., Chamberlain, M., R. Christian, J., P. Dunne, J., Gehlen, M., Ilyina, T., G. John, J., Lenton, A., Li, H., S. Lovenduski, N., C. Orr, J., Palmieri, J., Santana-Falcón, Y., Schwinger, J., Séférian, R., A. Stock, C., … Ziehn, T. (2020). Twenty-first century ocean warming, acidification, deoxygenation, and upper-ocean nutrient and primary production decline from CMIP6 model projections. *Biogeosciences*, 17(13), 3439–3470. https://doi.org/10.5194/bg-17-3439-2020

Lee, M.-C., Choi, B.-S., Kim, M.-S., Yoon, D.-S., Park, J. C., Kim, S., & Lee, J.-S. (2020). An improved genome assembly and annotation of the Antarctic copepod *Tigriopus kingsejongensis* and comparison of fatty acid metabolism between *T. kingsejongensis* and the temperate copepod *T. japonicus. Comparative Biochemistry and Physiology - Part D: Genomics and Proteomics*, 35, 100703. https://doi.org/10.1016/j.cbd.2020.100703

Lee, M.-C., Choi, H., Park, J. C., Yoon, D.-S., Lee, Y., Hagiwara, A., Park, H. G., Shin, K.-H., & Lee, J.-S. (2020). A comparative study of food selectivity of the benthic copepod *Tigriopus japonicus* and the pelagic copepod *Paracyclopina nana*: A genome-wide identification of fatty acid conversion genes and nitrogen isotope investigation. *Aquaculture*, 521, 734930. https://doi.org/10.1016/j.aquaculture.2020.734930

Lee, M.-C., Yoon, D.-S., Park, J. C., Choi, H., Shin, K.-H., Hagiwara, A., Lee, J.-S., & Park, H. G. (2022). Effects of salinity and temperature on reproductivity and fatty acid synthesis in the marine rotifer *Brachionus rotundiformis. Aquaculture*, 546(July 2021), 737282. https://doi.org/10.1016/j.aquaculture.2021.737282

Lee, S.-H., Lee, M.-C., Puthumana, J., Park, J. C., Kang, S., Han, J., Shin, K.-H., Park, H. G., Om, A.-S., & Lee, J.-S. (2017). Effects of temperature on growth and fatty acid synthesis in the cyclopoid copepod *Paracyclopina nana. Fisheries Science*, 83(5), 725–734. https://doi.org/10.1007/s12562-017-1104-2

Lin, Z., Hao, M., Zhu, D., Li, S., & Wen, X. (2017). Molecular cloning, mRNA expression and nutritional regulation of a Δ6 fatty acyl desaturase-like gene of mud crab, *Scylla paramamosain. Comparative Biochemistry and Physiology - Part B: Biochemistry and Molecular Biology*, 208–209, 29–37. https://doi.org/10.1016/j.cbpb.2017.03.004

Mah, M., Kuah, M., Yeat, S., Merosha, P., Janaranjani, M., Goh, P., Jayaram, A., & Shu-chien, A. C. (2019). Molecular cloning, phylogenetic analysis and functional characterisation of an Elovl7-like elongase from a marine crustacean, the orange mud crab (*Scylla olivacea*). *Comparative Biochemistry and Physiology - Part B: Biochemistry and Molecular Biology*, 232, 60–71. https://doi.org/10.1016/j.cbpb.2019.01.011

Malcicka, M., Visser, B., & Ellers, J. (2018). An evolutionary perspective on linoleic acid synthesis in animals. *Evolutionary Biology*, 45(1), 15–26. https://doi.org/10.1007/s11692-017-9436-5

Masclaux, H., Bec, A., Kainz, M. J., Perrière, F., Desvilettes, C., & Bourdier, G. (2012). Accumulation of polyunsaturated fatty acids by cladocerans: Effects of taxonomy, temperature and food. *Freshwater Biology*, 57(4), 696–703. https://doi.org/10.1111/j.1365-2427.2012.02735.x

Monroig, Ó., & Kabeya, N. (2018). Desaturases and elongases involved in polyunsaturated fatty acid biosynthesis in aquatic invertebrates: A comprehensive review. *Fisheries Science*, 84(6), 911–928. https://doi.org/10.1007/s12562-018-1254-x

Monroig, Ó., Shu-Chien, A. C., Kabeya, N., Tocher, D. R., & Castro, L. F. C. (2022). Desaturases and elongases involved in long-chain polyunsaturated fatty acid biosynthesis in aquatic animals: From genes to functions. *Progress in Lipid Research*, 86, 127248. https://doi.org/10.1016/j.plipres.2022.101157

Moreno, V. J., De Moreno, J. E. A., & Brenner, R. R. (1979). Fatty acid metabolism in the calanoid copepod *Paracalanus parvus*: 1. Polyunsaturated fatty acids. *Lipids*, 14(4), 313–317. https://doi.org/10.1007/BF02533413

Nanton, D. A., & Castell, J. D. (1998). The effects of dietary fatty acids on the fatty acid composition of the harpacticoid copepod, *Tisbe* sp., for use as a live food for marine fish larvae. *Aquaculture*, 163, 251–261. https://doi.org/10.1016/S0044-8486(98)00236-1

Nanton, D. A., & Castell, J. D. (1999). The effects of temperature and dietary fatty acids on the fatty acid composition of harpacticoid copepods, for use as a live food for marine fish larvae. *Aquaculture*, 175(1–2), 167–181. https://doi.org/10.1016/S0044-8486(99)00031-9

Nielsen, B. L. H., Gøtterup, L., Jørgensen, T. S., Hansen, B. W., Hansen, L. H., Mortensen, J., & Jepsen, P. M. (2019). n−3 PUFA biosynthesis by the copepod *Apocyclops royi* documented using fatty acid profile analysis and gene expression analysis. *Biology Open*, 8(2), bio038331. https://doi.org/10.1242/bio.038331

Nielsen, B. L. H., Van Someren Gréve, H., Rayner, T. A., & Hansen, B. W. (2020). Biochemical adaptation by the tropical copepods *Apocyclops royi* and *Pseudodiaptomus annandalei* to a PUA-poor brackish water habitat. *Marine Ecology Progress Series*, 655(655), 77–89. https://doi.org/10.3354/meps13536

R Core Team. (2020). *R: A language and environment for statistical computing (4.0.2)*. R Foundation for Statistical Computing. https://www.r-project.org/

Ribes-Navarro, A., Navarro, J. C., Hontoria, F., Kabeya, N., Standal, I. B., Evjemo, J. O., & Monroig, Ó. (2021). Biosynthesis of long-chain polyunsaturated fatty acids in marine gammarids: Molecular cloning and functional characterisation of three fatty acyl elongases. *Marine Drugs*, 19, 226. https://doi.org/10.3390/MD19040226

Sahota, R., Boyen, J., Semmouri, I., Bodé, S., & De Troch, M. (2022). An inter-order comparison of copepod fatty acid composition and biosynthesis in response to a long-chain PUFA-deficient diet along a temperature gradient. *Marine Biology*, 169, 133. https://doi.org/10.1007/s00227-022-04121-z

Sinensky, M. (1974). Homeoviscous adaptation: A homeostatic process that regulates the viscosity of membrane lipids in Escherichia coli. *Proceedings of the National Academy of Sciences of the United States of America*, 71(2), 522–525. https://doi.org/10.1073/pnas.71.2.522

Stamatakis, A. (2014). RAxML version 8: A tool for phylogenetic analysis and post-analysis of large phylogenies. *Bioinformatics*, 30(9), 1312–1313. https://doi.org/10.1093/bioinformatics/btu033

Sun, P., Zhou, Q., Monroig, Ó., Navarro, J. C., Jin, M., Yuan, Y., Wang, X., & Jiao, L. (2020). Cloning and functional characterization of an elovl4-like gene involved in the biosynthesis of long-chain polyunsaturated fatty acids in the swimming crab *Portunus trituberculatus*. *Comparative Biochemistry and Physiology - Part B: Biochemistry and Molecular Biology*, 242, 110408. https://doi.org/10.1016/j.cbpb.2020.110408

Ting, S. Y., Janaranjani, M., Merosha, P., Sam, K. K., Wong, S. C., Goh, P. T., Mah, M. Q., Kuah, M. K., & Chong Shu-Chien, A. (2020). Two Elongases, Elovl4 and Elovl6, fulfill the elongation routes of the LC-PUFA biosynthesis pathway in the Orange mud crab (*Scylla olivacea*). *Journal of Agricultural and Food Chemistry*, 68(14), 4116–4130. https://doi.org/10.1021/acs.jafc.9b06692

Ting, S. Y., Lau, N. S., Sam, K. K., Quah, E. S. H., Ahmad, A. B., Mat-Isa, M. N., & Shu-Chien, A. C. (2021). Long-read sequencing reveals the repertoire of long-chain polyunsaturated fatty acid biosynthetic genes in the purple land crab, *Gecarcoidea lalandii* (H. Milne Edwards, 1837). *Frontiers in Marine Science*, 8, 713928. https://doi.org/10.3389/fmars.2021.713928

Titocci, J., & Fink, P. (2022). Food quality impacts on reproductive traits, development and fatty acid composition of the freshwater calanoid copepod *Eudiaptomus* sp. *Journal of Plankton Research*, 44(4), 1–14. https://doi.org/10.1093/plankt/fbac030

Tocher, D. R. (2015). Omega-3 long-chain polyunsaturated fatty acids and aquaculture in perspective. *Aquaculture*, 449, 94–107. https://doi.org/10.1016/j.aquaculture.2015.01.010

Tripodi, K. E. J., Buttigliero, L. V., Altabe, S. G., & Uttaro, A. D. (2006). Functional characterization of front-end desaturases from trypanosomatids depicts the first polyunsaturated fatty acid biosynthetic pathway from a parasitic protozoan. *FEBS Journal*, 273(2), 271–280. https://doi.org/10.1111/j.1742-4658.2005.05049.x

Twining, C. W., Bernhardt, J., Derry, A., Hudson, C., Ishikawa, A., Kabeya, N., Kainz, M., Kitano, J., Kowarik, C., Ladd, S. N., Leal, M., Scharnweber, K., Shipley, J., & Matthews, B. (2021). The evolutionary ecology of fatty-acid variation: Implications for consumer adaptation and diversification. *Ecology Letters*, 24(8), 1–31. https://doi.org/10.1111/ele.13771

Twining, C. W., Taipale, S. J., Ruess, L., Bec, A., Martin-Creuzburg, D., & Kainz, M. J. (2020). Stable isotopes of fatty acids: Current and future perspectives for advancing trophic ecology. *Philosophical Transactions of the Royal Society B: Biological Sciences*, 375(1804), 20190641. https://doi.org/10.1098/rstb.2019.0641

Werbrouck, E., Bodé, S., Van Gansbeke, D., Vanreusel, A., & De Troch, M. (2017). Fatty acid recovery after starvation: Insights into the fatty acid conversion capabilities of a benthic copepod (Copepoda, Harpacticoida). *Marine Biology*, 164(7), 151. https://doi.org/10.1007/s00227-017-3181-2

Werbrouck, E., Van Gansbeke, D., Vanreusel, A., Mensens, C., & De Troch, M. (2016). Temperature-induced changes in fatty acid dynamics of the intertidal grazer *Platychelipus littoralis* (Crustacea, Copepoda, Harpacticoida): Insights from a short-term feeding experiment. *Journal of Thermal Biology*, 57, 44–53. https://doi.org/10.1016/j.jtherbio.2016.02.002

Wu, D. L., Huang, Y. H., Liu, Z. Q., Yu, P., Gu, P. H., Fan, B., & Zhao, Y. L. (2018). Molecular cloning, tissue expression and regulation of nutrition and temperature on Δ6 fatty acyl desaturase-like gene in the red claw crayfish (*Cherax quadricarinatus*). *Comparative Biochemistry and Physiology - Part B: Biochemistry and Molecular Biology*, 225, 58–66. https://doi.org/10.1016/j.cbpb.2018.07.003

Xie, D., Chen, C., Dong, Y., You, C., Wang, S., Monroig, Ó., Tocher, D. R., & Li, Y. (2021). Regulation of long-chain polyunsaturated fatty acid biosynthesis in teleost fish. *Progress in Lipid Research*, 82, 101095. https://doi.org/10.1016/j.plipres.2021.101095

Yang, Z., Guo, Z., Ji, L., Zeng, Q., Wang, Y., Yang, X., & Cheng, Y. (2013). Cloning and tissue distribution of a fatty acyl Δ6-desaturase-like gene and effects of dietary lipid levels on its expression in the hepatopancreas of Chinese mitten crab (*Eriocheir sinensis*). *Comparative Biochemistry and Physiology - Part B: Biochemistry and Molecular Biology*, 165(2), 99–105. https://doi.org/10.1016/j.cbpb.2013.03.010

Závorka, L., Blanco, A., Chaguaceda, F., Cucherousset, J., Killen, S. S., Liénart, C., Mathieu-Resuge, M., Němec, P., Pilecky, M., Scharnweber, K., Twining, C. W., & Kainz, M. J. (2023). The role of vital dietary biomolecules in eco-evo-devo dynamics. *Trends in Ecology & Evolution*, 38(1), 1–13. https://doi.org/10.1016/j.tree.2022.08.010

Závorka, L., Crespel, A., Dawson, N. J., Papatheodoulou, M., Killen, S. S., & Kainz, M. J. (2021). Climate change-induced deprivation of dietary essential fatty acids can reduce growth and mitochondrial efficiency of wild juvenile salmon. *Functional Ecology*, 35(9), 1960–1971. https://doi.org/10.1111/1365-2435.13860

Zheng, X., Ding, Z., Xu, Y., Monroig, O., Morais, S., & Tocher, D. R. (2009). Physiological roles of fatty acyl desaturases and elongases in marine fish: Characterisation of cDNAs of fatty acyl Δ6 desaturase and elovl5 elongase of cobia (*Rachycentron canadum*). *Aquaculture*, 290(1–2), 122–131. https://doi.org/10.1016/j.aquaculture.2009.02.010

Zhou, X. R., Horne, I., Damcevski, K., Haritos, V., Green, A., & Singh, S. (2008). Isolation and functional characterization of two independently-evolved fatty acid Δ12-desaturase genes from insects. *Insect Molecular Biology*, 17(6), 667–676. https://doi.org/10.1111/j.1365-2583.2008.00841.x

SUPPORTING INFORMATION

Additional supporting information can be found online in the Supporting Information section at the end of this article.